BIO-FOAMS FOR THERMAL PACKAGING APPLICATIONS

by

Virginia Martin Torrejon

A Thesis Submitted for the Degree of Doctor of Philosophy

College of Engineering, Design and Physical Sciences

Department of Mechanical Engineering

May 2018

Abstract

A liquid foaming technology was developed to produce bio-foams for packaging applications. Liquid foaming consists in the transformation of a liquid foamed solution into a porous solid polymer through liquid removal.

Five bio-based liquid foaming formulations systems were explored in this research: starch-PVA-calcium sulfate, starch-gelatine, gelatine hydrogel, gelatine-composites and hydrogel alternatives to gelatine. Gelatine hydrogel-composite foams secondary materials included bio-mass powders from agriculture waste, expanded vermiculite particles, silica aero-gel powders and honeycomb sandwich panels. The hydrogel foams alternative to gelatine were based on agar and gellan gum as main biopolymers.

The feasibility of each formulation system was explored, and the key parameters of formulation and process conditions were identified. The role of different formulation (e.g. biopolymer content, gelatine strength, surfactant type and content, among others) and processing (e.g. expansion ratio, processing temperature and drying process, among others) factors on foaming and drying behaviour of the liquid foam, and the impact on foam structure and properties (density, drying shrinkage and mechanical, thermal and acoustic properties) of the solid foams were investigated.

Hydrogel-foams with comparable densities and thermal conductivity to conventional polymeric foams were produced. Gelatine foams made with both surfactants "A" and C2 exhibited desirable properties for being a strong alternative to conventional plastic foams. Low densities (<20 kg/m^3), thermal conductivity (≈0.039 $W/k{\cdot}m$), and relatively low shrinkage level were achieved. Production upscale research would need to consider drying process optimization for drying time reduction and drying shrinkage minimization.

Keywords: liquid foaming, hydrogels, xerogels, gelatine, packaging foams, thermal conductivity, bio-based packaging

Acknowledgements

Firstly, I would like to express my sincere gratitude to my supervisor, Jim Song, for his guidance, continuous support and make the hard times look breezy. I am very grateful he gave me the opportunity to undertake this PhD project at Brunel University and guided me since the beginning to the completion of this thesis.

I would also like to thank Wolfson Centre for Materials Processing at Brunel University for supporting me during my experimental work, in particular, Karnik Tarverdi, Irene Resa, Paul Marsh, Kun Qi and Steve. I would like to especially thank Abdul Ghani for his support, continuously encouragement and altruistic daily biscuits for the whole Research Centre.

Undertaking this work gave me the opportunity to engage with exceptional colleagues from around the globe. I am very grateful to undergraduates, PhD colleagues, research technicians and Brunel University staff who contributed to this research. I especially thank Arjang, Fatullah, Henry, Inma, Myles and Uche for being a constant source of learning, positivity and support.

I am deeply grateful to my parents, my brother and my friend Elvira la de Yuncos for their unconditional support during the last four years.

Lastly, and foremost, I would like to thank my partner, Mario, for his immense help, endless patience and continuous emotional support. *Muchisimas gracias, Mar.*

TABLE OF CONTENTS

Nomenclature

γ	Surface tension (N/m)
	Shear strain ($\%$)
$\dot{\gamma}$	Shear rate (s^{-1})
ΔP	Pressure difference between two adjacent bubbles (Pa)
δ	Phase angle (rad)
δP	Pressure difference between cells inner and outer spaces (Pa)
ε	Strain ($\%$)
	Material emissivity
θ	Angular displacement (rad)
λ	Wavelength (m)
	Thermal conductivity ($W/m{\cdot}K$)
ρ^*	Density of the cellular material (kg/m^3)
ρ_s	Density of the solid from which the foam cell walls are made of (kg/m^3)
σ	Stephan-Boltzmann constant ($W{\cdot}m^{-2}{\cdot}K^{-4}$)
	Compression strength (Pa)
	Shear stress (Pa)
σ_y	Yield strength (Pa)
Ω	Angular velocity (rad/s)
τ	Sound transmission coefficient
ΔG	Free energy (J)
∇T	Temperature gradient (K)
A	Total gas-melt Interfacial Area (m^2)
	Surface Area of the barrier (m^2)

	Sound wave amplitude (*dB*)
	Wave amplitude (*m*)
a	Absorption coefficient
C	Surfactant concentration
$CaCO_3$	Calcium carbonate
CBL	Compression bonded loose fill
CEN	European Committee for standardisation
CMC	Critical Micelle Concentration
CTAB	Cetrimonium bromide
e	Radiant energy emitted (J)
E	Young's Modulus of the polymer (*Pa*)
E*	Young's Modulus of the foam (*Pa*)
EEC	European Economic Community
EIP	European Innovation Partnerships
EMC	Equilibrium moisture content
EPP	Expanded Polypropylene
EPS	Expanded Polystyrene
ER	Expansion Ratio
f	Frequency (*Hz*)
GMIA	Gelatin Manufacturers Institute of America
G*	Complex shear modulus (*Pa)*
G'	Storage modulus (*Pa)*
G''	Loss modulus (*Pa)*
G_{eq}	Equilibrium modulus

HA	High acyl
	Hydroxyapatite
HB	High bloom
h	Heat transfer coefficient ($W/m^2 \cdot K$)
HDPE	High Density Polyethylene
IEP	Isoelectric Point
k	Number of levels for a given factor in a factorial experiment
	Thermal conductivity ($W/m \cdot K$)
K_σ	Geometry stress constant
K_γ	Geometry strain constant
LDPE	Low Density Polyethylene
LA	Low acyl
LB	Low bloom
M	Torque ($N \cdot m$)
MER	Maximum Expansion Ratio
n	Number of factors analysed in a factorial experiment
p	Porosity *(%)*
P_L	Porosity of the liquid foam (%)
PA	Polyacrilate
PBAT	poly (butylene adipate-co-terephthalate)
PBS	Poly(butylene succinate)
PCL	Polycaprolactone
PE	Polyethylene
PEG	Polyethylene glycol

PET	Polyethylene Terephthalate
PHA	Polyhydroxyalkanoates
PHEE	Poly(hydroxy ester ether)
PHEMA	Polyhydroxyethylmethacrylate
PHVB	Poly(3-hydroxybutyrate-co-3-hydroxyvalerate)
POP	Plaster of Paris
PP	Polypropylene
PS	Polystyrene
PTT	Poly (trimethylene terephthalate)
PU	Polyurethane
PVA	Poly (vinyl alcohol)
PVAc	Poly (vinyl acetate)
PVC	Poly (vinyl chloride)
PVP	Polyvinylpyrrolidone
Q	Thermal flow (*W*)
q	heat flow (W/m^2)
R	Bubble radius (*m*)
	R-value
	Reflection coefficient (m)
R_1	Smaller cells radius (*m*)
R_2	Larger cells radius (*m*)
RPS	Regular Packaging and Stacking Process
SDS	Sodium Dodecyl Sulfate
SEM	Scanning Electron Microscope

STL	Sound Transmission Loss (*dB*)
T	Temperature of the body (K)
$T_1 - T_2$	Temperature differential (*K*)
T_f	Fluid temperature (*K*)
T_g	Glass transition temperature (*K*)
T_w	Surface temperature (*K*)
TGA	Thermogravimetric analysis
TPS	Thermoplastic starch
V_f	Volume of the liquid foam (ml)
V_s	Volume of the initial solution (ml)
x	Thickness of the barrier (m)
z	Material thickness (m)

1. CHAPTER 1.
INTRODUCTION TO THE PROJECT

Chapter 1.
INTRODUCTION TO THE PROJECT

1.1 BACKGROUND

Polymer foams are fossil fuel-derived materials and tend to be disposable (single use or trip). Although they are recyclable materials, this is not their usual end-life in practice (Razza *et al.*, 2015). They are difficult or expensive to recycle due to product contamination or lack of infrastructure. Therefore, foams waste management may depict a challenge for companies and authorities, involving litter and pollution issues (lack of biodegradability).

Various polymer foams are widely used for thermal packaging applications. The most common are Polyurethane (PU), Polyethylene (PE), Expanded Polypropylene (EPP) and Expanded Polystyrene (EPS). All of them are readily available in different densities and thicknesses. EPS and PE foams are the most extensively used plastic foams for thermal packaging for next day delivery products.

Thermal packaging is increasingly becoming a vital factor in new lifestyles, such as prepared foods, food delivery and online sales, which demand solutions that maintain the quality of the products without compromising cost. Besides, thermal packaging made of polymer foams can be used to mitigate or eliminate the negative impact of temperature fluctuation during distribution, where refrigeration is not required or available. However, it contributes to disposable culture as one-use containers are usually difficult and expensive to collect, separate and clean so they usually end up in landfills (Wang *et al.*, 2010).

Considerable efforts have been made in the last decades for the development of sustainable alternatives to polymeric foams. Packaging materials from biopolymers can be compostable and made from renewable resources.

Loose-fills, pieces of material for filling space around goods within shipment boxes, from starch-based materials are considered one of the most successful biopolymers applications (Zhou, Song and Parker, 2006) (Fang and Milford A Hanna, 2001). Bulk starch foams manufacturing technologies have also emerged, such as corrugated foam planks made by extrusion foaming of modified cornstarch. However, these materials are not widely used in packaging due to their high density and cost (Zhou, Song and Parker, 2006). Thus, there is still a need for bulk manufacturing of bio-based foams for packaging applications as a commercially-viable alternative to their fossil fuel counterparts.

Gelatine has extensive applications in different industries due to its biodegradability, nontoxicity and biocompatibility (Shyamkuwar *et al.*, 2010). Extensive research about gelatine films and coatings for packaging has been carried out (Ramos *et al.*, 2016) but its application as a substitute for polymeric foams has not been widely investigated.

This thesis reports the research work as part of a project between RCUK Centre for Sustainable Energy Use in Food Chains (CSEF) at Brunel University and Hydropak Ltd. to develop bio-based bulk foam materials for thermal packaging applications.

1.2 AIM AND OBJECTIVES

1.2.1 AIM

The aim of this research was to develop bio-based formulations for a liquid foaming technology to fabricate to manufacture bio-based bulk foams for thermal packaging of chilled foods, drinks and pharmaceutical products was developed.

1.2.2 OBJECTIVES

The objectives of this study were:

- To design bio-based formulations able to achieve high expansion ratios, high foam stability and low density solid foams on drying
- To prove the feasibility of liquid foaming in five different formulation systems: starch-PVAc-calcium sulfate, starch-gelatine, gelatine hydrogels, gelatine-composites hydrogels (i.e. biomass powders, expanded vermiculite particles, aero-gel powders and honeycomb boards) and hydrogel alternatives to gelatine (i.e. agar and gellan gum)
- To identify the key parameters of formulation and process conditions for the five different formulation systems studied
- To investigate the role of the different formulation (e.g. solid content, biopolymer content, surfactant content and plasticiser use, among others) and processing (e.g. expansion ratio, processing temperature, drying process) factors on foaming and stabilisation of the liquid foams, and their impact on foam structure and properties of the solid foams

1.3 EXPERIMENTAL DESIGN CONSIDERATIONS AND STRUCTURE OF THE THESIS

Liquid foaming consists in the transformation of a liquid foamed polymer into a porous solid polymer through liquid removal. Thus, the liquid foaming process consists of three different stages:

- **Liquid stage**, which corresponds with the formulation of the liquid. The formulation of the liquid consists of raw materials and solution/suspension preparation, involving the incorporation of the different materials, additives, and fillers into a liquid solution or suspension.

  The objective of the formulation design was to create a solution/suspension able to achieve a high expansion ratio, stable liquid and drying foams, uniform fine cell structure and ultimately low density solid foams. The formulation of the liquid determines liquid viscosity and surface tension, and thus influence the material behaviour in subsequent foaming, casting, gelling, drying and final product properties.

  The biopolymers used to produce the biofoams were a range of those compatible with water for the preparation and foaming of aqueous solutions/suspensions. These included wheat starch, high bloom gelatines, agar and gellan gum.

  Purified wheat starch was selected as a suitable polymer due to its low cost, high biodegradability and commercial availability.

  Gelatine was used as a foam stabiliser. It transforms the liquid foam into a liquid gel as temperature decreases to room temperature, so it preserved the liquid foam structure. Gelatine stabilised the liquid foams via gelling and lowered the shrinkage during the drying process. This hydrocolloid was used as a blend with starch or alone for gelatine hydrogel foams. Agar and gellan gum were used as alternative gelling agents to gelatine.

  Low liquid surface tension is desirable to maximise volume expansion during foaming and assist foam stabilisation. Surfactants assist the foaming process, increasing the foam volume produced from the initial solution by lowering its surface tension. Different surface tension modifiers were used: a bio-detergent and surfactants A, B, C1 and C2.

Two plasticisers, glycerol and sorbitol, were used to control the flexibility of the foams and modify the glass transition point of the biopolymers.

Fillers, such as biomass powders, aerogels or vermiculite, were incorporated into the formulation for different purposes (as it is discussed below). The fillers increase liquid viscosity and liquid heterogeneity and hence, the appropriate concentration needs to be defined.

Other formulation components included acetic acid (used as a preservative), Polyvinyl Acetate (PVAc), calcium sulfate hemihydrate and water.

PVAc was selected as stabilisation agent in system 1. It was used as a modifier of the biopolymer as at low concentrations may influence liquid bubble film stretchability and foam stability.

Calcium sulfate hemihydrate was used as foam hardener. Calcium sulfate hemihydrate is a cementitious solidifer which forms a moldable paste on hydration.

- **Liquid foam stage** (where foaming and casting take place). Once the liquid is formulated, gas is introduced into the liquid using a mechanical method and consequently cast into the desired shape (e.g. boards or 3D mouldings).

- **Gel to solid stage** (where the conversion from liquid foam to solid foam through foam gelling and drying occurs). The foam is stabilised by gelling and, following a drying process, the dried foam can be characterised in terms of density, shrinkage, foam cell structure and other properties (mechanical, thermal conductivity, among others).

This thesis consists of seven chapters which are arranged as follows:

- **Chapter one**, introduction to the project, gives the background, aim and objectives and structure of the thesis

- **Chapter two**, literature review, gives an overview of the relevant background information related to polymers and bio-foams

- **Chapter three**, experimental details, describes the materials, the procedures for liquid preparation, experimental details and characterisation details of raw materials, solution/suspensions, liquid and solid foams

- **Chapter four** reports the results of the investigation of starch-based foams: Systems 1 (starch-PVAc-calcium sulfate foams) and 2 (starch-gelatine foams).

  Liquid foams require stabilisation during the drying process. The additives used as stabilisers in System 1 were Polyvinyl Acetate (PVAc) and calcium sulfate (Plaster of Paris, POP) for stretchability and solidification enhancement, respectively. Through preliminary tests based on suitable liquid viscosity for mechanical foaming and stability of the liquid foams, a preliminary formulation was identified as a starting point for subsequent modification towards lower content of calcium sulfate and PVAc, lower drying shrinkage, absence of defects (such as cracks and large cavities) developed in the cast foam during drying and lower dry foam density. The scope of improvement in System 1 was limited by the requirement of high concentration of POP and PVAc, which, while proving the concept, led to relatively high-density and low-biodegradable materials.

  In System 2, gelatine was selected to replace POP and PVAc as foam stabilisers in attempt to achieve 100% biopolymer foams with a density comparable to their polymer counterparts, appropriate mechanical and thermal properties and to reduce the drying timescale obtained in System 1.

- **Chapter five** is focused on the investigation of hydrogel foams: systems 3 (gelatine-hydrogel foams) and 5 (hydrogel foams alternative to gelatine).

  System 3 studied the production of gelatine hydrogel foams without using starch to further decrease the density obtained in the foams from System 2. The experimental process for the formulation design of this system consisted in five studies:

  - Preliminary study on the influence of surfactant type (A, B and C2) and content on the properties of liquid (maximum expansion ratio) and solid (density, drying shrinkage, structure) foams to lay the groundwork for the subsequent experiments

  - Investigation of formulation (gelatine content, surfactant type and content) and processing (foaming temperature) influence on the foaming process, dry (density, drying shrinkage, compression behaviour, thermal conductivity and acoustic properties) and liquid (maximum expansion ratio) foams properties and structure

- Study on plasticisers incorporation into selected System 3 formulations to produce flexible foams

- Study on the influence of the formulated liquid expansion ratio on foam stability, morphology and dry foam density

- Drying process and timescale optimisation

System 5 discusses two alternative hydrogel foams manufactured using agar (System 5.1), a non-animal origin hydrocolloid, and gellan gum (System 5.2), produced by bacterium *Sphingomonas elodea*, to understand the key features of these systems in comparison with gelatine as a preliminary attempt to broaden the hydrogels choice.

- **Chapter six** presents and discusses the experimental results from the investigation of System 4 (gelatine-composite hydrogel foams), including the following subsystems:

  - Subsystem 4.1 (biomass-hydrogel foams), where biomass powders from agricultural waste (oat and straw fibres) were included for the formulation of cost-effective fully biodegradable composite foams for different applications.

  - Subsystem 4.2 (vermiculite-hydrogel foams), where expanded vermiculite particles, known for their fire resistance properties, where incorporated into selected System 3 formulations for thermal insulation and fire-resistance applications

  - Subsystem 4.3 (silica aero-hydrogel foams) studied the incorporation of silica aerogel powders into selected System 3 formulations for thermal insulation properties enhancement.

  - In Subsystem 4.4 (honeycomb structures infiltrated with hydro-gel foams), Nomex and cardboard honeycomb panels were filled with a selected formulation from System 3 for enhancement of mechanical properties in lightweight structures applications.

- **Chapter seven**, conclusion, summarises the project conclusions and suggests further work areas

1.4 RESEARCH INTELLECTUAL PROPERTY

For commercial sensitivity reasons some details regarding the materials used for experimental analysis (e.g. gelatine grade, surfactant type and gelatine and surfactant suppliers) are not provided.

2. CHAPTER 2.
LITERATURE REVIEW

Chapter 2.

LITERATURE REVIEW

2.1 INTRODUCTION

Modern organic chemical syntheses can be traced back to the mid-19th century with the evolution of the petrochemical industry. Petroleum polymers have a high chemical stability, desirable mechanical and physical properties and excellent processability and thus have become a major class of materials that are widely used in all industrial sectors (A.S. Ayoub and Rizvi, 2009). Polymer foams, in particular, are low-cost materials, lightweight and have many attractive properties and hence have found widespread applications for cushioning, thermal and acoustic insulations in construction, packaging, automotive, among other sectors. However, the excessive exploitation of petrochemical or conventional polymers has led to some environmental concerns such as waste production, greenhouse gasses emissions in addition to sustainability of the fossil resources (Montgomery, 2004).

In recent years, bio-foams have attracted the attention of research and development in the attempt to provide biobased alternatives to plastic foams to address such concerns and contribute to the long-term goal of more circular economy.

This chapter first reviews plastic foams, their manufacturing technologies, properties and applications. In comparison, developments in biopolymers and bio-foams are critically reviewed. The attention is then focused on a selected group of biopolymers which are of particular interest in the development of a novel technology, hydrogel liquid foaming technology, to fill the gaps in bio-foams and processing technologies identified.

2.2 PLASTIC FOAMS

Foams are cellular solids. They exist in many forms naturally (e.g. in animal bone structures, in marine organisms such as sponges and plants such as cork) or human-made from ceramics, metals and plastics. Plastic foams, the focus of this work, also known as cellular polymers/solids or expanded polymers, are multiphase porous materials consisting of a solid polymer phase and a dispersed gaseous phase.

2.2.1 TYPES OF PLASTIC FOAMS

Plastic foams may be classified in different ways based on e.g. their composition, cellular morphology, and mechanical properties, among others.

Based on the type of plastic, plastics foams can be categorised into thermoplastics, thermosets and elastomers. The main difference between thermoplastics and thermosets polymers is that the thermoplastics can be re-melted, while thermosets remain in a solid state on heating until thermally degraded. Examples of foams made with **thermoplastics** include polyethylene (PE), polystyrene (PS), and polypropylene (PP). Most polyurethane (PU) foams, on the other hand, are generally **thermosets** cross-linked with strong carbon bonds in a network (Gibson and Ashby, 1997). **Elastomeric foams** fall in between the above two with a certain degree of cross-linking which give them the ability to memorise their molecular structure below the stretch limit. Examples of elastomeric foams include neoprene and latex foams.

Based on **stiffness**, foams may be classified as rigid or flexible. Assuming they are used at room temperature, rigid foams are those with glass transition temperature (T_g), above room temperature while flexible foams T_g is below room temperature.

Regarding **cellular morphology**, foams may be classified according to their cells size (e.g. microcellular) and their structure (e.g. close-cell or open-cell foams).

2.2.2 FOAMING PROCESS AND RHEOLOGY OF POLYMERS

Different methods can be used to produce plastic foams but the most commonly used techniques for thermoplastics are based on the expansion of the polymer melt to a cellular state, using various ways to generate or inject gases. Other methods include leaching out of solid particles (Iannace, Di Maio and Nicolais, 2001) (McRae, Naguib and Atalla, 2010) and hollow particles dispersion in the polymer matrix (Bian, Tang and Li, 2008) (Luong *et al.*, 2014), which are irrelevant to this work, and thus will not be reviewed further. This section outlines the general principle of foaming and then reviews the analytical methods for characterisation of the key influential factors.

2.2.2.1 General principles of foaming

The foam structure of polymers is commonly created by incorporation of gas bubbles into the polymer in a viscous state, allowing the bubbles to nucleate, expand and, finally, solidify the foam by cooling or cross-linking (Suh and

Skochdopole, 1980). Thus, as shown in Figure 2.1, a foaming process consists of three main steps that may overlap: nucleation or initiation, growth and stabilization (or collapse and loss of the foam structure).

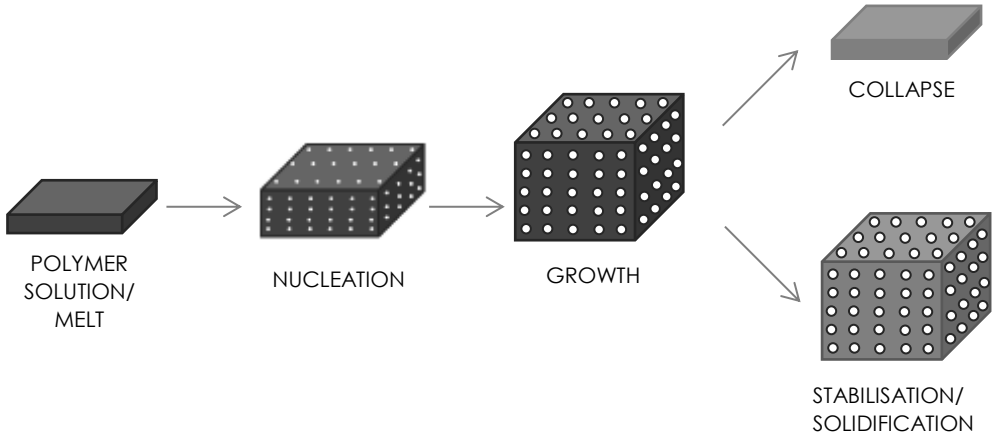

Figure 2.1 FLOW DIAGRAM OF A GENERAL FOAMING PROCESS

Nucleation is the initiation of cells, small gas bubbles, in a viscous polymer (liquid/molten)(Bonin, 2010). The gas may be incorporated into the polymer either by mechanical stirring, gas injection or by introducing a blowing agent (e.g. low-melting point liquids and physical or chemical blowing agents) into the polymer (Gibson and Ashby, 1997). The dominant processing parameter during nucleation is the gas solubility limit that, in turn, depends on pressure, temperature and the interaction with the polymer (Lee & Ramesh, 2004). The amount of gas generated and blended is a process parameter which may affect foaming dynamics and foam stabilisation (Lee, 2004). Other parameters affecting nucleation are the viscosity of the viscous polymer, surface tension and diffusivity of the gas. If the foam is stabilised at nucleation stage, the resulting foam may exhibit a relatively high density.

Once the cells have reached a critical size to start growing under the given conditions, cells growth takes place. Bubbles expand, remaining spherical until they come in contact with their neighbours and closely pack, where they get distorted into polyhedral structures (Weaire and Hutzler, 1999).

Energy is required to create bubbles in a viscous polymer (Rio *et al.*, 2014). The free energy, ΔG, increase during foaming (energy input) can be expressed by equation 2.1:

$$\Delta G = \gamma \cdot A \qquad \text{(Equation 2.1)}$$

Where γ is the surface tension and A is the total gas-melt interfacial area created. Liquid foams are thermodynamically unstable as the foam always tends to reduce

the free energy by reducing the surface area leading to coalescence, the formation of larger cells and cell collapse.

Driven by the absolute internal pressure in competition with the melt viscosity and surface tension of the polymer, cell growth continues as the competition approaches equilibrium and maximum foam volume expansion is achieved. While surface tension can be deemed constant, the bubble pressure varies with the bubble radius and diffusion of the blowing agent in or out of the bubbles. Viscosity plays a vital role in foaming. On the one hand, drainage can be retarded by viscosity increase. It restrains the bubble growth and the polymer flow from cell walls to intersections (known as drainage) which leads to cell wall thinning and cell collapse (Lee, 2004). Cell structure stabilisation can effectively be achieved by rapid viscosity increases when the required foam expansion is achieved, such as by cooling, solidification or cross-linking (Landrock, 1995). However, on the other hand, high viscosity may hinder foam expansion.

Bubbles with different sizes also coalesce or coarsen arising from pressure differences between neighbouring bubbles. The pressure difference between the inner and outer spaces of spherical cells, δP, can be calculated as in equation 2.2:

$$\delta P = \frac{2\gamma}{R} \qquad \text{(Equation 2.2)}$$

Where γ is surface tension and R is the radius of the bubble. The equation implies that the pressure is higher in smaller bubbles. There is a tendency to balance bubble pressures, either by breaking the cell walls or by diffusion of the blowing agent from the smaller cells (radius R_1) to the larger cells (radius R_2). The pressure difference between two adjacent bubbles, ΔP, is given by equation 2.3 (Herman, 2003):

$$\Delta P = 2\gamma \left(\frac{1}{R_2} - \frac{1}{R_1}\right) \qquad \text{(Equation 2.3)}$$

It is apparent from equation 2.3 that gas diffusion takes place from small to large bubbles, which results in small bubbles disappearance in benefit of large bubbles growth with time (Landrock, 1995). It can also be concluded from the equation that reduction in surface tension decreases the pressure difference between bubbles, leading to better foam stabilisation and smaller cell size (Landrock, 1995).

The temperature of the polymer melt is another parameter affecting foam stability (Landrock, 1995). An increase in temperature reduces both viscosity and surface tension, leading to cell walls thinning and collapse.

As a guideline, to achieve high volume expansion and stable foams, low surface tension, low gas diffusion and appropriate control of melt viscosity are required.

2.2.2.2 Characterisation of key factors influencing foaming

This section discusses the key parameter affecting foaming: rheology and surface tension of the melt.

2.2.2.2.1. Rheology of the polymer melt

Rheology studies the viscoelastic behaviour of polymers. As an illustration, in a typical shear rheometer, the motor can apply a given oscillating shear strain and frequency to the specimen and the sensors will measure its response (e.g. torque or stress). The shear stress and strain phase angle (δ) difference reflects the material behaviour, as shown in Figure 2.2. For purely elastic materials, stress is in phase with its strain whereas, for strictly viscous materials, stress is out of phase with its strain 90°. Intermediate stress-strain relationships (the most common behaviour) give rise to viscoelastic materials.

The parameters that can be measured by the rheometer motor are torque (*M*), angular displacement (*θ*) and angular velocity (Ω). The calculated parameters are shear stress (*Pa*), strain (%), shear rate (s^{-1}), viscosity (*Pa·s*) and modulus (*Pa*) (TA Instruments, 2017).

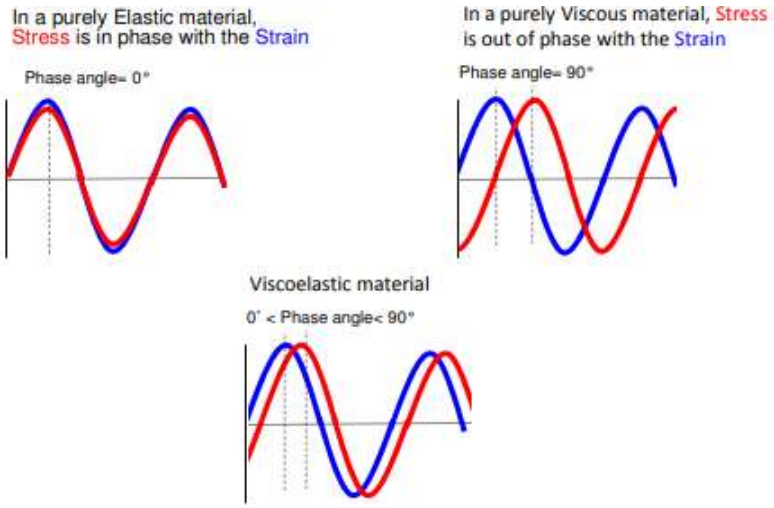

Figure 2.2 STRESS-STRAIN PHASE RELATIONSHIP IN OSCILLATORY TESTING (Cotts, 2016)

The shear stress is calculated from the torque measured, *M*, and geometry stress constant, K_σ, which depends on the measurement geometry and initial sample dimensions (see Equation 2.4) (TA Instruments, 2017).

$$\sigma = M \cdot K_\sigma \qquad \text{(Equation 2.4)}$$

Shear strain, γ, is calculated from the measured angular displacement (Θ) between two circular plates and the measuring geometry (represented by a strain constant, K_γ), as shown in Equation 2.5 (TA Instruments, 2017).

$$\gamma = (\theta \cdot K_\gamma) \cdot 100 \quad \text{(Equation 2.5)}$$

The shear rate, $\dot{\gamma}$, is calculated from the measured angular velocity, Ω, and the geometry strain constant, as shown in equation 2.6 (TA Instruments, 2017).

$$\dot{\gamma} = \Omega \cdot K_\gamma \quad \text{(Equation 2.6)}$$

Viscosity, the relationship between shear stress and shear rate, can be defined as the measure of the ability of a polymer to resist shear flow, reflecting the mobility of the molecules. There are two types of viscosity: dynamic, as shown in Equation 2.7 (measured in *Poises* or *Pa·s*) and kinematic (the ratio of dynamic viscosity to density, measured in *stokes* or m^2/s).

$$\eta = \frac{\sigma}{\dot{\gamma}} = \frac{M \cdot K_\sigma}{\Omega \cdot K_\gamma} \quad \text{(Equation 2.7)}$$

A Newtonian fluid is that which exhibits viscosity values dependent on temperature but independent of the shear rate. The viscosity of a non-Newtonian fluid can be shear-dependent (shear thinning or thickening) or time-dependent (thixotropic, decreasing with time; or rheopectic, increasing with time).

The complex (shear) modulus (G*) is the ratio of shear stress, τ, over shear strain, γ, and can be calculated from Equation 2.8.

$$G^* = \frac{\sigma}{\gamma} = \frac{M \cdot K_\sigma}{\theta \cdot K_\gamma} \quad \text{(Equation 2.8)}$$

The complex modulus can be separated into the elastic (G') and viscous components (G'') (Equation 2.9). G' is the storage modulus and represents the ability of the material to store energy (Equation 2.10), while G'' is the loss modulus and represents the ability of the material to dissipate energy (see Equation 2.11) (Cotts, 2016).

$$G^* = G' + G'' \quad \text{(Equation 2.9)}$$

Where:

$$G' = \frac{\sigma}{\gamma} \cdot \cos\delta \quad \text{(Equation 2.10)}$$

$$G'' = \frac{\sigma}{\gamma} \cdot \sin\delta \quad \text{(Equation 2.11)}$$

2.2.2.2.2 Surface tension

Du Nuoy ring (see Figure 2.3.A) and Wilhelmy plate (see Figure 2.3.B) are two widely used methods to measure the surface tension of fluids such as polymer solutions (Hu, Wang and Hartnett, 1991) (Grundke *et al.*, 1996). It is very common that both types are fitted with a tensiometer and use platinum for the ring or plate due to its high surface free energy which usually produces contact angles, θ, close to 0 (i.e. cosθ=1) (Kruss, 2018).

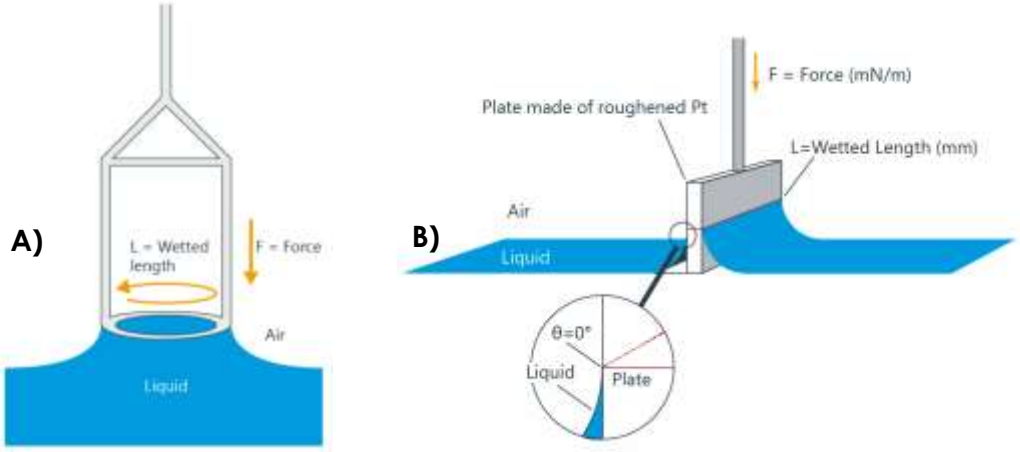

Figure 2.3 SCHEMATIC DIAGRAM SHOWING TWO FORCE TENSIOMETRY METHODS (A) DU NUOY RING METHOD (B) WILHELMY PLATE METHOD (CR, 2004)

The Wilhelmy method is similar to the Du Nuoy ring method. The first uses a plate and the latter, as its name states, a ring for measuring the surface tension. Both are placed vertically positioned touching the liquid surface, and surface tension can be calculated from the maximum force, F, wetted length, L, and contact angle, θ using Equation 2.12.

$$\gamma = \frac{F}{L \cdot \cos\theta} \qquad \text{(Equation 2.12)}$$

The Wilhelmy method is generally considered to be more accurate and suitable for aqueous-surfactant solutions as it is static (CR, 2004).

2.2.3 FOAMING TECHNOLOGIES

Polymer foams can be produced by mechanical, chemical or physical means (Landrock, 1995). Most thermoplastics and thermosetting plastics can be foamed with different foaming technologies. The foaming technology choice depends on the final product requirements (i.e. density, cell morphology and final product shape and dimension, among others). Table 2.1 summarises the most commercially significant processing technologies used for the foaming of different plastics foams.

Table 2.1 TECHNOLOGIES FOR PRODUCTION OF PLASTIC FOAMS (Herman, 2003)

POLYMER FOAM	EXTRUSION	EXPANDABLE FORMULATION	SPRAY	FROTH FOAM	COMPRESSION MOULDING	INJECTION MOULDING	SINTERING	LEACHING
Cellulose Acetate	x							x
Epoxy Resin		x	x	x				
Phenolic Resin		x						
Polyethylene	x	x			x	x	x	x
Polystyrene	x	x				x	x	
Silicones		x						
Urea-formaldehyde resin				x				
Urethane polymers		x	x	x		x		
Latex foam rubber				x				
Natural rubber	x	x			x			
Synthetic elastomers	x	x			x			
Polyvinyl chloride	x	x		x	x	x		x
Ebonite					x			
Polytetrafluroethylene							x	

The most common methods for foam generation include:

- Mechanical beating or **frothing**. Air is incorporated into a low viscosity polymer solution or low molecular weight precursor, and the foam is stabilised by chemical reaction (e.g. cross-linking) or gelling (e.g. urea-formaldehyde foams, natural rubber latex foams).

- **Gas incorporation** into the liquid polymer **under high pressure**. There are different technologies that produce foams from the decompression expansion process, including extrusion foaming, the most common (Park and Cheung, 1997) (Wang, Lee and Park, 2011), foam injection moulding (Chen, Liao and Chien, 2012) (Gomez-Gomez *et al.*, 2013) and foam compression moulding (Yao and Rodrigue, 2012). Extrusion is a technology widely used for the foaming of plastics such as PS, PE and PVC. Foams are produced by decompression expansion of a polymer melt-gas solution formed in the extruder under pressure and temperature. As the melt comes out of the extruder die, the pressure falls, which cause the gas bubbles to develop within the solution and the polymer to expand. For foam injection moulding, the polymer-gas melt is transferred from the pressurised injection cylinder to the mould cavity, where it expands until completely fills the mould.

Gas may be directly injected into the polymer in extrusion and injection moulding under pressure to form the melt-gas solution, but often the following methods using blowing agents are employed to generate gases within a polymer melt:

- **Thermal degradation of a blowing agent**. The blowing agent releases gas as it decomposes (e.g. azodicarbonamide).

- **Solvent vaporisation** (e.g. pentane, chlorofluorocarbons)**.** A given solvent is boiled to foam vapor within the polymer solution by the application of heat.

- **Chemical reactions** (e.g. water-blown PU foams). Foamable blends (such as EPS, expanded polystyrene) are compositions in which the cells pressure is increased relative to that of the surroundings (Herman, 2003) by gas generating chemical reactions. These foams can be stabilised by physical or chemical methods (Herman, 2003). For instance, spray foams are produced by two materials, a polyol resin and an isocyanate. They react when mixed and expand when sprayed up to sixty times their liquid volume.

- **Syntactic foams** (e.g. epoxy resin). Syntactic foams are produced by dispersing hollow microspheres in a polymer melt. The polymers used are usually coating resins, such as epoxy resins, polyesters, and urea-formaldehyde resins, among others (Herman, 2003). Some examples of dispersed hollow spheres are made from phenolic resins, urea-formaldehyde resins, glass and silica, among others (Herman, 2003).

- **Leaching.** A temporary phase (e.g. sucrose, starch, sodium chloride) is incorporated into the main polymer material, uniformly mixed and subsequently removed, yielding an open-cell structure. Some PE and PVC foams can be manufactured with this technology.

- **Sintering**. As leaching, sintering of solid plastic particles is a manufacturing method used for foaming high viscosity polymers such as ultra-high molecular PE, PP and PS (Mark, 2004).

2.2.4 FOAM STRUCTURE

It is crucial to understand how the solid is distributed in cell faces and edges as foam structure influences foams' properties (Gibson and Ashby, 1997). Optical and scanning electron microscopy (SEM) help to obtain this information from cross sections (Gibson and Ashby, 1997) but modern scanning techniques such as X-ray tomography can produce 3D images of the structure.

Foam morphology mainly depends on the cell topology, cell shape, cell size, and, in general, the distribution of the gas phase and the solid.

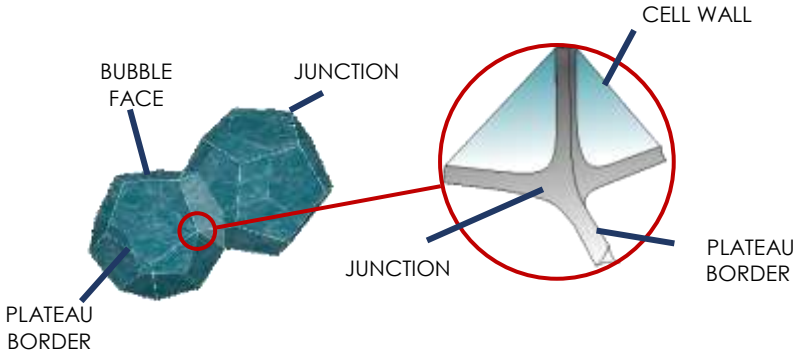

Figure 2.4 STRUCTURE OF POLYHEDRAL BUBBLES (Self elaboration)

Bubbles usually take a polyhedral shape (see Figure 2.4), with non-flat faces meeting in edges or Plateau borders and the edges meeting in vertices or junctions (Weaire and Hutzler, 1999). Several factors may shape foam cell structure, such as competitive growth, viscous forces, surface tension and the way the foam is made (Gibson and Ashby, 1997).

The cells topology characterises the number of faces, the cell connectivity and the cell walls curvature. Each cell consists of three different components: edges, vertices (which connect the edges) and faces (films or cell walls) (Mills, 2007). There may be differences in the number of faces and edges per face (Bhakta and Ruckenstein, 1997). The number of cell faces that meet at an edge is known by the connectivity of the cell faces, and it is usually three, though it can be higher, until six (Gibson and Ashby, 1997). The number of edges that meet at a vertex is known as the connectivity of cell edges, and it is usually four, but it may also be higher (Gibson and Ashby, 1997).

Foams are usually irregular packings that contain cells of different dimensions and shapes (Gibson & Ashby, 1997). Cell size is generally regarded as a significant parameter. Bing *et al.* (2010) stated that in thermoplastic foams, it is usually desirable to create uniform small size cells in order to achieve better mechanical properties.

Cell shape also influences the foam properties, as when the cells are equiaxed, the foam properties are isotropic, but when they are not, properties may depend on the direction (anisotropy). Anisotropy ratio for foams is determined from the ratio of the linear cell dimension in the rise direction to that normal to the rise direction. Materials with a value of 1 are isotropic (Granta, 2017). When polymer foams are created by foaming polymer melts or solutions in conditions that do not allow free

expansion in three dimensions, the cells are usually oriented to the rise direction due to viscous forces giving rise to anisotropic properties (Gibson and Ashby, 1997).

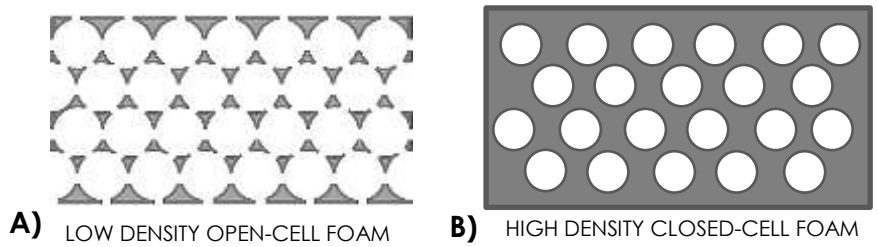

Figure 2.5 SCHEMATIC REPRESENTATION OF SECTION THROUGH (A) OPEN AND (B) CLOSED CELLED FOAMS (Self Elaboration)

Regarding the distribution of the gas phase, foams may have an open-celled structure, where both matrix and gas phases are continuous or interconnected; or a closed-celled structure, where the gas phase is disbursed (un-connected) within a continuous polymer matrix, as shown in Figure 2.5. Gas can flow through the system in open-celled structures, while in closed celled structures, gas movement can only occur by diffusion through the cell walls. The two cell structures may co-exist, and closed-cells may undergo a reticulation process, where they are ruptured, giving rise to open-cells (Gibson and Ashby, 1997). The stabilised cell structure can be quantified by "open to close cell ratio".

2.2.5 FOAM PROPERTIES

Foam properties mainly depend on the material of which the cell walls are made of, and the foam structure resulted from the foaming conditions which generated the foam (Gibson and Ashby, 1997) (Kaewtatip *et al.*, 2014)(Wang *et al.*, 2010). However, due to the complexity of foam structures, as Ceglia *et al.* (2012) stated, despite abundant literature dedicated to the foam structure and properties relationship, the interrelation is not entirely understood yet.

Figure 2.6 shows the comparison between solids and foams in density, thermal conductivity and Young's Modulus (Gibson and Ashby, 1997). The properties' extension generates new applications for foams that cannot be easily fulfilled by solids (e.g. lower density allows the creation of lighter and stiffer components, such as sandwich panels) (Gibson and Ashby, 1997).

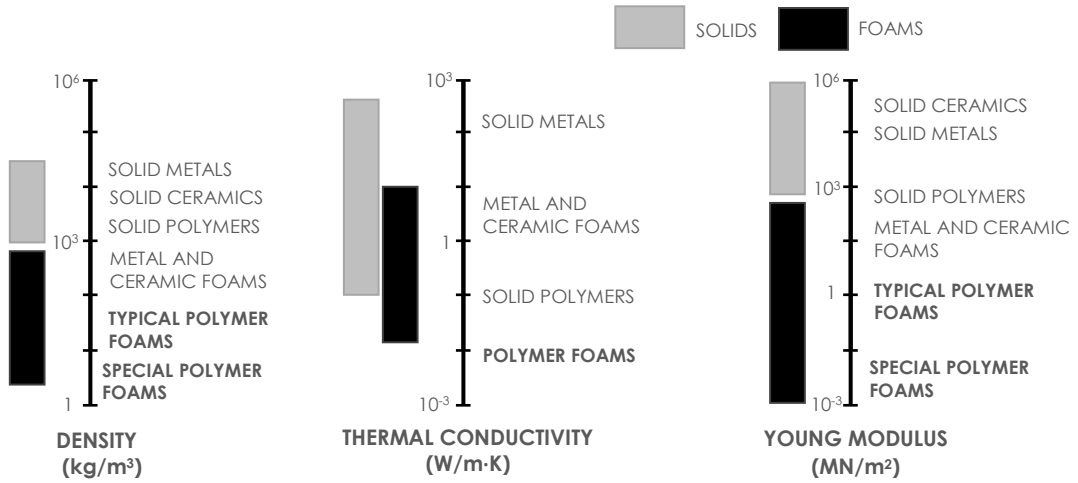

Figure 2.6 FOAM PROPERTIES (POLYMER FOAMS HIGHLIGHTED) IN COMPARISON WITH THAT OF SOLIDS (Gibson and Ashby, 1997)

Table 2.2 gathered data in density, relative density, thermal conductivity, Young's Modulus, compression strength at 25% and 50% strain for most commonly used PS, PU, PP, low-density polyethylene (LDPE) and high-density polyethylene (HDPE) foams.

Table 2.2 PROPERTIES OF PS, LDPE, HDPE AND PP POLYMER FOAMS (Granta, 2017)

POLYMER	DENSITY (kg/m³)	RELATIVE DENSITY	YOUNG'S MODULUS (MPa)	YIELD STRENGTH (MPa)	COMPRESSIVE STRENGTH AT 25% STRAIN (MPa)	COMPRESSIVE STRENGTH AT 50% STRAIN (MPa)	THERMAL CONDUCTIVITY (W/m·°C)
PS	18-22	0.017-0.021	3.4-7	0.11-0.16	0.15-0.17	0.21-0.23	0.033-0.036
	23-25	0.022-0.026	5.6-9.2	0.15-0.2	0.18-0.2	0.24-0.25	0.032-0.036
	28-32	0.027-0.031	7.7-11.3	0.2-0.25	0.21-0.23	0.26-0.28	0.031-0.035
	47-53	0.046-0.052	25-30	0.8-1	0.7-0.9	0.25-0.35	0.033-0.04
PU	23-25	0.015-0.02	0.01-0.001	$3e^{-3}$-$5e^{-3}$	$3.5e^{-3}$-$6e^{-3}$	$7e^{-3}$-$9e^{-3}$	0.025-0.028
	26-32	0.02-0.025	0.014-0.03	$2e^{-3}$-$3e^{-3}$	$2.5e^{-3}$-$3.3e^{-3}$	$6e^{-3}$-$8e^{-3}$	0.025-0.028
	30-34	0.02-0.025	0.04-0.06	$3.8e^{-3}$-$4.5e^{-3}$	$4.6e^{-3}$-$5.5e^{-3}$	$6e^{-3}$-$9e^{-3}$	0.025-0.028
	60-70	0.04-0.05	0.02-0.05	$1.2e^{-3}$-$2.5e^{-3}$	$1.5e^{-3}$-$3e^{-3}$	$5e^{-3}$-$5e^{-3}$	0.027-0.032
LDPE	16-20	0.017-0.022	0.25-0.3	0.01-0.015	0.031-0.035	0.09-0.1	0.036-0.038
	22-26	0.024-0.028	0.4-0.6	0.012-0.017	0.033-0.037	0.10-0.11	0.036-0.038
	27-31	0.029-0.033	0.5-0.7	0.015-0.018	0.036-0.04	0.11-0.12	0.038-0.04
	31-35	0.033-0.038	0.8-0.9	0.018-0.022	0.038-0.042	0.11-0.12	0.039-0.041
	43-47	0.046-0.051	1.5-1.8	0.02-0.025	0.048-0.052	0.13-0.14	0.042-0.044
HDPE	27-30	0.028-0.031	0.8-1	0.1-0.12	0.055-0.065	0.16-0.17	0.046-0.048
	57-60	0.058-0.061	3-4	0.25-0.3	0.1-0.12	0.3-0.31	0.055-0.059
PP	20-22	0.022-0.025	0.3-0.5	0.045-0.055	0.08-0.085	0.15-0.16	0.038-0.04
	28-32	0.03-0.035	0.6-0.9	0.095-0.105	0.14-0.15	0.22-0.24	0.039-0.041
	38-42	0.042-0.045	3-5	0.19-0.21	0.19-0.21	0.37-0.41	0.04-0.042

2.2.5.1 Foam characteristics associated with foam density

One of the most important characteristic parameters dominating foam properties is foam density. Relative density and porosity are closely related to foam density.

Foam density (ρ^*) as compared with that of the polymer, ρ, in mass per unit volume of foam, is a significant property of foams. Foam density depends on that of the solid polymer and the fraction of the polymer phase in a foam. Solid polymers are lighter than metals because the polymer chains are made of light carbon, and hydrogen and the chains are packed loosely in amorphous or semi-crystalline polymers. Generally speaking, the higher the crystallinity, the higher the density of a polymer is, as a result of better packaging of the chains (Granta, 2017).

Relative density (ρ_r) is considered as the primary property affecting cellular solids characteristics (Gibson and Ashby, 1997). It is the density of the cellular material, ρ^*, divided by the density of the solid from which the cell walls are made, ρ_S, as shown in equation 2.13 (Gibson and Ashby, 1997), in other words, the volume fraction of polymer within the foam (Bonin, 2010).

$$\rho_r = \frac{\rho^*}{\rho_S} \qquad \text{(Equation 2.13)}$$

Low-density foams usually have a relative density lower than 0.1 (Mills, 2007). Around 0.3 relative density, the cellular solid becomes a porous solid, rather than a foam (Gibson and Ashby, 1997). According to Gibson & Ashby (1997), polymer foams employed for cushion packaging and thermal insulation usually have relative densities ranging from 0.05 and 0.2. Granta (2017) suggested tighter ranges, from 0.017 to 0.021 and from 0.017 to 0.022 for PS and LDPE foams, respectively, with densities around 20 kg/m^3 (see Table 2.2).

Porosity (p). From Equation 2.13, the porosity of the foam, *p,* can be worked out as Equation 2.14, a useful parameter to quantify the fraction of gas phase in foams, or percentage of pore space in the foam (Gibson and Ashby, 1997). *p* is closely related to the mechanical properties of the foam and may fluctuate considerably in anisotropic foams when measured in different directions.

$$p = 1 - \frac{\rho^*}{\rho_S} \qquad \text{(Equation 2.14)}$$

2.2.5.2 Compressive behaviour

The compression behaviour of foams depends on the foam structure and the material which the cell walls are made of (Rusch, 1970) (Gibson and Ashby, 1997).

Foams tend to be loaded in compression for most of their applications. Thus, their compression properties need to be carefully characterised, especially for shocking absorbing, or cushioning applications.

Under uniaxial loading, compressive stress is applied to the foam material at a relatively low rate. The compressive stress-strain curves of plastic foams typically exhibit three areas: linear elastic zone, plateau zone and densification zone.

The **linear elastic zone** corresponds to the reversible deformation zone, where the foam stores energy by elastic deformation. In this zone, the compression stresses (σ) cause a proportional strain (ε). This zone is limited to small strains, usually 5% or less (Gibson and Ashby, 1997) (Granta, 2017), although elastomeric foams can be further compressed in the linear elastic zone (Gibson and Ashby, 1997). The more energy absorbed at this stage, the less available energy is to be transferred to the product to be protected by cushioning. The slope of the stress-strain curve is the Young's Modulus of the foam, E*, as compared with that, *E*, for the polymer, and represents the resistance to elastic deformation (Granta, 2017).

The linear elasticity ends at the yield strength (σ_Y) when a foam starts to deform plastically and hence beyond which permanent deformation occurs. For polymer foams, yield strength is the stress at which the gradient of the stress-strain graph is zero or the stress at which the stress-strain curve becomes no linear (Granta, 2017). The area below the stress-strain curve is the work done per unit volume of foam.

Ceglia *et al.* (2012) observed a substantial positive dependence of Young's Modulus on density, as previously Gibson and Ashby (1997) stated. In addition to this, for a given density, Ceglia *et al.* (2012) found a quasi-linear relationship between Young's modulus and pore size.

Deformation of open-cell foams, at low relative densities (<0.1) is controlled by cell wall bending in the linear elastic zone (Gibson and Ashby, 1997). At higher relative densities, simple compression of the cell walls is more relevant (Gibson and Ashby, 1997). Closed-cell foams deform by both bending and contraction of cell edges accompanied by stretching of the cell faces.

Beyond yielding, in the **crush plateau zone,** a plateau occurs where small stress increases lead to significant high strain increment. At this stage, the foam dissipates energy by cell collapsing at relatively constant stress values: cell wall crushing for brittle foams and elastic buckling in flexible foams (Gibson and Ashby, 1997).

In the **densification zone** further compression of foam results in sudden stress increase. Cell walls begin to collapse, provoking material densification.

Figure 2.7 shows the compressive stress-strain curves for elastomeric, elastic-plastic and brittle foams. Despite differences in details, the three zones can be easily identified.

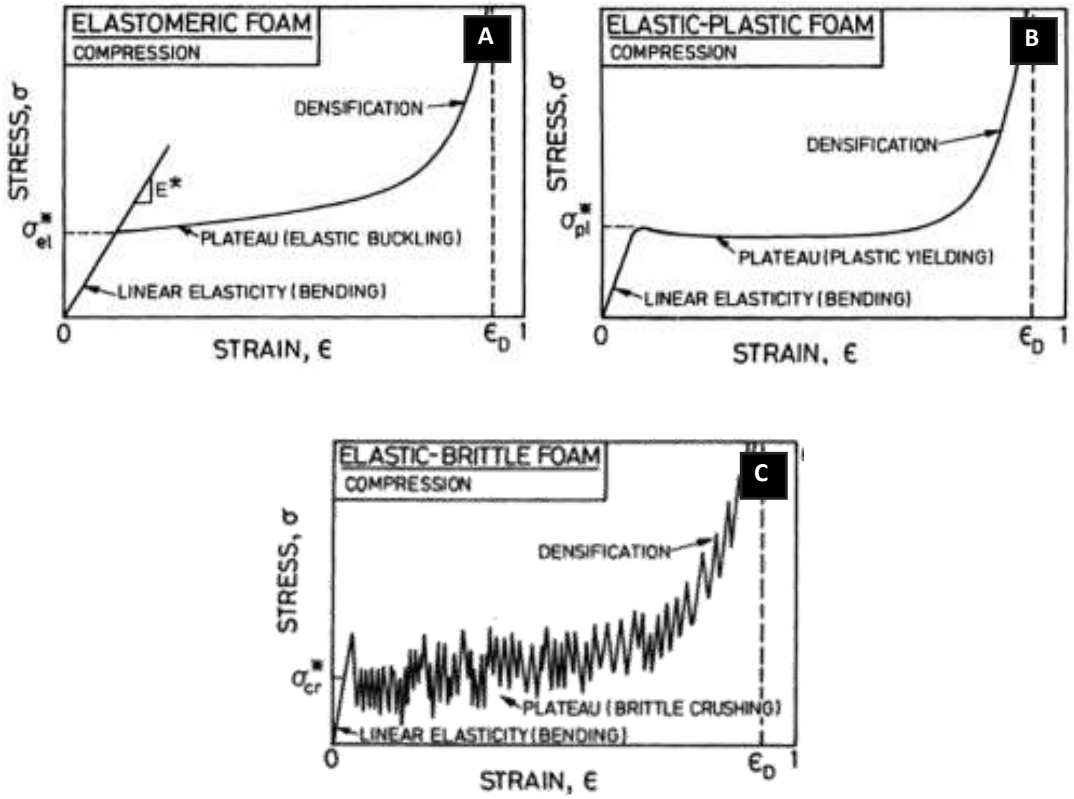

Figure 2.7 TYPICAL PSEUDO-STATIC COMPRESSION STRESS-STRAIN CURVES FOR (A) ELASTOMERIC FOAMS (B) ELASTIC-PLASTIC FOAM (C) ELASTIC-BRITTLE FOAM (Gibson and Ashby, 1997)

Compressive strength of foams is typically characterised by three measurements: compressive yield strength, compressive strength at 25% strain, which occurs approximately in the middle of cell-buckling plateau and compressive strength at 50% strain, which takes place nearly at the end of the plateau (Granta, 2017). They reflect the ability to withstand compressive stress at different stages of compression. Low-density foams exhibit almost horizontal plateaus (very weak strain hardening), and denser foams have rising stress-strain curves (stronger strain hardening) (Granta, 2017).

2.2.5.3 Thermal insulation property of foams

Plastic foams are good thermal insulators due to the low thermal conductivities of the polymer as well as the dispersed gas phase. Heat transfer is the flow of heat due to temperature differences. And heat transfer rate, or heat flux, depends on the temperature gradient and thermal conductivity of the medium through which

the heat is transferred (Rohsenow, Hartnett and Cho, 1998). This section first reviews the principles involved in thermal insulation, and then measurements of thermal insulation property of foams.

2.2.5.3.1 General principles of thermal insulation

Heat may be transferred by three fundamental mechanisms: conduction, convection and radiation. In practice, heat transfer is usually due to the combinations of two or more of these mechanisms (Rohsenow, Hartnett and Cho, 1998).

Conduction is the transfer of kinetic energy from one molecule to adjacent molecules, within or between bodies in contact. Thermal conduction is the main heat transfer mechanism through solids, while the dispersed gas phase in foams makes them relatively less conductive.

For steady-state heat flow, thermal conduction is defined by Fourier's law, as shown in Equation 2.15 (Rohsenow, Hartnett and Cho, 1998). The minus sign implies that heat flows towards lower temperature (Rohsenow, Hartnett and Cho, 1998).

$$q = -k\nabla T \qquad \text{(Equation 2.15)}$$

where:

- q: heat flux (W/m^2) or heat transfer rate per unit area of the area perpendicular to the flow direction.
- k: thermal conductivity ($W/m{\cdot}K$), the material property that characterise thermal conduction (Callister Jr. and Rethwisch, 2013).
- ∇T: temperature gradient (K/m)

The R-value is the resistance to heat flow through a given thickness, as in Equation 2.16 (Rohsenow, Hartnett and Cho, 1998). Materials with higher R-values, exhibit better insulating properties.

$$R = \frac{z}{k} \qquad \text{(Equation 2.16)}$$

where:

- z: material thickness (m)
- k: thermal conductivity ($W/m{\cdot}K$)

Convection is the physical transfer of heat from one site to another via mass transfer (i.e. coupled with fluids movement such as that in air or oil heating system). Convection can be categorised as forced convection (induced by a pump or a fan, among other devices) or natural convection (by density differences created by temperature gradient) (Rohsenow, Hartnett and Cho, 1998)

Newton's law of cooling states the amount of heat transfer from a body due to convection is proportional to the difference in temperature between the body and its surrounding fluid:

$$q = h(T_w - T_f) \qquad \text{(Equation 2.17)}$$

Where:

- q: heat flux (W/m^2)
- h: heat transfer coefficient (W/m^2·K)
- T_w: surface temperature (K)
- T_f: fluid temperature (K)

Radiation is the heat transfer through electromagnetic waves between two bodies which may or may not be in contact. Thermal radiation is electromagnetic radiation emitted by a body as a result of its temperature (Rohsenow, Hartnett and Cho, 1998). In contrast to conduction, radiation does not require a material medium for energy transfer, being transferred more efficiently in vacuum (Rohsenow, Hartnett and Cho, 1998).

Calculation of thermal radiation is based on the Stefan-Boltzmann law (Rohsenow, Hartnett and Cho, 1998). It relates the energy flux emitted by a blackbody to the fourth power of its temperature. However, real bodies do not perform as ideal radiators, and by this, Stefan-Boltzmann law is modified to equation 2.18 (Rohsenow, Hartnett and Cho, 1998), where ϵ is the material emissivity, the ability to emit infrared energy, with a value between 0 and 1 (blackbody).

$$e = \in \sigma T^4 \qquad \text{(Equation 2.18)}$$

Where:

- e: radiant energy emitted (J)

- σ: Stefan-Boltzmann constant, 5.669 x 10^{-8} W/(m^2·K^4)

- T: temperature of the body (*K*)

2.2.5.3.2 Thermal conductivity testing

Thermal conductivity can be measured under steady-state heat flow. ASTM C518, ISO 8301 and DIN 3N 12667 define the heat flow meter method for insulating materials.

The specimen (in plank form) is sandwiched between two temperature-controlled plates defining a temperature gradient (∇T) through the specimen. The heat flux (Q/A) from the steady-state heat transfer through the specimen is measured by two transducers placed in the upper and lower plates, in contact with the specimen surfaces. The average heat flux obtained is used to calculate the thermal conductivity (*k*).

2.2.5.4 Acoustic Properties

Polymer foams are widely used for acoustic insulation, and thus this section discusses fundamentals of sound propagation and acoustic properties of foams and its characterisation.

2.2.5.4.1 Sound propagation

Sound is a pressure wave generated by the source of vibration (Classroom, 2017). Sound waves are longitudinal waves moving in a parallel and anti-parallel direction to the propagation of the wave. This creates different regions in the propagation medium: compression regions (high-pressure areas), and, rarefactions regions (low-pressure areas) (Classroom, 2017), as seen in Figure 2.8.

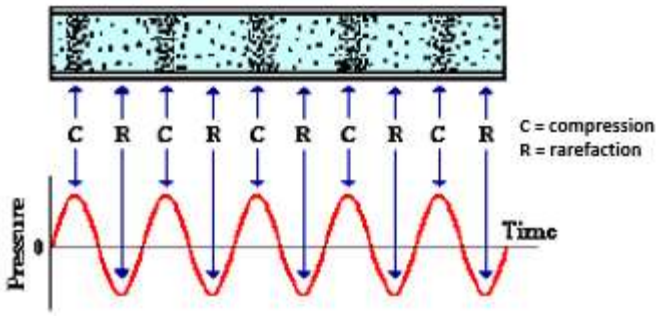

Figure 2.8 SOUND WAVE REPRESENTATION (Classroom, 2017)

Amplitude (*A*), wavelength (*λ*) and frequency (*f*) are the primary properties of sound waves. The amplitude, the wave height or pressure (*Pa*), determines how loud the sound is. Audible sounds vibrate at a wide range of pressure amplitudes,

ranging from the gentlest, at around 10^{-6} *Pa* and the loudest, approximately at 10^{2} *Pa*. Sound amplitude is measured in Decibels (*dB*), a logarithmic unit, that compares the intensity of two sounds, and thus not an absolute value for sound intensity (Liu *et al.*, 2014).

The sound wavelength (λ, measured in *m*), is the distance between two adjacent waves, in other words, the distance from a compression region to the next compression region or from a rarefaction region to the next rarefaction region (Classroom, 2017).

Frequency (*f*), measured in Hertz (*Hz*), is the number of wave cycles per second and determines the sound pitch. Sounds consisting of a single frequency are pure tones. However, these sounds are rare, and most of the sounds are made up of different frequencies, the so-called broadband noise. The audible frequency ranges from approximately 20 *Hz* to 20,000 *Hz* but distinguishable from 500-4,000 for most people (Liu *et al.*, 2014).

When required, noise can be reduced by controlling the source of vibration and the sound transmission (Liang and Jiang, 2012).

When any sound hits a surface, depending on the material which is made of and its thickness, the sound may be partly reflected and the remainder can be absorbed and/or transmitted. Sound insulating materials can be designed for sound absorption or insulation (against transmission) (Liang and Jiang, 2012).

When a material absorbs sound energy (the kinetic energy of vibration), it is converted to heat, known as acoustic attenuation. Most materials are adequate for attenuating sound within certain frequency ranges. For this reason, broad broadband noise attenuation usually requires composites or laminates to combine the sound attenuation properties of different materials at different frequencies.

Cellular solids are good sound absorbers but poor at providing insulation. PU is an example of a widely used polymer foam for sound absorption.

2.2.5.4.2 Characterisation of acoustic properties of foams

Sound absorption (α) coefficient is the ratio of sound absorbed energy to sound incident energy (Peng, 2016). If a material can absorb the acoustic energy entirely, then α=1 (Peng, 2016). The sound absorption coefficient varies with frequency, and it is commonly reported as an average at a specified set of frequencies (Peng, 2016) (Liu *et al.*, 2014).

One of the methods for measuring the sound absorption coefficient is the standing wave tube, known as impedance tube, see Figure 2.9. Impedance testing tubes expose substrates to sound waves at normal incidence (i.e. 90°). The measurement is based on measuring the sound reflected, using microphones, from the substrate (Bonin, 2010). A loudspeaker is positioned at one side of the tube and the sample to measure in the other. The sound source produces sound waves which travel along the tube, hit the sample and reflects from it.

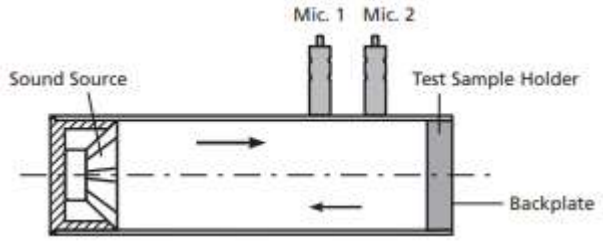

Figure 2.9 SCHEMATIC REPRESENTATION OF IMPEDANCE TUBE METHOD FOR SOUND ABSORPTION COEFFICIENT
(Bruel & Kjaer, 2018)

A standing-wave interference pattern forms due to the phase interference between the incident and reflected waves. The sound absorption is calculated from the sound pressure level measurement by the microphones. This method is described in both ISO 10534-2 and ASTM E1050-12 (Bruel & Kjaer, 2018). From *R*, the reflection coefficient measured, the absorption coefficient (α) can be obtained using Equation 2.19 (Suhanek, Jambroši and Horvat, 2008):

$$\alpha = 1 - |R^2| \qquad \text{(Equation 2.19)}$$

Sound transmission coefficient (τ) is the ratio of sound energy transmitted (through the substrate) to the incident sound energy to the surface (Peng, 2016). Sound Transmission Loss (STL), given by Equation 2.20 (Barnard and Rao, 2004) and measured in decibels (dB), is the sound insulation capacity of a material (Peng, 2016), which is usually greater at higher frequencies (Peng, 2016).

$$STL = 10 \cdot \log_{10} \frac{1}{\tau} \qquad \text{(Equation 2.20)}$$

An impedance tube with four microphones can be used to measure the transmission loss of a material, as shown in Figure 2.10. The speaker is at one end of the tube, and the sample is placed in a holder between the two pair of microphones. The impedance tube has an anechoic termination to prevent sound reflection. As the sound source generates the broadband, the sound waves propagate along the tube and hit the sample. The waves can be reflected back, absorbed by the material and transmitted through the material. The transmission

loss of the material can be derived from sound pressure measured at the four microphones. This method is described in ASTM E2611-17 (Bruel & Kjaer, 2018).

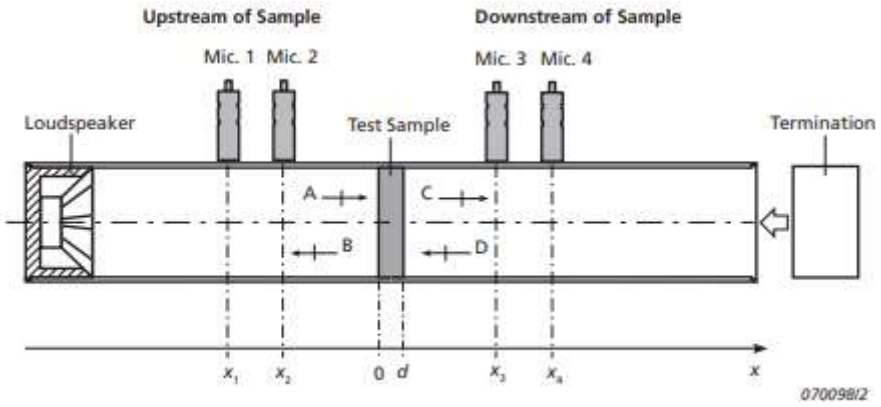

Figure 2.10 SCHEMATIC REPRESENTATION OF THE IMPEDANCE TUBE METHOD FOR STL (Bruel & Kjaer, 2018)

Sound insulation measurements are carried out at least from 100-3,150 frequency range, but extended measurements can be carried out up to 5000 *Hz* (Peng, 2016).

2.2.6 APPLICATIONS OF PLASTIC FOAMS

Plastic foams exhibit many interesting properties including shock absorbance, thermal and acoustic insulation, which make them attractive for different applications such as in automotive (seats, helmets), construction (insulation, sandwich panels), sports (shoes, sport mats, helmets), biomedical (hip protectors, scaffolds), aerospace and packaging industries, among others (Gibson and Ashby, 1997) (Wang *et al.*, 2010). As the focus of this work is on packaging applications, only a brief review in this sector is provided below.

2.2.7 FOAMS FOR PACKAGING APPLICATIONS

Polymeric foams are used for thermal and cushion packaging applications due to its low cost, light weight, good cushioning properties and low thermal conductivity (Wang *et al.*, 2010).

Foams are usually used for cushion packaging because they can absorb energy by deformation to minimise the stresses applied to the product (Bonin, 2010) during impacts. The cushioning material is then supposed to recover its original shape and dimensions to a certain degree, the degree of the recovery or resilience (Bonin, 2010). Cushion packaging is carefully designed to protect fragile products along the logistic chain to reduce damage from compression, shock or vibration by movement restriction and energy dissipation control within the package (Ceglia *et al.*, 2012). Cushion packaging is mostly for single-use and post-use plastic foams,

give rise to significant environmental issues due to the collection, returning and recycling difficulties and lack of biodegradability (Kaewtatip *et al.*, 2014).

Various polymer foams are widely used for thermal packaging applications. Thermal packaging refers to packaging that maintains temperature (cold or hot) of the products in cool boxes (e.g. for chilled foods, biological and pharmaceutical products) and thermal boxes (e.g. for hot meal delivery), respectively. The most common materials used are PU, PE, Expanded Polypropylene (EPP) and Expanded Polystyrene (EPS).

The most popular formats of EPS thermal packaging are bead-foamed, or steam chest molded rigid boxes. They are manufactured in different thicknesses, densities and interiors to meet the content requirements. For instance, EPS boxes are commonly used for fresh fish distribution. The lid and the box interlock, sealing the container. They provide good thermal insulation and are lightweight, water-resistant and stackable. They usually range from 0.5 to 40 *kg* capacities (Seafish Industry Authority, 2009) with different thicknesses, ranging from 30 to 70 *mm* (Topa Thermal, 2017). Molded boxes are very bulky to store and transport. A foldable EPS box has been recently developed (ICEE, 2017). It is a self-locking box that would require shrink-wrap or tape to fully close. This format saves storage and transport costs as it can be delivered in flat packs. This may also facilitate collection for recycling or sanitising to be safely reused. However, unlike classic EPS foam containers, the foldable EPS box is not watertight.

Some well-known tradenames for EPS foam used for packaging applications are Styropor® and Neopor®, both manufactured by BASF. Styropor® is a standard white EPS, patented in 1951 while Neopor® was patented in 1995. EPS Foam liners are usually used with cardboard boxes. They typically have a density of ~20 kg/m^3 and varying thickness, offering flexibility of design for low-volume uses.

PU foams exhibit outstanding insulation properties and are extensively used in insulation for construction and high-value packaging of biological or pharmaceutical products (Wang *et al.*, 2010). PU containers, combined with refrigerants, provide superior maintenance of internal payload temperatures for longer transit times and demanding weather conditions. One-piece moulded PU insulated packaging containers are held in an outer corrugated box sealed at the top with a soft foam polyurethane plug or rigid polyurethane friction fit lid. Sizes range from 2-1733 *L* of payload space (Topa Thermal, 2017).

PE foams are usually used as flexible foam liners with cardboard boxes. They typically exhibit a density of 20-30 kg/m^3 and a payload up to 60 *L* (Temperature Control Packaging, 2016).

2.3 BIOPLASTICS AND BIO-FOAMS

There is controversy regarding what a bioplastic is. While some authors consider bioplastics as plastics solely made from bio-based sources (Brodin *et al.*, 2017), other authors include compostable fossil fuel-derived plastics in the definition (Reddy *et al.*, 2013) (European Bioplastics Association, 2015) (Satish and KS, 2017). Bio-foams are therefore foams made from bioplastics.

The European Bioplastics Association (2015) defines the term "bioplastics" as those plastic materials that are bio-based, biodegradable or both. A bioplastic may be bio-based, i.e. derived from biological resources (e.g. crops or forestry materials) and/or biodegradable, that can be returned to nature in forms of water, carbon dioxide (CO_2) and biomass through biodegradation processes (European Bioplastics Association, 2015) (Reddy *et al.*, 2013).

The durability of petrochemical polymers is one of its main advantages and has contributed to its success during the latter half part of the twentieth century, supplanting more traditional but less durable materials, such as paper or wood (Bonin, 2010). This, however, has led to both economic and environmental concerns over resource sustainability and impact to the environment from waste (Reddy *et al.*, 2013). In the last few decades, developments in alternatives to fossil fuels derived plastic products have been made considerable progress (Cha *et al.*, 2001).

The key benefits of bioplastics and bio-foams developments materials are potential mitigation of fossil resources overdependence (Reddy *et al.*, 2013) (Stepto, 2009) and enhancement of biological waste management utilising their biodegradability (e.g. via composting and anaerobic digestion, AD).

2.3.1 OVERVIEW OF BIOPLASTICS

This section reviews the classification, drivers and policies, market, applications and challenges of bioplastics.

2.3.1.1 Classification

Bioplastics may be classified in different ways, such as their chemical composition, manufacturing process or applications (Coles and Kirwan, 2011). Reddy *et al.*

(2013) classify bioplastics according to the origin of the raw materials on which the polymers are based. Figure 2.11 identifies three categories: bio-based plastics (or bioplastics from renewable resources); bioplastics from petroleum resources and bioplastics from mixed sources.

Bioplastics from renewable resources are entirely or partially manufactured from biomass, such as those originated from plants and animals (Reddy *et al.*, 2013). This category includes materials such as starch, cellulose, chitosan or Polylactic Acid (PLA). Bio-based materials from harvesting are made from annually renewable crops that produce materials, such as starch, cellulose, lignin and hemicelluloses by photosynthesis (Coles and Kirwan, 2011).

Polylactic acid (PLA), one of the most extensively used bioplastics, is synthesised from lactic acids derived from fermentation of sugars in biomass (e.g. starch and other polysaccharides sources) while Polyhydroxyalkanoates (PHA), is extracted from that synthesised by microorganisms consuming sugar sources (Reddy *et al.*, 2013).

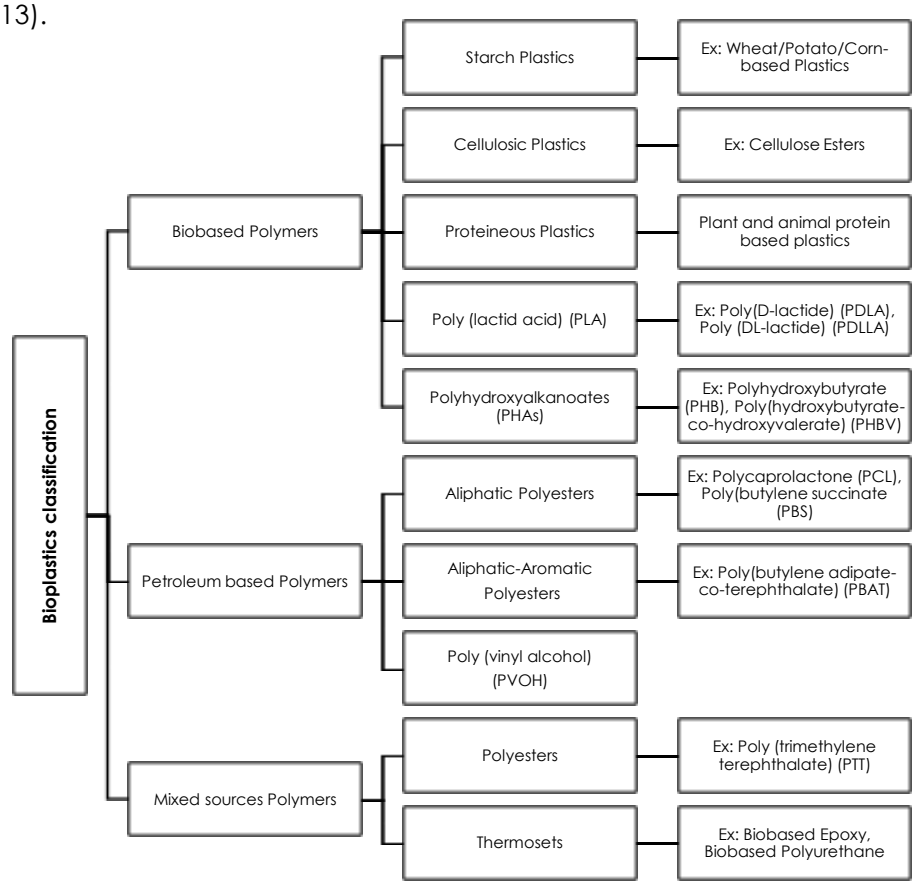

Figure 2.11 BIOPLASTICS CLASSIFICATION BASED ON ORIGINS (Reddy *et al.*, 2013)

Petroleum-based bioplastics are manufactured from chemicals of petroleum origins but are compostable. Plastics' compostability depends on the chemical composition, not on the source (Reddy *et al.*, 2013). Polycaprolactone (PCL) and

poly (butylene adipate-co-terephthalate) (PBAT) are examples of petroleum-based bioplastics (Reddy *et al.*, 2013).

Bioplastics can be made from **mixed sources** as copolymers, blends, or biocomposites to reduce costs or improve technical performance (Coles and Kirwan, 2011). Examples include polyesters like poly (trimethylene terephthalate) (PTT); or thermosets, like bio-based epoxy or bio-based PU (Reddy *et al.*, 2013).

In some cases, bioplastics are also classified according to its biodegradability and origin into three categories: bio-based and biodegradable, bio-based and not biodegradable and fossil-fuel based and biodegradable. (Coles and Kirwan, 2011).

During their evolution, bioplastics are traditionally classified into three generations (Robertson, 2008). **First generation** biopolymers were blends of traditional polymers with typically 5-15 *wt%* bio-based fillers, e.g. starch, natural fibres and other additives to accelerate its oxidative degradation (Robertson, 2008). They did not fully biodegrade but fragment into smaller pieces or particles, and thus the "biodegradability" was often interpreted as misleading to consumers (Bonin, 2010).

The **Second generation** had much greater bio-based content (40-75%) but, as the first generation, they did not meet the current definition of biodegradability (Robertson, 2008).

Third generation materials are either 100% bio-based materials or 100% biodegradable, as defined earlier. It includes bio-based synthetic polymers like Bio-PE, Bio-PET and Bio-PA, etc. which are bio-based but not biodegradable.

2.3.1.2 Drivers, Policies and Legislations in bio-based products and bioplastics

Since mid-1980s significant efforts have been made worldwide in the development and commercialisation of biobased products, including bioplastics (Whistler, (2009). Biobased products development is driven by improvements in the environment, resource security and in general, the sustainability of future economy (Philp, Ritchie and Guy, 2013).

Increasingly government policies, legislation or directives are established to encourage biopolymers. The primary relevant European policies include (European Comission, 2015):

- **The Commission's Lead Market Initiative** (2008-2011). It identified bio-based products as a lead market and aimed to promote their development by

standardisation, labeling and public procurement. It dictates some standards to the European Committee for Standardisation (CEN):

- **Mandate M/429**, for a standardisation programme elaboration for bio-based products
- **Mandate M/430**, on biopolymers and bio-lubricants
- **Mandate M/491**, on bio-solvents and bio-surfactants
- **Mandate M/492**, for standards development for bio-based products other than food or biomass for energy applications.

- **The European Union industrial policy** (28 October 2010). It aims to increment the manufacturing contribution to EU GDP from the current 15% to 20% by 2020. It prioritises the bio-based sector, considering it a key factor for sustainable growth.

- **Flagship initiative for a resource-efficient Europe** (26 January 2011). This is an initiative under the Europe 2020 strategy which aims to a more resource-efficient and low-carbon European economy, towards sustainable growth.

- **The Commission's bio-economy strategy** (13 February 2012). It intends to achieve a more sustainable use of renewable resources and to increase the bio-economy sector competitiveness.

- **The European Innovation Partnerships (EIP),** under the Commission's Innovation Union Flagship Programme. The EIP intends to stimulate Agricultural Productivity and Sustainability (EIP-AGRI) in which EIP on Raw Materials are more specific for bio-based products to promote sustainable agriculture and forestry and to increase recycling and reuse of materials.

European Standards have been developed regarding bio-based products (European Comittee for standardisation (CEN), 2014):

- European Standard **EN 16575:2004**, "Bio-based products – Vocabulary" (August 2014). It includes common terminology and definitions.

- Technical Report **CEN/TR 16721**, Technical Specification **CEN/TS 16640** and European Standard **EN 16785**. These are methods for bio-based content determination.

- European Standard **EN 16751**. Sustainability aspects

- European Standard **EN 16760**. Life Cycle Assessment.
- European Standard **EN 13432:2000**, Requirements for packaging recoverable through composting and biodegradation.
- European Standard EN **14995:2006**; Plastics, evaluation of compostability.

More specifically, in development of **bioplastics,** multiple factors act as driving forces including environmental friendliness, Corporate Social Responsibility (CSR), product differentiation, crude oil prices, technology advancements and legislation.

The main bioplastics industry driver is the rising awareness of environmental impact from food packaging. Plastic production imposes negative environmental impact, from resources consumption to disposal, as it ultimately generates landfill. Bioplastics could reduce landfill as they allow food waste to be composted with its packaging and, if anaerobic treated, they can also be employed to generate biogas. Bio-based plastics may also reduce greenhouse gases emissions, as plants absorb atmospheric carbon dioxide as they grow (Coles and Kirwan, 2011). However, one cannot assume zero carbon emission as they also consume fossil fuel from its production to transportation (Coles, et al., 2011). Other environmental consequences from biopolymers production should be considered, such as land and water usage, and eutrophication potential, among others.

Because of the consumers' increasing environmental awareness, some companies also see the development of biopolymers as an opportunity for marketing and brand differentiation.

The legislation is another significant driver for the development of bioplastics. Environmental policies and rising disposal costs may obligate industry to seek more sustainable alternatives (Fang and Milford A. Hanna, 2001). There are several policies regarding packaging made from biopolymers. The main areas covered are packaging waste legislation, biodegradable waste, and legislation on materials intended to come into food contact (Enguix, Imbernon and Ferrer, 2008).

The main European Directives regulating biopolymers for packaging applications are the following:

- **European Directive 94/62/EC** on packaging and packaging waste. The Directive aims to reduce packaging waste production and intends to

promote recycling, re-using and waste recovery for energy. The amending acts are:

- Directive 2004/12/EC on packaging and packaging waste
- Directive 2005/20/EC, an extension of deadlines for the attainment of the recycling and recovery targets for the Member States acceding the EU in 2004
- Commission Directive 2013/2/EU, amending Annex I of European Directive 94/62/EC
- Directive (EU) 2015/720 regarding lightweight plastic carrier bags consumption

- **Commission Regulation (EU) No 10/2011** on plastic materials and articles intended to contact food products.

The six main CEN standards for packaging, under Mandate 200 (M-200) are (Enguix, Imbernon and Ferrer, 2008):

- EN 13427 Packaging – Requirements for the use of European Standards in the field of packaging and packaging waste

- EN 13428 Packaging - Requirements specific to manufacturing and composition. Prevention by source reduction

- EN 13429 Packaging – Requirements for relevant materials and types of reusable packaging

- EN 13430 Packaging – Requirements for packaging recoverable by material recycling

- EN 13431 Packaging – Requirement for packaging recoverable in the form of energy recovery, including specification of minimum interior calorific value

- EN 13432 Requirements for packaging recoverable through composting and biodegradation. Test scheme and evaluation criteria for the final acceptance of packaging. This is the European Standard for biodegradability for polymers and packaging

Labeling is vitally important for waste separation and treatments. While EN 13432 mentioned above has become the general European Standard for biodegradability for polymers and packaging, other standards have been established for specified conditions and timeframe (European Bioplastics Association, 2015) (European Bioplastics Association, 2014). The European independent institutions involved in bioplastics certification are DIN CERTCO (Germany) and its associated institutes, such as AOR (UK), COBRO (Poland) and Vincotte (Belgium).

2.3.1.3 Bioplastic markets

Bioplastic industry is still in its implant stage. According to The European Bioplastics Association (European Bioplastics Association, 2018), the bioplastics market represents around 1% share of the ~320 million tonnes of global annual production of all plastics.

Bio-based PE, bio-based polyethylene terephthalate (PET) and bio-based polyamides (PA), all biobased but not biodegradable, represent ~56% of the global production capacities of bioplastics, followed by thermoplastic starch (TPS) blends (~18%) and PLA (~14%) (European Bioplastics Association, 2018). For bio-based and biodegradable materials, TPS, PLA and PHAs are the front runners (European Bioplastics Association, 2018).

As exhibited in Figure 2.12, the total bioplastics production represented around 820,000 hectares of agrarian land use in 2017, less than 0.02% of the total arable agricultural land of 13 billion hectares (European Bioplastics Association, 2018). Starch or sugar are the dominating raw materials used, but less land may be used in the future if more cellulosic biomass, non-food crops and food residues are utilised (European Bioplastics Association, 2014).

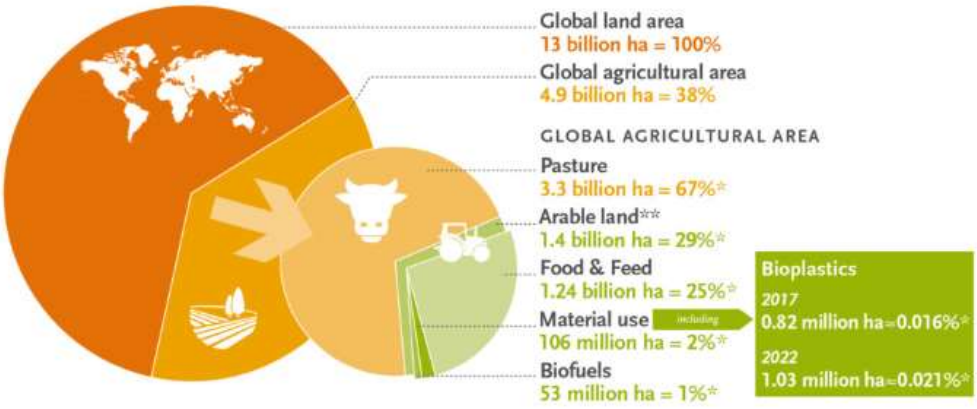

Figure 2.12 ESTIMATE OF LAND USE FOR BIOPLASTICS BETWEEN 2017 AND 2022
(European Bioplastics Association, 2018)

2.3.1.4 Application of bioplastics

A wide range of biopolymers are commercially available, and new ones are created continually (Coles and Kirwan, 2011). Bioplastics materials and products have found many applications (see Figure 2.13), such as packaging (the leading sector), textiles, consumer goods medicals anatomies, among others (European Bioplastics Association, 2018) (Willett and Shogren, 2002).

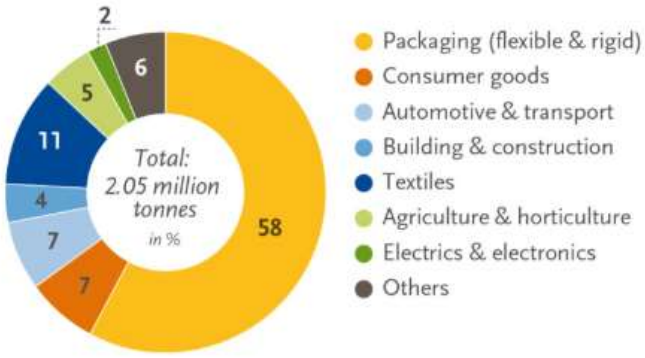

Figure 2.13 ESTIMATED APPLICATION OF BIOPLASTICS (2017-2022) IN DIFFERENT SECTORS (European Bioplastics Association, 2018)

An increasing number of brands and companies are introducing bioplastics in their products. Toyota introduced in its Prius model (2009) PLA-PP alloys in seven components, including the door trim and the scuff boards (Plastics Today, 2009). Coca-Cola has been using the *Plant Bottle*, a PET bottle with 30% bio-based content, since 2009 and in 2015, the company unveiled a 100% bio-based bottle (The Coca-Cola Company, 2015). Paperfoam®, injection molded starch-fibre blend foams, offers a more sustainable alternative to conventional cushioning packaging of high-value products (Paperfoam, 2018).

Table 2.3 shows a list of selective major bioplastic resin or blends manufacturers.

Table 2.3 A SELECTIVE LIST OF MAIN COMMERCIAL SUPPLIERS OF BIOPLASTIC RESIN AND BLENDS (Imam *et al.*, 2008)

Biodegradable polymer	Trade name	Company
Starch	Ecofoam	National Starch, USA
Starch	Novon	Ecostar GmbH, Germany
Modified starch	Evercorn	Japan Corn Starch Co. Ltd
Thermoplastic starch	Paragon	Avebe, The Netherlands
Starch/copolyester	Mater Bi	Novamont, Italy
PHAs	Nature's Plastic	Metabolix, USA
PHAs	Nodax	Proctor & Gamble, USA
Copolyester	Ecoflex	BASF, Germany
Copolyester	Biomax	Dupont, USA
Copolyester	Bionelle	Showa Highpolymer, Japan
Polylactc acid	NatureWorks	NatureWorks (Cargill-Dow), USA
Cellulose acetate	ACEPLAST	Acetati, Italy

Table 2.4 presents some examples of commercial food packaging from bioplastics, blends and composites.

Table 2.4 COMMERCIAL FOOD PACKAGING MADE FROM BIOPLASTICS, BLENDS AND COMPOSITES (Imam *et al.*, 2008)

Packaging product	Properties	Biopolymer(s)	Packaged material	Company
Trays	Convenience, moisture barrier	Virgin pulp	Beer, chicken	Pactiv, Omni-Pac, Germany
Wrapping films	Oxygen and moisture barrier	PE–starch (0–28%)	Ground meat	Europe
Tray/container	Convenience	Coated pulp and starch	French fries	Belgium
Container clamshells/ plates, soup bowls, beverage cups, etc.	Convenience, insulation, moisture barrier	Powdered starch, foam, baked foam	Hamburgers/sandwiches	Apack, Germany Earthshell, USA
Container	Mechanical protection, moisture barrier, carbon dioxide barrier	Cardboard/PLA	Yogurt	Dannon, Europe/ North America/ Asia
Packaging	Moisture barrier, light barrier, grease barrier	PLA–copolyester, starch–PLA, PLA–polycaprolactone	Butter/margarine	Europe
Packaging	Containment	Nets of starch-based plastics, pulp trays, corrugated board trays and transport boxes	Fruits and vegetables	Germany, Belgium/Europe
Packaging	Moisture and gas barrier	NatureSEAL™ (cellulose based)	Variety of fruits and vegetables	Europe/USA/Asia
Bags	Biodegradable	Starch/starch–polycaprolactone	General purpose	Europe – Finland, Italy, Denmark

2.3.1.5 Challenges in the bioplastic sector

The bioplastic industry is still young and thus is facing some main challenges (Coles and Kirwan, 2011). These include:

- Due to their relatively smaller production scale, the materials cost is still much higher than conventional plastics and hence less competitive

- Bioplastics must demonstrate acceptable physical and mechanical properties to replace their plastic counterparts, particularly in ductility, heat distortion, barrier properties and moisture sensitivity (Robertson, 2008)

- Effective consumer communication and labeling for easy identification of the materials, proper segregation and handling after use

- Effective demonstration of overall benefits to consumers in comparison to fossil-derived polymers

- Providing and/or enhancing biological waste management infrastructure for collection and separation at source of disposal or automatic, sorting at municipal waste management facilities

2.3.2 BIO-FOAMS

This section briefly reviews the significance, applications and types of bio-foams.

2.3.2.1 Introduction

There are some additional drivers for the development of bio-foams as an alternative to conventional plastic foams. Foams are lightweight and thus use less material which mitigate the relatively higher cost of bioplastics; they are also bulky and, in many cases, particularly when dispersed in rural households with the packed products, may be uneconomical to collect, sort and transport back to a central facility for recycling. Local composting would then become a much better option if foams are made biodegradable/compostable.

2.3.2.2 Types of bio-foams

Biological cellular solids can be easily found in nature such as in plants (e.g. straws and cork), marine lives (e.g. sponges) and in animals (e.g. beak of hornbill birds and bone structures) Synthetic bio-foams can be made using appropriate foaming technologies from bioplastics (Iannace and Sorrentino, 2016) and can substitute most conventional plastics foams where they have established uses. For instance, starch and PLA foams are used to replace EPS used for cushion packaging and PP foams in the automotive industry (Bergeret and Benezet, 2011) (Nofar and Park, 2016).

Starch foams are widely used for transit and shipping packaging as loose-fills (see Figure 2.14.A) or panels (See Figure 2.14.B). Starch foams will be further discussed in section 2.4.

Synbra Technologies (Netherlands) created BioFoam® (see Figure 2.14.C), a foam manufactured by the expansion of PLA beads. This was the first bio-based foam receiving the cradle-to-cradle certification (Synbra Technology, no date). PLA foams can also be manufactured by supercritical CO_2 extrusion (see Figure 2.14.D) for thermal packaging and containment of food products applications (Kelly *et al.*, 2014).

Bio-foams are also produced by blending biopolymers with conventional plastics. Vegetable oils (e.g. palm oil, soybean oil and rapeseed oil, among others) can substitute the fuel oil derived polyols for PU production (Prociak, 2016) and the bio-based PU foams can be used just like conventional PU. Oliveiro *et al.* (2015) produced gelatine/poly(butylene succinate) foams by supercritical foaming. BASF (Germany) developed Ecovio®, a packaging material compounded from BASF's Ecoflex® (PBAT based) and PLA (BASF, 2016). Figure 2.14.E shows an image of a box made with Ecovio®.

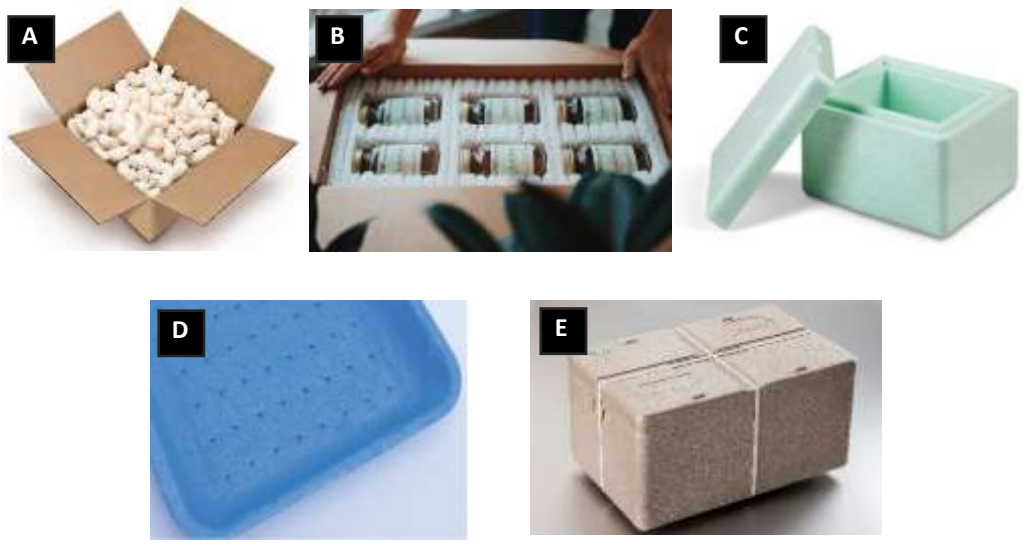

Figure 2.14 IMAGES OF BIO-FOAMS EXAMPLES (A) STARCH-LOOSE FILL (Sierra Suppy and Packaging, 2018) **(B) CORRUGATED STARCH PANEL** (Green Cell Foam, 2018) **(C) BIOFOAM®, PLA-ECOFLEX® FOAM (D) PLA FOAMS MANUFACTURED BY SUPERCRITICAL CO_2 EXTRUSION** (Pera Technology, 2014) **(E) ECOVIO® BOX** (BASF, 2016)

Bio-foams have found many biomedical applications. Sol-gel processing can create bio-foams in the form of organic-inorganic porous hybrids (e.g. xerogels, aerogels) (Lavorgna, Verdolotti and Mascia, 2016) to combine inorganic fillers (e.g. silicates, phosphates, carbonates) with different bioplastics (e.g. cellulose, hemicelluloses and proteins, among others) (Lavorgna, Verdolotti and Mascia, 2016) (Ruiz-Hitzky *et al.*, 2016). They are frequently used in tissue engineering which requires controlled biodegradation, and thus conventional plastic foams cannot perform.

Sections 2.4 and 2.5 reviews foams made from starch and gelatine, respectively. For further details about bio-foams, there is available literature, such as Iannace and Park (2014) book.

2.4 STARCH FOAMS

This section focuses on one of the most developed bio-foams systems, starch-based foams. First, the starch origins and its molecular structure are discussed. Then, the preparation of thermoplastic starch, followed by the discussion of the structure and properties of starch foams, is commented. Finally, the main foaming technologies are discussed.

2.4.1. INTRODUCTION

Starch is a raw material typically used in biodegradable polymers as a biodegradable filler. It is also the primary raw material to produce synthetic bioplastics such as PLA and PHA polymers using biological conversion processes

(Zhou et al., 2006) (Whistler, 2009). Thermoplastic starch, which has been treated to modify the original native starch structure to confer thermoplasticity, can be used alone or as compounds with other bioplastics, to manufacture a wide range of products, including bio-foams.

As mentioned in Section 2.3.1, considerable efforts have been made to develop materials from renewable resources (Willett and Shogren, 2002). Thermoplastic starch and compounds are among the most commercialised materials used to create bioplastics due to its cost-effectiveness, technical attributes (i.e. biodegradability and compostability) and nontoxicity (A. S. Ayoub and Rizvi, 2009) (Coles and Kirwan, 2011).

The perceived negative impact of EPS in foam packaging applications has stimulated the development of bio-foams, including starch-based foams and technologies to replace it (Whistler, 2009). These have been proved, in many cases, as an appropriate alternative to their fossil-based counterparts (Salgado *et al.*, 2008) (Peng *et al.*, 2013). Various patents of starch-based bioplastic compounds and bio-foams have been registered and commercialised (Zhou, Song and Parker, 2006) (Wang *et al.*, 2010).

Nevertheless, compared with EPS foams, starch foams may have some disadvantages, such as relatively higher densities, poorer resilience to plastic deformation and water sensitivity (Fang and Milford A. Hanna, 2001). This is why further research is needed to improve starch bio-foams, to penetrate deeper into the EPS market (Bonin, 2010). Starch loose-fill foams, free-flowing pieces for filling space around goods within shipment boxes, are considered one of the most successful bio-foams applications (Zhou, Song and Parker, 2006) (Fang and Milford A. Hanna, 2001). Packaging trays made of starch, cellulose fibers (20%) and sunflowers proteins (10%) as alternatives to EPS trays have also been reported (Salgado *et al.*, 2008).

Manufacturing technologies for starch foam planks have also been developed. Some of them produce corrugated foam planks by extrusion foaming of thermoplastic starch compounds (Novamont, 2018). However, these materials are not widely used in packaging due to their high density and cost (Zhou, Song and Parker, 2006)

2.4.2 STARCH

Starch is an abundant annually renewable low-cost resource. Historically it has been a major raw material for manufacturing of paper and boards, adhesives, fine chemicals, solvents and fuels , etc (Cha *et al.*, 2001). In recent years it has become one of the key raw materials for bioplastic production (Coles and Kirwan, 2011).

2.4.2.1 Starch Origins

Starch is a polysaccharide (Reddy *et al.*, 2013) produced in different plant tissues and numerous plant species, where it is accumulated as discrete semi-crystalline granules (Tester, Karkalas and Qi, 2004) (Cai and Wei, 2013). Its granules are synthesised in the cell cytosol from sucrose (50% glucose-50% fructose), that breaks down into fructose and uridine diphosphate glucose (UDP-glucose) (Tester, Karkalas and Qi, 2004). UDP-glucose undergoes subsequent transformation until it translocates into the amyloplast and is converted there into glucose-1-phospate (G-1-P), that is consequently converted to ADP-glucose, providing glucose residues for amylose and amylopectin biosynthesis (Tester, Karkalas and Qi, 2004).

Starch may come from different origins and botanic species (Reddy *et al.*, 2013), differing in the amylose-amylopectine ratio, molecular weight, crystallinity (type and degree) and size of granules. Genetical and environmental factors lead to properties differences during its synthesis process (Coles and Kirwan, 2011) (Song, 2014).

For single-use starch-based biodegradable materials, potato, corn, wheat or cassava starches, among others, have been used (Kaewtatip *et al.*, 2013).

2.4.2.2. Starch molecular structure

Starch is composed of highly branched molecules (Stepto, 2009). It is a hydrophilic polymer of D-glucose principally constituted, in turn, by two main types of polysaccharides, amylose and amylopectin, giving rise to around 98-99% of its dry weight (Tester, Karkalas and Qi, 2004) (Stepto, 2009) (Coles and Kirwan, 2011).

Amylose is a linear polymer of α-D-(1,4) glucopyranosyl that may be slightly branched by (1,6)-a-linkages (Bule, 1998). It has a molecular weight of 10^5-10^6 *g/mol* (Blanshard, 1987) (Avérous, 2004).

Amylopectin is a highly multiple-branched polymer composed of short α-(1,4) linked chains connected to each other by α-(1,6) glucosidic linkages with molecular weight 10^7-10^{10} *g/mol* (Blanshard, 1987) (Avérous, 2004). The

amylopectin units from high amylose starches have a relatively high number of very long chains (Yoshimoto et al. 2000).

The structures of amylose and amylopectin are shown in Figure 2.15.

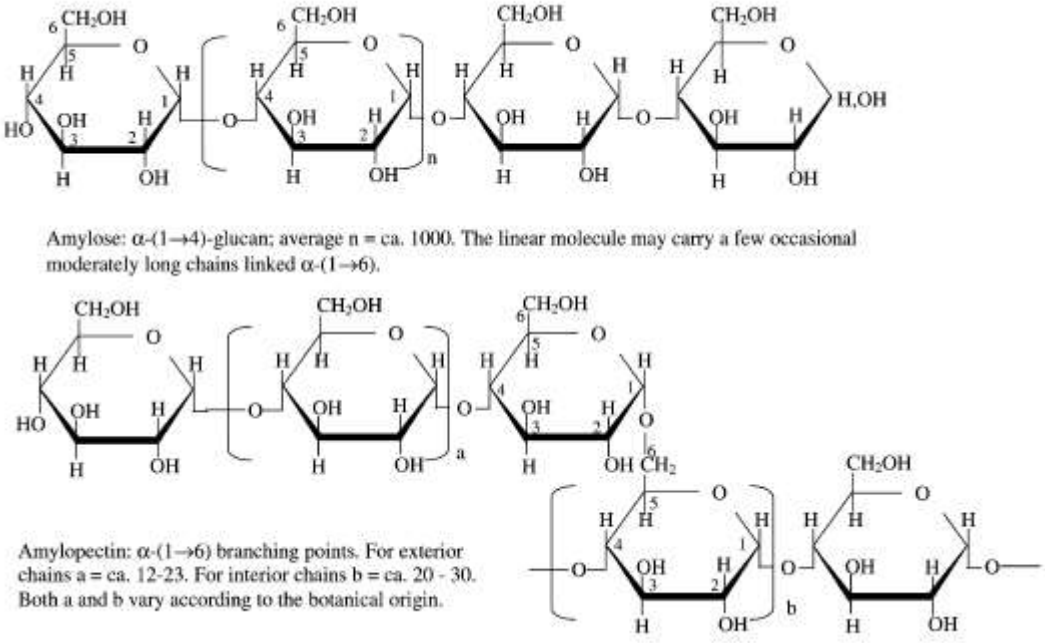

Figure 2.15 MOLECULAR STRUCTURE OF AMYLOSE AND AMYLOPECTINE (Tester, Karkalas and Qi, 2004)

Starch appears in granules ranging from 1-100 μm, depending on the botanic species and the granule shape (Tester, Karkalas and Qi, 2004). Starch granules structure consists of alternating rings with different crystallinity levels and amylose/amylopectin ratios. The core of the granule, also known as hilum, is the part where the granule starts to grow and it is the least organised area (Cai and Wei, 2013).

Starch has a semi-crystalline structure, crystallising in two polymorphic forms, A and B-type structures (Crochet *et al.*, 2005). The crystallised structure is based on left-handed double-stranded helices packed parallel into hexagonal and monoclinic unit cells (Crochet *et al.*, 2005). The A-type diffraction pattern is characteristic of cereal starches, B-type is usually shown in tube starches and high amylose starches. Besides, hybrid C-type patterns, a combination of A and B-type in X-ray diffraction (Tester *et al.,* (2004)), appear in some root, legume, fruit and seed starches (Tester, Karkalas and Qi, 2004) (Song, 2014).

Starch's overall crystallinity may vary from 15-45% depending on the origin, humidity content and technique used to measure it (Buléon *et al.*, 1998).

2.4.2.3 Characteristics of native starch granules

Starch granules characteristics include amylose/amylopectin ratio, size, shape (round, lenticular, polygonal), size, distribution (unimodal or bimodal), association (individual or granule clusters) and composition (moisture, lipid, mineral, protein and a-glucan content), among others (Tester, Karkalas and Qi, 2004). Table 2.5 shows some key characteristics of starch granules from different botanical sources.

Table 2.5 CHARACTERISTICS OF STARCH GRANULES FROM DIFFERENT BOTANICAL SOURCES (Tester, Karkalas and Qi, 2004)

Starch	Type	Shape	Distribution	Size (μm)
Barley	Cereal	Lenticular (A-type), spherical (B-type)	Bimodal	15–25, 2–5
Maize (waxy and normal)	Cereal	Spherical/polyhedral	Unimodal	2–30
Amylomaize	Cereal	Irregular	Unimodal	2–30
Millet	Cereal	Polyhedral	Unimodal	4–12
Oat	Cereal	Polyhedral	Unimodal	3–10 (single) 80 (compound)
Pea	Legume	Rentiform (single)	Unimodal	5–10
Potato	Tuber	Lenticular	Unimodal	5–100
Rice	Cereal	Polyhedral	Unimodal	3–8 (single) 150 (compound)
Rye	Cereal	Lenticular (A-type) Spherical (B-type)	Bimodal	10–40 5–10
Sorghum	Cereal	Spherical	Unimodal	5–20
Tapioca	Root	Spherical/lenticular	Unimodal	5–45
Triticale	Cereal	Spherical	Unimodal	1–30
Sago	Cereal	Oval	Unimodal	20–40
Wheat	Cereal	Lenticular (A-type)	Bimodal Spherical (B-type)	15–35 2–10

Native starches are usually composed of 70-85% amylopectin and 15-30% amylose (Reddy et al. 2013). The amylose-amylopectin ratio affects melt's rheological and mechanical behaviour of the product with time (Song, 2014). Ayoub and Rizvi (2009) stated that amylose typically constitutes around 30% of starch, but the ratio may vary with starch source. Corn possesses circa 25-28% amylose (high amylose corn can have up to 80%); tapioca, about 17%; and waxy maize, virtually none (Buléon *et al.*, 1998) (A.S. Ayoub and Rizvi, 2009).

Regarding moisture content, air-equilibrated starches present from 10-12% (cereals) to 14-18% (roots and tubers) content (Tester, Karkalas and Qi, 2004) (Whistler, 2009). Starch hydrophilicity is one of its major constraints (Calvert, 1997) and it is due to the three hydroxyl groups present in each D-glucosyl unit (Whistler, 2009) (Coles and Kirwan, 2011). The gain or loss of moisture in starch may provoke significant alterations in its mechanical and physical properties that may compromise the material utility (Whistler, 2009). This problem may be solved by converting the hydroxyl groups to esters via reaction with carboxylic acids (A.S. Ayoub and Rizvi, 2009).

Starches may include lipids and proteins (Tester, Karkalas and Qi, 2004). Other starch constituents are minerals (usually less than 0.4%), such as calcium, magnesium, phosphorus, potassium and sodium (Tester, Karkalas and Qi, 2004).

The crystallinity of some regions causes birefringence properties presented in the form of a Maltese cross when analysed under polarised light microscope (Song, 2014). Starch is not soluble in cold water (Cai and Wei, 2013) but in the presence of enough hot water or plasticiser, the amorphous regions of the starch granule disrupt, absorbing water and swelling (Cai and Wei, 2013) (Reddy *et al.*, 2013). This destabilises their crystalline structure, provoking birefringence loss (Cai and Wei, 2013) and leading to a non-reversible phenomenon called gelatinisation that produced a material called thermoplastic starch (TPS) (Reddy *et al.*, 2013).

2.4.3 PREPARATION OF THERMOPLASTIC STARCH

Native starches are rarely directly used for industrial applications. In terms of mechanical properties for material uses, they are brittle and cannot be processed by thermal processing as thermoplastic plastics. Starches used in industry are usually modified to change its characteristics (e.g. gelatinisation, retrogradation tendency, hydrophilic character, and cooking characteristics, among others) (A. S. Ayoub and Rizvi, 2009). This can be achieved by physical, chemical and enzymatic modifications to obtain the required characteristics (Tester, Karkalas and Qi, 2004).

Starch needs to go through some of the following procedures to be usable, transformed into TPS (see Figure 2.16): purification, gelatinization, destructuration and plastification described as follows.

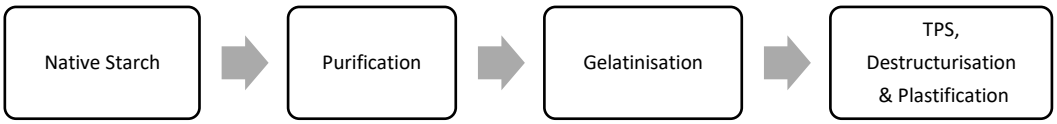

Figure 2.16 PREPARATION OF THERMOPLASTIC STARCH (TPS)

2.4.3.1 Purification

Some starch constituents, such as proteins and lipids, affect negatively the starch functionality (Tester, Karkalas and Qi, 2004). Thus, industrial starch (for non-food purposes) is normally purified to eliminate the non-starch elements (Song, 2014). Table 2.6 shows the composition differences between whole grain, milled flour and purified starch.

Table 2.6 COMPOSITION DIFFERENCES BETWEEN STARCH WHOLE GRAIN, STARCH FLOUR AND PURIFIED STARCH
(Tester, Karkalas and Qi, 2004)

COMPONENT	WHOLE GRAIN	MILLED FLOUR	PURIFIED STARCH
STARCH (wt%)	75	80	90
PROTEIN (wt%)	12	11	0.2
FIBRE (wt%)	8	1.5	1.5
LIPID (wt%)	2.5	1.5	1
ASH (wt%)	1.5	1	1.5

2.4.3.2 Gelatinisation

Starch gelatinisation is a widely studied process that significantly contributes to starch functionalities.

Native starch granules are insoluble in cold water, but when heated, in the presence of water, starch gelatinisation takes place (Song, 2014). When heated above their gelatinisation temperature (usually above 70°C), in excess of water, starch granules increase their size, provoking an irreversible disruption of molecular orders accompanied by water absorption and granular swelling, crystallinity loss, amylose leaching and increase in suspension viscosity (Song, 2014). Swelling is related to granule rupture, loss of birefringence and disruption of crystalline structure (Cai and Wei, 2013). Therefore, the typical Maltese cross disappears due to loss of D-glucosyl units regular orientation (Cai and Wei, 2013).

The gelatinisation results in a macromolecular aqueous gel constituted of an amylose-water solution with dispersed, swollen amylopectin-rich granules. (Song, 2014).

Gelatinisation may be affected by several factors, such as water presence, both internal and external to the starch granule; the content of amorphous and crystalline regions, processing temperature and starch's botanical origin, among others (Crochet *et al.*, 2005) (Song, 2014).

2.4.3.3 Destructuration and plasticisation

As mentioned in previous sections, natural starch is not a thermoplastic polymer. It is required to modify its structure to obtain a homogeneous melt with thermoplastic behaviour (Coles and Kirwan, 2011) (Song, 2014). Starch must be 'destructurised' (the granule structure destruction) and plasticised (for material flexibility) with the

application of heat, mechanical shear and plasticiser incorporation in an aqueous medium, destroying the swollen granules and producing amorphous TPS (Coles and Kirwan, 2011). Destructuration is desirable to achieve homogeneous compounding of starch with other additives and/or polymers for preparation of subsequent processes e.g. extrusion, moulding or foaming (Song, 2014).

Once plasticised, starch is ready for subsequent processing e.g. compounding with other bioplastics and processing additives (e.g. surfactants, blowing agents, fillers and pigments, among others (Song, 2014).

The structural changes during destructuration and plasticisation stages are (Song, 2014):

- Starch granules fragmentation
- The weakening of hydrogen-bond between starch molecules, provoking crystallinity loss
- Partial starch polymer chains depolymerisation

Thermoplastic starch preparation is usually made by extrusion, but TPS preparation can be carried out by other heating and shearing processes (Song, 2014).

Plasticisers assist thermoplastic starch in controlling the degree of gelatinisation and destructuration processes, assisting the polymer melt flow, increasing its ductility and toughness and reducing the glass transition temperature (Song, 2014). Water is a temporary plasticiser in starch processing, as it will be removed during subsequent drying. More permanent plasticisers for starch are glycerol, glucose, sorbitol, lactic amino acids, and urea, among others (Calvert, 1997).

2.4.4 STRUCTURE OF STARCH FOAMS

Starch foams structure depends on the composition and processing (see section 2.4.6, foaming technologies). For instance, granules relics may remain within the foam cell walls and results in surface roughness and/or bubble rupture due to heterogeneity (Shogren *et al.*, 1998).

Baked starch foams tend to exhibit a dense outer layer and a light inner open-cell core (Shogren *et al.*, 1998), as shown in Figure 2.17A. Microwaved and extruded starch foams usually exhibit a more regular structure (see Figures 2.17B and 2.17C, respectively) than baked foams, but their cell size and structure seems less regular than their plastic counterparts, owing probably to heterogeneity, among others,

mentioned earlier. Soykeabkaew *et al.* (2015) noticed that extruded foams tend to exhibit large and anisotropic cells, giving rise to low density and anisotropic properties. Zhou *et al.* (2006) described microwave starch foams as cellular solids with relatively thick cell walls, appropriate for applications requiring higher compression strength. Freeze-dried foams usually exhibit smaller and more uniform cell size than the extruded, microwaved and baked foams, as shown in Figure 2.17D.

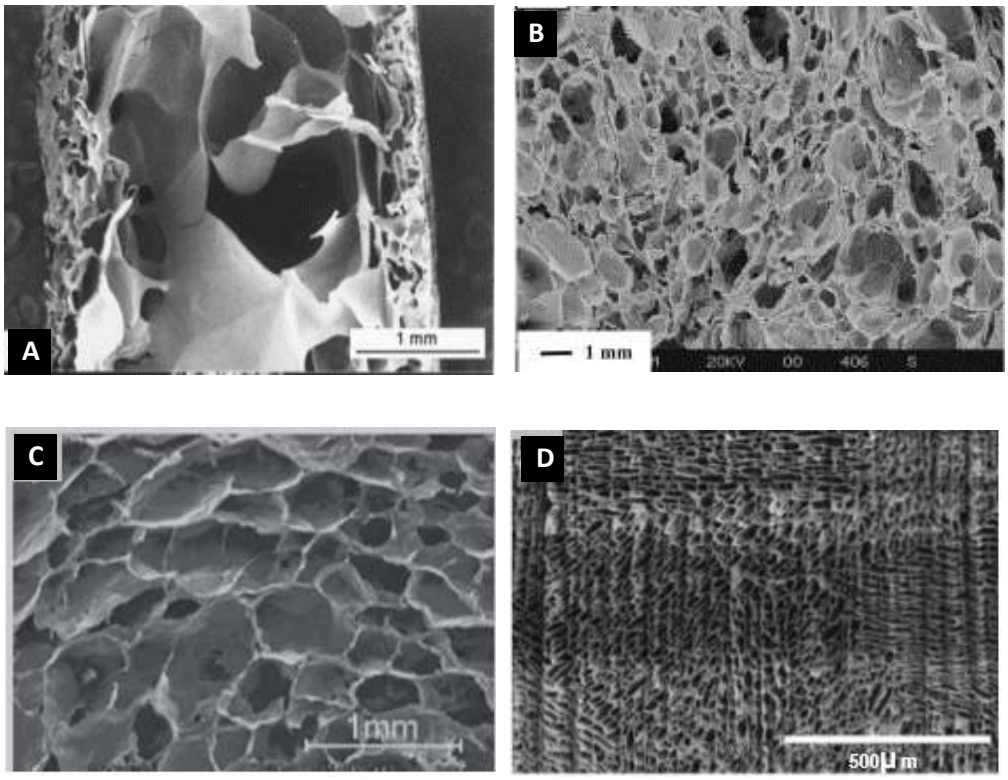

Figure 2.17 EXAMPLES OF STARCH FOAM STRUCTURE (A) BAKED STARCH FOAM (Shogren *et al.*, 1998) **(B) MICROWAVED FOAM STRUCTURE** (Zhou, Song and Parker, 2006) **(C) EXTRUDED STARCH FOAM** (Pushpadass *et al.*, 2008) **(D) FREEZE-DRIED STARCH FOAM** (Svagan, Samir and Berglund, 2008)

Highly viscous batters for any foaming technology impede bubbling during the expansion process, what leads to irregular structures and lower average cell sizes (Kaewtatip, Tanrattanakul and Phetrat, 2013). Purified starch materials produce finer cell structure in microwaved foams than wheat flour due to the presence of bran leading to heterogeneity in the latter (Zhou, Song and Parker, 2006).

2.4.5 PROPERTIES OF STARCH FOAMS

Extensive research has been carried out in the last decades or so to enhance starch foam properties (Cha *et al.*, 2001) as the properties that make it an environmentally attractive material (e.g. biodegradability), may also negatively influence its performance (A. S. Ayoub and Rizvi, 2009).

Foam properties are highly dependent on the raw materials and additives employed in the formulation (Zhou, Song and Parker, 2006). Increasing starch content in a bioplastic compound may give rise to deteriorations in expansion ratio and density increase, compressibility or processability, among others (Cha *et al.*, 2001) (Coles and Kirwan, 2011).

Brittleness of starch foams is highly dependent on the relative humidity conditions due to starch hydrophilic nature (Fang and Milford A. Hanna, 2001). Therefore, the use of coatings and additives, such as polysaccharides and biodegradable polyesters, may be necessary to produce more flexible starch foams (Fang and Milford A. Hanna, 2001) (Willett and Shogren, 2002).

Key factors influencing starch foam structure and properties include:

a. Formulation (e.g. starch type, native or modified starches; incorporation of bioplastics and additives)

b. Foaming techniques and the conditions used (Coles and Kirwan, 2011) (Soykeabkaew, Thanomsilp and Suwantong, 2015).

2.4.5.1 Influence of formulations

Native starches with different amylose-amylopectin ratio are available. This feature is known to influence expansion ratio and density of starch foams, which in turn, affects cell structure and mechanical properties (Fang and Milford A. Hanna, 2001). Willed & Shogren (2002) showed how the starch origin changed the properties of extruded starch foams. They found foam densities from corn, wheat, potato and high amylose starches vary from 61.4, 58.6, 40.6 and 35.5kg/m^3, respectively under the same processing conditions. Shey et al. (2006) also reported lower densities in potato starch foams (150kg/m^3) compared with wheat starch foams (200kg/m^3). Willed & Shogren (2002) correlated variation in the compressive strength of starch-*10wt%* PHEE foams (from 0.38, 0.35, 0.23 and 0.18MPa) to their starch origins for corn, wheat, potato and high amylose starch, respectively.

Starch can also be modified (e.g. crosslinked starch and acetylated starch, among others) or compounded with other bio-resins to improve water resistance and mechanical properties (Whistler, 2009) (Soykeabkaew, Thanomsilp and Suwantong, 2015). When starch is blended with petroleum-based plastics (e.g. PCL, PVA) or renewable bioplastics (e.g. PLA, chitosan and PHVB), the water resistance (Park and Cheung, 1997) (Pushpadass *et al.*, 2008) (Shey *et al.*, 2006), density (Willett

and Shogren, 2002) and mechanical properties (Kaisangsri, Kerdchoechuen and Laohakunjit, 2012) of the foams are usually enhanced (Soykeabkaew, Thanomsilp and Suwantong, 2015). The positive effect of PLA incorporation on the density of extruded starch foams has been widely discussed (Fang and Milford A. Hanna, 2001) (Willett and Shogren, 2002). Willed & Shogren (2002) reported that the density of corn-based foams decreased from 61.4kg/m^3 (starch only) to 47, 30.9 and 18.8 kg/m^3, for 5%, 10% and 20% PLA contents, respectively. Preechawong *et al.* (2004) studied the mechanical properties (tensile and flexural strengths) of starch-PLA foams revealing the influence of PLA content (and consequently, density) (see Figure 2.18).

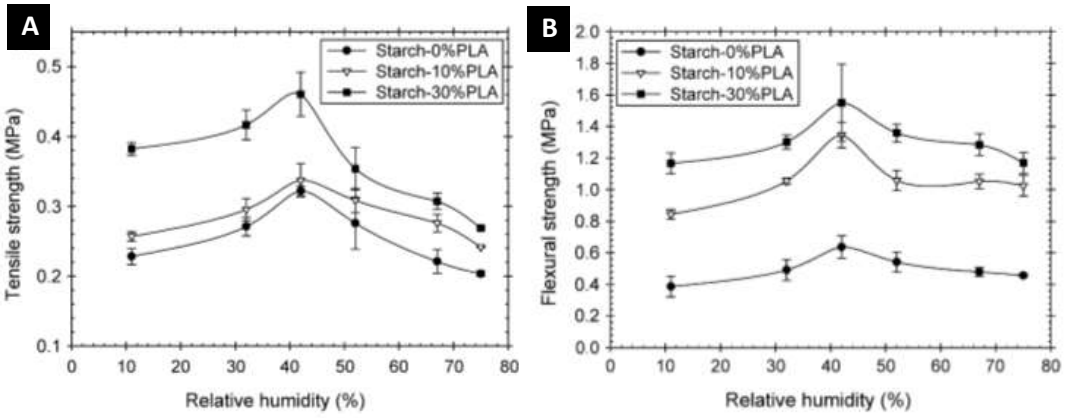

Figure 2.18 MECHANICAL PROPERTIES ((A) TENSILE STRENGTH (B) FLEXURAL STRENGTH) OF STARCH AND STARCH/PLA FOAMS AS A FUNCTION OF RELATIVE HUMIDITY (Preechawong *et al.*, 2004)

Starch foams may be susceptible to microbe spoilage when their water activity is high. Preservatives, such as acetic acid, are added to batters to decrease the pH and improve microbiology resistance (Willett and Shogren, 2002).

Starch foams properties may also be improved by the inclusion of processing additives, such as plasticisers, salts, nucleating agents and natural fibres, among others (Coles and Kirwan, 2011).

- Fillers are additives extensively used in the polymer industry to alter material properties, such as stiffness, strength, toughness, heat distortion, damping, permeability, electrical characteristics, density or cost. The properties provided by the fillers are dependent on the size and shape of the filler and the interfaces between the matrix polymer and the filler (Whistler, 2009). One must take into account however that the positive characteristics provided by the filler may counterpoise other properties of foams, such as foamability of the composites (Whistler, 2009). Natural fibres (e.g. hemp, flax, wood pulp) are often incorporated into starch suspensions to produce biocomposites. It is expected that fibres would improve mechanical

properties, water resistance and cell size distribution of starch foams (Soykeabkaew, Thanomsilp and Suwantong, 2015).

- Plasticisers are incorporated to adjust the brittleness/softness properties of starch-based materials (Preechawong *et al.*, 2004). Examples widely used for starch foams include glycerol, sorbitol and urea to adjust its glass transition temperature (T_g).

- Nucleating agents (e.g. talc, salts, $CaCO_3$) assist the foaming process by generating larger number of cells and narrowing the cell size distribution (Whistler, 2009) (Zeng *et al.*, 2014) (Soykeabkaew, Thanomsilp and Suwantong, 2015). The addition of nucleation agents may create denser foams and increase compressive strength, elastic modulus and elastic deformation energy (Zhou, Song and Parker, 2006). Thus, nucleation agents help to achieve more rigid foams, able to absorb more impact energy for cushioning foams (Zhou, Song and Parker, 2006) (Whistler, 2009).

- Starch foams can also be nano-reinforced with different materials such as nanoclays, nanocelluloses, and nanohydroxyapatite, among others, which may also act as nucleating agents.

2.4.5.2 Influence of foaming techniques

Various processing methods produce foams with different shapes, cellular structure and properties. Within each chosen technique, processing parameters (e.g. extrusion temperature and pressure, among others) will impact foam structure and properties (Cha *et al.*, 2001) (Zhang and Sun, 2007). Table 2.7 compares the structure features, density and mechanical properties of starch foams manufactured by different processing techniques. Compressive strength, the compressive modulus of elasticity and energy absorption during elastic deformation tend to be highly associated with foam density (Zhou, Song and Parker, 2006). Higher density foams usually have thicker cell walls or higher solid fraction and, therefore, they may withstand deformation better than lighter foams, which usually have thinner cell walls or lower solid fraction (Zhou, 2004).

Table 2.7 COMPARISON OF CELLULAR STRUCTURE, CELL SIZE, DENSITY, MECHANICAL PROPERTIES AND APPLICATIONS OF STARCH FOAMS MANUFACTURED BY DIFFERENT PROCESSING TECHNIQUES (Soykeabkaew, Thanomsilp and Suwantong, 2015)

PROCESSING	CELLULAR STRUCTURE	CELL SIZE	DENSITY (kg/m^3)	MECHANICAL PROPERTIES	APPLICATIONS
Extrusion	Relatively uniform with skin (open or closed cells)	Large (>100μm)	Low-medium (<100kg/m^3)	Low-medium	Loose-fill packaging, cushioning, insulating, biomedical
Baking/ Compression	Core-shell structure (closed cell at shell and opened cell at the core)	Large core (mm); dense shell (>100μm)	Medium (100-300kg/m^3)	Low-High	Foam panels, disposable packaging
Microwave	No uniform (open cell)	Large and wide distribution (>100 μm) (usually thick cell walls)	Medium-High (100-600kg/m^3)	Medium-High	Loose-fill packaging, cushion packaging, scaffolds
Freeze drying/solvent exchange	Uniform (opened cell)	Small (<100μm)	Medium-High (100-800kg/m^3)	Low	Scaffolds, drug delivery systems
Supercritical fluid extrusion	Radial gradient, large sizes at core	Small (<100μm)	Medium-High (100-900kg/m^3)	-	Biomedical applications, insulating, packaging

Yildirim *et al.* (2014) produced cellulose nanofibrils-starch foams by a freeze-drying process. The thermal conductivity of this material ranged from 0.041 to 0.054 $W/m{\cdot}K$ and its density ranged from 12 to 82 kg/cm^3 (i.e. porosities between 99.1 and 93.5%).

Extruded wheat foams developed for thermal insulation applications showed that the wheat foams (of density ~25 kg/m^3) exhibited thermal conductivity (~0.035 $W/m{\cdot}K$) comparable to EPS foams (~20 kg/m^3) and lower than PE (~30 kg/m^3) foams although not as low as some PU insulation panels (Wang, et al., 2010).

2.4.6 FOAMING TECHNOLOGIES

Starch gels/melt are non-Newtonian, and their viscosity is shear rate dependent and mainly influenced by temperature, starch concentration, amylose content, and degree of destructuration (Lagarrigue and Alvarez, 2001). Viscosity is one of the most important parameters in foaming of starch.

This section briefly discusses some of the most common starch foaming technologies, including baking, puff foaming, extrusion foaming and microwave foaming.

2.4.6.1 Baking

A water-starch mix is introduced in a closed mould at 175 - 235°C, where water acts as a gelatinisation agent, plasticiser and blowing agent (Song, 2014). Baking time, usually 60 seconds, varies with the size and thickness of the material (Song, 2014). This depicts a low production rate and limited thickness, which drives the use of multi-cavity moulds (Song, 2014).

Baked foams usually display a thin, dense outer layer as a result of a quick loss of water from the surface in contact with the hot mould, while the inner part is lighter and presents larger open cells (Song, 2014). Food trays are widely produced with this technology.

2.4.6.2 Puff foaming

It consists on extruded thermoplastic starch pellets heated (around 200°C) and pressurised in an mould which are subsequently expanded by water vapor (from the residual moisture) on release of the mould pressure (Song, 2014). Once the pressure is released, the starch feedstock expands in the mould and releases steam, obtaining closed cells typically ~ 1 mm in diameter.

Puffing technique uses much lower water content in the starch compared with baking, which implies a quicker processing time (Song, 2014). However, this technology is limited to moulding simple objects with rough finish due to poor flow of the expanding material and lack of control of the expansion process (Song, 2014).

2.4.6.3 Extrusion foaming

Extrusion foaming is a continuous process that generates a thermoplastic starch melt and creates the required foam structure as the melt leaves the extruder die. During the process, native starch is converted into thermoplastic starch with the assistance of plasticisers and other processing additives (Song, 2014).

As the melt passes through the extruder's die nozzle, the abrupt pressure change provokes the water vaporisation, increasing the viscosity of the extrudate also by rapid cooling (Song, 2014). Consequently, bubbles created and expanded in the extruded melt are stabilised by a rapid increase of viscosity (Song, 2014).

Starch loose-fill foams for packaging applications are commonly manufactured by extrusion foaming. When starch loose-fills are moistened and contact with each other under pressure, they form natural adhesion (Song, 2014). Several processes

to produce bulk starch foams have been successfully developed by using this property to produce starch block foams for cushioning and thermal insulation (Song, 2014), such as Regular Packaging and Stacking Process (RPS) and compression Bonded Loose fill (CBL) (Bonin, 2010) (Wang *et al.*, 2010).

Relatively thin sheet foams, around 10-20 mm thick, can also be produced by extrusion (Song, 2014), as Novamont (UK) foam based on Mater-Bi® (Novamont, 2018).

2.4.6.4 Microwave foaming

Prior to microwave foaming, the starch blend is gelatinised and extruded into thermoplastic starch pellets (Zhou, 2004) (Peng *et al.*, 2013). The equilibrium moisture left in the pellets acts as a blowing agent during microwave heating, foaming the starch pellets (Peng *et al.*, 2013).

Starch pellets' preparation is essential to achieve proper heat generation and activation of the blowing agent (Song, 2014). This technique has been demonstrated to produce foam blocks by expansion and fusion of the foamed pellets in an appropriate mould (Zhou, 2004), known as Microwave Assistant Moulding (MAM).

2.4.6.5 Other technologies

Other technologies producing starch foams include freeze-drying/solvent exchange and supercritical fluid extrusion (Soykeabkaew, Thanomsilp and Suwantong, 2015).

2.5 HYDROGEL FOAMS

Hydrogels are hydrophilic three-dimensional networks of polymer chains. There is a growing interest in the scientific community about hydrogels (Yahia, 2015). They can be found naturally in bacterial biofilms and some plant tissues (Ullah *et al.*, 2015) but they can also be synthetic. Examples like agar and gelatine have been widely known for centuries.

This section focuses on hydrogels foams. First, the characteristics of gels and hydrogels are discussed. Then, gelatine, a major gelling agent, is studied in detail by examining its main characteristics (e.g. production, origin, structure preparation and properties). Finally, gelatine-hydrogel foams preparation and features are discussed.

2.5.1 GELS

A gel is an intermediate material between a solid (with elastic behaviour) and a liquid (viscous behaviour) (Maity, 2007) (Banerjee and Bhattacharya, 2012). A gelator (the disperse phase in a solvent) creates an entangled three-dimensional network which traps the solvent (dispersion medium) within it to form a relatively more rigid structure (Maity, 2007)(Nishinari, 2009)(Banerjee and Bhattacharya, 2012).

Gels exhibit primary, secondary and tertiary structure. In the primary structure (angstrom to nanometer scale) the molecules are aggregated in one dimension. The secondary structure (nano to micrometer scale) corresponds to a molecular structure (e.g. micelles, vesicles, fibres, sheets, among others). The tertiary structure (micro to millimetre scale) implies the interaction of the molecular aggregates and it is responsible for the formation of the gel or, alternatively, the precipitation of the aggregates. Long, thin, flexible fibre networks can trap the solvent molecules, which also leads to gelation. On the contrary, shorter fibres may lead to precipitation rather than solvent trap (Maity, 2007).

Gels can be categorised according to the source, the gelling or crosslinking type and the solvent used (Maity, 2007). Based on their origin, they can be natural or synthetic gels. In turn, synthetic gels can generally be classified according to their structure into macromolecular or supramolecular gels (Maity, 2007). Marr & Marr (2015) suggested a third category for synthetic gels, colloidal gels, which are created by the growth or dispersion of colloidal particles in a liquid.

Supramolecular gels are usually prepared by heating the gelator and the solvent and cooling the saturated solution. Low molecular mass gelators (less than 3,000 *g/mol*) are generally included in this category (Marr and Marr, 2015). The gelator molecules interact with each other by non-covalent interactions to create a three-dimensional network which traps the solvent via physical interactions, surface tension or both (Marr and Marr, 2015). Three outcomes are possible: a highly ordered aggregation producing crystals, a random aggregation producing an amorphous precipitate and an intermediate result in between (Maity, 2007).

Assemble of polymer chains may also trap the solvent creating macromolecular or polymer gels (Marr and Marr, 2015). Macromolecular gels can be produced by chemical crosslinking or physical interactions. Crosslinked gels form strong chemical bonds which make them thermally irreversible while physical gels form weak or non-covalent bonds which make thermally reversible (Maity, 2007) (Marr and Marr,

2015). There are situations where chemical and physical interactions may co-occur (e.g. sol-gel processing) (Ullah *et al.*, 2015) (Marr and Marr, 2015).

Depending on the solvent used, gels can be categorised into hydrogels, which solvent is water, or organogels, made in organic solvents (Bhakta and Ruckenstein, 1997) (Maity, 2007). These, depending on the solvent removal/drying process, can result in aerogels, cryogels and xerogels (Maity, 2007).

Aerogels are highly (open) porous, solid materials (including silica, transition metal oxides, organic polymers, biopolymers or carbon nanotubes, among others) They are usually made by either supercritical (cryogels) or conventional evaporative drying techniques (xerogels). Xerogels, also referred to as "aerogels" by some researchers (Zanto, Al-Muhtaseb and Ritter, 2002), are produced when the liquid is removed by conventional drying, what usually implies substantial shrinkage (Maity, 2007) due to internal structure disturbance led by evaporation and capillary forces (Marr and Marr, 2015). Xerogels are less porous (maximum 95% of porosity), denser and higher thermal conductive materials than cryogels. In cryogels, solid structure is typically maintained when the solvent is replaced/removed by supercritical drying (Maity, 2007) and they may exhibit exceptional low densities and thermal conductivity (Bhakta and Ruckenstein, 1997). Cryogels properties are influenced by processing parameters such as freezing time, freezing rate and cooling rate, among others (Hixon, Lu and Sell, 2017).

2.5.2 HYDROGELS

Hydrogels are natural or synthetic three-dimensional polymer networks (disperse phase) which trap a considerable amount of water (dispersion medium) yielding a relatively rigid and flexible structure.

When the dry hydrogel is put into contact with water, the water molecules first hydrate the most hydrophilic groups, the so-called primary bound water. As the hydrophilic groups hydrate, the polymer network swells and exposes hydrophobic groups which now interact with the water molecules, the so-called secondary bound water. Primary and secondary bound water denominate the total amount of bound water. Once both the hydrophilic and hydrophobic molecules become saturated with bound water, the network absorbs additional water, the so-called free water, reaching an equilibrium swelling level and filling the space between the polymer chains (Yahia, 2015).

Factors such as crosslinker (type, and concentration), if incorporated, molecular physical entanglements and hydrogel net charge, among others, may influence

hydrogels properties (e.g. porosity, mechanical properties, hydrogel structure response to pH/temperature, biofunctionality, biocompatibility, biodegradability and water-insolubility) (Yahia, 2015).

2.5.3 TYPES OF HYDROGELS

Hydrogels can be classified in different ways (e.g. their physical properties, preparation methods, origins, charge, sources, environmental response and crosslinking nature, among others) (Laftah, Hashim and Ibrahim, 2011) (Ullah *et al.*, 2015).

Hydrogels can be cationic, anionic or neutral depending on the charges on their functional groups. Depending on their chain structure, they can be amorphous, semi-crystalline and hydrocolloid aggregates (Ullah *et al.*, 2015).

Bonding in hydrogels can be physical or chemical. Chemical crosslinking covalently bonds the polymer chains via a crosslinking agent, preventing the dissolution of the hydrogel structure into water, whereas physical crosslinking are from hydrogen bonding, hydrophobic interactions and ionic complexation (Ullah *et al.*, 2015). Physical crosslinking has several advantages compared to chemical crosslinking, such as ease of fabrication, biodegradation and non-toxicity (Ullah *et al.*, 2015), but may exhibit clusters of molecular entanglements or hydrophobically/ionically associated sections, which implies a non-homogenous structure (Yahia, 2015).

Depending on the origin, hydrogels can be natural or synthetic. Synthetic hydrogels are usually produced by solution or suspension polymerisation (Ullah *et al.*, 2015). Natural hydrogels are usually created by lithography, emulsion, extrusion, bioprinting, microfluidics or freeze-drying (Vieira *et al.*, 2007). Natural hydrogels have several disadvantages over synthetic hydrogels, such as batch variability due to their natural origin, which may affect reproducibility and mechanical properties negatively (Yahia, 2015). Artificial polymers exhibit more consistent properties but may impose challenges like low solubility, toxicity (due to the use of some crosslinkers), non-biodegradability and relatively poorer mechanical and thermal properties (Vieira *et al.*, 2007) (Ullah *et al.*, 2015).

Natural polymers used for hydrogels production include carbohydrates (alginate, chitosan, starch, agarose, gellan gum) and proteins (collagen, gelatine and silk fibre) (Vieira *et al.*, 2007) (Ullah *et al.*, 2015). Synthetic polymers include Polyvinylpyrrolidone (PVP), Polyhydroxyethylmethacrylate (PHEMA), Polyethylene

glycol (PEG) and derivatives, Poly (vinyl alcohol) (PVC), Polyacrylate (PA) hydrogels and PU hydrogels (Gibas and Janik, 2010) (Ullah *et al.*, 2015).

2.5.4 APPLICATIONS OF HYDROGELS

Hydrogels can be found not only in different forms in everyday products (e.g. shampoo, toothpaste, cosmetics, contact lenses, watering beads, diapers etc.) but also in industrial applications, such as in oil recovery, agriculture, pharmaceutical and medicine (Laftah, Hashim and Ibrahim, 2011) (Yahia, 2015) (Ullah *et al.*, 2015). Their dehydrated forms can also be found in applications such as biomedical and food packaging. The reason for the vast amount of hydrogel applications is their unique combination of properties: hydrophilicity, biocompatibility, biodegradability, and ease of processing, among others (Laftah, Hashim and Ibrahim, 2011).

Hydrogels have been widely studied and used for tissue engineering applications as they can maintain a considerable amount of water/biological fluids under physiological conditions and, especially natural hydrogels, possess a similar structure to living tissues (Vieira *et al.*, 2007) (Ullah *et al.*, 2015). They also exhibit other desirable properties, such as enzymatic degradation susceptibility or reversibility, making them ideal for tissue engineering, and drug delivery (Ullah *et al.*, 2015). Examples of biodegradable polymers used for biomedical applications include chitosan, chitosan-gelatine, chitosan-alginate, chitin, alginate, arabinogalactan, polyglycolide, hyaluronate and gelatine (Shyamkuwar *et al.*, 2010).

Hydrogels for food packaging have also been studied although not readily commercialised. Research on hydrogels for packaging applications includes films/sheets for gas and moisture barriers, antibacterial packaging, shelf life enhancement and oxidation protection, among others (Ullah *et al.*, 2015).

The following sections discuss gelatine and gelatine foams. The reasons to turn to the study of hydrogels made of gelatine, and no other materials, includes its commercial availability, relatively low cost and ease of production.

2.5.5 GELATINE

Gelatine is a hydrocolloid obtained from partial hydrolysis of animal tissues which contain collagen, the primary structural component in most connective tissues (skins, bones and tendons) (Shyamkuwar *et al.*, 2010) (GMIA, 2012). There are 27 varieties of collagen, the most common being type I, type II and type III (Schrieber

and Gareis, 2007). Type I collagen exists most commonly in connective tissues, such as skin, bone, and tendons (Schrieber and Gareis, 2007). Type II occurs primarily in cartilage tissue and type III depends on the animal age: young skin contains around 50%, but eventually it reduces to 5-10% (Schrieber and Gareis, 2007).

Gelatine produces thermally reversible hydrogels with good mechanical properties. Gelatine can form gels at various pH levels and be used in many applications where other gelling agents or stabilisers would fail.

2.5.5.1 Applications of Gelatine

A considerable amount of animal by-products, raw materials for gelatine production, are not appropriate for human consumption, resulting in a significant loss of material which may be overcome by promoting gelatine uses for non-food applications (Oliviero *et al.*, 2015).

Gelatine has extensive applications in different industries due to its biodegradability, nontoxicity and biocompatibility (Shyamkuwar *et al.*, 2010). Food grade gelatine is widely used in the food industry (e.g. in desserts, marshmallows, jellies, and canned meats, among others), pharmaceutical (e.g. capsules, tablets, bandages etc.), cosmetic (e.g. in shampoos, creams and lipsticks, etc.) and photographic industry in production of films.

The confectionery industry (making products from sugar and syrup) widely uses gelatine because it can produce foams, gels and solidifies easily. Some examples include gummy bears or marshmallows. Gummy products usually use about 7% of 175 Bloom (a measure of gel strength) gelatine and marshmallow producers generally use 2.5% of a 250 Bloom Type A gelatine (GMIA, 2012). Gelatine is not a vegetarian product and some religious groups may have issues with gelatine consumption. Kosher gelatine and gelatine from fish have been developed to mitigate this (Edwards, 2000).

The pharmaceutical industry has been using gelatine to manufacture hard and soft capsules since the 19th century (Zhang *et al.*, 2013). The typical formulation for a hard capsule is 30% of gelatine, 65% of water and 5% of dye with pigment and plasticiser added as necessary (GMIA, 2012).

Porous biopolymers are often used in biomedical applications for wound dressing, hemostatic agents, tissue engineering and as drug carriers (Shyamkuwar *et al.*, 2010) (Chen, 2011). These applications require a soft and elastic material that "vanish" by resorption after its functionality (Shyamkuwar *et al.*, 2010). Gelatine is

used for such biomedical applications as it, unlike collagen, does not express antigenicity, and it is resorbable in vivo (Shyamkuwar *et al.*, 2010) (Yan and Pochan, 2010).

Gelatine can also be used to produce biodegradable alternatives for fossil-based plastics (Oliviero *et al.*, 2015), which can be used for packaging applications as it can form clear and relatively impermeable films with varying flexibility depending on the level of plasticisation. Composite films, such as starch/gelatine or chitosan/gelatine, plasticised with glycerol and sorbitol have been studied for food packaging (Nur Hanani, Roos and Kerry, 2014).

Gelatine has also been used for ammunition testing, to mimic flesh. It helps to investigate the projectiles trajectory, penetration and fragmentation (Swain *et al.*, 2014).

2.5.5.2 Gelatine production

Gelatine is produced by thermal denaturation or physicochemical degradation of collagen from animal tissue (Fakhouri *et al.*, 2013).

First, the raw materials are washed and pretreated with acid or alkali soaking for partial hydrolysis of the peptide bonds and crosslinks in the collagen structure. This pre-treatments confer gelatine into type A gelatine, manufactured from acid-cured tissues and type B gelatine, obtained from alkali-cured tissues (Schrieber and Gareis, 2007). The process alters the amino acid composition and the molecular weight distribution of gelatine as required for different applications. Pig skins tend to react appropriately to acid treatment, and other skins (e.g. calf, beef or fish) respond better to lime soaking.

Once the soaking treatment is completed, the material is washed, its pH is adjusted to the desired value and it is rewashed. Afterwards, gelatine is extracted by either a continuous process or a series of warm water baths at progressively higher temperatures that yields gelatine of lower strength and viscosity for each successive extraction (Schrieber and Gareis, 2007). Therefore, the initial extraction generates higher quality products, with higher molecular weights, viscosity, gel strength and a lighter colour (GMIA, 2012).

Process variables, such as pH, time, temperature and number of extractions may vary from producers, depending on products requirements, type of equipment used and/or economic considerations (GMIA, 2012). The number of extractions ranges from 3-6. The first one tends to be at 56-60°C, and the successive steps

increase temperature by ~5-10°C each time until the final extraction, that takes place near the boiling point of water (GMIA, 2012). The different outputs of each extraction remain separated and are subsequently blended to meet the required specifications.

Then, the gelatine solutions are filtered, concentrated and sterilised. Later, the remainder solution is cooled to a gel and dried until the desired moisture content. Finally, the gelatine is ground and blend to meet the desired requirements.

2.5.5.3 Gelatine origins

The primary raw materials used for gelatine production are cattle bones, cattle hides, and pork skins (GMIA, 2012). However, there can be other sources, such as poultry and fish (GMIA, 2012) (Oliviero *et al.*, 2015). Its animal origin may be a disadvantage for consumers demanding vegetarian, kosher and halal products.

There are some differences in gelatine composition of placental land mammals. Pig skin gelatine has lower isoleucine content than ox skin gelatine. Whale and fish gelatines show a higher content of hydroxyamino acid, serine and threonine compared to land mammals (Zhao, Torley and Halley, 2008).

2.5.5.4 Gelatine structure

Collagen consists of three-coiled helical polypeptide chains connected by intermolecular crosslinks and organises in a triple helix (Schrieber and Gareis, 2007)(GMIA, 2012). As collagen is hydrolysed, the triple helix collagen structure is denatured to form three single-strand gelatine molecules (Yan and Pochan, 2010) (Frazier and Srubar, 2016).

Gelatine molecule possesses 18 different amino acids bonded by amide linkages (see Figure 2.19). However, it is not considered a complete protein because it lacks tryptophane, one of the nine essential amino acids. Gelatine composition varies depending on the raw materials, origins and processes used but the average amino acid content values are shown in Table 2.8.

Gelatine primary structure is formed by glycine-X-proline or glycine-X-hydroxyproline residues where X is a charged amino acid (Frazier and Srubar, 2016).

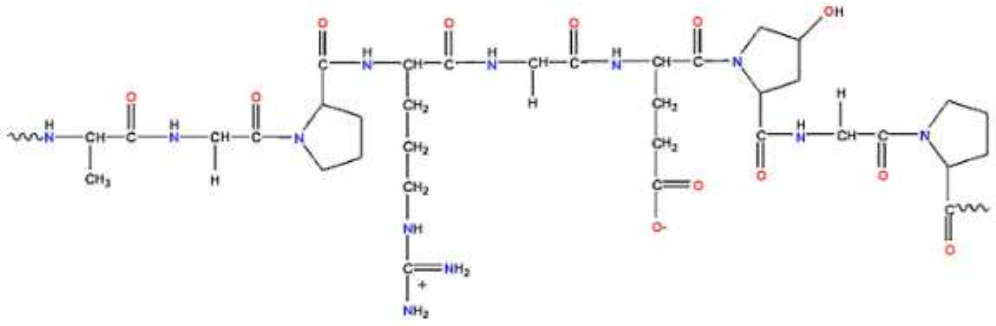

Figure 2.19. REPRESENTATIVE GELATINE STRUCTURE: ALA-GLY-PRO-ARG-GLY-GLU-4HYP-GLY-PRO (Nur Hanani, Roos and Kerry, 2014)

When dissolved in warm water, gelatine molecules exhibit a randomly coiled conformation but undergo a partial triple helix reformation on cooling (Yan and Pochan, 2010). Thus, gelatine-gel generation involves protein re-structuration from a disordered state to a more ordered structure (Sobral *et al.*, 2011).

Table 2.8. AMINO ACID COMPOSITION OF GELATINES, AVERAGE NUMBER OF AMINO ACIDS PER 1,000 AMINO ACIDS (Schrieber & Gareis, 2007)

Amino Acid	Gelatine Type A	Gelatine Type B
Alanine	112	117
Arginine	49	48
Asparagine	16	0
Aspartic acid	29	46
Cysteine	–	–
Glutamic acid	48	72
Glutamine	25	0
Glycine	330	335
Histidine	4	4.2
Hydroxyproline	91	93
Hydroxylysine	6.4	4.3
Isoleucine	10	11
Leucine	24	24.3
Lysine	27	28
Methionine	3.6	3.9
Phenylalanine	14	14
Proline	132	124
Serine	35	33
Threonine	18	18
Tryptophan	–	–
Tyrosine	2.6	1.2
Valine	26	22

Gelatine has several free or interconnected chains with a molecular mass from 1,000 *g/mol* to a hundred of thousands. Currently, it is widely accepted that gelatine structure consists of a linear chain with some ramifications (Zhao, Torley and Halley, 2008). Its linear chain shows chemical heterogeneity and dynamic properties, depending on the preparation method (Zhao, Torley and Halley, 2008).

2.5.5.5 Preparation of Gelatine solutions

A proper understanding of the rheological properties of the solution, the type of gelatine used, its interaction with other processing additives and the influence of the processing parameters is essential for an optimum processing of gelatine hydrogels (Schrieber and Gareis, 2007). The gelatine strength, the solution viscosity and the gelatine setting behaviour are the most important processing factors (Schrieber and Gareis, 2007). Gelatine solutions behaviour depend on temperature, pH, ash content, production process, thermal history, the composition of the liquid and gelatine concentration, among others

Gelatine is partially soluble in cold water, and it hydrates into swollen particles which, when heated, dissolves to form an aqueous solution (GMIA, 2012) over a wide pH range. It is noteworthy that greatly hydrolysed gelatine can dissolve better in cold water.

The dissolution process consists of different stages: gelatine powder dispersion, gelatine particles swelling, and gelatine dissolution (Schrieber and Gareis, 2007). The solution preparation may be a one-step or two-step process, where gelatine is initially stirred either in hot (directly) or cold water (as a first step), respectively (Schrieber and Gareis, 2007).

In the one-step process, gelatine is placed in a vessel or water bath at 50-70°C (Edwards, 2000) (Schrieber and Gareis, 2007). It is not advisable to heat the gelatine solution above 80°C, as gelatine may be over-hydrolysed and give rise to lower gel strength (Edwards, 2000). As the liquid surrounds the gelatine particles, they swell, gaining 5-10 times its dry weight (Edwards, 2000) (Schrieber and Gareis, 2007). At the same time, as the solution temperature surpasses 50°C, viscosity decreases, and water diffuses into the particles which then breaks down forming a random coil structure (Schrieber and Gareis, 2007).

Finally, if the gelatine solution is cooled, the sol-gel state transformation takes place when the polypeptide chains partially re-arrange in the collagen-like triple-helix.

2.5.5.6 Gelatine gelation

Gelatine gel formation is a controllable process which depends on conditions such as temperature, pH, thermal history, ash content interaction with other components, molecular weight and gelatine concentration, among others (Choi, Lim and Yoo, 2004) (Schrieber and Gareis, 2007) (Banerjee and Bhattacharya, 2012) (Tau and Gunasekaran, 2016). When heated, gelatine forms colloidal

solutions or sols consisting of polymer chains of different lengths. On cooling, gelatine sols transform into gels and melt when heated again. This, process reversibility, is one of the most significant gelatine properties.

Gelation occurs when locally ordered regions are formed because of the renaturation of the disordered gelatine molecules to the collagen-like helices (Choi, Lim and Yoo, 2004) (GMIA, 2012) which trap the water within them to create a more rigid structure (Banerjee and Bhattacharya, 2012). These locally ordered regions are known as junction zones, proline and hydroxyproline-rich areas in the polypeptide chains, where the sol-gel transition is triggered (Danks, Hall and Schnepp, 2016). As the continuous 3-dimensional network forms throughout the system, the number of junction zones and hydrogen and electrostatic bonds increases (Choi, Lim and Yoo, 2004) (GMIA, 2012).

The bonds formation is a slow process. The gel strength increases with time, as more bonds are generated (GMIA, 2012). Figure 2.20 shows the gel strength (in percentage) increase of a typical gelatine solution at 10°C as a function of time.

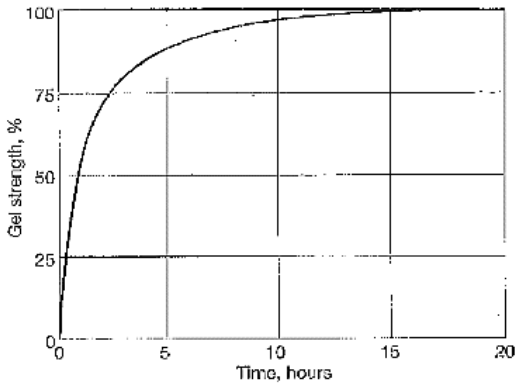

Figure 2.20. GELATINE GELLING BEHAVIOUR INFLUENCING GEL STRENGTH (%)-TIME (HOURS)
(GMIA, 2012)

2.5.5.7 Physical and chemical properties of gelatine hydrogels

One of the major features of gelatine is its role as a hydrocolloid, as it forms colloidal solutions with water. Among hydrocolloids, gelatine is considered as the most versatile one with functions including emulsion stabilisation, bind by adhesion, suspension stabilisation, beverage clarifying and foam and film creation (Schrieber and Gareis, 2007).

Gelatine is a vitreous, slightly yellow and brittle solid. It contains 85-92 *wt%* of protein, approximately 10 *wt%* moisture (it may vary from 5-14 *wt%*) and 2 *wt%* ash, which mainly comes from the curing and pH adjustment stages (Schrieber and Gareis, 2007).

Gelatine is hygroscopic; therefore, its moisture content depends on the relative humidity on the environment (Edwards, 2000). Gelatine gels are mediums that facilitate bacteria and mould growth due to its high water content (Edwards, 2000). Therefore, considerations to avoid contaminations need to be taken during manufacturing. However, dry gelatine has a considerably longer shelf life at low water content.

The gel physical properties depend on the degree of microcrystalline junctions formed, the speed of cooling and the degree of acidity (Zhao, Torley and Halley, 2008) (Sobral *et al.*, 2011). Slow cooling forms better-oriented gelatines and acidity increases setting time and lowers the gel liquefying temperature (Zhao, 2008).

The physical-chemical behaviour of gelatine gels is mainly influenced by the amino acid sequence, the spatial structure, the molecular mass distribution, the pH, the ionic strength and the reaction with other components (Schrieber and Gareis, 2007).

Gelatine forms strong ionic bonds with other substances. It generally constitutes coacervate with negatively charged hydrocolloids, such as Arabic gum, pectin, alginates, carrageenans and agar.

The main disadvantage of gelatine is its inherent poor mechanical properties (Shyamkuwar *et al.*, 2010).

- **Gel strength**

Gel strength or gelling power is measured by the Bloom test, a standardised analysis from the Gelatine Manufacturers Institute of America (GMIA). The Bloom test measures the weight in grammes required for a half-inch plunger to depress the gelatine surface by 4 *mm* (Schrieber and Gareis, 2007). The gelatine specimen for the test contains 6.67 *wt%* of gelatine, and it is conditioned for 17 hours at 10°C before measurement (Schrieber and Gareis, 2007). The mass obtained is the Bloom and usually ranges from 50 to 300 *grammes*. The ranges between 50-100, 100-200 and 200-300 are designated as low-Bloom, medium-Bloom and high-Bloom, respectively (Schrieber and Gareis, 2007). High Bloom gelatine typically exhibit higher melting and gelling points and shorter gelling times than lower Blooms (Schrieber and Gareis, 2007).

Gel strength mainly depends on pH, temperature, processing additives, concentration and casting temperature. Rapid cooling can lower the Bloom up to

10% whereas slow gelation can increase gel strength by the similar level (Schrieber and Gareis, 2007). The higher the gelatine concentration, the stronger the gel.

- **Viscosity**

The viscosity of the solution is an essential parameter for gelatine products. Depending on the applications, high viscosity gelatines (e.g. food stabilisers, pharmaceuticals, photographic emulsions) or lower viscosity gelatines (e.g. confectionary industry, where flowability is essential for production) may be required (Schrieber and Gareis, 2007).

Gelatine solutions tend to exhibit Newtonian behaviour. However, non-Newtonian behaviour may be observed at higher gelatine concentrations or use of high-Blooms. In any case, gelatine colloidal solutions are relatively shear stable and do not usually present problems related to piping or pumping (Schrieber and Gareis, 2007).

Solution viscosity generally depends on solution temperature, pH, gelatine concentration, temperature, time and molecular weight, among others. For solutions with the same Bloom, the viscosity of type B gelatines tend to be 30-50% higher than that of type A gelatines (Schrieber and Gareis, 2007). Higher polymer concentrations typically result in higher viscosities due to the formation of intertangled structures in the system. Viscosity decreases with temperature, being minimum at the isoionic point.

Gel strength and viscosity do not have a linear relationship due to the different molecular weight fractions. Gel strength mainly depends on the molecular weight fraction around 100,000 *g/mol*, while viscosity primarily depends on the range between 200,000-400,000 *g/mol*. Thus, same Bloom gelatines may exhibit different viscosities.

- **Molecular weight and molecular weight distribution**

Properties such as solubility, melting point, setting time and viscosity are dependent on the gelatine molecular weight. Generally, the lower the mean molecular weight of the gelatine, the lower the gel strength and viscosity of the solution (GMIA, 2012).

The molecular weight distribution depends on the type and intensity of the hydrolysis process. As an illustration, type B gelatine tends to have most of the molecular weight fraction in the region of 100,000 *g/mol* whereas type A gelatine usually exhibit a wider distribution (Schrieber and Gareis, 2007).

- **pH and Isoelectric Point (IEP)**

pH modification changes the net charge of the gelatine molecule and, consequently, the attractive or repulsive forces of the molecules and the molecules-solvent interactions (Schrieber and Gareis, 2007).

Gelatine is amphoteric, in other words, it has both acidic (carboxyl) and basic (amino and guanidine) groups (Osorio *et al.*, 2007). The IEP is the pH at which gelatine molecules do not migrate in an electrical field as they are in a neutral-charged state. In other words, the IEP is the pH at which the negative and positive charges are balanced, where the protein can precipitate more easily (Edwards, 2000) and the gelatine molecule exhibits a random coil structure (Schrieber and Gareis, 2007). IEP affects foaming capacity, the surface activity of the solutions, and gelatine interaction with other additives (Schrieber and Gareis, 2007). Gel strength reaches maximum and viscosity reaches minimum in an isoionic (at IEP) solution.

IEP and charge of gelatine molecules depend mostly on the carboxyl amino and guanidine groups in the side chains. Type A amino acid composition is virtually the same as collagen where glutamic and aspartic acids occur around 35% in their amidated form, glutamine and asparagine, whereas type B gelatine has most asparagine and glutamine converted to aspartic and glutamic acids, respectively. This composition difference explains the IEP difference for type A and type B gelatines. Type A and type B gelatine IEP ranges between pH 6-9.5 and 4.7-5.6, respectively (Schrieber and Gareis, 2007). Below the IEP the gelatine molecule has a positive charge, and above the IEP the gelatine molecule has a negative charge. Therefore, below pH 4.5 both Type A and B gelatines are positively charged, and over pH 9 they are negatively charged. Gelatine remains soluble throughout a wide pH range. However, gelation of both types A and B gelatine is inhibited outside the pH range 4-10 due to repulsive electrostatic forces inhibiting junction zones formation (Pang *et al.*, 2014).

- **Surface properties of gelatine solutions**

The surface properties of gelatine solutions depend on the molecule's charged side chains. Both hydrophobic and hydrophilic amino acids may migrate towards the surface, which reduces the colloidal solution surface tension. This is used for the stabilisation of surfaces in emulsions and foams. Table 2.9 lists the hydrophilic and hydrophobic amino acids found in gelatine molecules with information on their polarities.

Table 2.9 HYDROPHILIC AND HYDROPHOBIC AMINO ACIDS IN GELATINE (Schrieber and Gareis, 2007)

Amino Acid	Hydrophilic	Hydrophobic	Information
Alanine		+	Aliphatic, non-polar side chain
Arginine	+		Basic
Asparagine	+		Weak polar side chain
Aspartic acid	+		Acid
Glutamine	+		Weak polar side chain
Glutamic acid	+		Acid
Glycine		+	Aliphatic, non-polar side chain
Histidine	+		Basic
Hydroxyproline		+	Weak polar side chain
Hydroxylysine	+		Basic
Isoleucine		+	Non-polar side chain
Leucine		+	Non-polar side chain
Lysine	+		Basic
Methionine		+	Aliphatic, weak polar side chain
Phenylalanine		+	Aromatic, non-polar side chain
Proline		+	Non-polar side chain
Serine	+		Weak polar side chain
Threonine	+		Weak polar side chain
Tyrosine	+		Aromatic, weak polar side chain
Valine		+	Non-polar side chain

2.5.5.8 Rheology of gelatine solutions

Above the melting temperature of gel, gelatine solutions behave as Newtonian fluids (i.e. viscosity is independent of shear rate) (Schrieber and Gareis, 2007). As the temperature decreases, a sol-gel transition is reached, and a viscoelastic gel is formed which exhibits shear-thining behaviour. On cooling the sol-gel transition occurs where the *G''* (loss modulus, for viscous behaviour) and *G'* (storage modulus, for elastic behaviour) reached equilibrium (or "cross-over") (Schrieber and Gareis, 2007) and is considered the point (temperature) at which the 3-dimensional network first appears (Pang *et al.*, 2014). Once the gel forms, *G'* becomes higher than the loss modulus *G''*.

On the contrary, the gel-sol transition temperature is identifiable at the equilibrium of *G'* and *G''* on heating from a gel state (Schrieber and Gareis, 2007). The heating and cooling curves are non-congruent, and the melting process tends to be at a higher energy level (Schrieber & Gareis, 2007). Figure 2.21 represents the crossover points on cooling and heating, which represents the gelation and melting points, respectively.

Gelatine-water phase transitions (sol↔gel) are strongly influenced by the gelatine type, gelatine content, gelatine origin, temperature, and interactions with other processing additives, among others (Schrieber & Gareis, 2007). Both setting and

melting points depend on gelatine Bloom and concentration. Higher setting and melting points usually result from higher Blooms and gelatine concentrations.

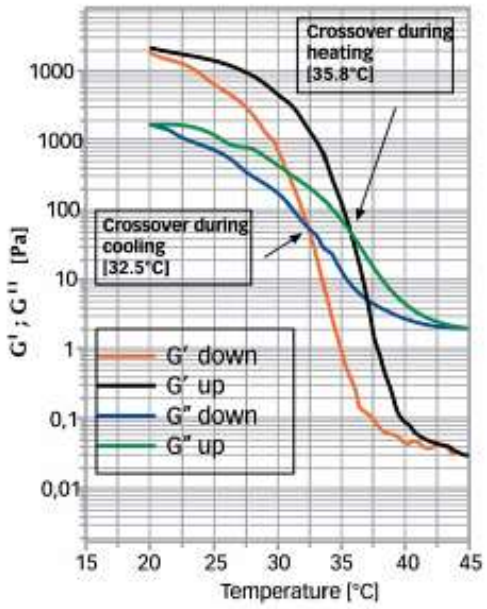

Figure 2.21. VARIATION OF G' AND G'' DURING COOLING AND HEATING OF A GELATINE SOLUTION SHOWING CROSS-OVERS OF THEM FOR IDENTIFICATION OF MELTING AND GELLING POINTS (Schrieber and Gareis, 2007)

At lower gelatine content, sol-gel transition temperature decreases but the gelling requires less setting time (Schrieber and Gareis, 2007). This can be attributed to the higher mobility of the gelatine molecules in less concentrated solutions. Consequently, the molecules can move more rapidly, achieving a faster spatial arrangement.

The thermal and mechanical history of the sample may modify the gelling setting and melting behaviour. For example, on rapid cooling, there will be greater differences between the setting and melting temperatures; gel strength will tend to be lower by 10-15% than slow cooling because the system does not have time to form a stable network by hydrogen bonds (Schrieber and Gareis, 2007). Significant rheological differences (e.g. gelling time and temperature) may also occur when preparing solutions at temperatures below 50°C or higher temperatures, over 80°C (Schrieber and Gareis, 2007), as gelatine may be over-hydrolysed and give rise to lower gel strength.

2.5.6 GELATINE FOAMS

A filled gel contains a second phase (e.g. particles, liquid droplets and gas bubbles) dispersed in the gel matrix (Banerjee and Bhattacharya, 2012). Thus, gelatine foams are filled gels where the dispersed phase are bubbles.

Proteins have been showed to be beneficial to the creation and stabilisation of foam structures in solutions (Foegeding, Luck and Davis, 2006). Therefore, protein foams can be found in many protein-containing foods such as meringue and nougat, among others, where foam stability must be kept after processing (Foegeding, Luck and Davis, 2006).

Proteins can be derived from plants (e.g. soy protein and pea protein isolates) or animals (e.g. gelatine, milk protein isolate, ß-lactoglobulin, bovine serum albumin etc.) (Niu *et al.*, 2014). These proteins can be compounded with polysaccharides such as starch, xanthan gum, carrageenan or chitosan, among others (Niu *et al.*, 2014).

This section discusses foams made with gelatine. First, the preparation of gelatine foams is discussed. Then, some of the additives used in gelatine foams foaming, followed by the discussion of gelatine foams properties, stability and drying are commented. Finally, the applications of gelatine foams are discussed.

2.5.6.1 Gelatine foams preparation

The main methods for production of porous materials based on the sol-gel route are (Lavorgna, Verdolotti and Mascia, 2016):

A. Aerogel production from a hydrogel;

B. Polymerisation-induced phase separation;

C. Solution foaming by either mechanical beating or gas solubilization. The liquid foam obtained can be dried by freeze-drying or conventional drying methods.

As discussed in Section 2.5.1, aerogels can be obtained by solvent removal using either conventional evaporative drying or supercritical drying (e.g. freeze-drying). Kang *et al.* (1999) and Wu *et al.* (2010) produced gelatine foams from gelatine hydrogels crosslinked with glutaraldehyde followed by subsequent sublimation of water using freeze-drying.

Polymerisation-induced phase separation has been widely used to produce cellular solids. The phase separation takes place in the hydrogel solution on polymerisation, followed by removal of the fluid phase (Lavorgna, Verdolotti and Mascia, 2016). This method may be combined with other techniques, depending on product needs. For example, (Liu and Ma, 2009) combined a thermally induced

phase separation (TIPS) technique with a paraffin leaching process to create nanofibrous gelatine scaffolds.

Mechanical foaming involves gas introduction and shearing of the solution which produces fine gas bubbles dispersed in the colloidal sol (Shyamkuwar *et al.*, 2010). Foaming by mechanical beating may require the use of surfactants as foam stabilisers and foaming process assistants. Catalysts may also be used as gelation accelerators (Lavorgna, Verdolotti and Mascia, 2016) to minimise shrinkage and maintain the cellular structure. Sharma *et al.* (2013) produced chitosan-gelatine-alginate bead-shape scaffolds by agitating the polymer solution and use of sodium bicarbonate (NaHCO) as a blowing agent. They used calcium chloride-glutaraldehyde to stabilise the foam by crosslinking without the use of any surfactant. Shyamkuwar *et al.* (Shyamkuwar *et al.*, 2010) made gelatine foams for biomedical applications by blending in air in a static mixer, followed by freeze-drying.

A gelatine foam can also be obtained by gas dissolution-precipitation using pressure changes. The solution is first heated at the desired temperature and saturated with gas at high pressure. Then, it is cooled to the required foaming temperature, and the pressure is dropped to release the gas and create the foam (Lavorgna, Verdolotti and Mascia, 2016). Oliveiro *et al.* (2015) prepared gelatine-PBS foams with this method, using CO_2 as blowing agent and drying the foam in ambient conditions.

Other drying methods, such as microwave vacuum drying have also been reported (Sundaram, Durance and Wang, 2008).

2.5.6.2 Additives in gelatine foaming

This section describes some of the main additives used to produce gelatine foams: plasticisers, polymers, surfactants and crosslinkers.

- **Plasticisers**

Plasticisers are to improve the flexibility of the otherwise brittle gelatine films or foams (Aydinli and Tutas, 2000) (Fakhouri *et al.*, 2013) by increasing intermolecular spacing and reducing intermolecular hydrogen bonding (Cao, Yang and Fu, 2009). Gelatine is commonly plasticised by hydroxyl compounds and polyols, such as glycerol (Cheng, Yang and Lin, 2011) (Oliviero *et al.*, 2015), sorbitol (Martucci, Espinosa and Ruseckaite, 2015), or ethylene glycol, among others (Cao, Yang and Fu, 2009).

- **Polymers**

Gelatine hydrogels can be combined with other polymers, such as PBS (Oliviero *et al.*, 2015), starch (Khomutov *et al.*, 1996), chitosan (Sharma, Dinda and Mishra, 2013), alginate (Balakrishnan *et al.*, 2014), among others, for modification of properties. Extensive research has been carried out regarding gelatine-starch aqueous systems, presumably due to the cost-effectiveness of the combination and the potential for high-volume industrial applications (Khomutov *et al.*, 1995).

- **Surfactants**

Surfactants are amphiphilic molecules which consist of a hydrophilic 'head' (or anchor group) and a hydrophobic 'tail'. Based on the charge groups in their head, they can be classified into cationic (positive charge), nonionic (no ionic charge), anionic (negative charge) and amphoteric surfactants (both positive and negative charges present in their head, being neutral in net charge) (Amaral *et al.*, 2008). Gelatine-ionic surfactant interactions are attributed to be both electrostatic and hydrophobic (Misra, Meher and Maharana, 2016). Anionic surfactants have a stronger interaction with gelatine than its cationic counterparts (Derkach, 2015). This is attributable to the gelatine molecule structure which is more likely to exhibit positive groups on the ends of the polymer chain and negatively charged ones at random along it (Derkach, 2015). Non-ionic surfactants show weak interactions with gelatine (Derkach, 2015) and hence are less attractive due to their limited facilitation to foaming (Misra, Meher and Maharana, 2016). The effectiveness of amphoteric surfactants depends on the pH of the solution. At their IEP, they behave like non-ionic surfactants; for acidic solutions like a cationic surfactant and for alkaline solutions like an anionic surfactant (Gelardi *et al.*, 2015). Common surfactants used for gelatine solutions include Sodium Dodecyl Sulfate (SDS) (Derkach, 2015) and CTAB (Mitra, Bhattacharya and Moulik, 2009).

Surfactants decrease the surface tension of aqueous solutions as they migrate to the liquid/gas (or liquid/oil) interfaces. The surfactant molecules tend to adsorb at the interface instead of remaining in the solution to minimise the free energy of the system. The hydrophilic head is oriented towards the solution molecules and the hydrophobic tail toward the gas (or oil) phases. This phenomenon reduces the surface tension of the liquid as the hydrophobic tails repel the water molecules, which weakens the surface hydrogen bonds and lowers the work required to increase the interfacial area. The adsorption properties can be studied by measuring the surface tension of the solution.

As the surfactant concentrations increases, the surface tension decreases until reaching the critical micelle concentration (CMC), where surfactant aggregates into micelles (Banerjee and Bhattacharya, 2012). The surface tension remains relatively constant, as more surfactant added will form micelles rather than migrating to the liquid/gas interfaces. CMC, a parameter specific for each surfactant, designates saturation of the surfactant's adsorption. Polymer chains may overlap with the micelles and form crosslinks (Bhakta and Ruckenstein, 1997).

Figure 2.22 shows the typical relationship between surfactant concentration and surface tension. As surfactant concentration increases, surface tension decreases until reaching CMC, where surface tension becomes relatively constant.

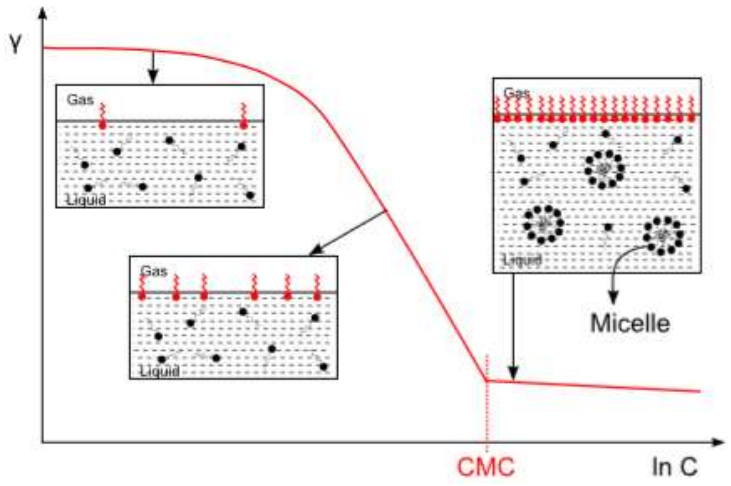

Figure 2.22. EQUILIBRIUM SURFACE TENSION (Y) AS A FUNCTION OF SURFACTANT CONCENTRATION (C) WHERE ABSORBED SURFACTANT MOLECULES AT INTERFACE ARE IN RED WHILE THOSE IN THE SOLUTION IN BLACK (Kawale, 2012)

Below CMC, the solution is said to be in a 'dynamic equilibrium' where the surfactant molecules are continuously moving within the surface. Thus, the surface tension measured at this stage is an average of the total activity of the molecules.

- **Crosslinkers**

Gelatine can be cross-linked to enhance both thermal and mechanical stability of the material (Shyamkuwar *et al.*, 2010). Physical crosslinking of gelatine has been carried out by thermal heating and UV crosslinking (Shyamkuwar *et al.*, 2010). It can also undergo chemical crosslinking with reagents such as glutaraldehyde (Kang, Tabata and Ikada, 1999) (Wu *et al.*, 2017), formaldehyde (Schrieber and Gareis, 2007), water-soluble carbodiimide and natural crosslinkers, such as Genipin, derived from gardenia fruit extract (Shyamkuwar *et al.*, 2010).

2.5.6.3 Properties of gelatine foams

Table 2.10 shows some examples of gelatine foams from gelatine hydrogels and some of their properties. Literature about physical and mechanical properties of gelatine foams is scarce as the primary focus is on biomedical applications. This implies the foam samples are usually small, in centimeters (e.g. for wound dressing sponges, scaffolds, etc.). A few works on gelatine-composite foams can also be found (Oliviero *et al.*, 2015), but gelatine foams for general industrial applications such as in construction, packaging and lightweight structures are not yet widely available in the literature. Patents may include some properties with indications (e.g. in thermal and packaging applications), but understandably, these data are usually given in extensive ranges, and it is difficult to check the credibility (Hartranft *et al.*, 1994) (Morrison, 1995)(Fidler and Simonton, 2000).

Reported gelatine foams exhibit varying densities ranging from ~9 to 102 kg/m^3 which falls into "low to medium density" polymer foams.

The pores size usually ranges from 100 to 550 μm and the porosity tends to be around 96-98 *vol%*. These parameters may vary depending on the formulations and processing conditions.

As mentioned in section 2.2.5, mechanical properties mainly depend on the foam density, foam cell structure and the cell-wall materials. The reported Young's modulus values vary from soft to rigid foams (0.86 to 6,031 *MPa)*. Gelatine foams usually possesses open-cell structures after drying (Liu and Ma, 2009) (Shyamkuwar *et al.*, 2010), with some exceptions (Frydrych *et al.*, 2011).

Table 2.10. EXAMPLES OF GELATINE FOAMS AND THEIR MAIN PROPERTIES REPORTED IN LITERATURE

FORMULATION	PROCESS	APPLICATIONS	DENSITY (kg/m³)	PORE SIZE (µm)	POROSITY (%)	YOUNGS's MODULUS (MPa)	REFERENCE
Gelatine Carbodiimide derivative	Crosslinking and freeze-drying at -20°C	Scaffolds for tissue engineering	56±0.13	400-500	89.8±1.8	0.86±0.19	(Kim, Knowles and Kim, 2005)
Gelatine-10% HA* Carbodiimide derivative	Crosslinking and freeze-drying at -20°C	Scaffolds for tissue engineering	102±0.12	200-300	87.5±2.2	2.28±0.1	(Kim, Knowles and Kim, 2005)
Gelatine, Formaldehyde SDS	Crosslinking, gas foaming and freeze-drying at -20°C	Absorbable sponge	22.4	500±50	97.80	9.1	(Shyamkuwar, et al., 2010)
Gelatine, Formaldehyde SDS	Crosslinking, gas foaming and freeze-drying at -40°C	Absorbable sponge	23.6	500±50	97.70	11.1	(Shyamkuwar, et al., 2010)
Gelatine, Glutaraldehyde	Crosslinking and freeze drying at -20°C	Scaffolds for tissue engineering	9±0.16	250±120	-	Weak/brittle	(Kang, et al., 1999)
Gelatine	Casting and freeze drying at -5°C	Drug delivery, wound dressing	31.9±0.9	159±7	97.60	1554±229.8	(Frydrych *et al.*, 2011)
Gelatine, Sepiolite *(9.1wt%)*	Casting freeze drying at -5°C	Drug delivery, wound dressing	50.8±1.2	102±7	96.4	6031±618.9	(Frydrych *et al.*, 2011)
Gelatine	Microwave foaming	-	39-56	332-1700	94	-	(Frazier, Aday and Srubar, 2018)

*Hydroxyapatite

Figure 2.23 compares the cell structure of different dried gelatine-based foams reported in the literature (Wu *et al.*, 2010). They vary a great deal in morphologies depending on formulation, foaming methods and conditions.

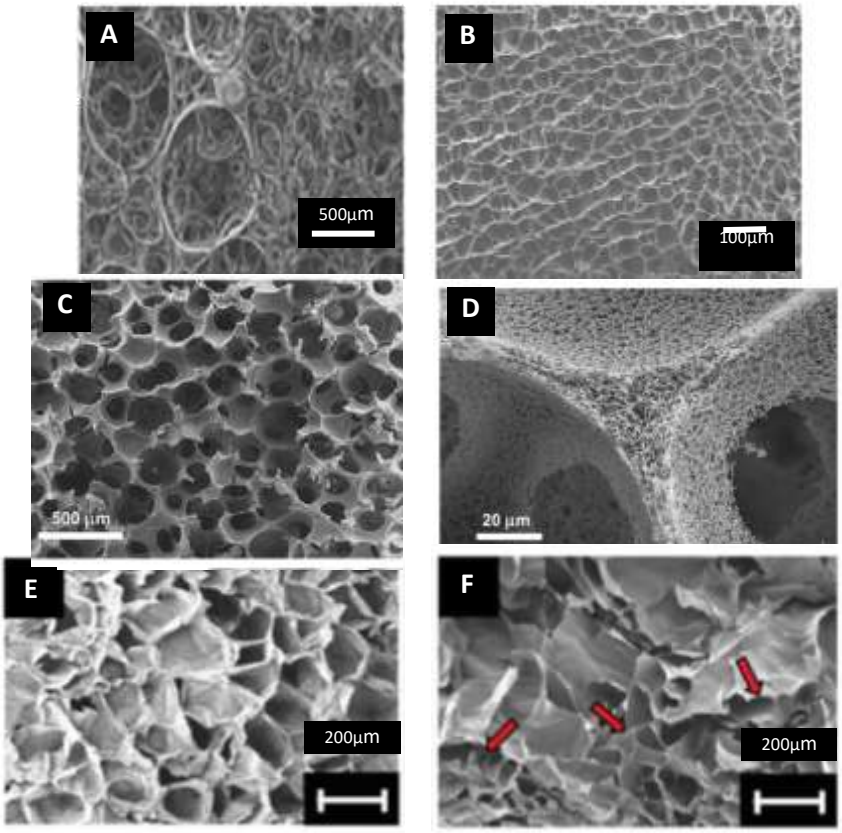

Figure 2.23. SEM IMAGES OF THE STRUCTURE OF (A) GELATINE-GLUTARALDEHYDE-SDS FOAM PRODUCED BY FREEZE-DRYING AT 40°C (Shyamkuwar, et al., 2010) (B) GELATINE-GLUTARALDEHYDE FOAM PRODUCED BY FREEZE DRYING (Wu, et al., 2017) (C) GELATINE FOAM PREPARED WITH A PHASE SEPARATION AND PARAFFIN-LEACHING TECHNIQUE (Liu and Ma, 2009) **(D) DETAILS OF A GELATINE FOAM STRUCTURE PREPARED WITH A PHASE SEPARATION AND PARAFFIN-LEACHING TECHNIQUE** (Liu and Ma, 2009) **(E) GELATINE FOAM PREPARED BY MECHANICAL FOAMING AND FREEZE DRYING AT -20°C (Frydrych, et al., 2011) (F) GELATINE-SEPIOLITE (9.1*wt%*) FOAM PREPARED BY MECHANICAL FOAMING AND FREEZE-DRYING AT -20°C** (Frydrych, et al., 2011)

2.5.6.4 Stability of liquid gelatine foams

Gelatine foams are mostly made from liquid hydrogel state. Liquid foams are metastable systems consisting of polyhedral bubbles, representing the minimum area for the system. Liquid foams have a natural tendency to minimise the liquid/gas interfaces by diminishing the bubbles. (Bhakta and Ruckenstein, 1997). When a liquid foam is prepared, the foam volume typically decreases with time accompanied by phase separation with floating of the foam on top of the liquid phase at the bottom (Bhakta and Ruckenstein, 1997). Within the foam, the total interfacial area decreases, as the mean size of the bubble increases (Bhakta and Ruckenstein, 1997). The phenomenon is known as aging of liquid foams. In most cases, it is desirable to prevent such aging by stabilisation of the liquid foam.

Foam stability may be improved by retarding or arresting the three main foam aging mechanisms: drainage, coalescence and coarsening (Foegeding, Luck and Davis, 2006)(Rio *et al.*, 2014). Figure 2.24 illustrates the four main factors that contribute to the instability of liquid foams. Drainage, coarsening and coalescence are interrelated. When foams drain until a given liquid fraction, coarsening and coalescence are facilitated. A fourth factor affecting foams stability is drying.

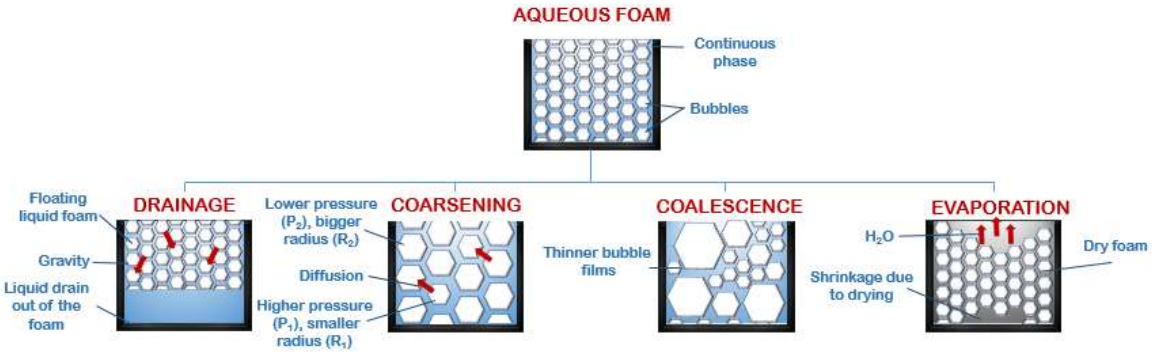

Figure 2.24. ILLUSTRATION OF THE 4 AGING MECHANISMS CONTRIBUTING TO INSTABILITY IN LIQUID FOAMS

Drainage is driven by two mechanisms: liquid flow in the films, which mainly occurs due to the capillary pressure created due to its curvature, and flow in the Plateau border channels, driven by gravity (Bhakta and Ruckenstein, 1997). Drainage eventually finishes when the gradient of the capillary pressure balances gravity (Bhakta and Ruckenstein, 1997). The more liquid content, the larger plateau border radius, the lower capillary pressure and, consequently, the more stable foams (Bhakta and Ruckenstein, 1997) which indicates that higher liquid foam expansion ratios lead to less stable foams. As drainage continues, film bubbles become thinner and eventually break. Drainage can be prevented by resistance to flow e.g. gelling or solidification of the liquid.

Coarsening originates as gas is transported between bubbles of different sizes, leading to the growth of the average bubble radius. Coarsening can be arrested at high films compression modulus and slowed down at thick or small films.

Coalescence usually occurs with drainage. The foam liquid phase is allocated in the films formed between the faces of the bubbles and the plateau border channels (Bhakta & Ruckenstein, 1997). The pressure at these edges is smaller than at the center of the film due to the curvature. This provokes a radial flow which leads to the reduction in film thickness with time (Bhakta & Ruckenstein, 1997). In this way, the liquid in the films is sucked by the plateau border channels under capillary pressure, and the films become thinner with time. Local void forms in the thinning films due to molecular thermal fluctuations and eventually bubble rupture, causing loss of gas at the foam surface or merge of bubbles in inner reigns (Bhakta & Ruckenstein, 1997). Coalescence

can be minimised by increasing the film strength and\or stretchability (e.g. incorporation of other polymers) and be slowed down by gelified films.

Foams can be stabilised using appropriate fillers, surfactants and polymers. A solid-like surface layer may be developed in the gas bubbles due to the attachment of the filler particles to the air-water interface. The filler concentrations in the dispersion must be large enough as high viscosity slows down foam aging.

Incorporation of hydrogels such as protein into the solution can produce highly stable foams. Proteins tend to adsorb at the air-water interface a thermodynamically favorable situation due to their amphiphilic nature (Foegeding, Luck and Davis, 2006). This leads to surface tension reduction (Foegeding, Luck and Davis, 2006). In addition, gelling of the protein hydrogel also slow done drainage and coalescence, as discussed earlier.

Foam stability can be improved by the addition of surfactants in sufficiently high concentrations (Bhakta & Ruckenstein, 1997). Shyamkuwar (2010) studied the stability of liquid gelatine foams prepared with SDS. It was noticed that foams are more stable and drainage rate decreases when SDS concentration increases. This ins mainly due to viscosity increase with the surfactant concentration and the formation of polymer-surfactant complexes (Petkova, Tcholakova and Denkov, 2012).

2.5.6.5 Drying of gelatine foams

Gelled hydrogel foams contain a considerable amount of water, so drying is a necessary step to obtain dry foams. Vaporisation of the liquid is the most common method of drying. It involves transitory heat and mass transfer alongside physical (e.g. shrinkage, puffing, crystallization or glass transitions) and chemical changes (e.g. progress of gelling and /or crosslinking) during the gel foam $\rightarrow$ dry foam transition. As gelatine gels lose moisture during drying, they exhibit retraction or shrinkage (Ruiz-Cabrera *et al.*, 2005). Shrinkage is associated with the compaction of the gelled chain network during migration of water in the drying process (Waje *et al.*, 2005).

Drying from a wet porous body takes place in several steps:

- Diffusion of water molecule within the gel to the cell wall surfaces or foam surface

- Vaporization of water molecules into the pore network or at the foam surface

- Mass transport of vapor through the channel network to the foam surface and away from the foam surface, allowing reduction of water vapor partial pressure and facilitate water vaporisation in the gel.

Drying rate, therefore, depends on many factors: diffusivity of water in the gels, heat transfer into the foam due to vaporisation of water from the interfaces and vapor mass transport through the porous channel network to the foam surface and from the surface.

Vaporisation of water molecules from the surface of the cell walls and foam surface is highly dependent on the heat provided. Heat may be provided by convection, conduction, radiation or volumetrically, by microwave or radio frequency electromagnetic field (Waje *et al.*, 2005). Mass transport is also essential to drive the water vapor away through the pore network (and open-cells facilitate such transport) within the foam to the foam surface.

The Equilibrium Moisture Content (EMC) is the moisture content where the gel neither gains nor loses moisture. During low-intensive evaporation (e.g. below boiling point), a significant amount of moisture migrates to the gel surface counterbalancing the water vapor partial pressure in the vapor phase before EMC is reached. As the drying process continues, moisture content decrease and the gel becomes harder, resulting in a lower drying rate (Waje *et al.*, 2005).

The contraction of the gel depends on the drying temperature, hydrogel concentration and crosslinker concentration. Waje *et al.* (2005) reported that higher crosslinker concentration leads to gel hardening what may complicate moisture loss. Therefore, increase in crosslinker concentration may decrease diffusivity and drying rate. Consequently, increase in cross-linker concentration leads to EMC increase (Waje *et al.*, 2005).

Most dryers are convective, where hot air is used to supply the heat for evaporation and to transport the evaporated moisture from the material. For heat sensitive materials, freeze and vacuum dryers are used, considerably more expensive than dryers operating near to atmospheric pressure.

2.5.6.6 Gelatine foams applications

Gelatine foams are widely used for culinary applications (e.g. espuma, marshmallows). They are also extensively used for biomedical and pharmaceutical purposes, such as in tissue engineering, wound dressing and drug delivery (Jaipan, Nguyen and Narayan,

2017). For instance, Gelfoam® (Pfizer, US) is a hemostatic absorbable wound dressing material commercially available in the form of compressed gelatine sponge (FDA, 2011).

The literature is currently dominated by those for biomedical applications. Brooks (1881) described one of the first patented foams made from gelatine. Most more recent patents also usually refer to formulations and preparation processes of gelatine foams for biomedical applications (Freedman, 1985) (Guenther, Katrin and Hanns, 1992) (Gunther, Borgschulte and Hanns, 1992). But patents cover other applications, such as agriculture (Neuman, 1976), thermal insulation (Hartranft *et al.*, 1994) (Fidler and Simonton, 2000) and packaging (Morrison, 1995).

The development of new applications for non-food and non-biomedical applications is still scarce (Jaipan, Nguyen and Narayan, 2017). Given the versatility of gelatine hydrogel and desirable characteristics (e.g. biodegradability and foam stabilisation), there is a great potential for more efforts of investigation and development of gelatine-based foams.

2.6 OTHER BIOBASED HYDROGELS

This section briefly discusses other biobased hydrogels and foams. It will focus on agar and gellan gum from two non-animal origins aimed at increasing diversity in materials origins.

2.6.1. AGAR

This section briefly discusses the characteristics of agar and agar foams.

2.6.1.1. Characteristics of agar

Agar is a gelling agent extracted from the cell walls of Rhodophyceae, a group of red seaweed (Vieira *et al.*, 2007). It is a polysaccharide composed of two different fractions: agarose and agaropectin.

Agarose usually contributes two-thirds of the total agar composition. It is a linear molecule which gives agar its gelling power and consists of repeated units of β-1,3-linked D-galactose and α-1,4-linked 3,6-anhydro-galactose (Vieira *et al.*, 2007). Agaropectin, the non-gelling fraction, is composed of agarose and different percentages of pyruvic acid, ester sulfate and D-glucoronic (Boral and Bohidar, 2009).

Agarose swells but not dissolves in cold water. It dissolves in hot water (~ 85°C) and cooled down to gel (Schrieber and Gareis, 2007) (Vieira *et al.*, 2007). The gelling

temperature depends on agarose concentration, pH, time and molecular weight, among others (Vieira *et al.*, 2007).

Agar gels are thermo-reversible and exhibit thermal hysteresis, a considerable temperature difference between melting (around 85°C) and gelling points (about 40°C) which is attributed to helices aggregation (Vieira *et al.*, 2007) (Boral and Bohidar, 2009).

Agar gel structure is complex. It forms fibre bundles bonded with intermolecular hydrogen which aggregate to generate three-dimensional structures (Boral and Bohidar, 2009).

Agar gels are firm and slightly elastic. Its gel strength is outstanding, being able to form gels at low concentrations. Agar may lose firmness in an acid medium (Schrieber and Gareis, 2007). Another relevant characteristic of agar is syneresis, a phenomenon which consists in the expulsion of liquid, usually water, from the gel.

2.6.1.2. Agar for foaming

Agar has been used as a vehicle to produce ceramic for thermal insulation of buildings. Cao *et al.* (2015) fabricated agar foams containing fly ash by mechanical beating and sintering. Jardim *et al.* (2016) produced amine-impregnated silica foams using agar as a gelling agent and SDS as a surfactant whereas Huo *et al.* (2017) used agar to improve the mechanical properties of alumina foams.

Solely agar foams have been less commonly reported. Lee and Lee (1997) prepared agar foams for packaging applications by freeze-drying. They found cell size of the agar foams was found significantly affected by the freezing rate.

2.6.2 GELLAN GUM

This section describes the main properties of gellan gum and the foams made from it.

2.6.2.1 Characteristics of gellan gum

Gellan gum is an anionic polysaccharide produced by the fermentation of the bacteria *Sphingomonas elodea* (Schrieber and Gareis, 2007) (Vieira *et al.*, 2007).

Its structure consists of the repetition of a tetrasaccharide composed of two D-glucose residues, one L-rhamnose and D-glucuronic acid (1,4-α-L-rhamnose,1,3-βD-glucose,1,4-β-D-glucuronic acid, and1,4-β-D-glucose (Vieira *et al.*, 2007).

There are two types of gellan gum: low or high acyl (LA and HA, respectively). HA gellan gum has two acyl substituents which appear in the glucose residue: acetyl (appearing,

on average, once per repeating unit) and L-glyceryl (appearing, on average, twice per repeating unit) (Vieira *et al.*, 2007). HA gels are more elastic, soft and ductile than LA gels (Schrieber and Gareis, 2007) because the acyl residues hinder polymer chain aggregation and, consequently, structure packaging (Vieira *et al.*, 2007). LA gellan gum has the two acyl residues removed by alkaline hydrolysis (Vieira *et al.*, 2007). It forms strong, clear and brittle gels (Schrieber and Gareis, 2007). LA and HA gellan gum can be combined to produce different textured gels (Schrieber and Gareis, 2007).

When heated at high temperatures (>75°C), gellan gum is in a disordered coiled state. As it cools (from 30°C-50°C), a threefold left-handed double helix stabilised by hydrogel bonding forms and junction zones aggregate to form a three-dimensional gel network (Vieira *et al.*, 2007)(Banerjee and Bhattacharya, 2012).

Gellan gum has a strong gelling power, even at a concentration as low as 0.05 *wt%* can produce strong gels (Schrieber and Gareis, 2007). Gellan gum gelation process depends on polymer concentration, and type of cation, among others (Banerjee and Bhattacharya, 2012).

2.6.2.2 Gellan gum-based materials

Gellan gum is the most recent discovered hydrocolloid (Morris, Nishinari and Rinaudo, 2012). This justifies that, while still relatively abundant, the scientific literature is relatively scarce compared to other hydrocolloids such as gelatine or agar.

Gellan gum has been researched for the development of tissue engineering hydrogels in isolation (Coutinho *et al.*, 2010) (da Silva *et al.*, 2013) and combined with other polymers, such as alginate (Akkineni *et al.*, 2016). Akkineni *et al.* (2016) found that the incorporation of gellan gum to alginate hydrogels improved shaping and mechanical properties while decreased swelling.

It has also been used for the manufacturing of ceramic-gellan gum composites. Zhang *et al.* (2014) and Manda *et al.* (2018) prepared gellan gum-alumina and gellan gum-hydroxyapatite xerogels, respectively, both for biomedical applications.

Not much literature can be found in gellan gum foams, and yet it is a promising and versatile material which offers a range of possibilities.

2.7 HONEYCOMB PANELS

Honeycomb panels consist of a hollow honeycomb structure core between two thin face-sheets bound by an adhesive. These panels are usually made by expanding strip-glued sheets where glued cell walls hold the structure together and have a thickness

2t and a length *l,* whereas free cell walls exhibit same length but thickness *t* (Gibson and Ashby, 1997).

Honeycomb panels can be made of different geometrical shapes (e.g. hexagonal, square, rhombic and triangular) and materials (e.g. cardboard, aluminium and thermoplastics). Nomex® (Dupont, US) is an extensively used material for sandwich materials. Nomex®, material, known for its outstanding fire-resistance properties, is made of meta-aramid fibres adhered by an epoxy adhesive which is dipped into a phenolic resin and cured (Roy *et al.*, 2014). Honeycomb panels, made from different materials, come in various cell sizes, core densities and thickness.

Honeycomb panels are widely used for different applications, including aerospace, automotive and packaging. They are an attractive alternative to conventional materials due to its high stiffness-weight ratio which assists reduction in fuel consumption and thus carbon emissions (Zinno *et al.*, 2011).

The panels offer excellent flexural strength and stiffness at low densities and exhibit orthotropic behaviour, i.e. they behave differently depending on the structure orientation (see Figure 2.25). For honeycomb structures manufactured by the corrugated method, the strongest orientation is the so-called L-direction (ribbon direction) while the weakest direction, in hexagonal honeycombs, is at 60° from L-direction. The other orientations are W-direction (transverse to the ribbon) and T (through the thickness) (Burlayenko and Sadowski, 2010). The strength of the panel mainly depends on the cell size (the distance between two parallel horizontal cell walls), the material the cell walls are made of and the panel thickness.

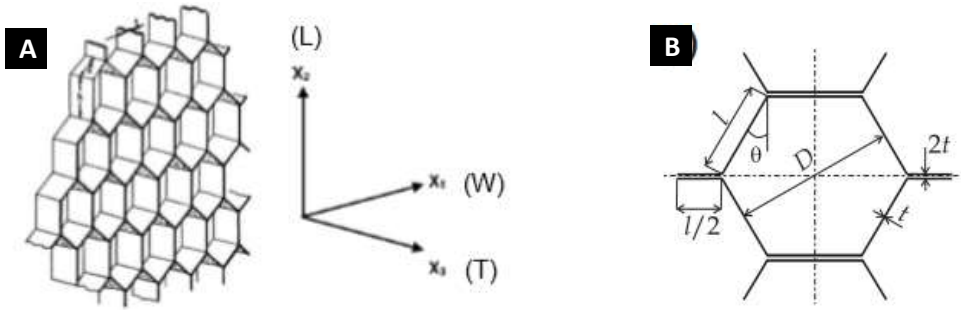

Figure 2.25. HONEYCOMB STRUCTURE. (A) HEXAGONAL HONEYCOMB STRUCTURE. L, W AND T PLANES (Gibson and Ashby, 1997) **(B) UNIT CELL** (Burlayenko and Sadowski, 2010)

Compression instabilities include panel buckling, intra-cell buckling and skin wrinkling but the weakest point of the panel is the point where the cell walls meet the adhesive-bonded face-sheet (Gibson and Ashby, 1997). The structure tends to buckle for relative densities lower than 0.1 while debonding tends to occur for relative densities higher

than 0.1 (Gibson and Ashby, 1997). Manufacturing defects may also contribute to panel debonding.

The compressive properties of honeycomb panels are usually studied by quasi-static compressive tests, where an increasing force is exerted slowly. The buckling in T direction takes place in different stages. First, the cell walls in T direction elastically bend and, as strain increases, depending on the material they are made of, they may collapse by elastic buckling, plastic yielding, creep or brittle fracture (Gibson and Ashby, 1997). As strain increases, cell wall densification occurs.

Honeycomb fillers, such as polymeric foams, may improve some of the unfilled panels' properties, such as impact, compression or fatigue (Burlayenko and Sadowski, 2010). Foam filling may increase the compression strength of honeycomb panels due to a decrease of the stress in the cell walls under compression. This effect is more evident as the foam density increases (Burlayenko and Sadowski, 2010). Increasing cell sizes decrease compression strength for both filled and unfilled panels. Burlayenko and Sadowski (2010) found the filling of aluminium honeycomb panels with PVC foam increased the stiffness and the debonding resistance to the panels. Bitzer (1997) stated that thermal insulation properties can be enhanced by filling the honeycomb structures but that it is not always true for mechanical properties, especially for denser cores.

Flexural bending failure modes include micro-buckling (Figure 2.26.A), core shear (Figure 2.26.B), core indentation (Figure 2.26.C) and face wrinkling (Figure 2.26.D) (Russell *et al.*, 2011).

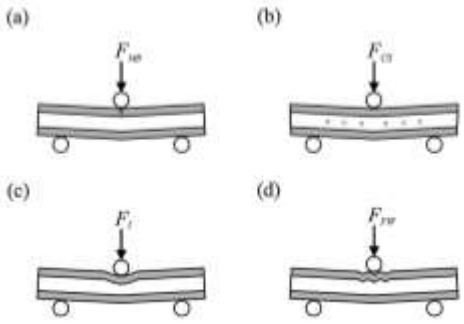

Figure 2.26 FLEXURAL BENDING FAILURE MODES (a) MICRO BUCKLING (b) CORE SHEAR (c) CORE INDENTATION (d) FACE WRINKLING (Russell *et al.*, 2011)

Micro buckling (face yielding) occurs when the top face sheet axial stress exceeds its compressive strength in bending (i.e. its micro-buckling strength). It may lead to bottom face sheet tearing as the axial stress exceeds the sheet maximum tensile stress. *Face wrinkling* is produced by local buckling on the face sheets due to compression forces.

Core shear involves the core damage due to shear stresses exceeding the core shear strength (Steeves and Fleck, 2004).

Yan *et al.* (2014) found that the maximum load bearing capacity and the bending stiffness of aluminium corrugated sandwich panels increased by four and two times, respectively, with a foam filler in 3-point bending tests.

2.8 GAPS IN TECHNOLOGY AND THE NEED FOR THIS WORK

There is a need for commercially viable bio-based foams as an alternative to their fossil fuel counterparts for different applications. This need is especially significant for packaging applications as society is increasingly concerned about the environmental impact of disposable foams, especially EPS. EPS can be recycled, but this is not usually economical due to product contamination or lack of waste management facilities. When recycling is possible, EPS is usually down-cycled to low-value products (Coles *et al.*, 2014). In addition to this, EPS is made of non-renewable sources which may exhibit oscillating prices due to oil prices' volatility and scarcity in the future. These reasons are demanding both legislation and producers to look for more environmental and cost sustainable solutions.

Bio-foams from bio-based materials can be an excellent substitute for conventional polymer foams. Plant-based biopolymers (e.g. starch, cellulose) are readily available, have been widely studied and have already been proved as effective substitutes for conventional polymers (e.g. starch-based loose-fill). But higher performing bio-foams are desirable. A range of bio-foams have become commercially available, but due mainly to high costs, industrial high-volume applications are yet to come.

Bio-based hydrogels are derived/extracted from natural materials and possess excellent biodegradability when necessary. Most hydrogel foams are currently made for biomedical applications, what it is not viable for mass production of packaging materials. Hydrogels made of gelatine were pursued on this research due to their high potential for bio-foams for packaging applications production due to gelatine desirable characteristics (e.g. biodegradability, bio-based origin, availability, performance and relative ease of manufacture).

Most plastics foaming involves high temperatures and pressures what involves a high use of energy and high capital cost for equipment. In contrast, hydrogels production involves low-temperature foaming, what requires less energy, and higher process versatility (i.e. foaming, sheet casting and moulding).

The following chapters aim to understand and investigate hydrogel foaming to lay the foundation for the mass production of biodegradable, cost-effective, low-density and high-performance foams for industrial applications. Systematic studies in formulation and processing (foaming, foam stabilisation and drying) were carried out to elucidate their influence on foams structure and properties. Different case studies were studied to demonstrate the technology versatility for different applications.

3. CHAPTER 3.
EXPERIMENTAL DETAIL

Chapter 3.

EXPERIMENTAL DETAILS

3.1 INTRODUCTION

This chapter describes the experimental details. The materials used in the solution preparation are described, followed by the sample preparation methods, experiment design and the analytical techniques used for characterisation of the solutions, solid foams and the foam matrix.

The liquid foaming process consists of three stages: solution preparation, foaming of the solution and drying. The following experimental studies aim to understand the role of the different formulation and processing factors on the foaming and foam stabilisation behavior to establish the process feasibility and its parameters influence on material properties.

The processing parameters studied included foaming temperature, drying temperature and mould design. The study of the processing parameters was to determine the operation windows for manufacturing low-density foams and, ultimately, to establish the optimum processing conditions.

The analytical techniques used in this research include SEM (Scanning Electron Microscopy), optical microscopy, rheology, viscosity, TGA (Thermogravimetric Analysis) and testing for mechanical, acoustic, and thermal properties of the solid foams.

3.2 DESCRIPTION OF MATERIALS

This section describes the materials used in this research. They are categorised into four sections: the biopolymers used, additives/modifiers, fillers and other materials.

3.2.1 BIOPOLYMERS

The biopolymers used to produce bio-foams are a range of those compatible with water for preparation and foaming of aqueous solutions/suspensions. These include starch, gelatine, agar and gellan gum.

3.2.1.1 Purified wheat starch

Purified wheat starch ($C_6H_{10}O_5$), with commercial name "Meritena 200", supplied by Tereos Syral (France) was selected as a suitable polymer due to its low cost, high biodegradability, and commercial availability.

Meritena 200 is a 99.7% purity starch with a real density of 1.43 g/cm^3 (in dry form) and containing 10-13% of moisture content (as-received). Table 3.1 shows the technical specification of the product.

Table 3.1 MERITENA 200 STARCH SPECIFICATION (Tereos Syral, 2014)

PARAMETER	VALUE
Moisture (%)	12.5*
Bulk Density (g/cm^3)	0.45-0.65
Real Density (g/cm^3)	1.43±0.12*
Amylose Content (%)	25
Protein Content (%)	<0.3
Sulfites (*mg/kg*)	<10
pH - 20% (*w/v*)	5-7
Sodium (*mg*)	<70
Calcium (*mg*)	<10
Iron (*mg*)	<2
Magnesium (*mg*)	<5
Zinc (*mg*)	<0.5
Shelf life (*months*)	24

*Parameters measured by the author (see Section 3.4.2, Characterisation of Raw Materials)

Figure 3.1.A shows an SEM (Scanning Electron Microscopy) image of Meritena 200 starch granules of around 10 µm size at lower magnification, while Figure 3.1.B, at higher magnification, reveals clusters of smaller and bigger granules.

As there is a lack of sufficient gelling power in aqueous solutions/suspensions of starch alone, to stabilise the liquid foam structure against drainage, bubble coarsening and rupture, two types of foam stabilisation agents were studied:

- The incorporation of strong bio-based gelling agents (gelatine, agar and gellan gum) either as blends with starch, or alone
- Solidification of liquid foams using calcium sulfate hemihydrate, or plaster of Paris (POP)

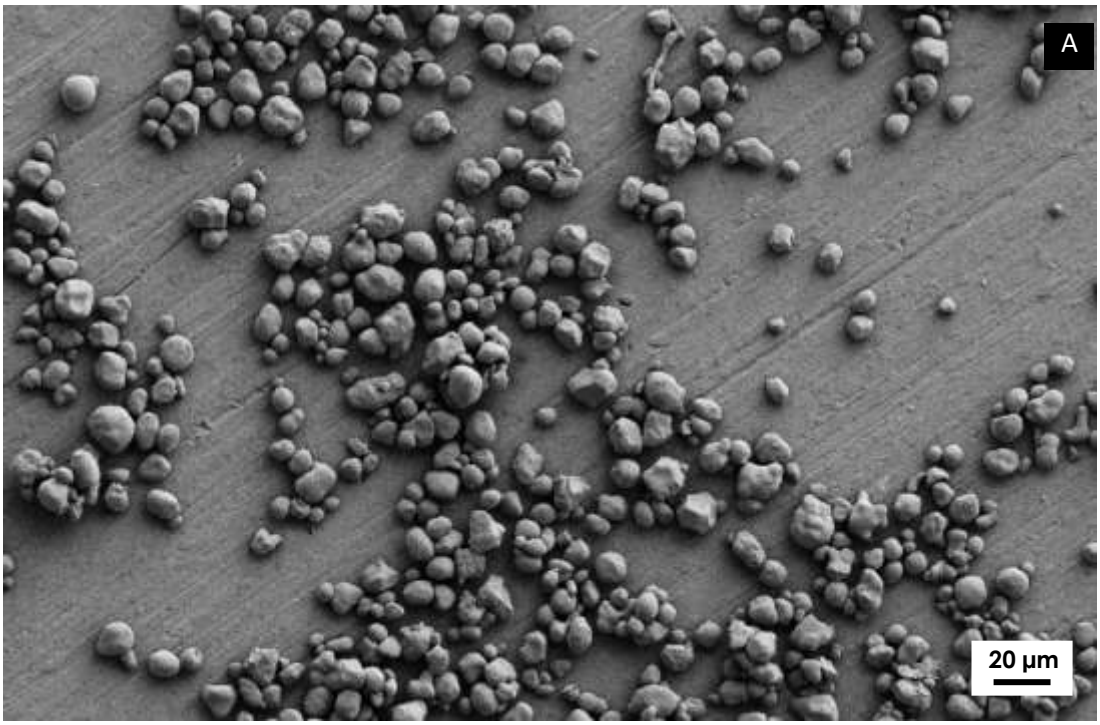

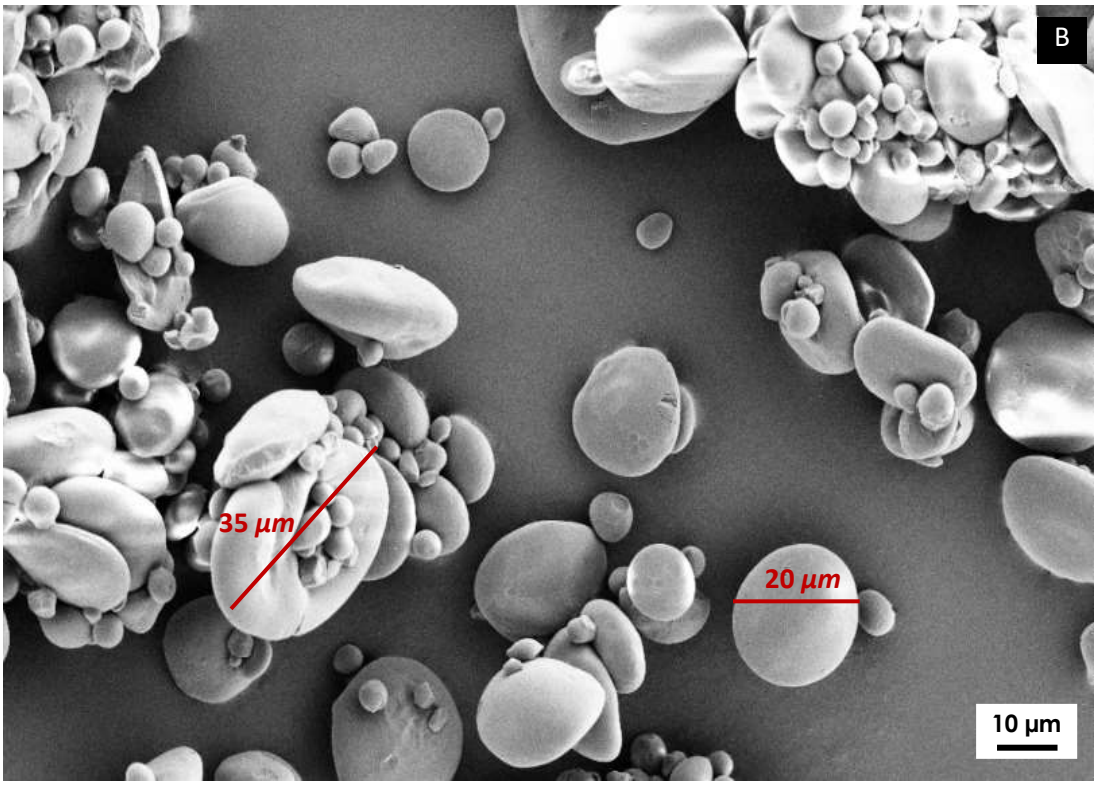

Figure 3.1 SEM IMAGES OF MERITENA 200 WHEAT FLOUR (A) 800x (B) 1750x

3.2.1.2 Gelatine

Gelatine was used as a foam stabiliser. Post-liquid foaming process, gelatine transforms the liquid foam into a liquid gel as temperature decreases to room temperature so as

preserves the foam structure. It was used as a blend with starch, or alone for gelatine hydrogel foams.

Two grades of type A (see Section 2.5.5.2 in Chapter 2) pigskin gelatine were used: high Bloom (HB) and low Bloom (LB), as shown in Table 3.2. The same supplier supplied both. This section does not include further information about both the bloom and the supplier due to commercial sensitivity.

Table 3.2. GELATINE TECHNICAL SPECIFICATION

PARAMETER	HB GELATINE	LB GELATINE
Real Density* (*g/cm³*)	1.27±0.05	1.35±0.02
Isoelectric Point	4.9	4.9
Clarity @6.67%	0.05	0.05
Moisture (%)	12	12
Moisture (%)*	13.3	12.5
pH 1% solution	4-6	4-6
Sulfur Dioxide *(ppm)*	<50	<50
Ash (%)	<2	<2
Arsenic (*ppm*)	<1	<1
Lead (*ppm*)	<5	<5
Cadmium (*ppm*)	<0.5	<0.5
Zinc (*ppm*)	<50	<50
Mercury (*ppm*)	<0.15	<0.15
Chromium (*ppm*)	<10	<10
Copper (*ppm*)	<30	<30
Shelf life (*years*)	5	5

*Parameters measured by the author (see Section 3.4.2)

Figure 3.2 shows optical microscope images of LB and HB gelatine particles. Figures 3.2.A and 3.2.B show LB gelatine particles, ranging from 5 to 175 *μm*. The HB gelatine particles were smaller, ranging from 5 to 78 μm, as shown in Figures 3.2.C and 3.2D.

Two other biopolymers (agar and gellan gum), described below, were also studied as alternatives to gelatine in attempt to extend the origins of the gelling agents.

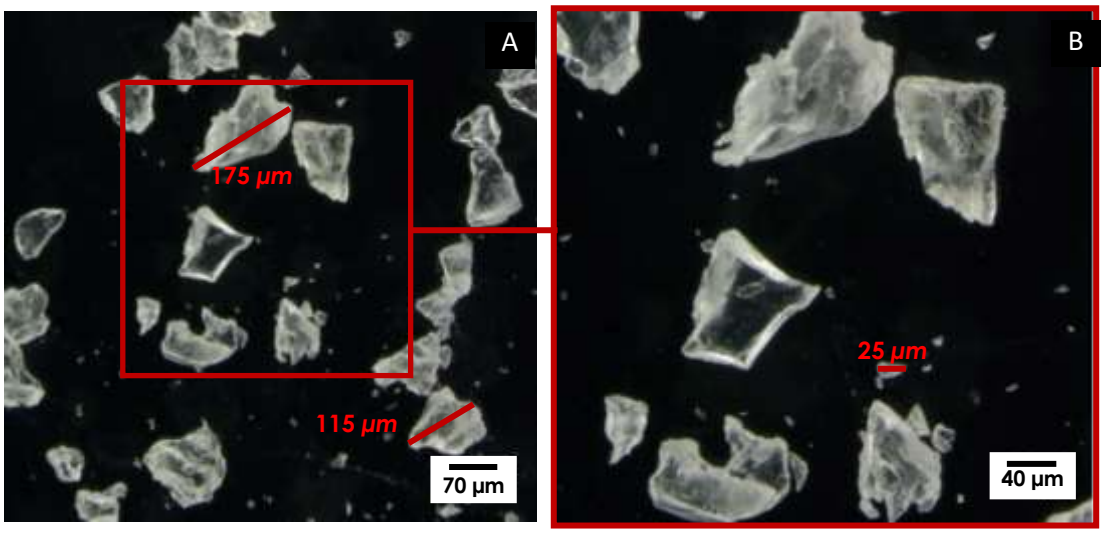

a. LB gelatine particles (8x) *b. LB gelatine particles detail (12.5x)*

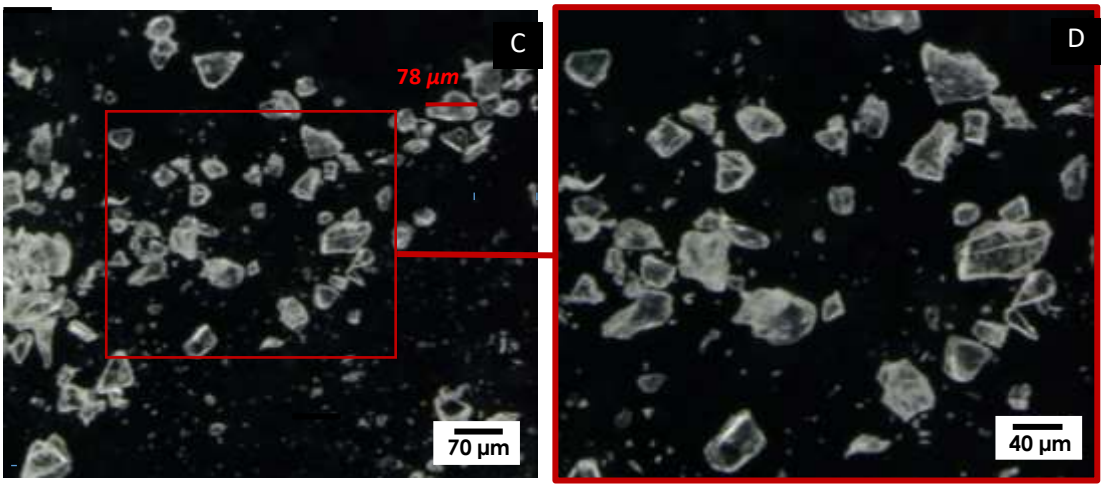

c. HB gelatine particles (8x) *d. HB gelatine particles detail (12.5 x)*

Figure 3.2 OPTICAL MICROSCOPE IMAGES OF (A) (B) LOW AND (C) (D) HIGH BLOOM GELATINE PARTICLES

3.2.1.3 Agar

Agar (E406) was used as the primary polymer for agar-hydrogel foams. It is a thickening and gelling agent that may stabilise foams, as it transforms the liquid foam into a liquid gel foam on cooling (see Section 2.6.1 in Chapter 2 for further details). It was supplied by Special Ingredients Ltd (UK) as a refined powder. Table 3.3 shows some agar parameters measured by the author.

Table 3.3. AGAR SPECIFICATION DETAILS

PARAMETER	VALUE
Moisture (%)*	8.42
Bulk Density (g/cm^3)*	0.40-0.55
Real Density (g/cm^3)*	1.23-1.45
Shelf life (*months*)	24

*Parameters measured by the author (see Section 3.4.2)

As shown in Figure 3.3.A, the agar particle size ranges from 20 to 300 *μm*. Figure 3.3.B shows a close-up image of an agar particle.

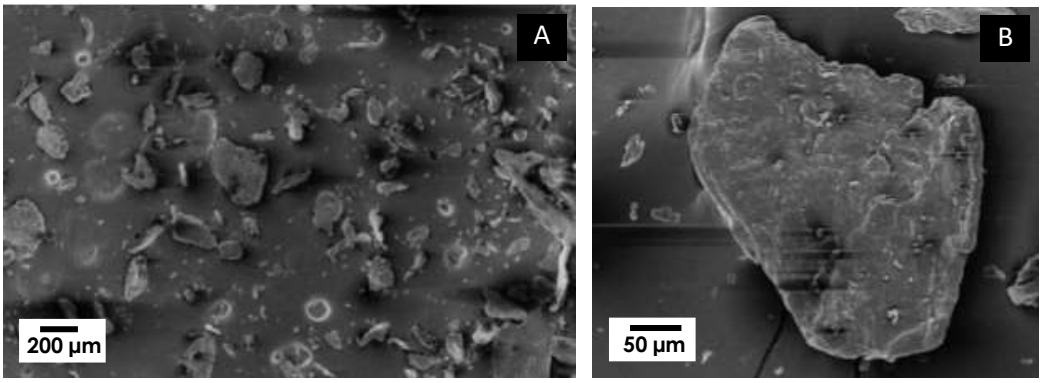

Figure 3.3 SEM IMAGES OF AGAR PARTICLES. (A) IMAGE SHOWING THE SIZE DISTRIBUTION OF AGAR PARTICLES (B) CLOSE-UP VIEW OF AN AGAR PARTICLE

3.2.1.4 Gellan gum

Gellan gum (E418) is a gelling agent used as the principal polymer for gellan gum hydrogel foams. The two types of gellan gum (supplied by Special Ingredients Ltd (UK)) were studied: LT100 (high acyl, HA) and type F (low acyl, LA). Further details about gellan gum can be found in Section 2.6.2.1 in Chapter 2.

Table 3.4. GELLAN GUM SPECIFICATION DETAILS

PARAMETER	LA GELLAN GUM	HA GELLAN GUM
Moisture (%)*	4.57	5.92
Bulk Density (g/cm^3)*	0.45-0.65	0.42-0.68
Real Density (g/cm^3)*	1.34-1.45	1.3-1.48
Shelf life (*months*)	48	48

*Parameters measured by the author (see Section 3.4.2)

Both gellan gum particles are shown in Figures 3.4 and 3.5. They have an irregular shape and a broad size distribution, ranging from 5 to 300 *μm*.

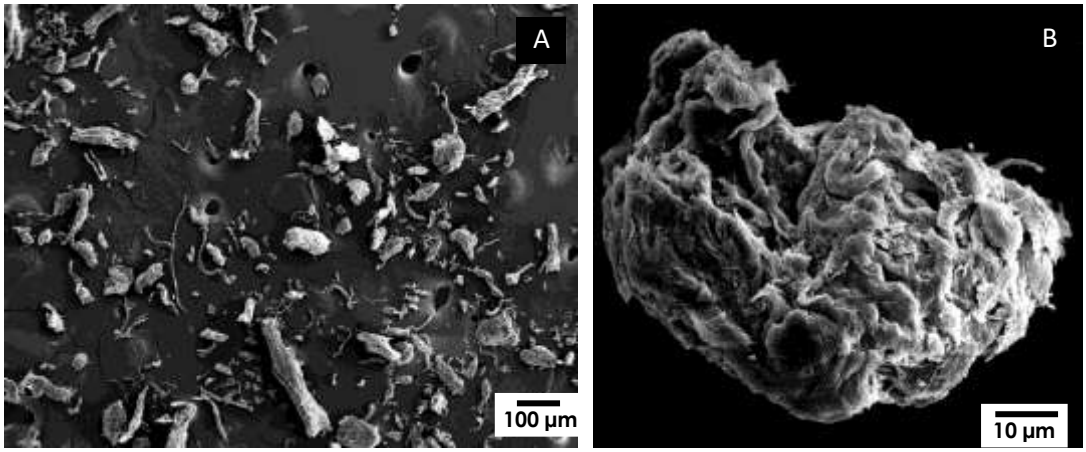

Figure 3.4 SEM IMAGES OF LA GELLAN GUM PARTICLES. (A) IMAGE SHOWING THE SIZE DISTRIBUTION (B) CLOSE-UP VIEW OF A PARTICLE

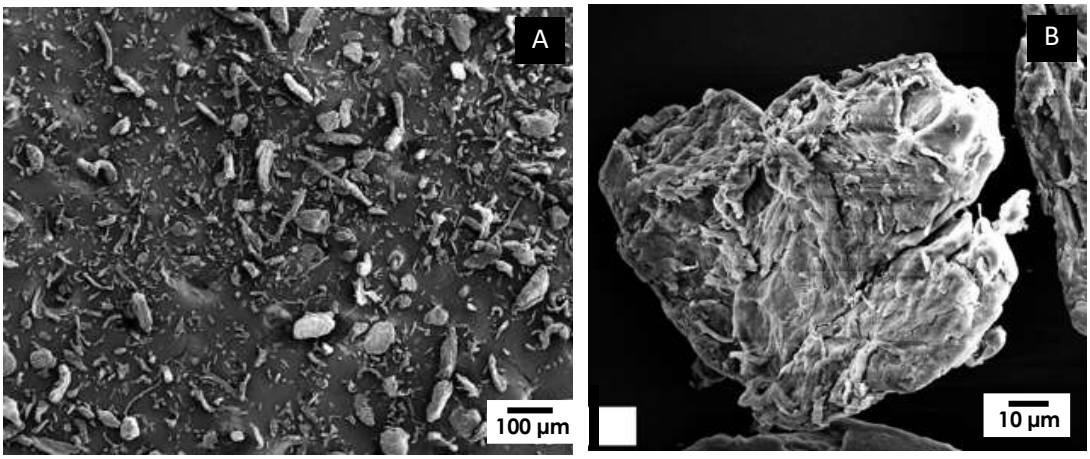

Figure 3.5 SEM IMAGES OF HA GELLAN GUM PARTICLES. (A) IMAGE SHOWING THE SIZE DISTRIBUTION (B) CLOSE-UP VIEW OF A PARTICLE

3.2.2 ADDITIVES/MODIFIERS

This section describes the additives used for the manufacturing of the bio-foams. These include plasticisers, stabilisers, fillers, surfactants and pH modifiers.

3.2.2.1 Glycerol

Two plasticisers, glycerol and sorbitol, were used to control the flexibility of the foams and modify the glass transition point of the biopolymers via the intermolecular hydrogen bonding (Yan and Pochan, 2010).

99+% pure glycerol ($C_3H_8O_3$), supplied by Fisher Scientific (UK) in a viscous liquid form at room temperature, was used as a plasticiser. Table 3.5 shows the specifications of the glycerol used.

Table 3.5. GLYCEROL TECHNICAL SPECIFICATION (Fisher Scientific, 2016)

PARAMETER	VALUE
Moisture (%)	<1
Density (g/cm^3)	1.26
Melting point (°C)	18
Boiling point (°C)	290

3.2.2.2 Sorbitol

Liquid sorbitol, supplied by MKS ingredients (UK), was used as a plasticiser to produce flexible gelatine foams. Sorbitol density was 1.4 g/cm^3, and its water content was 8%, both measured by the author following the procedures explained in Section 3.4.2 (Characterisation of Raw Materials).

3.2.2.3 Polyvinyl Acetate (PVAc)

An emulsion of polyvinyl acetate $(C_4H_6O_2)_n$, with commercial name *Unibond Super PVA Adhesive Sealer & Primer*, manufactured by Henkel Loctite Adhesives Limited (UK) and supplied by Screwfix Ltd (UK), was selected as stabilisation agent in System 1 (see Section 3.3.3.1). It was used as a modifier of the biopolymer as at low percentages may influence liquid bubble film stretchability and foam stability (Lai, Sun and Don, 2015). PVAc is usually used as a primer and bonding aid for plaster.

Table 3.6 shows the product specifications provided by the supplier.

Table 3.6. UNIBOND SUPER PVA ADHESIVE SEALER & PRIMER SPECIFICATION (Unibond, 2015)

PARAMETER	VALUE
Moisture (%)	65
Viscosity (*mPa·s*)	5-15
pH value	4.5
Density (g/cm^3)	1.05
Wet Colour	White
Colour as dries	Translucent

3.2.2.4 Calcium sulfate hemihydrate

Calcium sulfate hemihydrate (CaSO4 · 0.5H2O), with commercial name *Creation Station* and supplied by Artstraws Ltd (UK), was used as foam hardener. Calcium sulfate hemihydrate, also known as Plaster of Paris (POP) is a cementitious solidifier which forms a moldable paste on hydration and sets and develops strength (Singh and Middendorf, 2007).

Table 3.7 exhibits some properties of calcium sulfate, measured by the author following the procedures explained in section 3.4.2.

Table 3.7. CALCIUM SULPHATE HEMIHYDRATE PROPERTIES

PARAMETER	VALUE
Moisture (%)	1%
Bulk Density (g/cm^3)	1.45
Real Density (g/cm^3)	3.2

Figure 3.6 shows a SEM image of calcium sulfate particles. Their size distribution ranged from sizes smaller than 1*μm* to approximately 60*μm*.

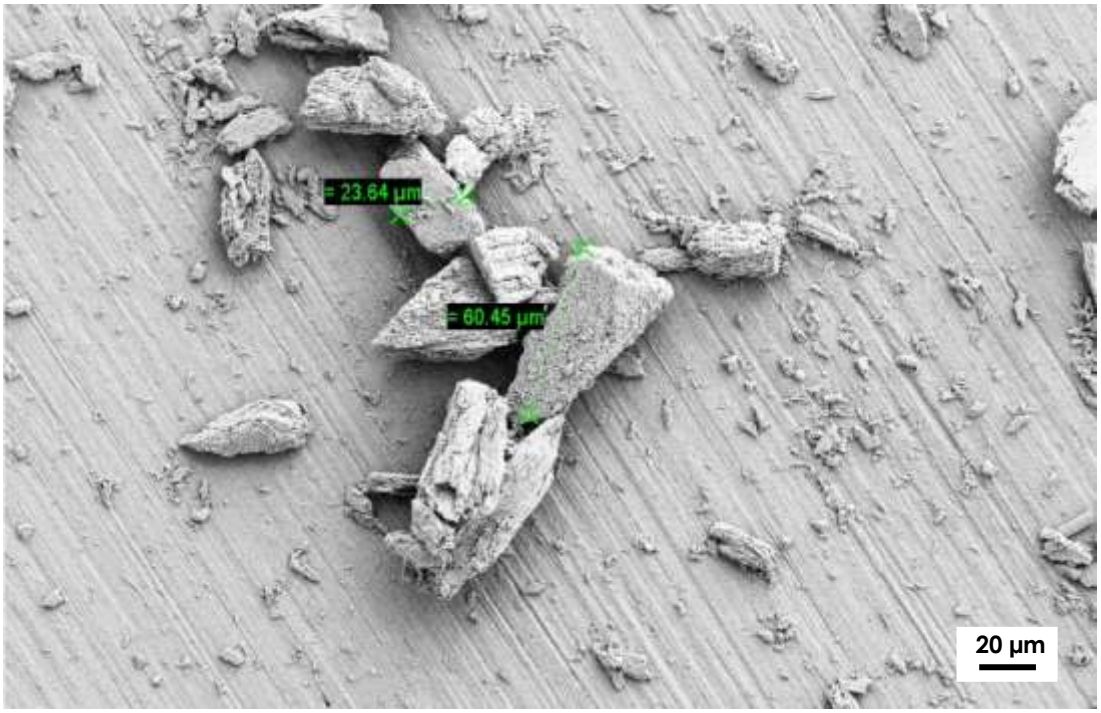

Figure 3.6. SEM IMAGE OF CALCIUM SULPHATE HEMIHYDRATE PARTICLES

3.2.2.5 Surface tension modifiers

As discussed in Chapter 2, Literature Review, foaming agents assist the foaming process, increasing the foam volume produced from the initial solution by lowering its surface tension. They may also support foam stabilisation.

Formil Biological Super Concentrated Liquid detergent, a conventional store bio-detergent, was selected as the foaming agent for calcium sulfate-PVAc-starch foams and gelatine-starch foams. It is claimed to be a biodegradable product according to Regulation (EC) No. 648/2004 for detergents. It contains less than 5% of soap, less than 5% of phosphonates, 5-15% of non-ionic surfactants and 15-30% of anionic surfactants. As measured by the author, its moisture content was 59% and its density, 1.05 g/cm^3.

Three different surfactants were used. For commercial sensitivity, their commercial names and suppliers are not revealed. They will be referred to as surfactants A, B, and C.

Surfactant A is an industrial amphoteric surfactant. It was used for hydrogel foams. It is a surfactant with excellent stability and hydrotropic characteristics over a wide pH range in hard or soft water. It is readily biodegradable and practically non-toxic.

Surfactant B, a cationic surfactant, was used for preliminary studies in hydrogel foams.

Surfactant C, an anionic surfactant, was used in starch-gelatine foams and hydrogel foams. It was supplied from two different sources. C1 (used in both starch-gelatine foams and hydrogel foams) was supplied from supplier 1 and C2 (only used for hydrogel foams) was supplied by supplier 2. C1 is more than ten times more expensive than C2, and thus the latter is likely to be a much more economical candidate for mass production. FTIR analysis was carried out for both C1 and C2 and confirmed both materials were surfactant C (the results are not shown in this thesis).

Table 3.8 summarises the technical information for the four surfactants used.

Table 3.8. SURFACE TENSION MODIFIERS TECHNICAL SPECIFICATIONS

PARAMETER	SURFACTANT A	SURFACTANT B	SURFACTANT C1	SURFACTANT C2
Surfactant type	Amphoteric	Cationic	Anionic	Anionic
Appearance	Clear colourless to light yellow liquid	Fine white solid granules	Fine white powder	Fine white powder
Density (g/cm^3)	0.98*	1	1.01	1.01
Cloud Point Elevation (°C)	35-45	-	>100	>100
CMC at 20°C (mM)	N/A	0.92	7-10	7-10
Moisture content* (%)	62.69±3.24	<0.1	<0.1	3

*Parameters measured by the author (see Section 3.4.2)

3.2.2.6 Acetic Acid

As discussed in Chapter 2, literature review, the pH of aqueous solutions affects the stability of liquid foams in terms of integrity and spoilage (Edwards, 2000) (Willett and Shogren, 2002). 99.5% pure acetic acid ($C_2H_4O_2$), supplied by Fisher Scientific (UK), was used as a pH modifier of gels for their rheological characterisation (see Section 3.4.3.4). It was also used as a preservative for starch-gelatine foams to prevent mould growth during drying. Table 3.9 shows acetic acid specification.

Table 3.9. TECHNICAL SPECIFICATION OF ACETIC ACID (Fisher Scientific, 2015a)

PARAMETER	VALUE
Moisture (%)	<0.5
Density (g/cm^3)	1.05
Melting point (°C)	16-16.5
Boiling point (°C)	117-118
pH	<0.1
Viscosity (cP)	1.22

Acetic acid is toxic to most of microorganisms at low concentrations, and its inhibitory effect is more significant than other organic acids, such as citric, in similar concentrations (Lund, Baird-Parker and Grahame W., 2000) (Trček, Mira and Jarboe, 2015).

In addition to this, acetic acid can degrade starch molecules and reduce the degree of crystallinity (Majzoobi and Beparva, 2014). Its incorporation into the gelatinised starch solution has been shown to produce flaws in the starch granules' surface and decrease the gelatinisation temperature and starch enthalpy of gelatinisation (Majzoobi and Beparva, 2014).

3.2.2.7 Sodium hydroxide

Sodium hydroxide (NaOH), supplied by Fisher Scientific (UK), was also used as pH modifier of gels and for their rheological characterisation (see Section 3.4.3.4). Table 3.10 shows some relevant parameters of Sodium hydroxide from the technical specification.

Table 3.10. TECHNICAL SPECIFICATION OF SODIUM HYDROXIDE (Fisher Scientific, 2015b)

PARAMETER	VALUE
Purity (%)	>97
Density (g/cm^3)	2.13
pH	14

3.2.3 FILLERS

Three fillers were used in hydrogel composite foams: biomass powders (from two different sources: oat and wheat straw), silicone oxide aero-gel powder and expanded vermiculite particles. Fillers were incorporated into hydrogel solutions for cost reduction and properties enhancement of the composite foams.

3.2.3.1 Biomass Powders

Fine Biomass powders, derived from oat husks and grey grain straw, were supplied by Biopower Technologies (UK). These powders were used as fillers for gelatine foams in

attempt to decrease costs while maintaining the biodegradability of the hydrogel-biomass composite foams. Table 3.11 shows the technical specification of both powders.

Table 3.11. TECHNICAL SPECIFICATION FOR POWDERS OF GREY GRAIN STRAW (Biopower Technologies, 2016a) **AND OAT HUSK** (Biopower Technologies, 2016b)

PARAMETER	GREY GRAIN STRAW	OAT HUSK
Appearance	Creamy light brown coloured loose powder	Light cream coloured loose powder
Bulk Density (g/m^3)	0.2	0.21
Real Density* (g/m^3)	1.29 ±0.04	1.55±0.11
Moisture content* (%)	4	7.5
Ash content (%)	3	3

*Parameters measured by the author (see Section 3.4.2)

SEM images of straw and oat powders are shown in Figures 3.7.A and 3.7.B. Straw and oat particles ranged approximately from 20 to 900*μm* and 5 to 600*μm,* respectively.

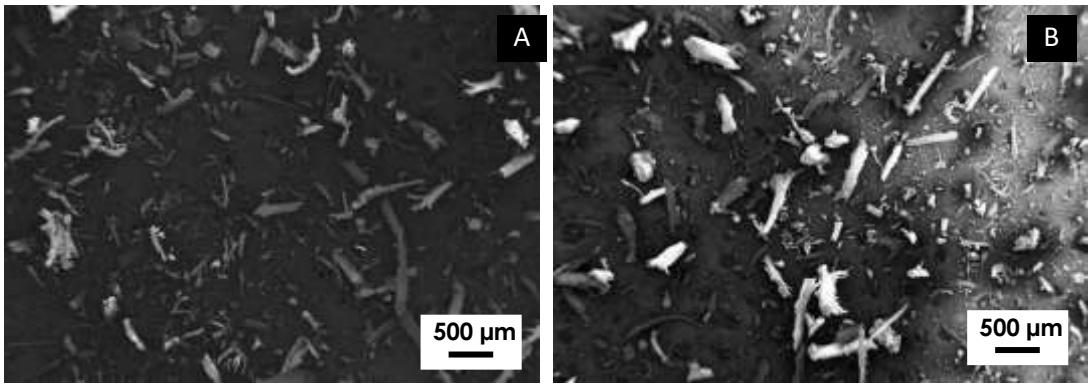

Figure 3.7. SEM IMAGES OF BIOMASS POWDERS. (A) GREY GRAIN STRAW, (B) OAT HUSK

3.2.3.2 Vermiculite

Expanded vermiculite ($(Mg, Fe^{+2}, Fe^{+3})_3[(Al, Si)_4O_{10}] (OH)_2 \cdot 4H_2O$) loose fill, supplied by Minelco Specialities Ltd (UK) was used to produce gelatine-composite foams. Expanded vermiculite is a low-density hydrous phyllosilicate mineral with good thermal insulation and fire resistance and thus selected to improve the composite foams' properties with construction applications in mind. "Coarse" (particles ranged approximately from 2 to 7 mm) and "fine" (particles ranged approximately from 0.5 to 2 mm) expanded vermiculite loose fill grades (shown in Figure 3.8) were selected. The author obtained the real density of 18 kg/cm^3 and moisture content of 5% following the procedures explained in Sections 3.4.2.

Figure 3.8. OPTICAL MICROSCOPE IMAGES OF THE EXPANDED VERMICULITE PARTICLES (A) COARSE VERMICULITE (B) FINE VERMICULITE

SEM images (Figure 3.9) of the expanded vermiculite loose fill reveals the porous laminated structure of the particles.

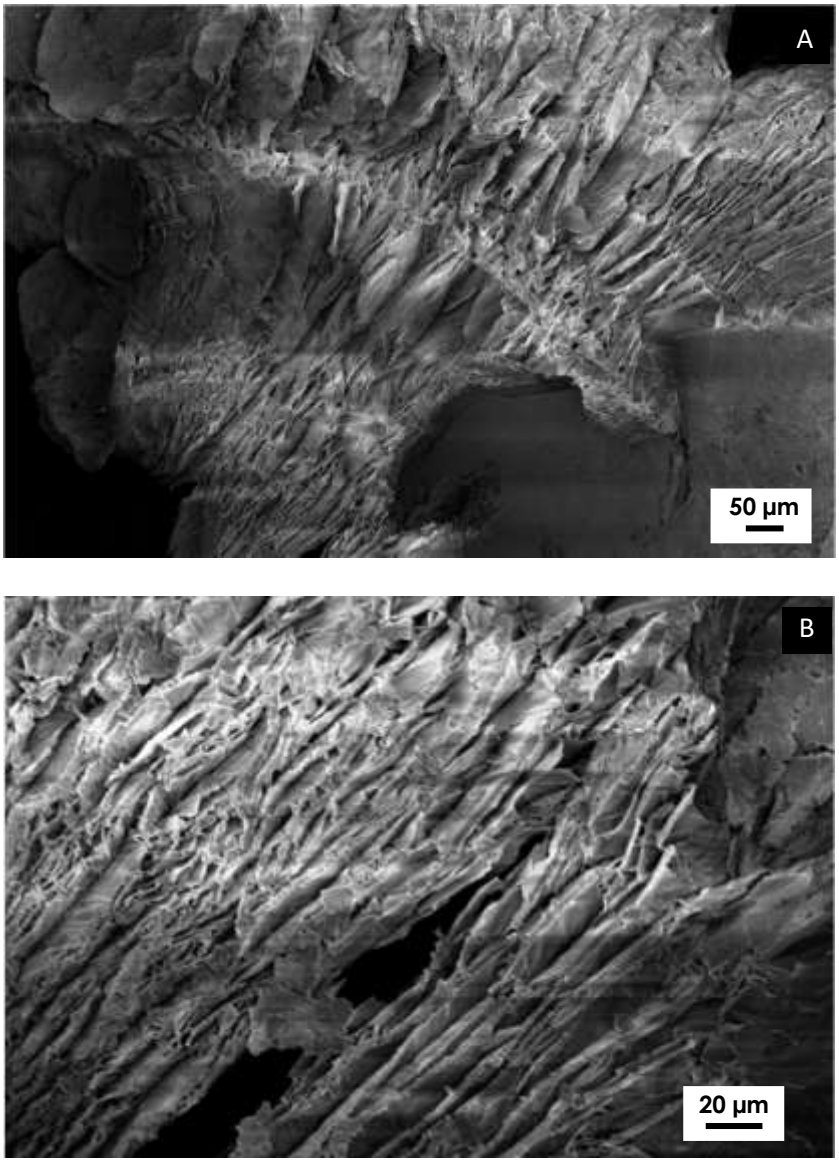

Figure 3.9. SEM IMAGES OF THE EXPANDED VERMICULITE PARTICLES SHOWING THE LAMINATED POROUS STRUCTURE

3.2.3.3 Silicon Dioxide Aerogel

Two Silicon dioxide (SiO_2) aero-gel powders, one hydrophobic and the other hydrophilic, were donated by Shenzhen Polytechnic University (China).

They were used to formulate gelatine hydrogel-aero-gel foams. The SiO_2 aerogel is ultra-light with excellent thermal insulation properties, and thus the incorporation of it into gelatine hydrogel foams is for the study of its influence in thermal conductivity of the composite foams. Table 3.12 shows technical specifications of the aerogel.

Table 3.12. TECHNICAL SPECIFICATION OF THE SILICON DIOXIDE AERO-GEL POWDERS

PARAMETER	HYDROPHOBIC AEROGEL	HYDROPHILIC AEROGEL
Appearance	White powder	White powder
Bulk Density (g/m^3)	0.08	0.08
Thermal conductivity ($W/m \cdot K$)	0.018±0.002	0.018±0.002
Granule size (μm)	1-20	1-20

Figure 3.10 shows SEM images of the hydrophilic and hydrophobic silica aerogel particles. The particle size ranged from less than 5 to 75*μm*.

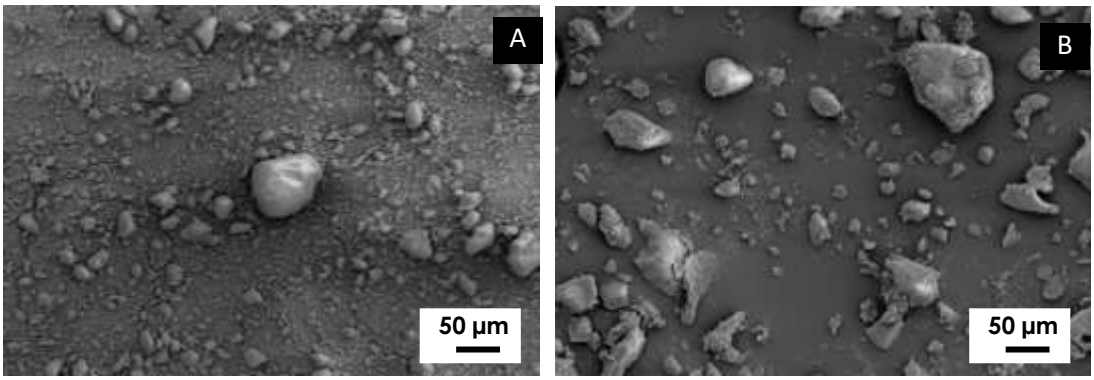

Figure 3.10. SEM IMAGES OF SILICA AERO-GEL PARTICLES (A) HYDROPHOBIC AEROGEL, (B) HYDROPHILIC AEROGEL

3.2.4 OTHER MATERIALS

This section describes materials which did not fall in any of the previous categories: water, used as a solvent for the liquid foams, and honeycomb boards.

3.2.4.1 Honeycomb boards

Gelatine-Hydrogel foams, in their liquid stage, were used to fill in cavities in cardboard and Nomex® honeycomb structures to enhance their mechanical (strength and stiffness) while maintaining the light-weight characteristics.

The Nomex® honeycombs boards were supplied from Easy Composites Ltd (UK) in two different cell sizes: 3.2 *mm* (aerospace grade), supplied in boards of 600 x 600 x 3 *mm*, and 4.8 *mm* (commercial grade), supplied in boards of 600 x 600 x 10 *mm*. Nomex® boards are made of woven aramid fibres of random orientations. Phenolic resin is used as adhesive. It would be ideal to experiment with boards with different cell sizes and same thickness, but it was commercially not possible.

The cardboard honeycombs boards were supplied in two different cell sizes (15 and 27 *mm*) by Dufaylite Development Ltd (UK). Both boards dimensions were 600 x 600 x 10 *mm*. They were supplied with glued top and bottom cardboard face sheets, but the

face-sheets specification was not available. The honeycomb boards were made from 100% recycled core and FSC certified faces.

Table 3.13 shows the technical specification of the honeycomb boards provided by the suppliers.

Table 3.13. TECHNICAL SPECIFICATION OF HONEYCOMB BOARDS (Dufaylite Ltd, 2017)

(Easy Composites Ltd, 2017)

PARAMETER	NOMEX 3.2*mm*	NOMEX 4.8*mm*	ULTRABOARD 15*mm*	ULTRABOARD *27mm*
Cell size (*mm*)	3.2	4.8	15	27
Thickness (*mm*)	3	10	10	10
Density (kg/m^3)	29	48	10.5	9.5
Wall thickness* (*t*) (mm)	0.1	0.12	0.25	0.25
Average wall length* (*l*) (mm)	2.3	3.6	7.4	11.7
Angle Θ (°)	50	35	45	40

*Parameters measured by the author (see Section 3.7)

The skins used for Nomex® honeycombs were supplied from Premier Paper (UK). They were A4 sized sheets with 1 *mm* thickness and 480 *gsm* grammage.

3.2.4.2 Solvent

Municipal water supplied by Affinity water to Brunel University was used as a low-cost solvent for the biopolymer solutions/suspensions.

Table 3.14 presents the published water quality parameters from the supplier for the period from 01/01/2016 to 31/12/2017. This water was categorised as 'hard water' due to the natural presence of high $CaCO_3$ concentration (from 151 to 300 *ppm*) (Affinity Water, 2017).

Table 3.14. WATER QUALITY CHARACTERISTICS (Affinity Water, 2017)

PARAMETER	VALUE
Alkalinity (*mg HCO_3/L*)	192
Calcium (*mg Ca/L*)	111
Chlorine (*mg Cl_2/L*)	0.59
Fluoride (*mg F/L*)	0.118
Total Hardness (*mg $CaCO_3$/L*)	278
pH value	7.4

3.3 PROCEDURES FOR LIQUID PREPARATION, FOAMING AND DRYING OF LIQUID FOAMS

This section describes the details of the experiments in formulation design of solutions, the liquid foaming, the conversion to gel foams and drying to achieve solid foams,

followed by the sample (in liquid, gel and solid states) preparation and characterisation.

This research aims to fill a gap in technology, as currently is not possible to produce commercially viable bio-foams in bulk sizes. Therefore, a liquid foaming technology to manufacture bio-based bulk foams for thermal packaging applications was developed.

Liquid foaming consists in the transformation of a liquid foamed polymer solution into a porous solid polymer through liquid removal. The liquid foaming process consists of 6 steps (Figure 3.11). In terms of physical state of the material, the process consists of three stages: liquid stage (formulation of the liquid), liquid foam stage (foaming and casting), and gel to solid stage (conversion of liquid foam to solid through foam gelling and drying).

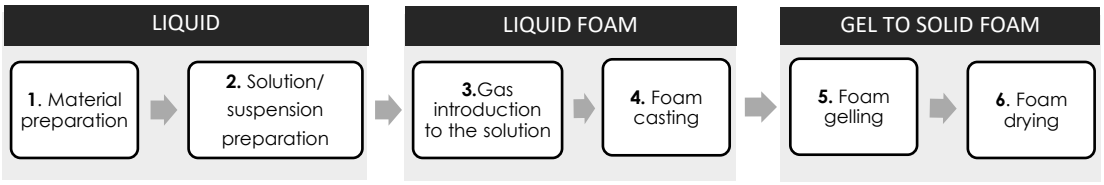

Figure 3.11. FLOW DIAGRAM OF LIQUID FOAMING TECHNOLOGY

The formulation of the liquid consists of raw materials and solution/suspension preparation, involving incorporation of materials, additives and fillers into a liquid solution or suspension. The rheological and gelling behavior of the liquid systems can be assessed. Gas is then introduced into the liquid (e.g. using a mechanical method or blowing agent) and cast into the desired shape (sheets, boards or 3D mouldings). The volume expansion of the liquid and stabilisation of the foam can be assessed at this point.

The cast foam was stabilised by gelling and, following a drying process, the dried foams were characterised in terms of density, shrinkage, foam cell structure and properties (mechanical, thermal conductivity, acoustic and fire resistance, depending on potential applications).

Five liquid foaming formulation systems were explored in this research:

- System 1. Starch-PVAc-Calcium sulphate foams
- System 2. Starch-gelatine foams
- System 3. Gelatine hydrogel foams

- System 4. Gelatine hydrogel-composite foams, including:
    - Subsystem 4.1. Biomass-hydrogel foams
    - Subsystem 4.2. Vermiculite-hydrogel foams
    - Subsystem 4.3. Silica aerogel-hydrogel foams
    - Subsystem 4.4. Honeycomb structures infiltrated with hydrogel foams
- System 5. Hydrogel foams alternative to gelatine, including:
    - System 5.1 Agar hydrogel foams
    - System 5.2. Gellan gum hydrogel foams

3.3.1 KEY CONSIDERATIONS IN FORMULATION DESIGN OF THE LIQUID

The aim of the formulation design was to create a solution/suspension able to achieve high expansion rate, stable liquid foams and ultimately low density solid foams on drying. Accordingly, the initial solution was required to produce high expansion ratio on foaming, with uniform fine cell structure and high foam stability during forming and casting/moulding stages.

Formulation of the liquid, solid content and concentration of additives determine liquid viscosity and surface tension, and thus influence their behavior in subsequent foaming, casting, gelling, drying and final product properties.

The liquid viscosity is dependent on the formulation, such as solid/water content, additives and concentration. Higher concentration of gelling agents, such as gelatine, agar and gellan gum was desirable to stabilise liquid foams (via gelling strength) and lower shrinkage during the drying process. However, high gelling agent concentration will also increase the solution/suspension viscosity considerably, resulting in lower expansion ratios. The use of fillers, such as biomass powders, aerogels or vermiculite, will also increase liquid viscosity and liquid heterogeneity and hence, the appropriate concentration needs to be identified. The other modifiers (e.g. PVAc, glycerol and sorbitol) may also affect the liquid viscosity.

In addition to formulation, processing conditions such as liquid temperature and agitation speed (shear rate) also affect liquid viscosity, which in turn influences the foam expansion ratio (degree of air incorporation) and the foam stability (e.g. via liquid film stretchability and reduction of drainage).

Low liquid surface tension was desirable to maximise volume expansion during foaming (via reduction of bubble expansion resistance) and assist foam stabilisation (via reduction of the bubble collapsing). This was mainly archived by effective use of surfactants in the solution/suspension.

The foam expansion ratio and stabilisation determine the density and properties of the solid foam and thus, were the key parameters in the formulation studies.

3.3.2 METHODOLOGIES IN EXPERIMENTAL DESIGN AND DATA ANALYSIS

The one-factor-at a time method of experimentation shows an estimate of the effect of a factor at given and fixed conditions of the other factors (Jiju, 2003). This experimental method was used in the feasibility study of calcium sulfate-PVAc-starch foams, starch-gelatine foams and after that in the in-depth studies of hydrogel foams (i.e. the effect of the liquid foams expansion ratio on dry foams and the study of drying conditions).

Full factorial experiment designs are extensively used in manufacturing (Jiju, 2003) and formulation optimisation (Chattopadhyay, De and Datta, 2015). They are then adapted in the formulation study of hydrogel gelatine foams and their composites foams, where the influence of the key factors in formulation and foaming behavior was analysed to identify desirable formulations to achieve the required material properties (low density, low shrinkage and high expansion ratio, among others).

Full factorial analysis consists in the following steps:

- Experimental Design. Factors, levels and number of replications choice to study a given outcome.

- Experimental work/measurement. At this stage, the outcome is measured for the different factors and level combinations.

- Statistical Analysis and interpretation. The results obtained in the experimental work are analysed using regression analysis and analysis of variance, usually by statistical software, like R, Minitab or SPSS.

A full factorial experiment consists of two or more factors studied at *k* levels. A factor is a controlled independent variable in the design. Each factor (*n*) has different discrete values or levels (*k*). As an illustration, Table 3.15 shows the settings for a full factorial design with three factors at three levels (3^3): low (-1), standard (0) and high (+1).

Table 3.15. LOW (-1), STANDARD (0) AND HIGH (+1) SETTINGS FOR A FULL FACTORIAL DESIGN WITH 3 FACTORS AT THREE LEVELS (3^3)

FACTOR LEVELS	LOW LEVEL	STANDARD LEVEL	HIGH LEVEL
Factor 1	-1	0	+1
Factor 2	-1	0	+1
Factor 3	-1	0	+1

Table 3.16 shows the settings for a full factorial design with three factors at two levels low (-1) and high (+1).

Table 3.16. LOW (-) AND HIGH (+) SETTINGS FOR A FULL FACTORIAL DESIGN WITH 3 FACTORS AT TWO LEVELS (3^2)

FACTOR LEVELS	LOW LEVEL	HIGH LEVEL
Factor 1	-	+
Factor 2	-	+
Factor 3	-	+

The factorial experiment consists of testing all the combinations of levels, *k*, for every factor (Antony, 2003). Therefore, the total number of samples to prepare for researching *n* factors at two levels is 2^n (k^n), and for *n* factors at three levels, 3^n. This allows investigating the effect of each factor on an outcome, as wells as the effect of interactions between factors on the outcome. Table 3.17 presents the full factorial design table ran in standard order for three factors at two levels.

Table 3.17. A 2^3 (THREE FACTORS, TWO-LEVEL) FULL FACTORIAL DESIGN TABLE SHOWING RUNS IN STANDARD ORDER

RUN NUMBER	FACTOR 1	FACTOR 2	FACTOR 3	OUTCOME 1 (y)
1	-	-	-	X_1
2	+	-	-	X_2
3	-	+	-	X_3
4	+	+	-	X_4
5	-	-	+	X_5
6	+	-	+	X_6
7	-	+	+	X_7
8	+	+	+	X_8

A factorial experiment can be analysed using regression analysis and analysis of variance (ANOVA). In this research, the ANOVA analysis was performed using Minitab 17 Statistical Software (2010).

ANOVA examined the null hypothesis (H_O), the assumption that the means of two or more populations were equal. The alternative hypothesis (H_1) stated that at least one of the means was different.

ANOVA also evaluated the significance of the different factors by contrasting the outcomes means at the different factor levels.

Table 3.18 shows an example of an ANOVA table for an experiment where three factors at three levels were analysed. The elements of the ANOVA table are:

- Degrees of freedom (DF) is the number of independent observations in the calculation.

- Adjusted sums of squares (Adj SS). It is a measure of variation for the different components of the model. It was used to calculate the p-value, and it is not usually interpreted.

- Adjusted mean squares (Adj MS). It measures how much variation a term or a model explains. As *Adj SS*, it was used to calculate the p-value and was not studied in isolation.

- F-value. It is a test statistic used to conclude if the term is associated with the response. It was used to calculate the p-value.

- p-value. To determine the statistical significance of the differences between the means, the null hypothesis was assessed comparing the p-value. This value helps to quantify the error in a hypothesis test as it provides support to decide whether to reject or accept the null hypothesis at a given accuracy or chance to make a correct conclusion. A significance level of 0.05 (i.e. a 5% risk of concluding that a difference exists when there is no actual difference) was used in all the analysis carried out in this project. This means a confidence level of 95%. When the p-value was less than or equal to the significance level, the null hypotheses was rejected, and it was concluded that not all population means were equal. When the p-value was greater than the significance level, there was not enough evidence to reject the null hypothesis that the population means were all equal.

Table 3.18. EXAMPLE OF ANOVA TABLE FOR 3^3 FACTORIAL DESIGN

SOURCE	DF	ADJ SS	ADJ MS	F-VALUE	P-VALUE
Model	**26**	**110.837**	**6.5198**	**29.57**	**0.000**
Linear	6	103.487	20.70	93.87	0.000
Factor 1	2	64.062	32.03	145.27	0.000
Factor 2	2	26.287	13.14	59.61	0.000
Factor 3	2	13.138	13.14	59.59	0.000
2-Way Interactions	**12**	**5.866**	**0.73**	**3.33**	**0.006**
Factor 1*Factor 2	4	4.623	1.16	5.24	0.002
Factor 1*Factor 3	4	0.993	0.50	2.25	0.572
Factor 2*Factor 3	4	0.25	0.12	0.57	0.120
3-Way Interactions	**8**	**1.485**	**0.37**	**1.68**	**0.175**
Factor 1*Factor 2*Factor 3	8	1.485	0.37	1.68	0.175
Error	54	7.938	0.22		
Total	**80**	**118.775**			

Main effect plots and interaction plots were also used as analysis tools for factorial designs. Main effects plots display how the categorical factors were related to the response. Interaction plots exhibit how the relationship between one factor and a response depended on the value of a second factor. Interaction plots show the means for the levels of one factor on the x-axis and separate curves for each level of a second factor. The analysis of these curves showed how the interaction affected the two factors and the outcome. Parallel lines imply no interaction, while non-parallel lines mean that interaction occurs. The higher the interaction, the more non-parallel the lines are. A 3-way interaction is interpreted as how one or more 2-way interactions are related to a third factor.

3.3.3 SAMPLE PREPARATION AND EXPERIMENTAL DETAILS

The sample preparation was conducted at typical laboratory conditions (22 ±5°C and 45±20% relative humidity).

This section describes the preparation of each system mentioned at the beginning of Section 3.3, as well as the experimental details.

3.3.3.1 System 1. Starch-PVAc-Calcium Sulfate foams

This section discusses the sample preparation and the experimental work carried out for system 1, Starch-PVAc-Calcium sulfate foams. Liquid foams require stabilisation during the drying process. The additives used as stabilisers were Polyvinyl Acetate (PVAc) and calcium sulfate (Plaster of Paris, POP) for stretchability and solidification enhancement, respectively.

The study aimed to prove the feasibility of starch-PVAc-POP foams. It consisted in three stages: the initial formulation development, the study of the increase in starch concentration in the initial solution and the study of the decrease in water content in the higher starch content formulations.

First, the experimental work carried out is discussed. Then, the sample preparation process for the initial recipe is explained.

3.3.3.1.1 Refinement 1. Increase in starch concentration

Through preliminary tests based on suitable liquid viscosity for mechanical foaming method (using a handheld power mixer with a whisking accessory) and stability of the liquid foams, a preliminary formulation was identified as a starting point (see Table 3.19) for subsequent modification of the formulation towards: lower content of calcium sulfate and PVAc, lower drying shrinkage, absence of defects (such as cracks and large cavities) developed in the cast foam during drying and lower dry foam density.

Table 3.19. INITIAL FORMULATION OF POP-PVA-STARCH FOAMS (*mass & wt%*)

ID	DETERGENT		PVAc		STARCH		WATER		POP		TOTAL MASS (g)
	g	*wt%*	g	*wt%*	g	*wt%*	g	*wt%*	g	*wt%*	
PO1	5	1.23	150	36.86	12	2.94	100	24.57	140	34.40	407

As seen in Table 3.19, PVAc and POP were the major solid components in PO1, the initial formulation. High starch content was desirable to improve the material biodegradability. Thus, this experiment aimed to study the increase in starch concentration in the initial formulation.

Two factors, detergent content and starch content, were studied at different levels. Starch and detergent concentrations were increased while the other parameters were kept constant.

Table 3.20 shows the experiment formulation matrix where the content of detergent, PVAc, starch and POP are in mass and weight percentage based on the mass of the total solution. The total mass of each batch was not kept constant because just one parameter of the formulation was changed each time on a weight basis.

Table 3.20. STARCH-PVA-POP FOAMS. FORMULATION MATRIX FOR INCREASE IN STARCH CONCENTRATION (MASS AND *wt%* ON BASIS OF TOTAL MASS OF SOLUTION)

ID	DETERGENT		PVAc		STARCH		WATER		POP		TOTAL MASS (g)
	g	*wt%*	g	*wt%*	g	*wt%*	g	*wt%*	g	*wt%*	
PO2	15	3.51	150	35.09	22.5	5.26	100	23.39	140	32.75	427.5
PO3	15	3.47	150	34.68	27.5	6.36	100	23.12	140	32.37	432.5
PO4	15	3.43	150	34.29	32.5	7.43	100	22.86	140	32.00	437.5
PO5	15	3.39	150	33.90	37.5	8.47	100	22.60	140	31.64	442.5
PO6	15	3.35	150	33.52	42.5	9.50	100	22.35	140	31.28	447.5
PO7	7.5	1.79	150	35.71	22.5	5.36	100	23.81	140	33.33	420
PO8	7.5	1.76	150	35.29	27.5	6.47	100	23.53	140	32.94	425
PO9	7.5	1.74	150	34.88	32.5	7.56	100	23.26	140	32.56	430
PO10	7.5	1.72	150	34.48	37.5	8.62	100	22.99	140	32.18	435
PO11	7.5	1.70	150	34.09	42.5	9.66	100	22.73	140	31.82	440

The detergent content was increased in an attempt to increase the expansion ratio of the foam and subsequently, decrease the dry foam density. The detergent content was studied at two levels:

- Low level, increase from 5 to 7.5 *g* (i.e. from 1.23 *wt%* to 1.70-1.79 *wt%)*
- High level, increase from 5 to 15 *g* (i.e. from 1.23 *wt%* to 3.35-3.51 *wt%)*

Starch content was studied at 5 levels, chosen on a weight basis and ranging from 22.5 *g* to 42.5 g (i.e. from ~5.3 *wt%* to ~9.7 *wt%*).

The outcomes measured in this experiment were:

- Liquid foam volume expansion (see Section 3.5)
- Drying time (see Section 3.6.1)
- Dry foam density (see Section 3.6.2)
- Moisture content of the dry foams (see Section 3.6.3)
- Dry foams shrinkage (see Section 3.6.4)

3.3.3.1.2 Refinement 2. The decrease in water concentration

PO7, PO8 and PO9 were the samples exhibiting lower cracking tendency in Refinement 1. To reduce the drying shrinkage/time and minimise the sample defects during drying (e.g. cracks) changes in water and detergent concentration were explored on the basis of the three formulations, as shown in Table 3.21.

Table 3.21. STARCH-PVA-POP FOAMS. FORMULATION MATRIX FOR DECREASED WATER CONCENTRATION (MASS AND *wt%* ON BASIS OF TOTAL MASS OF SOLUTION)

ID	DETERGENT		PVAc		STARCH		WATER		POP		TOTAL MASS (g)
	g	*wt%*	g	*wt%*	g	*wt%*	g	*wt%*	g	*wt%*	
PO7.2	10	2.52	150	37.74	22.5	5.66	75	18.87	140	35.22	397.5
PO8.2	10	2.48	150	37.27	27.5	6.83	75	18.63	140	34.78	402.5
PO9.2	10	2.45	150	36.81	32.5	7.98	75	18.40	140	34.36	407.5
PO7.3	7.5	1.90	150	37.97	22.5	5.70	75	18.99	140	35.44	395
PO8.3	7.5	1.88	150	37.50	27.5	6.88	75	18.75	140	35.00	400
PO9.3	7.5	1.85	150	37.04	32.5	8.02	75	18.52	140	34.57	405

The detergent and starch contents were refined at reduced water content levels.

Two levels of detergent content were studied:

- Low level. The detergent content was kept at 7.5 *g* (i.e. 1.85-1.90 *wt%)*
- High level. The detergent content was slightly increased to 10 *g* (i.e. 2.45-2.52 *wt%),* lower than the higher level in Refinement 1, which resulted in more defected samples compared with the lower detergent content level)

Starch content was refined at three levels, ranging from 22.5 *g* (i.e. 5.66-5.70 *wt%*) to 32.5 g (i.e. 7.98-8.02 *wt%*), following the starch content levels of samples PO7, PO8 and PO9.

Water content was reduced from 100 *g* (i.e. 23.26-23.81 *wt%*), used for PO7, PO8 and PO9, to 75 g (i.e. 18.40-18.99 *wt%*).

Perforated moulds were use in an attempt to reduce drying timescale. The PS moulds used in previous experiments were perforated with a vanadium-steel punch (perforation size 1*mm*) to expose all the liquid foam faces and facilitate their water removal.

The outcomes measured in this experiment were:

- Liquid foam volume expansion (see Section 3.5)
- Drying time (see Section 3.6.1)
- Dry foam density (see Section 3.6.2)
- Moisture content of the dry foams (see Section 3.6.3)
- Dry foams shrinkage (see Section 3.6.4)

3.3.3.1.3 Sample preparation methods

The preparation of all starch-PVAc-POP foams followed the procedures described below:

a. Solution preparation. First, a starch suspension in water was prepared in a glass beaker (covered with aluminium foil to minimise water evaporation) and heated on an IKA C-MAG HS 7 ceramic hot plate to 80±5°C for 10 minutes while magnetically stirred. Then, the liquid was mechanically sheared with a hand-held electric liquidiser (at 80±5°C for 20 minutes) to destructurise starch granules and transform the suspension into a thermoplastic starch (TPS) solution. Then, detergent, PVAc and POP, respectively, were incorporated at the required concentrations. The blend was mixed and magnetically stirred on the hot plate at 80±5°C for 10 minutes.

b. Foaming. The liquid formulated was foamed at 80±5°C by beating using a handheld electric mixer (Bosch MSM6700GB, 600 *W*) with a whisking accessory for about 15 minutes, when full volume expansion was achieved.

c. The liquid foam was then poured into a 100 cm^3 PS weigh boat (with dimensions 80 x 80 x 30 *mm*), used as a mould, and let to dry naturally in the laboratory. The dry sample was released from the mould and set aside for characterisation.

3.3.3.2 System 2. Starch-gelatine foams

This section describes the sample preparation and the experimental work carried out for system 2, the starch-gelatine foam systems.

This study aimed to prove the feasibility of starch-gelatine foams without the use of POP as foam solidification agent to reduce foam density and maintain high biodegradability. Section 3.3.3.2.1 describes the preliminary formulation study. Section 3.3.3.2.2, following the results from the previous section, carries out optimisation of the formulation. Finally, Section 3.3.3.2.3 reports the preparation of starch-gelatine foams.

The objectives of this study were the following:

- To identify the key parameters of formulation and process conditions for the starch-gelatine system, using gelatine as a gelling agent for liquid foam stabilisation
- To investigate the role of the different formulation factors (surfactant/detergent content, solid content, gelatine strength, gelatine-starch ratio) on foaming, drying behavior of the liquid foams and impact on foam structure and properties of the solid foams

3.3.3.2.1 Experiment 1. Preliminary study of starch-gelatine foams

This preliminary study aimed to understand the role of the key formulation factors (detergent content, gelatine strength and starch-gelatine ratio), on the liquid foaming behavior, foam stabilisation and solid foam properties.

The objectives of this preliminary study were:

- To test the sensitivity of liquid foaming behaviour to the formulation factors: detergent concentration, starch/gelatine ratio and gelatine strength
- To identify a workable range of formulation and process conditions for liquid foaming of the starch-gelatine system

In order to carry out a preliminary study, some simplifications were made. Three variables were studied at 2-levels. The chosen three factors were: detergent content, gelatine strength and the starch-gelatine ratio (see Table 3.22), while the total starch and gelatine concentration were fixed at 18 *wt%* which was expected to result in reasonable viscosity level for mixing and foaming.

Table 3.22. FACTORS AND LEVELS FOR THE PRELIMINARY STUDY OF STARCH-GELATINE FOAMS

VARIABLE	FACTOR ID	LOW LEVEL	HIGH LEVEL
1. DETERGENT (*wt%*)	A	0	1.2*wt%*
2.STARCH-GELATINE CONCENTRATION	B	5.4*wt%* starch 12.6*wt%* gelatine	9*wt%* starch 9*wt%* gelatine
3. GELATINE STRENGTH	C	Low Bloom	High Bloom

The reasons for the selected levels were:

Factor A, Detergent content.

Low level was without surfactant and high level at 1.2 *wt%*, found sufficient for enhancing volume expansion from the study of system 1 (see Table 3.19).

Factor B, Starch-gelatine ratio.

- Low level: the starch content of 5.4 *wt%* and gelatine content of 12.6 *wt%* (i.e. a 30/70 starch/gelatine ratio) represents a conservative high gelling agent concentration for effective gelation of the liquid foam and thus higher foam stability against foam collapsing
- High level: The 9 *wt%* each (i.e. 50/50 starch/gelatine ratio) represent significant starch concentration based on considerations of costs as starch is more than

ten times cheaper than gelatine. In bulk sizes, as an example, the high Bloom gelatine costs £5.8 per *kg* and purified wheat starch, £0.49 *per kg*, according to the supplier (Tereos Syral, UK)

Factor C, gelatine strength.

Higher gelatine strength reflects higher gelling power at a given concentration although it is also associated with higher costs. Both low level (low Bloom) and high level (high Bloom) of gelatine strength were chosen on recommendations from the supplier.

In addition to this, as starch and gelatine are both susceptible to microbial spoilage, 0.35 *wt%* acetic acid was added to avoid mould and bacteria growth during the slow natural drying, as recommended by Lund *et al* (2000).

Table 3.23 summarises the experiment design table. Runs of liquid preparation were randomised to minimise the bias induced due to human errors and environmental variations.

Table 3.23. FORMULATION DESIGN MATRIX FOR PRELIMINARY STUDY OF STARCH-GELATINE FOAMS

			FACTOR A	FACTOR B	FACTOR C
ID	**RUN NUMBER**	**RANDOM ORDER**	**DETERGENT CONTENT (*wt%*)**	**STARCH - GELATINE RATIO**	**GELATINE STRENGTH**
ST1	1	2	0	30-70	Low
ST2	2	6	1.2	30-70	Low
ST3	3	4	0	50-50	Low
ST4	4	8	1.2	50-50	Low
ST5	5	5	0	30-70	High
ST6	6	3	1.2	30-70	High
ST7	7	1	0	50-50	High
ST8	8	7	1.2	50-50	High

Table 3.24 summarises the formulation used for each run of the experiment, in mass and weight percentage.

Table 3.24. FORMULATION TABLE FOR THE PRELIMINARY STUDY OF THE STARCH-GELATINE SYSTEM

ID	DETERGENT		STARCH		GELATINE		GELATINE STRENGTH	WATER		ACETIC ACID		TOTAL MASS (g)
	g	wt%	g	wt %	g	wt%		g	wt%	g	wt%	
ST1	0	0	22.5	5.43	52.5	12.68	Low	337.5	81.52	1.5	0.36	414
ST2	5	1.19	22.5	5.37	52.5	12.53	Low	337.5	80.55	1.5	0.36	419
ST3	0	0	37.5	9.06	37.5	9.06	Low	337.5	81.52	1.5	0.36	414
ST4	5	1.19	37.5	8.95	37.5	8.95	Low	337.5	80.55	1.5	0.36	419
ST5	0	0	22.5	5.43	52.5	12.68	High	337.5	81.52	1.5	0.36	414
ST6	5	1.19	22.5	5.37	52.5	12.53	High	337.5	80.55	1.5	0.36	419
ST7	0	0	37.5	9.06	37.5	9.06	High	337.5	81.52	1.5	0.36	414
ST8	5	1.19	37.5	8.95	37.5	8.95	High	337.5	80.55	1.5	0.36	419

The outcomes measured in this experiment were:

- Liquid foam volume expansion (see Section 3.5)
- Drying time (see Section 3.6.1)
- Dry foam density (see Section 3.6.2)
- Moisture content of the dry foams (see Section 3.6.3)
- Volume shrinkage (see Section 3.6.4)
- The dry foam structure of sample ST8 (Section 3.6.5)
- The dry foam thermal conductivity of sample ST8 (Section 3.6.7)
- Assessment of the TPS liquids (see Section 3.4.3.1)

3.3.3.2.2 Experiment 2. Refinement of the starch-gelatine foams

This experiment investigates the use of industrial surfactant in starch-gelatine foams at different solid contents and starch-gelatine ratios.

This study aimed to investigate the effect of surfactant C2, as a known industrial surfactant, replacing the detergent without sufficient knowledge of its composition. The use of the organic acid preservative was expected to both hinder the gelation process (see Section 2.5.5.7 in Chapter 2) and reduce biodegradation of the solid foam, and thus, its elimination was investigated.

The objectives of this experiment were:

- To study the effect of surfactant C2 use on liquid foaming behaviour of the starch-gelatine system in terms of expansion ratio
- To study the drying process of starch-gelatine foams prepared with surfactant C2 regarding drying shrinkage
- To assess the impact of acetic acid elimination during drying
- To analyse the structure of starch-gelatine foams with surfactant C2 in terms of dry foam density, foam structure and properties

Three variables were studied at 2-levels (see Table 3.25). The chosen factors were: gelatine-starch ratio, total solid content and preservative content. Surfactant C2 content was kept constant at 0.75 *wt%* of the total mass of the starch-gelatine-water suspension, after preliminary trials followed by optimisation, as detailed in Chapter 5. High *Bloom* gelatine was found to generally produce lighter and less volume shrinkage-prone foams, so it was selected to use in this experiment.

Table 3.25. FACTORS AND LEVELS FOR THE REFINEMENT STUDY OF THE STARCH-GELATINE FOAMS

VARIABLE	FACTOR ID	LOW LEVEL	HIGH LEVEL
1.STARCH-GELATINE RATIO	A	30/70	50/50
2. SOLID CONTENT (*wt%*)	B	14	18
3. PRESERVATIVE CONTENT (*wt%*)	C	0	0.3

The reasons to focus on these factors and their selected levels were:

Starch-gelatine ratio. As seen in the results of the previous experiment, lower starch content foams exhibited lower densities and higher expansion ratios. Therefore, the starch content was not further increased, and a starch-gelatine ratio of 30/70 was chosen as low level and 50/50 as high level.

Solid content. The low level was adjusted at 14 *wt%* in an attempt to reduce the dry foam density. The high level was kept at 18 *wt%*, as from the preliminary study.

Preservative content. This is to clarify if the elimination of acetic acid would lead to mould growth problems during the natural dry process. The low level was chosen as no-preservative content, and 0.3 *wt%* (of the starch-gelatine solution) was chosen as high level, slightly lower than the previous experiment.

Table 3.26 summarises the formulation design matrix. Runs of liquid preparation were randomised to minimise the potential bias due to human error or environmental variations.

Table 3.26. FORMULATION DESIGN MATRIX FOR THE REFINEMENT STUDY OF STARCH-GELATINE FOAMS

		FACTOR A	FACTOR B	FACTOR C
RUN NUMBER	**RANDOM ORDER**	**STARCH-GELATINE CONTENT**	**SOLID CONTENT**	**PRESERVATIVE CONTENT**
ST9	1	-	-	-
ST10	7	-	-	+
ST11	6	-	+	-
ST12	2	-	+	+
ST13	3	+	-	+
ST14	5	+	-	-
ST15	8	+	+	+
ST16	4	+	+	-

Table 3.27 summarises the formulation used for each run of the experiment, in mass and weight percentage.

Table 3.27. FORMULATION TABLE FOR THE REFINEMENT STUDY OF STARCH-GELATINE FOAMS

RUN No	**STARCH**		**GELATINE**		**DETERGENT**		**WATER**		**ACETIC ACID**		**TOTAL MASS (g)**
	g	***wt%***	**g**	***wt%***	**g**	***wt%***	**g**	***wt%***	**g**	***wt%***	
ST9	30	24.60	70	57.07	4.17	3.77	455.5	14.57	0.00	0	559.67
ST10	50	41.31	50	41.07	4.17	3.80	455.5	13.82	0.00	0	559.67
ST11	23.33	24.51	54.45	56.87	4.17	4.83	455.5	13.79	0.00	0	537.45
ST12	38.89	41.19	38.89	40.96	4.17	4.87	455.5	12.98	0.00	0	537.45
ST13	30	24.27	70	56.31	4.17	3.72	455.5	14.68	1.02	1.11	560.78
ST14	50	41.40	50	41.17	4.17	3.81	455.5	12.58	1.04	1.11	560.78
ST15	23.33	24.11	54.45	55.96	4.17	4.75	455.5	13.87	1.30	1.11	538.56
ST16	38.89	39.83	38.89	39.61	4.17	4.71	455.5	14.56	1.29	1.11	538.56

The outcomes measured in this experiment were:

- Liquid foam volume expansion (see Section 3.5)
- Drying time (see Section 3.6.1)
- Dry foam density (see Section 3.6.2)

- Moisture content of the dry foams (see Section 3.6.3)
- Volume shrinkage (see Section 3.6.4)
- Dry foam structure (Section 3.6.5)
- Dry foam compression properties (Section 3.6.6) for samples ST9-ST12
- Dry foam thermal conductivity (Section 3.6.7) for samples ST9-ST12

3.3.3.2.3 Sample preparation methods

The stages for sample preparation of starch-gelatine foams were as follows:

a. Preparation of starch-gelatine suspensions. Purified starch was firstly heated on a IKA C-MAG HS 7 ceramic hot plate to 80±5°C and magnetically stirred for 10 minutes in a concentration that ranged from 10.28-14.73 *wt%*. Secondly, acetic acid, as a preservative, if required, was incorporated into the starch suspension. Then, at the same temperature, the liquid was sheared using a hand liquidiser, Bosch MSM6700GB, 600 *W*, for 20 minutes to assist the breakdown of the starch granules and form an aqueous TPS solution. Simultaneously, the gelatine solution (low or high Bloom, as required) was prepared by a one-step process, where the gelatine (at 20.95-28.57*wt%)* was directly stirred into water at 80°C and, subsequently, homogeneously mixed with the prepared TPS solution. while heated and magnetically stirred on a hot plate at 50°C. Surfactant, if required, was added at this stage into the solution.

b. Foaming. The liquid formulated was then foamed using a handheld electric mixer with a whisking accessory (Bosch MSM6700GB, 600*W*) for about 10 minutes at 50°C, when a maximum volume expansion was achieved.

c. Finally, at the *casting* stage, the liquid foam was poured into a mould and let to dry naturally at laboratory conditions (see Section 3.4.1). The sample was released from the mould and cut as required.

3.3.3.3 System 3. Hydrogel foams made from gelatine

This section describes the sample preparation and the experimental work carried out for system 3, hydrogel foams prepared from gelatine.

This study aimed to prove the feasibility to produce gelatine hydrogel foams without using starch. As indicated in the study of system 2 (see Chapter 4), higher starch/gelatine ratio led to high foam density.

The objectives of this study were the following:

- To assess the impact of starch elimination on foam density
- To identify key formulation factors and processing conditions for the gelatine hydrogel foams
- To investigate the role of the different formulation (gelatine content, surfactant types and content and plasticiser content) and processing factors (processing temperature) in foaming behavior (expansion ratio), foam structure and properties
- To identify workable windows for formulation and processing for formulation refinement and optimisation.

Section 3.3.3.3.1 describes Experiment 1, where a preliminary formulation study was carried out to identify the influence of different types of surfactants and concentrations on the hydrogel foaming process for subsequent refinements.

Section 3.3.3.3.2, Experiment 2, on the basis of Experiment 1, a refinement was carried out where gelatine content, surfactant types and concentration, and processing temperature were considered in more detail, laying the foundation for further optimisations.

Sections 3.3.3.3.3 and 3.3.3.3.4 explain the study of the optimisation of formulations from Experiment 2 (Section 3.3.3.3.2) taking account of varying liquid foam expansion ratios and plasticiser types and contents, respectively. Then, Section 3.3.3.3.5 describes the experimental details of the drying process of the foams.

Finally, Section 3.3.3.3.6 reports the preparation of gelatine-hydrogel foams.

3.3.3.3.1 Experiment 1. Influence of surfactant type and content on gelatine-hydrogel foams

This experimental study aimed to establish the feasibility of the liquid foaming process in gelatine foams using different types and contents of surfactant.

The objectives of this study were:

- To identify a workable preliminary formulation and the process conditions for the hydrogel foaming process.
- To investigate and determine the influence of surfactant type and concentration on the foaming behaviour of the aqueous hydrogel solutions and the solid foam structure and properties.

For the solution preparation, gelatine was kept constant at 15 *wt%*. The surfactant was incorporated into the solution at different concentrations (0.05, 0.5, 5 *wt%*). Two factors, surfactant content (Factor A) and surfactant type (Factor B) were studied. Both factors A and B were studied at 3 levels, as seen in Table 3.28. Processing temperature was kept constant at 80±5°C.

Table 3.28. FORMULATION FACTORS AND LEVELS FOR SURFACTANT TYPE AND CONTENT IN GELATINE-HYDROGEL FOAMS

VARIABLE	**ID**	**LOW LEVEL (-1)**	**INTERMEDIATE LEVEL (0)**	**HIGH LEVEL (+1)**
1. SURFACTANT CONTENT (*wt%*)*	A	0.05	0.5	5
VARIABLE	**ID**	**LEVEL 1**	**LEVEL 2**	**LEVEL 3**
2. SUFACTANT TYPE	B	Surfactant C2	Surfactant B	Surfactant A

*incorporated into the mixture in a gelatine-water weight basis

The reasons to focus on these factors and their selected levels were:

Factor A, surfactant content. Three different levels of surfactant content were assessed based on recommendations of the suppliers, from a low concentration at 0.05 *wt%* (-1), to an intermediate, 0.5 *wt%* (0), and a high concentration, 5 *wt%* (+1).

Factor B, surfactant type. Three types of industrial surfactants were selected for the study of their effectiveness in the processing of hydrogel foams: anionic (surfactant C2,), cationic (surfactant B) and amphoteric (surfactant A).

The outcomes of this study were expansion ratio, drying shrinkage, density of the solid foams and foam structure. The surface tension of the surfactant-water solutions at 22°C was also measured (see Section 3.4.3.2.1).

Table 3.29 shows the experimental design table of this study. A sample without surfactant, FH1, was included in the matrix as a control, for comparison. No statistical analysis was carried out for this experiment, as it was considered a preliminary study.

Table 3.29. FORMULATION MATRIX FOR INFLUENCE OF SURFACTANT TYPE AND CONTENT IN GELATINE-HYDROGEL FOAMS

	FACTOR A	FACTOR B
ID	**SURFACTANT CONTENT (*wt%*)***	**SURFACTANT TYPE**
FH1	n/a	n/a
FH2	0.05	C2
FH3	0.5	C2
FH4	5	C2
FH5	0.05	B
FH6	0.5	B
FH7	5	B
FH8	0.05	A
FH9	0.5	A
FH10	5	A

**Content based on the total weight of the gelatine-water solution*

Table 3.30 summarises the formulation used for each experiment.

Table 3.30. FORMULATION TABLE FOR INFLUENCE OF SURFACTANT TYPE AND CONTENT IN GELATINE-HYDROGEL FOAMS.

ID	SURFACTANT TYPE	SURFACTANT CONTENT (*wt%*)*	GELATINE CONTENT (*wt%*)	WATER CONTENT (*wt%*)
FH1	n/a	-	15	85
FH2	C2	0.05	14.99	84.96
FH3	C2	0.49	14.93	84.58
FH4	C2	4.76	14.29	80.95
FH5	B	0.05	14.99	84.96
FH6	B	0.49	14.93	84.58
FH7	B	4.76	14.29	80.95
FH8	A	0.05	14.99	84.96
FH9	A	0.49	14.93	84.58
FH10	A	4.76	14.29	80.95

**Content based on the total weight of the gelatine-water solution*

3.3.3.3.2 Experiment 2. Influence of foaming temperature, gelatine content and surfactant type and content on the foaming behaviour and properties of hydrogel-gelatine foams

This experimental study aimed to understand the role of processing temperature, surfactant type and content and gelatine content on the foaming process (expansion ratio) and hydrogel dry foams properties (density, foam structure, compression properties, thermal properties and acoustic damping).

The objectives of this study were:

- To refine the selection of surfactant type and content on liquid and dry hydrogel foams properties.
- To refine the selection of gelatine content based on influence on liquid and dry hydrogel foams properties.
- To study the effect of processing temperature on liquid and dry hydrogel foams properties.
- To assist further optimisation of formulations.

Three different experiments for three different surfactants were carried out, while surfactant B was dropped after Experiment 1 because it produced foams with non-uniform cell structure:

- Experiment 2.1. Gelatine hydrogel-Surfactant "A" foams
- Experiment 2.2. Gelatine hydrogel- Surfactant C2 foams
- Experiment 2.3. Gelatine hydrogel- Surfactant C1 foams

The study of surfactants A and C2 consisted of a full factorial design with three factors (gelatine content, surfactant content and processing temperature) at three levels. The study of C1 was simplified to two factors (gelatine content and surfactant content). No statistical analysis was carried out for C1. The reasons to focus on these factors and their selected levels were:

Factor A, gelatine content. Three different levels of gelatine content were assessed for the three surfactants studied: a relatively low level at 10 *wt%*, an intermediate level at 15 *wt%* and a relatively high level at 20 *wt%*. The low level (10 *wt%*) was chosen as an acceptable low-density foam was achieved. Gelatine concentrations lower than 10 *wt%* yielded low-quality foams, with high levels of drying shrinkage. The high level (20 *wt%*) was chosen to explore high-density rigid foams for broader applications other than thermal insulation.

Factor B, surfactant content. The three surfactant levels were refinements of the results obtained in Experiment 1 (discussed in Section 3.3.3.3.1). The chosen levels were adjusted to 0.5 *wt%* (low), 1.5 *wt%* (medium) and 4.5 *wt%* (high) for hydrogel-surfactant "A" foams. For both hydrogel-surfactant C1 and hydrogel-surfactant C2 foams, the chosen levels were adjusted to 0.75 *wt%,* 1.5 *wt%* and 3 *wt%*.

Factor C, Processing temperature. The processing temperature of hydrogel-surfactant "A" foams and hydrogel-surfactant C2 foams was studied at two levels: 50±5°C (low)

and 80±5°C (high). The low level, 50±5°C, was chosen because it was sufficient to dissolve gelatine to form a sol and yet more economical and energy efficient. The high level, 80±5°C, was chosen for its lower solution viscosity and ease of foaming than at 50±5°C.

The outcomes of this study were:

- MER (Section 3.5.1)
- Drying shrinkage (Section 3.6.4)
- Drying time and drying process (Section 3.6.1)
- Density of the solid foams (Section 3.6.2)
- Foam structure (Section 3.6.5)
- Rheological characterisation of gel samples A1, A7, C2.1 and C2.7 (see Section 3.4.3.4)
- Compression properties (Section 3.6.6)
- Thermal conductivity (Section 3.6.7)
- Thermal gravimetric analysis (TGA) of samples A7 and A9 (Section 3.4.3.3)
- Surface tension of the gelatine-surfactant "A" solutions (Section 3.4.3.2.2)
- Sound Insulation (Section 3.6.8).

Table 3.31 summarises the different factors and levels at which hydrogel-surfactant "A" foams experiment was adjusted.

Table 3.31. FACTORS AND LEVELS FOR HYDROGEL-SURFACTANT "A" FOAMS

VARIABLE	ID	LOW LEVEL (-1)	INTERMEDIATE LEVEL (0)	HIGH LEVEL (+1)
1. GELATINE CONTENT (*wt%*)	A	10	15	20
2. SURFACTANT CONTENT (*wt%*)*	B	0.5	1.5	4.5
3. PROCESSING TEMPERATURE (°C)	C	50	-	80

**Content based on the total weight of the gelatine-water solution*

Table 3.32 shows the different levels and factors studied for hydrogel-surfactant C2 foams.

Table 3.32. EXPERIMENT 2.2 FACTORS AND LEVELS FOR HYDROGEL-SURFACTANT C2 FOAMS

VARIABLE	ID	LOW LEVEL (-1)	INTERMEDIATE LEVEL (0)	HIGH LEVEL (+1)
1. GELATINE CONTENT (*wt%*)	A	10	15	20
2. SURFACTANT CONTENT (wt%)*	B	0.75	1.5	3
3. PROCESSING TEMPERATURE (°C)	C	50	-	80

**Content based on the total weight of the gelatine-water solution*

Table 3.33 exhibits the different levels and factors studied for hydrogel-surfactant C1 foams. As it was proved feasible foaming of hydrogel-surfactant C2 at 50±5°C, that temperature was chosen as a fixed parameter for hydrogel-surfactant C1 experiments.

Table 3.33. EXPERIMENT 2.3. FACTORS AND LEVELS FOR HYDROGEL-SURFACTANT C1 FOAMS

VARIABLE	ID	LOW LEVEL (-1)	INTERMEDIATE LEVEL (0)	HIGH LEVEL (+1)
1. GELATINE CONTENT (*wt%*)	A	10	15	20
2. SURFACTANT CONTENT (*wt%*)*	B	0.75	1.5	3

**Content based on the total weight of the gelatine-water solution*

Table 3.34 summarises the experiment design for the three subsystems: hydrogel-surfactant "A", hydrogel-surfactant C2 and hydrogel-surfactant C1 foams.

Table 3.34. FORMULATION/PROCESS MATRIX FOR HYDROGEL-SURFACTANT "A", HYDROGEL-SURFACTANT C2 AND HYDROGEL-SURFACTANT C1 FOAMS

			FACTOR A	FACTOR B	FACTOR C
SURF. A	SURF. C1	SURF. C2	GELATINE CONTENT	SURFACTANT CONTENT	PROCESSING TEMPERATURE
A1	**C1.1**	**C2.1**	-1	-1	-1
A2		**C2.2**	-1	-1	+1
A3	**C1.2**	**C2.3**	0	-1	-1
A4		**C2.4**	0	-1	+1
A5	**C1.3**	**C2.5**	+1	-1	-1
A6		**C2.6**	+1	-1	+1
A7	**C1.4**	**C2.7**	-1	0	-1
A8		**C2.8**	-1	0	+1
A9	**C1.5**	**C2.9**	0	0	-1
A10		**C2.10**	0	0	+1
A11	**C1.6**	**C2.11**	+1	0	-1
A12		**C2.12**	+1	0	+1
A13	**C1.7**	**C2.13**	-1	+1	-1
A14		**C2.14**	-1	+1	+1
A15	**C1.8**	**C2.15**	0	+1	-1
A16		**C2.16**	0	+1	+1
A17	**C1.9**	**C2.17**	+1	+1	-1
A18		**C2.18**	+1	+1	+1

Table 3.35 shows the formulation of gelatine-surfactant "A" foams and the processing temperature at which each sample was prepared.

Table 3.35. FORMULATION/PROCESS TABLE FOR HYDROGEL-SURFACTANT "A" FOAMS

ID	GELATINE CONTENT (*wt%*)	WATER CONTENT (*wt%*)	SURFACTANT CONTENT (*wt%*)*	PROCESSING TEMPERATURE (°C)
A1	9.95	89.55	0.50	50
A2				80
A3	14.93	84.58		50
A4				80
A5	19.90	79.60		50
A6				80
A7	9.85	88.67	1.48	50
A8				80
A9	14.78	83.74		50
A10				80
A11	19.70	78.82		50
A12				80
A13	9.57	86.12	4.31	50
A14				80
A15	14.35	81.34		50
A16				80
A17	19.14	76.56		50
A18				80

**Content based on the total weight of the gelatine-water solution*

Table 3.36 shows the formulation of gelatine-surfactant C2 foams and the processing temperature at which each sample was prepared.

Table 3.36. EXPERIMENT 2.2. FORMULATION/PROCESS TABLE FOR HYDROGEL-SURFACTANT C2 FOAMS

ID	GELATINE CONTENT (*wt%*)	WATER CONTENT (*wt%*)	SURFACTANT CONTENT (*wt%*)*	PROCESSING TEMPERATURE (°C)
C2.1	9.93	89.33	0.74	50
C2.2				80
C2.3	14.89	84.37		50
C2.4				80
C2.5	19.85	79.40		50
C2.6				80
C2.7	9.85	88.67	1.48	50
C2.8				80
C2.9	14.78	83.74		50
C.2.10				80
C.2.11	19.70	78.82		50
C2.12				80
C2.13	9.71	87.38	2.91	50
C2.14				80
C2.15	14.56	82.52		50
C2.16				80
C2.17	19.42	77.67		50
C2.18				80

**Content based on the total weight of the gelatine-water solution*

Table 3.37 shows the formulation of gelatine-surfactant C1 foams and the processing temperature at which each sample was prepared.

Table 3.37. EXPERIMENT 2.3. FORMULATION/PROCESS TABLE FOR HYDROGEL-SURFACTANT C1 FOAMS

ID	GELATINE CONTENT (*wt%*)	WATER CONTENT (*wt%*)	SURFACTANT CONTENT (*wt%*)*	PROCESSING TEMPERATURE (°C)
C1.1	9.93	89.33	0.74	50
C1.2	14.89	84.37		
C1.3	19.85	79.40		
C1.4	9.85	88.67	1.48	
C1.5	14.78	83.74		
C1.6	19.70	78.82		
C1.7	9.71	87.38	2.91	
C1.8	14.56	82.52		
C1.9	19.42	77.67		

**Content based on the total weight of the gelatine-water solution*

3.3.3.3.3 Experiment 3. Optimisation of liquid foaming expansion ratio

Liquid foam expansion ratio (ER) is an adjustable parameter during foaming, but maximum achievable expansion ratio does not necessarily lead to uniform low-density solid foams. The aim of this experiment was thus to study the effect of the ER on the post-casting behaviour of liquid foam leading to the solid hydrogel foams. The objectives were:

- To assess, for selected formulations, the impact of liquid foam ER on foam stability during gelation and drying, drying shrinkage, density and foam structure
- To select an optimum ER for each formulation

From the results of section 3.3.3.3.2, two formulations of hydrogel-surfactant "A" (Samples A7 and A9) and two formulations of hydrogel-surfactant C2 foams (Samples C2.1 and C2.3) were chosen to explore the effect of ER on the post-casting behaviour leading to solid hydrogel foams.

The outcomes of this study were post-cast shrinkage, drying time, density and foam structure. Table 3.38 shows the formulation and ER at which each sample was prepared.

Table 3.38. FORMULATION AND EXPANSION RATIO MATRIX TABLE FOR EXPANSION RATIO STUDY

ID	SURFACTANT	EXPANSION RATIO	GELATINE CONTENT (%)	WATER CONTENT (%)	SURFACTANT CONTENT* (%)	PROCESSING TEMPERATURE (°C)
ER1	A	6	9.85	88.67	1.48	50
ER2		8	9.85	88.67		
ER3		Max (9.7)	9.85	88.67		
ER4		6	14.78	83.74		
ER5		Max (7.39)	14.78	83.74		
ER6	C2	5	9.93	89.33	0.74	
ER7		Max (7.17)	9.93	89.33		
ER8		5	14.89	84.37		
ER9		Max (6.64)	14.89	84.37		

**Content based on the total weight of the gelatine-water solution*

3.3.3.3.4 Experiment 4. Influence of plasticiser type and content on gelatine-surfactants "A" and C2 foams

The aim of this study was to understand the role of the plasticiser type and content on the hydrogel foaming process and dry foam structure and properties.

The objectives were:

- To assess, for selected formulations, the impact of plasticiser type and content on foam stability during gelation and drying, ER, density, foam structure and compression properties of the dry foams
- To select an optimum formulation for each of the surfactant and gelatine levels

From the results of section 3.3.3.3.2, two formulations of hydrogel-surfactant "A" (samples A7 and A9) and two formulations of hydrogel-surfactant C2 (samples C2.1 and C2.3) foams were based upon to explore the effect of plasticiser type and content on liquid and solid hydrogel foams. The gelatine and surfactant contents were maintained for those formulations and plasticiser was added.

The study of the plasticiser for gelatine-surfactant "A" and gelatine-surfactant C2 foams was carried out at three factors (gelatine content, plasticiser type and plasticiser content). For gelatine-surfactant "A" foams, the plasticiser content was studied at four levels (see Table 3.39) and for gelatine-surfactant C2 foams, the plasticiser content was studied at two levels (see Table 3.40). The outcomes of this study were MER, drying shrinkage, density, foam structure and mechanical properties of the dry foams.

Table 3.39. EXPERIMENT 4. FORMULATION TABLE FOR EFFECT OF PLASTICISER IN GELATINE HYDROGEL-SURFACTANT "A" FOAMS.

VARIABLE	ID	LOW LEVEL		HIGH LEVEL	
1. GELATINE CONTENT (*wt%*)	A	10		*15*	
2. TYPE OF PLASTICISER	B	Sorbitol		Glycerol	
VARIABLE	**ID**	**LEVEL 1**	**LEVEL 2**	**LEVEL 3**	**LEVEL 4**
3. PLASTICISER CONTENT (*wt%*)*	C	1	2	3	4

**Content based on the total weight of the gelatine-water solution*

Table 3.40. EXPERIMENT 4 FORMULATION TABLE FOR EFFECT OF PLASTICISER IN GELATINE HYDROGEL-SURFACTANT C2 FOAMS

VARIABLE	ID	LOW LEVEL	HIGH LEVEL
1. GELATINE CONTENT (wt%)	A	10	15
2. PLASTICISER TYPE	B	Sorbitol	Glycerol
3. PLASTICISER CONTENT (*wt%*)*	C	2	4

**Content based on the total weight of the gelatine-water solution*

The reasons to focus on these factors and their selected levels were:

Factor A, gelatine content. Low to medium level (10-15 *wt%*) were chosen as the 20 *wt%* gelatine content gave rise to high-density and rigid foams

Factor B, plasticiser type. The two plasticisers, sorbitol and glycerol, are widely used for TPS based biopolymers and in gelatine (Cheng, Yang and Lin, 2011) (Oliviero *et al.*, 2015) (Martucci, Espinosa and Ruseckaite, 2015).

Factor C, plasticiser content. The plasticiser content was adjusted following preliminary experimental work (not shown in this research) based on foam usability (e.g. too much plasticiser may hinder sample preparation of dry foams due to excessive malleability). Hydrogel-surfactant C2 foams were studied at 2 levels to simplify the test.

Table 3.41 shows the experimental matrix for hydrogel-surfactant "A" foams.

Table 3.41. FORMULATION MATRIX FOR THE STUDY OF THE EFFECTS OF PLASTICISERS IN HYDROGEL-SURFACTANT "A" FOAMS

ID	PLASTICISER TYPE	GELATINE CONTENT (*wt%*)	WATER CONTENT (*wt%*)	PLASTICISER CONTENT (*wt%*)*
SA1	sorbitol	9.85	87.68	0.99
SA2		9.85	86.70	1.97
SA3		9.85	85.71	2.96
SA4		9.85	84.73	3.94
SA5		14.78	82.76	0.99
SA6		14.78	81.77	1.97
SA7		14.78	80.79	2.96
SA8		14.78	79.80	3.94
GA1	glycerol	9.85	87.68	0.99
GA2		9.85	86.70	1.97
GA3		9.85	85.71	2.96
GA4		9.85	84.73	3.94
GA5		14.78	82.76	0.99
GA6		14.78	81.77	1.97
GA7		14.78	80.79	2.96
GA8		14.78	79.80	3.94

**Content based on the total weight of the gelatine-water solution*
Note: Surfactant C2 content was constant at 1.48wt%
The processing temperature was kept constant at 50°C

Table 3.42 shows the experimental matrix for hydrogel-surfactant C2 foams.

Table 3.42. EXPERIMENT 4.2 FORMULATION MATRIX FOR EFFECT OF PLASTICISERS IN HYDROGEL-SURFACTANT C2 FOAMS

ID	PLASTICISER TYPE	GELATINE CONTENT (*wt%*)	WATER CONTENT (*wt%*)	PLASTICISER CONTENT* (*wt%*)
SS1	sorbitol	9.93	87.34	1.99
SS2		9.93	85.36	3.97
SS3		14.89	82.38	1.99
SS4		14.89	80.40	3.97
SG1	glycerol	9.93	87.34	1.99
SG2		9.93	85.36	3.97
SG3		14.89	82.38	1.99
SG4		14.89	80.40	3.97

**Content based on the total weight of the gelatine-water solution*
Note: Surfactant C2 content was constant at 0.74wt%
The processing temperature was kept constant at 50°C

3.3.3.3.5 Experiment 5. Study of the drying process of gelatine-surfactants "A" and C2 foams

The natural drying of samples prepared in Section 3.3.3.3.2 (A7, A9, A11, C2.1, C2.3, C2.5) and 3.3.3.3.4 was studied. Sample A7 was further studied, and different methods in comparison with the natural drying were investigated.

An experiment with three factors representing different drying methods (drying environment, refrigeration use and type of mould used) was designed.

The reasons to focus on these factors and their selected levels were:

Factor A. Two different drying environments were studied: in the oven (29°C, which was chosen following rheological test of the gel to avoid melting of the wet gel foams) and in an environmental chamber (26°C, 50% HR with air circulation).

Factor B. With or without refrigeration (at 4°C for 5 hours) after foam casting. This was an attempt to accelerate the gelling process under refrigeration in an earlier stage of drying.

Factor C. Two types of mould were assessed, a PS weigh boat of 120 x 120 x 20 *mm* supplied by Fisher Scientific (the "standard" mould used for most of the foam casting throughout this work) and a 120 x 120 x 20 *mm* mould made from aluminium wire mesh (hole size 1 x 2 *mm*), with the same dimensions, to allow drying from all sides. The aluminium mesh mould was initially covered by aluminium foil to prevent leakage of the sample after casting. The aluminium foil was removed from the mould one hour after casting, once the gelling process stabilised the liquid foam.

Table 3.43 shows the experiment design.

Table 3.43. EXPERIMENT 5. EXPERIMENTAL DESIGN FOR TESTING OF DRYING METHODS

ID	DRYING ENVIRONMENT	REFRIGERATION	MOULD
C1	Chamber (26°C)	No	Mesh
C2		No	PS mould
C3		Yes	Mesh
C4		Yes	PS mould
O1	Oven (29°C)	No	Mesh
O2		No	PS mould
O3		Yes	Mesh
O4		Yes	PS mould

Also, drying of sample A7 (see Table 3.35) was assessed using freeze-drying (see Section 3.6.1). Subsequently, foam structure (see Section 3.6.5) of the freeze-dried sample was analysed, and porosity was estimated.

3.3.3.3.6 Sample preparation methods

The stages of sample preparation of hydrogel foams based on gelatine were the following:

a. Hydrogel solution preparation. Low Bloom gelatine (at 10, 15, 20 *wt%)* was mixed and magnetically stirred with water at 50±5°C or 80±5°C, as required, for 15 minutes. Surfactants (at 0.05, 0.5, 0.75, 1.5, 3 and 4.5 *wt%*) and plasticisers (from 1 to 4 *wt%)*, if applicable, were added to the mixture in a gelatine-water weight solution basis and heated at 50±5°C or 80±5°C on a hot plate with magnetic stirring for 15 minutes

b. Foaming. The aqueous gelatine solution with selected additives was foamed at 50±5°C or 80±5°C by mechanical stirring using a blender Bosch MSM6700GB fitted with a whisking accessory until the desired liquid foam volume was obtained

c. Finally, at the *casting* stage, the hydrogel liquid foam was poured into a mould and let to dry naturally in laboratory conditions. Once the sample was dry, it was released from the mould and cut as required

3.3.3.4 System 4. Gelatine hydrogel composite-foams

This section describes the experimental work carried out for system 4, a range of gelatine hydrogel-composite foams to demonstrate various potentials applications of the hydrogel foaming techniques. Gelatine foams developed in System 3 were selected to combine with the second materials.

Four different **hydrogel composite** foams were produced:

- System 4.1. Biomass-hydrogel foams. Hydrogel foams filled with different types of powders from agro-biomass as low-cost, bio-based fillers for general applications.

- System 4.2. Vermiculite-hydrogel foams. Hydrogel foams dispersed with granules of expanded vermiculites, a low density, low-cost cellular filler with excellent thermal insulation and fire resistance properties aimed at construction applications.

- System 4.3. Aerogel-hydrogel foams. Hydrogel foams filled with ultra-low-density silicon dioxide aerogel particles with excellent thermal insulation aimed at thermal insulation applications.

- System 4.4. Hydrogel filled honeycomb. Cardboard and Nomex® honeycomb cavities infiltrated with hydrogel foam using foam casting method. This system aimed

to enhance combined mechanical, thermal and acoustic properties for high-performance and lightweight structural applications.

The objectives of this study were the following:

- To establish techniques for incorporation of secondary materials and identify suitable formulations in terms of the second phase contents and processing conditions.
- To assess the effects of the secondary materials on the behaviour of the combined composite materials during processing and in dry form.

3.3.3.4.1 Sample preparation

Preparation procedures for preparation of the liquid hydrogel-composites foams were as described in Section 3.3.3.3.6. Details in the incorporation of different secondary materials, composite sample preparations and analysis are described below.

3.3.3.4.2 Subsystem 4.1. Biomass-hydrogel foams

This experimental study aimed to understand the role of two types of powders from gramineous plants (oat and straw) when incorporated into gelatine hydrogel foams.

The objectives of this study were:

- To investigate the effect of type and content of biomass powders during the preparation of the composites in wet (MER and drying shrinkage), and dry stages (density, structure and mechanical and thermal properties)
- To identify optimum formulations and processing conditions for further exploitations.

From the results of section 3.3.3.3.2, samples A7, A9 and A11 (gelatine-hydrogel-surfactant "A") and samples C2.1 and C2.3 (gelatine-hydrogel-surfactant C2), see Table 3.35, were chosen to explore the effect of the biomass powders type and content on liquid and solid hydrogel foams.

The gelatine hydrogel-surfactant "A" foams (A7, A9 and A11) were studied for three gelatine concentrations (10, 15 and 20 *wt%*). The gelatine-hydrogel-surfactant C2 foams (C2.1 and C2.3) were studied for just two concentrations (10 and *15 wt%*) as the higher gelatine concentration previously studied (20 *wt%*) led to high-density foams. Each sample (A7, A9, A11, C2.1 C2.3) was studied using the following two factors at two levels:

- **Factor A.** Biomass Powder. Two powders were studied: oat and straw (see Section 3.2.3.1)

- **Factor B**. Biomass powder content. Two concentrations were studied: 1 *wt%* and 3 *wt%*

The biomass-hydrogel foams were prepared following the preparation procedure explained in Section 3.3.3.3.6. The biomass powders were incorporated, in weight percentage of the gelatine-water solution, along with the gelatine powder in the first production step and subsequently foamed and cast. Table 3.44 shows the formulation table for biomass-hydrogel composite foams.

Table 3.44. FORMULATION TABLE FOR BIOMASS-HYDROGEL COMPOSITE FOAMS

ID	FIBRE	FIBER CONTENT* (%)	GELATINE CONTENT (wt%)	WATER CONTENT (%)	SURFACTANT CONTENT* (%)	SURFACTANT TYPE
O1	oat	0.99	9.85	87.68	1.48	A
O2		2.96	9.85	85.71		
O3		0.99	14.78	82.76		
O4		2.96	14.78	80.79		
O5		0.99	19.70	77.83		
O6		2.96	19.70	75.86		
O7	oat	0.99	9.93	88.34	0.74	C2
O8		2.98	9.93	86.35		
O9		0.99	14.89	83.37		
O10		2.98	14.89	81.39		
W1	straw	0.99	9.85	87.68	1.48	A
W2		2.96	9.85	85.71		
W3		0.99	14.78	82.76		
W4		2.96	14.78	80.79		
W5		0.99	19.70	77.83		
W6		2.96	19.70	75.86		
W7	straw	0.99	9.93	88.34	0.74	C2
W8		2.98	9.93	86.35		
W9		0.99	14.89	83.37		
W10		2.98	14.89	81.39		

**Content based on the total weight of the gelatine-water solution*

The outcomes of this experiment were MER, the density of the dry foams, drying shrinkage, solid foam structure and mechanical and thermal properties.

3.3.3.4.3 Subsystem 4.2. Vermiculite-hydrogel foams

The aim of this experimental study was to understand the incorporation of vermiculite particles into gelatine hydrogel foams.

The objectives of this study were:

- To investigate the effect of the incorporation of vermiculite particles during the preparation of the composites in wet (expansion ratio and drying shrinkage), and dry stages (structure and mechanical, thermal, acoustic and fire resistance properties)
- To identify optimum formulations and processing conditions for further exploitations.

From the results of section 3.3.3.3.2, samples A7, A9 and A11 (see Table 3.35) were chosen to explore the effect of the incorporation of vermiculite particles into the gelatine hydrogel foams.

Two factors at different levels were studied for each gelatine concentration:

Factor A. Amount of vermiculite incorporated into the solution. Three vermiculite levels were incorporated into the solution at 6.5 *vol%*, 13 *vol%* and 19.5 *vol%* based on total volume of the liquid foams

Factor B. Vermiculite type. Two types of vermiculite with a different particle size ("Fine" and "coarse") were studied (see Section 3.2.3.2)

The vermiculite-hydrogel foams were prepared following the preparation procedure explained in Section 3.3.3.3.6. The vermiculite particles were incorporated, in volume percentage of the total expanded volume achieved after foaming, into the hydrogel foam after the foaming stage. Then, they were mixed with the hydrogel foam using the whisking accessory used in Section 3.3.3.3.6 for 1 minute.

Table 3.45 summarises the experiment design.

Table 3.45. FORMULATION TABLE FOR VERMICULITE-HYDROGEL FOAMS

ID	VERMICULITE TYPE	VERMICULITE CONTENT* (*vol%*)	GELATINE CONTENT (*wt%*)	WATER CONTENT (*wt%*)
VS1	Fine	6.5	9.85	88.67
VS2		6.5	14.78	83.74
VS3		6.5	19.70	78.82
VS4		13	9.85	88.67
VS5		13	14.78	83.74
VS6		13	19.70	78.82
VS7		19.5	9.85	88.67
VS8		19.5	14.78	83.74
VS9		19.5	19.70	78.82
VB1	Coarse	6.5	9.85	88.67
VB2		6.5	14.78	83.74
VB3		6.5	19.70	78.82
VB4		13	9.85	88.67
VB5		13	14.78	83.74
VB6		13	19.70	78.82
VB7		19.5	9.85	88.67
VB8		19.5	14.78	83.74
VB9		19.5	19.70	78.82

**Content based on the MER of A7, A9 and A11, depending on the gelatine content*
Note: Surfactant "A" content was constant at 1.48 wt%

The outcomes of this experiment were density of the dry foams, drying shrinkage and mechanical, acoustic, thermal and fire resistance properties.

3.3.3.4.4 Subsystem 4.3. Gelatine-surfactant C2-SiO_2 aerogel foams

The aim of this experiment was to understand the effect of two silicon oxide aerogel powders on properties of gelatine hydrogel foams. Particular attention was focused on whether the incorporation of aerogel powders at low concentrations (due to cost reason) will have a significant reduction in the thermal conductivity of the composite foams.

The objectives of this study were:

- To understand processing implications of the incorporation of the aerogel into gelatine hydrogel foams (expansion ratio and foam stability using different types at different loadings).

- To investigate the effect of aerogel powder type and content on liquid and dry hydrogel foams properties (dry density, foam structure and thermal conductivity)

- To identify desirable formulations windows for further development.

Two formulations of hydrogel-surfactant C2 (Samples C2.1 and C2.3, shown in Table 3.36) foams were chosen to explore the effect of aerogel powders. Three factors (gelatine content, type of aerogel powders and content) were studied at different levels. The studied levels were:

Factor A. Gelatine content: 10 and 15 *wt%*

Factor B. Type of powder: hydrophilic and hydrophobic

Factor C. The powder contents studied were 1 and 3 *wt%*

Table 3.46 shows the experiment design.

Table 3.46. EXPERIMENT DESIGN OF BIOMASS-HYDROGEL AND AERO-GEL COMPOSITE FOAMS

ID	GELATINE CONTENT *(wt%)*	WATER CONTENT *(wt%)*	AERO-GEL TYPE	AERO-GEL CONTENT* (*wt%*)
P1	9.93	89.33	Hydrophobic	1
P2				3
P3	9.93	89.33	Hydrophilic	1
P4				3
P5	14.89	84.37	Hydrophobic	1
P6				3
P7	14.89	84.37	Hydrophilic	1
P8				3

**Content based on the total weight of the gelatine-water solution*
Note: Surfactant C2 content was constant at 0.74 wt%

The aerogel-hydrogel foams were prepared following the preparation procedure explained in Section 3.3.3.3.6. The aerogel powders were incorporated, in weight percentage of the gelatine-water solution, along with the gelatine powder in the first production step and subsequently foamed and cast.

The outcomes of this experiment were MER, density of the dry foams, drying shrinkage, solid foam structure and thermal properties.

3.3.3.4.5 Honeycomb boards filled with hydrogel foams

The aim of this study was to investigate the change in mechanical properties of cardboard and Nomex® honeycomb boards when the honeycomb cavities were filled with a selected hydrogel foam, sample A11 (see Table 3.35).

The objectives were:

- To develop sample preparation methods, particularly in cavity filling and drying
- To assess the cavity filling on honeycombs boards structure (particularly defects associated with cavity filling, interfaces and distortions, if any), the density of the composite boards, and mechanical properties (bending stiffness and compression strength)

Three factors (type of material, filling and cell size) at two levels were studied. The gelatine content of the filling was kept constant to 20 *wt%* to maximise the sandwich panel mechanical properties enhancement.

The reason to focus on the studied levels were:

Factor A. Honeycombs board material. Two materials widely used in industry were tested: Nomex® (e.g. in aerospace) and cardboard (e.g. in packaging).

Factor B. Filling. Two levels were tested: unfilled and filled honeycomb boards with sample A11.

Factor C. Different cell sizes were tested to investigate the degree of potential performance enhancement. The cell size selected for each material was subjected to commercial availability.

The sample preparation consisted of four stages: core preparation, hydrogel foam production, foam infiltration and drying.

a. *Core preparation.* Nomex® boards were cut with a manual cutter. Cardboard sheets, considerably more rigid than Nomex®, were cut using a cardboard cutter

b. *Hydrogel foam production.* The hydrogel foam was prepared following steps *a* (hydrogel solution preparation) and *b* (foaming) from Section 3.3.3.3.6.

c. Foam infiltration

   - Nomex® boards. The honeycomb core was placed on top of a cardboard face sheet to avoid sample leaking after pouring, as shown in Figures 3.12A and

3.12B. Then, the hydrogel foam was poured into the honeycomb core, and a glass strip was used to even it out to ensure sample penetration and surface levelled. This process was repeated to ensure honeycomb filling. After filling, the honeycomb surface was covered with the top cardboard skin and subsequently pushed with a weight to guarantee core and skin fixing. The hydrogel foam served as an adhesive between the core and the skins.

- Cardboard boards. The honeycomb core was separated from its glued skins by hand, as shown in Figure 3.12C. Then, the panel was filled following the procedure explained for the Nomex® boards.

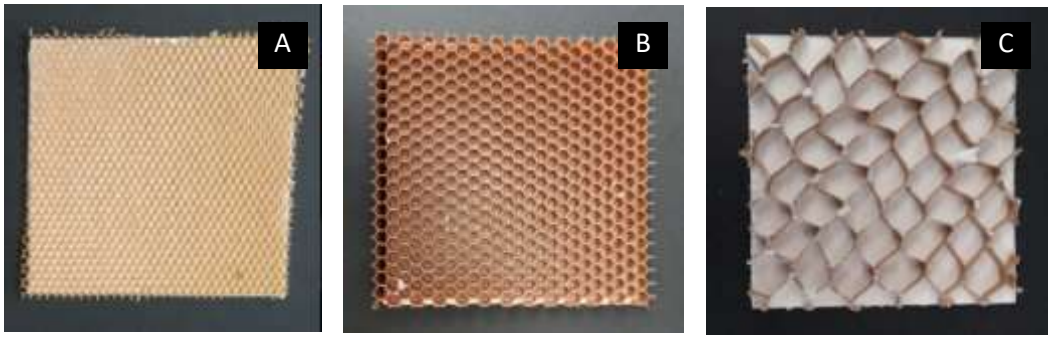

Figure 3.12. HONEYCOMB PANELS CORE VIEW (A) NOMEX 3.2*mm* CELL SIZE (B) NOMEX 4.8mm CELL SIZE (C) CARDBOARD 27*mm* CELL SIZE

d. Drying. The samples were let to dry naturally in laboratory conditions and 250 *g* weights were placed on top of the boards to avoid bending during drying and ensure skin-core glueing. Figure 3.13 illustrates the appearance of the honeycomb boards after sample preparation.

For the unfilled samples, cardboard honeycombs were cut into the desired size. The structure used was the one coming from the supplier: top cardboard layer + honeycomb layer + bottom cardboard layer.

For unfilled Nomex® boards, they were received without skins from the supplier. Thus, a thin layer of hydrogel foam was used as adhesive to adhere the cardboard skins described in Section 3.2.4.1.

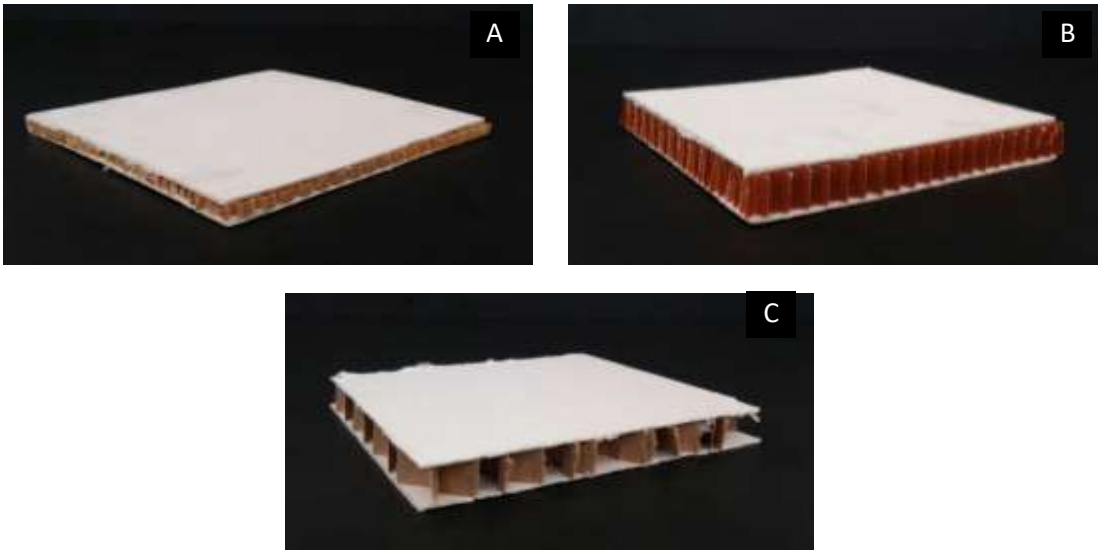

Figure 3.13. HONEYCOMB PANELS WITH TOP AND BOTTOM FACES GLUED (A) NOMEX 3.2*mm* CELL SIZE (SAMPLES N1.1 AND N1.2) (B) NOMEX 4.8mm CELL SIZE (SAMPLES N2.1 AND N2.2) (C) CARDBOARD 27*mm* CELL SIZE (SAMPLES H2.1 AND H2.2)

Table 3.47 shows the experimental matrix for this experiment.

Table 3.47. EXPERIMENT MATRIX FOR HONEYCOMB BOARDS FILLED WITH HYDRO-GEL FOAMS.

ID	HONEYCOMB BOARD MATERIAL	FOAM FILLING (Y/N)	HONEYCOMB BOARD CELL SIZE (mm)
H1.1	Cardboard	15	N
H1.2			Y
H2.1		27	N
H2.2			Y
N1.1	Nomex®	3.2	N
N1.2			Y
H2.1		4.8	N
N2.2			Y

Note: The filling material was Sample A11 (see Table 3.35)

The outcomes of this investigation were the dry density of the filled panels (see Section 3.7.2) and mechanical properties (static compression and static 3-point bending tests), as described in Sections 3.7.3 and 3.7.4.

3.3.3.5 System 5. Alternative hydrogel foams: agar and gellan gum

These studies aimed at developing hydrogel foams other than that based on gelatine to diversify the sources of hydrogel raw materials from animal origin to algae and bacterial origins.

3.3.3.5.1. Subsystem 5.1. Hydrogel foams from agar

This experimental study aimed to prove the feasibility of agar-hydrogel foams.

The objectives of this study were:

- To identify requirements in formulation (e.g. surfactant and agar concentrations) and process conditions (e.g. foaming/casting temperature) for agar-hydrogel foaming process
- To understand the impact of formulation and processing on the solid foam properties

Two factors (agar content and surfactant content) at three levels were studied. The reasons to focus on the studied levels were:

Factor A. Agar content. After preliminary testing on viscosity and foamability of the solution, three different agar concentrations were selected for the study: 5, 7.5 and 10 *wt%*.

Factor B. Surfactant C2 content was studied at 0.5, 1 and 1.5 *wt%*.

The formulation matrix is shown in Figure 3.48

TABLE 3.48. FORMULATION MATRIX FOR AGAR BASED HYDRO-GEL FOAMS

ID	AGAR (%)	SURFACTANT C2* (%)	WATER (%)
AS1	4.98	0.50	94.53
AS2	7.46	0.50	92.04
AS3	9.95	0.50	89.55
AS4	4.95	0.99	94.06
AS5	7.43	0.99	91.58
AS6	9.90	0.99	89.11
AS7	4.93	1.48	93.60
AS8	7.39	1.48	91.13
AS9	9.85	1.48	88.67

**Content based on the total weight of the agar-water solution*

The stages of sample preparation of agar foams were the following:

Agar dissolution preparation. Agar was mixed with water at concentrations between 5 to 10 *wt%*. The blend was heated on a beaker on a hot plate at 85±5°C and was stirred for 10 minutes by using a glass rod and a magnetic stirrer. The beaker was cover with aluminium foil to minimise evaporation.

Once the blend was homogeneous, the surfactant was incorporated

Foaming and casting. The liquid formulated was foamed using a blender (Bosch MSM6700GB, 600 *W* with a whisking accessory) for approximately 6 minutes at 85±5°C until a maximum expansion ratio was reached. The liquid foam was poured into a mould and let to dry naturally under laboratory conditions. The sample was released from the mould and cut as required.

The outcomes of this study were MER and the rheological characterisation of sample AS7 (see Section 3.4.3.4.2e).

3.3.3.5.2. Subsystem 5.2. Hydrogel foams made with gellan gum

The aim of this experimental study was to prove the feasibility of gellan gum-hydrogel foams.

The objectives of this study were:

- To identify requirements in the formulation (e.g. low and high acyl gellan gum and surfactant concentrations), type of surfactant used and process conditions (e.g. foaming/casting temperature) for gellan gum-hydrogel foaming process
- To understand the impact of formulation and processing on the solid foam properties

Two factors, high and low acyl gellan gum at two and four levels, respectively, were studied. Surfactant A was kept constant. The reasons to focus on the studied levels were:

Factor A. Low acyl gellan gum. After preliminary testing on viscosity and foamability of the solution, two different low acyl gellan gum concentrations were selected for the study: 3 and 4 *wt%*.

Factor B. High acyl gellan gum was studied at four levels: 0, 0.5, 1 and 1.5*wt%*.

The experimental design matrix is shown in Figure 3.49.

TABLE 3.49. EXPERIMENTAL DESIGN TABLE FOR GELLAN GUM BASED HYDROGEL FOAMS

ID	HA GELLAN GUM (*wt%*)	LA GELLAN GUM (*wt%*)
GG1	3	0
GG2	3	0.5
GG3	3	1
GG4	3	1.5
GG5	4	0
GG6	4	0.5
GG7	4	1
GG8	4	1.5

Note: Surfactant "A" was added at 10 wt% based on the gellan gum-water solution in weight

The formulation matrix is shown in Figure 3.50

TABLE 3.50. FORMULATION MATRIX FOR GELLAN GUM BASED HYDROGEL FOAMS

ID	HA GELLAN GUM (*wt%*)	LA GELLAN GUM (*wt%*)	WATER (*wt%*)	SURFACTANT (*wt%*)
GG1	2.73	0.00	88.18	9.09
GG2	2.73	0.45	87.73	9.09
GG3	2.73	0.91	87.27	9.09
GG4	2.73	1.36	86.82	9.09
GG5	3.64	0.00	87.27	9.09
GG6	3.64	0.45	86.82	9.09
GG7	3.64	0.91	86.36	9.09
GG8	3.64	1.36	85.91	9.09

The stages of sample preparation of gellan gum foams were the following:

Gellan gum dissolution preparation. HA gellan gum was mixed with LA gellan gum and water in a concentration that ranged from 3 to 4 *wt%*, The blend was heated on a beaker on a hot plate at 95±5°C and was stirred for 10 minutes by using a glass rod and a magnetic stirrer. The beaker was cover with aluminium foil to minimise evaporation.

Once the blend was homogeneous, the surfactant was incorporated on weight percentage based on the total mass of gellan gum-water solution.

Foaming. The liquid formulated was foamed by mechanical stirring until a maximum value. Air was introduced using a blender Bosch MSM6700GB, 600 *W* with a whisking accessory for approximately 5 minutes at 95±5°C.

Finally, at the **casting** stage, the liquid foam was poured into a mould and dry in an oven at 70°C for 24 hours.

The outcomes of this experiment were:

- Density
- Shrinkage
- Structure of sample GG4
- The thermal conductivity of samples GG3, GG4, GG6 and GG7.

3.4 CHARACTERISATION OF THE RAW MATERIALS, THE SOLUTION BEFORE FOAMING AND THE LIQUID AND DRY FOAMS SAMPLES

This section discusses the details about the characterisation of the raw materials, the solution before foaming and the liquid and solid foams.

3.4.1 SAMPLE CONDITIONING

Solid samples (powders, dry gels and dry foams) were conditioned at 20°C and relative humidity of 50% by using an environmental Chamber type DELTA 190 – 4HS (Design Environmental, UK) for 48 hours before characterisation.

3.4.2 CHARACTERISATION OF RAW MATERIALS

This section describes the characterisation of the raw materials regarding density (for powders and liquids), moisture content and morphologies.

3.4.2.1 Density of powders

The bulk density of raw materials in powder form was calculated from the mass per unit of bulk volume measured with graduated test tubes after gentle tapping.

The real density of raw materials in powder form was measured by volume displacement using a density bottle. The powders were dispersed in a non-polar solvent, acetone, and their real density was measured from the ratio between the mass and real volume of solvent displaced by the particles.

For both bulk and real density, the reported value was the average of five measurements.

3.4.2.2 Density of liquids

The density of liquids was calculated from mass and the volume measured with a manual pipette. The reported value was the average of five measurements.

3.4.2.3 Moisture content

An HR73 Halogen Moisture Analyser (Mettler Toledo, UK) was used to measure the moisture content of both the as-received liquids and solids after standard conditioning (section 3.4.1). Samples with a mass between 0.1-0.2 g were inserted into the equipment for a 30-minute analysis when the physically absorbed moisture was removed. The measurement error of ~0.25% was claimed by the manufacturer.

3.4.2.4 Microscopy

Three microscopes were used for raw material characterisation: an Olympus DP20 Microscope Digital Camera, a Zeiss optical microscope and Scanning Electronic Microscopy (SEM).

An Olympus DP20 Sterol Microscope (Olympus, UK) was used for gelatine and vermiculite particle size measurement and characterisation. The DP20 microscope features a 2-megapixel camera and outputs the image to a monitor.

A Zeiss Axioskop 2 MAT microscope (Zeiss, Germany) was used for starch particle size measurement and characterisation.

A FESEM Zeiss Supra 35VP Scanning Electron Microscope (SEM) at 5 kV was utilised for characterisation of the particle sizes and morphologies of the starch, calcium sulfate, agar, gellan gum, biomass powders, aero-gel powders and vermiculite particles. The particles were deposited on studs coated with a graphite conductive adhesive and coated for 120 seconds with gold using a sputter coating unit using the following parameters:

- Voltage: 1.2 *kV*
- Vacuum: 0.1 *torr*
- Electric current: *20 mA*
- Coating time: *90 s*

3.4.3 CHARACTERISATION OF THE FORMULATED LIQUIDS BEFORE FOAMING

The liquids before foaming were studied before, during and after gelling. The following sections describe the characterisation carried out for the formulated liquid before foaming.

3.4.3.1 Assessment of the TPS liquids

Destruction of the native starch granules (i.e. granule crystallinity destabilisation) is desirable to obtain a homogeneous thermoplastic starch solution (see Section 2.4.3.3 in Chapter 2 for further details). However, this often is not completely achieved as it requires very intensive thermal and mechanical treatments.

Starch granules structure was assessed at different processing stages:

a. The starch powder as received

b. Starch gel after heat treatment (80±5°C for 30 minutes on an IKA C-MAG HS7 ceramic hot plate). The starch gel was prepared from a 5.4 *wt%* starch-water solution; concentration used to produce samples ST1, ST2, ST5 and ST6 (see Tables 3.22 and 3.23)

c. Starch gel after the heat and shear treatment (80±5°C for 30 minutes on an IKA C-MAG HS7 ceramic hot plate: 10 minutes of magnetic stirring + 20 minutes of mechanical shearing). The starch gel was prepared from a 5.4 *wt%* starch-water solution, as the previous point. While heat treated, the starch solution was sheared using a hand liquidiser Bosch MSM6700GB, 600 *W* for 20 minutes. This was the most intensive thermal and mechanical treatment studied and the one used for preparing the liquids for systems 1 and 2.

A drop of liquid/powder sample was sandwiched between two thin glass slides under gentle pressure to form a thin layer for optical microscopy. The Zeiss optical microscope (discussed in Section 3.4.2.4.) under polarised light was then used to assess the breakdown of starch granules after mechanical and heating processes. If the relics of granules under polarised light exhibit a maltese cross birefringence, crystallinity remained (Chandrashekar, Savitri and Somashekar, 1987) and the thermal and mechanical treatments did not properly destroy the starch granules.

3.4.3.2 Surface tension of the hydrogel solutions

The surface tension of water-surfactants solutions was measured using the Du Nouy ring method for water-surfactant solutions at room temperature and the Wilhelmy plate method for gelatine-water-Surfactant "A" surfactant solutions at 50°C. Further information about the surface tension tests can be seen in Section 2.2.2.2.2, in Chapter 2.

3.4.3.2.1 Du Nouy ring method

The Du Nuouy ring tests were not carried out in gelatine solutions due to lack of temperature control measurement what meant the gelatine gelling around the ring due to natural cooling and the impossibility of achieving reliable surface data. Thus, the influence of the different surfactants used in this study on surface tension was studied in water.

Two factors, surfactant type and concentration, at three and six levels, respectively, were studied (see Table 3.51). The studied levels were:

Factor A. Surfactant type. The three surfactants used in the experiment described in section 3.3.3.3.1, surfactants A, B and C2, were selected

Factor B. Surfactant content. The three surfactants were studied at 6 concentrations (0.5, 1, 1.5, 2, 2.5, 3 *wt%*). A sample without surfactant (water) was also measured for comparison.

TABLE 3.51. EXPERIMENTAL MATRIX FOR THE MEASUREMENT OF SURFACE TENSION OF WATER-SURFACTANT SOLUTIONS AT 22°C

ID	SURFACTANT TYPE	SURFACTANT CONTENT* (*wt%*)
SF0	-	0
SF1	A	0.5
SF2		1
SF3		1.5
SF4		2
SF5		2.5
SF6		3
SF7	C2	0.5
SF8		1
SF9		1.5
SF10		2
SF11		2.5
SF12		3
SF13	B	0.5
SF14		1
SF15		1.5
SF16		2
SF15		2.5
SF16		3

**surfactants were added based on water weight percentage*

Table 3.52 shows the formulation matrix for this experiment.

TABLE 3.52. FORMULATION MATRIX FOR THE MEASUREMENT OF SURFACE TENSION OF WATER-SURFACTANT SOLUTIONS AT 22°C

ID	SURFACTANT TYPE	SURFACTANT CONTENT* (*wt%*)	WATER CONTENT (*wt%*)
ST0	-	0	100
ST1	A	0.5	99.5
ST2		0.99	99.01
ST3		1.48	98.52
ST4		1.96	98.04
ST5		2.44	97.56
ST6		2.91	97.09
ST7	C2	0.5	99.5
ST8		0.99	99.01
ST9		1.48	98.52
ST10		1.96	98.04
ST11		2.44	97.56
ST12		2.91	97.09
ST13	B	0.5	99.5
ST14		0.99	99.01
ST15		1.48	98.52
ST16		1.96	98.04
ST15		2.44	97.56
ST16		2.91	97.09

**surfactants were added based on water weight percentage*

The Experimental setup (see Figure 3.14) comprised the following components:

- Fisher Scientific accu-12D balance with 0.01 mg precision
- Faulhaber DC-Micro motor with high gear ratio
- Thurlby PL310 DC power supply
- Platinum ring. Its inner and outer dimeters were 9.201 and 9.770 mm, respectivelly
- Banana clip cables
- Retort stand and clamp
- 50 ml glass beaker

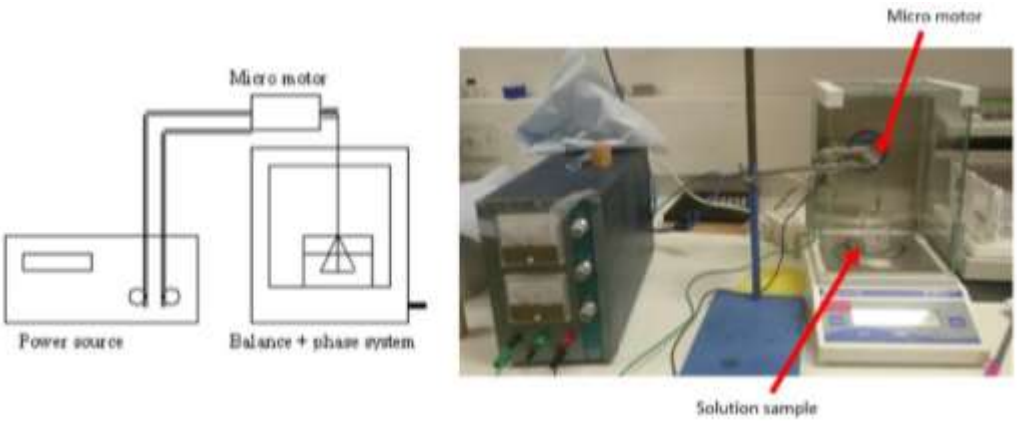

Figure 3.14. DU NUOY RING METHOD. EXPERIMENT SET UP FOR SURFACE TENSION MEASUREMENT

The ring was attached to a thread connected to the output shaft of the micromotor by a spindle. The ring was driven by the micromotor which was clamped above the beaker containing the solution on the balance. In turn, the micromotor was connected to the power supply, set to 11.55 V to pull the tread at 1mm/min. The Du Nuouy ring test procedure consisted in the following steps:

a. Sample preparation. Water solutions with Surfactants A, B and C2 at different concentrations were mixed by magnetic stirring for 10 minutes at 22°C. A 10-ml sample of each solution was syringed to a glass beaker for surface tension measurement.

b. Sample loading. After balance taring, the 10 ml-solution beaker was placed on the balance plate. The ring was submerged at the centre of the beaker just below the surface of the solution.

c. Measurement. Once the motor is turn on, the ring is pulled up what decreases the mass reading on the balance as the surface tension of the meniscus pulled the system up. When the meniscus reaches a maximum height, the mass reading stabilises for a few seconds at a considerably low value. This low value is the maximum tensile force exerted by the meniscus (m_1). The mass reading will continue decreasing until the meniscus breaks. The mass reading after meniscus breaking (m_2) was also recorded. Triplicate measurements were carried out and averaged for each sample.

The surface tension was calculated by the following equation:

$$\gamma = \frac{9.81 \cdot (m_2 - m_1)}{2\pi(r_i + r_0)} \qquad \text{(Equation 3.1)}$$

Where:

- r_1: inside radius of the ring

- r_0: outside radius of the ring

- m_1: lowest mass recorded before break point

- m_2: highest mass recorded after break point

3.4.3.2.2 Wilhelmy method

The surface tension measurements of gelatine-surfactant "A" solutions at 50°C were carried out by LPD Lab Services Ltd due to the equipment unavailability at Brunel University for the analysis of heated solutions.

The surface tension at 50°C of 10 *wt%* gelatine-water solutions was measured using a Data Physics DCAT 9 tensiometer and the Wilhelmy plate method. Six surfactant concentrations were measured. The surface tension of the 10 *wt%* gelatine-water solution without surfactant was also measured (sample TA0).

TABLE 3.53. EXPERIMENTAL DESIGN FOR THE SURFACE TENSION MEASUREMENT OF GELATINE-SURFACTANT "A" SOLUTIONS AT 50°C.

ID	SURFACTANT A* (*wt%*)
TA0	0.00
TA1	0.05
TA2	0.15
TA3	0.25
TA4	0.50
TA5	1.5
TA6	4.5

**Surfactant "A" was added based on water weight percentage*

Note: gelatine concentration was kept constant at 10wt%

Table 3.54 shows the experimental matrix for this experiment. Samples were prepared by heating water to 50°C, then add the required amount of surfactant A and gelatine. The mixture was stirred gently on a magnetic hot plate/stirrer for 15 minutes until the gelatine was fully dissolved. The temperature was monitored and maintained throughout. The surface tension of the sample was immediately tested in triplicate at 50°C.

TABLE 3.54. FORMULATION MATRIX FOR THE SURFACE TENSION MEASUREMENT OF GELATINE-SURFACTANT A SOLUTIONS AT 50°C.

ID	WATER (*wt%*)	GELATINE (*wt%*)	Surfactant A* (*wt%*)
TA0	90.00	10.00	0.00
TA1	90.00	10.00	0.05
TA2	90.00	10.00	0.15
TA3	90.00	10.00	0.25
TA4	90.00	10.00	0.50
TA5	90.00	10.00	1.50
TA6	90.00	10.00	4.50

**Surfactant A was added based on water weight percentage*

3.4.3.3 Thermogravimetric analysis (TGA)

Thermogravimetric analysis was carried out in a TA SDT Q600 (TA, UK). TGA was used to investigate the weight loss characteristics and decomposition of samples A7 and A11 (see table 3.35). Approximately 10 *mg* of sample was heated from room temperature to 450°C at 10°C/min under an air flow.

TGA consists in the monitoring of the mass of a substance as a function of time or temperature as it is subjected to a controlled temperature programme under a given atmosphere. Under this programme, the sample weight may decrease or increase.

3.4.3.4 Rheology

The gelatine and agar hydro-gel solutions were characterised by the sol-gel rheological behaviour and gelling and melting temperatures using an Advanced Rheometric Expansion System (ARES) (TA, UK) with a 50mm diameter parallel plate.

Gelatine and agar solutions were prepared and loaded to the rheometer at 70°C and 85°C, respectively. The beaker containing the solution was insulated with a PU foam sleeve, and the sample was transferred to the bottom plate of the rheometer using a 10-*ml* syringe, avoiding the formation of bubbles. The excessive solution was squeezed out of the gap, set to 0.5 *mm*, and was wiped off. A thin layer of silicone oil was applied around the edges of the parallel plates to minimise moisture loss. In the case where a gelled sample was required for analysis (strain, frequency and temperature sweeps), the sample was allowed to cool and gel between the plates for 45 minutes to ensure that the physical structure of the gel was naturally formed. Each hydrogel prepared was used for one test only. The tests were performed in triplicate and results were averaged. Table 3.55 summarises the gelatine rheology parameters of the tests discussed in the following sections.

TABLE 3.55. GELATINE RHEOLOGY TESTS PARAMETERS

TEST PARAMETER	FREQUENCY SWEEP	STRAIN SWEEP	TIME SWEEP	TEMPERATURE RAMP
gap (*mm*)	0.5	0.5	0.5	0.5
frequency (*Hz*)	1	1	1	1
strain (%)	1	1	1	1
temperature (°C)	23	23	23	23-40
points per decade	10	10	20	10
Max. applied strain (%)	-	-	-	2
Max. allowed torque (*g·cm*)	20	20	20	20
Min. allow torque (*g·cm*)	0.1	0.1	0.1	0.1

The agar rheology tests parameters are summarised in Table 3.56.

TABLE 3.56. AGAR RHEOLOGY TESTS PARAMETERS

TEST PARAMETER	FREQUENCY SWEEP	STRAIN SWEEP	TIME SWEEP
gap (*mm*)	0.5	0.5	0.5
frequency (*Hz*)	1	1	1
strain (%)	0.5	0.5	0.5
temperature (°C)	23	23	23
points per decade	10	10	20
Max. applied strain (%)	-	-	-
Max. allowed torque (*g·cm*)	20	20	20
Min. allow torque (*g·cm*)	0.1	0.1	0.1

3.4.3.4.1 Linear Viscoelastic Region (LVR)

The rheology tests were carried out following Zuidema *et al* (2014) procedure. The first test was the **linear viscoelastic (LVR)** determination for each of the selected formulations (see Table 3.58). The aim of this test was the selection of strain and frequency parameters for subsequent tests.

The LVR region was determined by frequency and strain sweeps to identify appropriate ranges that produce signals able to be recorded by the rheometer and, at the same time, do not destroy the gel structure. The end of the linear region for frequency and strain sweeps was considered a 10% deviation from the G' equilibrium plateau (TA Instruments, 2017). For both frequency and strain sweeps the sample was prepared as explained in Section 3.4.3.4 and left to gel on the plate for 45 minutes. This

time was found sufficient for gelling and it was identified in a preliminary time sweep that showed the time at which the sample reached equilibrium in *G'*.

Strain sweeps were conducted from 0.1 to 100% at a constant frequency (1 *Hz)* on the fully formed gel samples. The frequency sweep ranged from 0.01 to 81 *Hz*, the maximum allowed by the rheometer, at constant strain (0.5 and 1*%,* for agar and gelatine gels, respectively). For both strain and frequency sweeps, the rheometer chamber temperature was adjusted at 23°C, the temperature used for the foams drying in the environmental chamber.

The storage modulus (*G'*) and loss modulus (*G''*) were recorded for this analysis. The average equilibrium storage modulus (G'_{eq}), for each formulation was also recorded.

3.4.3.4.2 Time sweeps

Once the LVR was determined, **time sweeps** were conducted on the samples to determine the gelation time and temperature for each selected formulation (see Table 3.58). The gelation behaviour (i.e. gelation time at a given temperature and gelling temperature) of the gels may influence foam stabilisation and the drying process (e.g. drying temperature). Thus, it is essential to understand the influence of gelling agent, surfactant concentration and casting temperature on the gelation process.

The experiments carried out involving time sweep tests were:

a. Gelling time and temperature determination of gelatine sols at 23°C
b. Surfactant type and content influence on gelatine gelling behaviour at 23°C
c. Effect of curing temperature on the gelling behaviour of gelatine gels
d. Effect of the pH on the gelling behaviour of gelatine gels
e. Gelling behaviour of aqueous agar solutions at 23°C

The sample preparation was as explained in Section 3.4.3.4. The samples were loaded into the rheometer in a liquid state (at 70°C and 80°C for gelatine and agar, respectively) and let gel while the rheology tests were conducted and the temperature of the gel was decreasing. Constant strain and frequency parameters were chosen based on parameters found within the LVR as shown in Tables 3.55 and 3.56.

***a.* Gelling time and temperature determination of gelatine sols at 23°C**

The gelling of low and high bloom gelatine gels at three different concentrations (10, 15 and 20 *wt%)* was investigated at 23°C (rheometer chamber temperature). The

gelling time and temperature was measured with a time sweep (60 minutes) test following the parameters from Table 3.55. This allowed the study of the influence of gelatine content and gelatine strength on gelling characteristics of gelatine gels.

A full factorial design with two factors, gelatine strength and gelatine content, at two and three levels, respectively, was carried out to calculate the statistical significance of the two parameters in gelling temperature (see Table 3.57) by an ANOVA test, as described in Section 3.3.2. The reasons to focus on these factors and their selected levels were:

Factor A, gelatine content. The three different levels of gelatine content assessed in section 3.3.3.3 (for system 3) were investigated: low level, 10 *wt%*; intermediate level,15 *wt%;* and high level, 20 *wt%.*

Factor B, gelatine strength. The low and high *Bloom* gelatines used in System 2 were investigated to produce hydrogel foams.

Table 3.57. GELLING BEHAVIOUR OF GELATINE GELS AT DIFFERENT GELATINE CONCENTRATIONS AND GELATINE STRENGTHS. EXPERIMENTAL FACTORS AND LEVELS

VARIABLE	ID	LOW LEVEL (-1)	INTERMEDIATE LEVEL (0)	HIGH LEVEL (+1)
1. GELATINE CONTENT (*wt%*)	A	10	15	20
2. GELATINE STRENGTH	B	Low	-	High

The formulation matrix for the study of the influence of gelatine content and gelatine strength on the gelling behaviour of gelatine gels is shown in Table 3.58.

Table 3.58. GELLING BEHAVIOUR OF GELATINE GELS AT DIFFERENT GELATINE CONCENTRATIONS AND GELATINE STRENGTHS. EXPERIMENTAL FACTORS AND LEVELS

ID	GELATINE CONTENT (*wt%*)	GELATINE STRENGTH	WATER CONTENT (*wt%*)
J1	10	Low	90
J2	15		85
J3	20		80
J4	10	High	90
J5	15		85
J6	20		80

The gelling time was considered the zero-slope point of the G' curve, before the G' plateau and after the G' initial sharp increase. The gelling temperature was the temperature at which the G'-G'' cross-over took place.

b. Surfactant type and content influence on gelatine gelling behaviour at 23°C

The gelling of the gel samples (before foaming) of A1, A7, C2.1 and C2.7 (see Tables 3.35 and 3.36) was investigated at 23°C (rheometer chamber temperature). The gelling time and temperature was measured with a time sweep (60 minutes) test following the parameters from Table 3.55. This allowed the study of the influence of surfactants A and C2 incorporation at different levels on gelling characteristics of gelatine gels.

c. Effect of curing temperature on the gelling behaviour of gelatine gels

The gelling behaviour of sample J1 (see Table 3.58) was studied and compared at 23°C, 26°C and 29°C curing temperatures (set in the rheometer heating chamber). This test aimed to explore the influence of curing temperature increase in view of applying to the drying process (see Section 3.3.3.3.6).

***d.* Effect of pH on the gelling behaviour of gelatine gels**

The pH of the solution may affect gelling and melting temperatures of gelatine gels. To asses this, the gelling behaviour of sample J1 (see Table 3.58) was studied at different pH (see table 3.59).

TABLE 3.59. RHEOLOGY OF AQUEOUS GELATINE SOLUTIONS AT DIFERENT pH VALUES

ID	GELATINE CONTENT (*wt%*)	pH
PH4	10	4
PH5=J1	10	5
PH6	10	6
PH7	10	7
PH8	10	8

***e.* Gelling behaviour of aqueous agar solutions at 23°C**

The gelling behaviour of 5 *wt% a*gar solutions and sample AS7 (see Table 3.48) was studied at 23°C. Thus, the gelling behaviour of 5 *wt%* agar gels was compared to that when surfactant C2 was incorporated at 1.5 *wt%* (see table 3.60). The gelling point was measured with a time sweep at 0.5% strain and *1Hz* frequency (parameters obtained from the frequency and strain sweeps).

TABLE 3.60. FORMULATION MATRIX FOR THE MEASUREMENT OF GELLING POINT OF AGAR-WATER AND AGAR-SURFACTANT C-WATER SOLUTIONS

ID	AGAR CONTENT (*wt%*)	WATER CONTENT (*wt%*)	SURFACTANT CONTENT* (*wt%*)	SURFACTANT TYPE
AG1	5	95	0	-
AS7	9.85	88.67	1.48	C2

**Content based on the total weight of the agar-water solution*

3.4.3.4.3 Temperature sweeps

Temperature sweeps were conducted to determine the melting temperature of samples J1, J2, J3, J4, J5 and J6 (see sample 3.58). The tests were conducted from 25°C to 40°C. The Autostrain/autotension functions were used to allow the equipment to adjust the torque/stress applied as the material viscosity of the sample decreases and the signal weakens. An ANOVA test was carried out to analyse the statistical significance of gelatine strength and content on melting temperature.

3.4.3.5 Viscosity

A Haake Viscotester VT 550 (Thermofisher, UK) was used for viscosity measurement of the gelatine and gelatine-surfactant solutions. The liquid sample was placed in an NV cup (9 *ml* capacity), geometry mainly used for the measurement of low viscosity liquids. The NV system consists of the cup and a bell-shaped rotor. The sensor system was used with the temperature vessel which, in turn, was connected to a thermal liquid circulator and a temperature control unit. All the measurements were carried out at 50°C unless otherwise specified.

The following sections discuss the viscosity tests carried out.

3.4.3.5.1 Viscosity of gelatine solutions

The viscosity and shear stress dependence on shear rate (0-1000 s^{-1}) of gelatine solutions (at 50°C) at different concentrations (5, 10, 15 and 20 *wt%*) was measured. This test aimed to study solution behaviour and the viscosity dependence on gelatine concentration. Table 3.61 shows the formulation matrix for this test.

Table 3.61. FORMULATION MATRIX. VISCOSITY OF GELATINE SOLUTIONS

ID	GELATINE CONTENT (*wt%*)	GELATINE STRENGTH	WATER CONTENT (*wt%*)
J0	5	Low	95
J1	10		90
J2	15		85
J3	20		80

3.4.3.5.2 Influence of surfactant type and content on viscosity

The change of viscosity in gelatine solutions (10 *wt% gelatine)* with different surfactant at different concentrations was studied. The samples investigated were:

- For surfactant A. Samples A1, A7 and A13 (see Table 3.35)
- For surfactant C1. Samples C1.1, C1.4 and C1.7 (see Table 3.37)
- For surfactant C2. Samples C2.1, C2.7 and C2.13 (see Table 3.36)

3.4.3.5.3 Influence of processing temperature on gelatine-surfactant C2 solutions

The viscosity and shear rate (0-1000 s^{-1}) dependence of sample C2.1 was compared at 50°C and 70°C.

3.5 CHARACTERISATION OF LIQUID FOAMS

This section discusses the methods utilised to characterise the liquid foams.

3.5.1 Expansion ratio

Expansion ratio, ER, is the ratio between the liquid foam volume and the initial solution volume at a given time, as defined in Equation 3.2.

$$Expansion\ ratio(ER) = \frac{V_f}{V_s} \qquad \text{(Equation 3.2)}$$

Where:

- V_f: volume of the liquid foam
- V_s: volume of the initial solution

The volume of the initial solution and the liquid foam was measured using measuring cylinders of different capacities. The expansion ratio was reported as an average of three to five foaming experiments for each formulation. The maximum expansion ratio (MER) is the ratio of the maximum liquid foam volume achieved and the initial solution volume. The MER was recorded after 10 minutes of foaming, time at which all the liquid foams exhibited a constant foam height.

3.6 CHARACTERISATION OF DRY FOAMS

This section discusses the methods used to characterise the dry foams.

3.6.1 Drying and monitoring of mass loss

The drying time (conditioned at 23°C and 50% HR) of all the samples prepared for systems 3, 4 and 5 was recorded. For systems 1 and 2, the drying time was recorded in natural laboratory conditions.

The drying (conditioned at 23°C and 50% HR) of samples A7, A9, A11, C2.1, C2.3 and C2.5 (see Section 3.3.3.3.2) and ER1-ER9 (see Section 3.3.3.3.3) was studied by monitoring the weight loss every 24 hours. The drying time was considered that in which the sample mass remained constant from the previous day.

The drying process of sample A7 (see Table 3.35) was further studied by monitoring the mass loss every 24 hours under different conditions:

- Environmental chamber at 23°C and 50% HR
- Environmental chamber at 26°C and 50% HR
- Oven at 29°C. Humidity was monitored with a digital humidity/temperature meter

In addition to this, drying of sample A7 was assessed using freeze drying. The liquid foam was cast into a plastic vial of 5 ml, froze with liquid nitrogen immediately after casting and dried in a Telstar 50 (Lyoquest, Spain) freeze-drier at the following conditions:

- Freezing temperature: -45°C
- Pressure: 0.1 *mBar*
- Time frame: 8 hours

3.6.2 Density, relative density and porosity

The density (ρ) of all dry foams was measured after the samples were preconditioned at 20°C, 50% HR for 48 hours. Samples of approximately 50 x 50 x 15 *mm* were studied. Each sample was cut with a handsaw and sand to level both top and bottom faces. To minimise foam distortion and guarantee that the foam walls were perpendicular a device for guided cutting of the sample was used. The thin solid film at the bottom of some of the cast foams due to liquid drainage was removed before density measurement.

The foam density was calculated by measuring the mass per unit volume. The density was expressed as the average of five samples. The average mass of the given volume was calculated by weighing five times the sample using a Mettler Toledo AB204-S scale,

with an accuracy of 10^{-4} g. The volume of the sample was calculated from measurements using a digital calliper. Relative density ρ_r, the ratio between the density of the foam, ρ and that of the solid ρ_s, was calculated using Equation 3.3.

$$\rho_r = \frac{\rho}{\rho_s} \quad \text{(Equation 3.3)}$$

The porosity of the solid foam, p, was be found from Equation 3.4.

$$p = 1 - \rho_r \quad \text{(Equation 3.4)}$$

The porosity of the liquid foam (p_L) is given by the following formula:

$$p_L = 100 - (MER^{-1} \cdot 100) \quad \text{(Equation 3.5)}$$

3.6.3 Moisture content

The moisture content of the preconditioned dry foam samples (~0.1-0.2 *g)* was measured using an HR73 Halogen Moisture Analyser (Mettler Toledo), as described in Section 3.4.2.3.

3.6.4 Foam shrinkage and drying defects

Solid foams were produced from gelling and dehydration of the liquid foams cast in the mould. Volume shrinkage of the foam is associated with both any loss of volume in liquid stage, before significant gelling of the foam structure, and the cell wall shrinkage during drying, an undesirable phenomenon that needs to be minimised. No attempt was made to distinguish between the two sources of shrinkage. They were assessed combined and referred to as total volume shrinkage.

Foam drying shrinkage (S) was measured by the difference in cast foam volume (in moulds with known volume) and that of the dry cast foam which was measured by volume displacement of free-flowing 500-750 μm diameter glass beads (supplied by Fisher Scientific) using a graduated volume measuring glass cylinder (Zhou, 2004).

The shrinkage was calculated from Equation 3.6, where V_f is the measured volume of the foam and V_m is the mould capacity.

$$S = \left(1 - \frac{V_f}{V_m}\right) \cdot 100 \quad \text{(Equation 3.6)}$$

The cast foam volume was measured from two moulds sizes. Starch-PVAc-calcium sulphate foams used 100 cm^3 capacity moulds. The rest used 300 cm^3 moulds capacity.

The cracking tendency of starch-PVAc-calcium sulphate foams was categorised into null (no cracks), minor (small cracks in the sample surface which does not affect the

sample's integrity), medium (the sample presents big cracks in the surface which affect the sample's integrity) and severe (severe cracks which lead to collapse).

3.6.5 Foam structure analysis

SEM was utilised for structural characterisation of the dry foams from systems 2, 3, 4 and 5. The samples were selected from each batch and fractured after liquid nitrogen freezing to obtain fracture surfaces without distortions by, e.g. cutting. The sections were coated with gold using a Sputter Coater as described in Section 3.4.2.4.

The structure of samples ER1, ER2, ER3, ER4 and ER5 (see Section 3.3.3.3.3) was analysed by image analysis using *Image J* and following Pinto *et at* (2013) procedure.

3.6.6 Compression properties

The samples used for density measurement were also used for compression tests to measure compressive properties including the compressive modulus of elasticity, yield strength and compressive strength at 10, 25 and 50% strain. A Hounsfield Universal Testing Machine (Model H10KT, Hounsfield Test Equipment Ltd., UK) with a calibrated load cell of 100 *N* and two square compression plates (150 x 150 mm) was used to compress the samples up to 50% and 75% compression at a 10 *mm/min* compression speed. The stress-strain behaviour was recorded and used to extract the data mentioned.

The yield strength was determined for each averaged stress-strain curve by choosing the stress beyond the point where the elastic modulus stops being constant, indicating plastic deformation.

Compression recovery from 50% strain (recovery of the sample thickness as a percentage) was measured after the tested samples were reconditioned 48 hours in the environmental chamber at the standard conditions.

The compression behaviour of polymer foams was discussed in Section 2.2.5.2, in Chapter 2.

3.6.7 Thermal conductivity

Thermal conductivity (λ) measurement was by the standard test method for steady-state thermal transmission properties ASTM C-518. The equipment used was FOX200 from TA Instruments (UK), with an absolute thermal conductivity accuracy of ±2%. Material thermal properties principles were discussed in Section 2.2.5.3 in Chapter 2.

Samples with size 100 x 100 x 12 mm were cut and sanded using a belt sander to ensure the top and bottom faces of the samples were flat and parallel.

The samples were placed in contact with two plates set at different temperatures (0 and 20°C) and fitted with heat flux transducers. A temperature gradient established over the thickness of the sample resulted in steady-state uniaxial heat flux allowing the calculation of thermal conductivity. The test was repeated in triplicate, and the results were averaged.

The formulations studied for thermal conductivity were:

- **Starch-gelatine foams**

The thermal conductivity of samples ST8 (see Section 3.3.3.2.1), ST9, ST10, ST11 and ST12 was measured (see Section 3.3.3.2.2).

- **Hydrogel gelatine foams made with surfactants "A" and C2**

Three gelatine concentrations were studied at a constant surfactant "A" content (1.5 *wt%*) and processing temperature (50°C): 10 *wt%* (sample A7), 15 *wt%* (sample A9) and 20 *wt%* (sample A11).

Other three gelatine concentrations were studied at a constant surfactant C2 content (0.75 *wt%*) and processing temperature (50°C): 10 *wt%* (sample C2.1), 15 *wt%* (sample C2.3) and 20 *wt%* (sample C2.5).

A full factorial design with two factors, gelatine content (at three levels: 10, 15 and 20 *wt%)* and surfactant type (at two levels,"A" and C2) was carried out to calculate the statistical significance of the two parameters on thermal conductivity.

- **Biomass-hydrogel foams**

The thermal conductivity of samples O1-O6 and W1-W6 (see Section 3.3.3.4.2). ANOVA tests were carried out to study the statistical significance of the design parameters.

- **Aerogel foams**

The thermal conductivity of samples P1-P8 (see Section 3.3.3.4.4). ANOVA tests were carried out to study the statistical significance of the design parameters.

3.6.8 Sound Insulation

The airborne sound absorption coefficient and the airborne transmission loss in the audible frequency range of 50-800 Hz was measured for samples A7, A11, C2.1 and C2.5 (see Tables 3.35 and 3.36). These measurements were compared to PS 20 kg/m^3 (for both transmission loss and absorption coefficient) and PU (just for transmission loss).

Three cylindrical samples of 10 *mm* thickness were cut from each material to load them into the acoustic testing equipment.

The Brüel & Kjær impedance tube type 4206, large tube set-up was used for all absorption coefficient tests. The Brüel& Kjær sound transmission loss impedance tube type 4206-T, large tube set-up was used to measure the sound transmission loss.

The impedance tube parameters were:

- Tube diameter: 0.1 *m*

- Microphone spacing: 0.05 *m*

- Distance to sample from microphones: 0.1 and 0.15 *m*

For further information about material acoustic tests and properties, see Section 2.2.5.4 in Chapter 2.

3.6.9 Fire resistance assessment

The fire resistance performance of selected (VB7, VB9, VS3 and VS9, as seen in Section 3.3.3.4.3) dry vermiculite-hydrogel foams was evaluated and compared to that of PS (20 kg/m^3 and 10 *mm* thickness) and PU (14 kg/m^3 and 10 *mm* thickness). All the foams had the same dimensions 80 x 40 x 10 *mm*.

A photo comparison of the performance of the different materials when directly exposed to flame (produced by a hand torch) after 1, 3 and 10 *s* was analysed.

3.7 CHARACTERISATION OF THE HONEYCOMB PANELS

This section describes the characterisation of the filled and unfilled cardboard and Nomex® honeycomb panels.

3.7.1 Cell structure

The honeycomb panels cell walls were measured using Vernier Calipers and the value reported was the average of five measurements. The angle θ was calculated by trigonometry, using average values of the cell walls length.

3.7.2 Density

The reported panels density was the average of five specimens for each panel type. The sample size was 100 x 100 *mm*. The thickness reported in Table 3.13 does not include the thickness of Nomex® panels skins. The total panel thickness (core + skins) for samples N1 and N2 was 5 and 10 *mm*, respectively.

The relative density of the cores was calculated according to the following formula (Gibson & Ashby, 1999):

$$\frac{\rho}{\rho_s} = \frac{\frac{t}{l}\left(\frac{h}{l}+1\right)}{\left(\frac{h}{l}+\sin\theta\right)\cos\theta} \qquad \text{(Equation 3.7)}$$

Where:

- ρ_s: density of the material the honeycomb is made of
- t: cell wall thickness
- l: cell wall length
- h: cell height
- ϴ: cell wall angle

3.7.3 Quasi-static compression tests

The panels (core + skins) were compressed until 50% strain in an Instron 5969 Universal Testing System equipment (Instron, US). A calibrated load cell of 30 *kN* was used, and the compression speed was at 2 *mm*/min. The specimens used for compression tests were the ones used for density measurements. Five samples of each sample were tested.

The compression modulus and the maximum compressive strength were calculated from the stress-strain data.

3.7.4 3-Point Bending tests

The 3-point bending flexural tests for cardboard panels were carried out in a Zwick/Roell machine with a 5-mm radius circular head, whereas Nomex® panels were characterised in an Instron 5969, with a 5-*mm* radius roller, where the compression test was carried out.

The samples were cut at a length to thickness (l/h) ratio of 20, and the support span length to thickness ratio was 16. These ratios were in accordance with BS EN ISO 178:2010 A1:2013: Plastics-determination of flexural properties.

A 0.8 *N* preload was applied. The loading speed was 2 mm/min ± 20%, determined by the thickness of the samples. Three specimens of each panel type were tested.

The flexural modulus and the flexural strength were calculated from the stress-strain data obtained.

4. CHAPTER 4.
PRELIMINARY STUDY LEADING TO HYDROGEL FOAM

Chapter 4.

PRELIMINARY STUDY LEADING TO HYDROGEL FOAMS

4.1 INTRODUCTION

This chapter focuses on the results and discussions on the preliminary experiments carried out for production of bio-foams for thermal applications. Starch was selected as the primary biopolymer for this initial exploration due to its low cost, high biodegradability and commercial availability.

Starch must be mechanically and thermally processed in the presence of a plasticiser to convert it into a usable material, *Thermoplastic Starch* (TPS) with the required thermal plasticity and flexibility (Nafchi *et al.*, 2013). Section 4.2 analyses the effect of treatments on starch during the preparation of the liquid for foaming which would have an impact on the two formulation systems based on starch.

Section 4.3 moves on to describe the first formulation system explored based on starch-PVAc-calcium sulfate. Material characteristics, such as foam density, defects developed on drying and drying timeframe, are correlated with formulations and processing methods used.

Despite the success in proving the concept of liquid foaming and achieving foam stabilisation leading to dry foams, the density of the foams created in the first system was much higher than desired for thermal packaging applications mainly due to the use of calcium sulfate as the liquid foam stabiliser. In an attempt to reduce the foam density and the drying time, Section 4.4 examines the second formulation system, starch-gelatine foams using gelatine 1) to form part of the biopolymer matrix with starch and 2) to act as a liquid foam stabiliser. Two subsystems were explored here. Firstly, a preliminary study on starch-gelatine foams with detergent, for the liquid surface tension reduction, was carried out, and the foam structure and properties were briefly examined. Then, starch-gelatine foams were prepared with surfactant C2 to replace the detergent to eliminate the ambiguities due to incomplete knowledge of its composition.

4.2 MICROSCOPY ANALYSIS OF THE POST-PROCESSING STARCH

The starch was thermally and mechanically treated in the presence of water in attempt to transform it into a homogeneous TPS solution for subsequent liquid foaming, as described in Section 3.4.3.1 in Chapter 3.

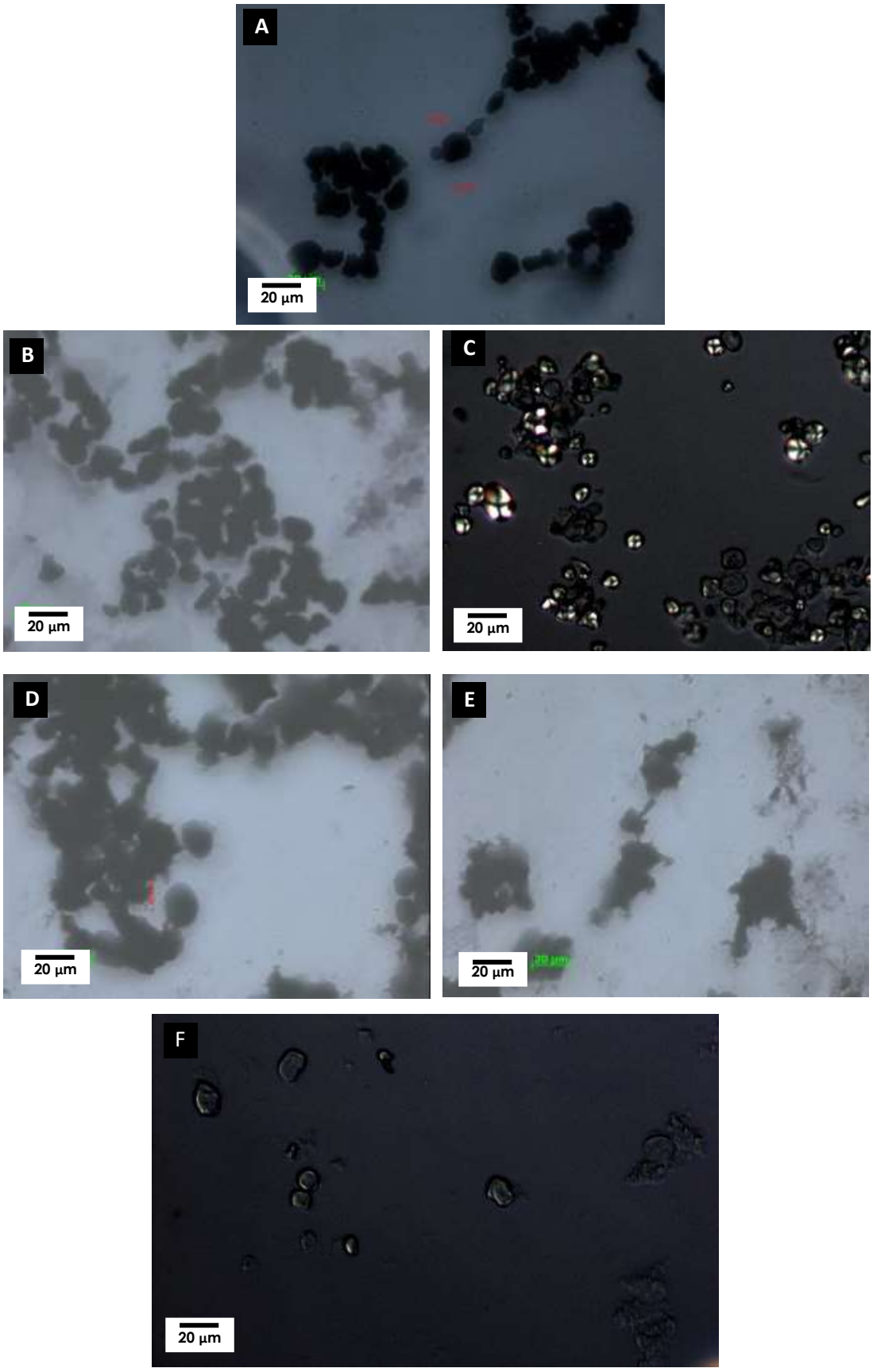

Figure 4.1. OPTICAL MICROSCOPE IMAGES OF STARCH AT DIFFERENT PROCESSING STAGES AND MICROSCOPE CONDITIONS (A) STARCH POWDER (B) STARCH GEL AFTER HEAT TREATMENT (C) STARCH GEL AFTER HEAT TREATMENT UNDER POLARISED LIGHT (D) (E) STARCH GEL AFTER HEAT AND SHEAR TREATMENT (E) STARCH GEL AFTER HEAT AND SHEAR TREATMENT UNDER POLARISED LIGHT

Figure 4.1.A shows the intact, as received, starch granules without any treatment. Thus, they exhibited the same size and shape as that of the SEM images presented in Section 3.2.1.1 (Chapter 3).

Figure 4.1.B presents an image of the starch gel after the heat treatment (cooking) alone. It shows that most of the granules were maintained, although there was considerable swelling and surface roughening of the granules. Figure 4.1.C shows the starch gel after the heat treatment under polarised light and the typical Maltese cross of some starch granules can be seen. This confirmed the remaining of crystallinity and suggested that the internal structure of a considerable number of granules resisted changes during the heat treatment and, thus gentle cooking only was not sufficient to transform starch into a homogenous TPS.

Figures 4.1.D, 4.1.E and 4.1.F shows the appearance of the starch gel after the combined heating and shearing treatment. The incorporation of shearing to the process considerably improved the starch structure destruction, resulting in a mixture of gel and relics of starch granules. As shown in Figure 4.1F, under polarised light, some starch relics still showed weaker crystallinity in comparison with Figure 4.1.C.

These assessments showed that the starch "solutions" prepared by the cooking and mechanical shearing treatments were not as homogeneous as expected and the heterogeneity in the liquid film may reduce the stretchability of the film leading to premature bubble rupture.

4.3 STARCH-PVAc-CALCIUM SULFATE FOAMS

After a series of preliminary testing based on suitability for foaming and foam integrity, an initial formulation, sample PO1 (see Table 3.19, Chapter 3) was selected as a starting point for further investigation, as described in 4.3.1. This was then extended to refinements for increasing starch content (section 4.3.2.) and further density reduction (section 4.3.3).

4.3.1. ASSESSMENTS OF THE INITIAL FORMULATION

Sample PO1 exhibited a maximum expansion ratio of 2.3 and gave rise to a density of 158 kg/m^3 after ~2 weeks of natural drying. As can be seen from Figure 4.2, PO1 foams maintained their integrity during the drying process and only showed a volume shrinkage of ~5% during drying without cracking. Both (low shrinkage and lack of drying defects) are desirable features for foam moulding.

The high density of the samples, compared with that for common low-density plastic foams of one order of magnitude lower, was however undesirable for thermal

packaging applications, it was associated with the relatively high content of calcium sulfate (~56.4 *wt%*) as shown in Table 4.1, among other factors.

Table 4.1. PO1 DRY COMPOSITION (*wt%*)

ID	CALCIUM SULFATE (*wt%*)	PVAc (*wt%*)	WATER (*wt%*)	STARCH (*wt%*)	DETERGENT (*wt%*)
PO1	56.37	21.14	16.85	4.83	0.81

The expansion ratio of the suspension also contributed to foam density (in liquid and dry stages). Expansion ratio represents the ability of air incorporation into the liquid and is related to several factors which are often interdependent. Low viscosity is commonly desirable for blending air into the liquid, but it implies low solid content formulations which may lead to high drying shrinkage and high drainage (what provokes film thinning and, ultimately, cell rupture (Bhakta and Ruckenstein, 1997). A low surface tension (i.e. lower resistance for bubble expansion and coarsening) is also desirable for air-liquid blending and foam stabilisation (Amaral *et al.*, 2008).

However, excessive high expansion ratios were observed to result in increased post-casting foam collapsing, i.e. before foam stabilisation. This may be attributable to the extension film thinning at high expansion ratios. High expansion ratios require a relatively high stretchability/strength of the liquid film to minimise cell rupture (Zhou, Song and Parker, 2006). PVAc was the additive intended to improve stretchability, but it was proved to be inefficient at relatively high expansion ratios.

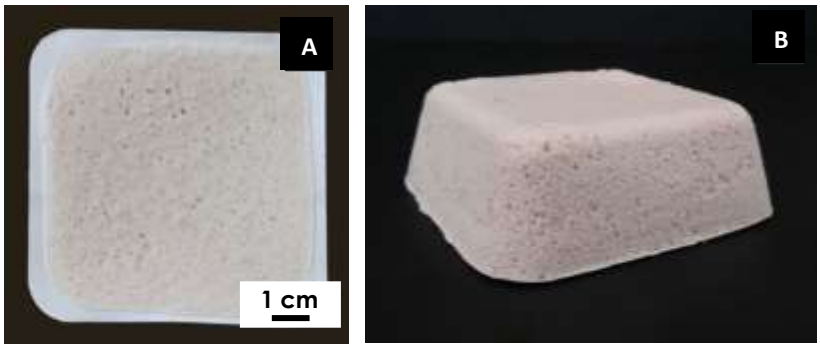

Figure 4.2 SAMPLE PO1. (A) AS CAST IN MOULD OF DIMENSIONS 80 x 80 x 30 *mm* (100cm^3 CAPACITY) (B) DRY STARCH-PVAc-CALCIUM-SULFATE FOAM

The low drying shrinkage (from the liquid foam casting to dry solid foam) can be attributed to the following:

a. Effective stabilisation of the liquid foam structure by cementation of the liquid phase into a rigid foam structure (Singh and Middendorf, 2007), which prevented changes in foam structure

b. Low shrinkage of the cemented structure during drying associated with the high solid content of POP and locking in of chemically bonded water

Low shrinkage reduces the risk of foam cracking. Non-uniform shrinkage leads to high stress in the cell walls which may generate cracking near the final stage of drying when the foam is more rigid and brittle (Turuallo and Soutsos, 2015). Stability of liquid foams refers to the resistance against volume reduction of foams by bubble ruptures following liquid drainage and film thinning (Bhakta and Ruckenstein, 1997).

Shrinkage is heavily influenced by the solution composition (Amaral *et al.*, 2008). For instance, it was observed during the preliminary investigations that higher contents of calcium sulfate and PVA produced dry foams with less shrinkage and cracking tendency than foams with higher starch contents. This is attributable to the rapid solidification and high film stretchability properties associated with higher POP and PVAc contents, respectively, whereas greater starch content correlated to solution/suspension heterogeneity and low film stretching. Higher water content helped to increase expansion ratios, but increased drying time and produced foams with higher drying shrinkage and crack tendency.

Based on the preceding discussions, further attempts were made to increase the starch content, decrease the water content and to reduce the drying effort. One should be mindful that changes in one formulation or processing factor may have multiple knock-on impacts.

4.3.2 REFINEMENT 1. INCREASE IN STARCH CONCENTRATION

This section discusses the attempt to increase the starch content and lower the foam density, based on the results from Section 4.3.1. The investigated starch content increased from 87.5% (samples PO2 and PO7) to 354% (samples PO6 and PO11) compared with that of the PO1 liquid formulation. The water was kept constant in weight as that in PO1 but slightly decreased in weight percentage of mass as the total mass of each batch was not kept constant (see Table 3.20 in Chapter 3).

Since low expansion ratios were expected, as starch content (and consequently, solid content) was increased, the surfactant (detergent) content was also increased by 50% (samples PO7-PO11) and 200% (PO2-PO6) compared with that in the PO1 liquid formulation, in an attempt to decrease the surface tension of the solution so as to assist the foaming process. All samples were dried naturally for ~16 days.

Table 4.2. EFFECT OF STARCH AND SURFACTANT CONCENTRATION INCREASED ON FOAMING/FOAM CHARACTERISTICS

ID	MER	DENSITY (kg/m^3)	CRACKING SIGNIFICANCE*	DRYING VOLUME SHRINKAGE (*vol%*)**
PO1	2.3	158	0	<5
PO2	2.69	-	3	-
PO3	2.36	-	3	-
PO4	2.46	-	3	-
PO5	2.33	-	2	-
PO6	1.69	-	3	-
PO7	2.19	135	1	<5
PO8	1.89	185	1	<5
PO9	1.71	211	1	<5
PO10	1.57	-	2	-
PO11	1.36	-	2	-

* See Section 3.6.4 (chapter 3) and Figure 4.3 for further details about levels definition
** For a cast foam ~ $100cm^3$ in volume

The results obtained are presented in Table 4.2. As expected, higher detergent concentration tended to produce higher MER. The group with higher detergent content (Samples PO2-PO6) exhibited slightly higher expansion ratios than the other group with lower detergent content (samples PO7-PO11).

However, all samples showed a different degree of cracking as in Figure 4.3. Figures 4.3A, 4.3B and 4.3C show samples exhibiting "minor, medium and severe" cracking, respectively. For only those with minor cracking (level 1), volume shrinkage and density can be measured with confidence and thus, the rest with a high level of cracking significance (levels 2-3) were omitted.

Sample group with higher detergent content and higher MER (PO2-PO6) exhibited a higher degree of cracking while those with the lower detergent contents exhibited less in general, especially at lower starch concentrations (samples PO7, PO8 and PO9). Higher MER and starch content implied a tendency to defect development due to film thinning and film stretchability decrease, respectively, as discussed in Section 4.3.1.

FIGURE 4.3 DIFFERENT DEGREE OF CRACKING IN THE DRY FOAMS A) MINOR B) MEDIUM AND C) SEVERE

Samples PO7, PO8 and PO9, with only minor cracking, achieved densities of 135, 185 and 211 kg/m^3, respectively. Compared with that of PO1, just PO7 was lighter, but PO1 did not present any cracking tendency, while PO7 had small cracks in its surface. Furthermore, dry PO7 foam main component was still calcium sulfate (*54.16 wt%*), followed by PVA (*20.51 wt%*) and starch (*7.74 wt%*). The measured moisture content was *17.59 wt%*.

In conclusion, insignificant improvement in density was achieved at the expenses of formation of drying defects-cracking.

4.3.3 REFINEMENT 2. DECREASE IN WATER CONCENTRATION

This section investigates the water content reduction and detergent adjustments based on PO7, PO8 and PO9 formulations which produced relatively better foams (see table 3.21 for formulations, Chapter 3). Water content was reduced by 25% compared with that in PO7, PO8 and PO9. Detergent was studied at the same level and by 33% increase with that in PO7, PO8 and PO9. The influence of using perforated moulds to reduce the drying time was also tested here.

As shown in Table 4.3, MER decreased at lower water and detergent concentrations, as expected. Sample PO9.3 could not be foamed due to the high solid content which hindered the air incorporation.

Samples PO9.2, PO7.3 and PO8.3, the ones exhibiting lower expansion ratios, were the ones displaying less formation of drying defects-cracking. But their low MER resulted in higher dry foam densities of 246, 247 and 289 kg/m^3, respectively compared with PO7, 8 and 9.

Table 4.3 EFFECT OF WATER AND DETERGENT CONCENTRATION DECREASE ON FOAMING/FOAM CHARACTERISTICS

ID	MER	DENSITY (kg/m^3)	CRACKING SIGNIFICANCE*	DRYING VOLUME SHRINKAGE (*vol%*)**
PO7.2	2.00	-	2	-
PO8.2	1.86	-	2	-
PO9.2	1.57	246	1	<5
PO7.3	1.29	247	1	<5
PO8.3	1.15	289	1	<5
PO9.3	-	-	-	-

* See Section 3.6.4 (Chapter 3) and Figure 4.3 for further details about levels definition
** For a cast foam ~ 100cm^3 in volume

The decrease in water concentrations did not reduce the foams drying time, but the use of the perforated moulds slightly reduced it by 2-3 *days* and hence from 16-17 days to 13-14 *days*.

In conclusion, there are fundamental restrictions on the system and no more scope for further improvements. A change in directions was carried out, and POP was substituted with bio-based hydrogel gelling agents.

4.4 STARCH-GELATINE FOAMS

This section studies starch-gelatine foams prepared with two different surfactants. In work described in section 4.4.1, the detergent remained as the surfactant agent but was replaced by Surfactant C2 in that of Section 4.4.2.

4.4.1 PRELIMINARY STUDY OF STARCH-GELATINE FOAMS

This preliminary experiment studied three factors: detergent content, the starch-gelatine ratio at a constant predetermined total solid (starch+ gelatine) content, and gelatine with different gelling strength (i.e. Bloom number).

Starch/gelatine formulation weight ratio was kept at nominally 30/70 for samples ST1, ST2, ST5 and ST6 and 50/50 for samples ST3, ST4, ST7 and ST8. Table 4.4 shows the dry foam compositions for this study. Further experimental details are shown in Section 3.3.3.2.1 in Chapter 3.

Table 4.4. DRY FOAMS COMPOSITION OF PRELIMINARY STARCH-GELATINE FOAMS

ID	DETERGENT (*wt%*)	STARCH (*wt%*)	GELATINE (*wt%*)	GELATINE STRENGTH
ST1	0.00	25.88	60.39	Low
ST2	1.97	25.30	59.04	Low
ST3	0.00	43.14	43.14	Low
ST4	1.97	42.17	42.17	Low
ST5	0.00	25.88	60.39	High
ST6	1.97	25.30	59.04	High
ST7	0.00	43.14	43.14	High
ST8	1.97	42.17	42.17	High

Notes: mean moisture content ~12*wt%*; acetic acid content 1.7*wt%;* total solid content 18*wt%* based on starch-gelatine suspension

As shown in Table 4.5, the use of detergent was proved useful in achieving higher liquid foam expansion ratio, lower volume shrinkage (although marginally) and dry foam densities. The drying time, compared with the previous system has halved from two weeks to 4-7 days and drying for the lower density foams in the pairs of samples (with/without detergent) generally requires less time by a day or two due most likely to the high porosities.

The starch/gelatine ratio also influenced the maximum expansion ratio (MER), especially in low strength gelatine. Relatively higher gelatine content gave rise to greater MER, and consequently, samples with higher starch/gelatine ratios exhibited higher densities. Density ranged from 85.2 kg/m^3 to 177.30 kg/m^3 for starch-gelatine ratios of 50/50 and 78.80 kg/m^3 to 120.10 kg/m^3 for starch-gelatine ratios of 30/70. Starch-gelatine ratio also affected the shrinkage values.

Table 4.5 FOAMING AND DRYING CHARACTERISTICS OF THE PRELIMINARY STARCH-GELATINE FOAMS

ID	STARCH/ GELATINE RATIO	DETERGENT (Y/N)	GELATINE STRENGTH	MER	Dry foam Density (kg/m^3)	Volume Shrinkage (*vol%*)*	Drying time (*days*)**
ST1	30-70	N	Low	3.47	120.10	56.86	6
ST2	30-70	Y	Low	4.57	91.8	56.53	5
ST3	50-50	N	Low	2.58	177.3	61.25	7
ST4	50-50	Y	Low	3.75	101	60.12	5
ST5	30-70	N	High	3.50	114	54.49	5
ST6	30-70	Y	High	4.29	78.8	52.42	4
ST7	50-50	N	High	3.14	118.2	55.43	4
ST8	50-50	Y	High	4.50	85.2	54.68	5

***for a cast foam ~ 300cm^3 in volume
****Time to reach equilibrium moisture content

Starch-gelatine foams resulted in slightly higher shrinkage (~10*vol%*) in comparison with starch-PVAc-POP foams (<5*vol%*) for a cast foam ~ 100cm^3 in volume. This may be

partially attributable to the substitution of POP by gelatine and starch. POP did not considerably shrink post-cementation reaction while gelatine shrank much more when losing water. The increase of the formulation water content and consequently, the increase in the amount of water to be evaporated during the drying process may be another factor influencing the higher shrinkage in starch-gelatine foams. However, higher shrinkage (~55*vol*%) was obtained for a cast foam ~ 300cm^3 in volume (no results for shrinkage in volume in 300cm^3 moulds for starch-PVAc-POP foams).

Starch-gelatine system gave rise to higher expansion ratios (2.58-4.57) than starch-PVA-POP system (1.15-2.69). This is due to the lower solid content of starch-gelatine foams and the homogeneous solution of gelatine compared to the heterogeneous liquid dispersed with POP particles and starch granule relics, allowing much higher film stretching.

Higher gelatine content resulted in lower volume shrinkage, more remarkably at high strength gelatine. This may be attributed to their relatively higher gelling power, compared to the foams with lower gelatine content, which reduced the bubble rupture (more details will be discussed in Rheological Characterisation, Chapter 5).

Also, as seen in table 4.5, higher gelling strength led to higher expansion ratios, shorter drying times, lower volume shrinkage and, more considerably, foam densities than that of the lower gelling strength, on average. This may be due to the higher gelling power of greater strength gel and the stronger foaming enhancement of gelatine at higher Bloom.

ST8 was deemed to be the promising formulation judged from its higher starch content (50/50 starch/gelatine ratio) and relatively low density (85 kg/m^3, approximately halved from that of the previous system).

Figure 4.4 shows the foam structure of sample ST8 under SEM microscopy. The image shows an open-cell structure with an average cell size of ~100 μm. This open-cell characteristic allows mass transport of moisture from the wet foam and supports the previous observation that lower density foams dried faster. The relics of the starch granules can be seen in the dry foam films, what confirms the conclusion obtained in Section 4.2.

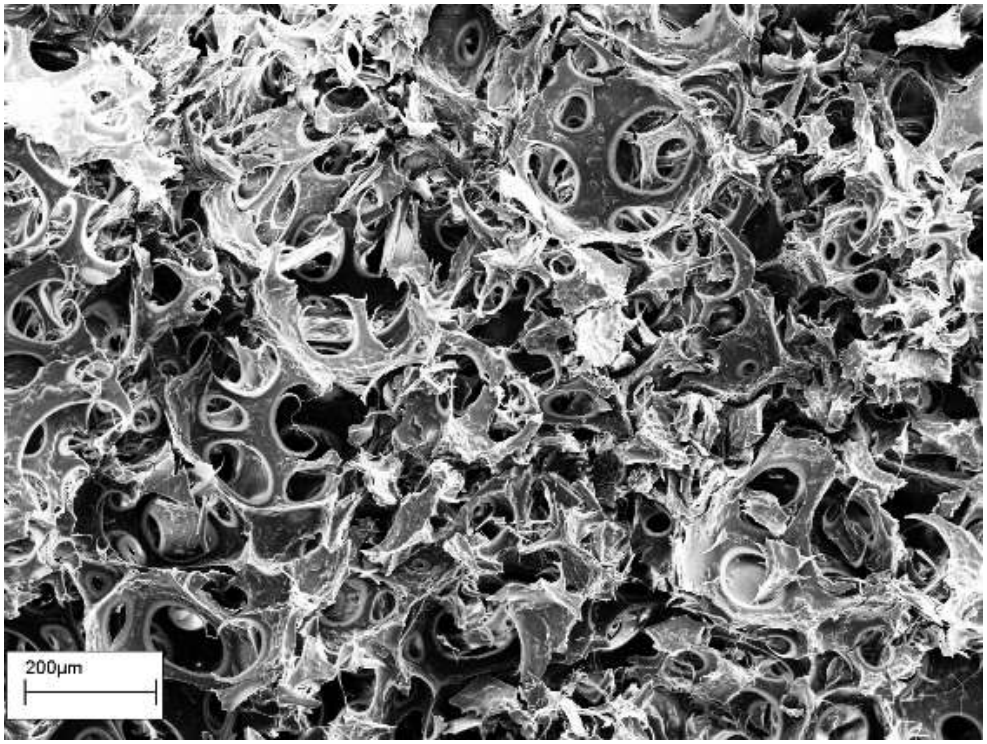

Figure 4.4. SEM IMAGE OF SAMPLE ST8

The thermal conductivity of ST8 was measured to be 0.074 *W/m·K*. It can be considered as a good thermal insulator judged from the general industrial consensus of <0.1 *W/m·K* but still higher when compared with conventional materials used for thermal packaging applications (e.g. PS ~0.03 *W/m·K*).

4.4.2 REFINEMENT OF THE STARCH-GELATINE FOAMS

This subsection investigates starch-gelatine foams prepared with surfactant C2. The surfactant content was selected after some preliminary trials followed by optimisation as detailed later in Chapter 5 for the study of hydrogel foams.

This refinement study investigated three factors: starch-gelatine ratio, starch-gelatine solid content and preservative content. Starch/gelatine formulation weight ratio was kept at nominally 30/70 for samples ST9, ST10, ST11 and ST12 and 50/50 for samples ST13, ST14, ST15 and ST16.

High Bloom gelatine was selected to use in this experiment as the results from Section 4.4.1 found that generally produced lighter and less volume shrinkage-prone foams. Further experimental details are shown in Section 3.3.3.2.2 in Chapter 3.

Table 4.6 shows the composition of the dry ST9-ST16 foams.

Table 4.6. DRY FOAMS COMPOSITION IN THE REFINED STARCH-GELATINE FOAMS

ID	STARCH-GELATINE CONTENT	SOLID CONTENT (*wt%*)*	ACETIC ACID (Y/N)	STARCH (*wt%*)	GELATINE (*wt%*)	SURFACTANT** C2 (*wt%*)	ACETIC ACID (*wt%*)
ST9	30/70	14	N	24.45	56.74	4.82	0.00
ST10	30/70	14	Y	24.08	55.88	4.74	1.30
ST11	30/70	18	N	24.76	57.45	3.79	0.00
ST12	30/70	18	Y	24.46	56.76	3.75	1.03
ST13	50/50	14	N	40.71	40.48	4.81	0.00
ST14	50/50	14	Y	40.09	39.87	4.74	1.30
ST15	50/50	18	N	41.22	40.99	3.79	0.00
ST16	50/50	18	Y	40.73	40.50	3.74	1.03

Notes: mean moisture content ~14*wt%*
**based on the starch-gelatine solution weight*
**Surfactant C2 content was kept constant at 0.75 *wt%* based on the starch-gelatine suspension weight

Table 4.7 shows the maximum expansion ratio (MER), dry density and shrinkage of samples ST9-ST16.

Table 4.7 FOAMING AND FOAM CHARACTERISTICS OF THE REFINED STARCH-GELATINE FOAMS

ID	STARCH-GELATINE CONTENT	SOLID CONTENT (*wt%*)*	ACETIC ACID (Y/N)	MER	DENSITY (kg/m^3)	VOLUME SHRINKAGE (*vol%*)**
ST9	30/70	14	N	4.22 ± 0.06	31.86 ± 4.81	35.83 ± 3.54
ST10	30/70	14	Y	4.00 ± 0.18	34.31 ± 3.14	42.29 ± 0.88
ST11	30/70	18	N	3.89 ± 0.09	47.17 ± 5.01	25.42 ± 2.36
ST12	30/70	18	Y	3.83 ± 0.06	47.51 ± 4.24	37.29 ± 0.88
ST13	50/50	14	N	3.40 ± 0.07	41.12 ± 7.27	40.42 ± 1.18
ST14	50/50	14	Y	3.38 ± 0.08	42.28 ± 3.65	40.83 ± 2.36
ST15	50/50	18	N	2.91 ± 0.06	62.33 ± 16.08	40.00 ± 0.59
ST16	50/50	18	Y	2.66 ± 0.05	73.08 ± 13.87	46.88 ± 0.29

*****based on the starch-gelatine solution weight
******for a cast foam ~ 300cm^3 in volume

As concluded in Section 4.4.1, higher gelatine contents resulted in higher expansion ratios and lower density and volume shrinkage.

MER ranged from 2.66 (sample ST16) to 4.22 (sample ST9). Highest MER was for ST9 at higher gelatine content, lower solid content and without acetic acid.

Substitution of detergent with C2 surfactant led to a decrease in MER. ST15 and ST16 exhibited a MER of 2.91 and 2.66, respectively, whereas ST8 in the earlier tests gave rise

to MER of 4.50. This may be attributable not only to the difference between surfactants and content but also their format. C2 came in powder form with less than 3% moisture content. The detergent came in liquid form, with 59% moisture content. C2 incorporation into the solutions noticeably resulted in a higher viscosity than that of the detergent, which may negatively impact on foaming. The impact of the surfactant C2 content on viscosity of the gelatine solutions will be further discussed in Chapter 5.

There was a considerable improvement in the dry foam densities using surfactant C2 compared with that of ST8 in the preliminary study using the detergent (85 kg/m^3). Density ranged from 31.86 (ST9) to 73.08 kg/m^3 (ST16). ST9 exhibited a density comparable to that of some rigid PS and PE, as shown in Table 2.2 in the Literature Review (Chapter 2).

When compared between similar formulations, foams prepared with surfactant exhibited considerably lower density than their detergent counterparts (despite the differences in contents): ST6 density was 78.80 kg/m^3 compared with that of ST12, at 47.51 kg/m^3. Similarly, ST8 density was 85.28 kg/m^3, whereas ST16 was 73.08 kg/m^3.

The volume shrinkage of the refined foam formulations was considerably lower (38.62%, on average) than that in the preliminary study (56.47%, on average). Additionally, in foams prepared without acetic acid, the shrinkage was generally relatively lower (~15-30%)than those containing acetic acid, which exhibited shrinkage levels of ~40%. The use of acetic acid decreased the pH of the solution (pH~4), which hindered, to a certain degree, the gelling of the cellular structure (this will be discussed in more details in the rheological study in Chapter 5). Despite this, the acetic acid was found necessary as visual inspections detected mould growth in ~17% of the samples produced without it. The natural drying (without forced ventilation) of all the samples in conventional *PS* moulds took ~6 days during which the wet foam provided favourable sites for growth of spoilage microorganisms. This may not be the case in a well-ventilated environment (drying with circulating air) or with the use of perforated moulds to shorten the drying time.

Figure 4.5 shows a typical cross-section for all formulations. This image corresponds to sample ST10. It shows the shrinkage as compared with dimensions of the casting mould and free of defects (cracks or large central voids).

Figure 4.5. TYPICAL CROSS-SECTION TO ALL THE CASTS OF STARCH-GELATINE FOAMS SHOWING THE SHRINKAGE FROM THE MOULD OUTLINED AND FREE OF DEFECTS.

As expected, higher solid content produced foams with lower expansion ratios and volume shrinkage and higher density. The viscosity of the solution increased with higher solid content what affected foaming, hindering the air incorporation into the solution and affecting the density of the dry foam. The lower shrinkage resulted in foams with higher solid content may be attributed to their higher gelling power derived from a higher gelling content which arrested foam aging.

Figure 4.6 compares the SEM images of the cross-section of sample ST10. No significant variation can be noticed in cell structure and density at the positions, apart from a thin layer of relatively higher density at the bottom of the cast foam, due most likely to the drainage (Figure 4.6C).

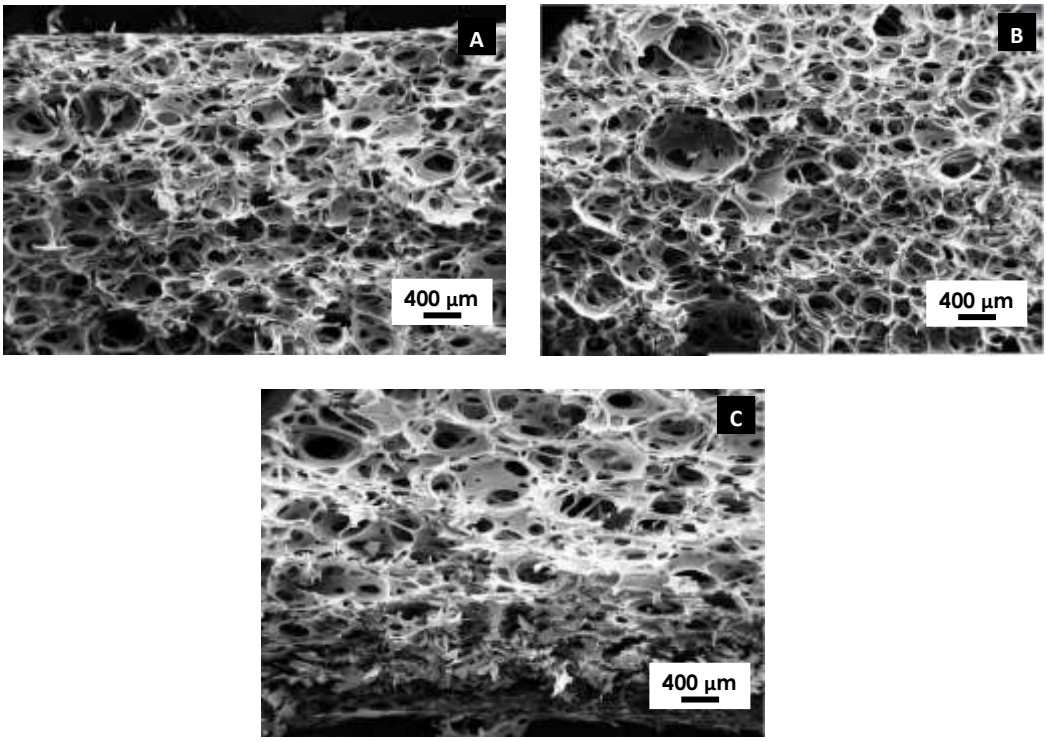

Figure 4.6. SEM IMAGES SHOWING THE CELL STRUCTURE OF STARCH-GELATINE FOAMS (SAMPLE ST10) AT DIFFERENT POSITIONS (A) TOP, IN CONTACT WITH AIR (B) CENTRE (C) BOTTOM, IN CONTACT WITH THE MOULD

Figure 4.7 illustrates a close-up image of the cells. An open cell structure with interconnected pore network can be seen. The wall surface roughness can be attributed to the granule relics. This will be compared with systems without starch in Chapter 7.

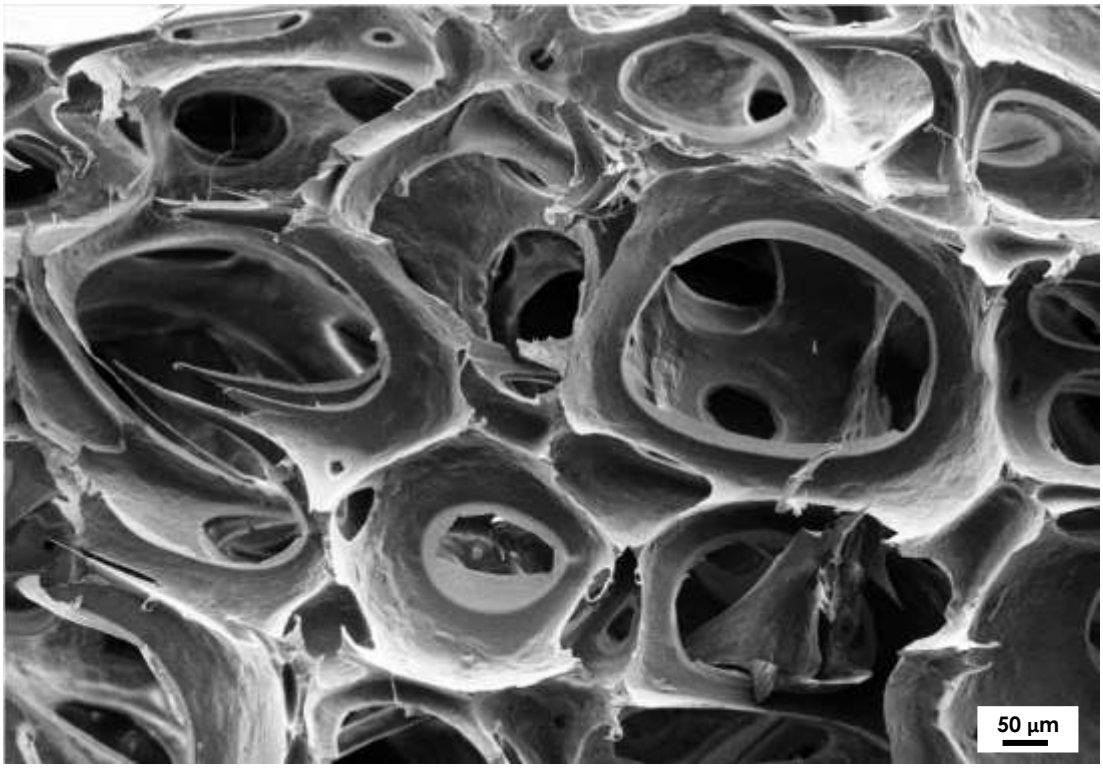

Figure 4.7 SEM IMAGES OF ST10 AT HIGH MAGNIFICATION SHOWING THE CLOSEUP OF THE INTERCONNECTED CELLS AND SURFACE ROUGHNESS OF THE CELL WALLS

Table 4.8 shows the compression modulus and stress at 10, 25 and 50% strain of samples ST9, ST10, ST11 and ST12 (i.e. samples with higher gelatine content and lower shrinkage and density). The results agreed with general observations that the compression modulus and stress at different strain values increase with density of the foams (Gibson and Ashby, 1997).

The starch-gelatine foams exhibited an average Young's Modulus of 2 *MPa* and 2.5 *MPa* for densities ~ 32.5 and ~47 kg/m^3, respectively. Thus, starch-gelatine foams Young's Modulus was considerably lower than PS Young's modulus foams (7.7-11.3 and 25-30 *MPa* for 38-32 kg/m^3 and 47-53 kg/m^3, respectively), higher than LDPE foams (0.8-0.9 and 1.5-1.8 MPa for 31-35 kg/m3 and 43-47 kg/m3, respectively) and comparable to HDPE foams (Granta, 2017).

TABLE 4.8. COMPRESSION MODULUS AND STRESS AT GIVEN STRAINS FOR SELECTED STARCH-GELATINE FOAMS

ID	DENSITY (kg/m^3)	SOLID CONTENT (*wt%*)*	E (kPa)	STRESS AT 10% (kPa)	STRESS AT 25% (kPa)	STRESS AT 50% (kPa)
ST9	31.86	14	1861.67 ± 263.60	88.34 ± 11.16	106.34 ± 13.63	142.18 ± 22.29
ST10	34.31	14	2068.67 ± 445.35	120.10 ± 6.08	133.15 ± 6.86	183.80 ± 16.12
ST11	47.17	18	2505.33 ± 402.06	147.03 ± 14.01	170.55 ± 18.10	216.15 ± 22.15
ST12	47.51	18	2409.67 ± 542.26	115.22 ± 17.63	144.84 ± 25.65	206.06 ± 36.21

***based on the starch-gelatine solution weight

The compression strength at 25 and 50% strain was lower than that for PS foams (210-230 and 700-900 *kPa* for 38-32 kg/m^3 and 47-53 kg/m^3, respectively) and higher than that of LDPE foams (38-42 and 48-52 *kPa* for 31-35 kg/m^3 and 43-47 kg/m^3, respectively).

Table 4.9 shows the yield strength and the recovery rate of samples ST9-ST12. No considerable difference was found in yield strength of this study but, generally, lower densities imply slightly lower yield strengths. The yield strength was lower than that for PS foams (200-250 and 800-1000 *kPa* for 38-32 kg/m^3 and 47-53 kg/m^3, respectively) and higher than that of LDPE foams (18-22 and 20-25 *kPa* for 31-35 kg/m^3 and 43-47 kg/m^3, respectively).

The recovery rate when the foams were compressed at 50% strain ranged from 72.92% to 82.34%. All the samples were flexible enough at the end of the compression tests without crumbling. Higher densities (i.e. higher solid content) and lower solid content implied lower recovery rates (Gibson and Ashby, 1997).

TABLE 4.9. YIELD STRENGTH (kPa) AND RECOVERY RATE (%) OF STARCH-GELATINE FOAMS

ID	DENSITY (kg/m^3)	SOLID CONTENT (wt%)*	YIELD STRENGH (kPa)	RECOVERY (%)
ST9	31.86	14	86.98	77.84
ST10	34.31	14	119.85	72.92
ST11	47.17	18	135.88	82.34
ST12	47.51	18	115.44	79.54

***based on the starch-gelatine solution weight

Figure 4.10 shows the thermal conductivity of samples ST9-ST12. The measured values are considerably lower for those measured for sample ST8 in the preliminary study. This can be attributable to the substantially high density (thus, low porosity) in sample ST8.

The thermal conductivity was comparable to that for 28-32 kg/m^3 and 47-53 kg/m^3 density PS foams (0.031-0.035 W/m·K and 0.033-0.04 W/m·K, respectively) and slightly

lower than that for 31-35 kg/m^3 and 43-47 kg/m^3 LDPE foams (0.039-0.041 and 0.042-0.044 W/m·K, respectively) (Granta Design Limited, 2014).

Table 4.10 THERMAL CONDUCTIVITY OF STARCH-GELATINE FOAMS

ID	DENSITY (kg/m^3)	THERMAL CONDUCTIVITY (W/m·K)
ST9	31.86	0.0356 ± 0.0003
ST10	34.31	0.0366 ± 0.0003
ST11	47.17	0.0356 ± 0.0005
ST12	47.51	0.0352 ± 0.0007

4.5 CONCLUSION

Two formulation systems were developed for liquid foaming. Both were starch-containing foams but with different methods of foam stabilisation from the liquid state.

The method for starch preparation combining cooking and mechanical shearing was effective but not sufficient to produce granule-free homogeneous solutions, which may limit the stretchability of the liquid film and expansion ratio. In further studies, either more energy extensive methods, such as extrusion compounding (Zhou and Hanna, 2006) would be required to destroy the starch granules. Alternatively, starch can be removed from the system using an alternative bio-polymer.

Starch-PVAc-Calcium sulfate foams use POP cementation reaction (Singh and Middendorf, 2007) for the stabilisation of the liquid foams (liquid to rigid wet foam). The system required higher non-biodegradable content (POP) to maintain foam integrity as significant cracking was associated with formulations with higher starch and solid contents. The lowest density achieved was around 135 kg/m^3, considerably higher than desirable for thermal packaging applications, and the drying timeframe was 16 days for the cast foam ~ 100cm^3 in volume. It was considered that the scope for high biopolymer incorporation was limited by the fundamental requirement of high concentration of the compendious material and thus will not be pursued further. However, it proved the concept of liquid state foaming and transition to solid foams.

A hydrocolloid was selected to replace POP in the second system to combine with starch in an attempt to achieve 100% biopolymer foams with a density comparable with polymer counterparts, appropriate mechanical and thermal properties and to reduce drying effort. The system obtained higher MER and lower shrinkage and density with surfactant C2 than detergent. Starch-gelatine system gave rise to higher MER (~4) than the starch-PVAc-POP system due to the homogeneous, lower solid content suspension achieved for the former compared to the heterogeneous suspension for

the latter. The density was considerably reduced to ~32 kg/m^3, slightly higher than that used for packaging plastic foams (~20 kg/m^3). Shrinkage was similar for a cast foam ~ 100cm^3 in volume (~10%) but increased to ~38% for a casted foam ~ 300cm^3 in volume. The drying time at ambient conditions considerably decreased to 4-6 *days*.

Starch-gelatine foams exhibited an open-cell structure with cell size 50-600 μm. The mechanical properties were comparable to that on HDPE foams, ~2 *MPa* Young's Modulus and ~100 kPa Yield Strength for ~32 kg/m^3 density. The thermal conductivity was reasonably low (~0.036 $W/m{\cdot}K$), exhibiting a comparable performance to PS foams and slightly better than LDPE and HDPE foams, with same densities.

Good all-round properties bio-foams were achieved for starch-gelatine foams. These results successfully proved the concept of using hydrocolloids as foam stabilisers for liquid foaming and transition of liquid foams to gelled foams leading to solid foams by drying. However, there is scope for further improvement. Insufficient starch treatment, relatively high density and drying times suggested starch exclusion and exploration of hydrogel foams.

5. CHAPTER 5.

PROPERTIES AND STRUCTURE OF HYDROGEL FOAMS BASED ON GELATINE

Chapter 5.

PROPERTIES AND STRUCTURE OF HYDROGEL FOAMS BASED ON GELATINE

5.1 INTRODUCTION

This chapter presents feasibility studies of hydrogel foaming and systematic investigations on the formulation, processing, structure and properties of hydrogel foams.

The chapter is divided into four main sections. Section 5.2 studies the fundamentals of gelatine solutions and gels covering rheology, viscosity and surface tension of the gelatine solutions for the selection of gelatine and surfactant concentrations suitable for liquid state foaming.

Section 5.3 includes a preliminary study on the influence of surfactant type and content on the properties of gelatine foams. This laid the groundwork for the subsequent sections to refine the selection of surfactant type and dosage.

Section 5.4 studies the influence of formulation and processing on foaming process and dry foam properties and structure. It also examines their compliance with the performance required for different applications. The properties analysed included maximum expansion ratio (MER), drying shrinkage, foam density, compressive strength and stiffness of the dry foams, thermal properties (thermal conductivity and mass loss in the thermogravimetric analysis) and acoustic properties (transmission loss and absorption coefficient).

Sections 5.5, 5.6 and 5.7 further investigate selected formulations from subsection 5.4 in terms of modifications in the formulation (plasticisers inclusion) and processing conditions (varying expansion ratio and drying process).

Section 5.8 briefly discusses two alternative hydrogel foams manufactured using agar, a non-animal origin hydrocolloid, and gellan gum, produced by bacterium *Sphingomonas elodea*, to understand the key features of these systems in comparison with gelatine as a preliminary attempt to broaden the hydrogels choice.

5.2 FUNDAMENTS OF GELATINE SOLUTIONS AND GELS

The manufacturing of hydrogel foams based on gelatine requires the preparation of an aqueous solution. The understanding of this solution is crucial for formulation and process development.

This section includes the characterisation of the rheological properties of the solutions and/or gels and surface tension, properties governing the capacity of gas incorporation (expansion ratio) and foam stabilisation.

5.2.1 RHEOLOGICAL CHARACTERISATION OF GELATINE HYDROGELS

It is essential to understand the rheological properties of gelatine gels: the equilibrium storage (*G'*) and loss (*G''*) moduli and the melting and gelling points as they influence the foaming processing and evolution of the foam structure.

The rheological characterisation procedure was described in detail in Section 3.4.3.4 (Chapter 3). Rheology principles were discussed in Section 2.2.2.2 (Chapter 2).

First, the Linear Viscoelastic Region (LVR) of the material was determined. Then, the gelling point of the gelatine solutions and its dependence on solution pH and surfactant incorporation were studied. Finally, the melting point of the gelatine gels was investigated.

5.2.1.1 Linear Viscoelastic Region (LVR)

The first step of the rheological characterisation of gelatine gels was the LVR determination. Strain sweeps from 0.1 to 100% strain were carried out on a fully formed gel at a constant frequency, 1 *Hz* (6.28 $rad \cdot s^{-1}$) (see Section 3.4.3.4.1 in Chapter 3 for further details).

The results obtained from the average strain sweeps of low and high Bloom gelatine gels are presented in Figure 5.1. The gels exhibited a viscoelastic behaviour, where *G'* values were higher than *G''* at all strain values, showing the predominance of a solid-like behaviour.

The gelatine gel exhibited constant *G'* values in a wide range of strains. The 10% linearity deviation finished at 1.26%, 2%, 17.19% and 1.41% strain for 10 *wt%* low *Bloom*, 20 *wt%* low Bloom, 10 *wt%* high *Bloom* and 20 *wt%* high Bloom, respectively. A strain level of 1% was selected for further rheological characterisation for all the samples.

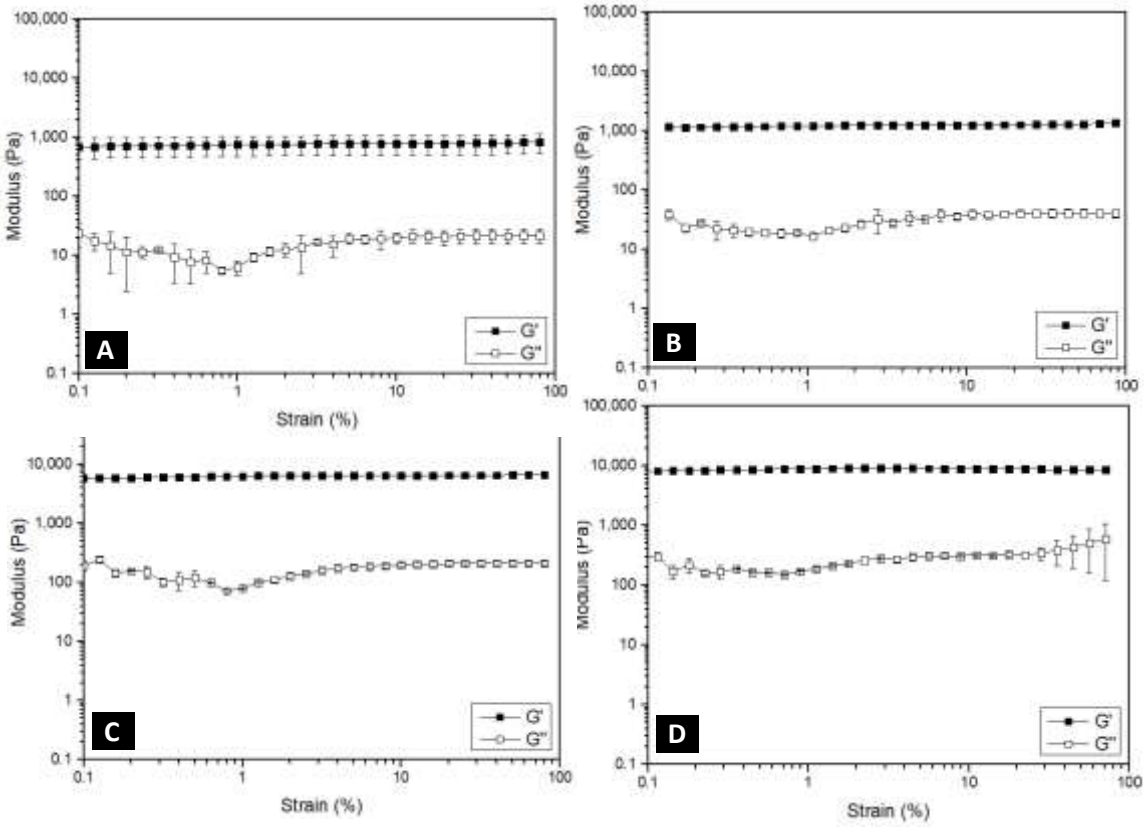

Figure 5.1 STRAIN SWEEPS. AVERAGE *G'* (*Pa*) AND *G''* (*Pa*) DETERMINATION WITH RESPECT TO STRAIN AT DIFFERENT GELATINE CONCENTRATIONS AND BLOOMS (A) SAMPLE J1, 10 *wt%* LOW *BLOOM* (B) SAMPLE J4, 10 *wt%* HIGH *BLOOM* (C) SAMPLE J3, 20 *wt%* LOW BLOOM (D) SAMPLE J6, 20 *wt%* HIGH BLOOM

Frequency sweeps (varying shear rate) from 0.1 to 81 *Hz* were carried out at 1% strain, the LVR strain value selected. The tests, as seen in Figure 5.2, revealed the gelling behaviour at different frequencies for 10 *wt%* and 20 *wt%* gelatine content gels.

The 10% linearity deviation finished at 5.01*Hz*, 6.31*Hz,* 5.01Hz and 2*Hz* frequency *for* 10 *wt%* LB, 20 *wt%* LB, 10 *wt%* HB and 20 *wt%* HB, respectively. A frequency of 1*Hz* (6.28 $rad \cdot s^{-1}$) was adopted for further characterisation.

Therefore, the LVR parameters selected for further assessment were 1% strain and 1*Hz*.

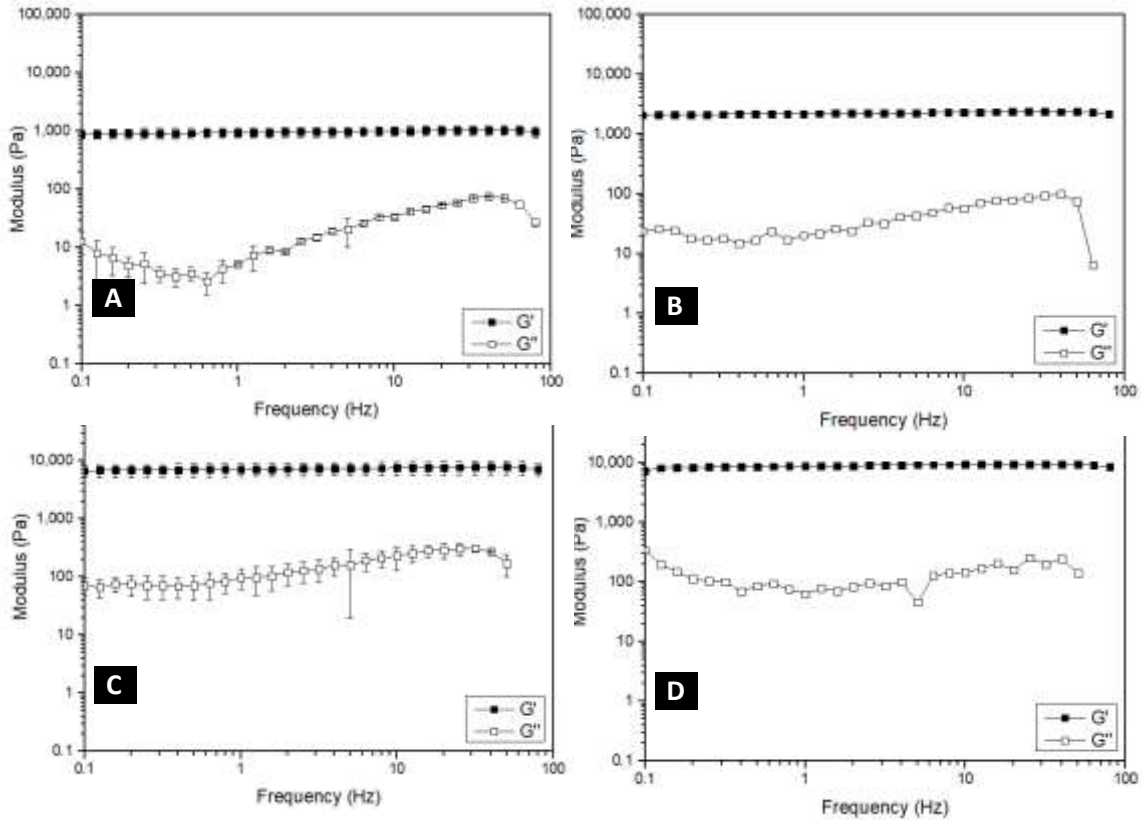

Figure 5.2 FREQUENCY SWEEPS. AVERAGE *G'* AND *G''* DETERMINATION WITH RESPECT TO FREQUENCY AT DIFFERENT GELATINE CONCENTRATIONS AND BLOOMS (A) SAMPLE J1, 10 *wt%* LOW *BLOOM* (B) SAMPLE J4, 10 *wt%* HIGH *BLOOM* (C) SAMPLE J3, 20 *wt%* LOW BLOOM (D) SAMPLE J5, 20 *wt%* HIGH BLOOM

As expected, the equilibrium storage modulus, G_{eq} (see Table 5.1), increased with increasing gelatine concentrations at both low and high *Bloom*. It was also slightly higher at HB degrees. 10 *wt%* gelatine gels were relatively soft gels, and 20 *wt%* were relatively stiff gels. 15 *wt%,* as expected, presented intermediate mechanical properties.

Table 5.1 AVERAGE EQUILIBRIUM STORAGE MODULUS G' FOR LOW AND HIGH BLOOM GELATINE GELS AT 10 wt%, 15 wt% AND 20 wt% GELATINE CONTENTS

LOW BLOOM			HIGH BLOOM		
J1 (10 *wt%*)	**J2 (15 *wt%*)**	**J3 (20 *wt%*)**	**J4 (10 *wt%*)**	**J5 (15 *wt%*)**	**J6 (20 *wt%*)**
926 ± 36 Pa	3,470 ± 943 Pa	7,060 ± 295 Pa	1,549 ± 610 Pa	4,344 ± 433 Pa	8,228 ± 638 Pa

5.2.1.2 Gelling time and temperature determination

Time sweeps for gelatine gels were conducted for 60 minutes at the LVR, 1% strain and 1 *Hz* at 23°C to identify their gelling time and temperature.

Gelation time is a relevant parameter for hydrogels. For hydrogel foams production, more rapid gelation (i.e. low gelling time) would be desirable to minimise foam drainage and coalescence.

As the gelatine solution (in a sol state, at 70°C) was loaded in the rheometer (rheometer chamber set at 23°C), a gel slowly formed from a sol state between the parallel plates, and its gelling behaviour was recorded (see Section 3.4.3.4.2a in Chapter 3 for further details). Table 5.2 shows the average time at which the gelation was completed for the different formulations. Lower gelatine concentrations tended to exhibit higher gelling times than higher gelatine contents generally.

Table 5.2 AVERAGE TIME AT WHICH GELATION WAS ACHIEVED FOR LOW AND HIGH *BLOOM* GELATINE GELS AT 10 *wt%*, 15 *wt%* AND 20 *wt%* GELATINE CONTENTS

LOW BLOOM			**HIGH BLOOM**		
J1 (10 *wt%*)	**J2 (15 *wt%*)**	**J3 (20 *wt%*)**	**J4 (10 *wt%*)**	**J5 (15 *wt%*)**	**J6 (20 *wt%*)**
595 ± 28 s	425 ± 78 s	322 ± 116 s	422 ± 97 s	527 ± 41 s	362 ± 46 s

Figure 5.3 shows the gelatine hydrogel evolution from sol to gel. The relatively slow gelation kinetics of gelatine at 23°C allowed the G' and G'' cross-over measurement. When the loss modulus is greater than the storage modulus, the sample is considered to be in a sol state. At this state, both G' and G'' are relatively low. As the sample gels, both G' and G'' increase. The G'-G'' cross-over indicates the material transition from a liquid-dominant state to a solid-dominant state. As gelation progresses, the sample viscosity increases and G' (elastic behaviour) become higher than G'' (viscous behaviour) and reaches the equilibrium modulus.

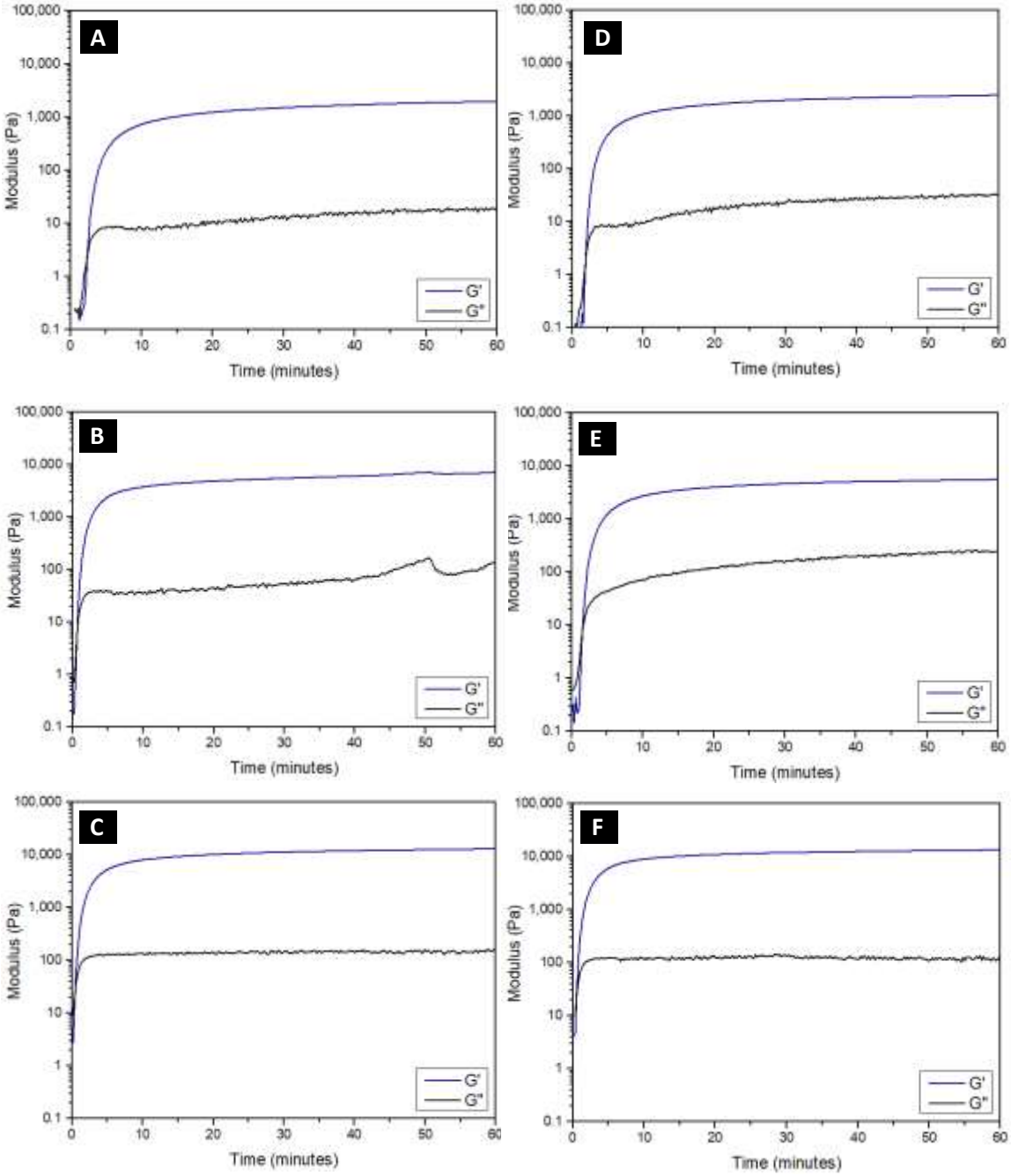

Figure 5.3 TIME SWEEPS. G' AND G'' EVOLUTION WITH TIME AT DIFFERENT GELATINE CONCENTRATIONS AND BLOOMS SHOWING THE GELLING BEHAVIOUR FOR (A) SAMPLE J1, 10 *wt%* LOW *BLOOM* (B) SAMPLE J2, 15 *wt%* LOW *BLOOM* (C) SAMPLE J3, 20 *wt%* LOW *BLOOM* (D) SAMPLE J4, 10 *wt%* HIGH *BLOOM* (E) SAMPLE J5, 15 *wt%* HIGH *BLOOM* (F) SAMPLE J6, 20 *wt%* HIGH *BLOOM*

Figure 5.4 shows the time sweep G'-G'' cross-over at different gelatine concentrations and Blooms (close-up of the time sweep graphs shown in Figure 5.3). The temperature at those cross-overs was the gelling temperature of the samples when the rheometer chamber was 23°C.

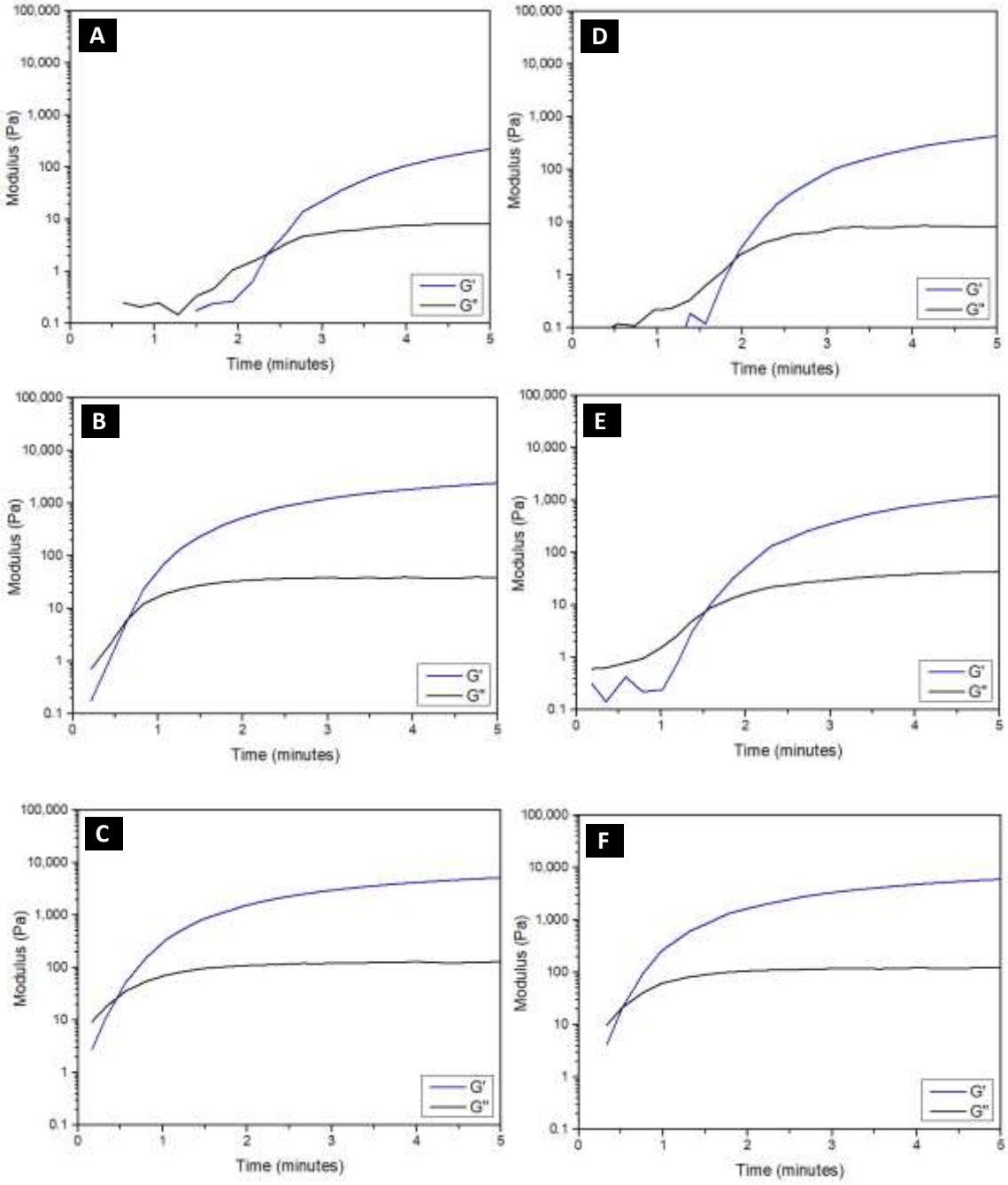

Figure 5.4 TIME SWEEPS. G' AND G'' EVOLUTION WITH TIME AT DIFFERENT GELATINE CONCENTRATIONS AND BLOOMS SHOWING THE SOL/GEL TRANSITION (THE CROSS-OVER OF G' AND G") FOR (A) SAMPLE J1, 10 *wt%* LOW *BLOOM* (B) SAMPLE J2, 15 *wt%* LOW *BLOOM* (C) SAMPLE J3, 20 *wt%* LOW *BLOOM* (D) SAMPLE J4, 10 *wt%* HIGH *BLOOM* (E) SAMPLE J5, 15 *wt%* HIGH *BLOOM* (F) SAMPLE J6, 20 *wt%* HIGH *BLOOM*

A full factorial 3x2 design with three replicates was used to calculate the statistical significance of the design parameters (gelatine strength and gelatine content) in gelling temperature for the set chamber temperature of 23°C. The hypotheses for this experiment were:

A. The null hypotheses (H_O): there is no difference in mean gelling temperature for different combinations of gelatine strength and gelatine content

B. The alternative hypotheses (H_1): there is a difference in mean gelling temperature for different combinations of gelatine strength and gelatine, content.

As shown in Table 5.3, and according to the ANOVA study (see Table A.1 in Appendix A), gelation temperature tended to increase with gelatine concentration (statistically significant, P<0.001) and gelatine strength (non-statistically significant, P=0.068, greater than the selected significant level, 0.05). The gelatine strength*gelatine content interaction (how the relationship between one of them and the gelling temperature depended on the other one) was not statistically significant (P=0.724).

These findings were consistent with the literature (Osorio *et al.*, 2007) (Pang *et al.*, 2014). Higher gelatine concentrations facilitate bond formation what justifies gelling temperature increase (Osorio *et al.*, 2007).

Table 5.3 AVERAGE GELLING TEMPERATURE FOR LOW AND HIGH *BLOOM* GELATINE GELS AT 10, 15 AND 20 *wt%* GELATINE CONTENTS

LOW BLOOM			**HIGH BLOOM**		
J1 (10 *wt%*)	**J2 (15 *wt%*)**	**J3 (20 *wt%*)**	**J4 (10 *wt%*)**	**J5 (15 *wt%*)**	**J6 (20 *wt%*)**
25.83±0.75°C	26.89±1.01°C	27.89±0.38°C	25.93±0.99°C	27.80±0.59°C	28.75±0.21°C

5.2.1.3 Surfactant type and content influence on gelatine gelling time and temperature

This section studies the impact of surfactant type and content on gelation time and temperature for 10 *wt%* gelatine content solutions (see Section 3.4.3.4.2.b for further details). Table 5.4 shows the average time at which the gelation was completed for the different formulations. Surfactant incorporation considerably delayed the gelling time of the solutions, and the delay was more significant at higher surfactant contents. Surfactant "A" had a more detrimental effect on gelatine gelling time than surfactant C2.

Table 5.4 AVERAGE TIME AT WHICH GELATION WAS ACHIEVED FOR LOW *BLOOM* GELATINE GELS AT 10 *wt%*, GELATINE CONTENT AND DIFFERENT SURFACTANT TYPES AND CONTENTS

NO SURFACTANT	**SURFACTANT "A"**		**SURFACTANT C2**	
	A1 (0.5 *wt%*)	**A7 (1. 5 *wt%*)**	**C2.1 (0.75 *wt%*)**	**C2.7 (1.5 *wt%*)**
595 ± 28 s	1,187.4 ± 106.03 s	1,385.2 ± 106.73 s	863.8 ± 158.88 s	1,034 ± 135.07 s

Figure 5.5 compares the time sweeps for 10 *wt%* gelatine solutions without and with surfactants. It shows that the solutions containing surfactants, especially, surfactant "A", exhibit slower gelation kinetics than the solution without surfactant. The use of

surfactant C2 does not seem to affect the equilibrium G' modulus negatively. In fact, at low surfactant C2 concentrations, 0.75 *wt%*, it even slightly increased G' (i.e. stiffer gels). Surfactant "A" not only considerably delayed the gelation time but also lower the equilibrium G' modulus of the gel (i.e. less stiff gels).

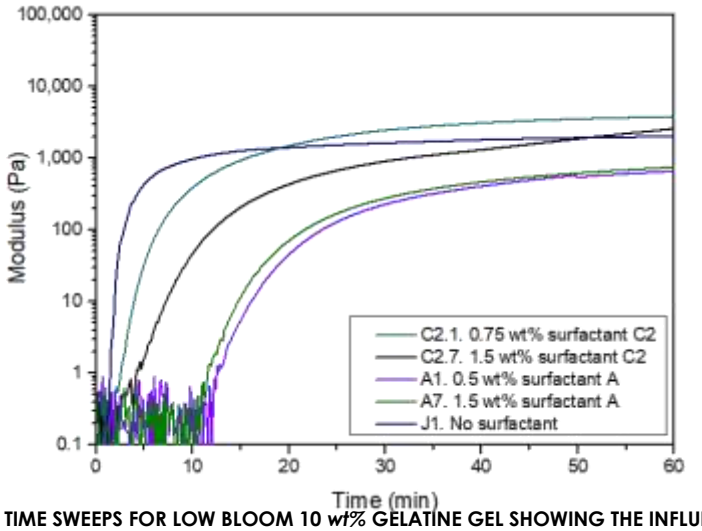

Figure 5.5 TIME SWEEPS FOR LOW BLOOM 10 *wt%* GELATINE GEL SHOWING THE INFLUENCE OF DIFFERENT SURFACTANTS AND CONCENTRATIONS ON GELLING TIME AND GEL STIFFNESS G'

Table 5.5 compares the gelling temperature (G'-G'' crossover) of gelatine solutions with and without surfactants. The surfactant incorporation into the formula significantly increased the gelling temperature (i.e. the temperature at which the first gel associations occur) of the gelatine sols. This might be attributed to the gelatine chains overlapping with the surfactant micelles, forming crosslinks (Bhakta and Ruckenstein, 1997).

Table 5.5 AVERAGE GELLING TEMPERATURE FOR LOW *BLOOM* GELATINE GELS AT 10 *wt%* GELATINE CONTENT AND DIFFERENT SURFACTANT (A, C2) CONCENTRATIONS

NO SURFACTANT	SURFACTANT "A"		SURFACTANT C2	
	A1 (0.5 *wt%*)	**A7 (1. 5 *wt%*)**	**C2.1 (0.75 *wt%*)**	**C2.7 (1.5 *wt%*)**
25.83±0.75°C	28.11 ± 1.07°C	28.18 ± 1.23°C	28.27 ± 0.98°C	28.07 ± 1.15°C

5.2.1.4 Effect of curing temperature on the gelling behaviour of gelatine solutions

As seen in Section 5.2.1.2, the gelling temperature of sample J1 (low *Bloom* and 10 *wt%* gelatine) was 25.83°C when the chamber temperature was set at 23°C (see Section 3.4.3.4.2c for further details). Figure 5.6 compares *G'* of sample J1 at different curing temperatures. Gelatine is a heat-sensitive hydrocolloid, what implies that the curing temperature influences their gelling behaviour.

From time sweeps adjusting the rheometer chamber at 26°C and 29°C, the gelling temperature of sample J1 was found to be 26 and 28.7°C, respectively. At 26°C, G'

dramatically increased until getting to a first and brief plateau, lower than the one achieved at 23°C (see Figure 5.6). Then, after some artefacts, the G' slightly tended to a second plateau. All the curves obtained at this concentration showed a similar behaviour what may be due to the hardening of the edges of the 50-mm plate, as time advanced. Therefore, the first plateau of the curve is considered more reliable than the second plateau what implies that the equilibrium modulus slightly decreased when the rheometer chamber temperature increased.

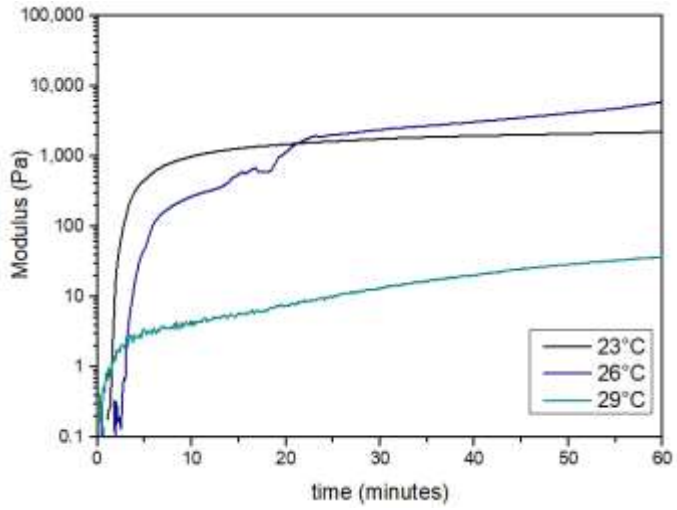

Figure 5.6 TIME SWEEPS FOR LOW BLOOM *10 wt%* GELATINE GEL SHOWING THE EFFECT OF CURING TEMPERATURE ON G' WITH TIME

At 29°C, the sample gelled considerably more slowly than the other foaming temperatures studied, and the equilibrium *G'* modulus was not achieved within the 60 minutes test. As the equilibrium *G'* modulus was obtained faster at lower temperatures, foams cured at lower temperatures should be more stable against drainage and coalescence than the ones cured at higher temperatures. This finding limits the use of high temperatures to accelerate the foams drying during the initial stage of curing (and drying) of the relatively high-moisture-content gel. At late stage as moisture content decrease, the gel will be stiffer and may be able to withstand an increase in drying temperature.

5.2.1.5 Effect of the pH on the gelling behaviour of gelatine gels

Studies have found pH range from 4.6-8 (Pang *et al.*, 2014) or 5-9 (Osorio *et al.*, 2007) favourable for the gelling of type A gelatine. As seen in Figure 5.7, the gelatine solution/gel behaved similarly at pH 5 and 7 (Figures 5.7B and 5.7C, respectively).

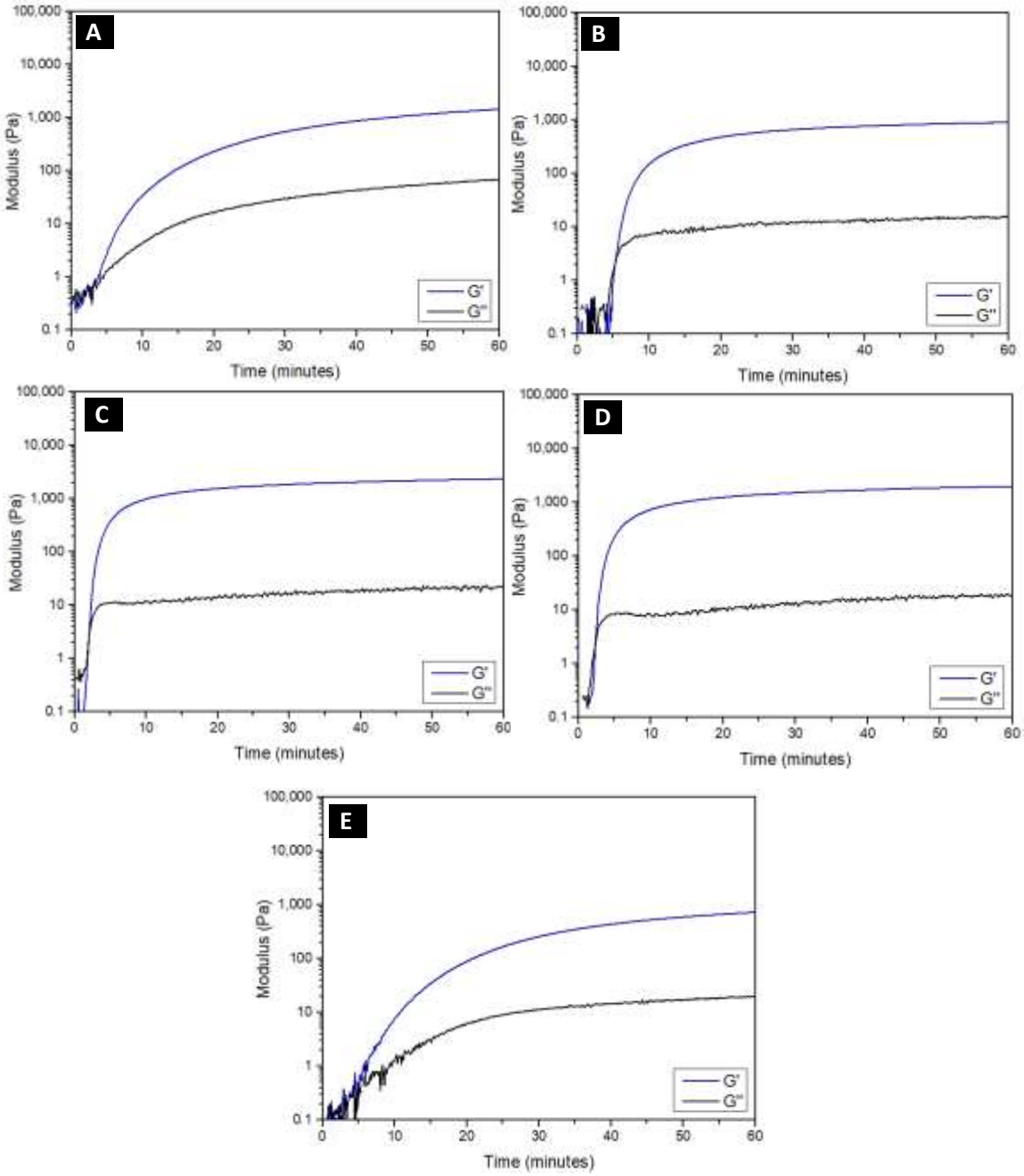

Figure 5.7 TIME SWEEPS FOR 10 *wt%* LOW BLOOM GELATINE GEL SHOWING THE G' AND G'' EVOLUTION WITH TIME AT DIFFERENT PH (A) PH=4 (B) PH=5 (C) PH=7 (D) P=8 (E) PH=10

At pH4 (Figure 5.7A) and pH10 (Figure 5.7E) however, the gelling was considerably slower than the intermediate pH range. This may be attributed to protonation of amino acids at low pH which hinders hydrogel bonds formation (Pang *et al.*, 2014).

5.2.1.6 Melting point determination

Temperature sweeps from 25°C to 40°C were carried out to determine the gelatine gels' melting temperature (see Figure 5.8).

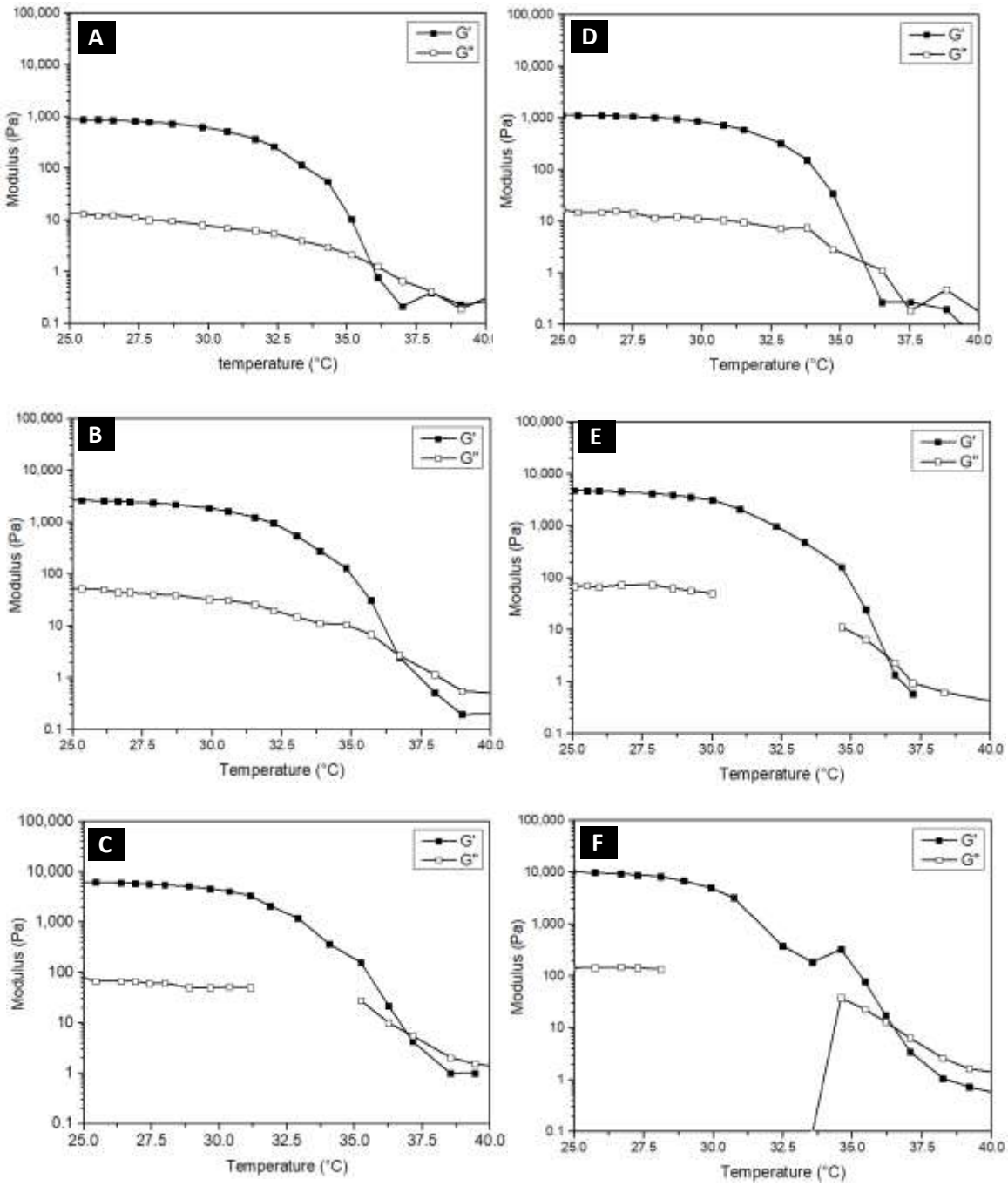

Figure 5.8 TEMPERATURE RAMPS FOR LOW AND HIGH *BLOOM* GELATINE GELS SHOWING G' AND G'' EVOLUTION WITH TEMPERATURE AT DIFFERENT GELATINE CONCENTRATIONS AND BLOOMS (A) SAMPLE J1, 10 *wt%* LOW *BLOOM* (B) SAMPLE J2, 15 *wt%* LOW *BLOOM* (C) SAMPLE J3, 20 *wt%* LOW *BLOOM* (D) SAMPLE J4, 10 *wt%* HIGH *BLOOM* (E) SAMPLE J5, 15 *wt%* HIGH *BLOOM* (F) SAMPLE J6, 20 *wt%* HIGH *BLOOM*

Figures 5.8.C, 5.8.E and 5.8F shows discontinuities in the G'' curve. This occurred as the viscosity of the gel decreases and the signal received in the rheometer decreased, producing low torques (<0.1 *g·cm*), what influenced the results reliability at those points.

The tests started with *G'* at its equilibrium value. As temperature increased, both *G''* and *G'* (but this one more dramatically), decreased. As the temperature continued to increase, a *G'-G''* cross-over occurred at a given temperature, the melting point of the gel, where the sample was transformed from its gel predominant state to a liquid

predominant state. The melting temperatures of the gelatine gels are summarised in Table 5.6.

Table 5.6 AVERAGE MELTING TEMPERATURE FOR LOW AND HIGH *BLOOM* GELATINE GELS AT 10, 15 AND 20 *wt%* GELATINE CONTENTS

LOW BLOOM			HIGH BLOOM		
J1 (10 *wt%*)	**J2 (15 *wt%*)**	**J3 (20 *wt%*)**	**J4 (10 *wt%*)**	**J5 (15 *wt%*)**	**J6 (20 *wt%*)**
35.38±1.10°C	36.66±0.10°C	37.07±0.21°C	35.95±0.77°C	36.45±0.33°C	36.67±0.4°C

A full factorial 3x2 design with three replicates was used to calculate the statistical significance of the design parameters (gelatine strength and gelatine content) in melting temperature. The hypotheses for this experiment were:

a. The null hypotheses (H_O): there was no difference in mean melting temperature for different combinations of gelatine strength and gelatine content

b. The alternative hypotheses (H_1): there was a difference in mean melting temperature for different combinations of gelatine strength and gelatine, content.

Table A.2 (see Appendix A) shows the ANOVA table for the study of the influence of gelatine strength and concentrations on the melting point of gelatine solutions. Melting temperatures tended to increase slightly with gelatine concentration (no significantly, P=0.051 as P>0.05). Higher concentration gelatine gels exhibited stronger bonds and junction zones which required higher temperatures for breaking, resulting in higher melting temperatures (Osorio *et al.*, 2007) (Pang *et al.*, 2014).

Surprisingly, gel strength did not show a strong influence on melting temperature (P=0.643, P>0.05). It was expected that greater gelatine strength exhibited higher melting points, as it is supposed to have a more significant number of crosslinks.

As Osorio *et al* (2007) pointed out, gelatine concentration has a greater influence on gelling temperature than on melting temperature. Gel melting temperatures were, on average, 9.2°C greater than gelling temperatures. These results are comparable to the ones observed by Osorio *et al* (2007), where an average difference of 10.5°C was found.

5.2.2 VISCOSITY

The study of the viscosity of the gelatine solutions is essential for the liquid foaming process and foam stability (drainage). The viscosity measurement procedure was explained in detail in Section 3.4.3.5 in Chapter 3.

This subsection analyses the viscosity of low Bloom gelatine solutions at different gelatine concentrations and assess the influence of surfactant incorporation and temperature on viscosity.

5.2.2.1 Viscosity of gelatine solutions

Figure 5.9 shows the dependence of apparent viscosity and shear stress on the shear rate of the aqueous gelatine solutions (J0, J1, J2 and J3, see formulation in Table 3.61 in Chapter 3) at different gelatine concentrations at 50°C. The solution at low gelatine content (J0, at 5 *wt*%) exhibited a Newtonian behaviour as its viscosity was independent of shear rate. For higher gelatine concentrations (J1, J2, J3 samples, at 10, 15 and 20 *wt*%, respectively) the solutions showed increasing shear thinning behaviour with the increase in gelatine concentration as its apparent viscosity decreased with shear rate. The reduction of viscosity with shear rate is related to the destruction of structures (e.g. entanglement of the molecules) at high shear rates (Ludmila and Dyshlyuk, 2016).

As typically found in polymer solutions, the viscosity of the solution increased with polymer concentration. This can be related to the structure formation in the gelatine solutions (Ludmila and Dyshlyuk, 2016). Figure 5.10 presents the apparent viscosity of the solutions at a fixed shear rate, 125 s^{-1}, where the influence of gelatine concentration on the apparent viscosity is revealing.

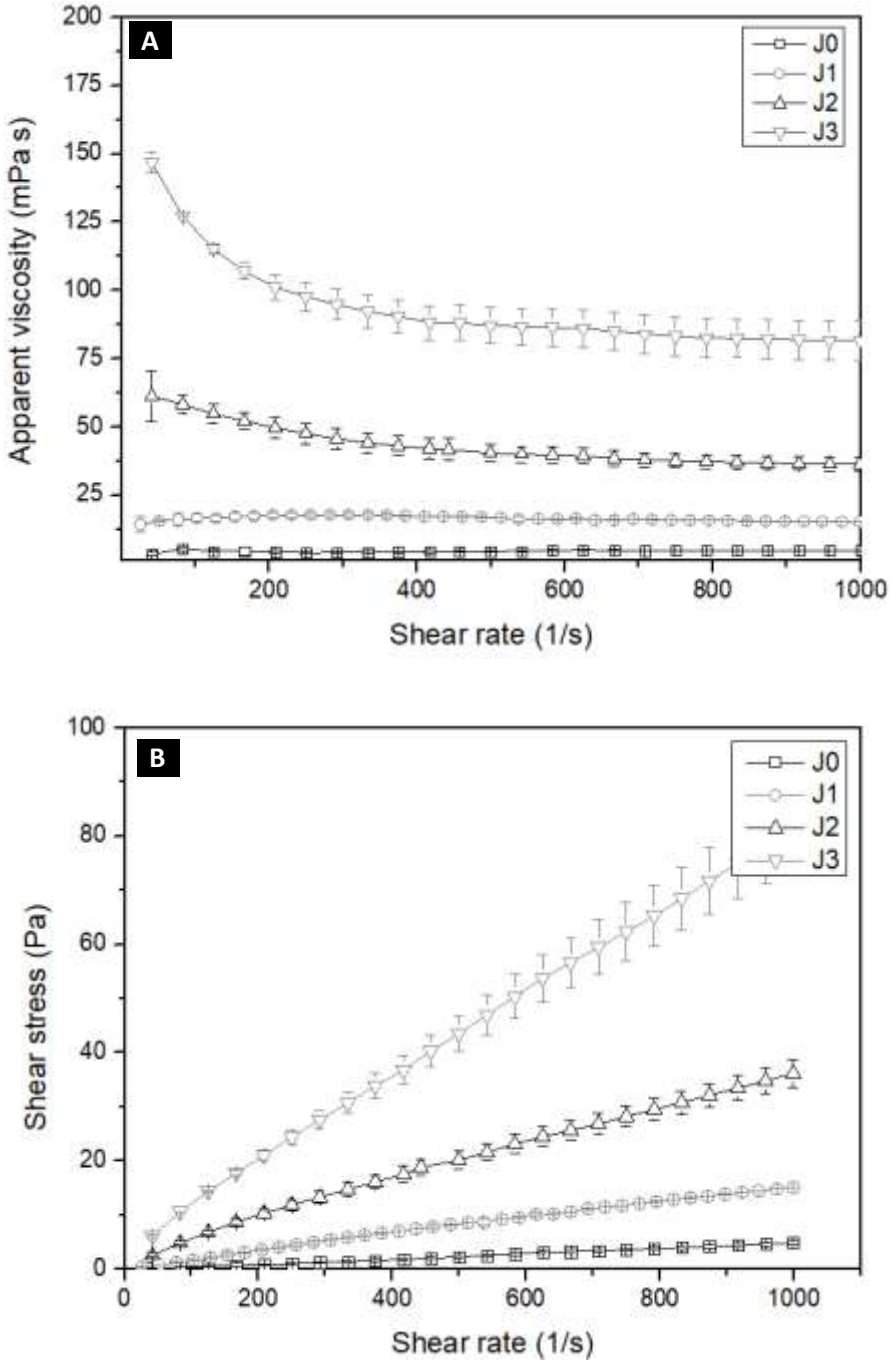

Figure 5.9 INFLUENCE OF SHEAR RATE ON (A) THE APPARENT VISCOSITY AND (B) THE SHEAR STRESS OF GELATINE OF GELATINE SOLUTIONS AT 50°C

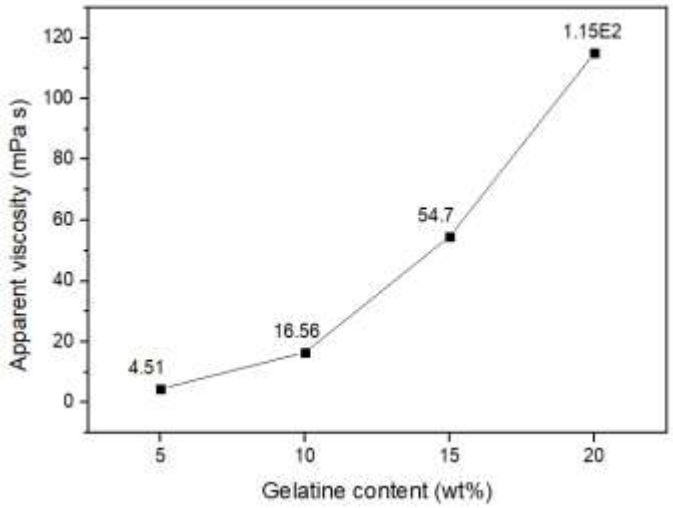

Figure 5.10 DEPENDENCE OF APPARENT VISCOSITY OF GELATINE AQUEOUS SOLUTIONS ON GELATINE CONCENTRATIONS MEASURED AT A FIXED SHEAR RATE (125 s^{-1}) AND AT 50°C

5.2.2.2 Influence of surfactant type and content on viscosity

Figure 5.11 shows the changes of apparent viscosity of gelatine solutions with different surfactant types and concentrations. The gelatine concentration was kept constant at 10 *wt%*. The investigated solutions were samples A1, A7, A13, C1.1, C1.4, C1.7, C2.1, C2.7 and C2.13 (see Tables 3.35, 3.36 and 3.37 in Chapter 3 for formulation details)

The incorporation of surfactants C1 and C2 depicted a steady increase in viscosity of the solutions with surfactant concentration (Figures 5.11A and B). The shear thinning behaviour also increased as surfactants C1 and C2 concentrations increased.

The viscosity of solutions prepared with surfactant C2 was slightly higher than the viscosity of gelatine solutions with surfactant C1 (comparing Fig 5.11A and B).

Surfactant "A" use had a relatively weaker effect on viscosity compared with surfactants C1 and C2 (Figure 5.11.C). This was most likely due to dilution of the as-received surfactant "A". The moisture contents in surfactants C1 and C2 were <0.1%, 3%, respectively, while it is approximately 63% for surfactant "A". Surfactant "A" incorporation into the formula had little effect at both 0.5 and 1.5 *wt%*. However, at 4.5 *wt%,* the viscosity roughly doubled that at 0.5*wt%* surfactant content.

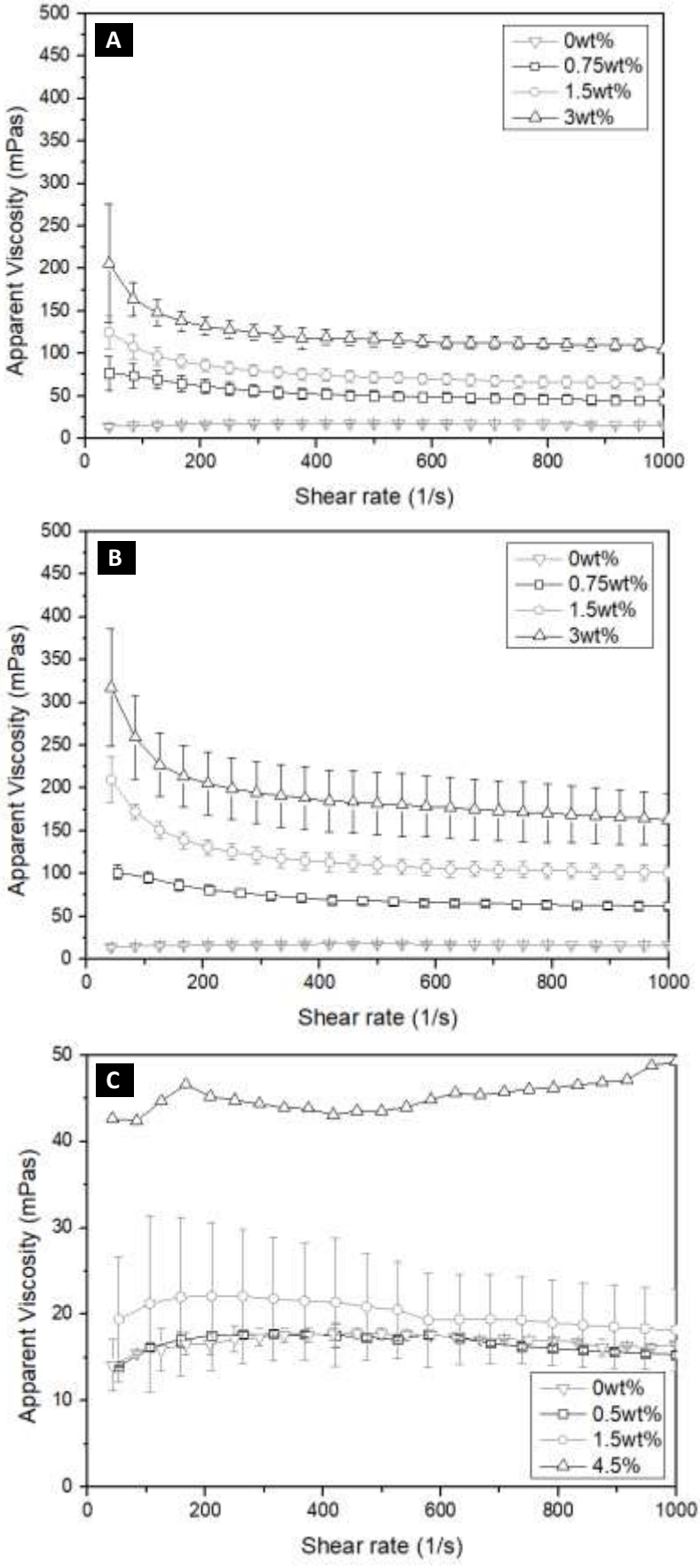

Figure 5.11 INFLUENCE OF SHEAR RATE ON VISCOSITY OF THE GELATINE (LOW BLOOM AT *10wt%*) SOLUTIONS PREPARED WITH (A) C1 (B) C2 and (C) "A" SURFACTANTS TESTED AT 50°C

Figure 5.12 presents the apparent viscosity of the gelatine solutions with the different surfactants (C1 C2 and A) at a fixed shear rate ($125s^{-1}$) at different surfactant concentrations (on a wet basis). It is clear that both type and concentration of surfactants have a significant influence on solution viscosity and the choice and concentration of surfactants must be taken into account to achieve suitable viscosity for liquid foaming.

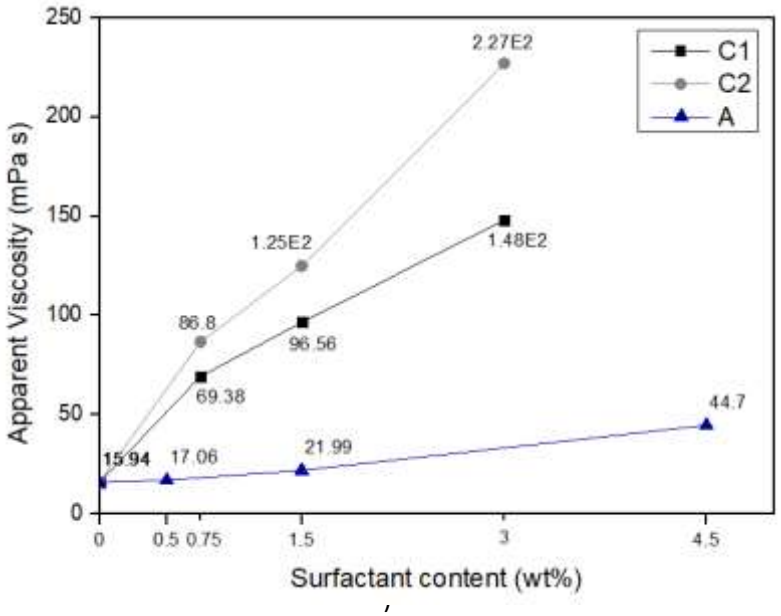

Figure 5.12 VISCOSITY VARIATION OF GELATINE SOLUTIONS WITH SURFACTANT TYPES AND CONCENTRATIONS TESTED AT 50°C AND FIXED SHEAR RATE ($125s^{-1}$)

5.2.2.3 Influence of foaming temperature on the viscosity of gelatine solutions with surfactants

As expected, the viscosity of gelatine solutions decreased with increasing temperature. Figure 5.13 illustrates the difference in viscosity in a solution of 10 *wt%* gelatine and 0.75 *wt%* surfactant C2 (sample C2.1, see Table 3.36 in Chapter 3) tested at 50°C and 75°C.

At lower temperature, the partially gelled solution exhibited shear-thinning behaviour, as anticipated. At higher temperatures, the creation of gel structure in the gelatine solutions was hindered, which decreased the solution viscosity and led to a Newtonian behaviour. The decrease in viscosity was also partially due to the reduction of the internal friction coefficient (Asyakina & Dyshlyuk, 2016).

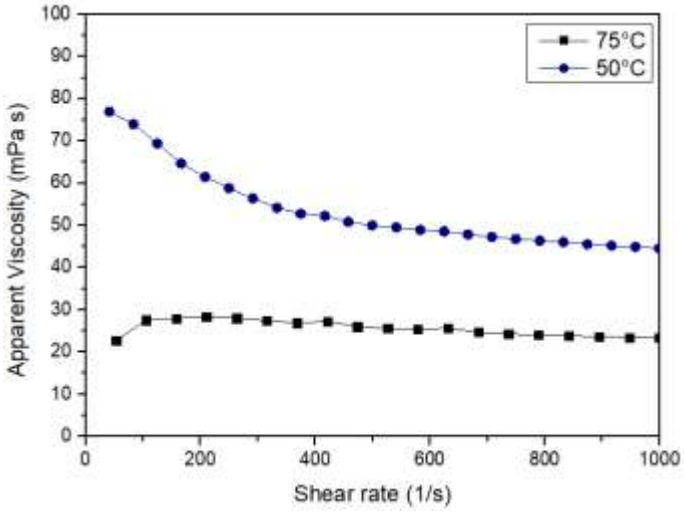

Figure 5.13 VISCOSITY/SHEAR RATE RELATIONSHIP FOR THE GELATINE SOLUTION (SAMPLE C2.1) TESTED AT 50°C AND 70°C

5.2.3 SURFACE TENSION

Along with rheology and viscosity of the gelatine solutions, surface tension is a crucial parameter for the liquid foaming process (e.g. assisting bubble nucleation and growth) and foam stability (e.g. decreasing the differential pressure between bubbles of different sizes, minimising coalescence and coarsening). The procedures for surface tension measurement were described in detail in Section 3.4.3.2, Chapter 3.

This subsection analyses the surface tension of water-surfactant solutions (at 22°C) and 10 *wt%* gelatine-surfactant "A" solutions at 50°C (above the melting point).

5.2.3.1 Surface tension of water-surfactant solutions at 22°C

Table 5.7 shows the surface tension measurements of the water-surfactant solutions (see formulations in Table 3.52, chapter 3) at 22°C. The measured water surface tension, sample ST0, was 71.72 *mN/m*, sufficiently close to standard values and comparable to 71.60 *mN/m*, reported by Pallas & Harrison (1990) at 25°C. This also was treated as satisfactory calibration of the device.

The three surfactants were effective to reduce surface tension at concentrations as low as 0.5 *wt%* (by 45.91 to 49.39%), and beyond this level, further surface tension reduction was rather limited.

The starting point of the plateaus of the curves shown in Figure 5.14 indicated that the concentration at which the water-surfactant solutions were studied reached Critical Micelle Concentration (CMC), i.e. the value at which the surfactant molecules start to form micelles. Both surfactants C2 and B reached CMC at ~2.5 *wt%* (achieving 45.5 and 50.8% reduction in surface tension, respectively relative to that of pure water),

while surfactant "A" reached CMC at ~1.5*wt%* (~47.0% relative surface tension reduction).

Table 5.7 SURFACE TENSION OF WATER-SURFACTANT (A, C2, B) SOLUTIONS AT 22°C

ID	SURFACTANT TYPE	SURFACTANT CONTENT* (*wt%*)	AVERAGE SURFACE TENSION (mN/m)
SF0	-	0	71.73
SF1	Surfactant "A"	0.5	38.80
SF2		1.0	38.25
SF3		1.5	38.00
SF4		2.0	38.09
SF5		2.5	38.01
SF6		3.0	38.00
SF7	Surfactant C2	0.5	40.91
SF8		1.0	40.72
SF9		1.5	40.36
SF10		2.0	39.92
SF11		2.5	39.07
SF12		3.0	39.02
SF13	Surfactant B	0.5	36.30
SF14		1.0	35.81
SF15		1.5	35.67
SF16		2.0	35.43
SF15		2.5	35.32
SF16		3.0	35.32

**Surfactant content on a wet basis. Surfactant content was based on total gelatine-water solution weight*

Surfactant B was relatively more effective, exhibiting lower surface tension values at all the concentrations studied, followed by surfactant "A" and C2.

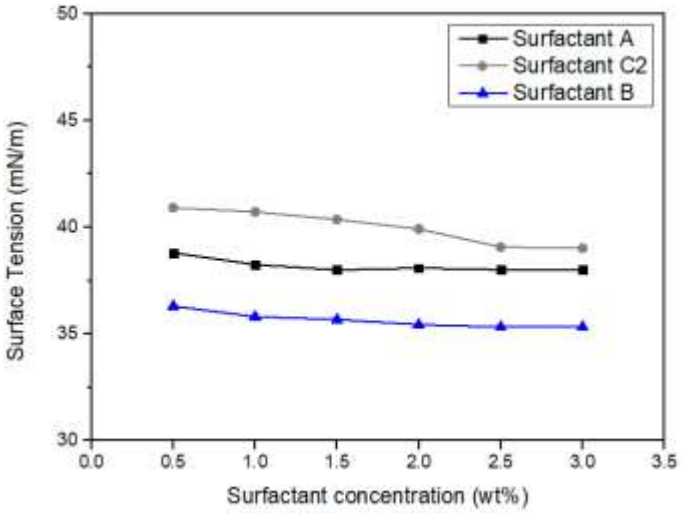

Figure 5.14 SURFACE TENSION VARIATION OF WATER-SURFACTANT (A, C2 AND B) SOLUTIONS WITH SURFACTANT CONCENTRATION AS TESTED AT 22°C

5.2.3.2 Surface tension of gelatine-surfactant "A" solutions at 50°C

Table 5.8 shows the surface tension of the gelatine-surfactant "A" solutions measured at 50°C. The samples formulation are shown in Table 3.54, Chapter 3.

Table 5.8 SURFACE TENSION OF GELATINE-SURFACTANT "A" SOLUTIONS AT 50°C

ID	SURFACTANT "A"* (*wt%*)	AVERAGE SURFACE TENSION (mN/m)
TA0	0.00	41.49
TA1	0.05	29.88
TA2	0.15	30.32
TA3	0.25	31.04
TA4	0.50	31.72
TA5	1.5	33.16
TA6	4.5	35.02

**Surfactant content on a wet basis and based on total gelatine-water solution weight*
Note: gelatine concentration was kept constant at 10 wt%

The measured surface tension for the 10 *wt%* gelatine solution (without any surfactant, sample TA0), was 41.49 *mN/m in comparison* with 67.9 *mN/m*, that of water at 50°C (The Engineering Toolbox, 2005). This decrease was attributable to the surface activity of gelatine molecules as they adhere to the water/air interface (Hyono *et al.*, 2004).

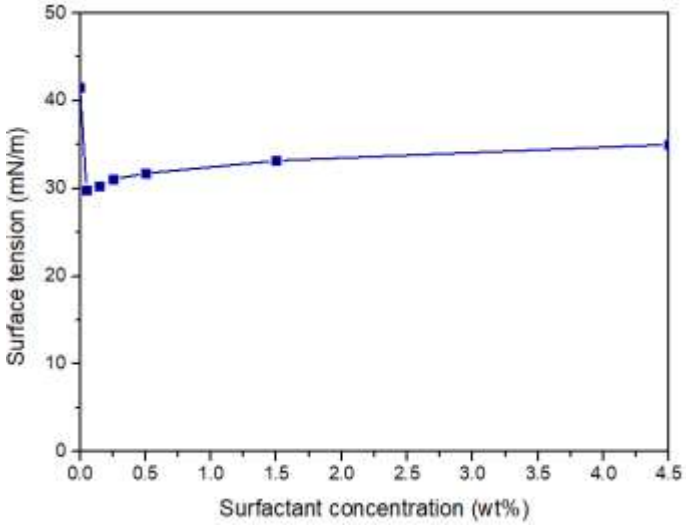

Figure 5.15 SURFACE TENSION OF GELATINE-SURFACTANT SOLUTIONS TESTED AT 50°C

As seen in Table 5.8 and Figure 5.15, the surface tension of the gelatine solution with the addition of surfactant "A" at 0.05 *wt% was* decreased by 26.90%, relative to that without surfactant. However, from 0.05 *wt%,* the surface tension of the gelatine-surfactant solutions slowly but steadily increased, approaching a plateau. Hyono *et al* (2004) attributed this behaviour to hydrophobic associations among the hydrophobic sections of gelatine molecules at the interface, which lead to an association of these hydrophobic segments. This provokes desorption of gelatine molecule as it becomes more hydrophilic.

5.2.4 SUMMARY

This section argued the viscosity, surface tension and rheological properties of gelatine, surfactant and gelatine-surfactant solutions. These properties may affect foam generation and stabilisation and, consequently, may also have a significant effect on the dry foams characteristics.

The understanding of the rheological properties (e.g. equilibrium modulus, gelling time and gelling and melting temperatures) of gelatine gels is essential as they influence processing (e.g. foaming, drying temperature) and dry foam properties (e.g. drying shrinkage, mechanical properties).

Gelatine gels exhibited a viscoelastic behaviour. As gelation proceeded from a gelatine-sol (liquid-like behaviour predominance, *G''>G'*) to a gelatine gel (solid-like behaviour predominance, G'>G'') state, *G'* rapidly increased and surpassed *G''*, which cross-over represents the gelling point (i.e. gelling temperature). As gelation continued, *G'* gradually increased (and *G''* stabilises at lower values) up to reaching a plateau (G_{eq}, equilibrium modulus). Conversely, when a gelatine gel melted, *G'*

sharply decreased, reaching a cross-over point with *G''* (melting temperature) and further decreased below *G''*, when the gelatine-sol consolidated.

The G_{eq}, gelling time and gelation and melting temperatures were studied for gelatine sols/gels. For all the parameters studied, gelatine concentration had a more significant impact on rheological properties than gel strength.

The equilibrium modulus represents the gel strength, a parameter which influences the stabilisation of gelatine foams. It was expected that higher strength gels lead to stronger plateau borders able to hold together the foam structure during the drying process. G_{eq} slightly increased at higher *Bloom* and considerably increased with increasing gelatine concentrations (i.e. higher bloom and, most significantly, higher gelatine content gave rise to higher strength gels), as expected.

Gelation time also impacts foams stabilisation as it is the time at which the gelatine liquid foam 'freezes', arresting drainage and coalescence. For hydrogels foams production, more rapid gelation (i.e. low gelling time) would be desirable to minimise foam drainage and coalescence. For low *Bloom* gels, the gelation time was 595 and 322 *s* for 10 and 20 *wt%* gelatine content, respectively. Gelling time decreased at higher gelatine concentrations, but not a clear trend was found for gelatine strength. Gelling time was also influenced by curing temperature and the pH of the solution. Gelatine exhibited an optimum gelling behaviour at the pH range 5-7. However, as the pH increased/decreased to extremes (i.e. pH=4 and pH=10), gelling considerably slowed down.

Hydrogel-gelatine foams include surfactants to assist the foaming process and the foam stabilisation, so their influence on gelation time is crucial. Surfactant incorporation into 10 *wt%* low *Bloom* gels considerably delayed gelling time and this behaviour was more significant at higher surfactant content and when surfactant "A" (amphoteric) was used (approximately, the gelation time doubled). The lower gelation times achieved compared to those for surfactant C2 may be attributable to the surfactants charge. Surfactant C2 is anionic, the type of surfactant which presents stronger interaction with gelatine due to gelatine structure, which tends to exhibit positive groups on the ends of the polymer chains (Derkach, 2015).

The gelation temperature of low *Bloom* gels at 10 and 20 *wt%* was 25.8°C and 27.9°C, respectively. Gelation temperature increased with gelatine concentration ($P<0.001$), gelatine strength (no statistically significant, $P>0.05$), curing temperature and surfactant content. Higher gelatine concentrations facilitate bond formation what justifies gelling temperature increase (Osorio *et al.*, 2007). The surfactant micelles overlap with the

gelatine chains, creating cross-links which require a higher temperature for denaturation (Bhakta and Ruckenstein, 1997). The gelling temperature increased as curing temperature increased but gelling time was obtained faster at lower curing temperatures. This limits the use of high temperature to speed up the drying process.

Gel melting temperatures were, on average, 9.2°C greater than gelling temperatures. The melting temperature of low *Bloom* gels at 10 and 20 *wt%* was 35.4°C and 37.07°C, respectively. Melting temperature slightly increased with gelatine concentration (no significantly, P>0.05). Higher concentration gelatine gels exhibited stronger networks which required higher temperatures for breaking (Osorio *et al.*, 2007) (Pang *et al.*, 2014). Contrary to expectations, gel strength did not show any influence on melting temperature (P>0.05).

Table 5.9 summarises the rheological results produced in Section 5.2.1.

Table 5.9 EQUILIBRIUM MODULUS, GELATION TEMPERATURE, MELTING TEMPERATURE AND GELLING TEMPERATURE AT DIFFERENT CURING TEMPERATURES FOR GELATINE GELS AND GELATINE SURFACTANT GELS

ID	G_{EQ}* (*Pa*)	GELATION TIME* (s)	GELLING TEMP. (°C) AT 23°C	GELLING TEMP. (°C) AT 26°C	GELLING TEMP. (°C) AT 29°C	MELTING TEMP.* (°C)
J1	926 ± 36	595 ± 28	25.83±0.75	26.00±0.34	28.70±0.54	35.38±1.10
A1	-	1,187.4± 106.03	28.11±1.07	-	-	-
A7	-	1,385.2±106.73	28.18±1.23	-	-	-
C2.1	-	863.8± 158.88	28.27±0.98	-	-	-
C2.7	-	1,034±135.07	28.07±1.15	-	-	-
J2	3,470 ± 943	425 ± 78	26.89±1.01	-	-	36.66±0.10
J3	7,060 ± 295	322 ± 116	27.89±0.38	-	-	37.07±0.21
J4	1,549 ± 610	422 ± 97	25.93±0.99	-	-	35.95±0.77
J5	4,344 ± 433	527 ± 41	27.80±0.59	-	-	36.45±0.33
J6	8,228 ± 638	362 ± 46	28.75±0.21			36.67±0.4

* Rheometer chamber set at 23°C

It is also fundamental to understand the influence of foam formulation parameters (i.e. gelatine content, surfactant content and surfactant type) on the viscosity of the gelatine solution as it is a critical factor for foaming processing and foam stabilisation.

Gelatine solutions exhibited a Newtonian behaviour at low concentrations (5 *wt%*). However, the concentrations used for the production of hydrogel-gelatine foams (10, 15 and 20 *wt%*) exhibited a non-Newtonian behaviour due to the destruction of gelatine structures at high shear rates (Ludmila and Dyshlyuk, 2016).

The viscosity of the gelatine solution increased at the lower processing temperature and greater polymer and surfactant concentrations. The viscosity increase related to

a greater gelatine content (by 267%, 845% and 1,337% for an increase of gelatine concentration from 5 *wt%* to 10, 15 and 20 *wt%*, respectively) was due to gelatine networks formation (Ludmila and Dyshlyuk, 2016),

Surfactants C1 and, more significantly, C2 considerably increased the viscosity of the gelatine solutions. Surfactant "A" showed a weaker effect on viscosity compared to surfactants C1 and C2. The viscosity of the solution increased by ≈444% and ≈1% when surfactants C2 (at 0.75 *wt%*) and "A" (0.5 *wt%*) were incorporated to the gelatine solution, respectively. This result is explained by the high water content of surfactant "A" and the higher interaction of surfactants C1 and C2 with gelatine, which contributed to structures development.

Surface tension decrease assists the foaming process and stabilises the foam by reducing the pressure difference between bubbles. Surfactants "A", B and C2 were proved effective to reduce the surface tension of water solutions. Surfactant "A" reached CMC at ~1.5 *wt%* and both surfactants B and C2 reached CMC at 2.5 *wt%*. Surfactant B, the most effective, exhibited the lowest surface tension values at all the concentrations studied.

Gelatine showed to decrease the surface tension of solutions due to its surface activity. When surfactant "A" at 0.05 *wt%* was incorporated into a 10 *wt%* gelatine solution, the surface tension considerably decreased, but as surfactant concentration increased, surface tension slightly increased, approaching a plateau. Hyono *et al* (2004) attributed this behaviour to the desorption of the gelatine molecule as it becomes more hydrophilic due to hydrophobic associations between gelatine molecules.

5.3 INFLUENCE OF SURFACTANT TYPE AND CONTENT ON GELATINE-HYDROGEL FOAMS

This subsection analyses the effect of surfactant type and content on the properties of gelatine hydrogel foams. The Maximum Expansion Ratio (MER), density, drying shrinkage and structure were studied, but no statistical analysis was carried out.

As discussed in Section 3.3.3.3.1, in Chapter 3, the influence of surfactant type (at three levels: surfactants A, B and C2) and content (at three levels: 0.05 *wt%*, 0.5 *wt%* and 5 *wt%*) on gelatine hydrogel foams was studied. The gelatine content in the solution and the starting foaming temperature were kept constant at 15 *wt%* and 80°C, respectively. Sample FH1, hydrogel foam prepared with no surfactant was included in the experiment as a control. Table 5.10 shows the formulation design table.

Table 5.10 EXPERIMENTAL DESIGN TABLE FOR THE STUDY OF THE INFLUENCE OF SURFACTANT TYPE AND CONTENT ON HYDROGEL FOAMS

	FACTOR A	FACTOR B
ID	**SURFACTANT CONTENT (*wt%*)***	**SURFACTANT TYPE**
FH1	n/a	n/a
FH2	0.05	C2
FH3	0.5	C2
FH4	5	C2
FH5	0.05	B
FH6	0.5	B
FH7	5	B
FH8	0.05	A
FH9	0.5	A
FH10	5	A

**Content based on the total weight of the gelatine-water solution*

5.3.1 FOAMABILITY

As shown in Figure 5.16, at lower concentrations (0.05 *wt%*), all three surfactants showed significant increase in MER and the effectiveness can be ranked as (from high to low): surfactants B, C2 and A. At medium concentration (0.5 *wt%*), the three surfactants presented similar MER levels, around 7.5.

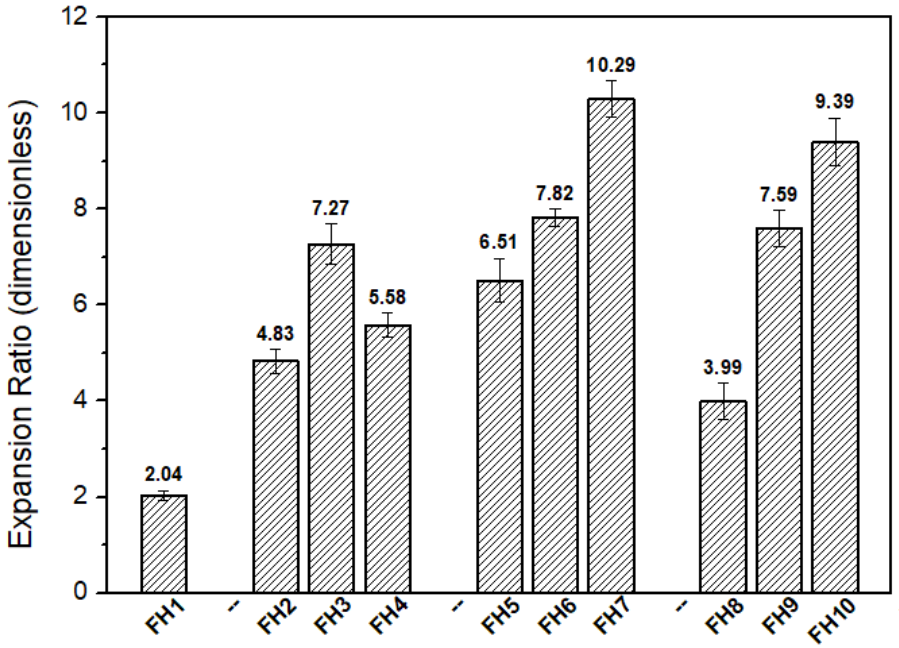

Figure 5.16 INFLUENCE OF SURFACTANT TYPE AND CONTENT ON MER OF THE HYDROGEL SOLUTIONS

At the highest surfactant concentration studied (5 *wt%*), the MER increased further to 9.39 for surfactant "A" (sample FH10) and 10.29 for surfactant B (sample FH7), which represented a wet foam porosity of 89.4% and 90.30%, respectively. Foam generation tends to increase as surfactant concentration increases up to CMC, the concentration at which further surfactant incorporation has little effect on foamability (Osama Al, 2015). Section 5.2.3.1 studied the surface tension of aqueous-surfactant solutions at 22°C. Section 5.2.3.2 studied the surface tension of 10 *wt%* gelatine-surfactant "A" solution but not conclusive results about its CMC were found.

Surfactant C2's behaviour was different from that observed in surfactants "A" and B. It gave rise to a drop in MER at the highest surfactant concentrations (5 *wt%*). This was due to a significant increase in the solution viscosity, as discussed in Section 5.2.2.2, leading to the hindrance of air incorporation into the solution.

Figures 5.17.A, 5.17.B and 5.17.C show a comparison of the expansion ratio increase with beating time during the foaming process for surfactant concentrations of 0.05, 0.5 and 5*wt%,* respectively.

As seen in Figure 5.17A, at low surfactant concentrations (0.05 *wt%*), the foam volume sharply increased within the first ~100s. Then the foam volume expansion slowed down and approached a plateau, the MER for each system.

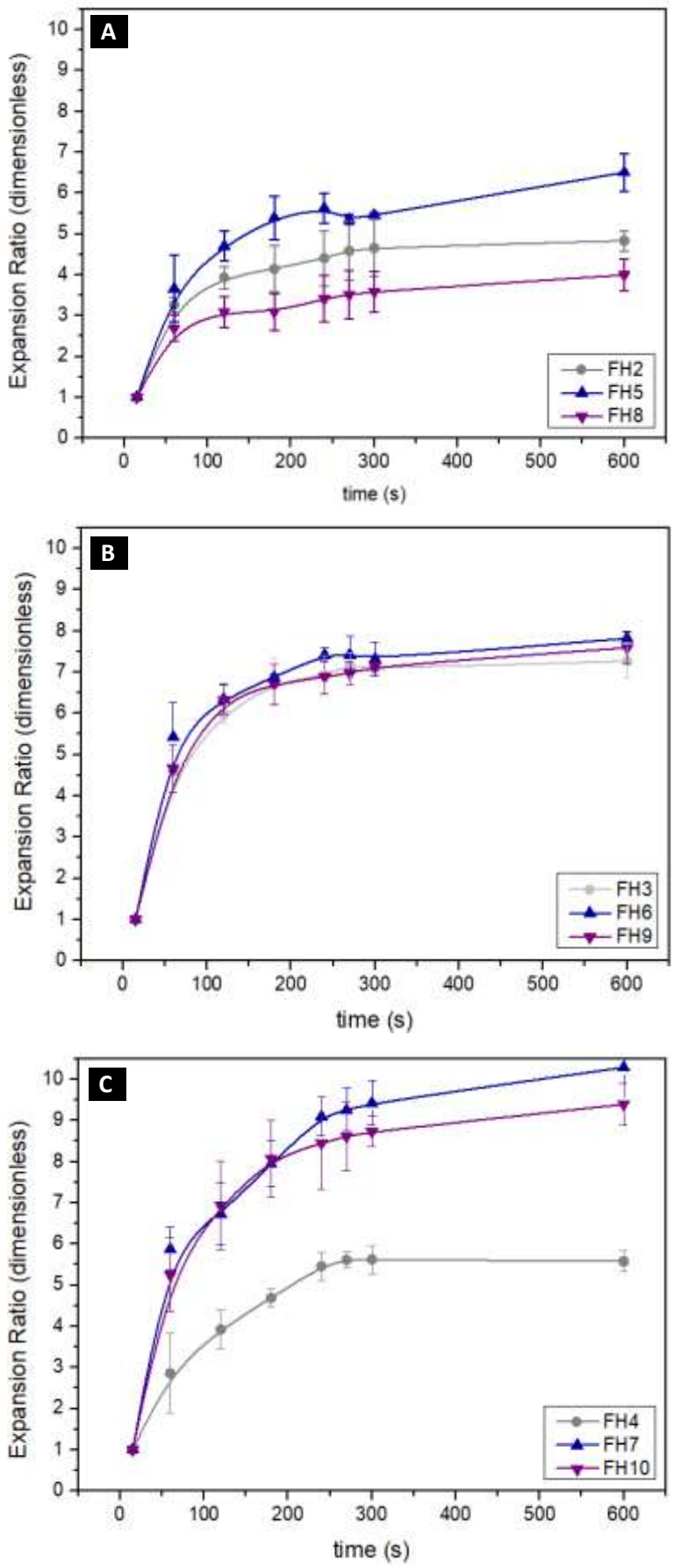

Figure 5.17 EXPANSION RATIO WITH FOAMING TIME FOR SOLUTIONS PREPARED WITH SURFACTANTS AT CONCENTRATIONS AT (A) 0.05 *wt%*; (B) 0.5 *wt%* AND (C) 5 *wt%*

At intermediate surfactant concentrations, 0.5*wt%* (see Figure 5.17B), rapid foam expansion occurred for all solution systems in the first ~100*s,* followed by a slow-down of the expansion. The three surfactants studied reached similar MERs at intermediate surfactant concentration.

At the highest surfactant concentration studied, *5 wt%*(see Figure 5.17C), the initial sharp expansion period was delayed to ~250*s*. Surfactants A and B gave rise to higher MERs, compared to those at lower surfactant concentrations, whereas surfactant C2 exhibited much slower expansion and MER. Surfactant C2 at higher concentrations resulted in solutions with higher viscosity, as mentioned earlier, which hindered air incorporation into the solution.

An increase in surfactant concentration was expected to decrease surface tension and assist the foaming process, but one should also consider their influence of solution viscosity on foaming and the total solid content distribution in the foam structure.

5.3.2 FOAM SHRINKAGE

Hydrogel foams shrinkage is the overall volume shrinkage from that of the cast liquid foam to that of the dried foam. It involves two mechanisms:

a) Volume loss due to lack of stability of the liquid foam (leading to loss of air entrapped in the foam) before sufficient gelling of the foamed liquid. As the gelatine liquid foam cools down, gelling takes place but until the foam walls "freeze", foam ageing processes such as drainage, coalescence and coarsening will result in changes in foam structure, leading to volume reduction.

b) Shrinkage of the cell walls during dehydration and the volume shrinkage associated with it.

Practically, however, it is rather difficult to characterise the two mechanisms separately, and thus, Figure 5.18 presents the total shrinkage of the foams. It is referred to as "drying shrinkage" in this work.

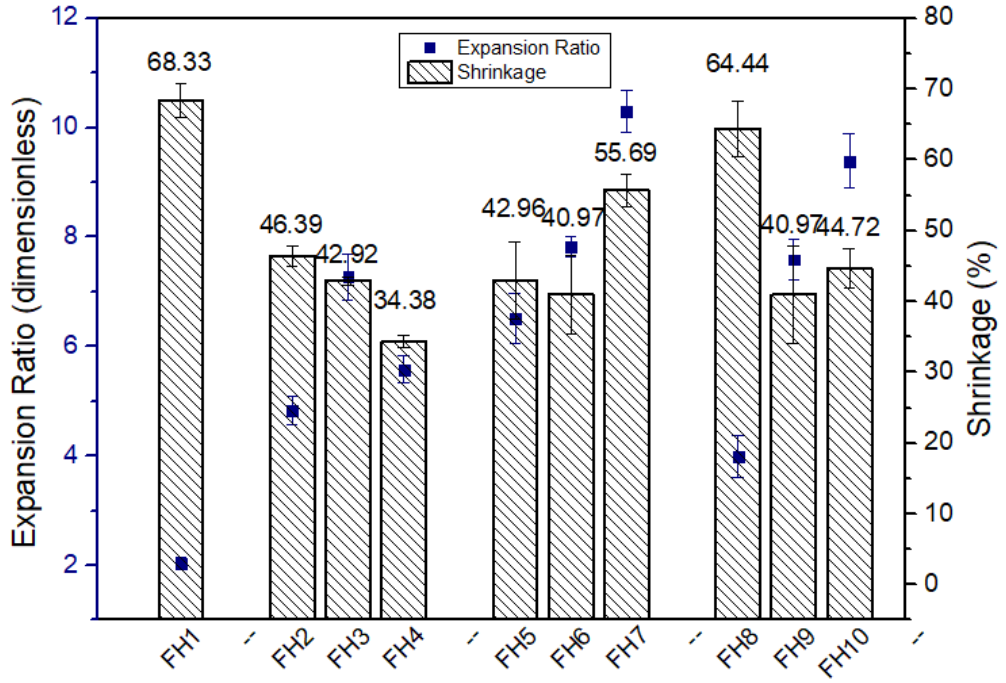

Figure 5.18 INFLUENCE OF SURFACTANT TYPE AND CONTENT ON DRYING SHRINKAGE OF THE HYDROGEL FOAMS BASED ON GELATINE. THE LIQUID FOAM MER WAS ALSO PRESENTED FOR REFERENCE

In comparison with FH1 (without surfactant), incorporation of surfactant into the solution reduced the overall shrinkage from 68.3% to levels ranging from 34.4% (FH4) to 64.4% (FH8).

Foams prepared with surfactant C2 exhibited shrinkage inversely proportional to the surfactant content, from the highest, 46.4% (FH2), to the lowest shrinkage, 34.4% (Sample FH4).

Surfactant B foams presented slightly lower shrinkage values for low and intermediate surfactant contents, (from 43%, FH5, to 41%, FH6). Shrinkage increased, up to 55.7% for sample FH7, at higher surfactant concentration due most likely to poorer liquid foam stability associated with the high expansion ratio achieved. As discussed in section 2.5.6.4 in Chapter 2, higher expansion ratios may lead to less stable foams due to film thinning and breaking if the gelling process is not fast enough.

In contrast, surfactant "A" containing foams exhibited high shrinkage at low surfactant "A" concentrations (64.4%, FH8) and considerably lower shrinkage at medium and higher surfactant concentrations (41%, FH9 and 45%, FH10, respectively). This shows surfactant "A" was less effective at low concentrations compared to both surfactants B and C2 and more concentration was needed to achieve relatively low shrinkage values.

Low shrinkage alone does not necessarily lead to low dry foam density, as it relies on both low shrinkage and high liquid foam expansion ratio. In general, surfactant

inclusion increased liquid foam expansion (Figure 5.16) and reduced foam drying shrinkage (Figure 5.18), and thus, helped to achieve low-density foams (see section 5.3.3). However, foam expansion and shrinkage did not only depend on surfactant concentration but also on other parameters such as viscosity and surface tension. Thus, as shown in Figure 5.18, there is not a clear relationship between shrinkage and MER. Samples with low MER can exhibit very high shrinkage, such as sample FH8, because the amount of surfactant is not sufficiently high to stabilise the cell walls before gelling occurs. However, samples with high MER can also exhibit high values of shrinkage, such as sample FH7, due to the production of thin walls which cannot withstand the forces generated during the drying process.

Figure 5.19 shows a visual assessment of the dry foams. It compares the cross-section of the dry foam samples, which illustrates the shrinkage patterns. Shrinkage tended to be maximum in the centre of the sample. A convex deformation tended to develop in the surface in contact with the mould, and a concave deformation tended to form in the surface in contact with the atmosphere.

The foam shrinkage was not even because the water was not removed uniformly as the gelled foam dehydrated and the cell walls did not have a constant elasticity. First, water was removed from the surface of the foam, followed by gradual dehydration of deeper layers until reaching the centre, which caused a concave shrinkage (Potter & Hotchkiss, 2012).

FH1. 15 *wt%* Gelatine

FH2. 15 *wt%* Gelatine. 0.05 *wt%* C2

FH5. 15 *wt%* Gelatine. 0.05 *wt%* B

FH8. 15 *wt%* Gelatine. 0.05 *wt%* A

FH3. 15 *wt%* Gelatine. 0.5 *wt%* C2

FH6. 15 *wt%* Gelatine. 0.5 *wt%* B

FH9. 15 *wt%* Gelatine. 0.5 *wt%* A

FH4. 15 *wt%* Gelatine. 5 *wt%* C2

FH7. 15 *wt%* Gelatine. 5 *wt%* B

FH10. 15 *wt%* Gelatine. 5 *wt%* A

Figure 5.19. VISUAL ASSESSMENT OF THE CROSS-SECTIONS OF THE DRY FOAMS SHOWING DRYING SHRINKAGE FROM LIQUID FOAMS CAST TO THE SAME VOLUME AND SHAPE.

5.3.3 DENSITY OF THE DRY HYDROGEL FOAM

The density of the dry hydrogel foam is more important than the maximum expansion ratio achieved during liquid foaming. Density depends on not only MER but also the stability of liquid foams during subsequent gelling and drying processes. Therefore, the influence of surfactants on foaming may not necessarily correlate directly to the density of dry foams. Other factors such as the total solid content of the solution and gelatine content may also influence density.

Figure 5.20 shows the correlation of surfactant incorporation to dry foam density. In general, as compared to the dry foam density of sample FH1 (no surfactant), 61.8 *kg/m*^{3}, the incorporation of surfactants at increasing levels produced lighter foams.

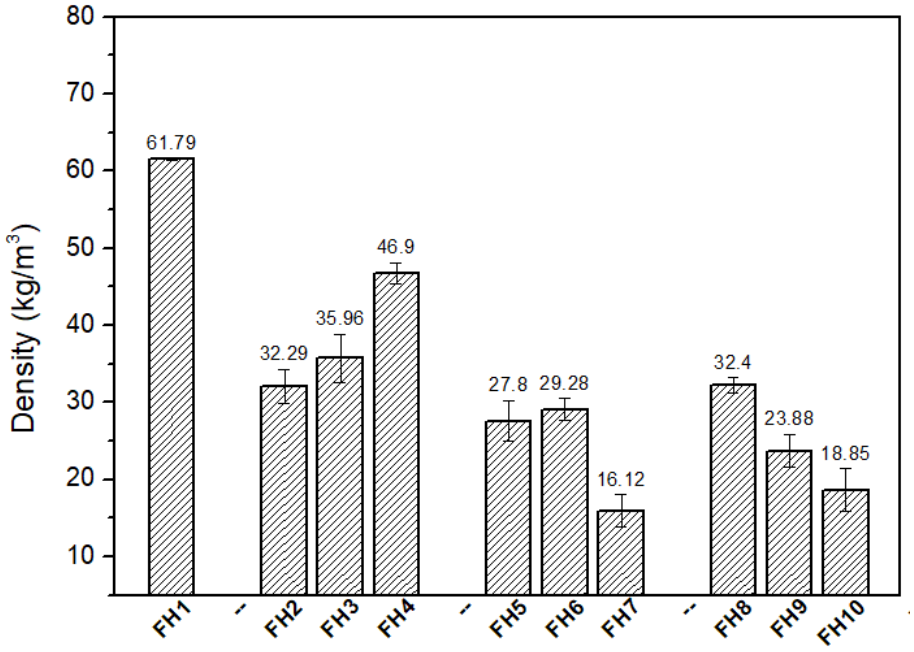

Figure 5.20 CORRELATION OF SURFACTANT TYPE AND CONTENT TO DRY FOAM DENSITIES

Foams prepared with surfactant C2 exhibited a slightly increase from low to medium, surfactant concentrations (from 32.3 *kg/m*^{3}, FH2, to 36.0 *kg/m*^{3}, FH3) and considerable density increase at higher concentration (46.9 kg/m^3, sample F4). The considerable density increase was due to an increase in the viscosity of the solution that hindered the air incorporation, and consequently, considerably decreased the expansion ratio.

Surfactant B at low and medium surfactant concentrations exhibited similar densities (27.8 *kg/m*^{3}, FH5, and 29.3 *kg/m*^{3}, FH6) but the density considerably decreased at higher concentrations (16.1 kg/m^3, FH7).

Foams prepared with surfactant "A", presented a similar trend to that of surfactant B. They manifested a density decrease with increasing surfactant content (from 32.4 *kg/m*^{3}, FH8; 23.9 *kg/m*^{3}, FH9; and 18.9 *kg/m*^{3}, FH10)

Although these observations did not mirror the results in Figure 5.16 for MER exactly, the general trend agreed high expansion ratio led to low foam density, and thus, what achieved in liquid foam expansion was larger transferred to the density reduction of the dry foams. It may also be extended to argue that there were no drastic differences in foam stability during gelling and drying stages from the different surfactant concentration.

5.3.4 FOAM STRUCTURE

Optical microscope images of the cross-section of the hydrogel foams are presented in Figure B1 (see Appendix B). All the foams exhibited an open-cell structure as the cells were interconnected. The top layer cells generally manifested a relatively smaller cell size and distorted shape. This may be partially due to the faster gelling and drying of the top layer. The central and bottom layers exhibited bigger cell sizes indicating relatively longer duration in a liquid state and possible coarsening. In general, the foams showed cell sizes ranging from 0.1 to 5 mm diameter. Foams with surfactant C2 had slightly smaller cells and denser structure than that with surfactants B and A.

Figure 5.21 shows the cell structure of the top layer of the dry foams, the layer in contact with air. The dyed cells on the surface showed an open cell structure in all the foams, confirming the observations on the cross-section (discussed above). This feature allows gas flow through the foams, assisting the drying process.

Foams with surfactant C2 (FH2-FH4) resulted in fine cells at all concentrations, foams with surfactant B (FH5-FH7) exhibited coarsening, more considerably at higher surfactant contents (FH6 and FH7) and foams with surfactant "A" produced intermediate (between surfactants B and C2) cell size at all concentrations.

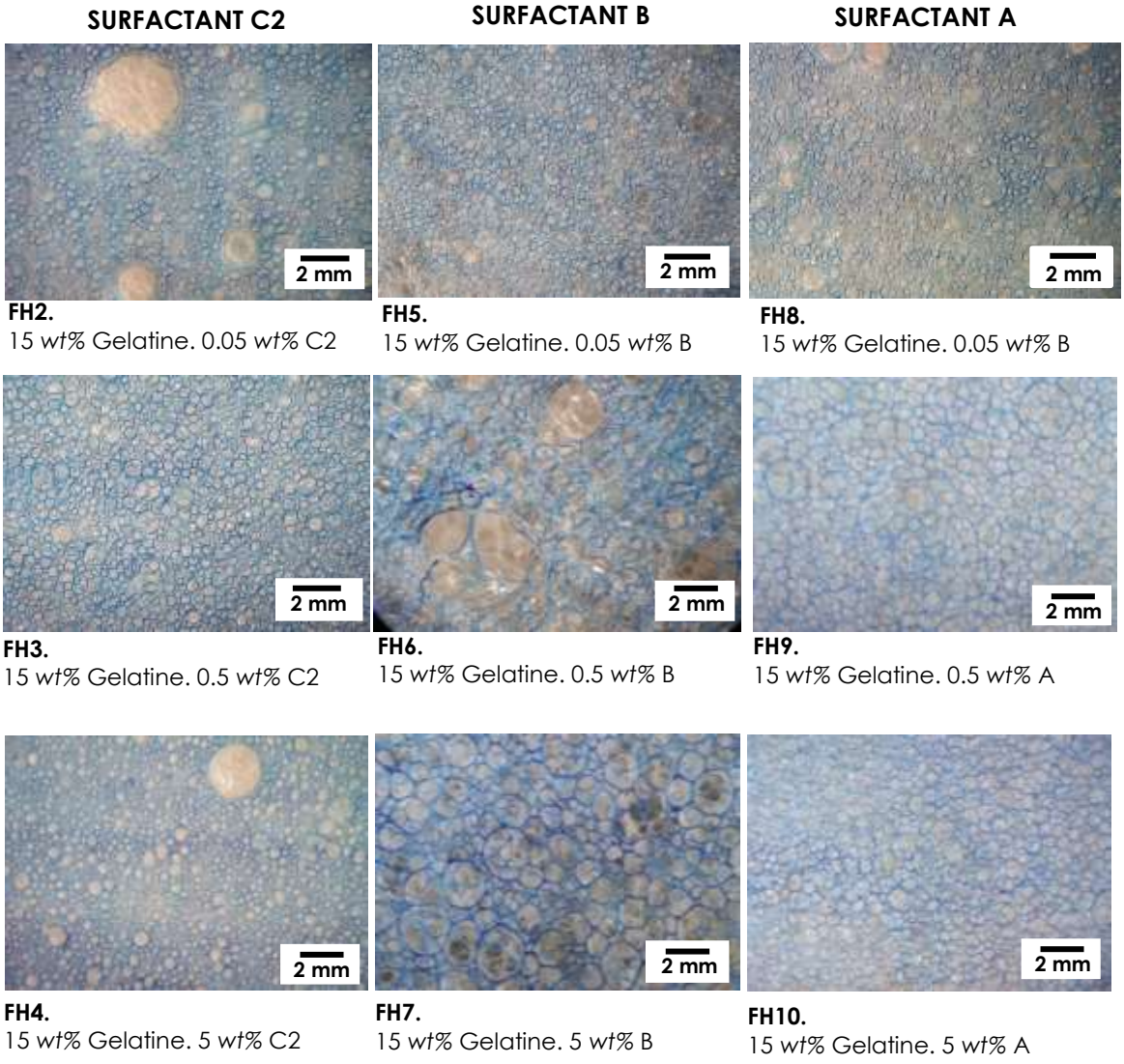

Figure 5.21 OPTICAL MICROSCOPE IMAGES OF THE TOP SURFACE OF GELATINE FOAMS SHOWING INFLUENCE OF SURFACTANT TYPE AND CONTENT ON CELL STRUCTURE

5.3.5 SUMMARY

This study aimed to investigate the influence of the surfactant type and content on MER, density, shrinkage and structure of hydrogel-gelatine foams. This was carried out mainly for narrowing down the selection of surfactant type and content range to lay the foundations for further study.

Table 5.11 summarises the influence of surfactant type and concentration on liquid foam maximum expansion ratio (MER), drying shrinkage and density of dry foams.

Table 5.11 SUMMARY OF INFLUENCE OF SURFACTANT TYPE AND CONTENT ON FOAMING, DRYING AND DRY DENSITY OF HYDROGEL FOAMS.

ID	SURFACTANT TYPE	SURFACTANT CONTENT* (*wt%*)	MER (dimensionless)	DRYING SHRINKAGE (%)	DRY FOAM DENSITY (*kg/m³*)
FH1	N/A	N/A	2.04 ± 0.10	68.33 ± 2.36	61.79 ± 7.60
FH2	C2	0.05	4.83 ± 0.25	46.39 ± 1.37	32.29 ± 2.26
FH3		0.5	7.27 ± 0.42	42.92 ± 0.59	35.96 ± 3.15
FH4		5	5.58 ± 0.25	34.38 ± 0.88	46.90 ± 1.38
FH5	B	0.05	6.51 ± 0.46	42.96 ± 5.46	27.80 ± 2.67
FH6		0.5	7.82 ± 0.18	40.97 ± 5.59	29.28 ± 1.44
FH7		5	10.29 ± 0.38	55.69 ± 2.29	16.12 ± 2.07
FH8	A	0.05	3.99 ± 0.38	64.44 ± 3.93	32.40 ± 1.03
FH9		0.5	7.59 ± 0.38	40.97 ± 6.85	23.88 ± 2.14
F10		5	9.39 ± 0.5	44.72 ± 2.75	18.85 ± 2.78

*Surfactant content based on the total gelatine-water solution weight

All the foams exhibited an open cell structure throughout, and at the surface, this structural feature may be utilised for forced gas transport to assist drying.

For packaging applications, low-density foams around 20 kg/m^3 are desirable. As seen in Table 5.11, this is achievable. Low volume shrinkage, below 10%, is desirable and thus, this feature needs further attention.

In foams containing surfactant C2, FH2 was the one exhibiting the lowest density, 32.29 kg/m^3, but also the highest shrinkage, 46.39%. FH4 exhibited the lowest shrinkage, 34.38%, but highest density, 46.90 kg/m^3. FH3 presented intermediate values in both shrinkage, 42.92%, and density, 35.96 kg/m^3.

In foams with surfactant B, FH7 achieved the lowest density, 16.12 kg/m^3, but the highest shrinkage, 55.69%. Both FH5 and FH6 manifested similar values in both density and shrinkage.

In foams with surfactant "A", FH10 achieved the lowest density, 18.85 kg/m^3, followed by FH9, 23.88 kg/m^3. Both exhibited similar shrinkage values (44.72% and 40.97%, respectively) while F8 showed the highest density, 32.40kg/m^3, and shrinkage, 64.44%.

Surfactant B will not be followed for further experimentation. Despite the relatively low density and shrinkage achieved, surfactant B containing foams exhibited tendencies to produce non-uniform and coarse cells structures. Surfactants C2 and A were selected for further research (see Section 5.4).

5.4 INFLUENCE OF FOAMING TEMPERATURE, GELATINE CONTENT AND SURFACTANT TYPE AND CONTENT ON THE FOAMING BEHAVIOUR AND PROPERTIES OF HYDROGEL-GELATINE FOAMS

This section focuses on the study of the effects of different formulation factors, type and concentration of surfactants "A", C1 and C2, gelatine concentration and processing parameters (foaming temperature) on the foaming behaviour of the hydrogel drying shrinkage, density, foam structure and their mechanical, thermal and acoustic properties. Figure 5.22 summarises the properties characterised in this section.

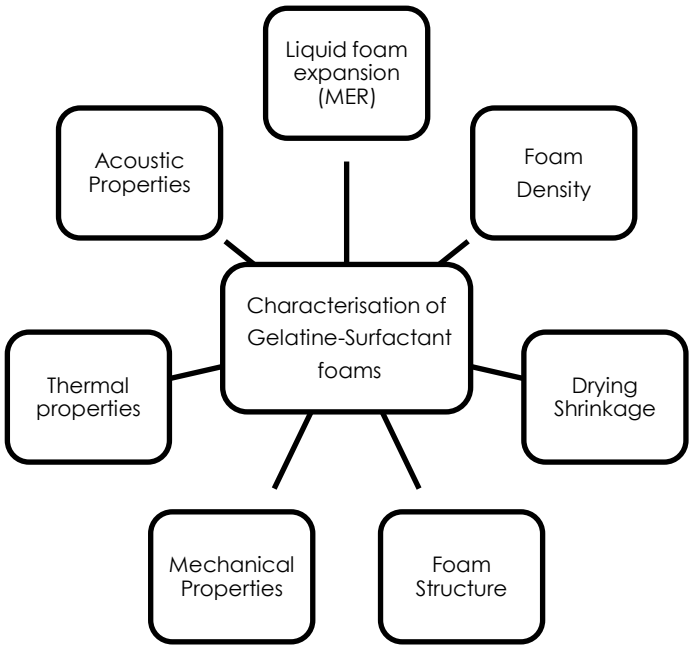

Figure 5.22 CHARACTERISATION OF HYDROGEL FOAMS BASED ON GELATINE CONTAINING SURFACTANTS "A" AND C2

As discussed in section 3.3.3.3.2, in Chapter 3, the following experimental factors and levels were considered during the preparation of the hydrogel foams studied in this section:

a. Gelatine content. Three levels were investigated: low (10 *wt%*), medium (15 *wt%*), and high (20 *wt%*) using surfactants A, C1 and C2

b. Surfactant content. Three levels were analysed:

- Surfactant "A": low (0.5 *wt%*), medium (1.5 *wt%*) and high (4.5 *wt%*)

- Surfactants C1 and C2: low (0.75 *wt%*), medium (1.5 *wt%*) and high (3 *wt%*)

c. Foaming temperature: low (50°C) and high (80°C) for surfactants "A" and C2. Surfactant C1 was solely studied at a foaming temperature of 50°C.

In addition to characterisation of foams made with surfactants "A" and C2, the performance (in terms of MER and dry density) of surfactants C1 and C2 (sourced by two different suppliers) was also compared.

Table 5.12 shows the experimental matrix of this experiment. It shows the levels at which each factor was prepared. (-1), (0) and (1) correspond to the low, intermediate and high levels analysed for each factor, as explained above.

Table 5.12 EXPERIMENTAL MATRIX FOR HYDROGEL-GELATINE-SURFACTANT FOAMS

			FACTOR A	FACTOR B	FACTOR C
SURF*. A	**SURF*. C1**	**SURF*. C2**	**GELATINE CONTENT**	**SURFACTANT CONTENT**	**PROCESSING TEMPERATURE**
A1	**C1.1**	**C2.1**	-1	-1	-1
A2		**C2.2**	-1	-1	+1
A3	**C1.2**	**C2.3**	0	-1	-1
A4		**C2.4**	0	-1	+1
A5	**C1.3**	**C2.5**	+1	-1	-1
A6		**C2.6**	+1	-1	+1
A7	**C1.4**	**C2.7**	-1	0	-1
A8		**C2.8**	-1	0	+1
A9	**C1.5**	**C2.9**	0	0	-1
A10		**C2.10**	0	0	+1
A11	**C1.6**	**C2.11**	+1	0	-1
A12		**C2.12**	+1	0	+1
A13	**C1.7**	**C2.13**	-1	+1	-1
A14		**C2.14**	-1	+1	+1
A15	**C1.8**	**C2.15**	0	+1	-1
A16		**C2.16**	0	+1	+1
A17	**C1.9**	**C2.17**	+1	+1	-1
A18		**C2.18**	+1	+1	+1

**Surfactant*

Section 5.4.1 investigates the relationship between liquid foam maximum expansion, MER, and the experimental factors in an attempt to identify conditions that lead to maximum foam expansion for low-density foams. Section 5.4.2, focuses on the relationship of post-casting foam shrinkage with the experimental factors in an attempt to identify conditions that lead to desirable low foam shrinkage levels. Then, Section 5.4.3 looks into the relationship between dry foam density and the experimental factors. This is a key section as foam selection for packaging applications is usually dictated by foam density due to its impact on logistics.

The cell structure of the solid foams was characterised in Section 5.4.4 with SEM and optical microscopy.

Finally, Section 5.4.5 reports the characterisation of the following solid foam properties:

1) Compression properties
2) Thermal conductivity
3) Acoustic properties

5.4.1 MER OF GELATINE-SURFACTANT FOAMS

All the gelatine-surfactant solutions were foamed for 10 minutes and the expansion ratio, ER, with time and the final maximum value, MER, were recorded, as explained in section 3.5.1, in chapter 3.

ANOVA testing was carried out for surfactants "A" and C2 separately. A full factorial 3x3x2 design with three replicates was used to calculate the statistical significance of *the design parameters* (gelatine content, surfactant content and foaming temperature) in MER. Further information about the statistical analysis can be found in section 3.3.2 in Chapter 3.

The hypotheses for this experiment were:

a. The null hypotheses (H_O): there was no difference in MER for different combinations of the three design parameters.

b. The alternative hypotheses (H_1): there was a difference in MER for different combinations of the three design parameters.

A second ANOVA test was carried out for the comparison between surfactants C2 and C1. A full factorial design 2x2x3 with three replications was used to calculate the statistical significance of the surfactant type (C1 and C2) in MER.

5.4.1.1 Foams containing surfactant "A"

As shown in Figure 5.23, the MER of gelatine-surfactant "A" foams ranged from 5.7 (sample A5, with the highest gelatine content, 20 *wt%*; the lowest surfactant content, 0.5 *wt%*, and low foaming temperature, 50°C) to 10.25 (sample A14 with the lowest gelatine content, 10 *wt%*; the highest surfactant content, 4.5 *wt%*; and high foaming temperature, 80°C). These results were as expected. MER tended to increase as gelatine content decreased, surfactant content increased and foaming temperature increased, as these conditions favoured liquid foaming: low viscosity and low surface tension. More detailed influence on MER from the categorical variables and the interactions between them will be given below.

The results of this experiment were comparable to the results in section 5.3.1 where both ER and MER of surfactant "A" foams were analysed. F12 (MER=7.59) and A4 (MER=6.99), with the identical formulation and prepared at the same temperature, and FH13 (MER=9.39) and A16 (MER=9.15) differing only slightly in surfactant concentrations (4.5*wt%* and 5*wt%,* respectively) demonstrated the repeatability of the foaming process.

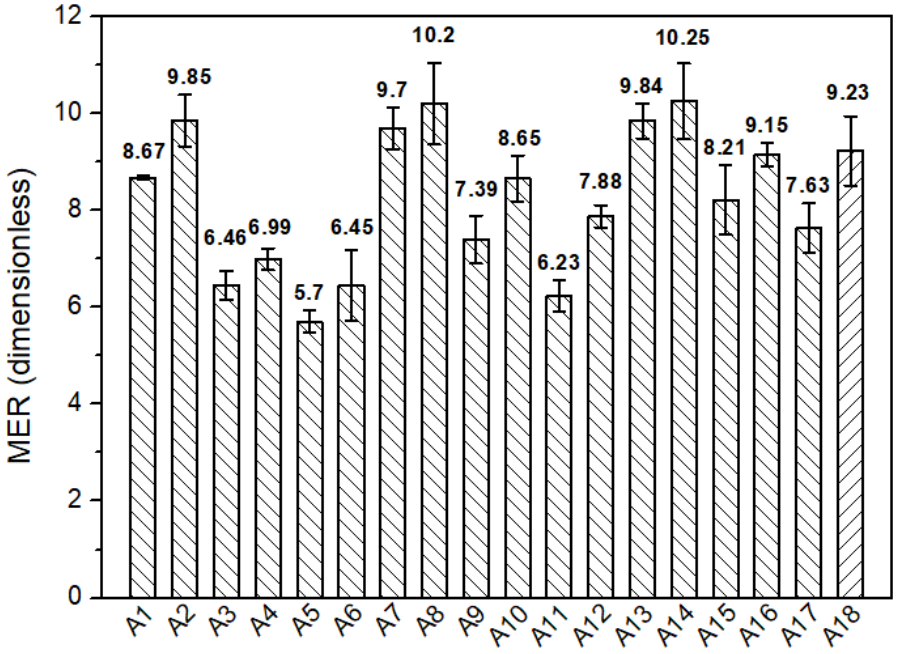

Figure 5.23 MER OF GELATINE-SURFACTANT "A" FOAMS

Figure 5.24 (for more detailed data, see Table C1, in Appendix C) shows the evolution of ER with time for the different formulations of this study.

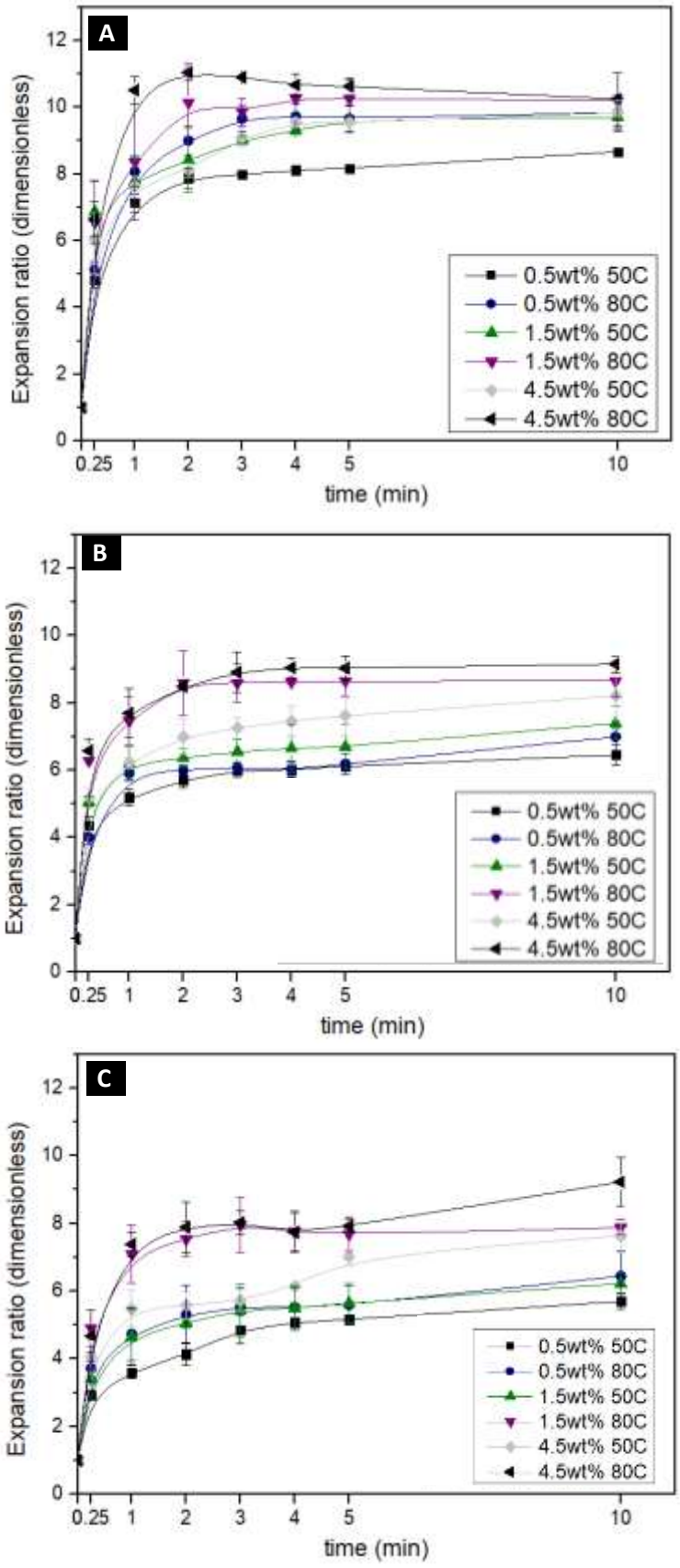

Figure 5.24 VARIATION OF EXPANSION RATIO (ER) WITH TIME FOR GELATINE-SURFACTANT "A" FOAMS PREPARED AT DIFFERENT SURFACTANT CONCENTRATIONS AND FOAMING TEMPERATURES (A) 10 *wt% GELATINE FOAMS* (B) 15 *wt% GELATINE FOAMS* (C) 20 *wt%* GELATINE FOAMS

The foams underwent a rapid expansion during the first 1-2 minutes for the three gelatine concentrations studied. Then, approximately after a foaming time of three minutes, a plateau corresponding with the MER was reached.

As previously discussed, higher gelatine concentrations led to lower ER and MER. The sample prepared at the highest surfactant concentration (4.5 *wt%*) and highest foaming temperature (80°) exhibited the highest ER at all the gelatine concentrations studied, followed by the sample prepared at intermediate surfactant concentration (1.5 *wt%*) and highest foaming temperature. The sample prepared at the lowest surfactant concentration (0.5 *wt%*) and low foaming temperature (50°C) corresponded to the bottom curve in Figures 5.24.A, 5.24.B and 5.24.C. This behaviour, as previously discussed, is attributable to a lower viscosity at higher foaming temperatures, and lower surface tension at higher surfactant contents.

The ANOVA table for the MER with a level of significance of 0.05 can be seen in Table A.3 (Appendix A). A small p-value (<0.05, the level of significance) indicated that the factor and/or interactions had a statistically significant effect on the MER. The ANOVA table gave F statistics=145.27, $p<0.001$; F=59.61, $p<0.001$; and F=59.59, $p<0.001$ for gelatine content, surfactant content, and foaming temperature, respectively. From these results, it can be said that there was strong evidence that the MER varied with the three studied parameters. Similarly, MER was influenced by the gelatine content-surfactant content interaction (F=5.24, p=0.002) (see Figures 5.26.B and 5.26.C). The null hypotheses can, therefore, be rejected, concluding that the three factors had a significant effect on the MER.

Figure 5.25 exhibits the main effect plots that show the means of each value for a categorical variable. Figure 5.25A shows MER increased as gelatine concentration decreased. The MER decreased from 10 *wt%* gelatine content foams (MER=9.75) to 15% (MER=7.81) was more significant than from 15% to 20% (MAER=7.19). This is attributable to a more considerable increase in viscosity at 20 *wt%* gelatine content, as shown in Section 5.2.2.1.

Figure 5.25B shows the increase in MER with surfactant content. The increase was higher from 0.5 *wt%* (MAER=7.35) to 1.5 *wt%* (MAER=8.34) than from 1.5 *wt%* to 4.5 *wt%* (MAER=9.04). This may be due to the interfaces saturation with the surfactant molecules, as the solution approaches CMC. Figure 5.25.C shows the increase in MER with foaming temperature, from 7.76 for 50°C to 8.74 for 80°C.

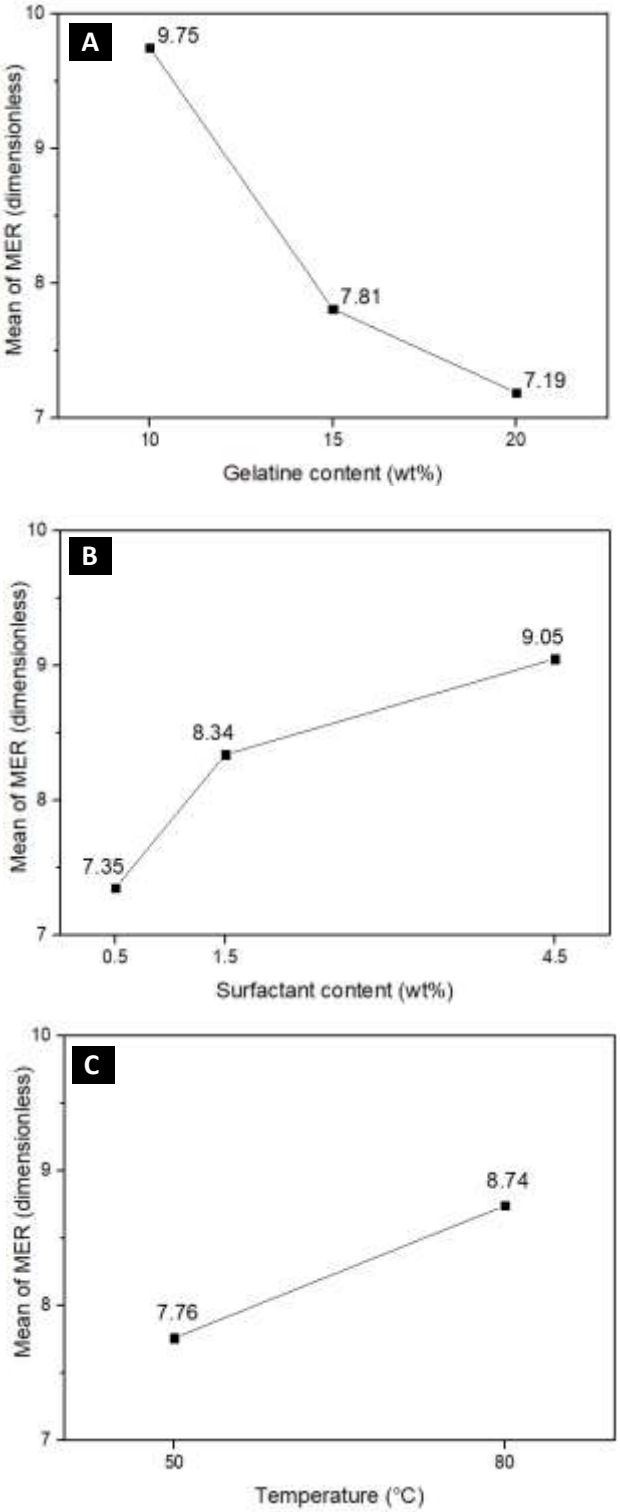

Figure 5.25 MAIN EFFECTS PLOTS FOR MER OF GELATINE-SURFACTANT "A" LIQUID FOAMS (A) GELATINE CONTENT (%); (B) SURFACTANT CONTENT (%) (C) FOAMING TEMPERATURE (°C)

As seen in Figures 5.26.A and 5.26.D, the curves representing the two studied foaming temperatures are nearly parallel, which implies a slight interaction effect between foaming temperature and surfactant and gelatine concentration, respectively (no statistically significant, P>0.05). MER was higher at 80°C than 50°C for all the surfactant

and gelatine concentrations studied. The trend shown in Figures 5.26.A and 5.26.D was the same described for Figures 5.25.B and 5.25.A, respectively.

Figure 6.25.B and 6.25.C show the gelatine content-surfactant content interaction ($P<0.05$). As discussed, lower gelatine content and higher surfactant content exhibited higher expansion ratios. However, the surfactant content had a stronger positive effect on MER when increasing from lower to medium concentrations than medium to higher concentrations due to the surfactant reaching CMC at relatively low surfactant content. This trend was less remarkable at higher gelatine concentrations, where the MER increased from 1.5 to 4.5 *wt%* surfactant content more than observed al lower concentrations. This may be due to surfactant "A" nature, which provided extra water to the formulation, assisting the foaming process of higher gelatine content foams by slightly lowering its viscosity.

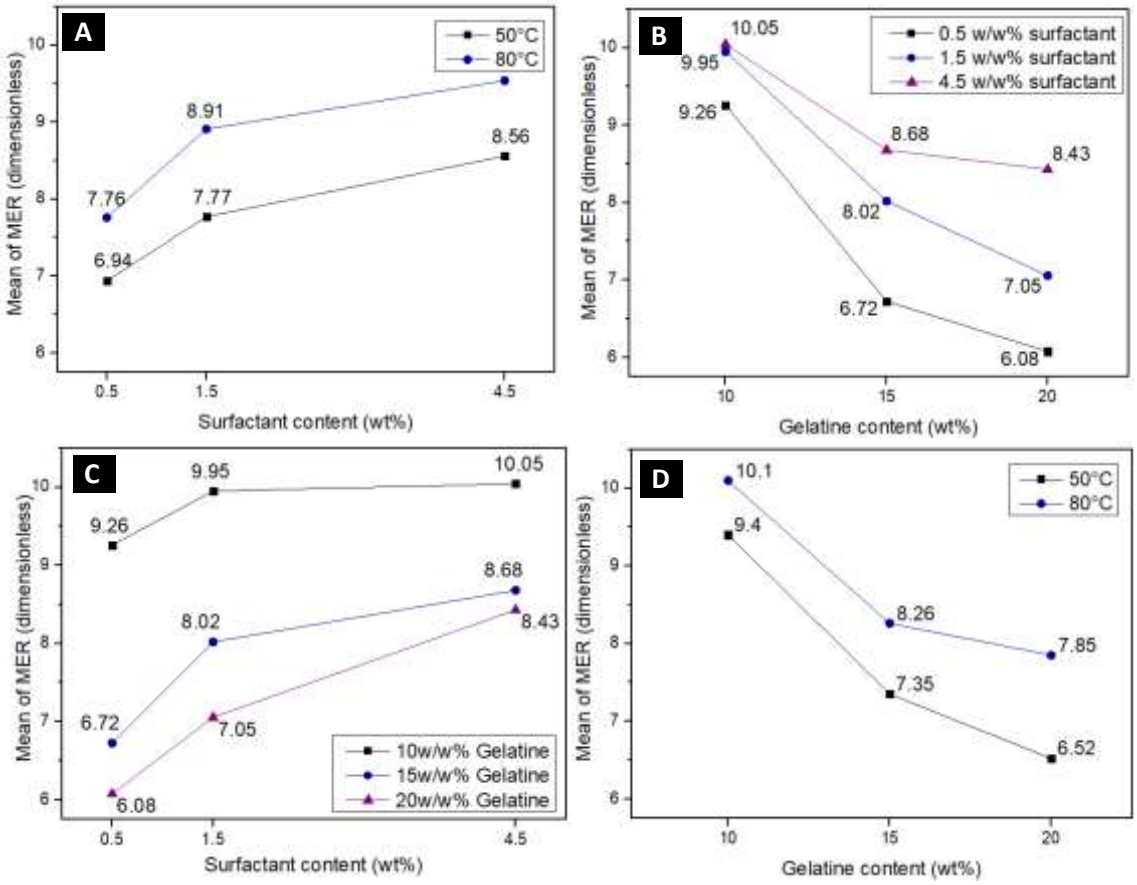

Figure 5.26 ESTIMATED MARGINAL MEANS FOR GELATINE-SURFACTANT "A" MER (A) SURFACTANT CONTENT-FOAMING TEMPERATURE (B) GELATINE CONTENT-SURFACTANT CONTENT (C) SURFACTANT CONTENT-GELATINE CONTENT (D) GELATINE CONTENT-FOAMING TEMPERATURE

5.4.1.2 Foams containing surfactants C1 and C2

As shown in Figure 5.27, the MER of gelatine-C2 foams ranged from 4.5 (sample C2.17, with the highest gelatine content, 20 *wt%*; the highest surfactant content, 3 *wt%*, and low foaming temperature, 50°C) to 8.52 (sample C2.8, with the lowest gelatine content,

10 *wt%*; intermediate surfactant content, 1.5 *wt%*; and high foaming temperature, 80°C). As observed in gelatine-surfactant "A" foams, MER tended to increase as gelatine content decreased and foaming temperature increased. More detailed influence on ER and MER from the categorical variables and the interactions between them will be given below.

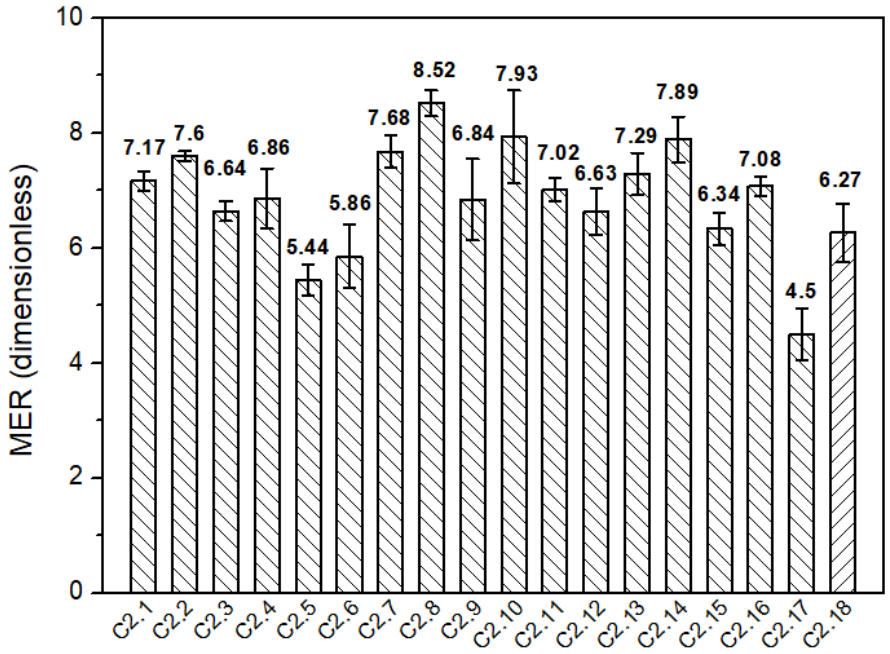

Figure 5.27 MER OF GELATINE-C2 FOAMS

Figure 5.28 (for more detailed data, see Table C2, in Appendix C) shows the evolution of ER with time for the different formulations of this study. The foams underwent a rapid expansion during the first 3 minutes for the three gelatine concentrations studied. Then, a plateau corresponding with the MER was reached. As observed for gelatine-surfactant "A" foams, higher gelatine concentrations tended to produce lower ER and MER.

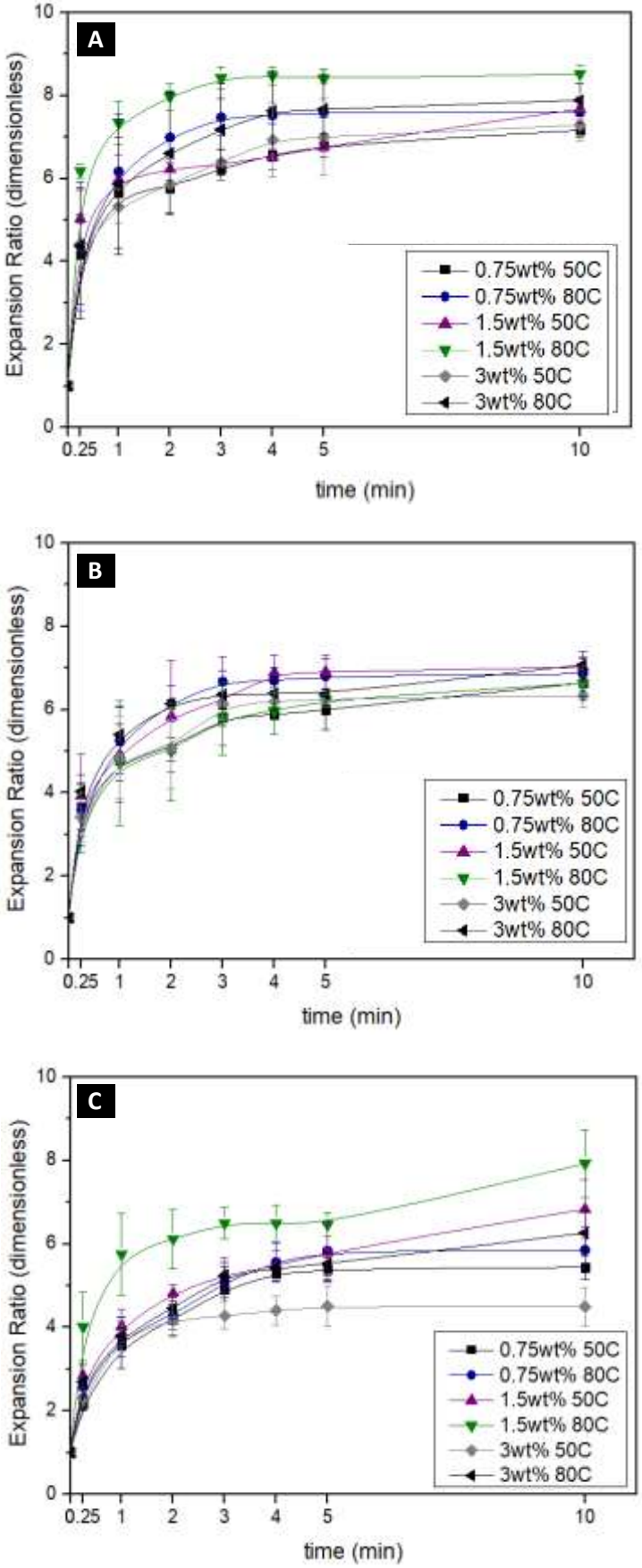

Figure 5.28 VARIATION OF EXPANSION RATIO (ER) WITH TIME FOR GELATINE-SURFACTANT C2 FOAMS PREPARED AT DIFFERENT SURFACTANT CONCENTRATIONS AND FOAMING TEMPERATURES (A) 10 *wt% GELATINE* FOAMS (B) 15 *wt%* GELATINE FOAMS (C) 20 *wt%* GELATINE FOAMS

The ANOVA table for the MER of gelatine-surfactant C2 foams, with a level of significance of 0.05, can be seen in Table A.4 (Appendix A). The table gave F statistics=80.08, $p<0.001$; F=25.90, $p<0.001$; and F=31.89, $p<0.001$ for gelatine content, surfactant content, and foaming temperature, respectively. From these results, it can be said that there is strong evidence that the MER varied with the three studied parameters. Similarly, MER was also influenced by the gelatine content-foaming temperature interaction (F=0.05, p=0.047) and the gelatine content-surfactant content-foaming temperature 3-way interaction (F=4.56, p=0.004) The null hypotheses can, thus, be rejected, concluding that all factors had a significant effect on MER.

Figure 5.29 exhibits the main effect plots that show the means of each value for a categorical variable. Figure 5.29.A shows the decrease in MER as gelatine concentration increases. The decrease in MER from 10 *wt%* gelatine content foams (MER=7.69) to 15 *wt%* (MAER=6.95) was almost linear to 15 *wt%* to 20 *wt%* (MAER=5.95) due to a relatively constant increase in the solution viscosity as surfactant C2 content increased.

Figure 5.29.B shows the MER for different surfactant concentrations. The highest MER corresponded to intermediate surfactant levels (MER=7.44). At lower and higher surfactant contents, MER was lower, 6.59 and 6.56, respectively. These results may be attributable to an optimum viscosity-surface tension balance for the solutions with an intermediate level of surfactant, which were closer to CMC than the solutions with the lowest level of surfactant and exhibited less viscosity than the solution with the highest level of surfactant, situation which facilitated the foaming process.

Figure 5.29.C shows the increase in MER with foaming temperature, from 6.54 (for 50°C) to 7.18 (for 80°C). As shown in Figure 5.25.C, gelatine-surfactant "A" foams MER increased by around 12.6% with foaming temperature (from 50 to 80°C). The MER increase with foaming temperature was slightly lower for gelatine, surfactant C2 foams, approximately 9.8%.

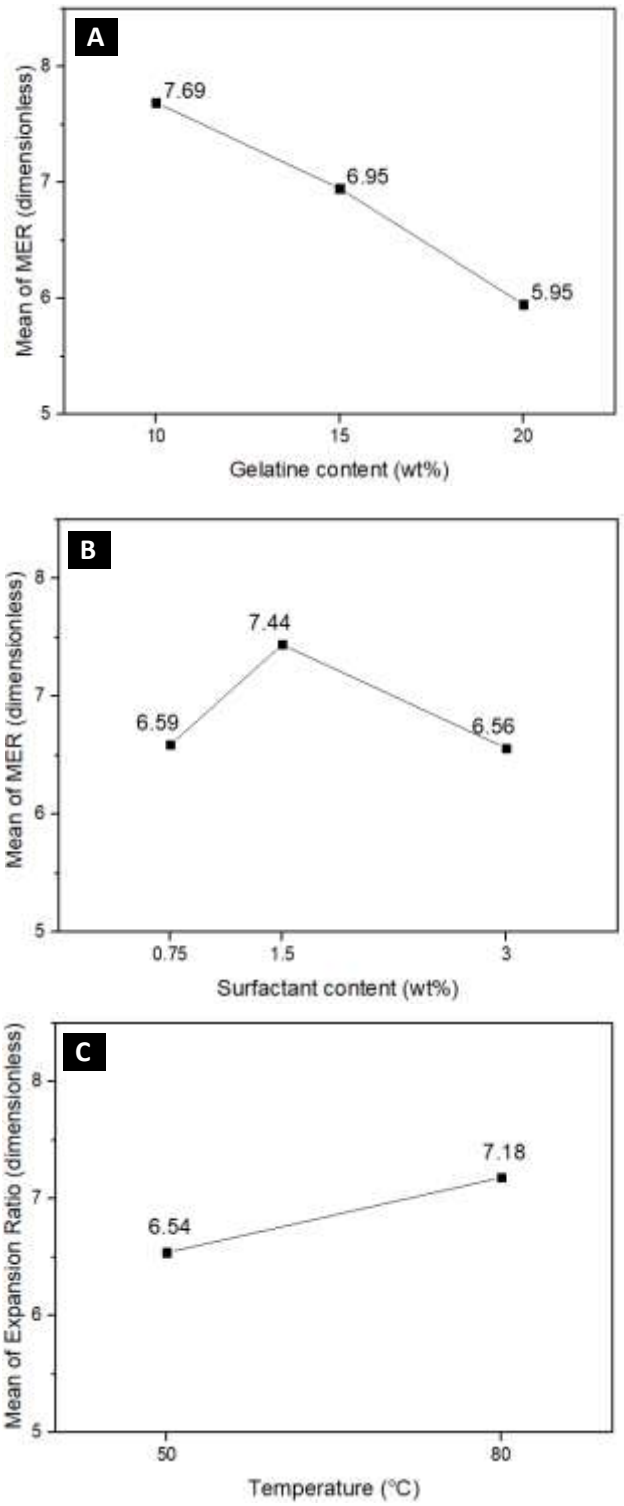

Figure 5.29 MAIN EFFECTS PLOTS FOR MER OF GELATINE-SURFACTANT C2 LIQUID FOAMS (A) GELATINE CONTENT (%); (B) SURFACTANT CONTENT (%) (C) FOAMING TEMPERATURE (°C)

Figure 5.30 shows the *estimated marginal means* for the MER. Figure 5.30D shows the gelatine content-foaming temperature interaction ($p<0.05$). As previously discussed, MER decreased as gelatine content increased. At 50°C, the decrease was virtually linear, but at 80°C, the MER decreased less sharply due to the higher viscosity at higher temperature. The three-way interaction ($p<0.05$) related the gelatine content-foaming

temperature interaction with surfactant content. MER decrease at lower foaming temperatures was more significant at higher gelatine and surfactant contents, what agrees to an increase in viscosity.

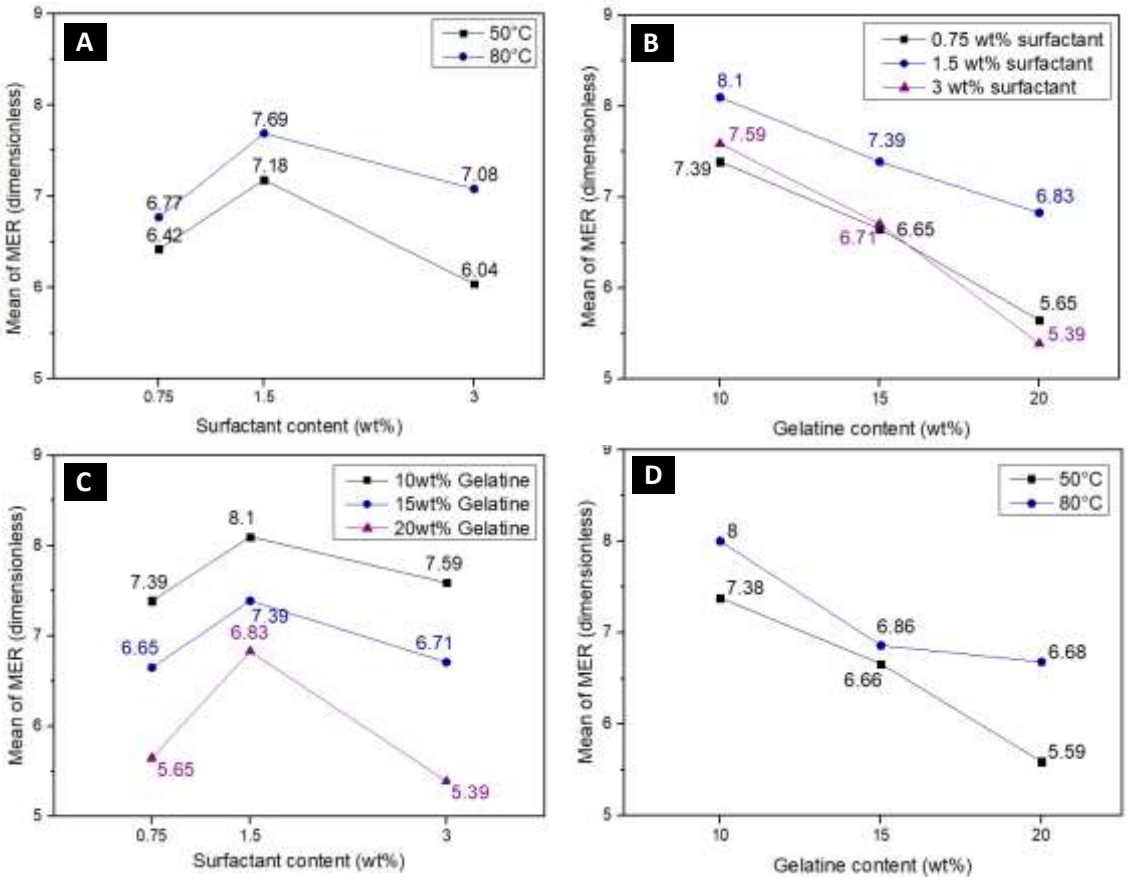

Figure 5.30 ESTIMATED MARGINAL MEANS FOR GELATINE-SURFACTANT C2 MER (A) SURFACTANT CONTENT FOAMING TEMPERATURE (B) GELATINE CONTENT-SURFACTANT CONTENT (C) SURFACTANT CONTENT-GELATINE CONTENT (D) GELATINE CONTENT-FOAMING TEMPERATURE

Figure 5.31 compares the MER between foams prepared with C2 and C1 surfactants (see Tables 3.36 and 3.37, respectively, in Chapter 3, for the formulations of the foams), which only difference was the sourcing (they were acquired from different suppliers). The difference in MER between foams prepared with C1 and C2 was not statistically significant (i.e. the surfactant type, C1 and C2, did not significantly affect the MER of the gelatine foams). The ANOVA table (see Table A.5 in Appendix A) gave F statistics=1.50, p<0.233 for surfactant type.

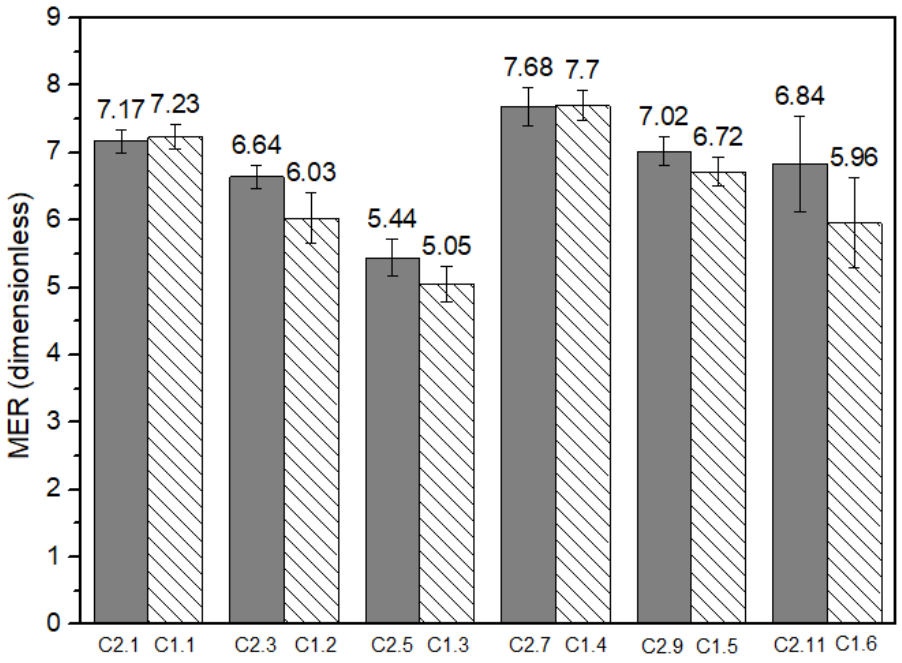

Figure 5.31 COMPARISON OF THE MER (DIMENSIONLESS) OF GELATINE FOAMS CONTAINING SURFACTANTS C1 AND C2

5.4.2 POST-CASTING VOLUME SHRINKAGE

This section studies the total shrinkage of foams containing surfactants A, C1 and C2 from the volume difference between that of the cast liquid foam and that of the dry foam, as described in section 3.6.4 in Chapter 3.

A full factorial 3x3x2 design with three replicates was used to calculate the statistical significance of the three design parameters (gelatine content, surfactant content and foaming temperature) in shrinkage. The hypotheses for this experiment were:

a. The null hypotheses (H_O): there was no difference in mean total shrinkage for different combinations of the design parameters for the gelatine-surfactant "A" and gelatine-surfactant C2 foams

b. The alternative hypotheses (H_1): there was a difference in mean shrinkage for different combinations of the design parameters for the gelatine-surfactant "A" and gelatine-surfactant C2 foams.

5.4.2.1 Foams containing surfactant "A"

As shown in Figure 5.32, gelatine-surfactant "A" foams shrinkage ranged from, the minimum, 31% (samples A3 and A9, with 15 *wt%* gelatine content, 50°C foaming temperature and surfactant contents 0.5 and 1.5 *wt%*, respectively) to the maximum 56% (sample A2, with 10 *wt%* gelatine content, 0.5 *wt%* surfactant and 80°C foaming temperature).

In general, lower gelatine concentration gave rise to higher total shrinkage. Shrinkage also tended to increase as foaming temperature increased, as further discussed below.

The ANOVA table for total shrinkage with a level of significance of 0.05 can be seen in Table A.6 (Appendix A). The ANOVA table gave statistics: F=0.08, p=0.921; F=54.91, p<0.001; and F=36.14, p<0.001 for surfactant content, gelatine content and foaming temperature, respectively. From these results, it can be said that there is strong evidence that the shrinkage varied with gelatine content and foaming temperature but not the surfactant content. However, shrinkage was significantly influenced by interactions between the gelatine-surfactant contents (F=5.62, p=0.001), the surfactant content-foaming temperature (F=3.76, p=0.033) and the gelatine content-foaming temperature (F=9.26, p=0.001). Thus, surfactant had not a significant effect on shrinkage solely, but it had an effect on it when combined with the other two factors (gelatine content and foaming temperature).

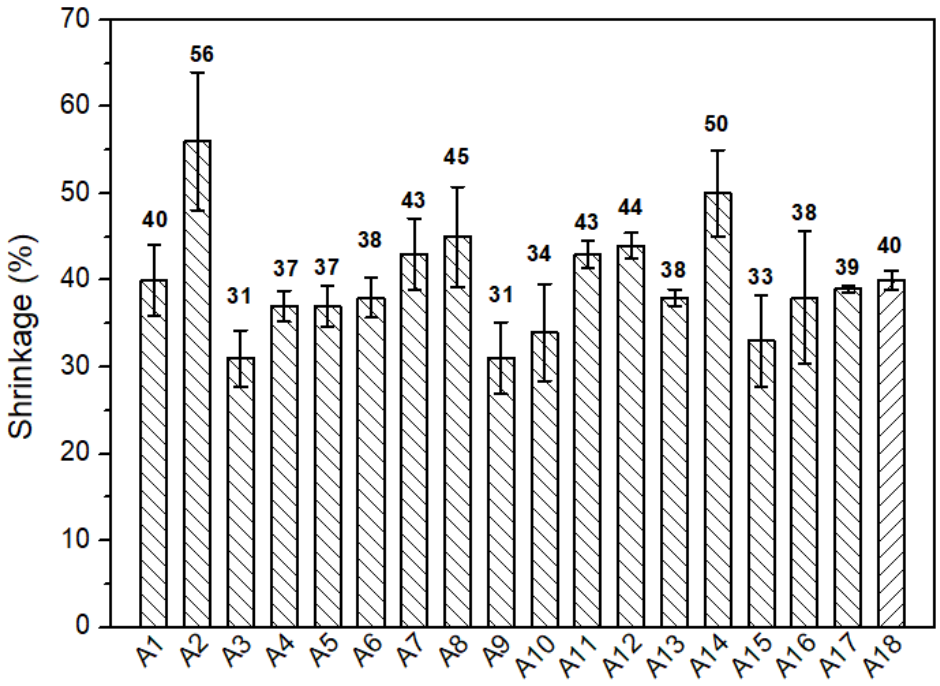

Figure 5.32 TOTAL SHRINKAGE OF THE GELATINE-SURFACTANT "A" FOAMS

Figure 5.33 exhibits the main effect plots for the total shrinkage of the gelatine-surfactant "A" foams. Figure 5.33A shows the effect of gelatine content on total shrinkage. On contrary to anticipated, higher gelatine foams did not show the lowest shrinkage but those at intermediate gelatine content level were the ones showing the lowest shrinkage. This result may be explained but the fact that gel hardening of the plateau borders of the 20 *wt%* gelatine foams may complicate moisture loss and hinder diffusivity, as reported by Waje (2005) for the drying of hydrogels including cross-linkers.

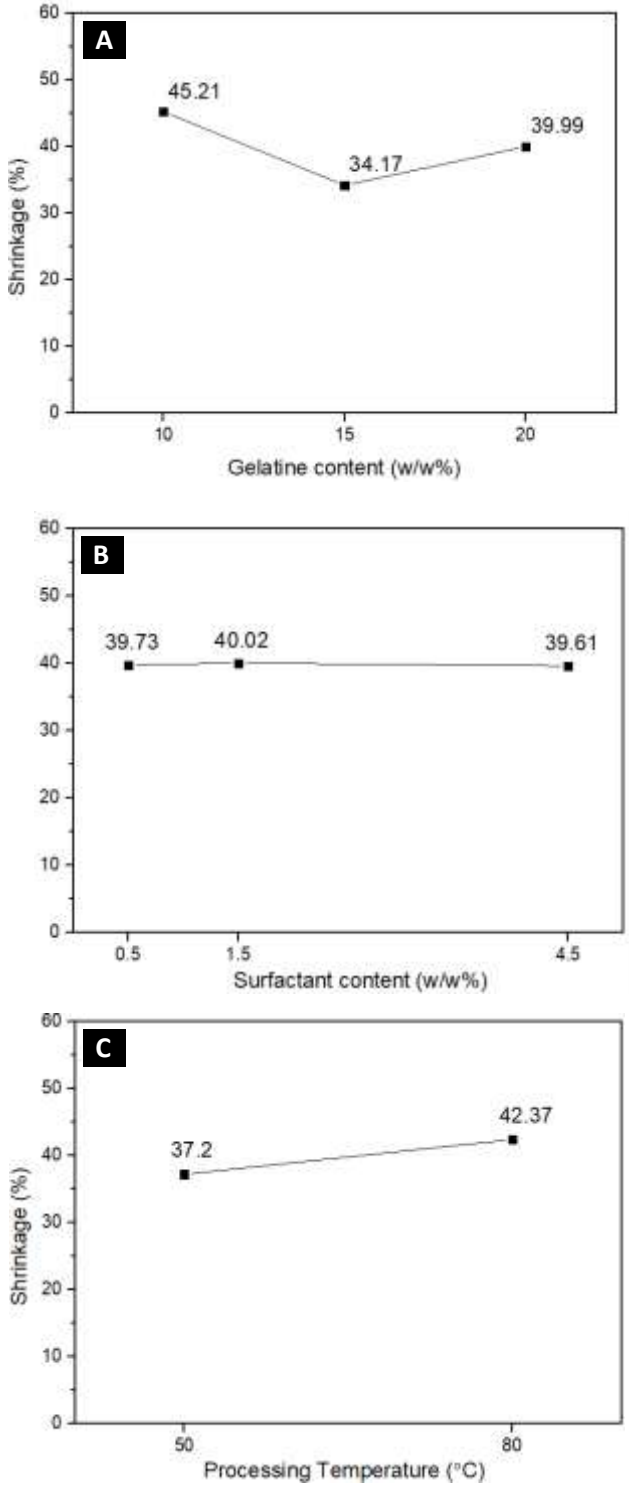

Figure 5.33 MAIN EFFECTS PLOTS FOR TOTAL SHRINKAGE OF GELATINE-SURFACTANT "A" LIQUID FOAMS (A) GELATINE CONTENT (*WT%*); (B) SURFACTANT CONTENT (WT%); (C) FOAMING TEMPERATURE (°C)

As expected (see Section 2.5.6.4 in Chapter 2), Section 5.3.2 proved the stabilising effect of surfactant "A" on gelatine foams, as the sample prepared without surfactant depicted a significantly higher shrinkage, 68%, compared to that of the gelatine foams including surfactant. This stabilising effect was attributable to the creation of polymer-surfactant complexes in the interfaces (even at very low surfactant concentrations) (Petkova, Tcholakova and Denkov, 2012) and not considerably to the surface tension

reduction (Kristen *et al.*, 2009). However, as seen in Figure 5.33B, the effect of surfactant content in total shrinkage was not significant at the studied levels. The average total shrinkage at different surfactant concentrations was virtually the same. This behaviour may be due to the interfaces saturation by surfactant molecules in the gas-liquid interfaces.

Figure 5.33C shows that the average shrinkage increased at higher foaming temperature, what may be related to the expected higher gelling time (and consequently longer 'stabilisation' time) of the gelatine foams foamed at higher temperature.

Figure 5.34 shows the estimated marginal means for shrinkage. Figures 5.34B and 5.34F show the gelatine content-foaming temperature interactions. Total shrinkage tended to be higher with foams processed at higher temperatures and lower gelatine content. However, the increase of foaming temperature had a less negative impact on the shrinkage of higher gelatine foams. A possible explanation for this might be that the gelling time of 20 *wt%* was considerably faster than the lower gelatine concentrations, which can minimise the drainage of high foaming temperature (see Section 5.2.1.2). (see Table 5.2).

Figure 5.34C shows a nearly parallel response of total shrinkage to surfactant content for both 10 and 15 *wt%* gelatine concentrations. However, at higher gelatine concentrations (20 *wt%*), intermediate surfactant concentration (1.5 *wt %*) exhibited a slightly more negative response in shrinkage. Figure 5.34E shows the surfactant content-foaming temperature interaction. At all surfactant concentrations, higher temperatures led to higher shrinkage. However, this trend was less significant at intermediate surfactant content (1.5 *wt%*).

The shrinkage of surfactant "A" foams was minimum at lower foaming temperatures ($p<0.001$), especially at lower gelatine concentrations ($p<0.001$). The temperature influence on shrinkage was due the expected higher gelling time of the gelatine foams foamed at higher temperature. Regarding gelatine content, higher gelatine content may have a detrimental effect on shrinkage due to its higher equilibrium modulus which produced stronger plateau borders which may hinder moisture loss.

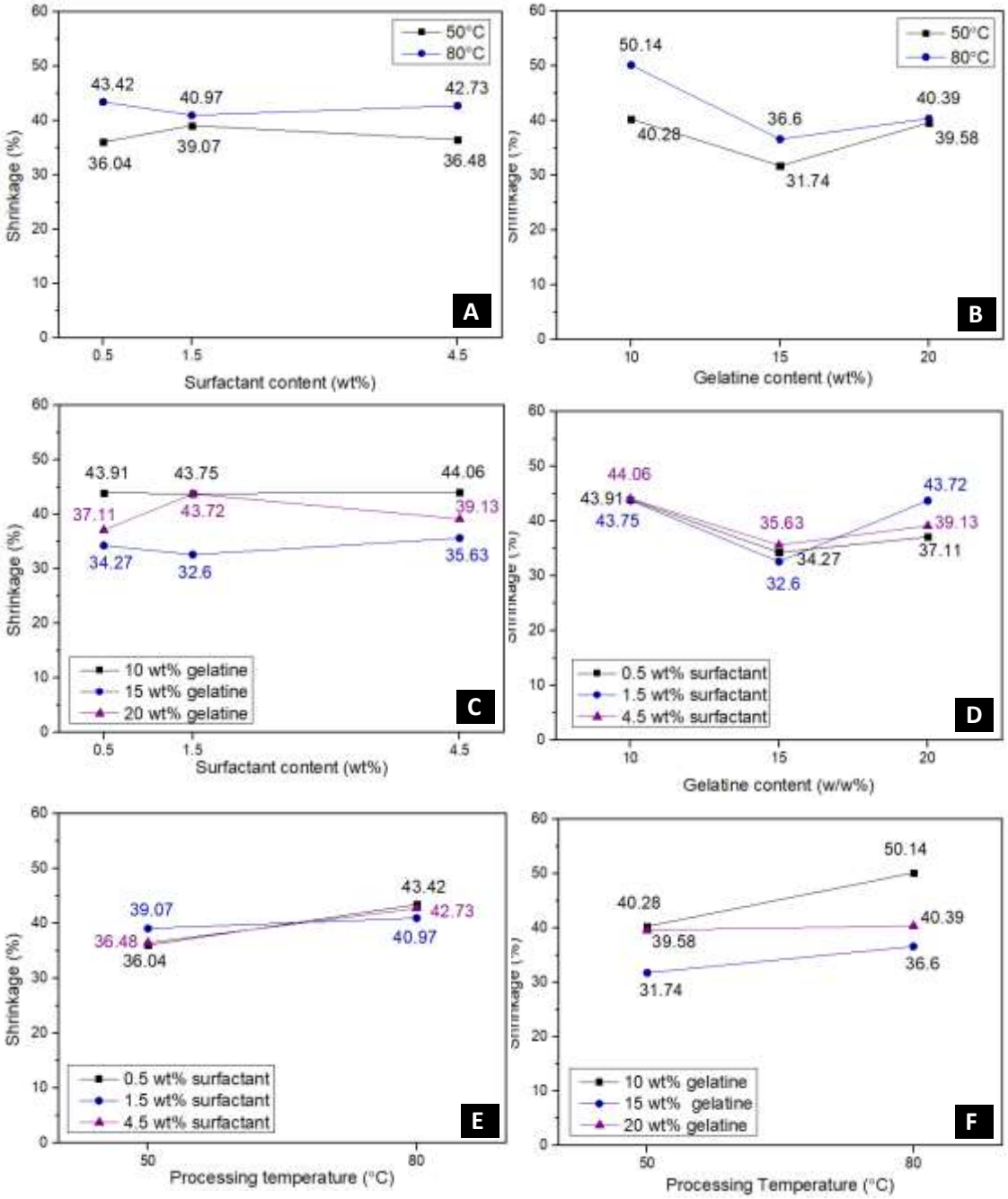

Figure 5.34 ESTIMATED MARGINAL MEANS FOR GELATINE-SURFACTANT "A" TOTAL SHRINKAGE (A) SURFACTANT CONTENT-FOAMING TEMPERATURE (B) GELATINE CONTENT-FOAMING TEMPERATURE (C) SURFACTANT CONTENT-GELATINE CONTENT (D) GELATINE CONTENT-SURFACTANT CONTENT (E) FOAMING TEMPERATURE-SURFACTANT CONTENT (F) FOAMING TEMPERATURE-GELATINE CONTENT

Figure 5.35 shows the cross-section of all dry samples, where the shrinkage patterns (concave, on the top surface, and convex, on the bottom) and no central voids are shown. The overall shrinkage was comparable to that on section 5.3.2 for samples FH9 and FH10, but considerably better than that compared to FH8 (0.05 *wt%* surfactant "A"). A surfactant "A" concentration of 0.5 *wt%* was proved effective for drainage arresting.

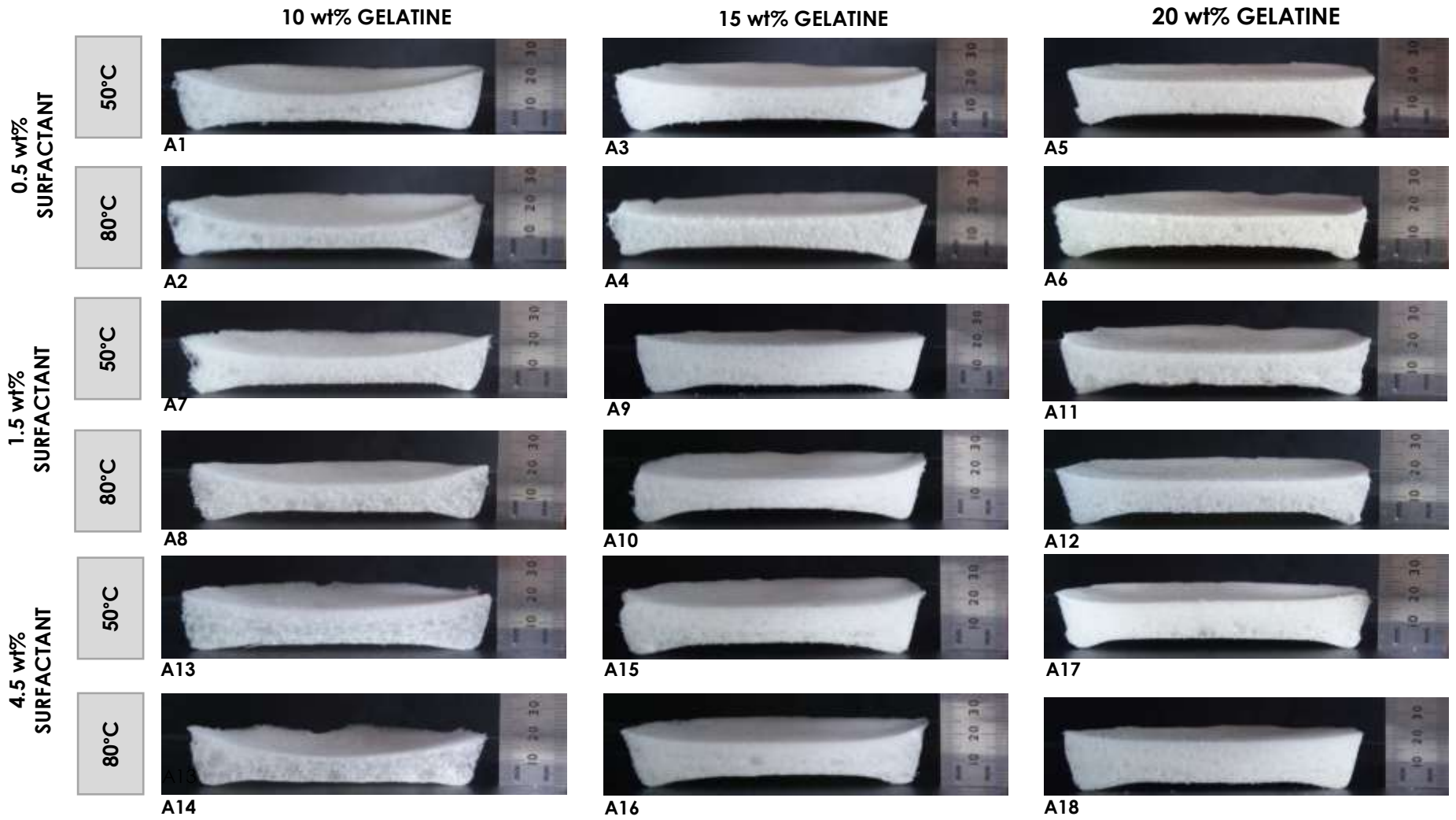

Figure 5.35 CROS-SECTIONS OF THE GELATINE-SURFACTANT "A" DRY FOAMS

5.4.2.2 Foams containing surfactant C2

As shown in Figure 5.36, gelatine-surfactant C2 foams total shrinkage ranged from a minimum 11.22% (sample C2.13, with 10 *wt%* gelatine content, foamed at 50°C foaming temperature and surfactant content 3*wt%*) to a maximum of 33.97% (sample C2.6, 20 *wt%* gelatine content, 0.75 *wt%* surfactant content and foamed at 80°C). In comparison with the gelatine-surfactant "A" system (Figure 5.32), the total shrinkage drastically improved and was closer to the target of <10%. The shrinkage decrease in the hydrogels prepared with surfactant C2 was attributable to both higher viscosities (see Section 5.2.2.2) and lower gelling times (see Section 5.2.1.3) compared to that in hydrogels foams prepared with surfactant "A".

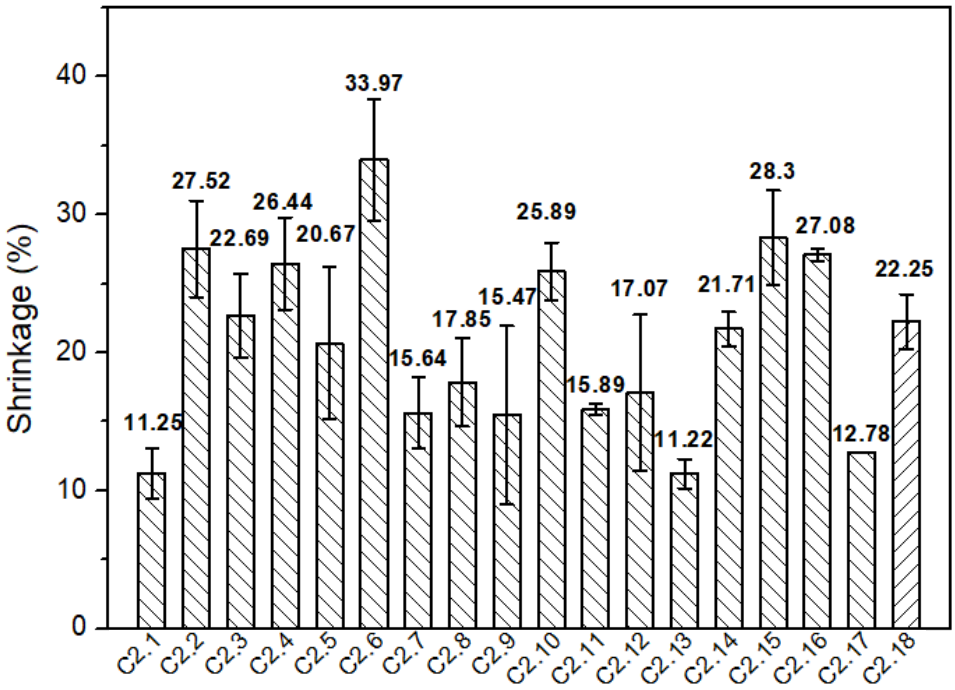

Figure 5.36 TOTAL SHRINKAGE OF THE GELATINE-SURFACTANT C2 FOAMS

The ANOVA table for total shrinkage with a level of significance of 0.05 can be seen in Table A.7 (Appendix A). ANOVA table gave statistics F=13.66, p<0.001; F=18.81, p<0.001; and F=65.27, p<0.001 for surfactant content, gelatine content and foaming temperature, respectively. It can be said that there is strong evidence that the shrinkage was affected by all the 3 parameters. Similarly, total shrinkage was also significantly influenced by the interactions between: gelatine-surfactant content (F=76.48, p<0.001), the surfactant content-foaming temperature (F=4.64, p=0.016) and the gelatine content-surfactant content-foaming temperature interaction (F=5.96, p=0.001).

Figure 5.37 exhibits the main effect plots for the total shrinkage of the gelatine-surfactant C2 foams.

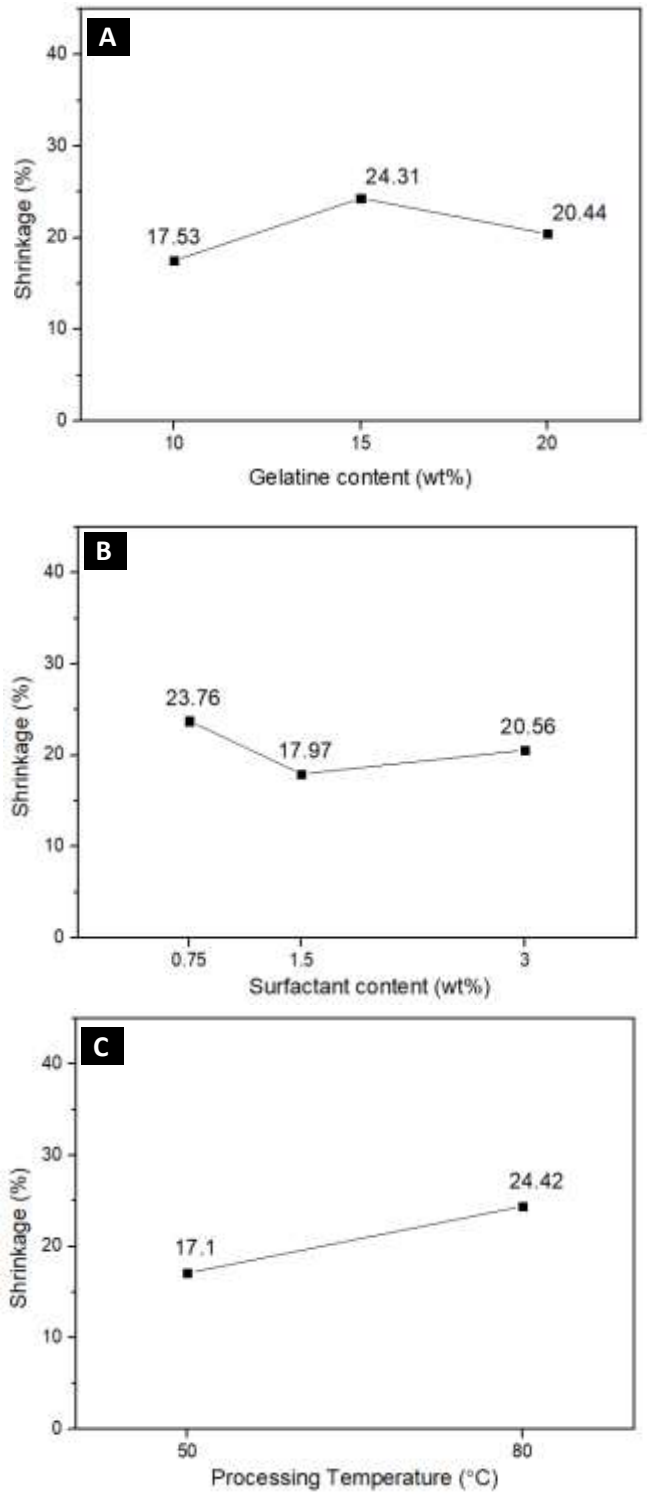

Figure 5.37 MAIN EFFECTS PLOTS FOR TOTAL SHRINKAGE OF GELATINE-SURFACTANT C2 LIQUID FOAMS (A) GELATINE CONTENT (*wt%*); (B) SURFACTANT CONTENT (wt%); (C) FOAMING TEMPERATURE (°C)

Figure 5.37A shows the effect of gelatine content on total shrinkage. The mean shrinkage was slightly higher at intermediate gelatine content (15 *wt%*) than at both ends; and was minimum at lower (10 *wt%)* gelatine content. These results contrasted with the results from Section 5.4.2.1 where the shrinkage of gelatine-surfactant "A" foams was minimum at intermediate (15 *wt%*) gelatine content and maximum at

lower (10 *wt%*) gelatine content. This inverse trend between the two surfactants may be explained by the increase in viscosity of 10 *wt%* gelatine when surfactant C2 was used, considerably lower when surfactant "A" was used. This viscosity increase contributed to a more effective foam stabilisation of the 10 *wt%* gelatine foam. The higher shrinkage level at higher gelatine concentration for foams produced with surfactant C2 may be attributable to the formation of gelatine-surfactant complexes and the hardening of the foam plateau borders, which may hinder the drying process. This can produce higher deformation as higher tensile stresses would be generated.

As seen in Figure 5.37B, the total shrinkage was higher at low (0.75 *wt%*) surfactant content (0.75*wt%*) and slightly decreased as surfactant content increased due to an increase in viscosity.

As expected, from the results from Section 5.4.2.1, Figure 5.37C shows that the total shrinkage increased at higher foaming temperature (80°C*)*.

Figure 5.38 shows the estimated marginal means for shrinkage. Figure 5.38A and 5.38E show the surfactant content-foaming temperature interaction ($p<0.05$). All the foams exhibited similar shrinkage levels when processed at 50°C. However, at higher foaming temperature, the surfactant content influenced the level of shrinkage, being maximum at lower surfactant content (0.75 *wt%*), where solution viscosity was minimum.

Figures 5.38C and 5.38D shows the gelatine-surfactant content interaction ($p<0.05$) and how the gelatine foams shrinkage decreased when increasing the surfactant content from low (0.75 *wt%*) to intermediate (1.5 *wt%)*. However, when surfactant was further increased the shrinkage level had an erratic response due to the formation of central voids (see Figure 5.39), especially for the foams produced at the lower foaming temperature. The formation of these voids at higher surfactant content (3 *wt%*) and lower foaming temperature (50°C) was attributable to a higher liquid foam viscosity, an expected gelling time increase (due to the higher surfactant content) and a considerable number of protein-surfactant complexes which hindered the drying process and difficulted the water removal from the inner part of the foam (in contact with the mould).

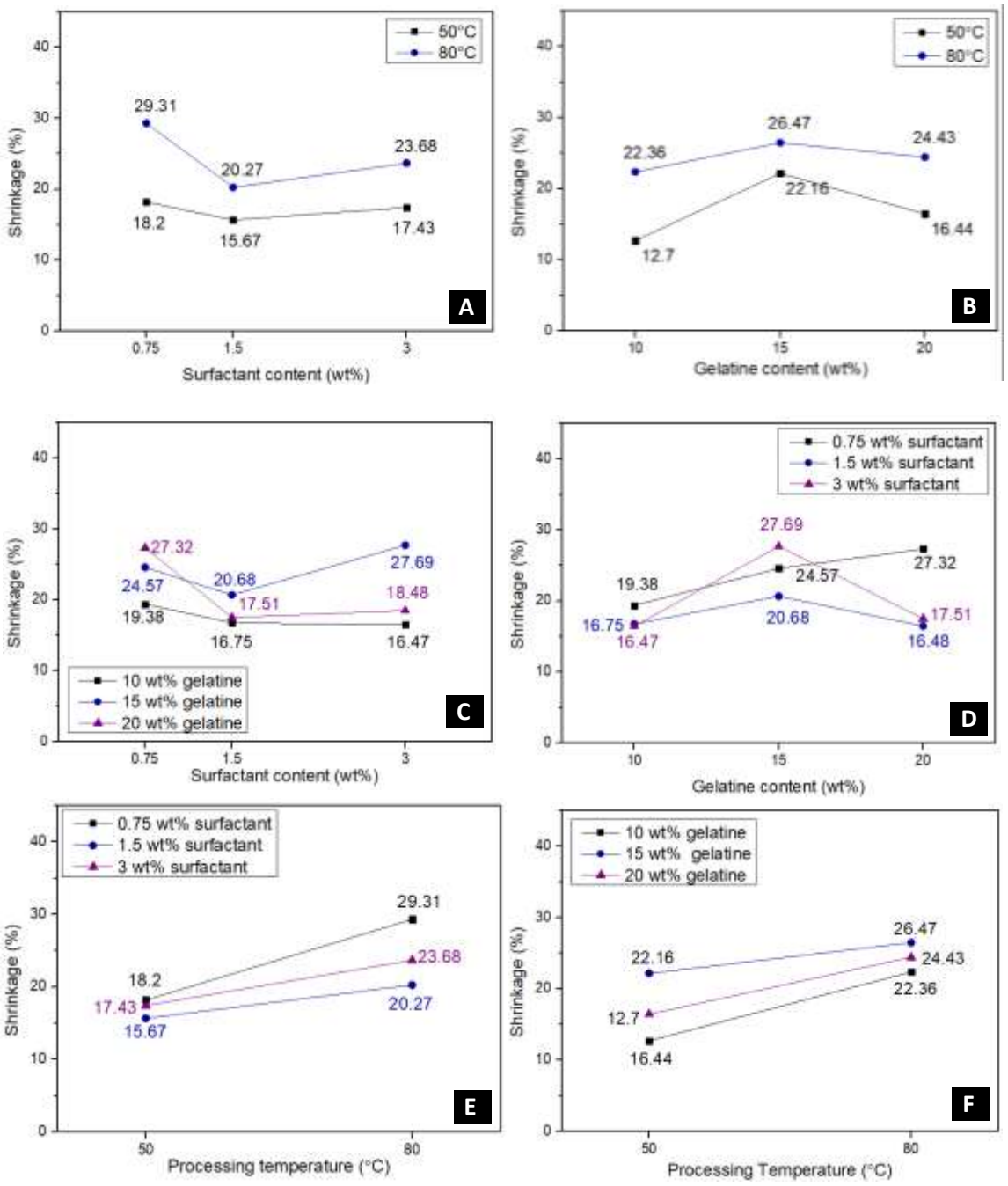

Figure 5.38 ESTIMATED MARGINAL MEANS FOR GELATINE-SURFACTANT C2 TOTAL SHRINKAGE (A) SURFACTANT CONTENT-FOAMING TEMPERATURE (B) GELATINE CONTENT-FOAMING TEMPERATURE (C) SURFACTANT CONTENT-GELATINE CONTENT (D) GELATINE CONTENT-SURFACTANT CONTENT (E) FOAMING TEMPERATURE-SURFACTANT CONTENT (F) FOAMING TEMPERATURE-GELATINE CONTENT

Figure 5.39 shows the cross-section of all the samples. They exhibited considerable less shrinkage to that in Figure 5.35. C2.1 showed a remarkably low shrinkage and minimum convex (on the bottom) and concave (on the surface) deformations, which is desirable for sheet and mould casting.

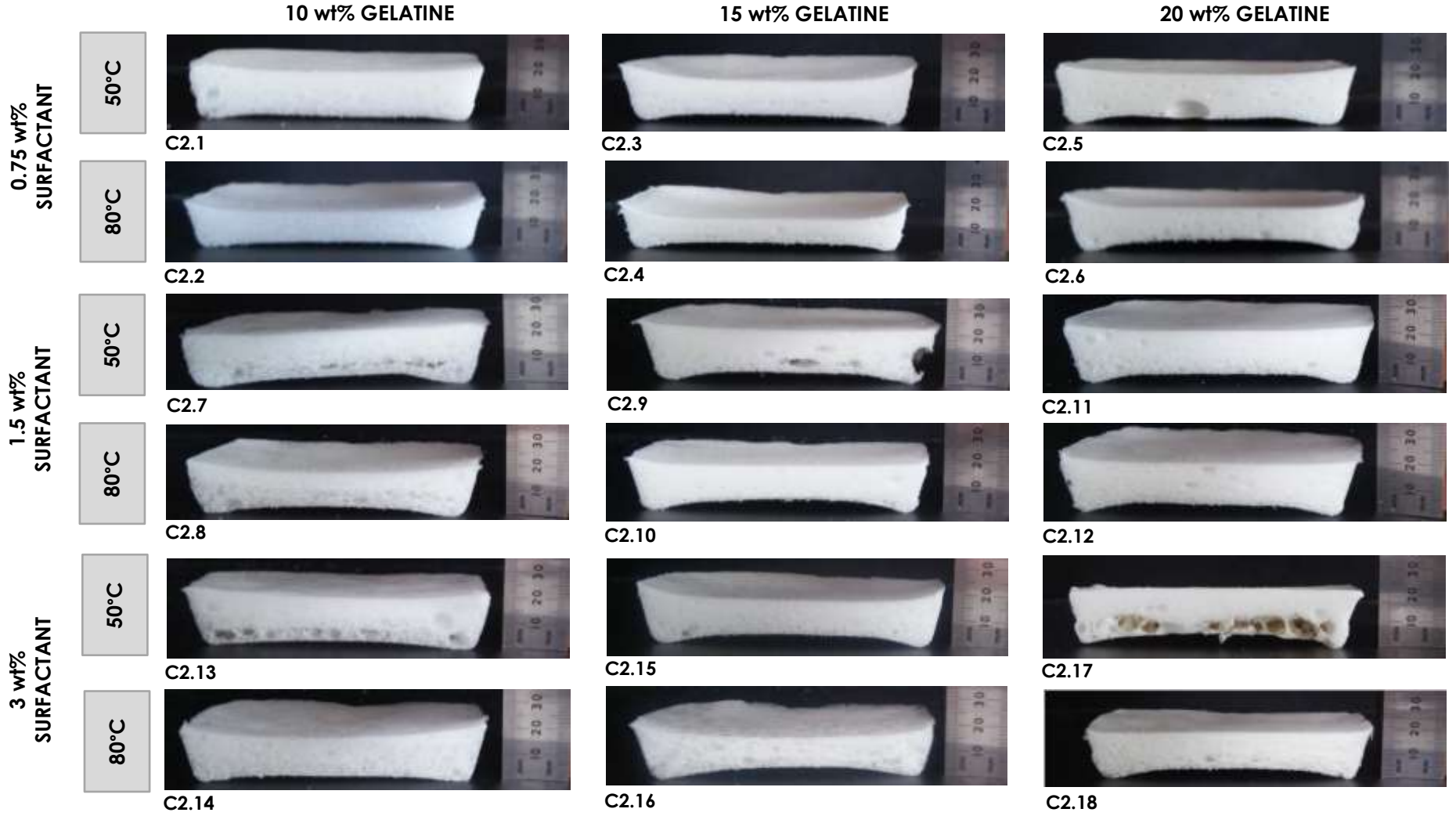

Figure 5.39 CROS-SECTIONS OF THE GELATINE-SURFACTANT C2 DRY FOAMS

5.4.3 DRY FOAMS DENSITY, RELATIVE DENSITY AND POROSITY

This section studies the density, relative density and porosity of the dry gelatine-surfactant foams. Foam density was measured post the standard conditioning at 20°C and 50% RH following the procedure described in section 3.6.2 in Chapter 3.

A full factorial 3x3x2 design with five replicates was used to calculate the statistical significance of the three design parameters (gelatine content, surfactant content and foaming temperature) in density. The hypotheses for this experiment were:

a. The null hypotheses (H_O): there was no difference in mean density for different combinations of the design parameters for the gelatine-surfactant "A" and gelatine-surfactant C2 foams.

b. The alternative hypotheses (H_1): there was a difference in mean density for different combinations of the design parameters.

The following equation was derived to predict the approximated density of the formulated foams according to different parameters. The reason to its development was to facilitate formulation design for further work. Appendix D show how the formula was derived.

$$\rho_{df} = \frac{\rho_l \cdot \sum wt\%}{ER \cdot (1-S)} \qquad \text{(Equation 5.1)}$$

Where:

- ρ_{df}: dry foam density
- ρ_l: density of the liquid
- $\sum wt\%$: total solid content
- ER: Expansion ratio
- S: Total shrinkage

5.4.3.1 Foams containing surfactant "A"

The density, density of the matrix (the density of the dried hydrogels with surfactant, without foaming), relative density and porosity of the solid foams are studied in this section.

As seen in Table 5.13, the foams porosity ranged from 95.78% (sample A5 and exhibiting the highest density) to 99.16% (sample A8 and with the lowest density).

Porosity tended to be higher at lower gelatine concentrations and slightly higher at higher surfactant concentrations and foaming temperatures.

Density, relative density and porosity were interdependent and derived from each other when the density of the cell wall material (matrix) was known.

Table 5.13 DENSITY, MATRIX DENSITY, RELATIVE DENSITY AND POROSITY OF DRY GELATINE-SURFACTANT "A" FOAMS

ID	FOAM DENSITY (kg/m^3)	MATRIX DENSITY (kg/m^3)	RELATIVE DENSITY	POROSITY (%)
A1	14.03 ± 0.72	1,030 ± 36.06	1.36	98.64
A2	13.49 ± 0.83	1,030 ± 36.06	1.31	98.69
A3	25.99 ± 1.46	1,090 ± 50.00	2.38	97.62
A4	23.76 ± 2.14	1,090 ± 50.00	2.18	97.82
A5	47.32 ± 3.18	1,120 ± 36.06	4.22	95.78
A6	43.27 ± 3.46	1,120 ± 36.06	3.86	96.14
A7	11.09 ± 1.43	1,060 ± 36.06	1.05	98.95
A8	8.88 ± 0.18	1,060 ± 36.06	0.84	99.16
A9	26.10 ± 1.02	1,120 ± 36.06	2.33	97.67
A10	23.75 ± 2.69	1,120 ± 36.06	2.12	97.88
A11	37.08 ± 4.8	1,160 ± 23.09	3.20	96.80
A12	31.60 ± 3.15	1,160 ± 23.09	2.72	97.28
A13	10.52 ± 1.11	1,160 ± 40.00	0.91	99.09
A14	11.82 ± 0.34	1,160 ± 40.00	1.02	98.98
A15	26.95 ± 2.19	1,200 ± 40.00	2.25	97.75
A16	23.58 ± 1.53	1,200 ± 40.00	1.97	98.03
A17	44.66 ± 2.39	1,260 ± 56.86	3.54	96.46
A18	32.53 ± 4.51	1,260 ± 56.86	2.58	97.42

It is worth noting that all matrices had different compositions, as shown in Table 5.14, including slightly different residual moisture content (see Section 3.6.3, Chapter 3, for details in moisture content measuring). Accordingly, their densities varied (Table 5.14).

Table 5.14 COMPOSITION OF DRY GELATINE-SURFACTANT "A" FOAMS

ID	GELATINE CONTENT (*wt%*)	MOISTURE CONTENT (*wt%*)	SURFACTANT CONTENT (*wt%*)
A1	80.30	15.68	4.02
A2	81.02	14.93	4.05
A3	81.94	15.33	2.73
A4	82.69	14.55	2.76
A5	83.55	14.36	2.09
A6	81.10	16.87	2.03
A7	74.36	14.49	11.15
A8	74.03	14.87	11.10
A9	77.53	14.72	7.75
A10	77.59	14.65	7.76
A11	79.02	15.05	5.93
A12	78.68	15.42	5.90
A13	57.33	16.87	25.80
A14	58.64	14.97	26.39
A15	64.68	15.91	19.41
A16	65.09	15.38	19.53
A17	68.84	15.67	15.49
A18	68.59	15.98	15.43

As shown in Figure 5.40, foam densities of the gelatine-surfactant "A" foams ranged from as low as 8.8 kg/m^3 (sample A8, with 10 *wt%* gelatine, 1.5 *wt%* surfactant content and 80°C foaming temperature) to 47.32 kg/m^3 (sample A5, with 20 *wt%* gelatine, 0.5 *wt%* surfactant and 50°C foaming temperature). In general, higher gelatine concentrations led to higher densities. Density also tended to increase with lower foaming temperature.

The low density achieved was considered remarkable for bio-foams which tend to have higher density than conventional plastic foams (see Table 2.7 in Chapter 2). Density <10 kgm^{-3} or >99% porosity, enters the range of low-density expanded polystyrene (EPS), and thus, a breakthrough achievement enabling the bio-foams to compete in similar area of applications.

The results of this experiment were comparable to the results in Section 5.3.3. Samples FH12 and A4 (with same formulation) achieved almost identical density, ≈24 kg/m^3. Samples FH13 and A16, having a similar formulation (same gelatine content but slightly difference in surfactant concentrations 5 *wt%* and 4.5 *w%,* respectively) achieved similar density values, 18.85 kg/m^3 (FH13) and 23.58 kg/m^3 (A16). This again demonstrated the good repeatability of the foaming processes.

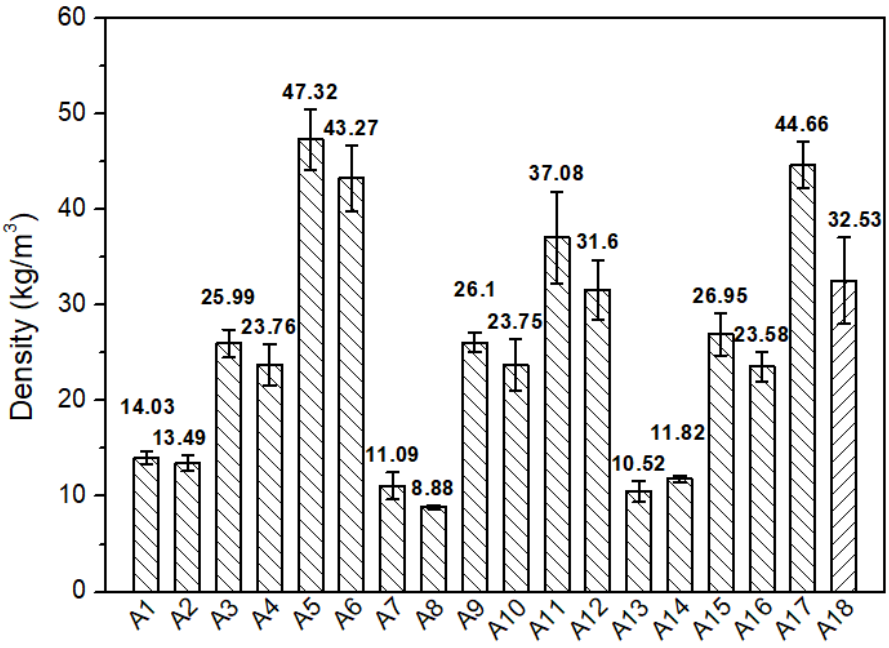

Figure 5.40 DENSITY OF THE DRY GELATINE-SURFACTANT "A" FOAMS

The ANOVA table for density with a level of significance of 0.05 can be seen in Table A.8 (Appendix A). The ANOVA table gave statistics F=41.13, p<0.001; F=1356.82, p<0.001; and F=63.81, p<0.001 for surfactant content, gelatine content and foaming temperature, respectively. From these results, it can be said that there is strong evidence that the density varied with the three studied parameters. Similarly, the density was significantly influenced by the following interactions: gelatine content-surfactant content (F=18.68, p<0.001), gelatine content-foaming temperature (F=20.42, p<0.001) and the three-way interaction (F=4.85, p=0.002). The null hypotheses can be rejected, concluding that some factors had a significant effect on the density of the dry gelatine-surfactant "A" foams.

Figure 5.41 exhibits the main effect plots for the density of the dry gelatine-surfactant "A" foams. The solid content in the foams' plateau borders, the MER (see Section 5.4.1.1) and shrinkage (see Section 5.4.2.1) were the most significant parameters influencing density.

Figure 5.41A shows the linear increase in density for different gelatine concentrations, from 11.69 *kg/m³* for 10 *wt%* gelatine foams to 39.41 *kg/m³* for 20 *wt%* gelatine foams. Figure 5.41B shows that lower densities were achieved by increasing surfactant content, despite of a slight density increase at the highest surfactant concentration.

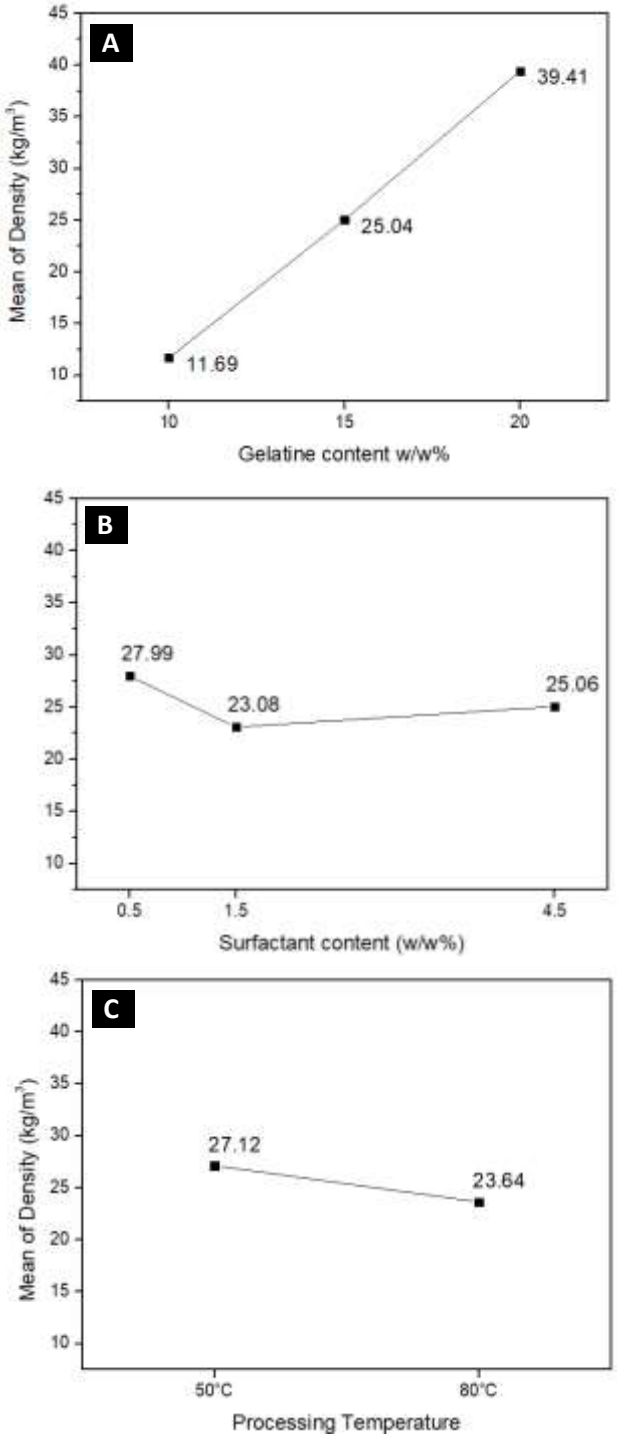

Figure 5.41 MAIN EFFECTS PLOTS FOR THE DENSITY OF THE DRY GELATINE-SURFACTANT "A" FOAMS (A) GELATINE CONTENT (*wt%*); (B) SURFACTANT CONTENT (wt%); (C) FOAMING TEMPERATURE (°C)

Figure 5.41C shows that the average density decreased at higher foaming temperature. This agreed with the results shown in Section 5.4.1.1., where MER exhibited an inverse trend (increasing as foaming temperature increased). Shrinkage increased with foaming temperature (see Section 5.4.2.1). Thus, it had a less significant

impact on the density of the dry foams as it did not considerably affect their density at higher foaming temperatures.

Figure 5.42 shows the estimated marginal means for density. Figures 5.42A and 5.42B show that density was higher in foams processed at lower temperatures. Figures 5.42A and 5.42E shows the surfactant content-foaming temperature interaction (p>0.05).

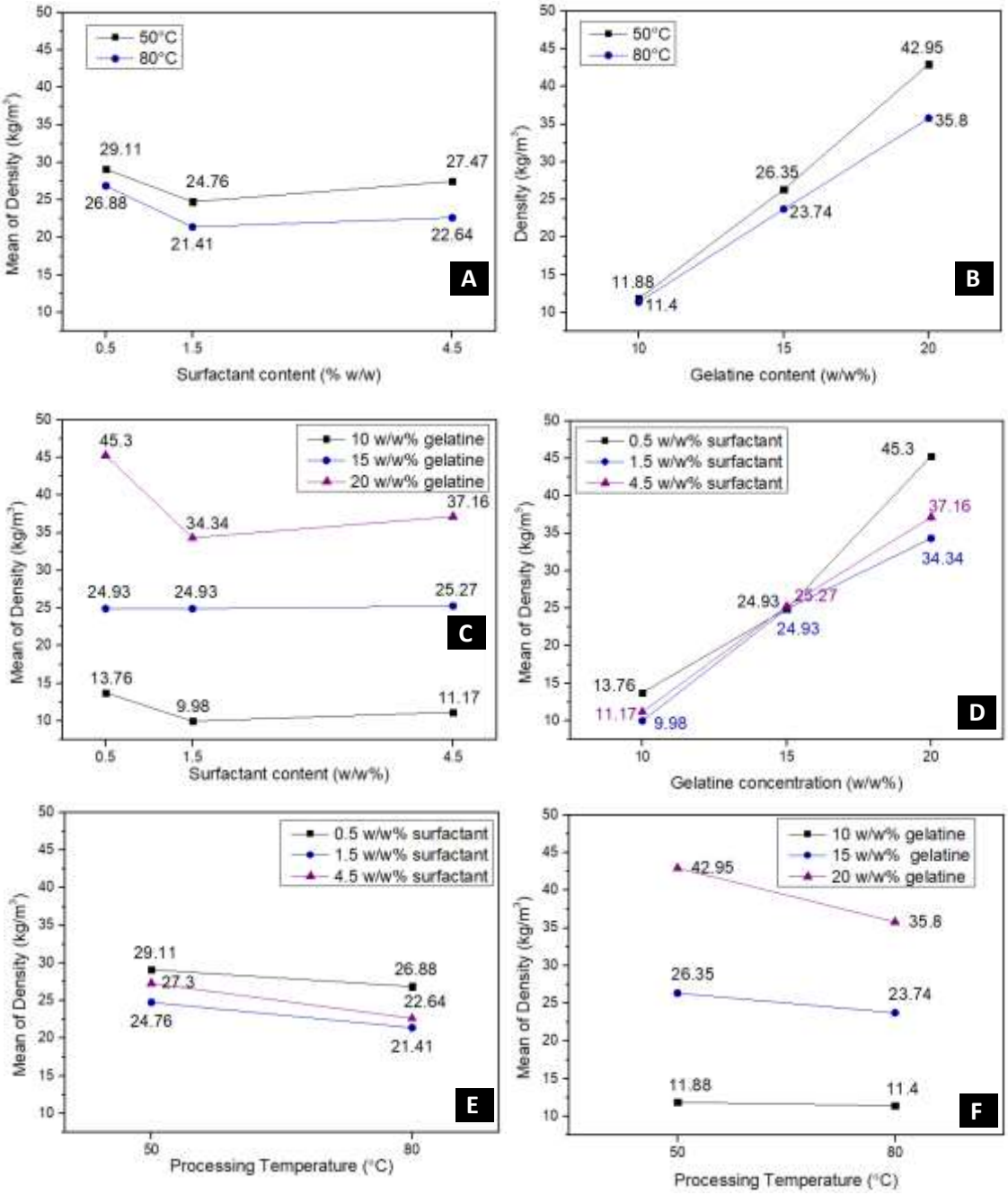

Figure 5.42 ESTIMATED MARGINAL MEANS FOR GELATINE-SURFACTANT "A" FOAMS DRY DENSITY (A) SURFACTANT CONTENT-FOAMING TEMPERATURE (B) GELATINE CONTENT-FOAMING TEMPERATURE (C) SURFACTANT CONTENT-GELATINE CONTENT (D) GELATINE CONTENT-SURFACTANT CONTENT (E) FOAMING TEMPERATURE-SURFACTANT CONTENT (F) FOAMING TEMPERATURE-GELATINE CONTENT

Figures 5.42C and 5.42D present the gelatine content-surfactant content interaction (p<0.001). As shown in Figure 5.42D, lower (0.5 *wt%*) and higher (4.5 *wt%*) surfactant

concentrations produced higher densities foams and an intermediate surfactant content (1.5 *wt%*) was the optimum to achieve lower density foams, closely followed by the highest surfactant content (4.5 *wt%*). However, this was mainly due to the more significant effect of surfactant content on foams made with higher gelatine content (20 *wt%*). Surfactant content increase had little effect on the density of 10 *wt%* and 15 *wt%* gelatine foams.

Figures 5.42B and 5.42F show the gelatine content-foaming temperature interaction ($p<0.001$). The positive effect of foaming temperature on density increased at higher gelatine concentrations. Therefore, at low gelatine concentrations, average density was similar for both samples produced at 50°C (11.88 kg/m^3) and 80°C (11.4 kg/m^3) but, at higher gelatine concentrations the density difference was more remarkable, 41.12 kg/m^3 for 50°C and 34.85 kg/m^3 for 80°C. This is attributable to the higher viscosity of the 20 *wt%* gelatine content solutions, which were more susceptible to the benefits of viscosity decrease when foaming takes place at higher temperatures.

The gelatine content-foaming interaction interacted, in turn, with surfactant content ($p<0.05$). As previously discussed, both higher surfactant contents and higher foaming temperatures more considerably decreased the density of 20 *wt%* foams than that of 10 *wt%* and 15 *wt%* foams.

5.4.3.2 Foams containing surfactants C1 and C2

The density, density of the matrix, relative density and porosity of the solid foams are studied in this section. As seen in Table 5.15, the foams porosity ranged from 94.93% (sample C2.6) to 98.27% (sample C2.13, with also the lowest density).

As observed in Section 5.4.3.1, porosity tended to be higher at lower gelatine concentrations and slightly higher at higher surfactant concentrations and foaming temperatures. Porosity and density of the dry gelatine-surfactant C2 foams were slightly lower and higher, respectively, than that of the foams made with surfactant "A".

Table 5.15 DENSITY, MATRIX DENSITY, RELATIVE DENSITY AND POROSITY OF DRY GELATINE-SURFACTANT C2 FOAMS

ID	DENSITY (kg/m^3)	MATRIX DENSITY (kg/m^3)	RELATIVE DENSITY	POROSITY (%)
C2.1	20.85 ± 0.79	1070 ±42.26	1.95	98.05
C2.2	23.12 ± 1.52	1070 ± 42.26	2.16	97.84
C2.3	36.91 ± 0.77	1100 ± 49.82	3.36	96.64
C2.4	38.51 ± 0.81	1100 ± 49.82	3.50	96.50
C2.5	55.54 ± 1.28	1140 ± 38.25	4.87	95.13
C2.6	57.80 ± 1.78	1140 ± 38.25	5.07	94.93
C2.7	19.60 ± 1.69	1100 ± 35.78	1.78	98.22
C2.8	21.42 ± 2.25	1100 ± 35.78	1.95	98.05
C2.9	33.17 ± 0.79	1150 ± 63.64	2.88	97.12
C2.10	40.08 ± 2.30	1150 ± 63.64	3.49	96.51
C2.11	48.64 ± 1.03	1180 ± 47.22	4.12	95.88
C2.12	46.25 ± 2.64	1180 ± 47.22	3.92	96.08
C2.13	19.76 ± 1.89	1,140 ± 51.37	1.73	98.27
C2.14	22.06 ± 1.74	1,140 ± 51.37	1.94	98.06
C2.15	39.70 ± 2.38	1180 ± 39.65	3.36	96.64
C2.16	42.71 ± 2.38	1180 ± 39.65	3.62	96.38
C2.17	57.58 ± 3.99	1200 ± 54.76	4.80	95.20
C2.18	59.70 ± 2.81	1200 ± 54.76	4.98	95.02

As mentioned before, the dry foams had different compositions, including residual moisture (see Table 5.16). Thus, the density of the matrix was also different (Table 5.15).

Table 5.16 COMPOSITION OF DRY GELATINE-SURFACTANT C1 FOAMS

ID	GELATINE CONTENT (*wt%*)	MOISTURE CONTENT (*wt%*)	SURFACTANT CONTENT (*wt%*)
C2.1	77.27	17.31	5.42
C2.2	77.95	16.59	5.46
C2.3	80.19	16.44	3.37
C2.4	80.90	15.70	3.40
C2.5	80.66	16.91	2.43
C2.6	81.82	15.72	2.46
C2.7	78.90	10.84	10.26
C2.8	76.66	13.37	9.97
C2.9	78.64	14.81	6.55
C2.10	80.32	12.99	6.69
C2.11	80.87	14.35	4.78
C2.12	80.99	14.22	4.79
C2.13	69.88	11.81	18.31
C2.14	69.99	11.67	18.34
C2.15	74.03	13.78	12.19
C2.16	75.46	12.11	12.43
C2.17	77.14	12.89	9.97
C2.18	77.58	12.40	10.02

As shown in Figure 5.43, foam density of the gelatine-surfactant C2 foams ranged from 19.60 *kg/m³* (sample C2.7, with 10 *wt%* gelatine, 1.5 *wt%* surfactant content and 50°C foaming temperature) to 59.70 kg/m³ (sample C2.18, with 20 *wt%* gelatine, 3 *wt%* surfactant and 80°C foaming temperature). Higher gelatine concentrations led to higher densities and, contrary to the analysis carried out for gelatine-surfactant "A" foams, higher foaming temperature generated denser foams.

The use of surfactant C2 produced denser foams than those produced with surfactant "A" but still exhibited comparable densities than conventional plastic polymers. The results of this experiment were comparable to the results in Section 5.3.3. Samples FH3 and C2.4 (same gelatine concentration and 0.5 and 0.75 *wt%*, respectively) achieved similar density values, 32.29 *kg/m³* and 38.51 *kg/m³,* respectively. Samples FH4 and C2.16, having similar formulation (same gelatine content but slightly different in gelatine concentrations, 5 *wt%* and 4.5 *w%,* respectively) achieved similar density values, 46.9 *kg/m³* (FH4) and 42.71 *kg/m³* (C2.16).

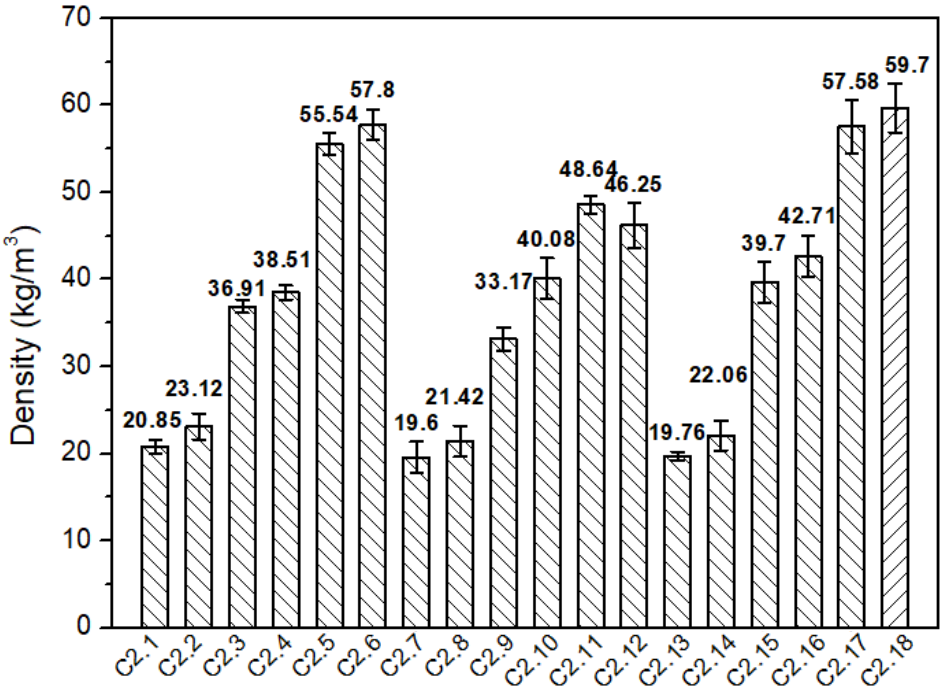

Figure 5.43 DENSITY OF THE DRY GELATINE-SURFACTANT "C2" FOAMS

The ANOVA table for density with a level of significance of 0.05 can be seen in Table A.9 (Appendix A). ANOVA table gave the statistics F =66.99, p<0.001; F=2392.88, p<0.001; and F=30.56, p<0.001 for surfactant content, gelatine content and foaming temperature, respectively. From these results, it can be said that there is strong evidence that the foam density varied with the three studied parameters. Similarly, the density was significantly influenced by the following interactions: gelatine content-surfactant content (F=27.05, p<0.001), the gelatine content-foaming temperature (F=5.54, p=0.006) and the three-way interaction (p<0.05). The null hypotheses can be rejected, concluding that some factors had a significant effect on the density of dry gelatine-surfactant C2 foams.

Figure 5.44 exhibit the main effect plots for the density of gelatine-surfactant C2 foams. Figure 5.44A shows the linear increase in density as gelatine concentration increases, from an average of 21.07 kg/m^3 for 10 *wt%* gelatine foams to 54.25 kg/m^3 for 20 *wt%* gelatine foams.

Figure 5.44B shows the decrease in average density when using 1.5 *wt%* surfactant content, compared to 0.75 *wt%.* As the surfactant content increased to 3 *wt%*, density also increased due to a decrease in MER (see Section 5.4.1.2) associated with a viscosity increase.

As previously mentioned, foam density slightly increased at higher foaming temperature (Figure 5.44C). This may be attributable to the higher shrinkage level

produced at higher foaming temperatures. As seen in Sections 5.4.2.1 and 5.4.2.2 the higher foaming temperature negative effect on shrinkage was more significant in gelatine-surfactant C2 foams. The average increase in shrinkage from a low to a high foaming temperature was 13.9% and 42.81% for foams made with surfactant "A" and surfactant C2, respectively.

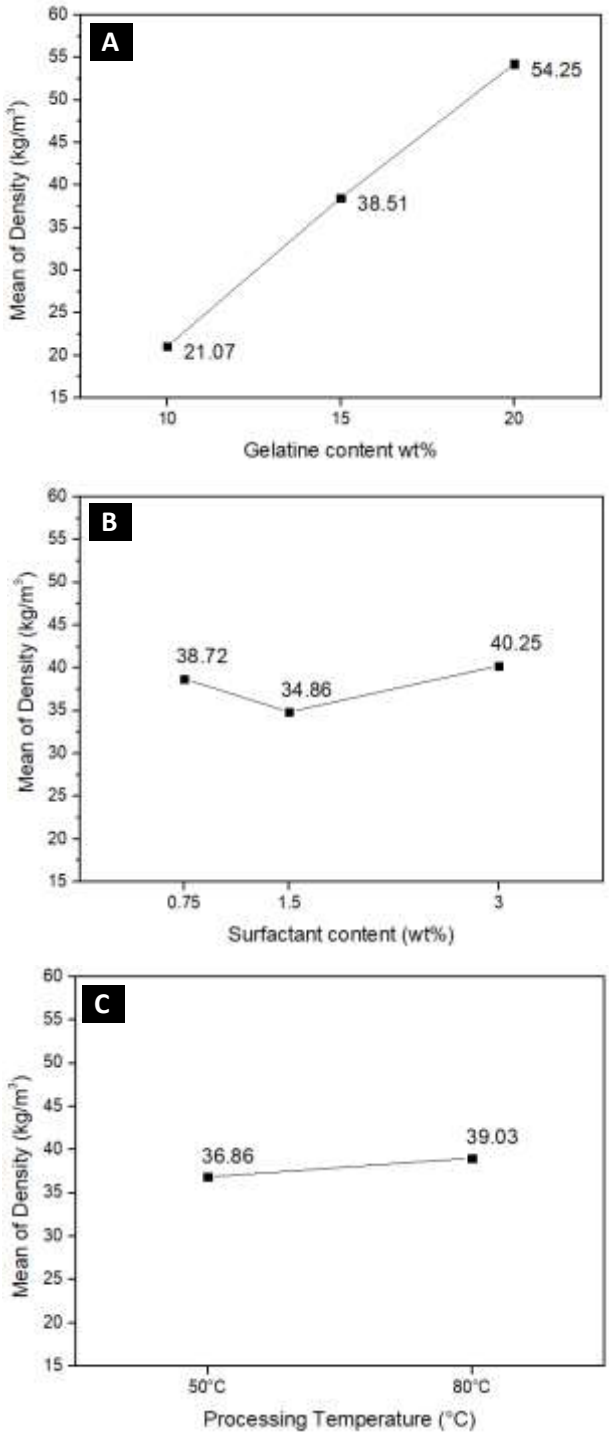

Figure 5.44 MAIN EFFECTS PLOTS FOR THE DENSITY OF THE DRY GELATINE-SURFACTANT C2 FOAMS (A) GELATINE CONTENT (*wt%*); (B) SURFACTANT CONTENT (wt%); (C) FOAMING TEMPERATURE (°C)

Figure 5.45 shows the estimated marginal means for foam density. Figure 5.45A and 5.45B show that density tended to be higher in foams processed at higher temperatures. Figures 5.45A and 5.45E show the same trend of foam density variation at 50°C and 80°C (i.e. no interaction between surfactant content and foaming temperature) ($p>0.05$). Lower density was achieved at intermediate and lower surfactant concentrations.

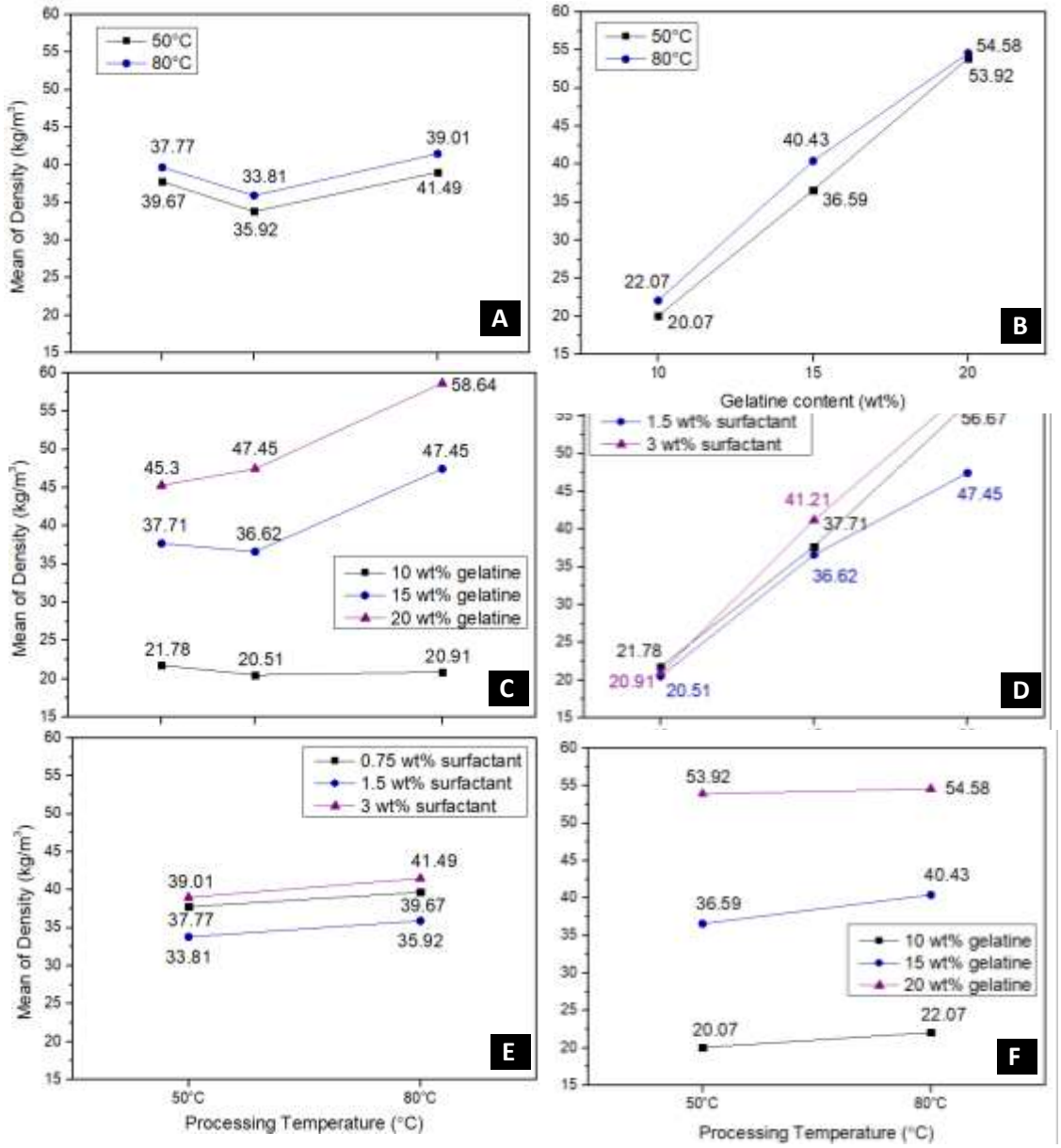

Figure 5.45 ESTIMATED MARGINAL MEANS FOR GELATINE-SURFACTANT C2 FOAMS DRY DENSITY (A) SURFACTANT CONTENT-FOAMING TEMPERATURE (B) GELATINE CONTENT-FOAMING TEMPERATURE (C) SURFACTANT CONTENT-GELATINE CONTENT (D) GELATINE CONTENT-SURFACTANT CONTENT (E) FOAMING TEMPERATURE-SURFACTANT CONTENT (F) FOAMING TEMPERATURE-GELATINE CONTENT

Figures 5.45C and 5.45D show the gelatine-surfactant contents interaction ($p<0.001$). As shown in Figure 5.45C, an increase of surfactant content from 1.5 *wt%* to 3 *wt%* considerably increased density of high (20 *wt%*) and intermediate (15 *wt%*) gelatine foams. However, this surfactant increase had little effect on the density of 10 *wt%*

foams. In fact, surfactant content did not significantly affect foam density at 10 *wt%* gelatine content. Intermediate surfactant content (1.5 *wt%*) led to a slightly lower density compared to lower surfactant content (0.75 *wt%*) for 10 *wt%* and 15 *wt%* gelatine content. However, lower densities were achieved at the lowest surfactant concentration for 20 *wt%* gelatine content foams.

Figures 5.45B and 5.45F present the gelatine content-foaming temperature interaction ($p<0.05$). The effect of foaming temperature was very weak at high gelatine concentrations. Foaming temperature played a more significant role at lower and, especially, intermediate gelatine concentration foams.

The gelatine content-foaming interaction interacted, in turn, with surfactant content ($p<0.05$). The combination of lower surfactant content and lower foaming temperature considerably decreased the density of 15 *wt%* foam. However, this behaviour was not found for 20 *wt%* gelatine foams (their density was influenced by the surfactant content but not by the foaming temperature).

The composition of surfactant C1 containing foams is shown in Table 5.17. Figure 5.46 compares the influence of the two surfactants, C1 and C2 on density. It shows that the foams made with surfactant C2 tended to exhibit lower foam densities than those made with surfactant C1, under identical conditions of use. Based on these results, one should give priority to surfactant C2 use not only for the lower density foams produced but also for its lower cost compared to C1. FTIR results (not shown here for confidenciality reasons) confirmed the two surfactants were the same material, so no significant differences in performance were expected.

Table 5.17 COMPOSITION OF DRY GELATINE-SURFACTANT C1 FOAMS

ID	GELATINE CONTENT (*wt%*)	MOISTURE CONTENT (*wt%*)	SURFACTANT CONTENT (*wt%*)
SA1	80.88	13.05	6.07
SA3	84.55	11.22	4.23
SA5	82.54	14.37	3.10
SA7	72.91	16.15	10.94
SA9	80.43	11.53	8.04
SA11	81.52	12.37	6.11

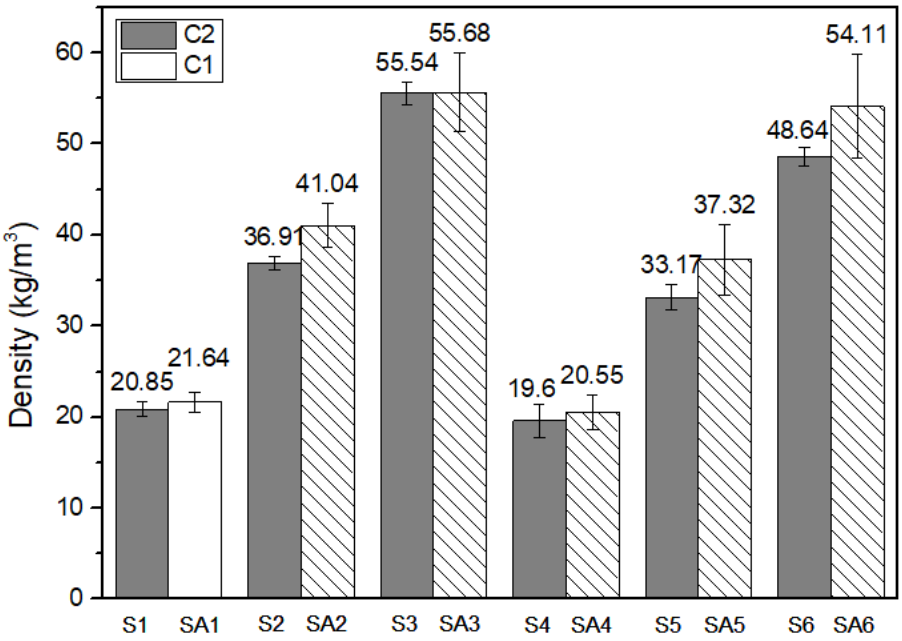

Figure 5.46 COMPARISON OF FOAM DENSITY CONTAINING SURFACTANTS C1 AND C2 WHILE OTHER CONDITIONS WERE IDENTICAL

5.4.4 FOAMS STRUCTURE

This section analyses the structure of hydrogel foams made with gelatine using surfactants "A" and C2.

First, for each surfactant separately, SEM micrographs of the foams prepared at 50°C and 80°C were compared. Then, the cross-section of the foams was analysed and, finally, the structure of the top surface of the dry foams was investigated.

5.4.4.1 Foams containing surfactant A

SEM micrographs of cross-sections of hydrogel foams made with gelatine and surfactant A are shown in Figures 5.47 (foamed at 50°C) and 5.48 (foamed at 80°C).

All the foams exhibited an open-cell structure and were clearly gas-permeable through its structure. The reason of an open-cell structure was the gelling time was not sufficient rapid to prevent the cell walls rupture.

The foam structure mainly consisted of cells (macropores) and interconnecting "windows" of smaller sizes (micropores). Each single cell was connected via multiple channels to its surrounding cells. As seen in Figures 5.47 and 5.48, the relatively higher density foams (e.g. those made at 20 *wt%* gelatine content, A5, A6, A11, A12, A17 and A18) exhibited a more uniform cell size, thicker edges and vertexes and higher fraction of retained cell walls. Lower gelatine foams (e.g. those made at 10 wt% gelatine content, A1, A2, A7, A8, A13 and A14), tended to exhibit fibrous-like thin edges and vertexes with little cell walls left.

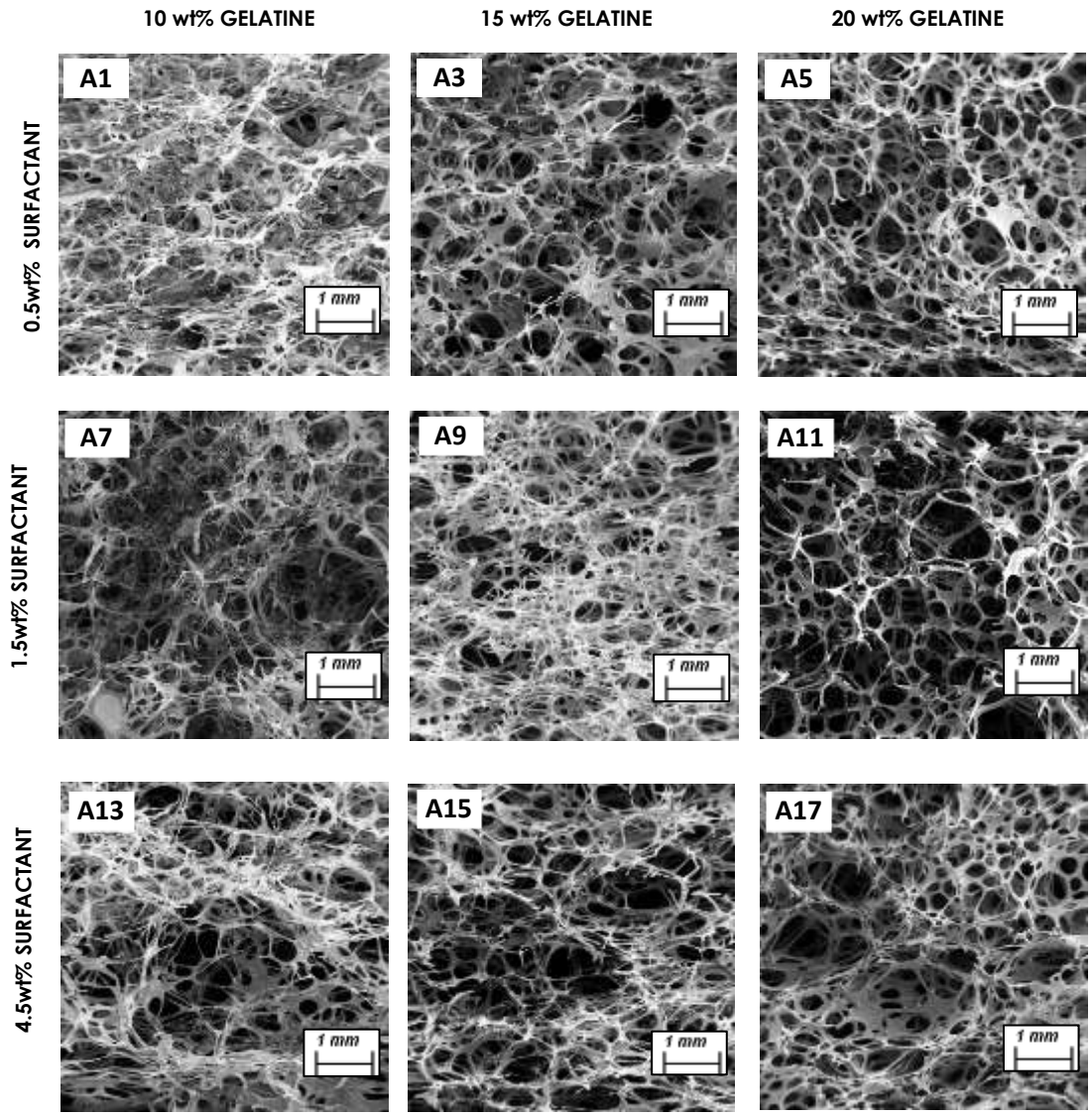

Figure 5.47 SEM MICROGRAPHS OF CELL MORPHOLOGIES OF GELATINE-SURFACTANT "A" FOAMS MADE AT 50°C

Foams made at 80°C (Figure 5.48) exhibited relatively bigger macropores and thinner edges and vertexes than those processed at lower temperature. The 10 *wt%* gelatine foams generated at 80°C also exhibited considerably larger micropores and thinner vertex and plateau borders ~10-70 μm compared with that of 20 *wt%* gelatine foams ~20-100 μm. The typical cell size range was 0.2-0.8 *mm*. Higher gelatine content (20 *wt%*) foams presented slightly smaller cells (0.2-0.7 mm) than low gelatine content (10 *wt%*) foams (0.3-0.8 *mm*). Thus, cells size was usually less than 1 *mm*, but bigger cell sizes (1.4-4.8 mm) can be rarely found.

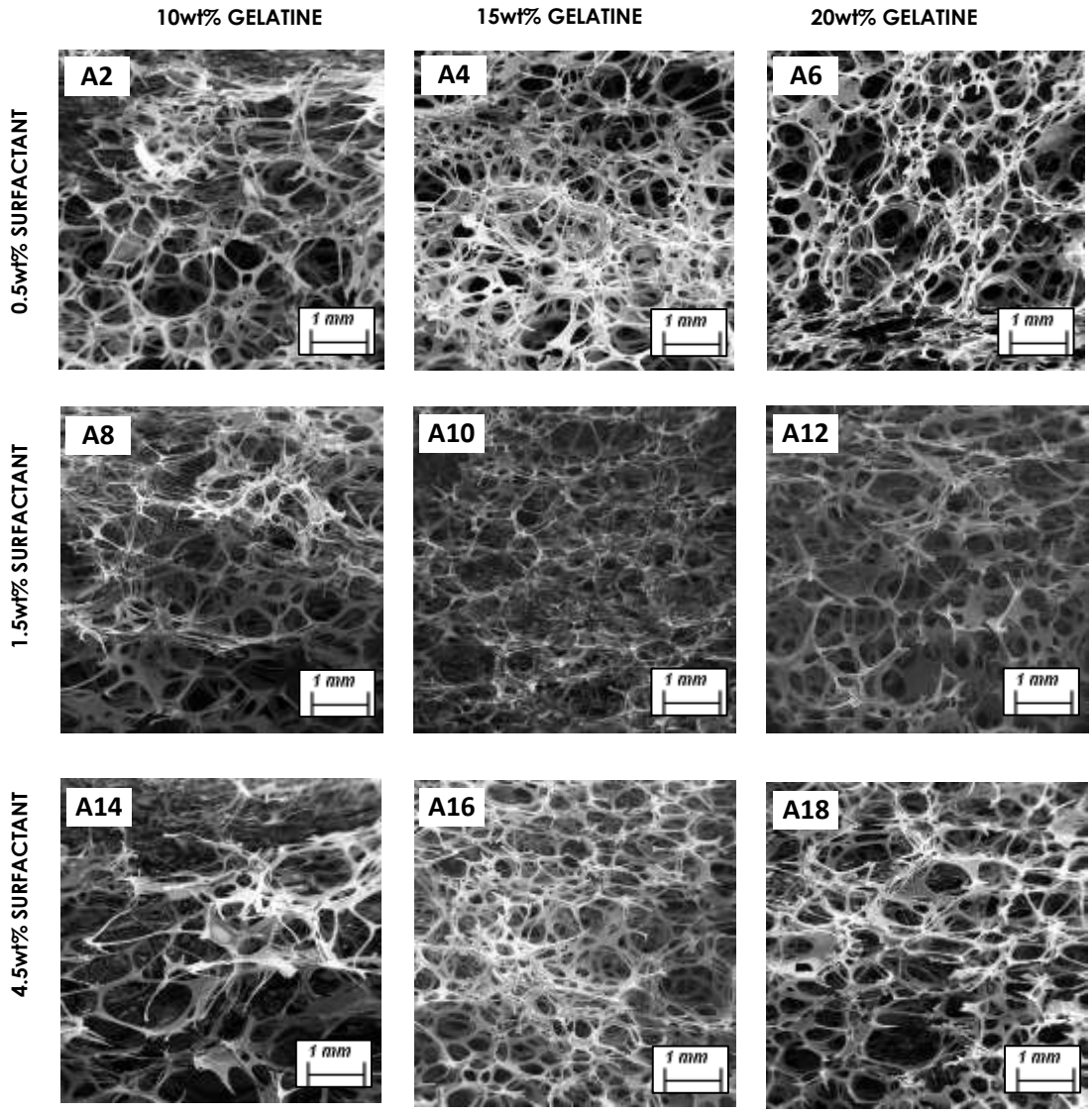

Figure 5.48 SEM MICROGRAPHS OF CELL MORPHOLOGIES OF GELATINE-SURFACTANT "A" FOAMS MADE AT 80°C

Figures 5.49 shows close-up views of the cell structure of A1, A3 and A5 foams. The foams were slightly denser at the top (in contact with air), where the open-cell structure prevailed but exhibited certain cell distortion due to drying shrinkage. This implies gas permeation from the inner to the outer layers was allowed, which it is important for the drying process, but it can be slightly compromised at high gelatine content, where the cell distortion is more considerable.

A1 exhibits a fibre-like cell structure and thinner plateau borders. However, its plateau borders are thicker in the bottom due to gravity shrinkage. A3 and, more considerably, A5 exhibit thicker plateau borders and less distorted structure than A1, due to the higher viscosity effect, which arrested drainage, and higher gelatine content, which reduced the gelling time of the foam, and consequently, speed up the foam stabilisation process via gelling.

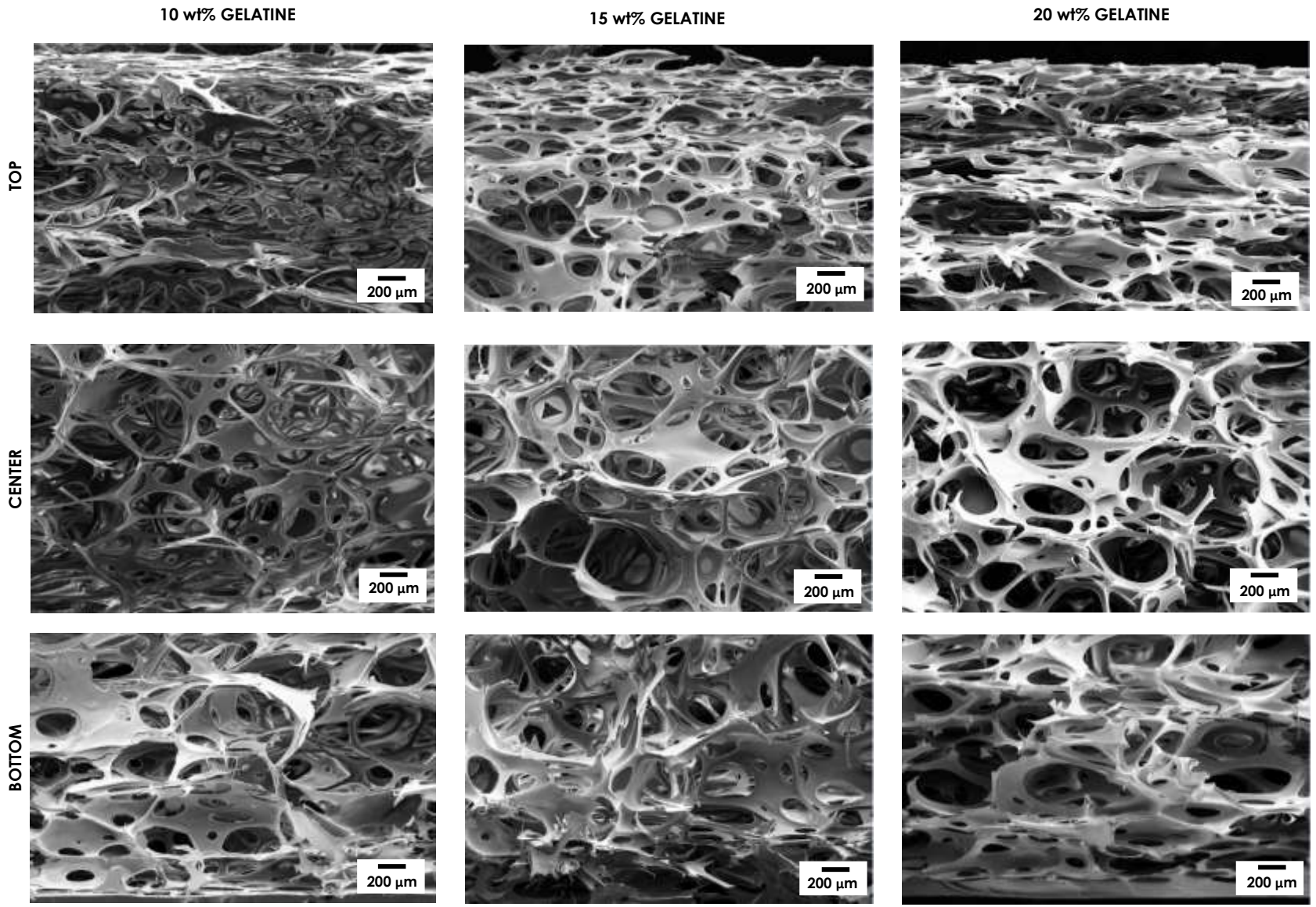

Figure 5.49 SEM IMAGES OF GELATINE-SURFACTANT A FOAMS (A1, A3 AND A5) SHOWING THE VARIATION OF THE CELL STRUCTURE AT TOP, MIDDLE AND THE BOTTOM AREAS OF THE CAST FOAMS

Figure 5.50 presents the 2D cell morphology on the top surface of the cast gelatine-surfactant "A" foams. The top layer of the foam gelified relatively more rapidly as it was in direct contact with the air, and thus, at lower temperature and lower moisture contents than the internal pores. These helped to "freeze" the surface pores. Although the pores may be relatively finer than the internal pores, they gave revealing information on the foam structures.

The dyed 2D surface facilitated the structure assessment. As previously observed, all the foams exhibited an open-cell structure.

The cell shape of the foams tended to be more polyhedral at lower gelatine content, whereas higher gelatine content foams led to more spherical cells shape with thicker plateau borders.

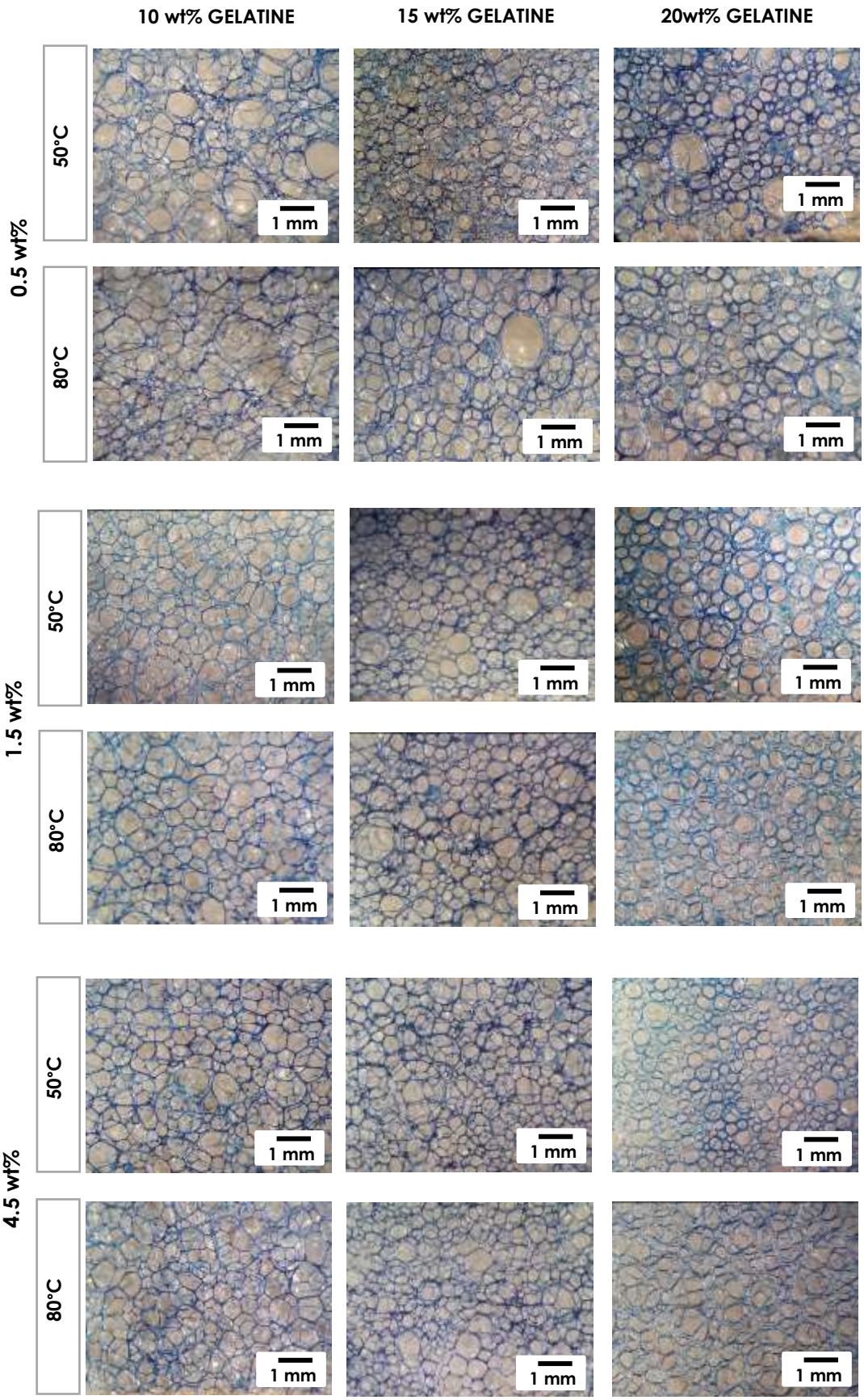

Figure 5.50 OPTICAL MICROSCOPE IMAGES OF 2D PORE MORPHOLOGY ON THE TOP SURFACE OF THE CAST GELATINE-SURFACTANT "A" FOAMS

5.4.4.2 Foams containing surfactant C2

Figures 5.51 and 5.52 show SEM images of the cell structure of gelatine-surfactant C2 foams made at 50°C and 80°C, respectively. Just 10 and 20 *wt%* gelatine content micrographs are shown. 15 *wt%* gelatine content foams exhibited an intermediate behaviour between them.

All the foams exhibited an open-cell structure but showed a greater number of closed-cells than the foams in Section 5.4.4.1 due to the higher viscosity (and consequently, stability) of the liquid plateau borders and cell walls during both gelling and drying. As observed in gelatine-surfactant "A" foams, the foam structure consisted in macropores and micropores. However, as a result of their higher density compared to that of foams made with surfactant "A", foams containing surfactant C2 exhibited thicker plateau borders and vertexes. The predominant cell shape was oval, with little presence of polyhedral cells.

As seen in Figures 5.51 and 5.52, the relatively higher density foams (e.g. those made at 20 *wt%* gelatine content, C2.5, C2.6, C2.11, C2.12, C2.17 and C2.18) exhibited a slightly smaller cell size, a more uniform cell size, thicker edges and vertexes and higher fraction of retained cell walls. Lower gelatine comtent foams (e.g. those made at 10 wt% gelatine content, C2.1, C2.2, C2.7, C2.8, C2.13 and C2.14, did not exhibit the fibrous-like structure observed in Section 5.4.4.2.

The 10 *wt%* gelatine foams exhibited considerably larger microspores and thinner vertex and plateau borders ~20-130 μm compared with that of 20 *wt%* gelatine foams ~30-180 μm. The typical cell size range was 0.05-0.9 *mm*. Higher gelatine content (20 *wt%*) foams presented slightly smaller cells (0.05-0.8 mm) than low gelatine content (10 *wt%*) foams (0.1-0.9 *mm*). Thus, cells size was usually less than 1 *mm*, but bigger cell sizes (1-3.5 mm) also were found, especially at intermediate surfactant concentrations.

The foams containing an intermediate (1.5 *wt%*) surfactant content showed a relatively bigger cells size than those made at lower (0.75 *wt%*) and higher contents (3 *wt%*). This agrees with the results from Sections 5.4.2.2 and 5.4.3.2 which found that intermediate surfactant content achieved higher MER and lower density.

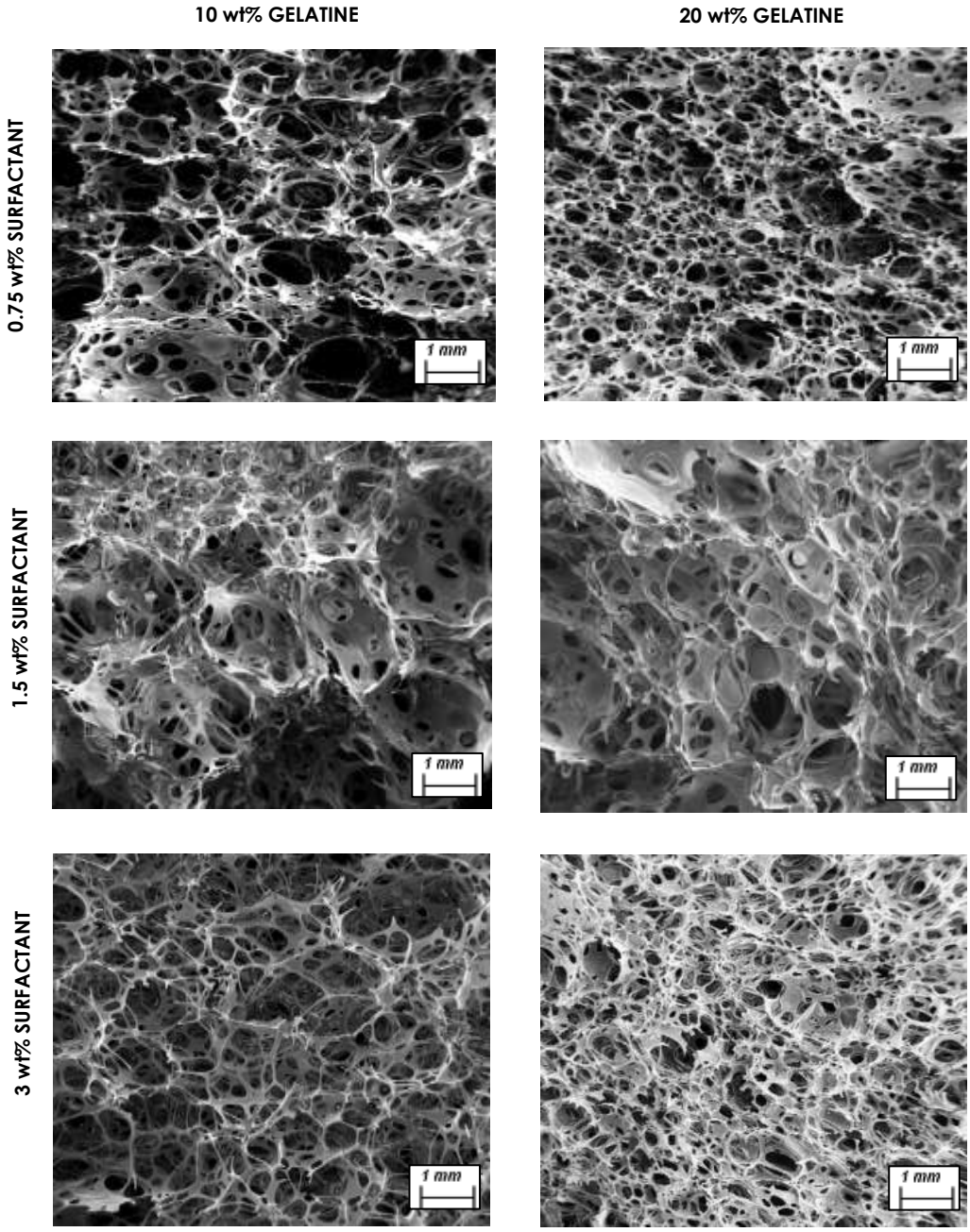

Figure 5.51 SEM MICROGRAPHS OF CELL MORPHOLOGIES OF GELATINE-SURFACTANT C2 FOAMS MADE AT 50°C

Foams made at 80°C (Figure 5.52) tended to exhibit relatively bigger macropores, less number of close-cell walls and thinner edges and vertexes than those processed at lower temperature, as also observed in Section 5.4.4.1.

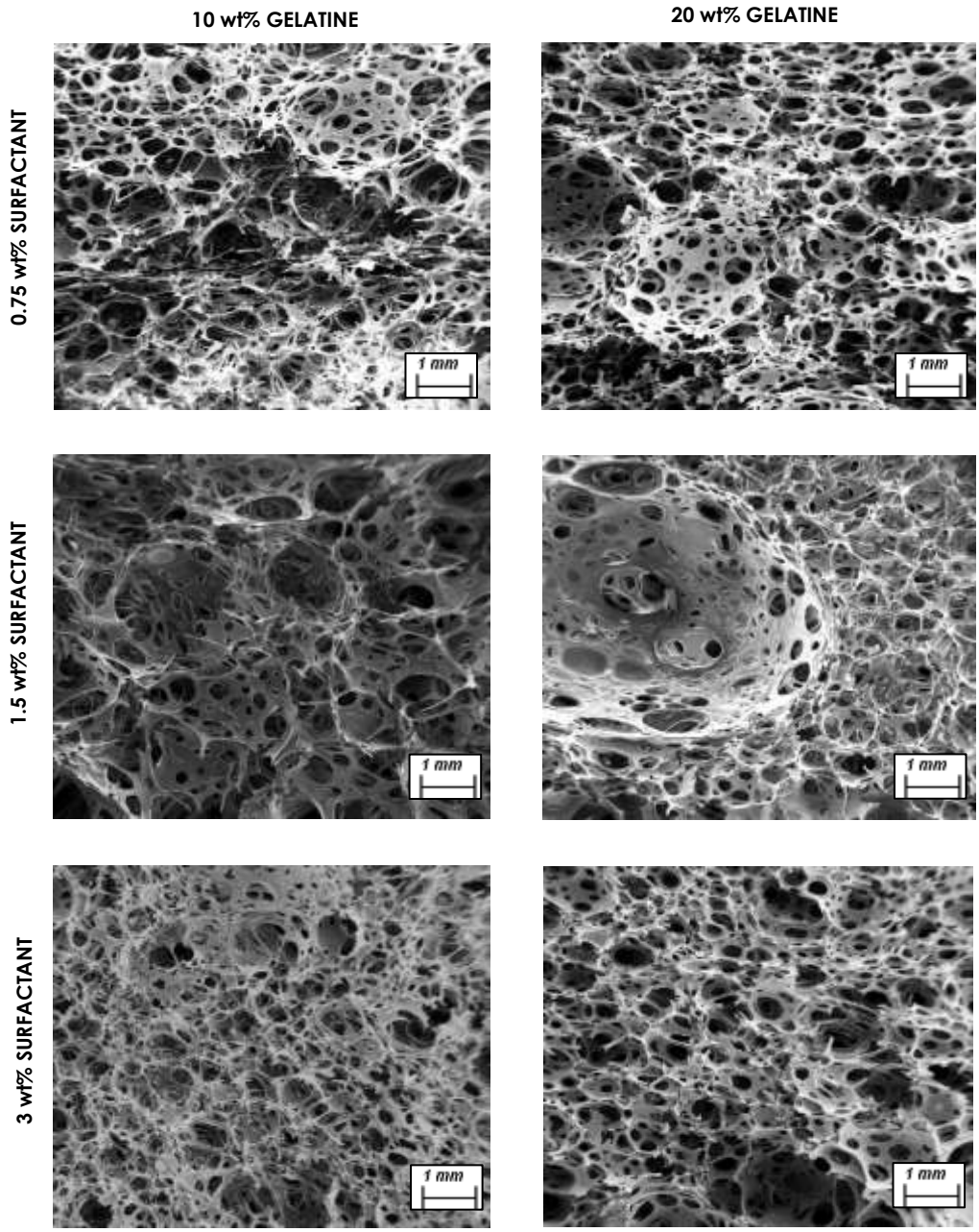

Figure 5.52 SEM MICROGRAPHS OF CELL MORPHOLOGIES OF GELATINE-SURFACTANT C2 FOAMS MADE AT 80°C

Figure 5.53 compare SEM images at different positions (top, centre and bottom) of the cross-section of samples C2.1 (10 *wt%* gelatine and 98.05% porosity and C2.5 *(*20 *wt%* gelatine and 95.13% porosity), both processed at 50°C and containing 0.75 *wt%* surfactant C2.

The cell size and the plateau borders thickness were relatively smaller and bigger, respectively, in sample C2.5 than sample C2.1, as expected due to its higher density.

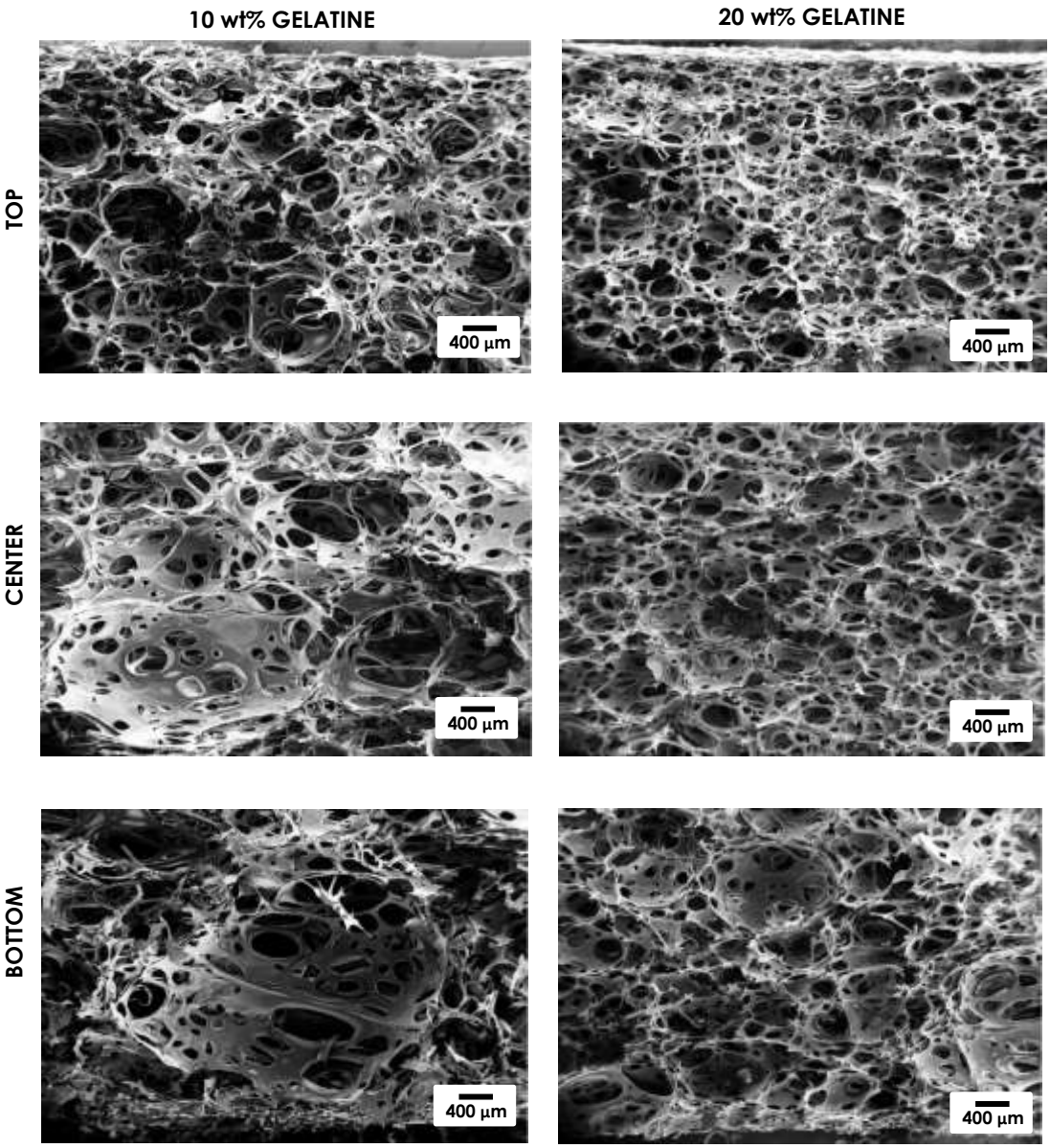

Figure 5.53 SEM IMAGES OF GELATINE-SURFACTANT C2 FOAMS (C2.1 AND C2.5) SHOWING THE VARIATION OF the CELL STRUCTURE AT THE TOP, MIDDLE AND BOTTOM AREAS OF THE CAST FOAMS

Figure 5.54 exhibit the SEM micrographs of samples C2.1 and C2.5 at higher magnification than those showed in Figure 5.53. Figure 5.54 illustrates the denser top of foam C2.5 due to drying shrinkage and the relatively rigidity that this sample exhibits, which made it vulnerable to plastic deformation when, during vaporisation, forces higher than the yield strength of the plateau borders/cell walls where generated.

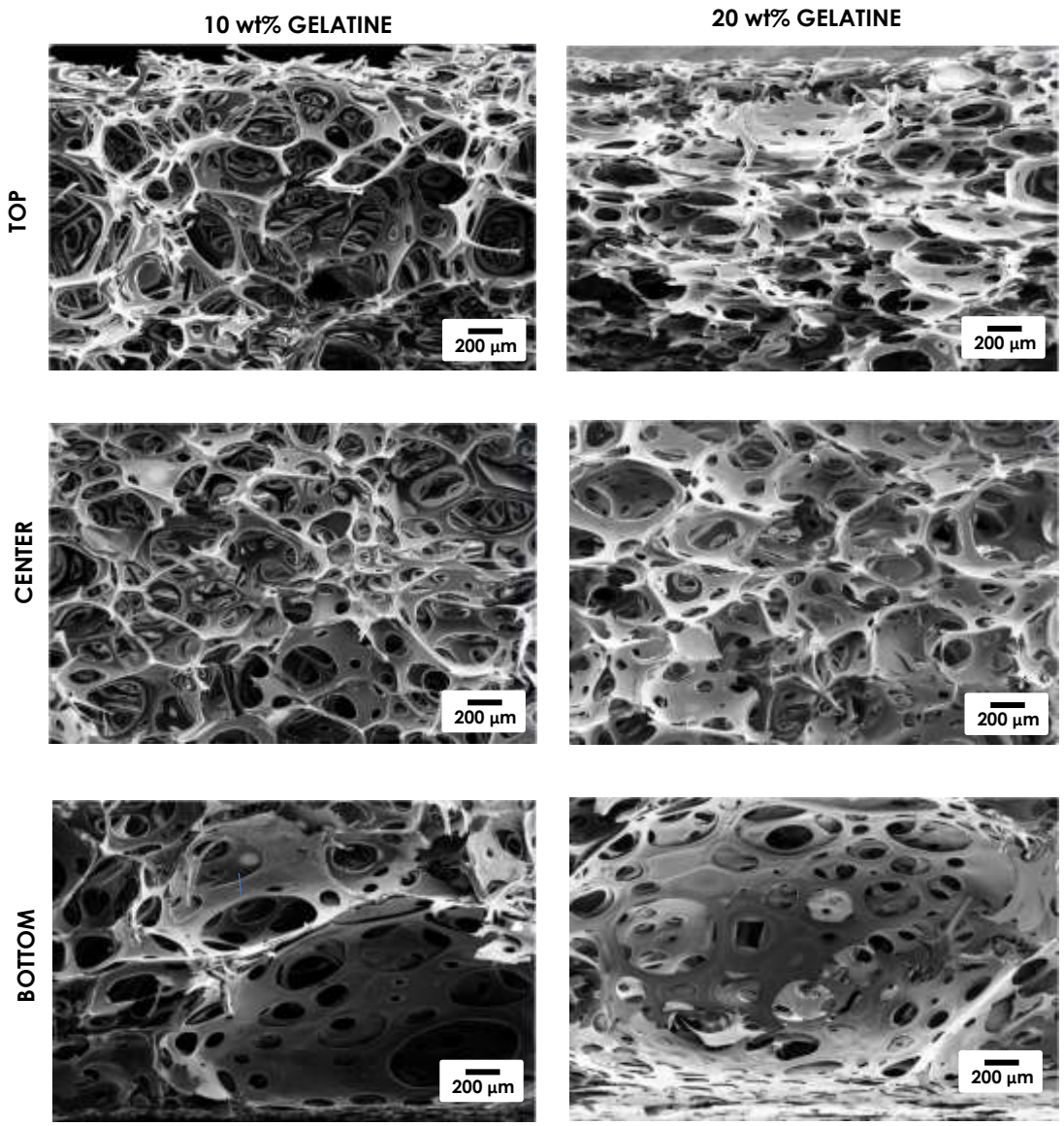

Figure 5.54 SEM IMAGES SHOWING GELATINE-SURFACTANT C2 FOAMS (C2.1 AND C2.5) SHOWING IN-DETAIL THE CELL STRUCTURE AT THE TOP, MIDDLE AND BOTTOM AREAS OF THE CAST FOAMS

Figure 5.55 presents the cell morphology of the top surface of the cast gelatine-surfactant C2 foams which was "frozen" due to rapid gelification, as discussed in section 5.4.4.1.

As discussed, all the foams exhibited an open-cell structure. The cell shape of the foams tended to be more oval than polyhedral, especially at lower surfactant and gelatine contents. The plateau borders were thicker at higher gelatine and surfactant content, so does the number of closed-cells.

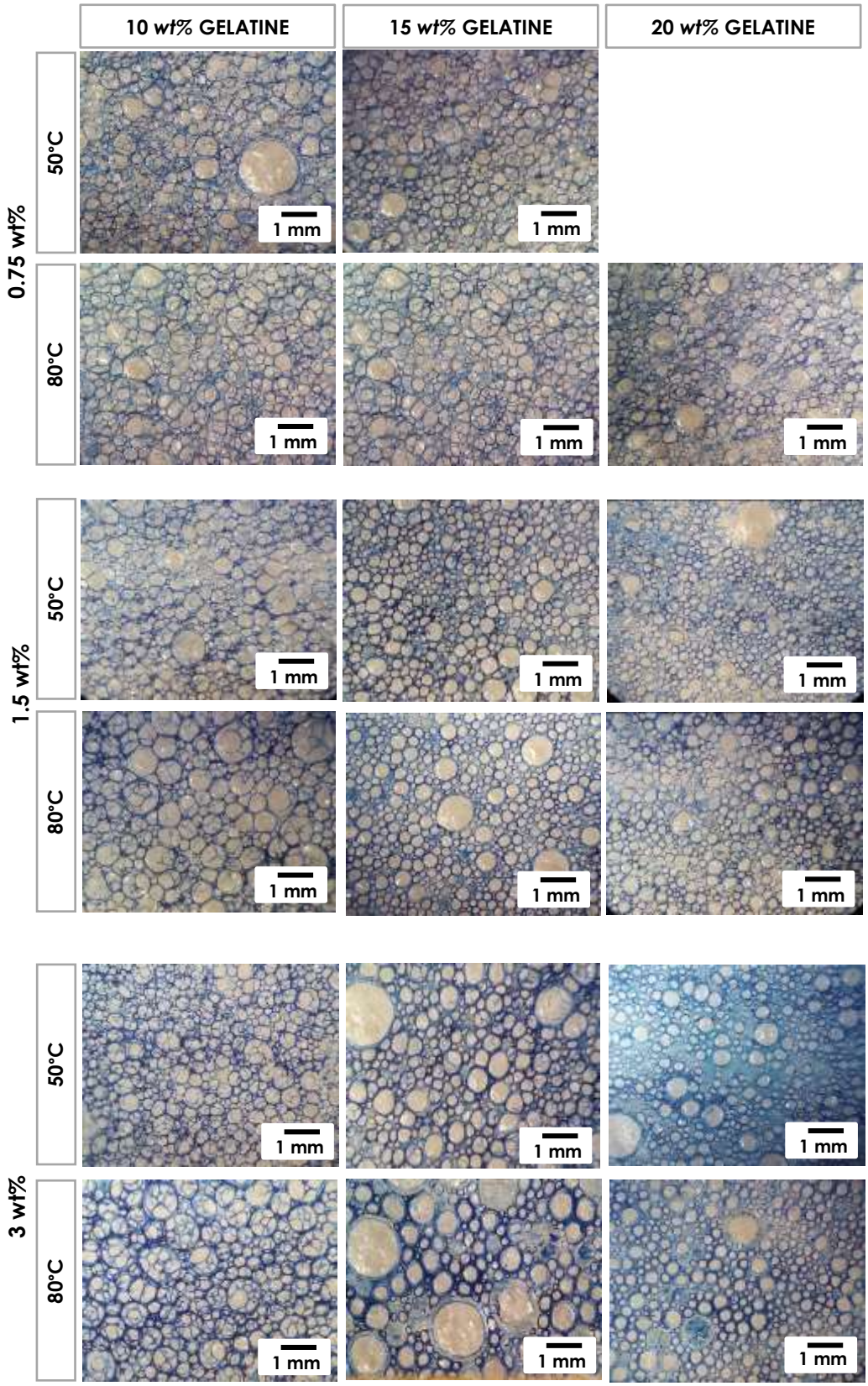

Figure 5.55 OPTICAL MICROSCOPE IMAGES OF 2D PORE MORPHOLOGY ON THE TOP SURFACE OF THE CAST GELATINE-SURFACTANT C2 FOAMS

5.4.5 FOAM PROPERTIES

This section discusses the compression, thermal and acoustic properties of gelatine foams made with surfactants "A" and C2.

Compression properties of foams are essential for their selection in cushioning packaging as well as thermal and acoustic insulations applications. Thus, firstly the yield strength, compression modulus, compression strength and recovery after compression of gelatine foams were characterised.

Secondly, the thermal conductivity of selected gelatine-surfactant "A" and C2 foams were studied to investigate the thermal insulation performance. The thermal stability of selected gelatine-surfactant "A" foams was studied to investigate their maximum service temperature.

Finally, the sound absorption and transmission loss of selected foams prepared with both surfactants "A" and C2 was analysed and compare with those for PS.

5.4.5.1 Compression properties

The averaged stress-strain curves for gelatine-surfactant "A" foams obtained from compression tests are shown in Figure 5.56. The tests details can be seen in Section 3.6.6, in Chapter 3.

As the dry foam composition differed slightly (see Tables 5.16 and 5.14), some differences in the mechanical behaviour of the solids were expected. However, foams mechanical properties are largely controlled by foam density as commonly reported (Gibson and Ashby, 1997). As shown in Figures 5.56 A, B and C, the dependence of stress-strain behaviour on density (which is related closely with gelatine concentration) was clearly shown.

The stress-strain response of lower density gelatine-surfactant "A" foams (~10 kgm^{-3}) (Figure 5.56A) was similar to that of elastomeric foams behaviour. They exhibited low elastic compression modulus without clear yielding or "crush plateau". Instead of exhibiting a plateau, they displayed a steady increase of stress and gradual transition to the densification zone.

For the intermediate density foams (~25 kgm^{-3}), higher elastic compression modulus can be seen, clear yielding and crush plateau appeared and transition to the densification zone was more identifiable (Figure 5.56B).

For higher density foams (>30 kgm^{-3}), Figure 5.56C exhibits the behaviour of typical more rigid foams, with higher elastic compression modulus, clearly definable yield strength, crush "plateau" and much sharper transition to the densification zone.

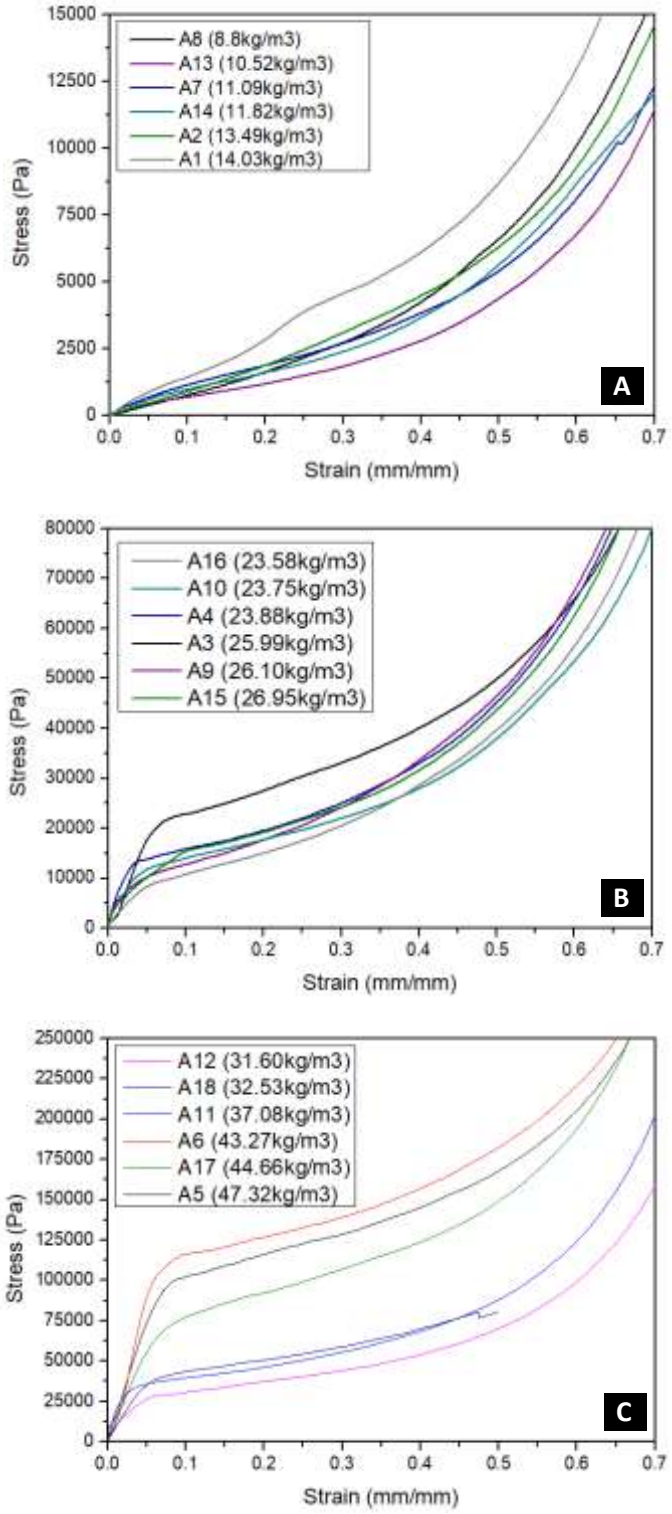

Figure 5.56 STRESS-STRAIN CURVES OF GELATINE-SURFACTANT "A" FOAMS (A) 10 *wt%* GELATINE CONTENT (B) 15 *wt%* GELATINE CONTENT (C) 20 *wt%* GELATINE CONTENT

Figures 5.57A and 5.57B presents the relationship between elastic compression modulus and yield strength, respectively, with foam densities of gelatine-surfactant "A" foams.

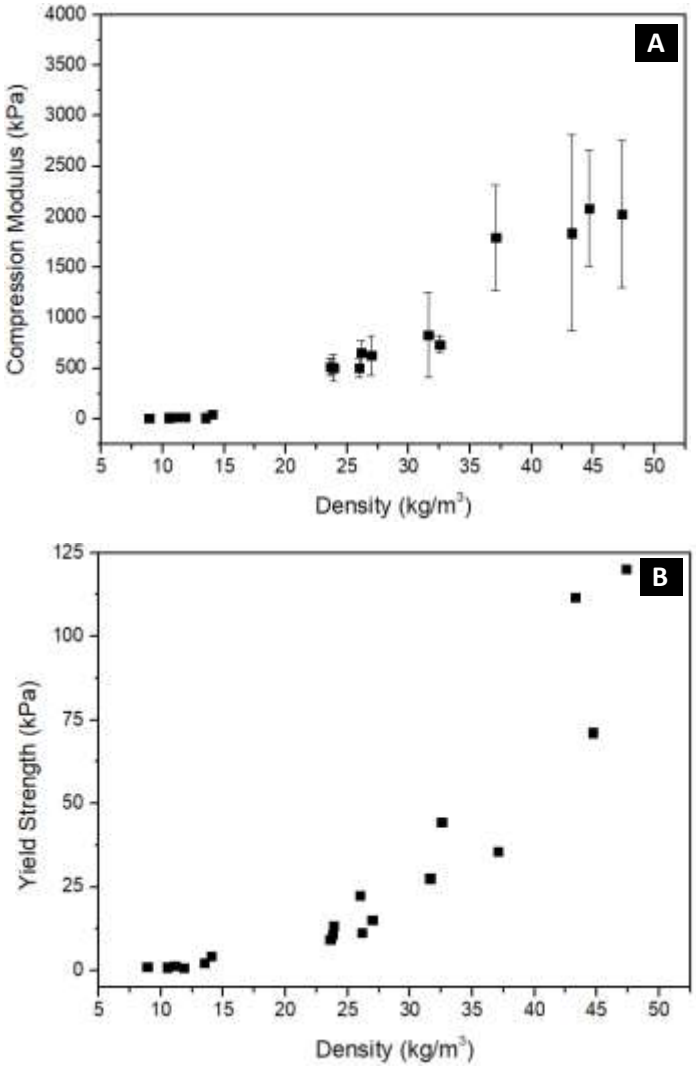

Figure 5.57 RELATIONSHIP BETWEEN (A) ELASTIC COMPRESSION MODULUS (B) YIELD STRENGTH AND FOAM DENSITIES (GELATINE-SURFACTANT "A" FOAMS)

Figure 5.58 shows the compression strength of gelatine-surfactant "A" foams at 10, 25 and 50% and illustrates that the mechanical properties were closely related to foam density as expected (Gibson and Ashby, 1997).

Figure B.3 (see Appendix B) compares the structure of sample A11 before and after compression at 50% strain. The cells buckling and bending after compression can be seen in detail in Figure B.5.A (Appendix B).

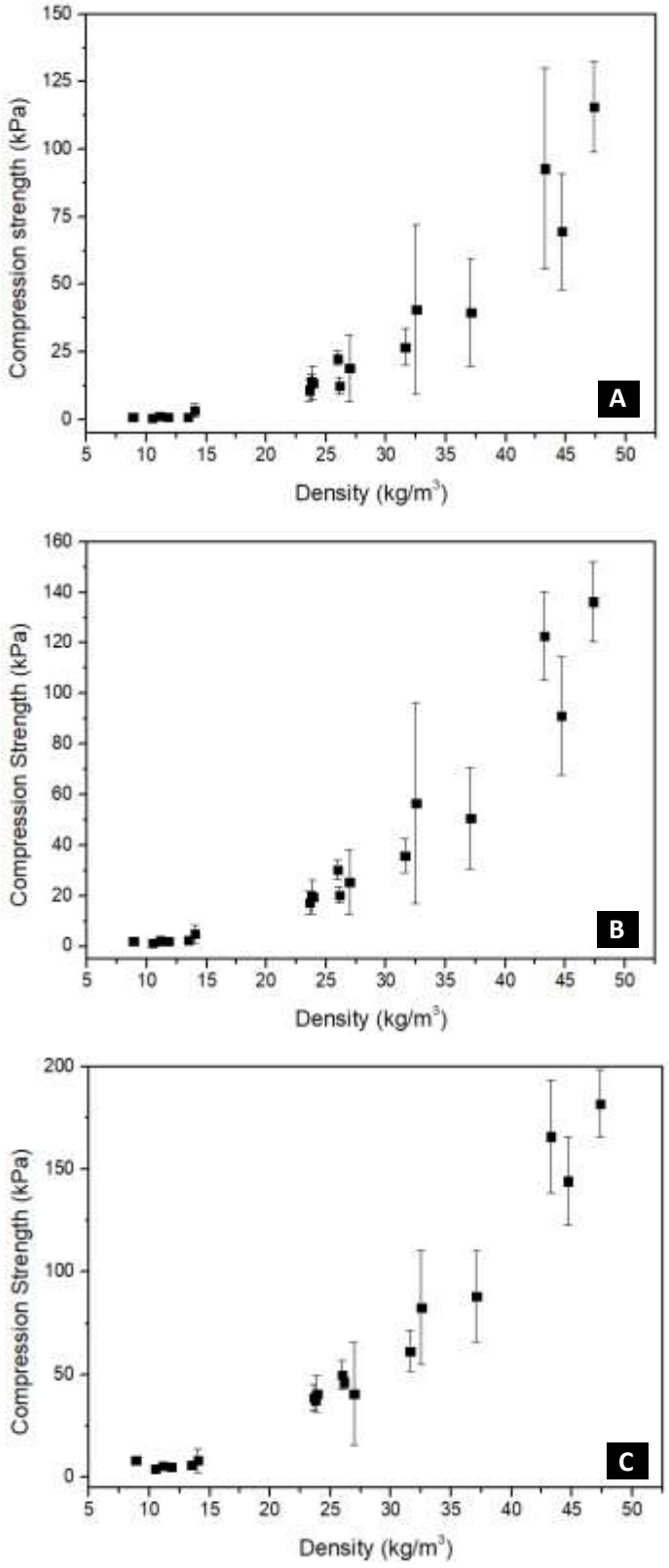

Figure 5.58 COMPRESSION STRENGTH OF THE GELATINE-SURFACTANT "A" FOAMS AT DIFFERENT COMPRESSION STRAINS A) 10% B) 25% C) 50%

Yield strength, elastic compression modulus and compression strength at given strains (10, 25 and 50%) were determined from the stress-strain data and are presented in

Table 5.18. The table also includes the foam recovery after 50% strain compression. The recovery depended on the foams density. Lower density foams exhibited higher recovery rates, while intermediate and higher densities led to similar recovery rates.

Table 5.18 COMPRESSION MODULUS, YIELD STRENGTH, RECOVERY AND COMPRESSION STRENGTH (AT 10, 25 AND 50% STRAINS) OF THE GELATINE-SURFACTANT A FOAMS

ID	DENSITY (kg/m³)	MODULUS (kPa)	YIELD STRENGTH (kPa)	STRESS AT 10% (kPa)	STRESS AT 25% (kPa)	STRESS AT 50% (kPa)	RECOVERY (%)
A8	8.88	7.80±1.11	1.12	0.90±0.05	2.15±0.05	8.40±0.40	100.00±0.00
A13	10.52	11.20±1.87	0.98	0.67±0.12	1.40±0.20	4.23±0.49	95.84±3.22
A7	11.09	19.37±2.00	1.35	1.13±0.06	2.27±0.15	5.43±0.57	94.29±2.47
A14	11.82	20.45±11.76	0.85	0.95±0.07	1.95±0.07	5.10±0.85	100.00±0.00
A2	13.49	11.05±0.35	2.25	0.90±0.28	2.45±0.07	6.15±0.64	96.05±3.58
A1	14.03	43.15±24.50	4.37	3.23±2.43	4.93±3.60	8.23±5.78	97.00±2.87
A16	23.58	514.21±82.90	9.42	10.85±3.99	17.25±4.50	38.83±6.58	76.47±2.29
A10	23.75	511.64±85.40	10.84	14.07±2.41	19.70±2.21	37.93±2.62	77.42±3.10
A4	23.88	503.39±136.68	13.48	13.54±6.38	19.44±6.69	40.66±8.94	76.73±1.87
A3	25.99	504.11±89.12	22.46	22.60±2.59	30.38±3.64	50.00±6.99	79.86±2.08
A9	26.10	660.53±117.05	11.32	12.40±3.18	20.36±3.22	46.36±3.47	73.00±2.89
A15	26.95	628.59±196.73	15.21	18.90±12.29	25.30±12.71	40.70±24.77	72.22±2.71
A12	31.60	829.90±424.42	27.56	26.78±6.79	35.94±6.71	61.56±9.98	75.41±7.74
A18	32.53	738.37±83.69	44.52	40.56±31.41	56.61±39.70	82.59±27.75	76.34±2.78
A11	37.08	1,795.13±521.05	35.68	39.76±19.96	50.70±20.03	88.16±22.03	76.26±1.23
A5	47.32	2,027.33±729.68	120.33	115.80±16.75	136.30±15.63	181.95±16.35	76.80±1.34
A6	43.27	1,839.22±971.71	111.67	92.83±37.17	122.60±17.45	165.93±27.53	78.48±3.06
A17	44.66	2,082.75±576.74	71.18	69.50±21.39	91.25±23.45	144.23±21.58	71.12±1.14
A5	47.32	2,027.33±729.68	120.33	115.80±16.75	136.30±15.63	181.95±16.35	76.80±1.34

The averaged stress-strain curves for 10, 15, 20 *wt%* gelatine-C2 foams obtained from compression tests are shown in Figure 5.59 (all exhibiting an elastomeric behaviour). As observed in gelatine-surfactant "A" foams, stress-strain behavior was dependent on density. Stiffness and elastic compression modulus increased as density and gelatine content increased. The three stress-strain curves shown in Figure 5.59 exhibited a clear yielding, plateau and densification zones.

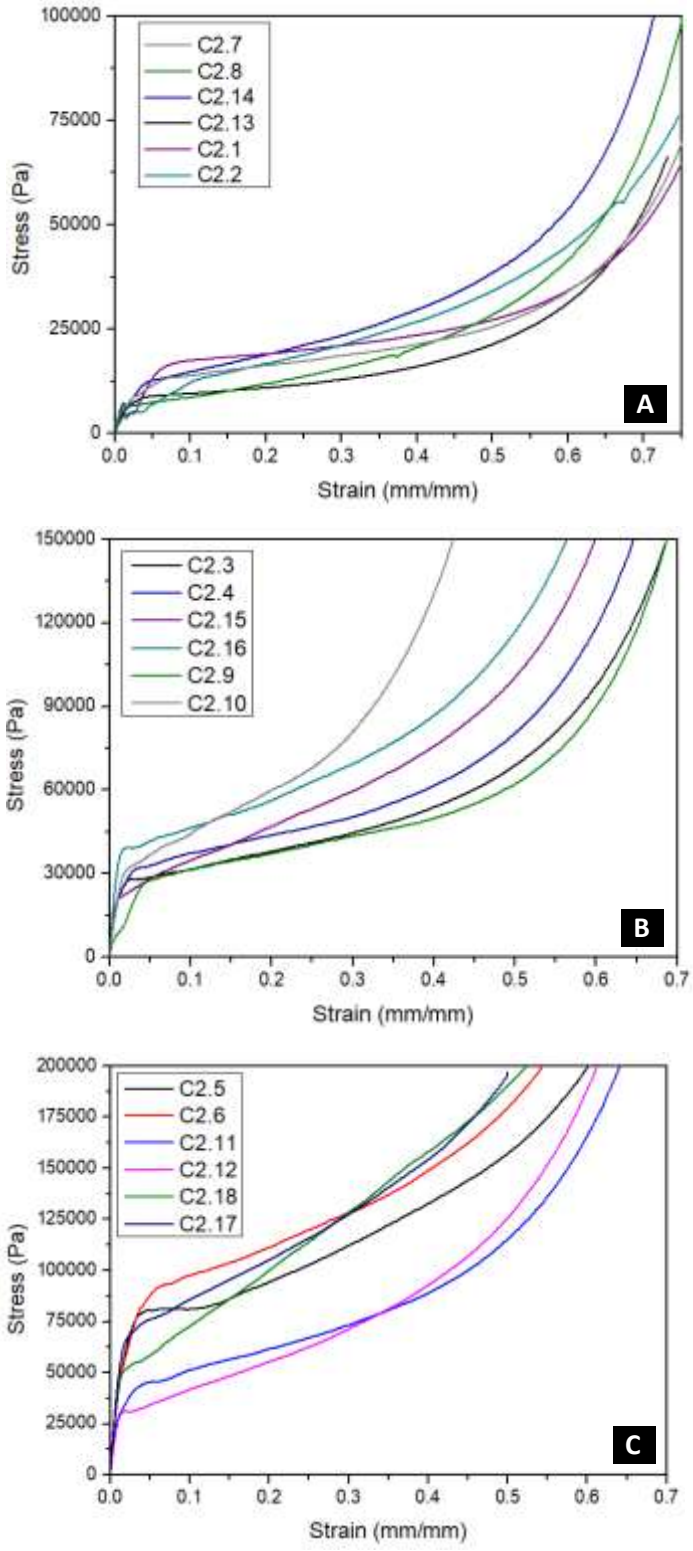

Figure 5.59 STRESS-STRAIN CURVES OF GELATINE-SURFACTANT C2 FOAMS (A) 10 *wt%* GELATINE CONTENT (B) 15 *wt%* GELATINE CONTENT (C) 20 *wt%* GELATINE CONTENT

Figures 5.60A and 5.60B presents the relationship between elastic compression modulus and yield strength, respectively, with foam densities of gelatine-surfactant C2 foams. Both were dependent on foam density.

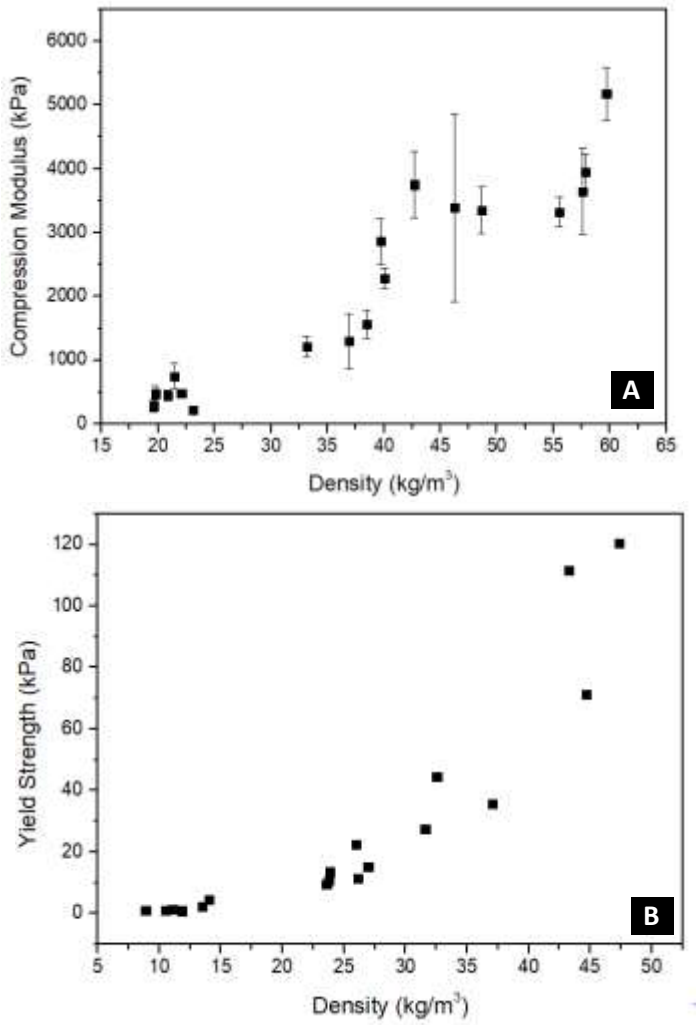

Figure 5.60 RELATIONSHIHP BETWEEN (A) ELASTIC COMPRESSION MODULUS (B) YIELD STRENGTH AND FOAM DENSITIES (GELATINE-SURFACTANT C2 FOAMS)

Figure 5.61 shows the compression strength of gelatine-surfactant C2 foams at 10, 25 and 50% strain. They exhibited the same density dependence trend observed for compression modulus and yield strength

Figure B.4 (see Appendix B) compares the structure of sample C2.5 before and after compression at 50% strain. The cells buckling and bending after compression can be seen in detail in Figure B.5.B (Appendix B).

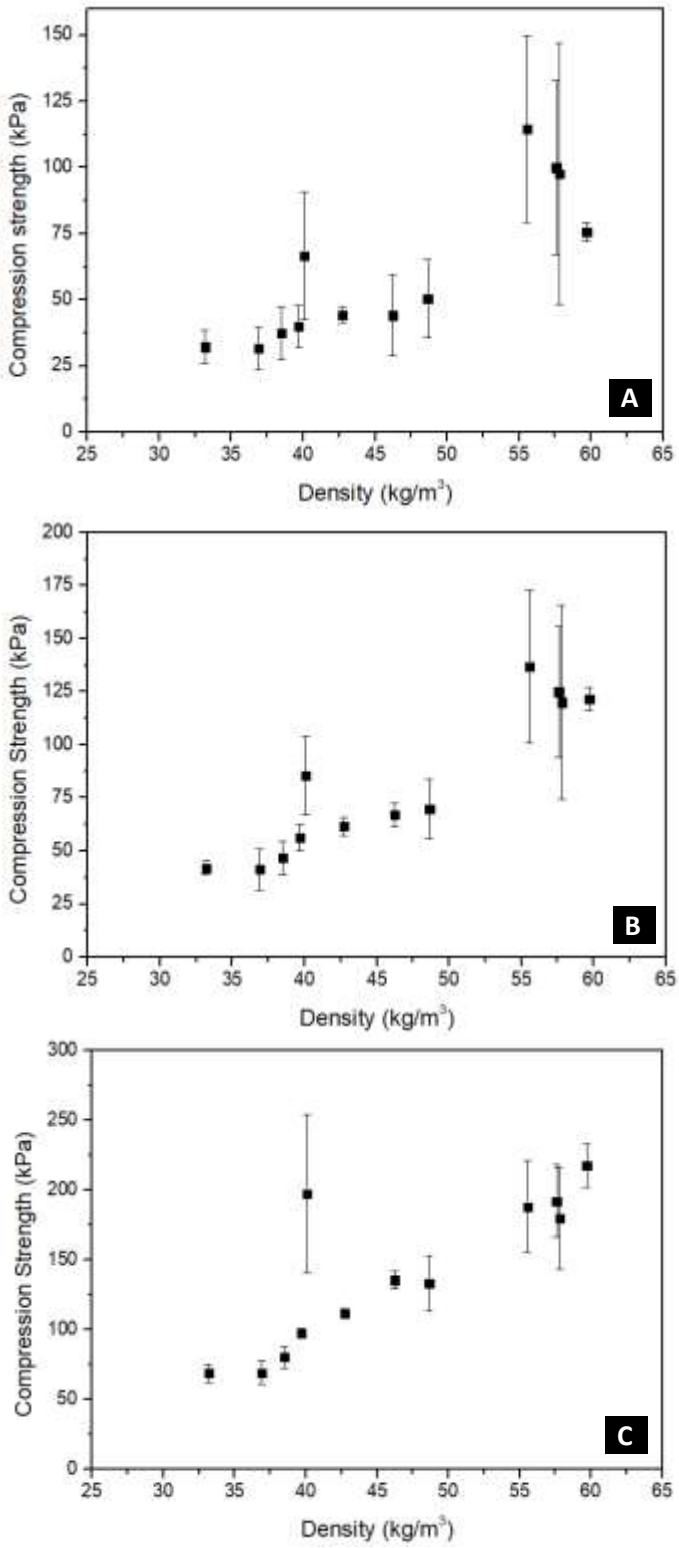

Figure 5.61 COMPRESSION STRENGTH OF THE GELATINE-SURFACTANT "A" FOAMS AT DIFFERENT COMPRESSION STRAINS A) 10% B) 25% C) 50%

Table 5.19 summarises the compression modulus, yield strength, recovery and stress at 10, 25 and 50% of the different foam samples. The recovery rate of gelatine-surfactant C2 foams was considerably lower than that of foams made with surfactant "A" at low

gelatine concentrations (10 *wt%*). This is attributable to a decrease in foam flexibility when surfactatant C2 was used. The recovery rate for 15 *wt%* and 20 *wt%* gelatine foams was slightly lower than that reported for foams made with surfactant "A".

Table 5.19 COMPRESSION MODULUS, YIELD STRENGTH, RECOVERY AND COMPRESSION STRENGTH (AT 10, 25 AND 50% STRAINS) OF THE GELATINE-SURFACTANT C2 FOAMS

ID	DENSITY (kg/m³)	YOUNG'S MODULUS (kPa)	YIELD STRENGTH (kPa)	STRESS AT 10% (kPa)	STRESS AT 25% (kPa)	STRESS AT 50% (kPa)	RECOVERY (%)
C2.7	19.60	284.10±99.32	12.94	13.95±2.38	17.45±2.28	26.40±2.23	79.61
C2.13	19.76	475.75±122.65	8.26	9.55±4.71	11.70±4.67	20.55±3.98	87.83
C2.1	20.85	446.50±77.03	16.78	19.70±3.53	22.40±3.46	29.67±3.56	89.84
C2.8	21.42	749.16±194.49	5.42	8.90±0.31	15.50±0.11	36.10±1.80	84.72
C2.14	22.06	477.70±28.20	11.28	19.90±2.82	26.60±4.01	40.80±3.34	81.67
C2.2	23.12	222.67±53.24	12.82	12.15±3.09	18.78±3.12	34.16±1.47	73.42
C2.9	33.17	1213.83±161.12	26.58	32.20±6.25	42.00±3.29	68.70±6.26	69.19
C2.3	36.91	1297.91±429.78	27.92	31.56±7.88	41.19±9.79	68.94±8.42	74.40
C2.4	38.51	1564.74±223.81	30.64	37.33±9.80	46.68±8.00	80.15±7.69	74.83
C2.15	39.70	2864.00±356.35	21.52	39.93±8.02	56.30±6.47	97.40±3.05	72.42
C2.10	40.08	2280.00±158.95	30.17	66.65±24.02	85.55±18.40	197.25±56.80	67.25
C2.16	42.71	3751.83±517.68	38.95	44.15±2.86	61.48±4.45	111.63±3.72	67.98
C2.12	46.25	3389.87±1469.25	31.96	44.09±15.43	67.13±5.23	135.45±6.31	64.30
C2.11	48.64	3348.50±363.14	40.34	50.50±14.76	69.83±13.93	133.03±19.85	64.64
C2.5	55.54	3319.14±236.18	79.61	114.43±35.23	136.92±36.10	187.97±32.51	76.49
C2.7	57.58	3646.40±681.41	52.93	99.94±32.94	124.88±30.74	192.02±25.94	72.63
C2.6	57.80	3944.71±290.25	92.47	97.57±49.37	119.92±45.75	179.62±36.54	72.60
C2.18	59.70	5173.44±415.96	71.83	75.57±3.63	121.57±5.32	217.40±15.31	65.19

5.4.5.2 Thermal properties

This section discusses the thermal conductivity of selected formulations of gelatine foams made with surfactant "A" at 1.5 *wt%* (samples A7, A9 and A11 with 10 *wt%,* 15 *wt%* and 20 *wt%* gelatine content, respectively), and C2 at 0.75 *wt%* (samples C2.1, C2.3, C2.5 with 10 *wt%,* 15 *wt%* and 20 *wt%* gelatine content, respectively.

A full factorial 3x2 design with three replicates was used to calculate the statistical significance of *the design parameters* (gelatine content and surfactant type) in thermal conductivity. Further information about the statistical analysis can be found in section 3.3.2 in Chapter 3.

The hypotheses for this experiment were:

a. The null hypotheses (H_O): there was no difference in thermal conductivity for different combinations of the two design parameters.

b. The alternative hypotheses (H_1): there was a difference in thermal conductivity for different combinations of the two design parameters.

The thermal stability of samples A7 and A9 was studied by Thermogravimetric Analysis (TGA).

5.4.5.2.1 Thermal conductivity

Thermal conductivity is a crucial property for materials which intended use is thermal insulation. Due to the large number of samples produced and time limitation, the thermal conductivity measurements were simplified to three samples per subsystem (i.e. three samples for each surfactant, "A" and C2).

As presented in Table 5.20, thermal conductivity of gelatine-surfactant "A" and gelatine-surfactant C2 foams ranged from 0.0398-0.0415 and 0.0381-0.0393 *W/m·K*, respectively. Thermal conductivity was slightly dependent on foam density and surfactant content, but the two design parameters (gelatine content and surfactant type) influence on thermal conductivity was not statistically significant (see ANOVA table in Table A.10, Appendix A). Surfactant C2 foams produced foams with slightly lower thermal conductivity, and for each surfactant separately, higher densities (higher gelatine content) led to slightly higher thermal conductivities, as expected.

Table 5.20 THERMAL CONDUCTIVITY COEFFICIENT, *k*, (W/m·K) OF SELECTED FOAMS FOR GELATINE FOAMS MADE WITH SURFACTANTS "A" AND C2

ID	DENSITY (kg/m^3)	THERMAL CONDUCTIVITY (W/m·K)
A7	11.09	0.0398 ± 0.0019
A9	26.10	0.0403 ± 0.0025
A11	37.08	0.0415 ± 0.0032
C2.1	20.85	0.0381 ± 0.0016
C2.3	36.91	0.0387 ± 0.0021
C2.5	55.54	0.0393 ± 0.0018

The low thermal conductivity achieved was considered remarkable as it was comparable to that in conventional plastic foams (see Table 2.2 in Chapter 2). A thermal conductivity of ≈0.039 *W/m·K* enters the range of relatively high-insulating foams, like EPS and, thus, it enables bio-foams to compete conventional plastics for thermal applications.

5.4.5.2.2 Thermal stability

TGA was used to determine the thermal stability of the dry foams. Figures 5.62A and 5.62B show the TGA curves for the samples A7 (10 *wt%* gelatine content) and A11 (20 *wt%* gelatine content), respectively. The dry gel (before foaming) was used for the measurements. The initial stage represented loss of moisture in both samples and then the material mass remained at constant up to approximately 250°C, where the material started thermal degradation.

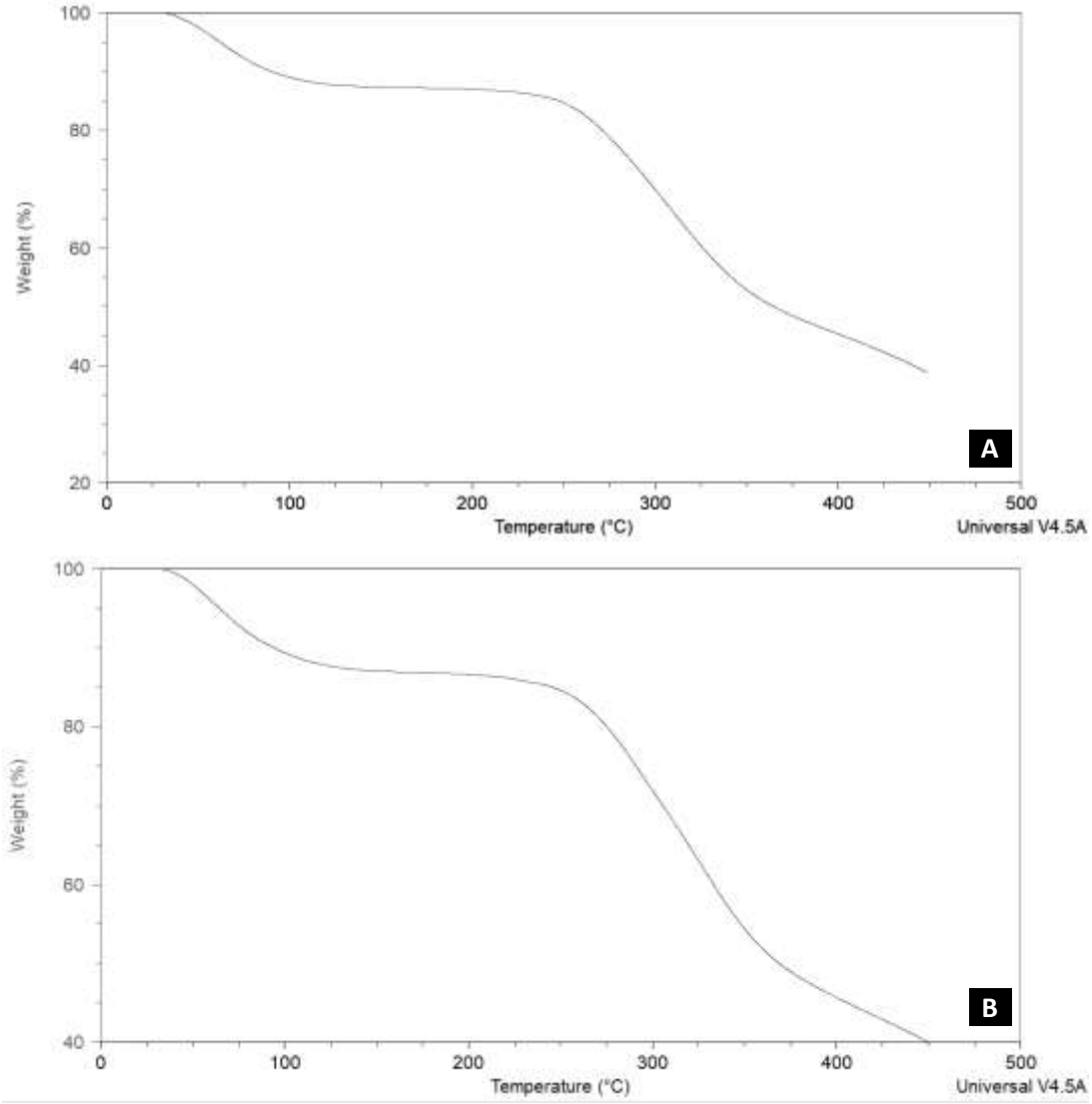

Figure 5.62 TGA SHOWING THERMAL STABILITY OF GELATINE-SURFACTANT "A" FOAMS A) SAMPLE A7 (11.09 *kg/m*^{3}) B) SAMPLE A11 (37.08 *kg/m*^{3})

Therefore, the maximum service temperature of the gelatine-surfactant foams was ≤250°C. Gelatine content did not affect considerably to the thermal stability of the material.

5.4.5.3 Acoustic properties

Figure 5.63 compares the coefficient of absorption of 10 *mm* thickness gelatine foam samples (A7, 11.09 kg/m^3; A11, 37.08 kg/m^3; C2.1, 20.85 kg/m^3; and C2.5, 55.54 kg/m^3) and a 10 *mm* thick PS foam (20kg/m^3) for frequencies from 0 to 800 *Hz*. It is desirable to perform this test to a frequency range 100-3150 *Hz,* as discussed in Chapter 2 (see Section 2.2.5.4) but this was not possible due to equipment unavailability.

C2.5, the highest density foam, achieved the best performance, followed by A11, second largest density, A7 and C2.1. Thus, it can be concluded that the coefficient of absorption depended on the foams density.

The bio-foams exhibited better performance than PS at all the frequencies (excepting for C2.1 in the range 600-700 *Hz*).

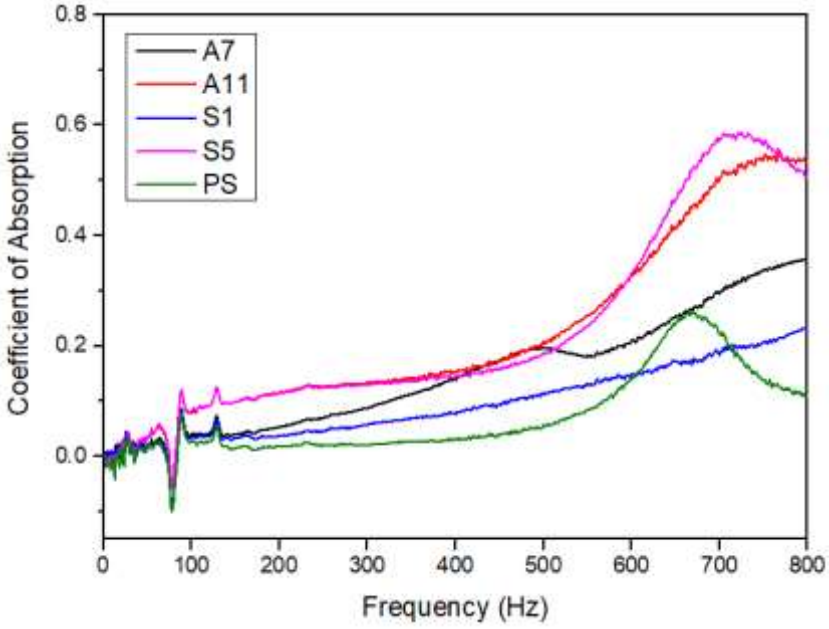

Figure 5.63 COEFFICIENT OF SOUND ABSORPTION OF SELECTED GELATINE-SURFACTANT "A" (A7, 11.09 *kg/m^3*; A11, 37.08 *kg/m^3*) AND GELATINE-SURFACTANT C2 (C2.1, 20.85 *kg/m^3*; C2.5, 55.54 *kg/m^3*) FOAMS IN COMPARISON WITH PS FOAM

Figure 5.64 compares the transmission loss of the same 10-*mm* thickness samples analysed for the coefficient of absorption (A7, A11, C2.1, and the PS) plus a 10-*mm* thickness PU (14kg/m^3) sample for frequencies from 0 to 800Hz. Sample C2.5 data was not included due to measurement artifacts which produced defective data.

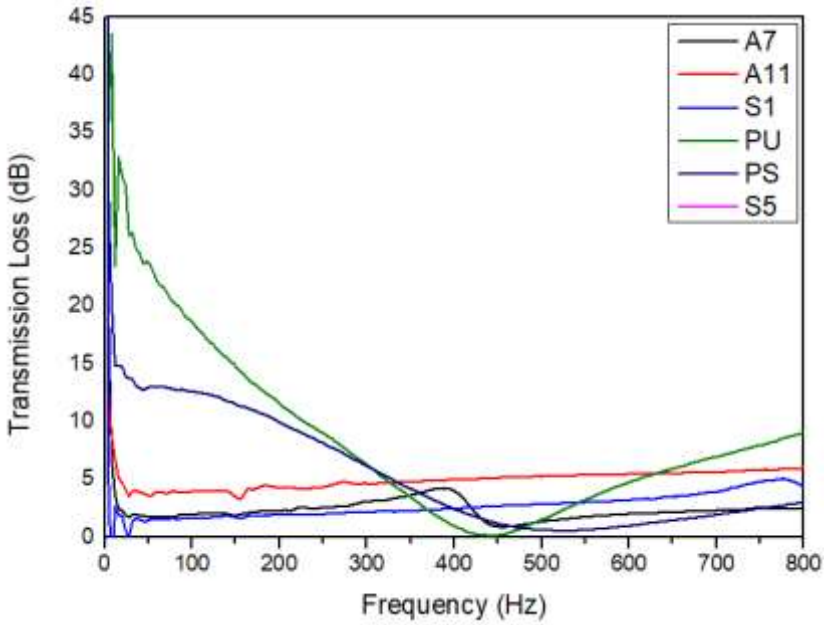

Figure 5.64 TRANSMISSION LOSS FOR THE GELATINE FOAM SAMPLES (A7, A11, C2.1) IN COMPARISON WITH PS AND A PU FOAMS.

As illustrated in Figure 5.64, PU outperformed all the bio-foams at the low (0-350 *Hz*) and high frequencies (650-800 *Hz*) studied; but was outperformed by all the biofoams at 350-550 *Hz.* PS exhibited a relatively good performance for frequencies <350 *Hz* but it was outperformed by the other foams at higher frequencies.

The bio-foams did not generally exhibit a considerable sound blocking but they may be used in combination with other materials in sandwiched structures to mitigate this. Their relatively low transmission loss may be attributable to their open-cell structure.

5.4.6. SUMMARY

This section investigated the effect of different formulation and processing (foaming temperature) parameters on the properties and structure of hydrogel-gelatine foams made with two different surfactants: "A" and C2. This study was based on the findings found in Section 5.3, where surfactant type and content selection was narrowed down.

Table 5.21 compares the main properties of selected samples from the two systems. The higher surfactant level was omitted in the table due to drying defects development (surfactant C2) and similar performance as lower surfactant content foams (surfactant "A"). The foams processed at higher temperatures were also not included in the summary table as the lower foaming temperature was found to be optimum (i.e. lower shrinkage level, lower or similar density and lower energy demanding process than production at higher temperatures).

The selected samples for further experimentation were A7, A9 and A11, for surfactant "A" foams; and C2.1 and C2.3 for surfactant C2 foams. The selected surfactant "A" foams formulations exhibited an outstanding density, moderate shrinkage values and a homogeneous cell structure. The selected surfactant "C2" foams exhibited outstanding density and shrinkage values and they did not exhibit defects. C2.7 and C2.9 exhibited lower shrinkage and density than C2.1 and C2.3, but, in some cases, they showed central voids.

Table 5.21 MER, SHRINKAGE, DENSITY, YOUNG'S MODULUS, RECOVERY AND THERMAL CONDUCTIVITY OF SELECTED FOAMS MADE WITH SURFACTANTS "A" AND C2

ID	MER	SHRINKAGE (%)	DENSITY (kg/m^3)	YOUNG'S MODULUS (KPa)	RECOVERY (%)	THERMAL CONDUCTIVITY (W/m·K)
A1	8.67	40	14.03 ± 0.72	43.15±24.50	97.00±2.87	-
A3	6.46	31	25.99 ± 1.46	504.11±89.12	79.86±2.08	-
A5	5.70	37	47.32 ± 3.18	2,027.33±729.68	76.80±1.34	-
A7	9.70	43	11.09 ± 1.43	19.37±2.00	94.29±2.47	0.0398 ± 0.0019
A9	7.39	31	26.10 ± 1.02	660.53±117.05	73.00±2.89	0.0403 ± 0.0025
A11	6.23	43	37.08 ± 4.8	1,795.13±521.05	76.26±1.23	0.0415 ± 0.0032
C2.1	7.17	11.3	20.85 ± 0.79	446.50±77.03	89.84	0.0381 ± 0.0016
C2.3	6.64	22.7	36.91 ± 0.77	1297.91±429.78	74.40	0.0387 ± 0.0021
C2.5	5.44	20.7	55.54 ± 1.28	3319.14±236.18	76.49	0.0393 ± 0.0018
C2.7	7.68	15.6	19.60 ± 1.69	3646.40±681.41	72.63	-
C2.9	6.84	15.5	33.17 ± 0.79	1213.83±161.12	69.19	-
C2.11	7.02	15.9	48.64 ± 1.03	3348.50±363.14	64.64	

The study of MER and total shrinkage showed the importance of relatively low changes in viscosity.

MER was favoured at low surface tension and viscosity. It increased as gelatine content decreased ($p<0.001$) and foaming temperature increased ($p<0.001$) for both surfactants "A" and C2. However, surfactant content influence depended on the surfactant type. MER was maximum at the highest surfactant "A" and intermediate surfactant C2 levels ($p<0.001$). This discrepancy was attributable to the viscosity differences between the two surfactants solutions. At higher surfactant C2 content, the viscosity of the solution considerably increased, which hindered the foaming process.

Gelatine-surfactant C2 foams exhibited less shrinkage (11.22-33.97%) level than foams made with surfactant "A" (31% to 56%), but all the samples exhibited the same drying shrinkage deformation patterns (concave, on the top surface, and convex, on the

bottom). Both surfactants generally exhibited lower shrinkage values at lower foaming temperature ($p<0.001$) due to shorter gelling time and higher viscosity.

The two surfactants exhibited an opposite shrinkage trend with gelatine content. Surfactant "A" exhibited maximum and minimum total shrinkage at lower and intermediate gelatine contents, respectively; while surfactant C2 showed maximum and minimum total shrinkage at intermediate and minimum gelatine contents, respectively.

Surfactant content did not considerably affected surfactant "A" foams total shrinkage (excepting at high gelatine and intermediate surfactant contents), but the use of higher surfactant content considerably affected surfactant C2 foams, leading to the development of central voids. Thus, lower surfactant contents were desirable when producing C2 foams.

The most significant factors influencing density were the solution solid content, MER and shrinkage. Surfactant "A" exhibited lower densities (from 8.8 kg/m^3 to 47.32 kg/m^3) than surfactant C2 (19.60 kg/m^3 to 59.70 kg/m^3). However, both systems produced low-density bio-foams, comparable to that of conventional plastic foams. Lower gelatine content decreased the density of foams made with the two surfactants ($p<0.001$) but foaming temperature influence was the opposite between them. Surfactant "A" foams gave rise to lower density foams at higher foaming temperatures ($p<0.001$), while surfactant C2 produced lower density foams at lower foaming temperatures. It was discussed in Section 5.2.1.3 that surfactant "A" considerably influenced gelling time and that gelling time was dependent on curing temperature. As higher MER may accelerate the temperature decrease within the gelled plateau borders and accelerate stabilisation, higher foaming temperature may produce lower density foams. For foams made with surfactant C2, the lower shrinkage exhibited at lower foaming temperature led to lower density foams.

Both surfactants exhibited minimum density values at intermediate surfactant concentrations ($p<0.001$) where, in the case of surfactant C2, the shrinkage was minimum.

All the foams exhibited an open-cell structure but the foams made with surfactant C2 exhibited a greater number of closed-cells due to the higher viscosity of both the plateau borders and the cell walls, which increased the stability during both gelling and drying. The foam structure mainly consisted of macropores and interconnecting micropores. Foams made at higher foaming temperatures, lower gelatine content and surfactant "A" exhibited relatively bigger macropores and thinner plateau

borders than that processed at lower temperature, higher gelatine content and containing surfactant C2.

Table 5.22 compares the typical plateau borders and cell size range of both gelatine foams made with surfactants "A" and C2 at 10 and 20 *wt%*. Higher gelatine content led to slightly smaller cells than lower gelatine content foams. Cell size was usually less than 1 *mm*, but bigger cell sizes (1.4-4.8 mm) were rarely found.

Table 5.22 TYPICAL PLATEAU BORDERS THICKNESS AND CELL SIZE RANGE OF GELATINE-SURFACTANT "A" AND GELATINE-SURFACTANT C2 FOAMS

	10 *wt%* GELATINE		**20 *wt%* GELATINE**	
	SURFACTANT A	**SURFACTANT C2**	**SURFACTANT A**	**SURFACTANT C2**
Plateau Borders Thickness (μm)	10-70	20-130	20-100	30-180
Typical cell size range (*mm*)	0.3-0.8	0.1-0.9	0.2-0.7	0.05-0.8

The foams were slightly denser at the top layer, in contact with air, due to the drying shrinkage. However, the open-cell structure, although, distorted, prevailed, allowing gas permeation from the inner to the outer layers and facilitating the drying process.

The stress-strain response of gelatine foams made with surfactants "A" and C2 was elastomeric. At lower gelatine content (low-density foams), foams exhibited a low elastic compression modulus without clear yielding or "crush plateau". As gelatine concentration increased, the elastic modulus increased, ant the yielding and the crush plateau were more evident.

Higher gelatine content and the use of surfactant C2 (instead of surfactant "A") led to higher compression modulus and, generally, lower recovery rates. Lower gelatine foams were more flexible, especially those made with surfactant "A" than those made with surfactant C2.

The thermal conductivity achieved was considered remarkably low as it was comparable to that in conventional plastic foams (e.g. EPS, PE). A thermal conductivity of ≈0.039 $W/m \cdot K$ enters the range of relatively high-insulating foams, and, thus, it enables bio-foams to compete conventional plastics for thermal applications.

Regarding acoustic properties, the bio-foams did not generally exhibit a considerable sound blocking but they may be used in combination with other materials in sandwiched structures to mitigate this. Their relatively low transmission loss may be attributable to their open-cell structure.

In conclusion, gelatine foams made with both surfactants "A" and C2 exhibited desirable properties for being a strong alternative to conventional plastic foams. Low densities (<20 kg/m^3), thermal conductivity (≈0.039 $W/k{\cdot}m$), and relatively low shrinkage level were achieved.

5.5. OPTIMISATION OF LIQUID FOAMING EXPANSION RATIO

Liquid foaming expansion ratio has direct impact on foam stability, morphology and dry foam density, and in turn, affect the foam properties. Previous studies recorded the foam expansion with time and the maximum MER (see Section 5.4.1). Based on selected formulations from earlier studies, foams were made at varying final expansion ratios to identify the optimum levels that give rise to foams with desirable combination of density, cell structure and properties.

It was also intended to answer a question: is the use of maximum achievable expansion ratio always beneficial? In other words, would it lead to poor liquid foam stability, and thus, have negative impact on final foam density and structure?

This study covers the investigation of the influence of the expansion ratio on total shrinkage, foams density, and foam structure/morphologies. Table 5.23 shows the experimental matrix for this study.

Table 5.23 EXPERIMENTAL MATRIX FOR THE OPTIMISATION OF EXPANSION RATIO

ID	SURFACTANT	EXPANSION RATIO	GELATINE CONTENT (wt%)	WATER CONTENT (wt%)	SURFACTANT CONTENT (wt%)
ER1	A	6	9.85	88.67	1.48
ER2		8			
ER3		Max (9.7)			
ER4	A	6	14.78	83.74	1.48
ER5		Max (7.39)			
ER6	C2	5	9.93	89.33	0.74
ER7		Max (7.17)			
ER8	C2	5	14.89	84.37	0.74
ER9		Max (6.64)			

From studies in section 5.4, two gelatine-surfactant "A" formulations: A7 (10 *wt%* gelatine content) and A9 (15 *wt%* gelatine content*)* were selected for this study. Formulation A7 was studied at three expansion ratios levels: 6, 8 and 9.7 (the maximum

value achievable for this formulation), whereas formulation A9 was studied at two levels: 6 and 7.39 (the maximum value achievable for formulation A9).

Similarly, formulations C2.1 (10 *wt%* gelatine content) and C2.3 (*15 wt%* gelatine content) were selected from the gelatine-C2 system. Both formulations were studied at two levels. C2.1 was studied at 5 and its maximum achievable expansion ratio, 7.17; whereas C2.3 was studied at 5 and its maximum achievable level, 6.64.

5.5.1 TOTAL SHRINKAGE

As seen in Figure 5.65, the higher (or maximum) expansion ratios tended to give rise to lower total shrinkage. It seems possible that these results were due to the fact that foams prepared at higher expansion ratios exhibited shorter drying times, what minimise the shrinkage values. However, foams made with surfactant "A" and low (10 *wt%*) gelatine content exhibited little effect of expansion ratio on shrinkage. 10 *wt%* gelatine foams made with surfactant "A" gave rise to similar shrinkage levels (≈40%) for the three expansion ratios studied. This result may be related to the relatively low solid content of ER1, ER2 and ER3, which did not considerably difficult the drying process and, consequently, the development of defects related with drying was similar for the three expansion ratios studied.

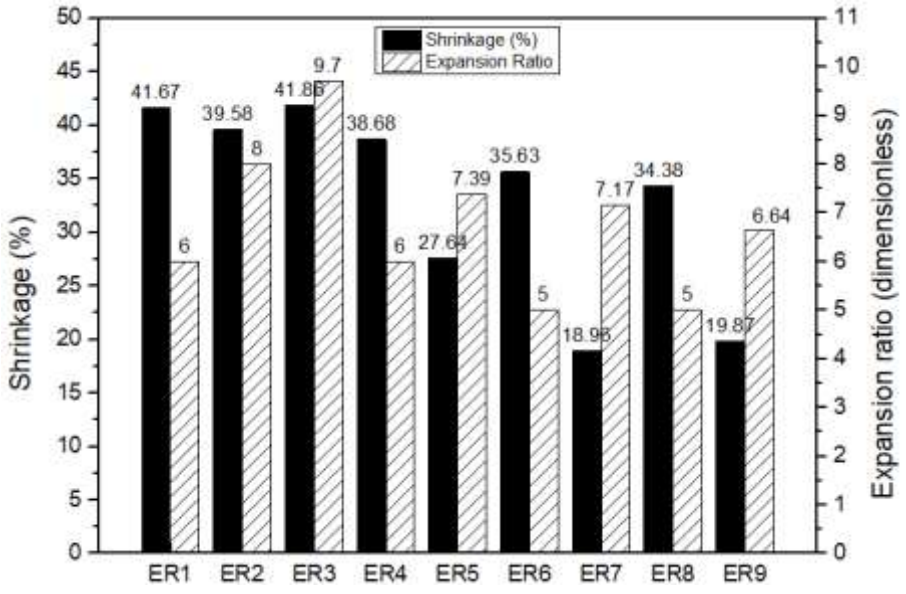

Figure 5.65 TOTAL SHRINKAGE OF THE SAMPLES COMPARED TO THE EXPANSION RATIOS

When foams made with surtactant "A" were prepared with higher gelatine content (15 *wt%*), total shrinkage increased when prepared at lower expansion ratio. This behaviour was also observed in foams made with surfactant C2 at the two gelatine concentrations studied. This may be partially attributable to a lower liquid foam porosity, which slower water removal from the plateau borders of the bottom layers

to the surface. This involves longer drying time which may provoke the development of drying defects and mould development.

Figure 5.66 presents the cross-sections of the dry gelatine foams, showing a visual comparison of the total shrinkage for gelatine foams made with surfactants "A" and C2 at different expansion ratios.

FIGURE 5.66 CROSS-SECTIONS OF THE DRY GELATINE FOAMS SHOWING VISUAL COMPARISON OF TOTAL SHRINKAGE FOR SURFACTANT A) "A" B) C2

5.5.2 DENSITY, RELATIVE DENSITY AND POROSITY

Table 5.24 summarises foam density, relative density and porosity of the dry foams.

For surfactant "A", the relative density of foams made with 10 *wt%* gelatine slightly decreased as expansion ratio was increased. However, for foams made at 15 *wt%* the relative density of foams decreased more significantly as expansion ratio increased.

For surfactant C2, the relative density of the foams (prepared at both 10 *wt%* and 15 *wt%* gelatine content) significantly decreased as expansion ratio increased.

Table 5.24 FOAM DENSITY, MATRIX DENSITY, RELATIVE DENSITY AND POROSITY OF THE DRY FOAMS

ID	FOAM DENSITY (kg/m³)	LIQUID FOAM ER	MATRIX DENSITY (kg/m³)	RELATIVE DENSITY	POROSITY (%)
ER1	12.54±0.25	6	1060	1.18	98.82
ER2	11.54±8	8	1060	1.09	98.91
ER3	11.02±1.12	9.7	1060	1.04	98.96
ER4	21.91±6	6	1120	1.96	98.04
ER5	17.18±7.39	7.39	1120	1.53	98.47
ER6	31.13±5	5	1070	2.91	97.09
ER7	20.85±7.17	7.17	1070	1.95	98.05
ER8	42.87±5	5	1100	3.9	96.10
ER9	36.91±6.64	6.64	1100	3.36	96.64

To reveal the correlation between the liquid foam expansion ratio, ER, to the foam density, the relative density of the foams was plotted against ER in Figure 5.67.

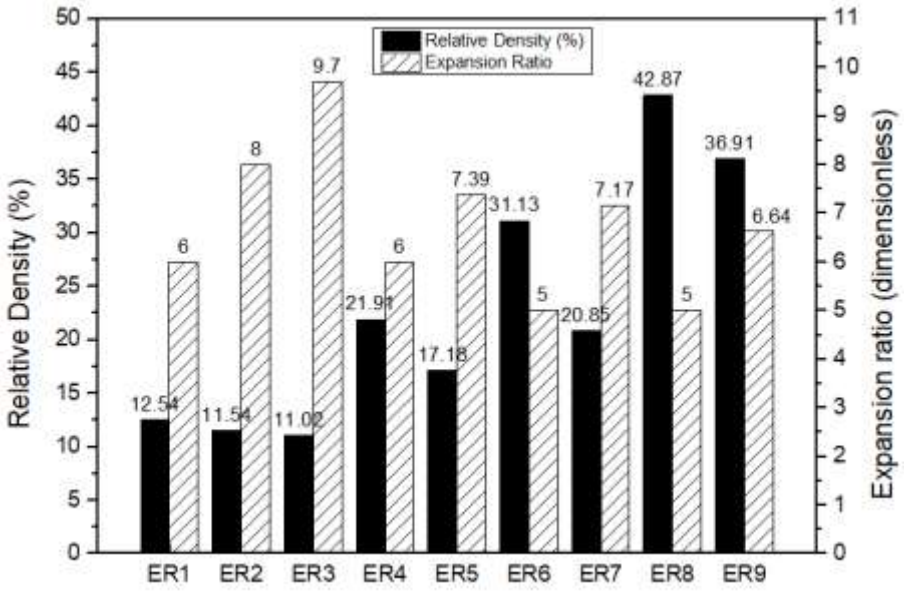

Figure 5.67. CORRELATION OF RELATIVE FOAM TO EXPANSION RATIOS

5.5.3 STRUCTURE

Figure 5.68 exhibits SEM micrographs of the cross-sections of ER1, ER2 and ER3. They did not show much differences in foam structure, as they had similar relative densities (see Table 5.24).

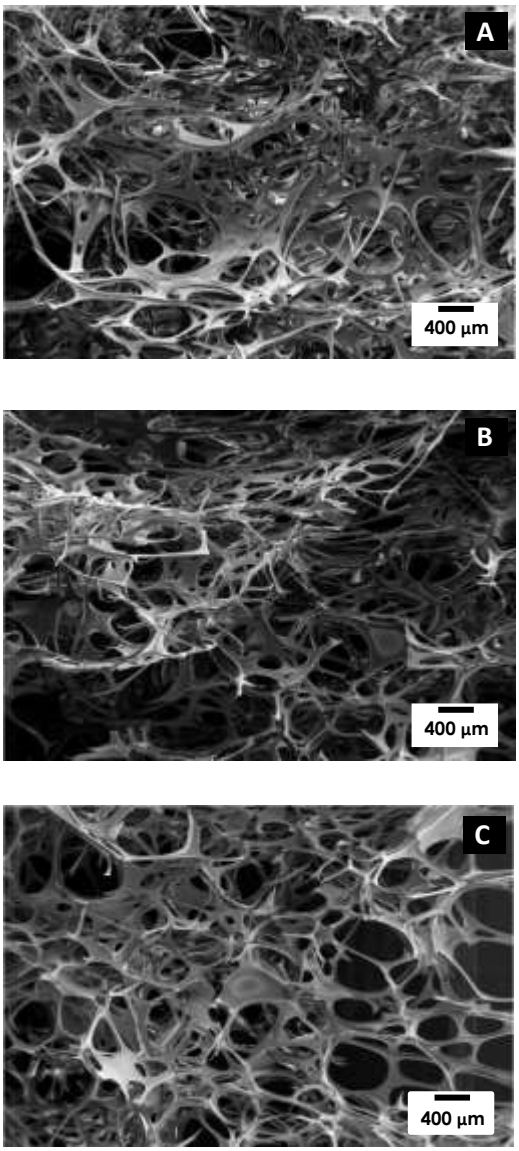

Figure 5.68. SEM IMAGES OF CELL STRUCTURES OF GELATINE–SURFACTANT "A" FOAMS PREPARED WITH IDENTICAL FORMULATION (10 *wt%* GELATINE 1.5 wt% SURFACTANT "A") BUT AT DIFFERENT EXPANSION RATIOS: A) ER=6, DENSITY = 12.54 kgm^{-3}; B) ER= 8, DENSITY = 11.54 kgm^{-3}; C) ER=9, DENSITY = 11.09 kgm^{-3}

Figure 5.69 presents SEM micrographs of the cross-sections of ER4 and ER5 (15 *wt%* gelatine, 1.5 *wt%* surfactant "A") but prepared at two expansion ratios: 6 and 7.39. The higher expansion ratio resulted a fibrous-like low density open-cell structure whereas the lower expansion ratio gave rise to a denser cell structure with relative small "windows" (micropores) connecting the surrounding cells (macropores).

There was only a slight cell densification at the top and the bottom positions due to the reasons explained before (gelling and evaporation, at top surface; and drainage at the bottom.

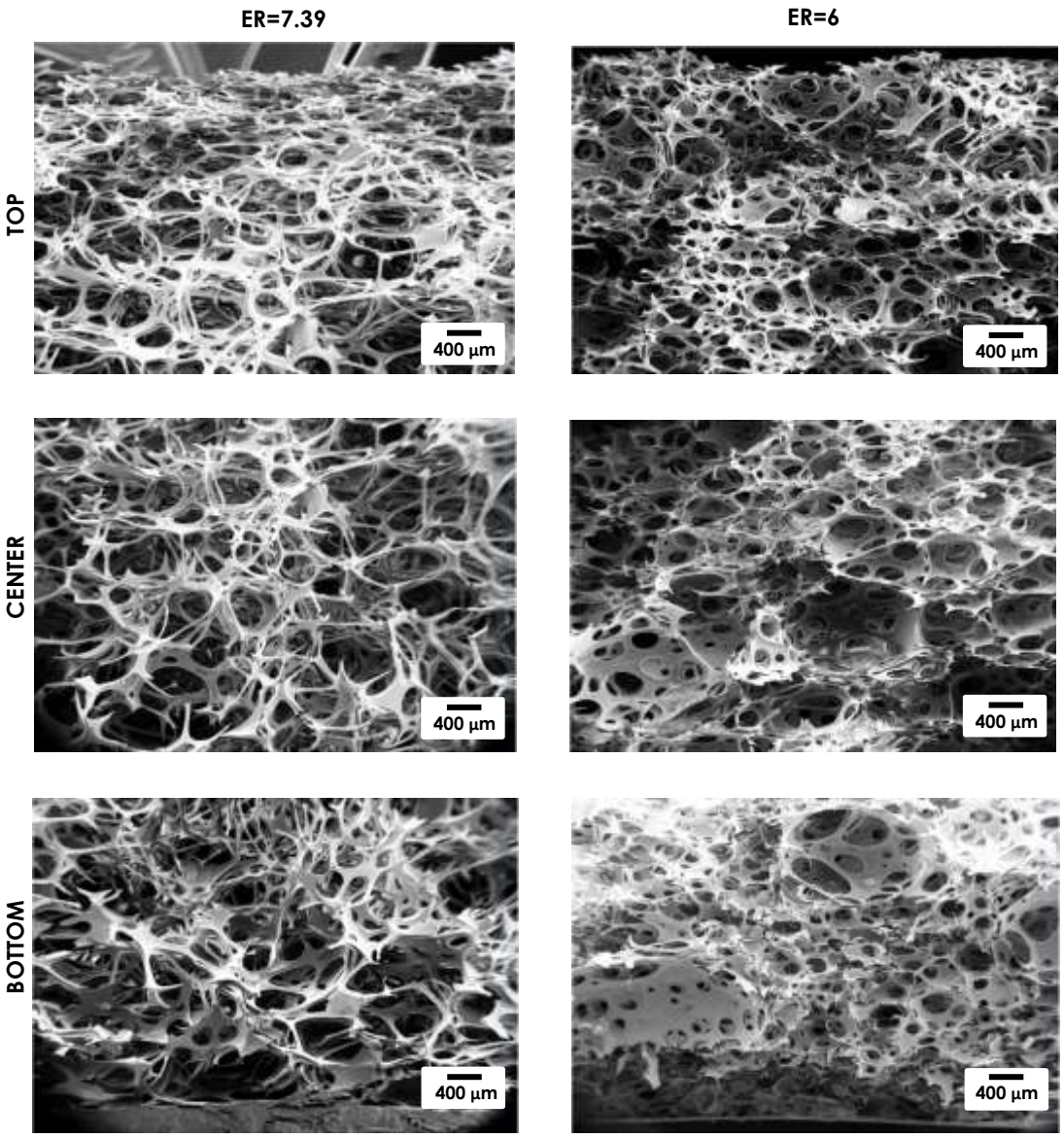

Figure 5.69. SEM IMAGES OF CELL STRUCTURES OF GELATINE–SURFACTANT "A" FOAMS PREPARED WITH IDENTICAL FORMULATION (15 *wt%* GELATINE 1.5 wt% SURFACTANT "A") BUT AT DIFFERENT EXPANSION RATIOS: LEFT COLUMN: ER=7.39, DENSITY = 17.78 kgm^{-3}; RIGHT COLUMN: ER=6, DENSITY = 21.91 kgm^{-3}

Figure 5.70 presents the SEM micrographs of the cross-sections of the gelatine-surfactant C2 foams prepared from identical formulations but different expansion ratios.

The lower expansion ratio gave rise to a denser cell structure, with thicker plateau borders, a greater number of oval-shape cells and less micropores.

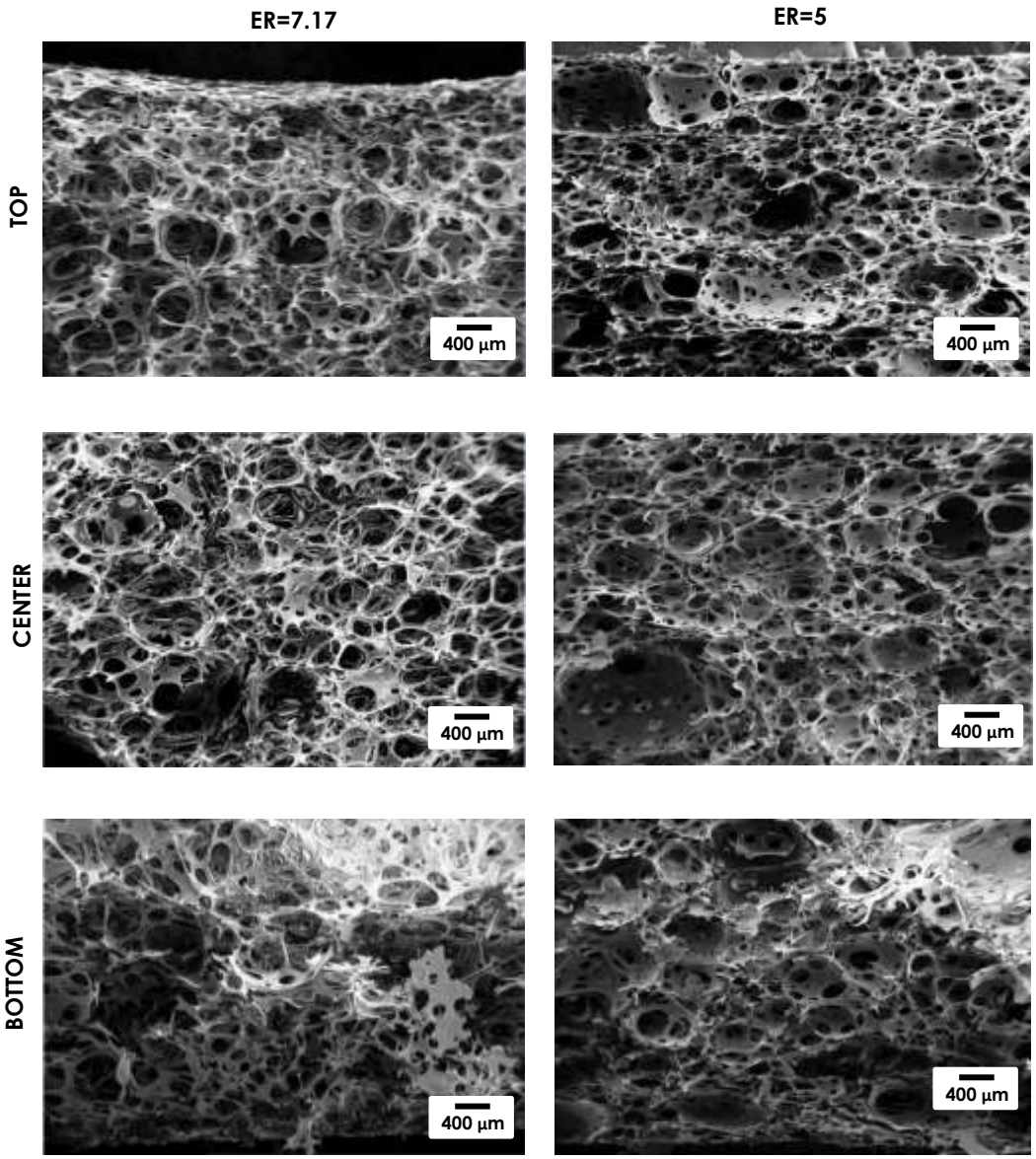

Figure 5.70. SEM IMAGES OF CROSS-SECTIONS AT TOP, MIDDLE AND BOTTOM POSITIONS OF GELATINE-SURFACTANT C2 FOAMS MADE FROM IDENTICAL FORMULATION (10 wt% GELATINE 0.75 wt% SURFACTANT "A") BUT PREPARED AT 2 EXPANSION RATIOS. LEFT COLUMN: ER=7.17, DENSITY=20.85 *kgm*$^{-3}$; RIGHT COLUMN: ER=5, DENSITY=30.13 *kgm*$^{-3}$

Table 5.25 summarises the structure characteristics of the gelatine foams made with surfactants "A" and C2 prepared at different expansion ratios.

Table 5.25 SUMMARY OF STRUCTURE CHARACTERISTICS OF GELATINE-SURFACTANT "A" AND GELATINE-SURFACTANT C2 FOAMS AT DIFFERENT EXPANSION RATIOS

ID	MAXIMUM CELL SIZE RANGE (mm)	TYPICAL CELL SIZE RANGE (mm)	MINIMUM CELL SIZE (mm)	PLATEAU BORDERS THICKNESS (mm)
ER1	1.6-4	0.2-0.6	0.06	0.02-0.06
ER2	1.6-4	0.2-0.6	0.06	0.02-0.06
ER3	1.6-4	0.3-0.7	0.06	0.02-0.06
ER4	1-4	0.2-0.6	0.07	0.02-0.07
ER5	1-4	0.2-0.5	0.06	0.02-0.1
ER6	1-3.5	0.2-0.5	0.06	0.01-0.06
ER7	1-3	0.15-0.3	0.05	0.01-0.8
ER8	1-3.5	0.2-0.5	0.05	0.01-0.07
ER9	1-3	0.1-0.3	0.05	0.01-0.1

The foam structure of the two gelatine-surfactant "A" formulations was studied with an image process technique (as explained in section 3.6.5 in Chapter 3) in an attempt to identify further influence of the expansion ratio on foam structure. Details of the table on cell size distribution of the gelatine-surfactant "A" foams can be found in Tables C.3 and C.4 in Appendix C.

The cell size distribution of the foams in each group was very similar. Most cells were below 0.5 *mm*. Higher ER ratios created less cells, leading to a less number of cells per unit area. However, the cells created exhibited similar sizes and not considerably cell size differences (cell growth) was found. This confirms the gelling process efficiency in stabilising the cellular structures.

The above arguments were supported by the visual assessment of the microscope images on the top surface of the dry foams. Figures 5.71 and 5.72 show similar cell sizes for different groups. ER3 shows slightly greater cell size than ER. This observation was also reflected in the image analysis carried out.

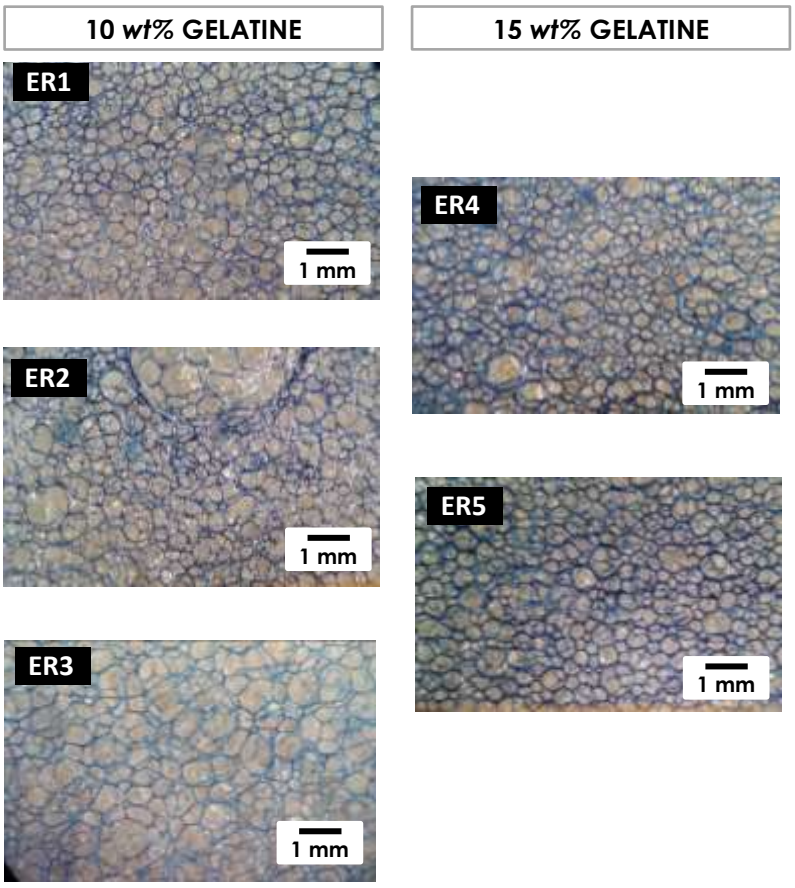

Figure 5.71. OPTICAL MICROSCOPE IMAGES OF THE TOP SURFACES OF THE DRY GELATINE-SURFACTANT "A" FOAMS AT DIFFERENT EXPANSION RATIOS (ER1 AT 6, ER2 AT 8, ER3 AT 9.7); AND (ER4 AT 6 AND ER5 AT 7.39)

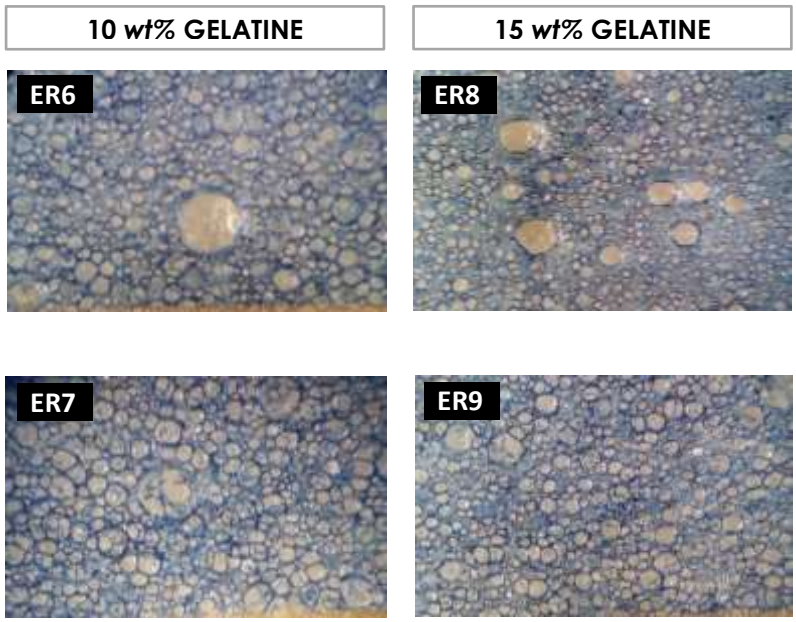

Figure 5.72. OPTICAL MICROSCOPE IMAGES OF THE TOP SURFACES OF THE DRY GELATINE-SURFACTANT C2 FOAMS AT DIFFERENT EXPANSION RATIOS (ER6 AT 5, ER7 AT 7.17); AND (ER8 AT 5 AND ER9 AT 6.46)

5.5.4 SUMMARY

This section aimed to identify the optimum expansion ratio levels for gelatine-surfactants "A" and C2 foams to produce the desired combination of density, low shrinkage and defects-free structure.

The maximum expansion ratios (MER) gave rise to lower total shrinkage and, generally, lighter foams for the two surfactants. Higher expansion ratios exhibited shorter drying time, which minimised total shrinkage, and higher porosity, which reduced density.

The lower expansion ratio gave rise to a denser cell structure, with thicker plateau borders, a greater number of oval-shape cells and less micropores.

In conclusion, the MER was identified as the optimum expansion ratio for gelatine surfactants "A" and C2 foams.

5.6. INFLUENCE OF PLASTICISER TYPE AND CONTENT ON GELATINE-SURFACTANTS "A" AND C2 FOAMS

This section focuses on the study of the effects of the incorporation of plasticisers (glycerol and sorbitol) on the foam structure and mechanical properties of gelatine-surfactant "A" and gelatine-surfactant C2 foams.

As discussed in Section 3.3.3.3.5, in Chapter 3, the following experimental factors and levels were considered during the preparation of the hydrogel foams studied in this section:

a. Gelatine content. Two levels were investigated: low (10 *wt%*) and high (15 *wt%*)

b. Plasticiser type. Two types of plasticisers were used: glycerol and sorbitol

c. Plasticiser content. For gelatine surfactant "A" foams, four levels were studied. For gelatine-surfactant C2 foams, two levels were studied to simplify the experiments.

This investigation was based on formulations A7 and A9, for foams made of surfactant "A"; and C2.1 and C2.3 for foams made of surfactant C2.1. Tables 5.26 and 5.27 show the experimental matrix of gelatine foams made with-surfactants "A" and C2, respectively. The formulation details can be seen in Section 3.3.3.3.5, in Chapter 3.

Table 5.26 EXPERIMENTAL MATRIX FOR THE STUDY OF THE EFFECTS OF PLASTICISERS IN HYDROGEL-SURFACTANT "A" FOAMS

ID	PLASTICISER TYPE	GELATINE CONTENT (*wt%*)	PLASTICISER CONTENT * (*wt%*)
SA1	sorbitol	10	1
SA2			2
SA3			3
SA4			4
SA5		15	1
SA6			2
SA7			3
SA8			4
GA1	glycerol	10	1
GA2			2
GA3			3
GA4			4
GA5		15	1
GA6			2
GA7			3
GA8			4

**Content based on the total weight of the gelatine-water solution*
Notes: Surfactant "A" content was constant at 1.5wt%
The processing temperature was kept constant at 50°C

Table 5.27 EXPERIMENTAL MATRIX FOR THE STUDY OF THE EFFECTS OF PLASTICISERS IN HYDROGEL-SURFACTANT C2 FOAMS

ID	PLASTICISER TYPE	GELATINE CONTENT (*wt%*)	PLASTICISER CONTENT* (*wt%*)
SS1	sorbitol	10	1
SS2		10	4
SS3		15	1
SS4		15	4
SG1	glycerol	10	1
SG2		10	4
SG3		15	1
SG4		15	4

**Content based on the total weight of the gelatine-water solution*
Note: Surfactant C2 content was constant at 0.74wt%
The processing temperature was kept constant at 50°C

Section 5.6.1 investigates the relationship between MER and the experimental factors. Section 5.6.2, focuses on the relationship between drying shrinkage and the

experimental factors in an attempt to identify conditions that lead to desirable low foam shrinkage levels. Then, Section 5.6.3 assess the effect of plasticer type and content on foam density. The cell structure of the solid foams was characterised in Section 5.6.4 with SEM and optical microscopy. Finally, Section 5.6.5 reports the analysis of the mechanical properties.

5.6.1 EXPANSION RATIO OF GELATINE-SURFACTANT-PLATICISER FOAMS

The gelatine-surfactant-plasticisers solutions were foamed for 10 minutes and their MER was recorded, as explained in section 3.5.1, in chapter 3.

ANOVA testing was carried out for surfactants A and C2 separately. Full factorial 2x2x3 (for foams made with surfactant "A") and 2x2x2 (for foams made with surfactant C2) designs with two replicates were used to calculate the statistical significance of *the design parameters* (gelatine content, plasticiser type and plasticiser content) in MER. The foams containing surfactant "A" were studied at four plasticiser content levels but for statistical analysis just three levels were studied, as the higher level implied some difficulties in measuring some of the outcomes (i.e. density). Further information about the statistical analysis can be found in section 3.3.2 in Chapter 3.

The hypotheses for these experiments were:

a. The null hypotheses (H_O): there was no difference in MER for different combinations of the three design parameters.

b. The alternative hypotheses (H_1): there was a difference in MER for different combinations of the three design parameters.

5.6.1.1 Foams containing surfactant "A"

The maximum MER of the surfactant "A" foams prepared with sorbitol and glycerol was 8.04 and 9.17, respectively; while their minimum MER was 6.34 (sorbitol) and 6.83 (glycerol), as presented in Figure 5.73.

Lower MER was achieved for foams made with sorbitol than those made with glycerol at both gelatine concentrations studied, as shown in Figure 5.73. Thomazine, Carvalho and Sobral (2016) studied the rheology of gelatine-plasticisers solutions and found that gelatine blends plasticised with glycerol exhibited higher tan(d) and lower storage modulus (G') than those plasticised with sorbitol due to the glycerol lower molecular weight compared to sorbitol's. This means glycerol solutions exhibit lower viscosities and a more 'liquid-like' behaviour than sorbitol.

The incorporation of sorbitol/glycerol slightly decreased the expansion ratio achieved when compared with the formulations they were based on (A7, MER=9.7, and A9, MER=7.39). This may be attributable to a higher solid content (and consequently slight viscosity increase) of the foams containing sorbitol/glycerol.

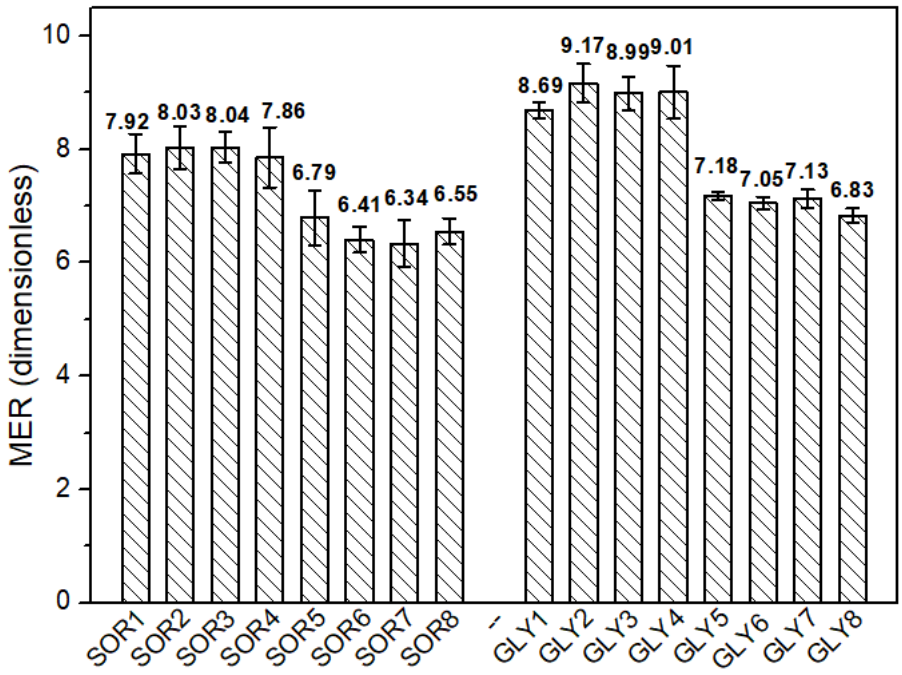

Figure 5.73. EXPANSION RATIO OF THE GELATINE-SURFACTANT "A"-SORBITOL FOAMS (SOR1-8) AND GELATINE-SURFACTANT "A"-GLYCEROL FOAMS (GLY1-8)

The ANOVA table for the MER of gelatine-surfactant "A"-plasticisers foams with a level of significance of 0.05 can be seen in Table A.11 (Appendix A). From the ANOVA test results, it can be said that there was a strong evidence that the MER varied just with gelatine content ($F=47.14$, $p<0.001$), as discussed in Section 5.4,1 but not the other two parameters studied, plasticiser type and content.

5.6.1.2 Foams containing surfactant C2

The maximum MER of the surfactant C2 foams prepared with sorbitol and glycerol was 7.07 and 7.02, respectively; while their minimum MER was 6.26 (sorbitol) and 6.37 (glycerol), as presented in Figure 5.74.

The MER of foams made with sorbitol and glycerol exhibited similar values, so a not considerable effect of plasticiser type on MER was found. In addition to this, the incorporation of sorbitol/glycerol into foams made with surfactant C2 did not considerable affect the MER compared with the formulations they were based on (C2.1, MER=7.17, and C2.3, MER=6.64). These results may be attributable to a lower contribution to density increase from the plasticisers compared to the one from the surfactant C2 incorporation.

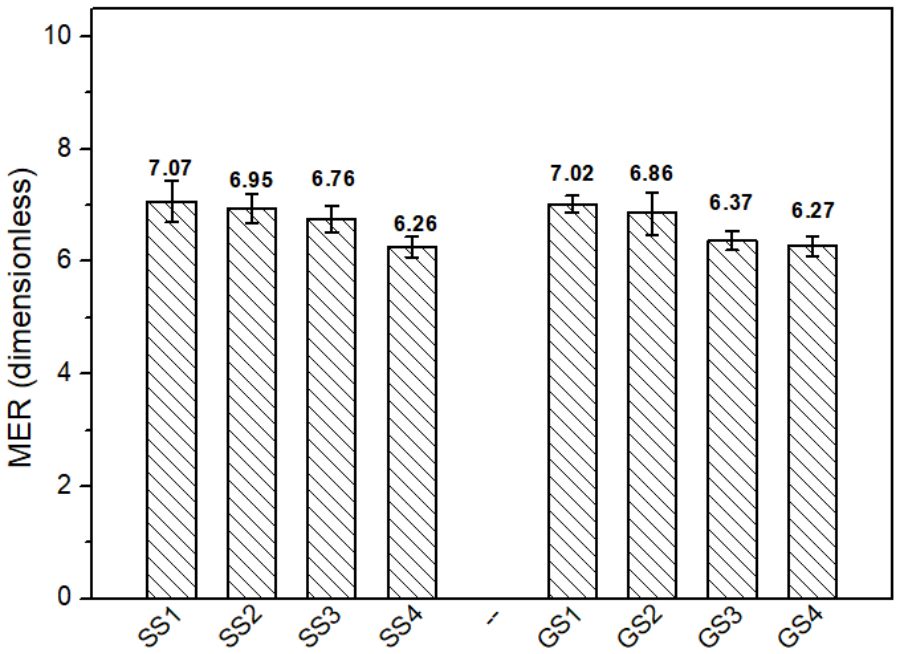

Figure 5.74. EXPANSION RATIO OF THE GELATINE-SURFACTANT C2-SORBITOL FOAMS (SS1-SS4) AND GELATINE-SURFACTANT C2 GLYCEROL FOAMS (GS1-GS4)

The ANOVA table for the MER of gelatine-surfactant C2-plasticisers foams with a level of significance of 0.05 can be seen in Table A.12 (Appendix A). From the ANOVA test results, it can be said that there was a strong evidence that the MER varied with gelatine content (F=20.33, p=0.002), as discussed in Section 5.4,1 but not the other two parameters studied, plasticiser type and content.

5.6.2 TOTAL SHRINKAGE

This section studies the total shrinkage of foams containing surfactants "A" and C2 from the volume difference between that of the cast liquid foam and that of the dry foam, as described in section 3.6.4 in Chapter 3.

ANOVA testing was carried out for surfactants "A" and C2 separately. Full factorial 2x2x3 (for foams made with surfactant "A") and 2x2x2 (for foams made with surfactant C2) designs with three replicates were used to calculate the statistical significance of *the design parameters* (gelatine content, plasticiser type and plasticiser content) in total shrinkage. The foams containing surfactant "A" were studied at four plasticiser content levels but for statistical analysis just three levels were studied, as the higher level implied some difficulties in sample measuring. The higher plasticiser content samples were too soft and their handling involved sample distortion which affected the total volume of the sample. Further information about the statistical analysis can be found in section 3.3.2 in Chapter 3.

The hypotheses for these experiments were:

a. The null hypotheses (H_O): there was no difference in total shrinkage for different combinations of the three design parameters.

b. The alternative hypotheses (H_1): there was a difference in total shrinkage for different combinations of the three design parameters.

5.6.2.1 Foams containing surfactant "A"

The total shrinkage of the surfactant "A" foams prepared with sorbitol and glycerol at 10 *wt%* gelatine content was 42.36-45% and 34.72-38.61% for sorbitol and glycerol, respectively, while the total shrinkage of 15 *wt%* gelatine foams was 30.42-33.19% and 22.78-34.58% for sorbitol and glycerol, respectively. These results did not include the shrinkage of foams including 4 *wt%* plasticiser as they were considerably malleable and sample preparation was not possible without affecting the sample volume, which may affect the test reliability. However, this issue confirmed the effectivity of the plastification process.

Figure 5.75 illustrates the total shrinkage of the gelatine-surfactant "A"-plasticisers foams.

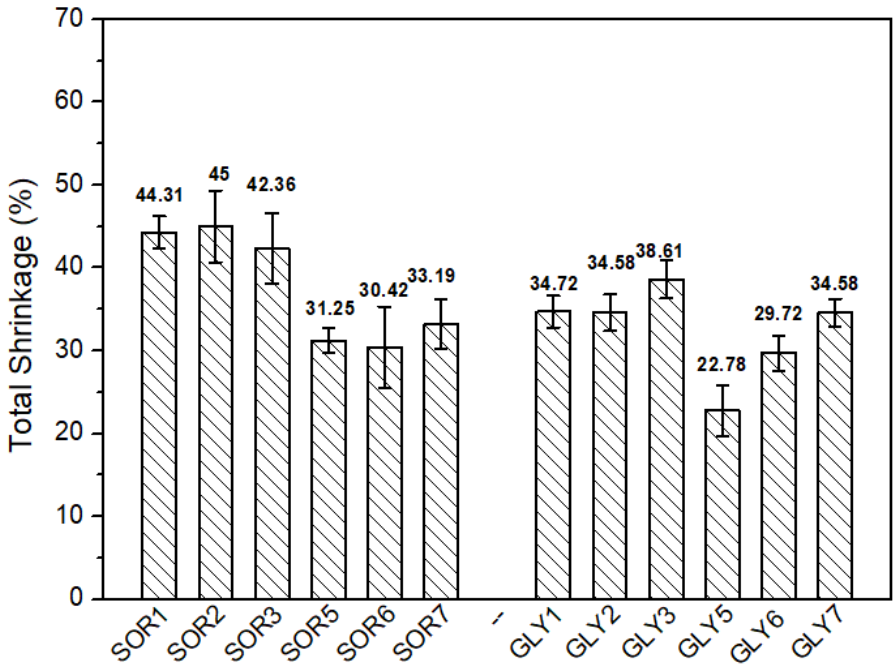

Figure 5.75. TOTAL SHRINKAGE OF THE GELATINE-SURFACTANT "A"-SORBITOL FOAMS (SOR1-3 AND SOR 5-7) AND GELATINE-SURFACTANT "A"-GLYCEROL FOAMS (GLY1-3 AND GLY 5-7)

As previously mentioned, this experiment was based on samples A7 (10 *wt%* gelatine content and shrinkage=43%) and A9 (15 *wt%* gelatine content and shrinkage=31%). Thus, the incorporation of sorbitol did not seem to affect the shrinkage of both 10 *wt%* and 15 *wt%* gelatine content foams, as foams including sorbitol exhibited virtually the

same shrinkage than samples A7 and A9. Glycerol, incorporation, however, considerably decreased 'A7' shrinkage and decreased or maintained that from A9.

Total shrinkage generally increased as plasticiser content increased, and more considerably for glycerol.

The ANOVA table for the total shrinkage of gelatine-surfactant "A"-plasticisers foams with a level of significance of 0.05 can be seen in Table A.13 (Appendix A). The ANOVA test confirmed the conclusions carried out above, and it can be said that there was a strong evidence that the total shrinkage varied with the three factors studied, gelatine content ($F=47.69$, $p<0.001$), plasticiser type ($F=31.89$, $p<0.000$) and plasticiser content ($F=24.49$, $p<0.001$). Figure B.6 (see Appendix B) shows the main effects plot for the shrinkage of foams made with surfactant "A"

The gelatine content-plasticiser type ($F=5.44$, $p<0.028$), gelatine content-plasticiser content ($F=19.08$, $p<0.001$) and plasticiser type-plasticiser content interactions ($F=3.92$, $p<0.034$) interactions were also statistically significant.

As seen in Figure B.7.A (gelatine content-plasticiser type interaction), the shrinkage level difference between sorbitol and glycerol foams was more significant at lower gelatine concentrations.

Regarding the gelatine content-plasticiser content interaction, at 10 *wt%* gelatine content, the plasticiser content had little effect but, at 15 *wt%* gelatine content the different plasticiser concentrations incorporated into the formula led to considerable differences in shrinkage level.

At 10 *wt%* gelatine content, plasticiser content did not have a significant effect on total shrinkage, but at 15 *wt%*, shrinkage increased as plasticiser content increased (see Figure B.7.B in Appendix B, gelatine content-plasticiser content interaction).

Finally, the interaction between plasticiser type and content (see Figure B.7C) meant that as plasticiser content increased, the shrinkage decrease effect of glycerol was less significant tan that in sorbitol.

As illustrated in Figure 5.76 the shrinkage patterns were the same as those observed in Section 5.4.2.1 (i.e. concave, on the top surface, and convex, on the bottom) and no central voids were shown. The overall shrinkage was generally comparable to that on section 5.4.2 for samples A7 and A9, excepting at the highest plasticiser contents, where total shrinkage surpassed 50% (estimated).

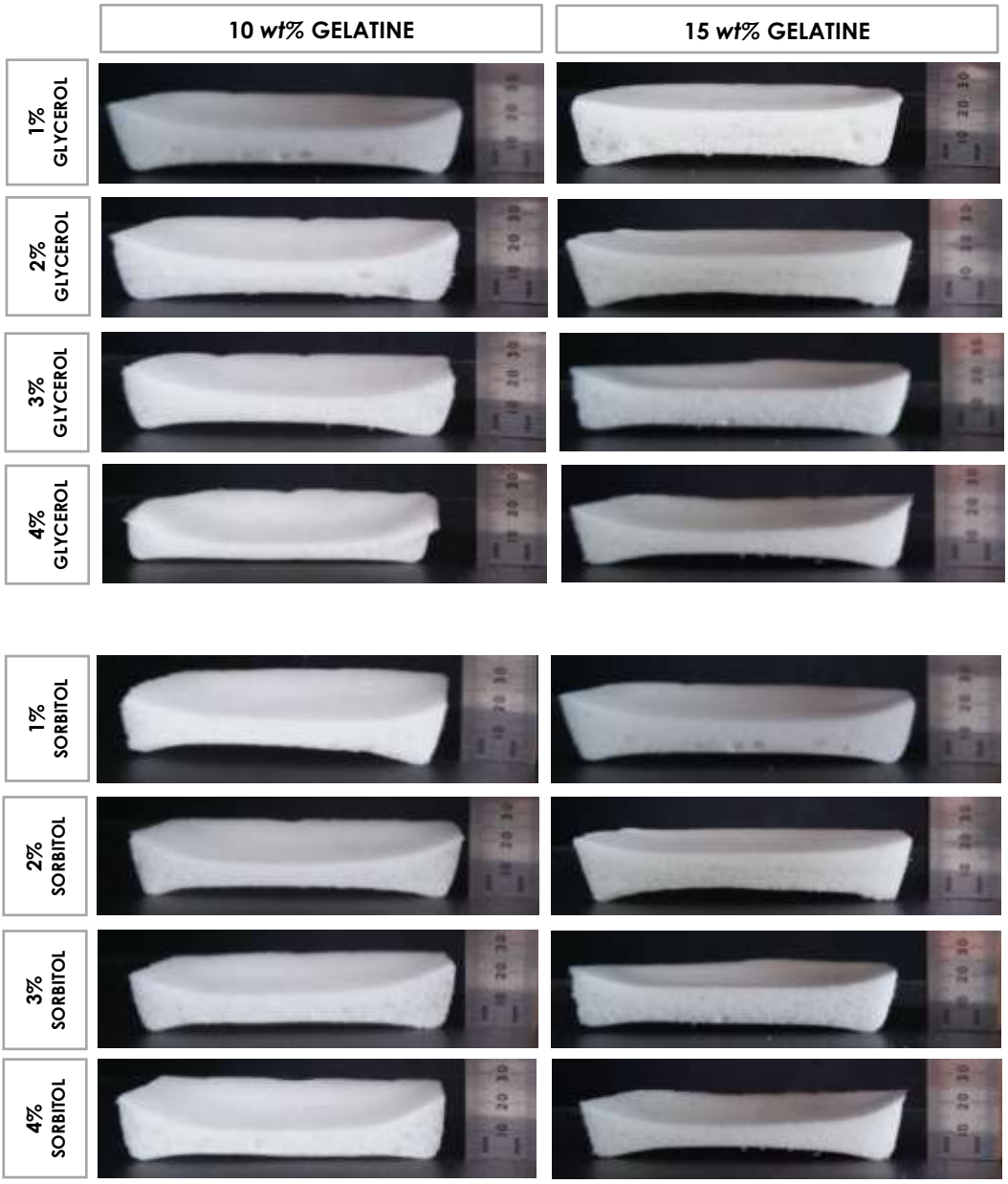

Figure 5.76 CROS-SECTIONS OF THE GELATINE-SURFACTANT "A" DRY FOAMS CONTAINING DIFFERENT PLASTICISERS (A) GLYCEROL (B) SORBITOL

5.6.2.2 Foams containing surfactant C2

This section compares the shrinkage of surfactant C2 foams prepared with plasticisers at 2 and 4 *wt%.* The *plasticiser content* factor was studied at two levels instead of four due to the relatively low differences found in the previous section when the plasticiser varied 1 *wt%*. In this case, the samples prepared at 4 *wt%* were still more malleable than those prepared at 2 *wt%,* but in contrast to the experience with surfactant "A" foams (4 *wt%* plasticiser foams were too deformable to handle), sample preparation was allowed without compromising reliability.

However, the comparison between the shrinkage of surfactants "A" and C2 might be ambiguous due to the difference between the test design (e.g. different plasticiser content levels studied).

This experiment was based on samples C2.1 (10 *wt%* gelatine content and shrinkage=11.25%) and C2.3 (15 *wt%* gelatine content and shrinkage=22.69%). Thus, the incorporation of both sorbitol and glycerol considerably increased the foams shrinkage. This effect was higher as plasticiser content increased. This trend was not in accordance with the one observed for surfactant "A" foams where sorbitol did not have a considerable effect on the original total shrinkage, but glycerol actually decreased it. However, mentioned before the results between the two surfactants might not be comparable.

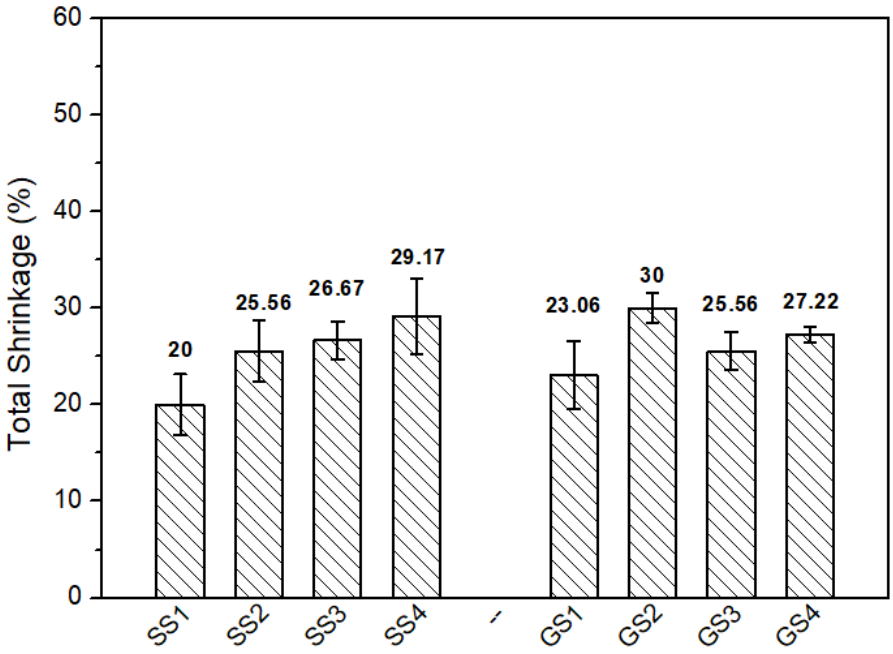

Figure 5.77. TOTAL SHRINKAGE OF THE GELATINE-SURFACTANT C2-SORBITOL FOAMS (SS1-SS4) AND GELATINE-SURFACTANT "A"-GLYCEROL FOAMS (GS1-GS4)

The ANOVA table (see Table A.14 in Appendix A) for the total shrinkage of gelatine-surfactant C2-plasticisers foams shows there was a strong evidence that the total shrinkage varied with gelatine ($F=11.75$, $p<0.001$) and plasticiser content ($F=27.67$, $p<0.001$) contents. However, plasticiser type was not found statistically significant, in other words, the type of plasticiser used did not significantly affect the total shrinkage. Table B.8 (Appendix B) shows the main effect plots for the total shrinkage.

The gelatine-plasticiser content interaction ($F=7.84$, $p<0.039$) was also found significant. At higher plasticiser contents, the increase in total shrinkage was more significant at lower gelatine content (10 *wt%*), as opposed to findings in Section 5.6.2.1. Table B.9 (Appendix B) shows the interaction plots for gelatine-plasticiser content.

As presented in Figure 5.78 the shrinkage patterns were the same as those observed in Section 5.4.2.2. 10 *wt%* gelatine-C2-plasticiser foams exhibited slightly higher shrinkage than that on sample C2.1.

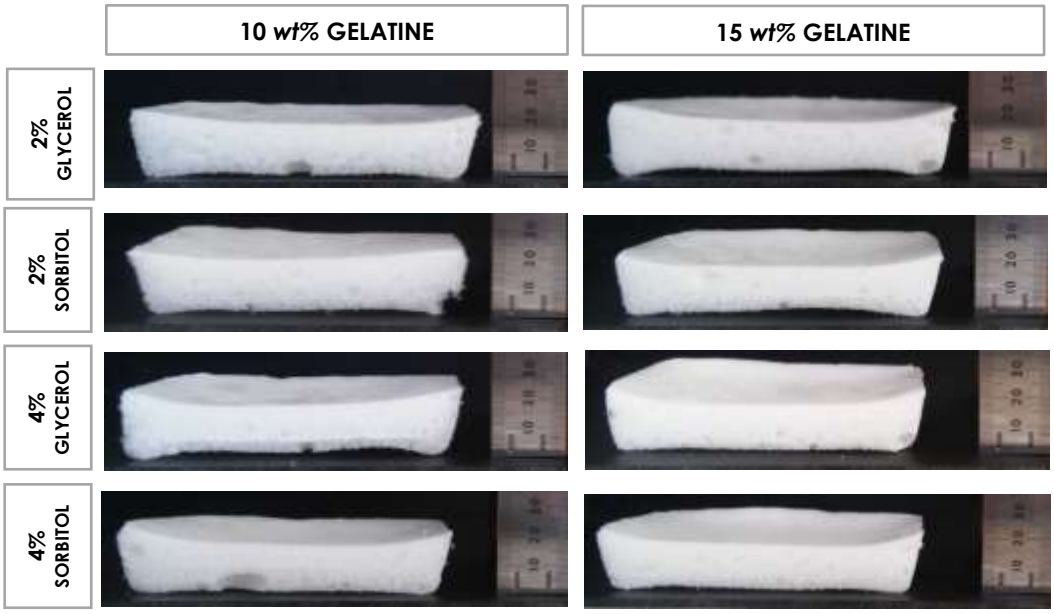

Figure 5.78 CROS-SECTIONS OF THE GELATINE-SURFACTANT C2 DRY FOAMS CONTAINING DIFFERENT PLASTICISERS

5.6.3 MATRIX DENSITY, FOAM DENSITY, RELATIVE DENSITY AND POROSITY

This section studies the density, relative density and porosity of the dry gelatine-surfactant-plasticisers foams. The measurements were carried out following the procedures described in section 3.6.2 in Chapter 3.

ANOVA testing was carried out for surfactants "A" and C2 separately. Full factorial 2x2x3 (for foams made with surfactant "A") and 2x2x2 (for foams made with surfactant C2) designs with three replicates were used to calculate the statistical significance of *the design parameters* (gelatine content, plasticiser type and plasticiser content) in density.

The hypotheses for these experiments were:

a. The null hypotheses (H_O): there was no difference in density for different combinations of the three design parameters.

b. The alternative hypotheses (H_1): there was a difference in density for different combinations of the three design parameters.

5.6.3.1 Foams containing surfactant "A"

As shown in Table 5.28, plasticised low densities foams were produced. For 10 *wt%* gelatine content-sorbitol foams, density ranged from 15.06 kg/m^3 (sample SOR1, with 98.66% porosity) to 18.40 kg/m^3 (Sample SOR4, with 98.44% porosity). For 10 *wt%* glycerol containing foams, density ranged from 16.47 *wt%* (sample GLY1, with 98.48% porosity) to 17.37 kg/m^3 (sample GLY4 density was not measured because of the difficulties in sample cutting, as previously stated). Compared to A7 density, (11.09 kg/m^3), foams made with plasticiser gave rise to denser foams. The same trend was found for foams made at 15 *wt%* gelatine.

Thus, foam density steadily increased (when compared to that for A7 and A9) as plasticiser content increased, but the type of plasticiser used did not seem to considerably affect the foam density increase.

Table 5.28 DENSITY, MATRIX DENSITY, RELATIVE DENSITY AND POROSITY OF DRY GELATINE-SURFACTANT "A"-PLASTICISERS FOAMS

ID	FOAM DENSITY (kg/m^3)	MATRIX DENSITY (kg/m^3)	RELATIVE DENSITY (%)	POROSITY (%)
SOR1	15.06±1.91	1,120±46.29	1.34	98.66
SOR2	15.89±1.38	1,150±21.92	1.38	98.62
SOR3	17.05±1.57	1,160±10.86	1.47	98.53
SOR4	18.40±1.25	1,180±107.46	1.56	98.44
SOR5	28.44±1.54	1,120±95.73	2.54	97.46
SOR6	32.02±1.47	1,150±100.33	2.78	97.22
SOR7	32.36±2.42	1,150±74.48	2.81	97.19
SOR8	34.73±1.41	1,200±56.09	2.89	97.11
GLY1	16.47±0.70	1,080±75.78	1.52	98.48
GLY2	17.37±0.68	1,060±27.18	1.64	98.36
GLY3	16.83±0.86	1,110±23.09	1.52	98.48
GLY4*		1,170		
GLY5	26.91±1.19	1,160±67.32	2.32	97.68
GLY6	30.10±2.71	1,160±46.85	2.59	97.41
GLY7	32.84±3.57	1,200±39.65	2.74	97.26
GLY8	43.15±1.67	1,200±68.42	3.60	96.40

*No data available

Figure 5.79 illustrates the density of the dry gelatine-surfactant "A"-plasticiser foams.

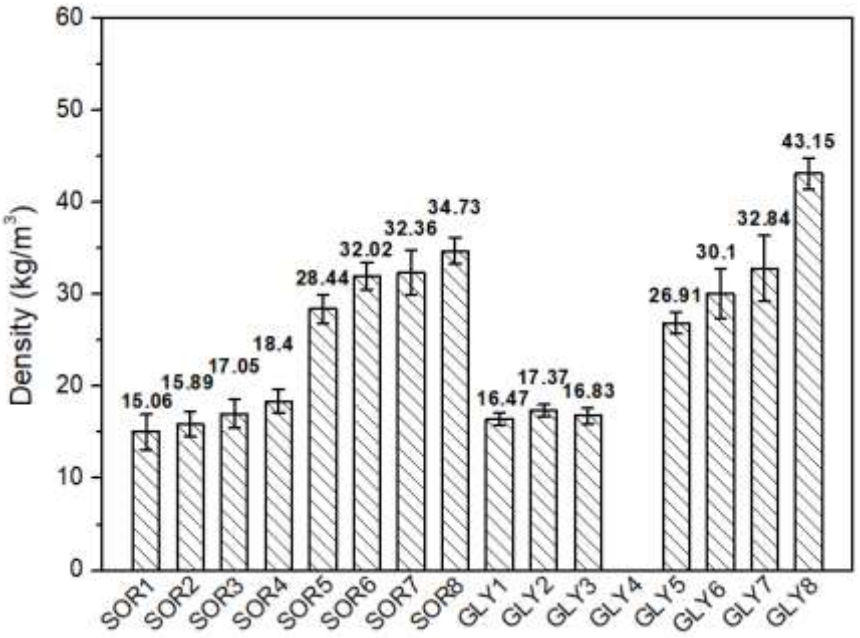

Figure 5.79 DENSITY OF THE DRY GELATINE-SURFACTANT "A"-PLASTICISER FOAMS

All matrices had different compositions, as shown in Table 5.29, including slightly different residual moisture content (see Section 3.6.3, Chapter 3, for details in moisture content measuring).

Table 5.29 COMPOSITION OF DRY GELATINE-SURFACTANT "A"-PLASTICISER FOAMS

ID	GELATINE CONTENT (wt%)	WATER CONTENT (wt%)	SURFACTANT CONTENT (wt%)	PLASTICISER TYPE	PLASTICISER CONTENT (wt%)
SOR1	67.50	15.62	10.13	Sorbitol	6.75
SOR2	63.90	13.74	9.58		12.78
SOR3	57.96	15.96	8.69		17.39
SOR4	56.62	12.24	8.49		22.65
SOR5	73.28	14.51	7.33	Sorbitol	4.89
SOR6	69.71	14.02	6.97		9.30
SOR7	67.66	12.04	6.77		13.53
SOR8	63.10	13.76	6.31		16.83
GLY1	68.25	14.69	10.24	Glycerol	6.82
GLY2	65.36	11.76	9.80		13.07
GLY3	61.45	10.9	9.22		18.43
GLY4	54.21	15.97	8.13		21.69
GLY5	73.30	14.48	7.33	Glycerol	4.89
GLY6	70.00	13.67	7.00		9.33
GLY7	65.24	15.19	6.52		13.05
GLY8	62.52	14.56	6.25		16.67

The ANOVA table for density of gelatine-surfactant "A"-plasticisers foams with a level of significance of 0.05 can be seen in Table A.15 (Appendix A). The ANOVA test

confirmed the comments above as there was evidence that density varied with gelatine content ($F=847.71$, $p<0.001$) and plasticiser content ($F=14.25$, $p<0.001$). Plasticiser type was not statistically significant. Figure B.10 (see Appendix B) shows the main effects plots for density of foams made with surfactant "A".

The gelatine content-plasticiser content ($F=5.16$, $p=0.009$) interaction was also statistically significant. The plasticiser content had a greater effect at higher gelatine content (15 *wt%*). Figure B.11 (see Appendix B) shows the main effects plot for this interaction.

5.6.3.2 Foams containing surfactant C2

As presented in Table 5.30, sorbitol containing foams density ranged from 22.63 kg/m^3 (sample SS1, with 98.05% porosity) to 49.24 kg/m^3 (Sample SS4, with 95.93% porosity). Glycerol foams density ranged from 22.90 kg/m^3 (sample GS1, with 97.96% porosity) to 47.65 kg/m^3 (sample GS4, with 96% porosity).

As presented in Table 5.30, 10 *wt%* gelatine content-sorbitol foams, density ranged from 22.63 kg/m^3 (sample SS1, with 98.05% porosity) to 31.77 kg/m^3 (Sample SS2, with 97.31% porosity). For 10 *wt%* glycerol containing foams, density ranged from 22.90 *wt%* (sample GS1 with 97.96% porosity) to 30.86 kg/m^3 (sample GS2, with 97.27% porosity). Compared to C2.1 foams density (20.85 kg/m^3), foams made with lower plasticiser content (2 *wt%*) had little effect on density, but at higher plasticiser content (4 *wt%*) density increased compared to that of C2.1. The same trend was generally found for foams made at 15 *wt%* gelatine. Thus, foam density steadily increased (when compared to that for C2.1 and C2.3 as plasticiser content increased. Sorbitol led to slightly higher densities compared to glycerol.

Table 5.30 DENSITY, MATRIX DENSITY, RELATIVE DENSITY AND POROSITY OF DRY GELATINE-SURFACTANT C2-PLASTICISERS FOAMS

ID	DENSITY (kg/m^3)	MATRIX DENSITY (kg/m^3)	RELATIVE DENSITY (%)	POROSITY (%)
SS1	22.63±0.56	1,160±57.86	1.95	98.05
SS2	31.77±0.96	1,180±62.87	2.69	97.31
SS3	44.16±2.63	1,200±21.83	3.68	96.32
SS4	49.24±2.67	1,210±54.12	4.07	95.93
GS1	22.90±0.83	1,120±94.75	2.04	97.96
GS2	30.86±0.87	1,130±58.79	2.73	97.27
GS3	36.89±0.81	1,160±37.56	3.18	96.82
GS4	47.65±0.89	1,190±36.06	4.00	96.00

Figure 5.80 illustrates the density of the dry gelatine-surfactant C2-plasticiser foams.

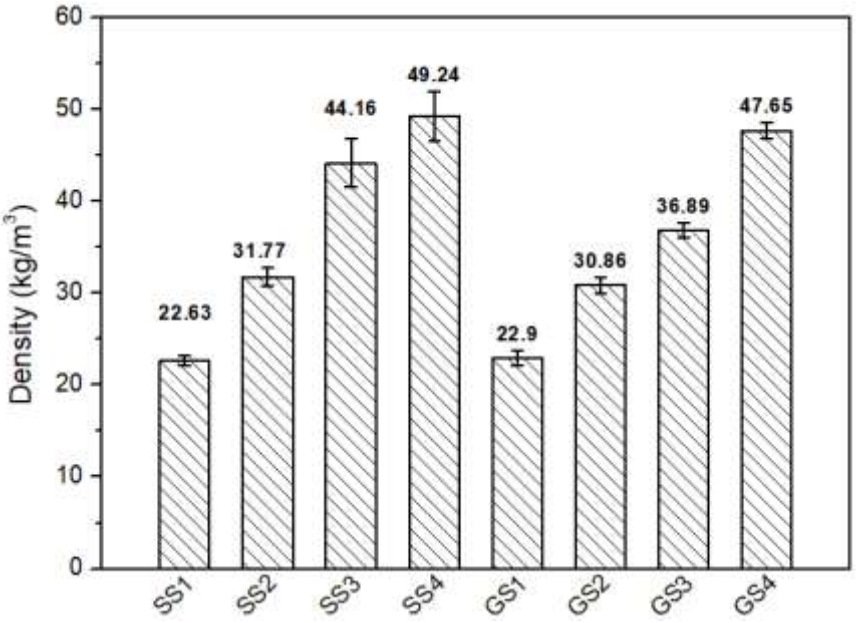

Figure 5.80 DENSITY OF THE DRY GELATINE-SURFACTANT C2-PLASTICISER FOAMS

Table 5.31 presents the composition of the dry gelatine-surfactant C2-plasticiser foams.

Table 5.31 COMPOSITION OF DRY GELATINE-SURFACTANT C2-PLASTICISER FOAMS

ID	Gelatine content (wt%)	Water content (wt%)	Surfactant content (wt%)	Plasticiser type	Plasticiser content (wt%)
SS1	67.82	13.53	5.09	Sorbitol	13.56
SS2	59.58	12.12	4.47		23.83
SS3	73.04	13.57	3.65		9.74
SS4	67.78	10.75	3.39		18.08
GS1	67.22	14.29	5.04	Glycerol	13.44
GS2	55.79	17.71	4.18		22.32
GS3	72.67	14.01	3.63		9.69
GS4	65.10	14.29	3.25		17.36

ANOVA (see Table A.16, in Appendix A) shows there is evidence that density varied with gelatine content ($F=1342$, $p<0.001$), plasticiser type ($F=24.89$, $p<0.001$) and plasticiser content ($F=299.19$, $p<0.001$). Figure B.12 (see Appendix B) shows the main effects plot for density of foams made with surfactant C2.

The gelatine content-plasticiser type ($F=18.63$, $p<0.001$) and the plasticiser type-plasticiser content ($F=5.60$, $p<0.001$) interactions were also statistically significant. Plasticiser type had a more significant effect at higher gelatine and plasticiser content. Sorbitol produces higher density foams than glycerol at both higher and plasticiser content (see Figure B.13, in Appendix B).

5.6.4 STRUCTURE

Figure 5.81 compares the structure of 15 *wt%* gelatine foams with 4 *wt%* content of each plasticiser (i.e. sorbitol and glycerol). As observed in Section 5.4.4, all the foam exhibited an open-cell structure arranged in macropores holding micropores. The incorporation of the plasticisers at 4 *wt%* into all the foams solutions produced relatively more ordered cellular structures compared to A9 (for those made with surfactant "A") and C2.3 (for those made with surfactant C2) with thicker edges and vertexes. Cells in the top layers were relatively elongated and distorted due to the considerable shrinkage. No considerable difference was found between foams made with glycerol and sorbitol.

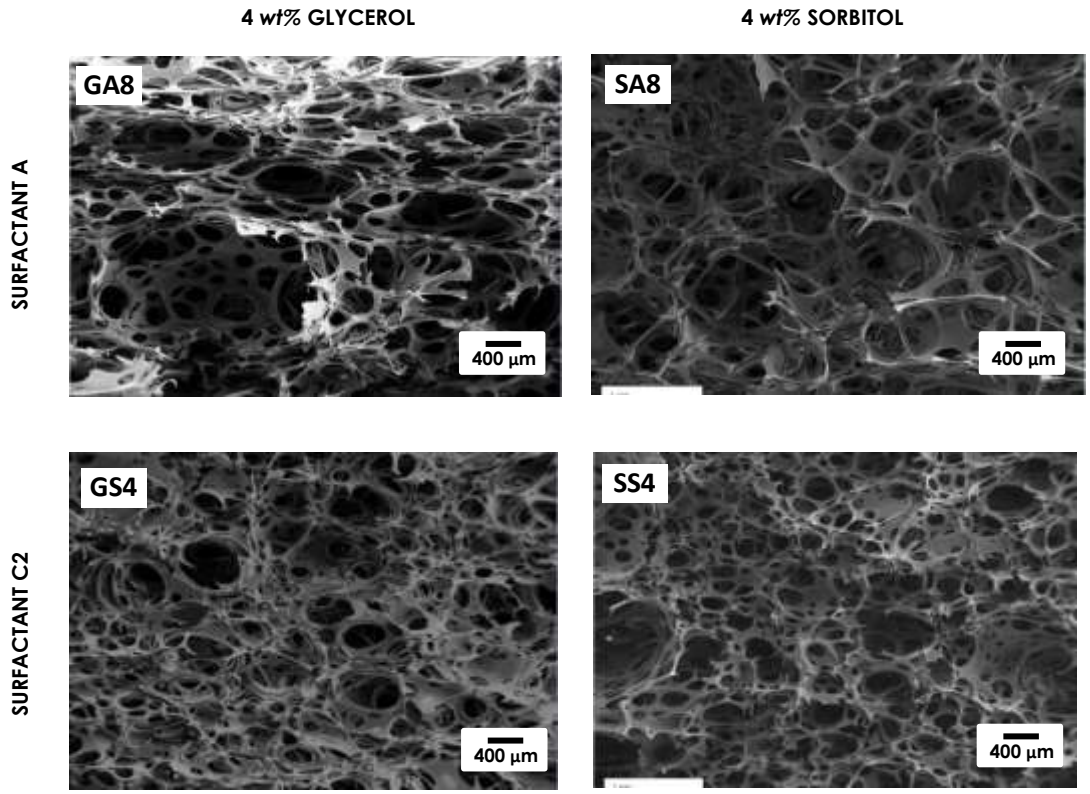

Figure 5.81 COMPARISON OF 15 *wt%* GELATINE FOAMS MADE WITH SURFACTANTS "A" AND C2 AND 4 *wt%* GLYCEROL AND SORBITOL

Figure 5.82 and 5.83 exhibit the optical microscope images of the surface of the surfactant "A" foams made with sorbitol and glycerol, respectively. No considerable effect of plasticiser type and content on microstructure was found.

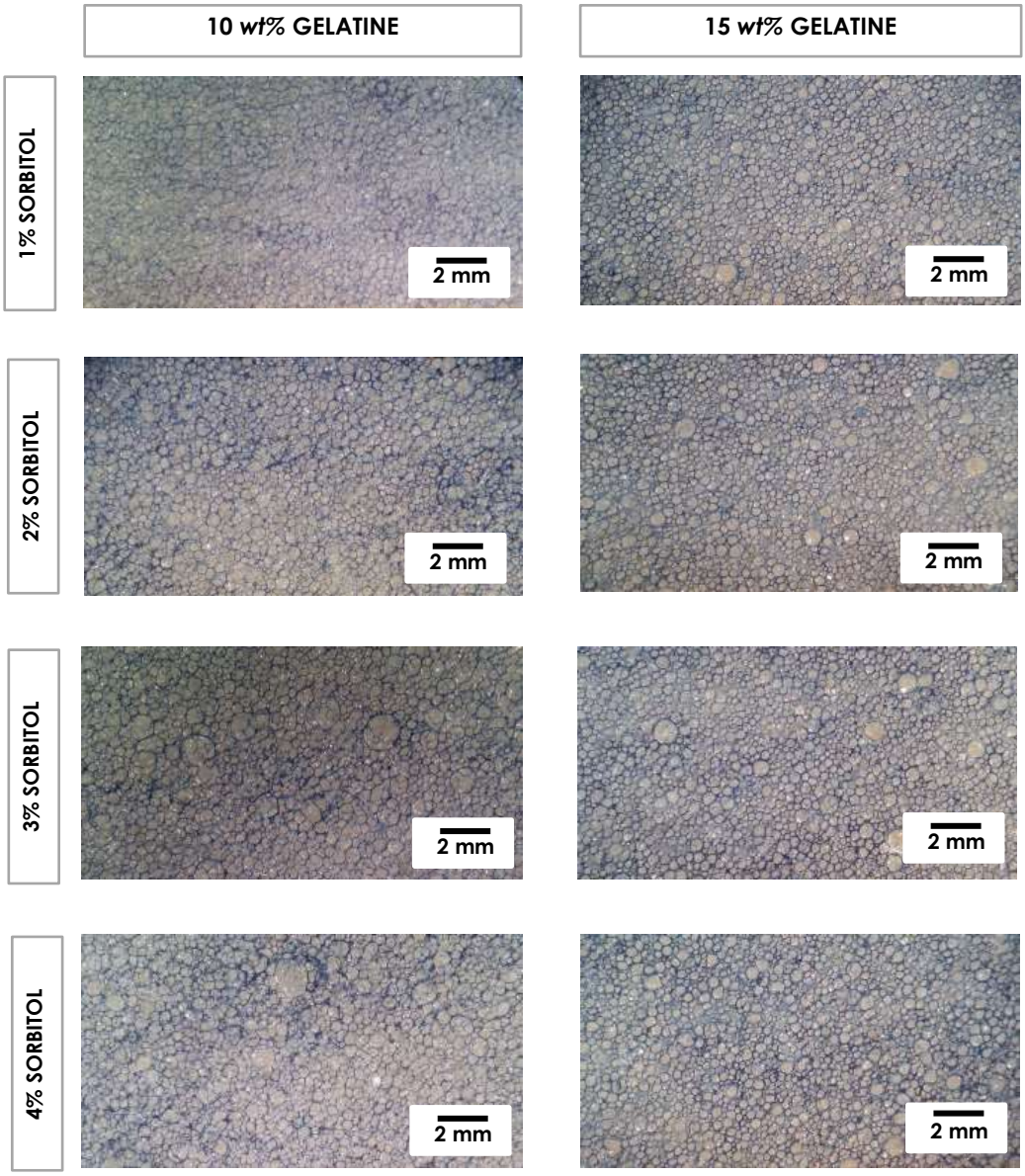

Figure 5.82. TOP SURFACE OF THE GELATINE-SURFACTANT "A"-SORBITOL FOAMS

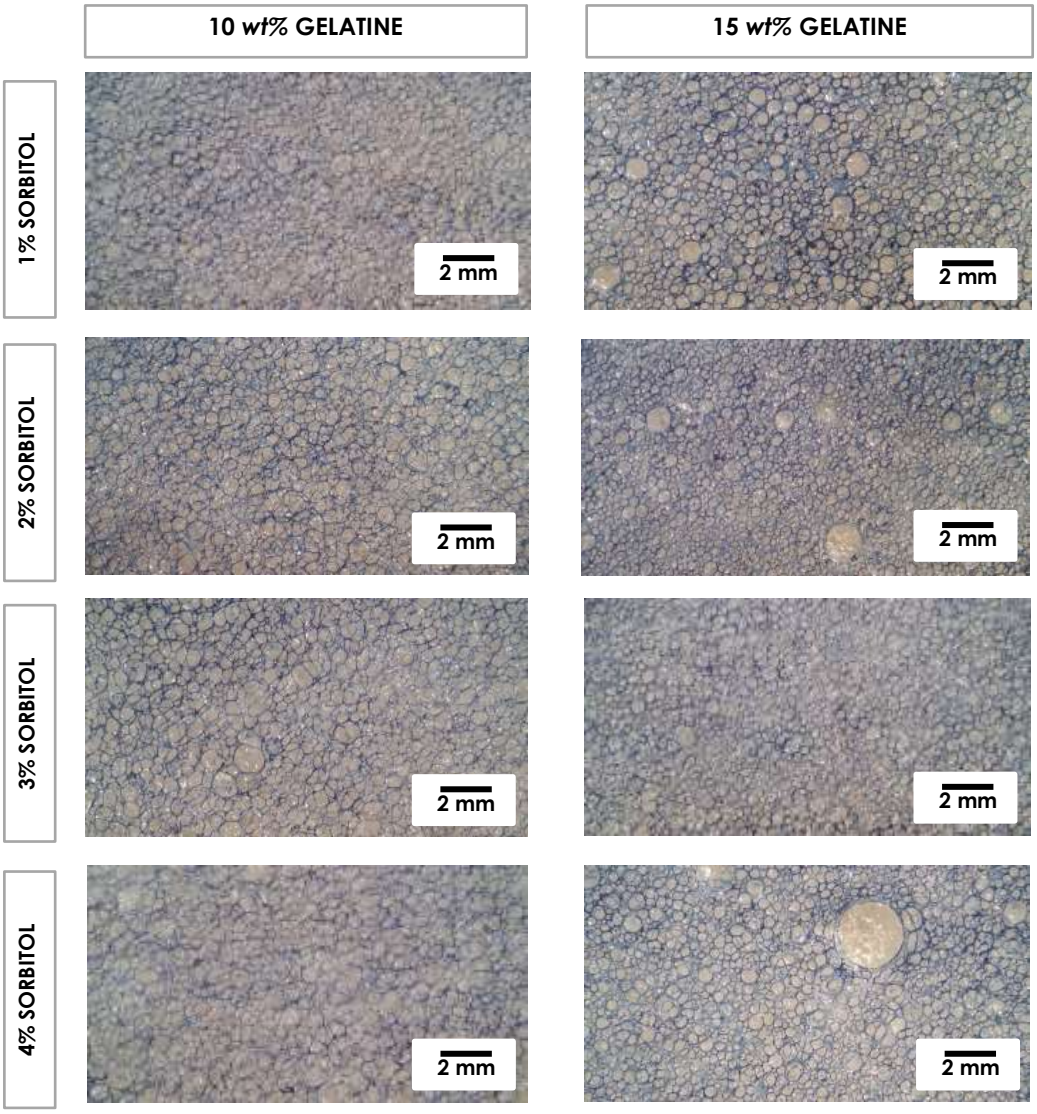

Figure 5.83. TOP SURFACE OF THE GELATINE-SURFACTANT "A"-GLYCEROL FOAMS

Figure 5.84 exhibits the top surface of gelatine-surfactant C2-plasticisers foams. No significant effect of plasticiser type and content was found between them and samples C2.1 and C2.3.

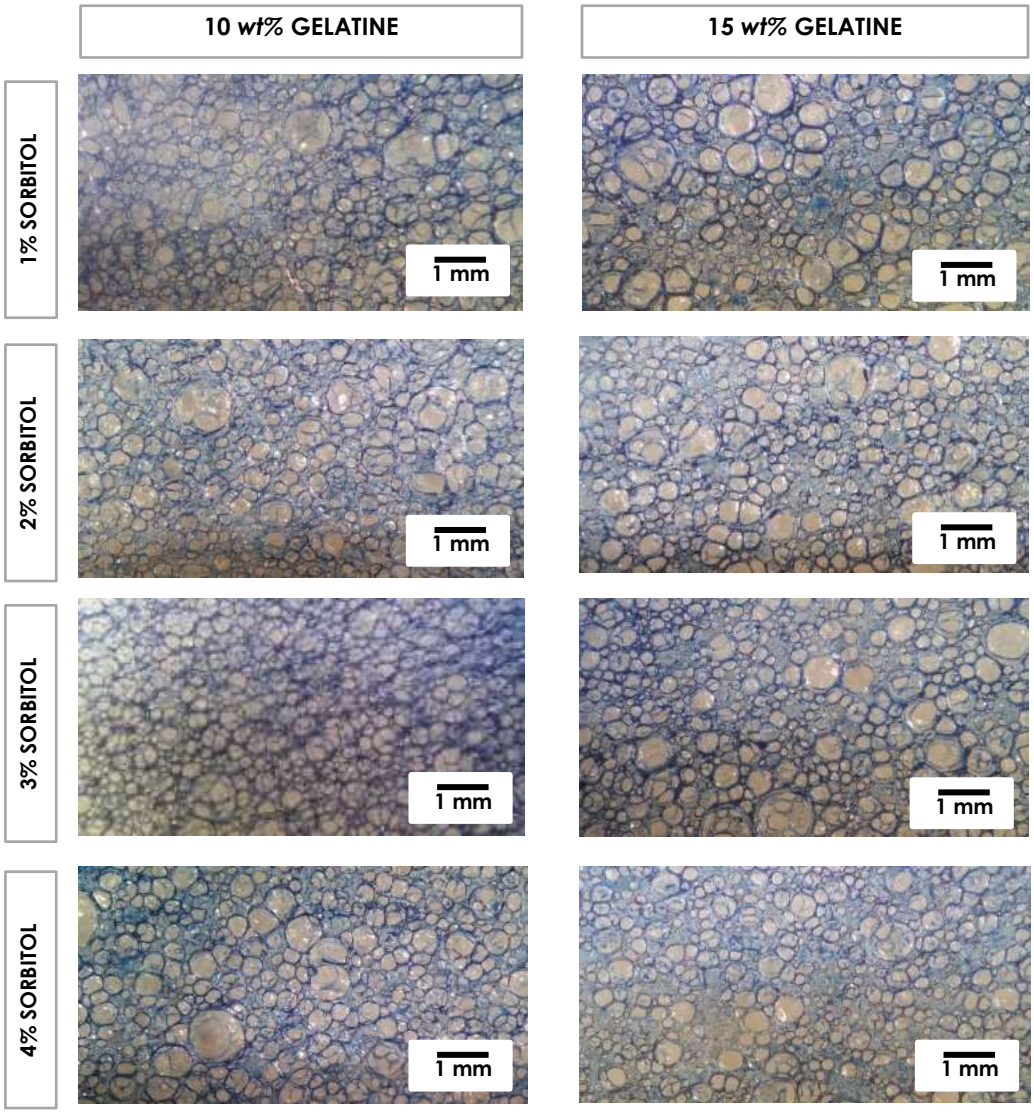

Figure 5.84. TOP SURFACE OF THE GELATINE-SURFACTANT C2-PLASTICISERS FOAMS

5.6.5 COMPRESSION PROPERTIES

As previously discussed (see Section 5.4.5.1), the mechanical properties heavily depend on foam composition and density, so it was expected differences in compression properties for the foams made with plasticisers.

5.6.5.1 Foams containing surfactant "A"

The averaged stress-strain curves for gelatine-surfactant "A"-plasticisers are shown in Figures 5.85 (for those made of glycerol) and 5.86 (for those made of sorbitol). The Young's modulus of the foams generally decreased as plasticiser content increased, which confirmed the plastification effect, as softer, more flexible foams were produced.

Contrary to what was expected, the foams (Figures 5.85.A, 5.86.A and 5.86.B) generally exhibited higher Young's modulus and a more obvious yielding and plateau than A7 (19.37 *kPa)* and A9 (660.53 *kPa)*, the samples they were based on. However, the foams including plasticisers were considerably softer than those without it. This may be attributable to the plasticisation of the cell walls but not the plasticisation of the actual foam.

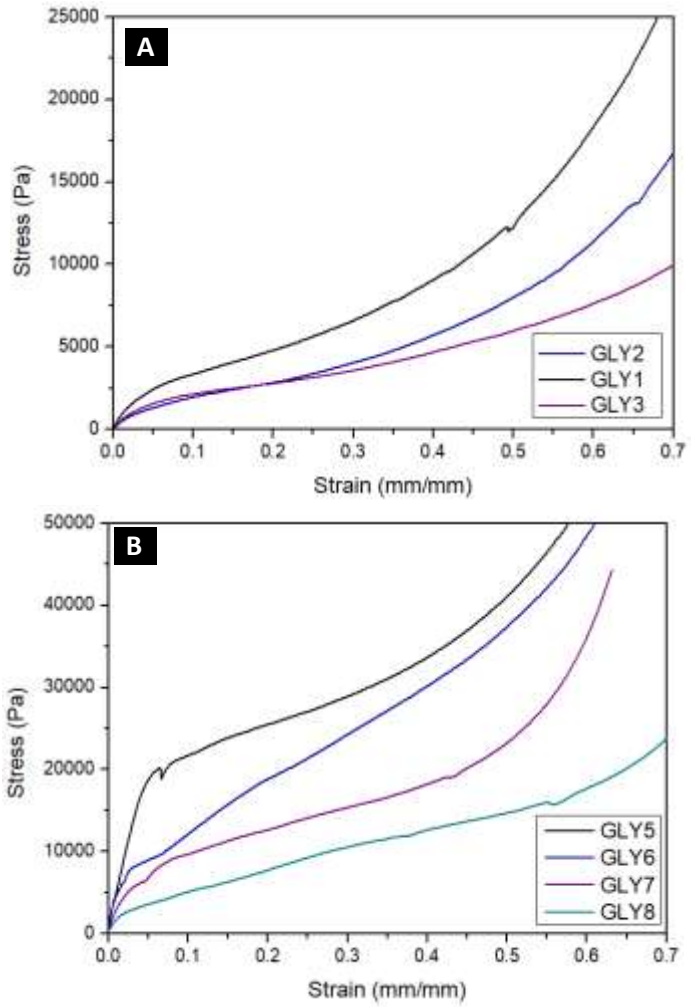

Figure 5.85 STRESS-STRAIN CURVES OF GELATINE-SURFACTANT "A"-GLYCEROL FOAMS (A) 10 *wt%* GELATINE -SURFACTANT "A"-GLYCEROL (B) 15 *wt%* GELATINE CONTENT-SURFACTANT "A"-GLYCEROL

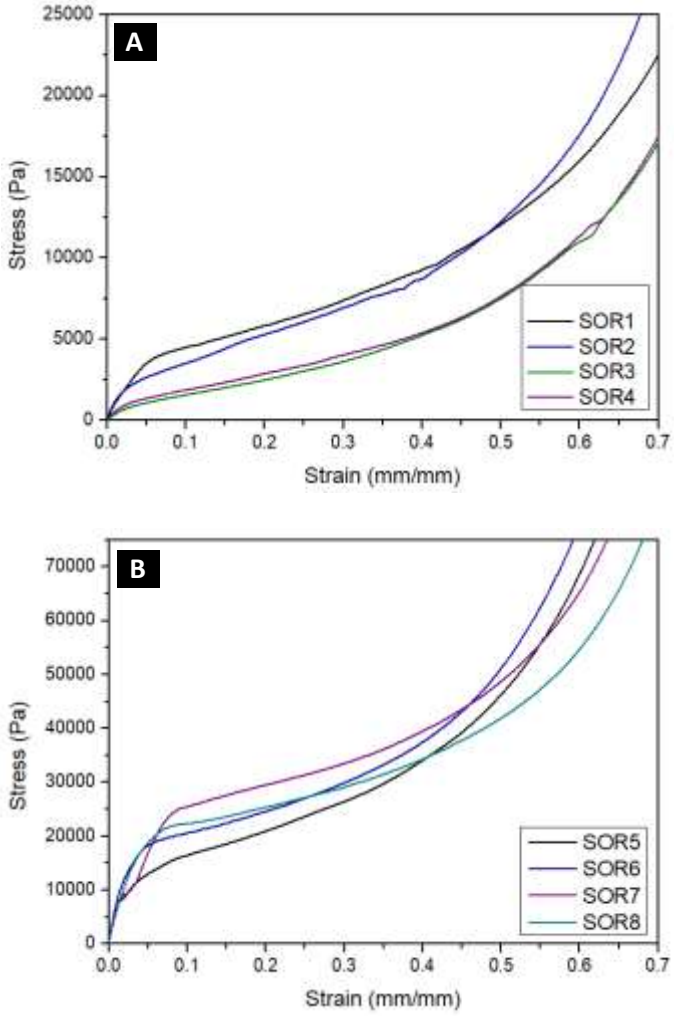

Figure 5.86 STRESS-STRAIN CURVES OF GELATINE-SURFACTANT "A"-SORBITOL FOAMS (A) 10 *wt%* GELATINE -SURFACTANT "A"-SORBITOL (B) 15 *wt%* GELATINE CONTENT-SURFACTANT "A"-SORBITOL

Table 5.32 summarises the compression modulus and stress at 10, 25 and 50% of the different foam samples. These values tended to decrease as plasticiser concentration increased, proving the plastification effect.

Table 5.32 COMPRESSION MODULUS, YIELD STRENGTH AND COMPRESSION STRENGTH (AT 10, 25 AND 50% STRAINS) OF THE GELATINE-SURFACTANT "A"-PLASTICISERS FOAMS

ID	DENSITY (kg/m^3)	E (kPa)	YIELD STRENGHT (kPa)	STRESS AT 10% (kPa)	STRESS AT 25% (kPa)	STRESS AT 50% (kPa)
SOR1	15.06	104.26±4.65	4.00	4.47±1.68	6.53±1.40	12.10±0.75
SOR2	15.89	101.48±16.13	2.23	3.13±0.71	5.30±1.32	11.30±1.81
SOR3	17.05	39.51±15.44	0.87	1.57±0.50	3.03±0.50	7.33±0.15
SOR4	18.40	55.54±14.06	1.02	1.87±0.25	3.37±0.47	7.63±0.78
SOR5	28.44	738.20±176.89	10.17	16.37±5.62	23.67±6.15	46.23±5.48
SOR6	32.02	770.67±121.51	15.17	20.57±7.33	27.10±6.54	51.07±9.51
SOR7	32.36	641.24±146.64	17.97	25.43±12.40	31.40±11.71	48.80±8.64
SOR8	34.73	672.56±111.31	16.48	22.37±5.69	27.13±5.87	41.93±5.76
GLY1	16.47	80.17±8.10	3.28	3.37±0.91	5.67±0.93	12.23±0.93
GLY2	17.37	47.36±3.37	2.60	2.03±0.06	3.57±0.12	8.13±0.75
GLY3	16.83	48.58±6.32	2.03	2.15±0.07	3.15±0.21	5.95±0.35
GLY4	n/a	n/a	n/a	n/a	n/a±	n/a
GLY5	26.91	564.02±143.93	21.20	21.67±5.71	27.07±5.19	41.03±3.55
GLY6	30.10	489.50±202.12	8.63	12.23±3.01	21.40±6.45	37.33±9.29
GLY7	32.84	254.70±150.05	7.83	9.23±3.97	12.93±3.74	18.97±4.16
GLY8	43.15	184.13±17.92	3.85	5.10±0.89	9.27±0.50	14.73±1.91

5.6.5.2 Foams containing surfactant C2

The averaged stress-strain curves for gelatine-surfactant C2-plasticisers are shown in Figure 5.87. The Young's modulus of the 4 *wt%* plasticiser content foams generally significantly decreased when compared to that in foams C2.1 and C2.3 (with no plasticiser). However, in some cases, the compression properties did not decrease with plasticiser content/foam density. This may be attributable to the considerably foam softness which complicated sample preparation.

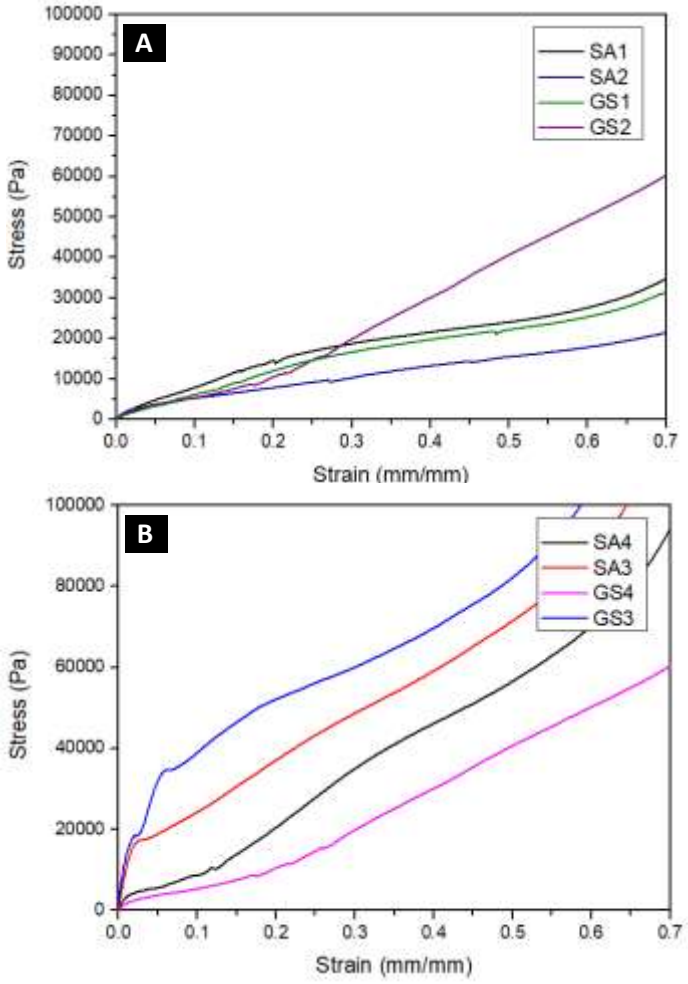

Figure 5.87 STRESS-STRAIN CURVES OF GELATINE-SURFACTANT-PLASTICISERS FOAMS (A) 10 *wt%* GELATINE -SURFACTANT "A"-PLASTICISERS (B) 15 *wt%* GELATINE CONTENT-SURFACTANT "A"-PLASTICISERS

Table 5.33 summarises the compression modulus and stress at 10, 25 and 50% of the different foam samples. As discussed, these values tended to decrease as plasticiser concentration increased.

Table 5.33 COMPRESSION MODULUS, YIELD STRENGTH AND COMPRESSION STRENGTH (AT 10, 25 AND 50% STRAINS) OF THE GELATINE-SURFACTANT C2-PLASTICISERS FOAMS

ID	DENSITY (kg/m^3)	E (kPa)	YIELD STRENGTH (kPa)	STRESS AT 10% (kPa)	STRESS AT 25% (kPa)	STRESS AT 50% (kPa)
SA1	22.63	77.56±0.18	15.70	7.87±1.37	16.87±1.76	24.03±0.95
SA2	31.77	39.52±9.59	8.17	5.30±0.46	9.20±0.79	15.53±1.64
SA3	44.16	325.00±64.66	7.63	8.57±1.5	27.80±2.79	56.47±2.31
SA4	49.24	985.44±138.81	17.50	24.23±1.51	43.27±4.2	71.40±7.48
GS1	22.90	60.17±5.01	12.93	6.13±1.62	14.67±0.35	22.20±0.44
GS2	30.86	26.30±13.52	1.43	1.97±0.64	4.87±0.95	11.63±1.16
GS3	36.89	1464±222.32	33.77	38.80±9.99	56.10±11.40	82.00±6.45
GS4	47.65	149.00±71.13	3.30	5.37±0.96	14.50±3.44	49.83±19.82

5.6.6 SUMMARY

This section studied the effects of plasticiser incorporation into the structure and the properties of gelatine-surfactant "A" and gelatine-surfactant C2 foams.

The incorporation of sorbitol/glycerol did not considerably affect the expansion ratio ($P>0.05$) achieved when compared with the foams prepared without plasticiser (for the two surfactants).

For surfactant "A" foams, shrinkage decreased with glycerol incorporation at both 10 and 15 *wt%* gelatine concentrations ($p<0.001$) and at lower plasticiser contents ($p<0.001$). The increase of shrinkage with plasticiser content was considerably more evident in 15 *wt%* gelatine foams. However, the incorporation of sorbitol did not seem to considerably affect the shrinkage of the foams.

Regarding surfactant C2 foams, the incorporation of both sorbitol and glycerol considerably increased the foams shrinkage but not considerable difference between the plasticiser type used was found ($p>0.05$). The detrimental effect of plasticiser incorporation on shrinkage was more significant at higher plasticiser contents ($p<0.001$) and this was more evident at lower gelatine content ($p=0.039$) (i.e. the negative effect of plasticiser content increase was more significant at 10 *wt%* gelatine concentrations.

The foam density of surfactant "A" foams steadily increased (when compared to that for A7 and A9) as plasticiser content increased ($p<0.001$), but the type of plasticiser ($p>0.05$) used did not seem to considerably affect the foam density increase. The plasticiser content had a greater effect at higher gelatine content (15 *wt%*) than lower ($p=0.009$).

The foam density for surfactant C2 foams increased as plasticiser content ($p<0.001$) increased. Sorbitol led to slightly higher densities compared to glycerol ($p<0.001$). The plasticiser content and type had little effect at lower gelatine concentrations (P,0.05). However, at higher gelatine concentrations, glycerol gave rise to lower density foams compared to those of sorbitol at any plasticiser concentration.

The incorporation of the plasticisers at 4 *wt%* into all the foams solutions produced relatively more ordered cellular structures compared to those without plasticisers. Not significant differences were found between the structure of glycerol and sorbitol foams.

The plasticification effect of glycerol and sorbitol was proved as Young's Modulus decreased as plasticiser content increased. However, the results obtained did not seem consistent with those for A7 and A9 foams.

5.7. STUDY OF THE DRYING PROCESS OF GELATINE-SURFACTANTS "A" AND C2 FOAMS

This section discusses the drying process and timescale for foams discussed in Sections 5.4 (gelatine foams made with surfactants "A" and C2) and 5.5 (foams prepared at different expansion ratios). Then, different drying conditions were investigated, including heating use and freeze-drying.

5.7.1 NATURAL DRYING OF CAST FOAMS

The foams produced in section 5.4 were dried under natural drying conditions (at 23°C and 50%HR), for cast foams ~300 cm^3 in volume in PS weight boats and hence loss of moisture was only from the top surfaces (see section 3.6.1 in Chapter 3, for further details).

5.7.1.1 Gelatine-surfactant "A" and Gelatine-surfactant C2 foams

Figure 5.88 shows the weight loss of both gelatine-surfactant "A" and gelatine-surfactant C2 foams under natural drying conditions. The foams moisture contents reached equilibrium in ~2-3 days.

Although weight loss was a continuous process, it was practically convenient to treat the average loss in terms of days:

- Day 1. An initial relatively fast drying during which the material lost most of its moisture content

- Day 2. Continued drying at an intermediate rate at which the product continued losing mass gradually.

- Day 3. Drying at a much slower rate towards the equilibrium.

The gelatine-surfactant "A" foams lost around 55%, 49.5% and 46% of the added water in the first day for 10 *wt%,* 15*wt%* and 20*wt%* gelatine contents, respectively which, as expected, also governed the total moisture levels. Gelatine-surfactant "A" foams dried in 3 days, excepting sample A7 (10 *wt%* gelatine) which dried in 2 days. This faster drying is attributable to a higher sample porosity, which facilitates vaporisation.The foams prepared with surfactant C2 exhibited a similar behavior and completed drying in day 3.

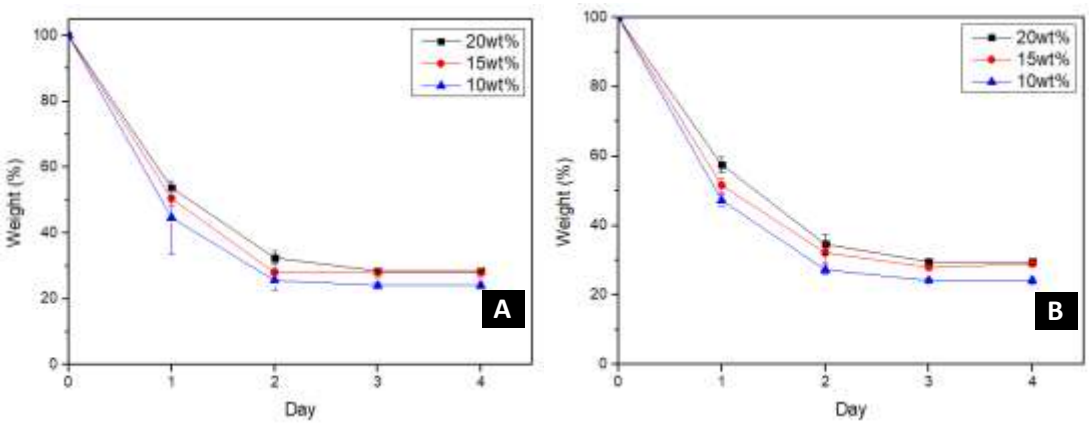

Figure 5.88 WEIGHT LOSS-TIME FOR (A) GELATINE-SURFACTANT "A" FOAMS (B) GELATINE-SURFACTANT C2 FOAMS

5.7.1.2 Foams made with different expansion ratios

As discussed in Section 5.5 liquid foam expansion ratios were largely inherited by porosities of the dry foam. And thus, weight loss was assessed using gelatine-surfactants "A" and C2 made at different expansion ratios, as described in section 5.5.

As shown in Figure 5.89, samples prepared at its maximum possible expansion ratio exhibited shorter drying times. For instance, Fig 5.89A showed that gelatine-surfactant "A" foams (with 10 *wt%* gelation content) completed their drying in 2, 4 and 5 days for ER=9.7 (the maximum), ER=8 and ER=6, respectively. All foams at ER=max dried faster than those produced at lower expansion ratios. The *5 wt%* gelatine content difference between the groups did not seem to have marked effect on drying time.

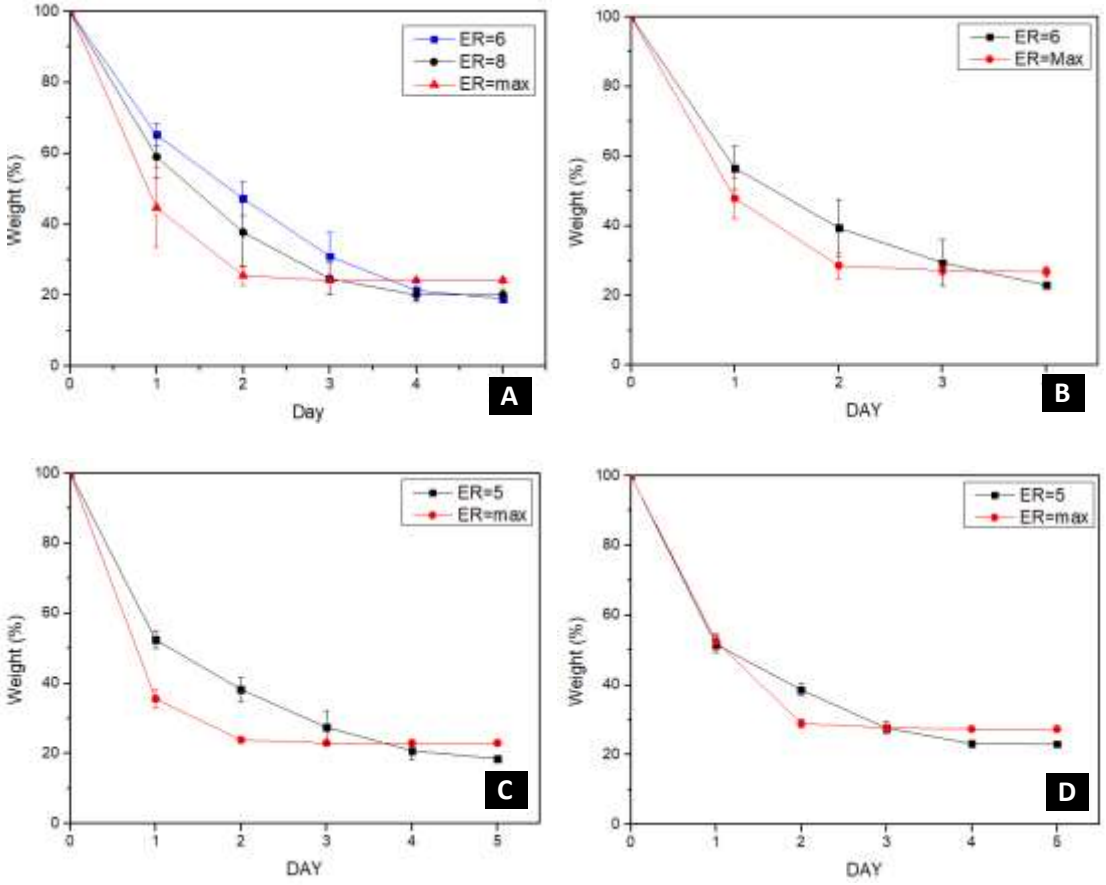

Figure 5.89 DRYING CURVES FOR FOAMS PREPARED AT DIFFERENT EXPANSION RATIOS (A) 10*wt%* GELATINE-SURFACTANT "A" FOAMS (B) 15*wt%* GELATINE-SURFACTANT "A" FOAMS (C) 10*wt%* GELATINE-SURFACTANT C2 FOAMS (D) 15*wt%* GELATINE-SURFACTANT C2 FOAMS

5.7.2 STUDY OF THE DRYING CONDITIONS

As discussed in Section 3.6.1 in Chapter 3, experimental details, several other drying conditions were studied in an attempt to speed up the drying process.

These included:

a. Use of chamber drying at higher temperatures above room temperature but below the melting point of gels

b. Use of porous moulds to assist loss of moisture from all directions.

c. Use of refrigeration to assist rapid gelling before drying

For the chamber drying environments, the drying was set at 26°C and 50%HR, and 29°C and 35±6%HR. Cast foam samples were dried either in a PS mould, as in section 6.7.1, or in a porous mould made of mesh material, as described in section 3.3.3.3.6, in Chapter 3. Table 5.34 shows the experimental table.

Table 5.34 DRYING CONDITIONS STUDIED

ID	CHAMBER /OVEN TEMPERATURE	REFRIGERATION	MOULD
C1		No	Mesh
C2		No	PS mould
C3	26°C	Yes	Mesh
C4		Yes	PS mould
O1		No	Mesh
O2		No	PS mould
O3	29°C	Yes	Mesh
O4		Yes	PS mould

Figure 5.90 shows the drying curves of samples C1, C2, C3 and C4 at 26°C and 50%HR. The use of the aluminium mesh mould accelerated the drying process. Foams dried in a PS mould dried in approximately 48 hours (at both 23°C natural drying and 26°C in the chamber), while foams dried in an aluminium mesh mould dried in 36 hours, shortening the process by 25%. As expected, a mould design that facilitates water evaporation from all directions accelerated drying. The increase of temperature from 23°C (see Section 6.7.1) to 26°C did not seem to reduce the drying time. Although helped to speed up gelling, refrigeration did not seem to affect the drying process

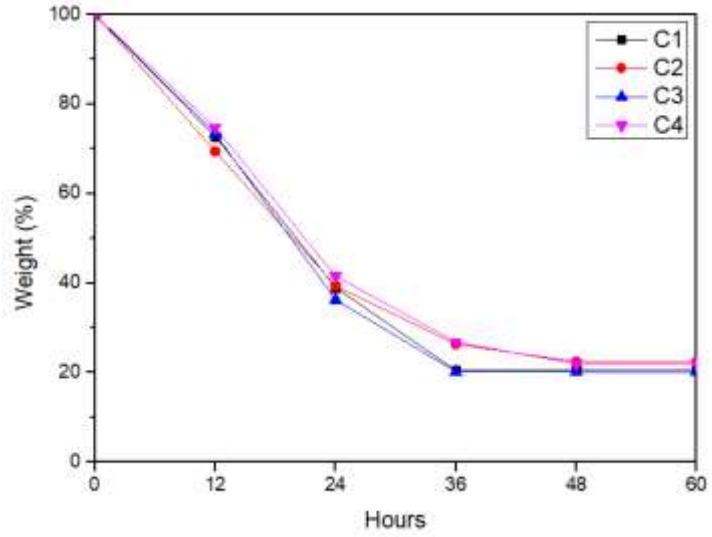

Figure 5.90 DRYING CURVES FOR CHAMBER DRYING AT 26°C OF SAMPLES C1 (IN MESH MOULD), C2 (IN PS MOULD), C3 (IN MESH MOULD WITH PRE-COOLING) AND C4 (IN PS MOULD WITH PRE-COOLING)

Figure 5.91 shows the drying curves for samples O1, O2, O3 and O4. All the samples dried in 48 hours. The drying trend of O1 and O3 (porous moulds) lost more moisture at any given time, which was consistent with C1 and C3, also in porous moulds. The samples dried at 29°C exhibited the formation of a denser outer surface layer (see

Figure 5.92), which reduced water evaporation and vapor transport to the surface. They also showed a coarser cell structure (see Figure 5.92.B) and, in some cases, extreme shrinkage (see Figure 5.92C). The extreme shrinkage may be due to the less moisture loss in the first hours when the foams were refrigerated, which make the material more sensitive to high temperatures.

O3 completed the drying in 36 hours in comparison with O1, in 48 hours. This seems to indicate that fast gelling using pre-cooling might help to maintain higher porosity and thus assist more rapid drying. In contrast, O2 and O4, in non-porous PS moulds, exhibited slower drying compared with O1 and O3 (or C2 and C4). A possible explanation for this is the drying hindering by both the denser outer layer and the use of PS moulds.

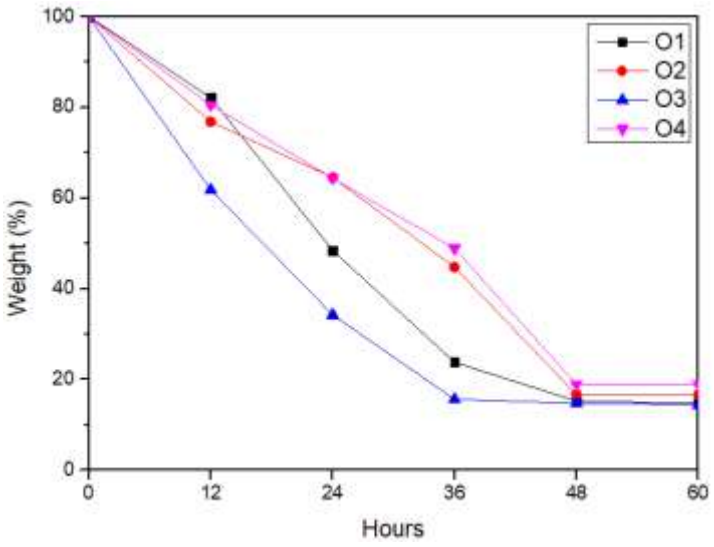

Figure 5.91 DRYING CURVES FOR CHAMBER DRYING AT 29°C OF SAMPLES O1 (IN MESH MOULD), O2 (IN PS MOULD), 03 (IN MESH MOULD WITH PRE-COOLING) AND O4 (IN PS MOULD WITH PRE-COOLING)

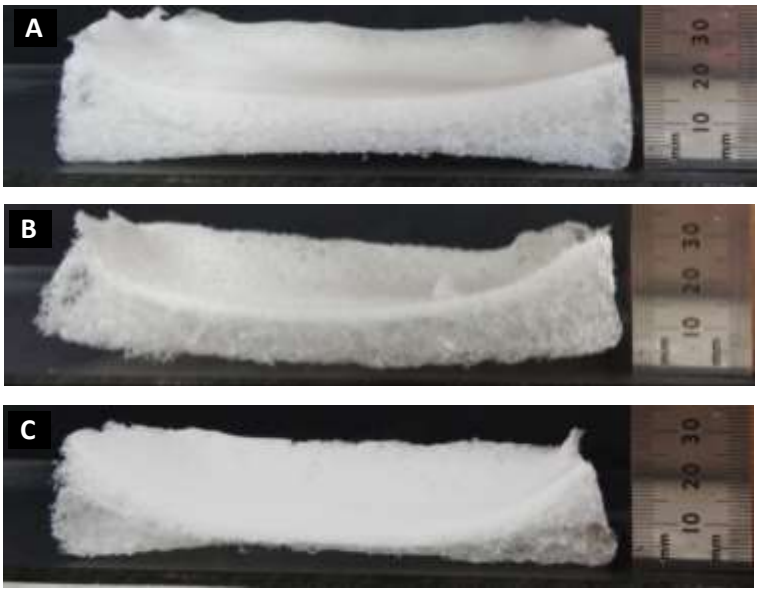

Figure 5.92 COMPARISON OF THE DRYING OF (A) SAMPLE C1 (DRIED AT 26°C) (B) SAMPLE O1 (DRIED AT 29°C IN A MESH MOULD) (C) SAMPLE O3 (DRIED AT 29°C IN A MESH MOULD AFTER PRE-COOLING)

Figure 5.93 compares the total shrinkage of the foams in natural drying at 23°C (in a PS mould) and chamber drying at higher temperatures. All samples chamber dried at 26°C exhibited less shrinkage than the natural drying (at 23°C, A7) Shrinkage decreased from 42.92% (sample A7, dried in a PS mould) to 32.5% (sample C2, also dried in the PS mould). In particular, samples dried in the aluminium mesh mould exhibited lower total shrinkage (C1 and C3) than in the PS moulds (C2 and C4). The metal mesh mould may have assisted more rapid cooling and gelling and restricted shrinkage, as there was certain penetration of foam into the apertures of the mash.

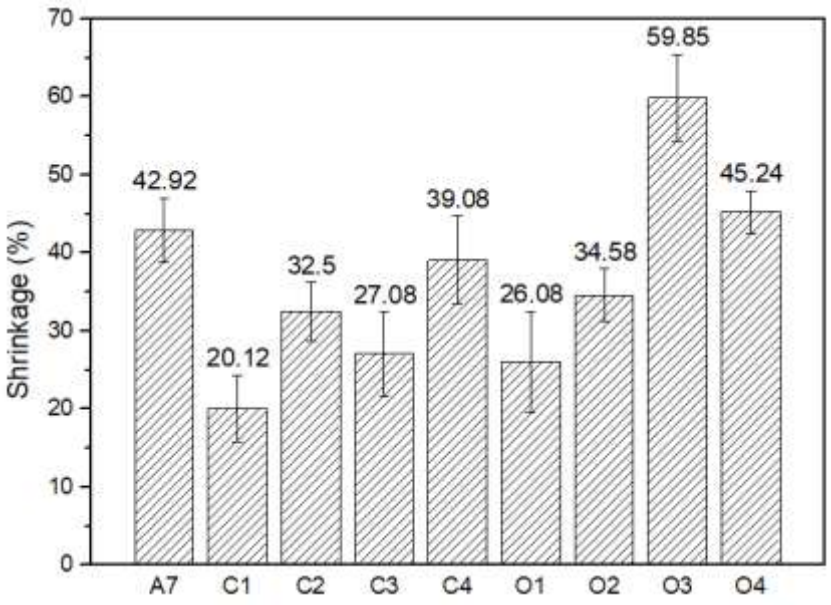

Figure 5.93 COMPARISON OF TOTAL SHRINKAGE FOR FOAMS DRIED AT DIFFERENT CONDITIONS

The drying at 29°C was proved less effective, with the development of higher shrinkage and undesirable structure changes.

5.7.3 FREEZE DRYING

The most common drying techniques combine application of heat and vapor transport, as described in the literature review. The conditions studied in section 5.7.2, however, were limited in the use of higher temperature by the melting point of the hydro-gels as gelling is thermally reversible. This may be addressed by using stronger chemical crosslinking (e.g. formaldehyde (Shyamkuwar *et al.*, 2010), glutaraldehyde (Kang, Tabata and Ikada, 1999) or carbodiimides (Kim, Knowles and Kim, 2005)) of the hydrogels. In addition, there is also considerable scope for increasing the vapor transport rate to speed up drying, by e.g. forced gas flow techniques, such as fans.

Freeze drying of sample A7 was also explored. Unlike conventional evaporative drying, water was removed through direct transformation from solid (ice) to vapor state i.e. *sublimation*. This drying method may not only reduce shrinkage to minimum without the otherwise contraction due to water diffusivity, but can also significantly affect the foam substructure (cell walls, plateau edges and vertex).

A cast foam sample was prepared and freeze dried as described in section 3.6.1 in chapter 3. No noticeable volume shrinkage was observed at the end of drying.

As shown in Figure 5.94, the cell walls (Figure 5.94A) exhibited highly porous substructure, revealing the porous morphology on the surface and throughout the thickness of the cell walls (5.94B) with sub-pore size in the range of 8-20 *μm* and sub-walls of *1-2 μm* thick (5.94C). The foam was indeed a microcellular solid and should have extraordinary specific surface area, leading to potential applications as a super absorbent.

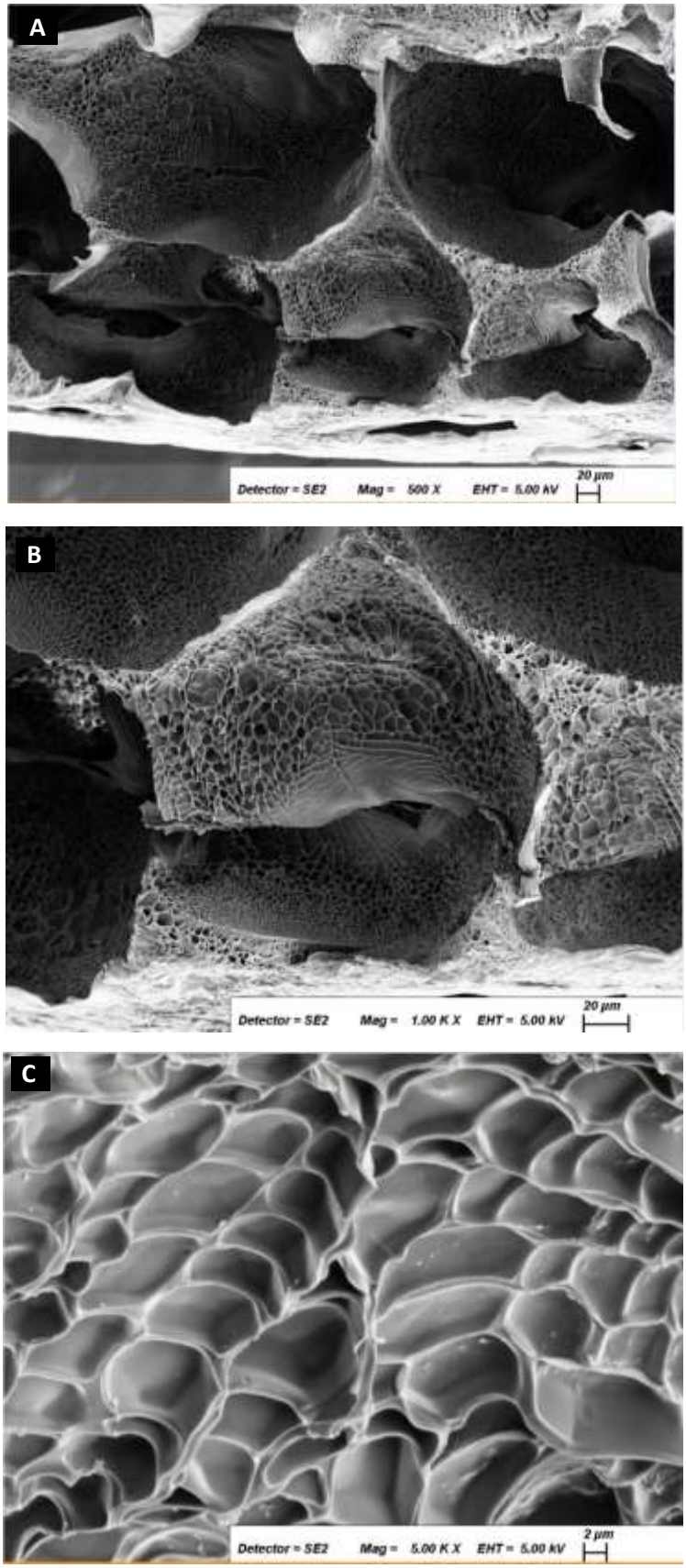

Figure 5.94 SEM MICROGRAPHS OF THE SUBSTRUCTURE ON SURFACE AND WITHIN THE CELL WALLS FOR THE FREEZE-DRIED SAMPLE A7 AT DIFFERENT MAGNIFICATIONS.

In theory, extraordinarily high porosity can be achieved. Assuming a foam density (under natural drying condition) of $\rho = 10\ kg/m^{-3}$ (proved possible earlier, see Table 5.14 in Section 5.4.3.1), the relative density, ρ_r can be found from ρ and the matrix density ρ_m (see Table 5.14):

$$\rho_r = \rho / \rho_m = 10/1150 = 0.869\% \qquad \text{Equation 5.1}$$

and "nominal" foam porosity, p, will be

$$p = 1 - \rho_r = 99.131\% \qquad \text{Equation 5.2}$$

Then, assuming the same porosity was achieved in the cell walls (by freeze frying), the additional porosity from the cell walls, p' would be

$$p = \rho_r\, p = 0.869\% \times 99.131\% = 0.861\% \qquad \text{Equation 5.3}$$

This leads to a theoretical total porosity *(p)*:

$$p = p + p' = (99.131 + 0.861) = 99.992\% \qquad \text{Equation 5.4}$$

5.7.4 SUMMARY

Drying time is a limiting factor for liquid foaming. The selected formulations from Section 5.4 exhibited drying times between 2-3 days at 23°C and 50% HR. This was a considerable improvement from the previous systems studied but there is still room for drying optimisation.

There are several processing parameters which may affect the drying of the hydrogel foams. Samples prepared at its MER exhibited shorter drying times, regardless their gelatine concentration. The use of perforated moulds was also proved to slightly reduce (by approximately 25%) the drying time by allowing water migration from all the mould walls. However, the use of slightly higher curing temperatures (26°C) did not have a considerably effect on drying.

The use of convection drying is limited by the thermo-sensitivity of gelatine (as shown in Section 5.2.1.4). This may be addressed by using stronger chemical crosslinking (e.g. formaldehyde (Shyamkuwar *et al.*, 2010), glutaraldehyde (Kang, Tabata and Ikada, 1999) or carbodiimides (Kim, Knowles and Kim, 2005)) of the hydrogels. In addition to this, there is also considerable scope for increasing the vapor transport rate to speed up drying, by, for example, forced gas flow techniques, such as fans.

Freeze-drying may be another route to explore for further work. This drying method may not only reduce shrinkage to minimum without the otherwise contraction due to water diffusivity, but can also significantly affect the foam substructure, as shown in Section 5.7.3.

5.8. BIO-BASED HYDROGEL FOAMS ALTERNATIVES TO GELATINE

This section discusses the results of the preliminary exploration of two other bio-based hydro-gels, agar and gellan gum. The main objective was to diversify the hydro-gels alternatives from non-animal origins.

5.8.1 AGAR HYDROGEL FOAMS

Table 5.35 shows the composition of agar-surfactant C2 foams, prepared as described in section 3.3.3.5.1 in Chapter 3, and their associated MER during the liquid foaming stage.

Table 5.35 AGAR LIQUID FOAMS FORMULATION AND MER

ID	Agar *(wt%)*	C2 *(wt%)*	Water *(wt%)*	MER
AS1	4.98	0.50	94.53	10.25±0.35
AS2	7.46		92.04	8.38±0.53
AS3	9.95		89.55	6.38±0.53
AS4	4.95	0.99	94.06	9.38±0.53
AS5	7.43		91.58	8.25±0.35
AS6	9.90		89.11	5.50±0.71
AS7	4.93	1.48	93.60	8.75±0.35
AS8	7.39		91.13	7.63±0.53
AS9	9.85		88.67	2.38±0.18

It was feasible to produce liquid agar-surfactant C2 foams. However, during subsequent gelling and drying process, cell structure of the agar-surfactant C2 foams collapsed significantly and almost lost the foam structure, as shown in Figure 5.95 at the end of drying. Stable liquid agar foam gels were formed but the gel structure was not consolidated and instead of exhibiting a continuous matrix (i.e. like the one observed in gelatine foams) the matrix was connected in a fibrous-like structure as seen under optical microscope and agreed by Boral and Bohidar (2009). As the water removal of the agar fibre-like gel proceed, the gel structure weaken, collapsed and exhibited a considerable shrinkage.

Considering the high MERs achieved, such significant loss of foam structure was most likely due to lack of foam stability and agar gel strength. Agar is well known to form gel (as discussed in section 2.6.1, in Chapter 2) and thus the incorporation of C2 surfactant might have negatively affected the gelling process, as observed in Section 5.2.1.3 for gelatine gels. To clarify this, the agar gelling behaviour with the incorporation of surfactant C2 was investigated, as illustrated in Figure 5.95.

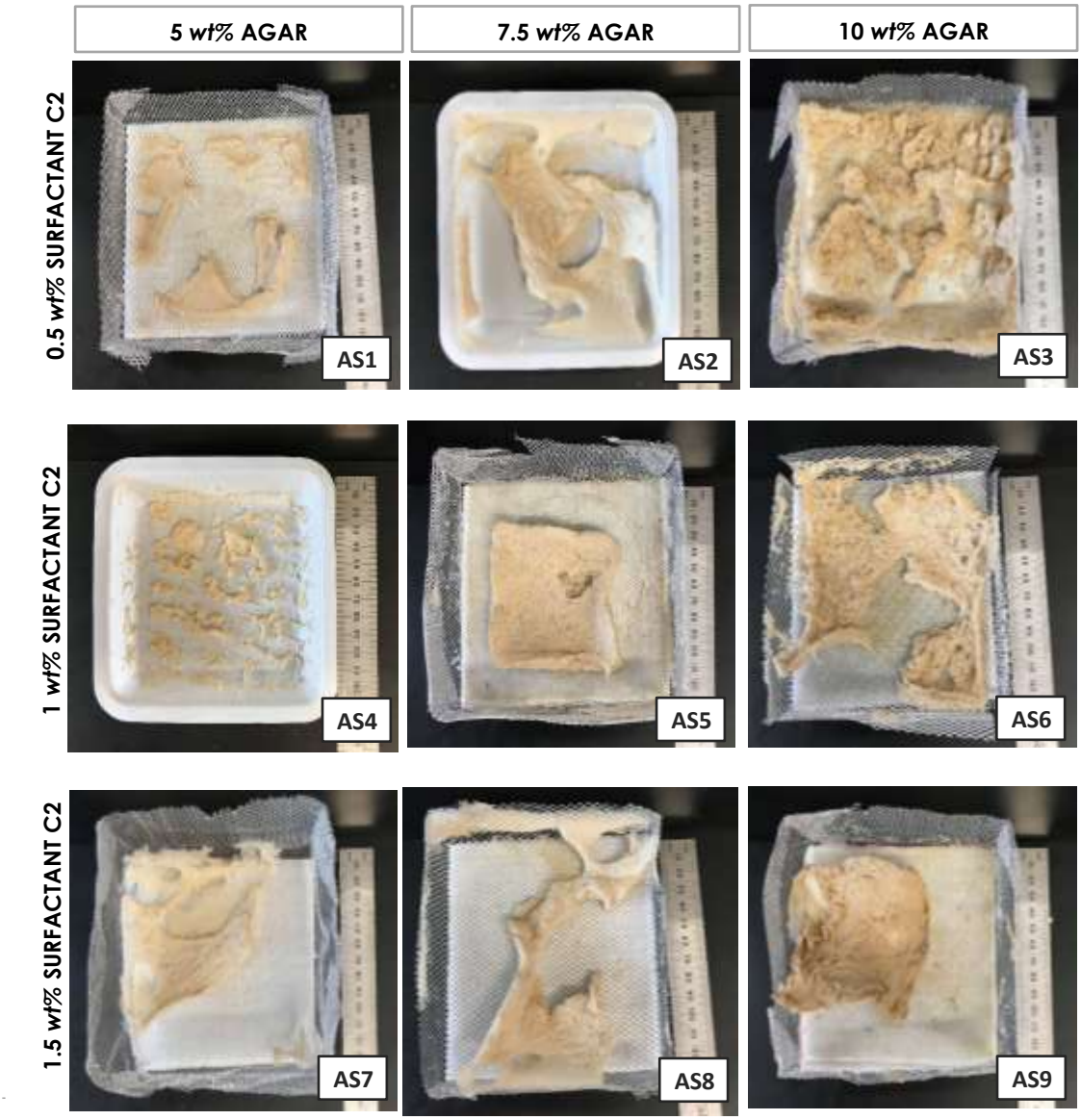

Figure 5.95 AGAR-SURFACTANT C2 FOAMS AFTER DRYING

In the LVR identification, a strain of 0.5% and a frequency of 1 *Hz* were chosen for further characterisations. Figure 5.96 shows the time sweep during which solution temperature decreased naturally from 80°C. It compares the gelling behaviour of a 5 *wt%* agar without any surfactant and the 5 *wt%* agar-surfactant C2 (formulation AS7). Figure 5.96A shows the gelling behaviour of the agar gel without surfactant. *G'* gradually increased implying gelling of the sample solution. The gelling took place at ~55°C (or after ~15 minutes). The gelling time considerably increased to that observed for gelatine gels (see Section 5.2.1.3).

The noise obtained in the *G''* curve may be due to the agar syneresis.

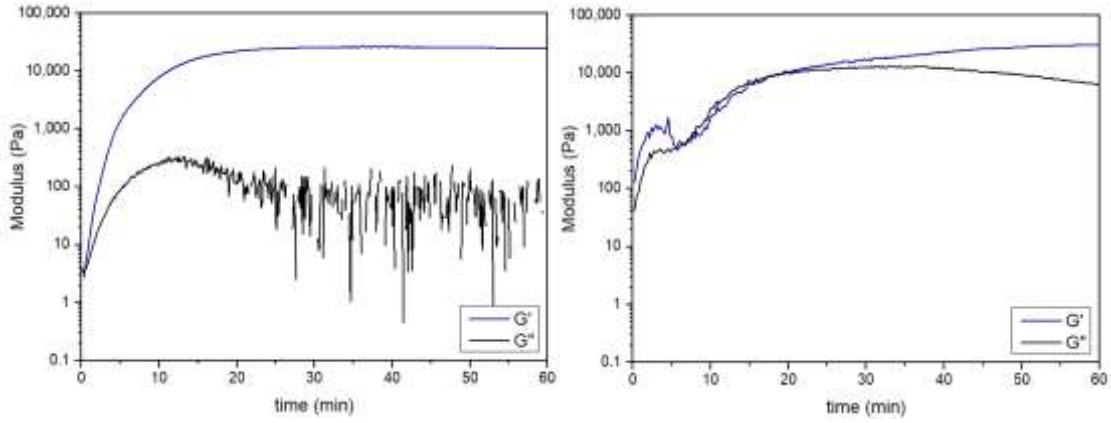

Figure 5.96 TIME SWEEPS COMPARISON BETWEEN TWO HYDROGELS: (A) 5 *wt%* AGAR; (B) 5 *wt%* AGAR-SURFACTANT C2

Figure 5.96B shows the gelling behaviour of the agar gel with the surfactant C2. Both *G'* and *G''* increased gradually without clear separation between them. This implies the formation of a very weak gel. This strongly suggests that the loss of gelling power due to the surfactant incorporation may be partially responsible for the foam collapsing of the agar-surfactant C2 liquid foams. No attempt for further investigation was made but focus of future research should ensure the compatibility of processing additives with the hydrogel of interests.

5.8.2 HYDROGEL FOAMS FROM GELLAN GUM

This study investigated two gellan gums:

1) LA (low acyl) gellam gum at two concentrations (3 and 4 *wt%*)

2) HA (high acyl) gellan gum at three concentrations (0.5, 1, 1.5 *wt%)*

he MER of the gellan gum foams was not recorded because its foaming took place at water boiling point, what hindered the measurement.

As shown in Table 5.36, higher HA gellan gum foams generally increased the foam density and decreased shrinkage. LA incorporation generally increased the density of the foams but not a clear trend was found for this type of gellan gum when increasing its concentration. Density ranged from 11.53 kg/m^3 (sample GG1) to 45.45 kg/m^3 (sample GG8) and drying shrinkage from 32% to 64.66%.

The thermal conductivity of the samples exhibiting lower shrinkage (GG3, GG4, GG6 and GG7) was investigated. It ranged from 0.0329 (sample GG4) to 0.0373 $W/m{\cdot}K$ (sample GG7). They can be considered as good foam insulators, comparable to conventional plastics foams.

Table 5.36 GELLAN GUM FOAMS DENSITY, SHRINKAGE AND THERMAL CONDUCTIVITY

ID	HA GELLAN GUM (*wt%*)	LA GELLAN GUM (*wt%*)	Foam DENSITY (kg/m^3)	Total SHRINKAGE (*vol%*)	THERMAL CONDUCTIVITY (*W/m·K*)
GG1	3	0	11.53	64.66	-
GG2	3	0.5	39.22	54	-
GG3	3	1	31.04	34.67	0.0347
GG4	3	1.5	32.23	35.33	0.0329
GG5	4	0	36.6	60	-
GG6	4	0.5	38.59	41.33	0.035
GG7	4	1	35.82	32	0.0373
GG8	4	1.5	45.45	51.33	-

The drying time, compared to the other systems was considerably reduced. Convective drying was carried out in an oven at 70°C, resulting in a drying time <24 hours, which is a significant improvement from gelatine-based foams.

Figure 5.97 shows SEM images of sample GG4. It exhibited a relatively closed structure and its porosity ranged from 0.4-1.2 mm. This was due to an immediate gelling after foaming, which complicated processing at atmospheric conditions.

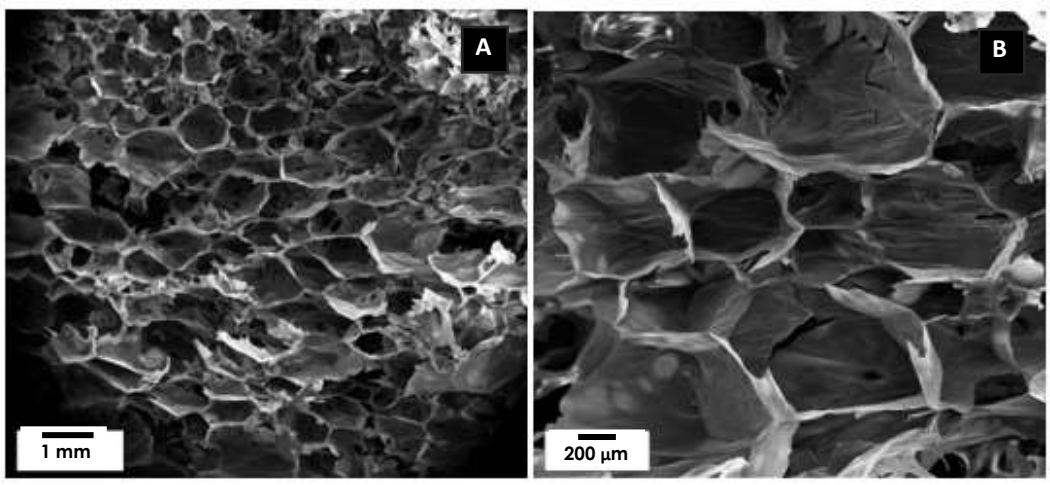

Figure 5.97 SEM IMAGES SHOWING THE CELL STRUCTURE OF SAMPLE GG4 (A) GENERAL VIEW (B) CLOSE-UP

5.8.3 SUMMARY

Alternative hydrogels (agar and gellan gum) to gelatine were studied in this section.

It was feasible to product liquid agar foams. However, during subsequent gelling and drying process, cell structure of the agar-surfactant C2 foams collapsed significantly. Rheological characterisation suggested that the loss of gelling power due to the surfactant incorporation may be partially responsible for the foam collapsing of the

agar-surfactant C2 liquid foams. No attempt for further investigation was made, but focus of future research should ensure the compatibility of processing additives with the hydrogel of interests. In addition to this, as mentioned for hydrogel foams made with gelatine, agar can benefit from the use of cross-linkers or process, such as freeze-drying.

Regarding gellan gum, it was feasible to produce both liquid and solid foam. It is a promising solution for bio-materials as it gels at very low concentrations and can be dried by convective methods. However, further work needs to focus in minimise shrinkage (e.g. crosslinkers) and processing improvement. Gellan gum melts around 95°C, which difficults processing at atmospheric conditions.

6. CHAPTER 6.
CASE STUDIES: APPLICATIONS OF GELATINE BIO-FOAMS

Chapter 6.

CASE STUDIES: APPLICATIONS OF GELATINE BIO-FOAMS

6.1 INTRODUCTION

The previous chapter studied the properties of hydrogel foams based mainly on gelatine. This chapter explores applications aspects of the gelatine based bio-foams in four case studies:

a. The inclusion of biomass powders from agricultural waste in the gelatine bio-foams for the generation of cost-effective fully biodegradable composite foams in general applications.

b. The incorporation of silica aerogel powders in the gelatine foams for thermal insulation and thermal packaging applications.

c. The inclusion of expanded vermiculite particles in the gelatine foam for thermal insulation and fire-resistant composites in construction applications.

d. The bio-foam filled honeycomb structures for enhancement of properties in lightweight structure applications.

The case studies made use of the advantages of the liquid foams, low viscosity and ease to flow, to blend with second materials or filling in complex cavities.

6.2 FULLY BIODEGRADABLE COMPOSITE GELATINE BIOFOAMS CONTAINING POWDERED BIOMASS FILLERS

This section explores the incorporation of biomass powders into the liquid gelatine foams to produce more cost effective biofoam composites for general applications (e.g. cushion and thermal packaging).

From the investigations carried out in Chapter 5, a few base gelatine foams were selected to combine with the lignocelluloses biomass powders. Formulations **A7** (10 *wt%* gelatine content), **A9** (*15 wt%* gelatine content) and **A11** (20 *wt%* gelatine content), from the gelatine-surfactant "A" subsystem; and formulations **C2.1** (*10 wt%* gelatine content) and **C2.3** (15 *wt%* gelatine content), from the gelatine-surfactant C2 subsystem, were selected.

Three factors were studied at different levels for this experiment (see Section 3.3.3.4.2 for further details):

- Factor A. *Gelatine content*. This factor was studied at two (gelatine-C2 foams) or three (gelatine-surfactant "A" foams) levels
- Factor B. *Biomass Powder type*. Two different types of biomass powder were studied, oat and straw (see Section 3.2.3.1)
- Factor C. *Biomass powder content*. Two biomass powder concentrations were investigated, 1 *wt%* and 3 *wt%*

Table 6.1 shows the experimental matrix for the biomass-hydrogel composite foams. Details about formulation and sample preparation can be seen in Section 3.3.3.4.2.

Table 6.1 EXPERIMENTAL MATRIX FOR BIOMASS-HYDROGEL COMPOSITE FOAMS

ID	FIBRE TYPE	FIBRE CONTENT* (wt%)	GELATINE CONTENT (wt%)	SURFACTANT CONTENT* (wt%)	SURFACTANT TYPE
O1	oat	1	10	1.5	A
O2		3	10		
O3		1	15		
O4		3	15		
O5		1	20		
O6		3	20		
O7	oat	1	10	0.75	C2
O8		3	10		
O9		1	15		
O10		3	15		
W1	straw	0.9	10	1.5	A
W2		2.96	10		
W3		0.99	15		
W4		2.96	15		
W5		0.99	20		
W6		2.96	20		
W7	straw	0.99	10	0.75	C2
W8		2.98	10		
W9		0.99	15		
W10		2.98	15		

**Content based on the total weight of the gelatine-water solution*

Expansion ratio of the liquid foams, dry foam density, foam structure, mechanical properties and thermal conductivity of the composite foams were measured and compared with that of the base foams. Process-related attributes, such as shrinkage and drying were also investigated.

6.2.1 MER

Full factorial 3x2x2 and 2x2x2 (for gelatine "A" and gelatine C2 systems, respectively) designs with two replicates were used to calculate the statistical significance of the design parameters (gelatine content, biomass powder type and content) in MER of the composite foams. Further information about the statistical analysis can be found in section 3.3.2 in Chapter 3.

6.2.1.1 Composite foams based on gelatine-surfactant "A" formulations

As seen in Figure 6.1, in comparison with the base foams A7, A9 and A11, MER of the liquid composite foams ranged from 4.96 (sample O6, with 20 *wt%* gelatine content and 3 *wt%* oat fibre) to 9.41 (sample O1, 10 *wt%* gelatine content and 1 *wt%* oat fibre). The incorporation of the fibres generally resulted in decrease in expansion ratio.

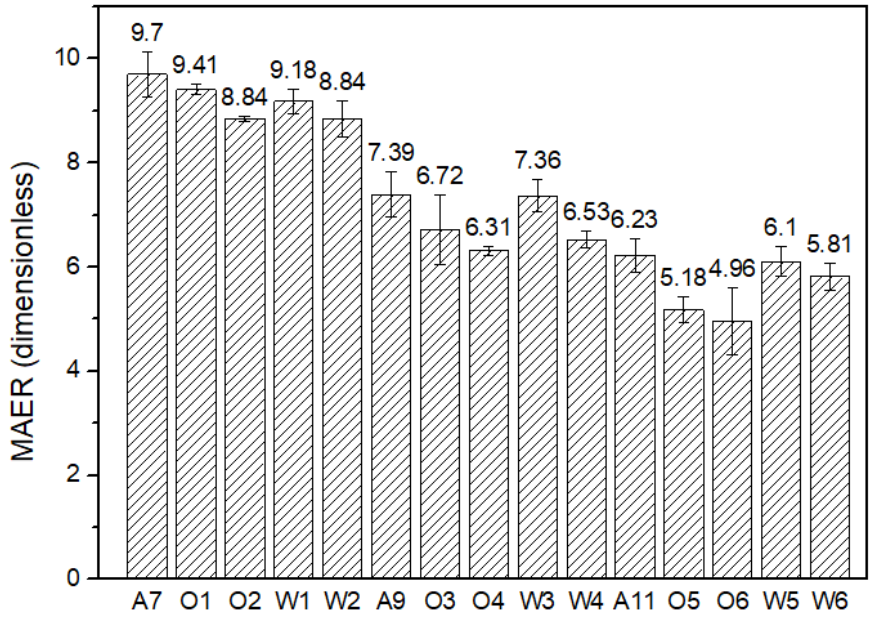

Figure 6.1. MER OF GELATINE-SURFACTANT "A"-FIBRE COMPOSITE FOAMS AND COMPARISON WITH THE BASE FOAMS A7, A9 AND A11

Table A.17 (see Appendix A) shows the ANOVA table for MER with a level of significance of 0.05. The table gave F statistics=226.58, $p<0.001$, F=8.4, p=0.013, F=10.13, p=0.008 for gelatine content, fibre type and fibre content, respectively. The null hypothesis can be rejected as there is a strong evidence that the MER varied with the three studied parameters. There was also evidence that MER was influenced by the gelatine content-fibre type interaction (F=4.35, p=0.038).

Figure B.14 (see Appendix B) shows the main effects plots for the MER. As previously found in Section 5.6.1 (in Chapter 5), MER tended to decrease as gelatine content increased in a quasi-linear trend ($p<0.001$).

Fibre type slightly affected MAER ($p<0.05$). Foams prepared with straw generally led to slightly higher MER. This may be partially due to the particle size difference. Straw particles are slightly bigger than those in oat, which can assist nucleation. Foams prepared with *1 wt%* and *3 wt%* fibre exhibited an average MER of 7.32 and 6.88, respectively. As expected, an increase in fibre content had a detrimental effect on MER ($p<0.05$).

The gelatine content-fibre type interaction ($p<0.05$) was found in 15 *wt%* and 20 *wt%* gelatine content foams, whereas 10 *wt%* gelatine foams showed virtually the same response in MER for both oat and straw. Straw nucleation assisting was more significant in solutions with higher viscosities.

6.2.1.2 Composite foams based on gelatine-surfactant C2 formulations

As seen in Figure 6.2, MER of the liquid composite foams made with surfactant C2 ranged from 5.69 (sample W10; 15 *wt%* gelatine, 3 *wt%* straw powder) to 7.37 (sample W7, 10 *wt%* gelatine, 1 *wt%* straw powder). The incorporation of the fibers was generally associated with a slightly MER decrease, excepting for sample W7, which exhibited a slight increase compared with sample C2.1.

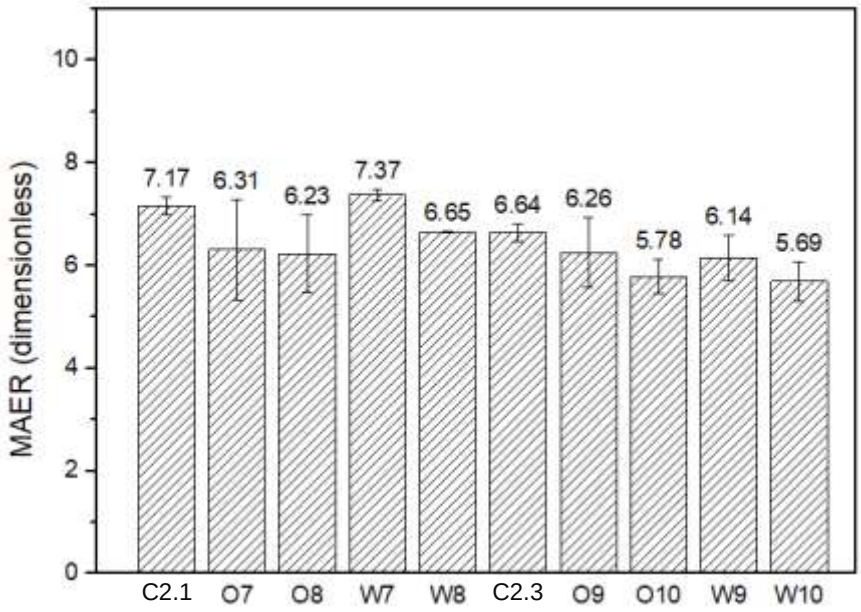

Figure 6.2. MER OF GELATINE-SURFACTANT C2-FIBRE COMPOSITE FOAMS AND COMPARISON WITH THE BASE FOAMS C2.1 AND C2.3

The ANOVA test (Table A.18 in Appendix A) gave F statistics=2.38, p=0.161, F=0.54, p=0.485, F=0.98, p=0.351 for gelatine content, fibre type and fibre content, respectively. The null hyphotheses can be accepted as there is a strong evidence that MER did not vary with the three studied parameters. Gelatine was the most significant factor ($p>0.05$) and its no statistically significance in this test may be due to the exclusion of 20 *wt%* gelatine content in the experimental matrix (due to the high-

density foams 20 wt% gelatine-surfactant C2 led to) and the relatively significant standard deviation of samples O7 and O8.

6.2.2 TOTAL SHRINKAGE

Full factorial 3x2x2 and 2x2x2 designs with two replicates were used to calculate the statistical significance of the design parameters (gelatine content, fibre type and fibre content) in total shrinkage of the composite foams.

6.2.2.1 Composite foams based on gelatine-surfactant "A" formulations

As shown in Figure 6.3, the total shrinkage of the composite foams containing oat ranged from 27.08% (Sample O2; 10 *wt%* gelatine content, 3 *wt%* oat content) to 42.71% (Sample O3, 15 *wt%* gelatine content, 1 *wt%* oat content). For foams containing straw powder, shrinkage ranged from 20.83% (Sample W4; 15 *wt%* gelatine content, 3 *wt%* straw content) to 34.58% (Sample W1; 10 *wt%* gelatine content, 1 *wt%* straw content).

In comparison with the base foams, when fibres were incorporated into the formula, shrinkage tended to decrease when compared with A7 (10 *wt%* gelatine) and A11 (20 *wt%* gelatine). The filler powder did not absorb in the matrix and helped to maintain the cell structure. For A9 (15 *wt%* gelatine), the incorporation of straw powder also decreased the shrinkage level but the incorporation of oat powder increased it. Further investigation is needed to investigate the increase in shrinkage for 15 *wt%* gelatine foams made with oat.

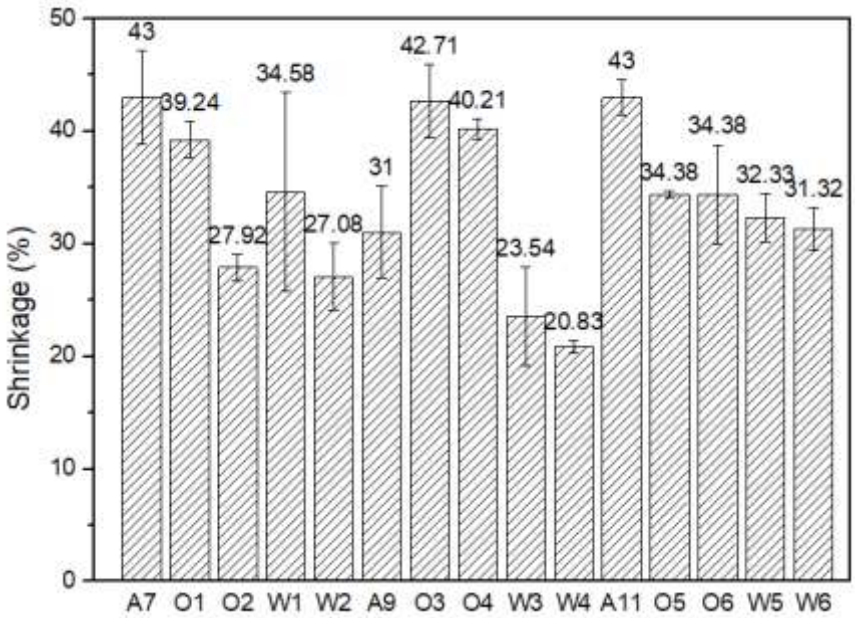

Figure 6.3. SHRINKAGE OF GELATINE-SURFACTANT "A"-FIBRE COMPOSITE FOAMS AND COMPARISON WITH THE BASE FOAMS A7, A9 AND A11

The ANOVA test (Table A.19 in Appendix A) for shrinkage of the composite foams gave F statistics=0.29, p=0.751, F=35.82, p<0.001, F=8.92, p=0.011 for gelatine content, fibre

type and fibre content, respectively. It can be said that there is a strong evidence that the shrinkage varied with fibre type and content. Surprisingly, the influence of gelatine content on shrinkage was not significant due to high shrinkage found in 15 wt% gelatine foams made with oat. However, the gelatine content-fibre type interaction was significant ($F=7.58$, $p=0.001$) due to the same reason why gelatine was not significant. Figure B.16, in Appendix B, shows the gelatine content-fibre type interaction.

The use of straw powder led to lower shrinkage levels compared to the use of oat ($p<0.001$). Higher fibre content (*3 wt%*) gave rise to slightly lower shrinkage than lower fibre content (*1 wt%*). The main effect plots can be seen in Figure B.15 (Appendix B).

Figure 6.4 illustrates the cross-section of the cast gelatine-surfactant "A"-fibres dry foams.

Figure 6.4. CROSS-SECTION OF CAST GELATINE-SURFACTANT "A"–FIBRE COMPOSITE FOAMS SHOWING THE EFFECTS OF BIOMASS FILLERS AND CONCENTRATION ON TOTAL SHRINKAGE

6.2.2.2 Composite foams based on gelatine-surfactant C2 formulations

As shown in Figure 6.5, the total shrinkage ranged from 28.33% to 36.67% and 26.46% to 43.54% for foams prepared with oat and straw, respectively.

In contrast to the gelatine-surfactant "A"-fibre composite foams, (Section 6.2.4.1), fibre incorporation into the foams made with surfactant C2, increased their shrinkage compared to the base foams (C2.1 and C2.3).

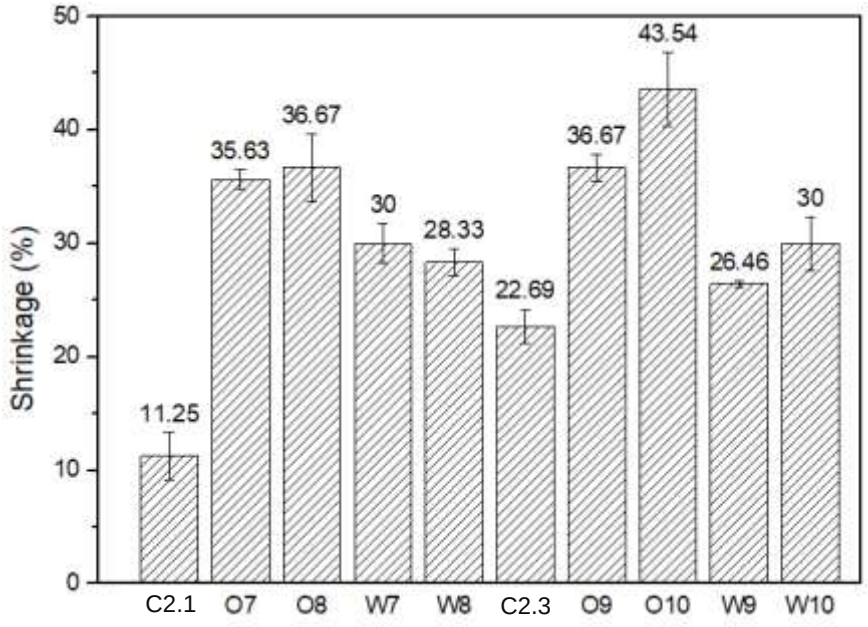

Figure 6.5. SHRINKAGE OF GELATINE-SURFACTANT C2-FIBRE COMPOSITE FOAMS AND COMPARISON WITH THE BASE FOAMS C2.1 AND C2.3

The ANOVA test (Table A.20 in Appendix A) for shrinkage of the composite foams gave F statistics=2.31, p<0.167, F=90.12, p<0.001, F=6.08, p=0.039 011 for gelatine content, fibre type and fibre content, respectively. It can be said that there is a strong evidence that the shrinkage varied with fibre type and content. As observed for gelatine-surfactant "A"-fibre foams the influence of gelatine content on shrinkage was not significant (p>0.05).

The use of straw powder led to lower shrinkage levels compared to the use of oat (p<0.001), as also observed in foams made with surfactant "A". Higher fibre content (*3 wt%*), however, gave rise to slightly higher shrinkage than lower fibre content (*1 wt%*), opposed to found for surfactant "A" (p<0.05). The main effect plots can be seen in Figure B.17 (Appendix B).

The gelatine content-fibre type (p=0.039) and gelatine content-fibre content (p=0.024) interactions were also statistically significant (interaction plots can be seen in Figure B.18, in Appendix B). The higher shrinkage produced with foams containing oat was more significant at higher gelatine content (15 *wt%*). At 10 *wt%*

gelatine content, both 1 *wt%* and 3 *wt%* fibre content exhibited virtually the same shrinkage level. However, at higher gelatine concentration, higher biomass powder concentrations produced less shrinkage.

Figure 6.6 shows the cross-section photos of the cast gelatine-surfactant C2-fibre dry composite foams. The incorporation of fibres into the foam seems to generate a higher number of cells with a cells size greater than 2 *mm*.

Figure 6.6. CROSS-SECTION OF CAST GELATINE-SURFACTANT C2-FIBRE COMPOSITE FOAMS SHOWING THE EFFECTS OF BIOMASS FILLERS AND CONCENTRATION ON TOTAL SHRINKAGE

6.2.3 DENSITY OF THE COMPOSITE FOAMS

Full factorial 3x2x2 and 2x2x2 designs, respectively for surfactant "A" and surfactant C2 foams, with five replicates were used to calculate the statistical significance of the design parameters (gelatine content, fibre type and fibre content) in density of composite foams.

The matrices had different compositions, as shown in Table 6.2, including slightly different residual moisture content (see Section 3.6.3, Chapter 3, for details in moisture content measuring). The fibre content in the dry foams ranged from ~4 *wt%* to a maximum ~20 *wt%*.

Table 6.2 COMPOSITION OF THE COMPOSITE GEL BIOFOAMS CONTAINING POWDERED BIOMASS FILLERS

ID	FIBRE	FIBRE CONTENT (wt%)	SURFACTANT	SURFACTANT CONTENT (*wt%*)	GELATINE CONTENT (*wt%*)	WATER CONTENT (wt%)
O1	oat	6.71	A	10.03	66.76	16.50
O2	oat	17.40	A	8.70	57.90	16.00
O3	oat	4.84	A	7.24	72.31	15.60
O4	oat	12.77	A	6.38	63.75	17.10
O5	oat	3.69	A	5.51	73.35	17.45
O6	oat	10.12	A	5.06	67.33	17.50
O7	oat	7.28	C2	5.45	73.07	14.20
O8	oat	18.43	C2	4.58	61.40	15.60
O9	oat	5.08	C2	3.79	76.33	14.80
O10	oat	13.64	C2	3.39	68.17	14.80
W1	straw	6.81	A	10.19	67.80	15.20
W2	straw	17.19	A	8.60	57.21	17.00
W3	straw	4.76	A	7.11	71.03	17.10
W4	straw	13.11	A	6.55	65.44	14.90
W5	straw	3.73	A	5.57	74.20	16.50
W6	straw	10.25	A	5.13	68.22	16.40
W7	straw	7.30	C2	5.46	73.24	14.00
W8	straw	18.29	C2	4.54	60.96	16.20
W9	straw	5.11	C2	3.82	76.87	14.20
W10	straw	13.51	C2	3.36	67.53	15.60

6.2.3.1 Composite foams based on gelatine-surfactant "A" formulations

Densities of the gelatine-surfactant "A"-fibre composite foams ranged from 15.59 kg/m^3 (sample O1; 10 wt% gelatine, 1 wt% oat fibre) to 59.34 kg/m^3 (sample O6, 10 wt% gelatine, 3 wt% oat fibre), as illustrated in Figure 6.7. Compared to the base foams (A7, A9 and A11) all the formulations including fibres exhibited a considerable increase in density.

The 10 *wt%* foams densities increased by 40.83% and 83.47% when oat fibre was used at 1% and 3 *wt%*, respectively; and by 50.32% and 88.71% when straw was used at 1% and 3%, respectively.

The 15 *wt%* foams densities increased by 24.9% and 50.08% when oat fibre was used at 1% and 3 *wt%*, respectively; and by 7.28% and 32.30% when straw was used at 1% and 3%, respectively.

The 20 *wt%* foams densities increased by 47.09% and 60.03% when oat fibre was used at 1% and 3 *wt%*, respectively; and by 40.53% and 53.37% when straw was used at 1% and 3%, respectively.

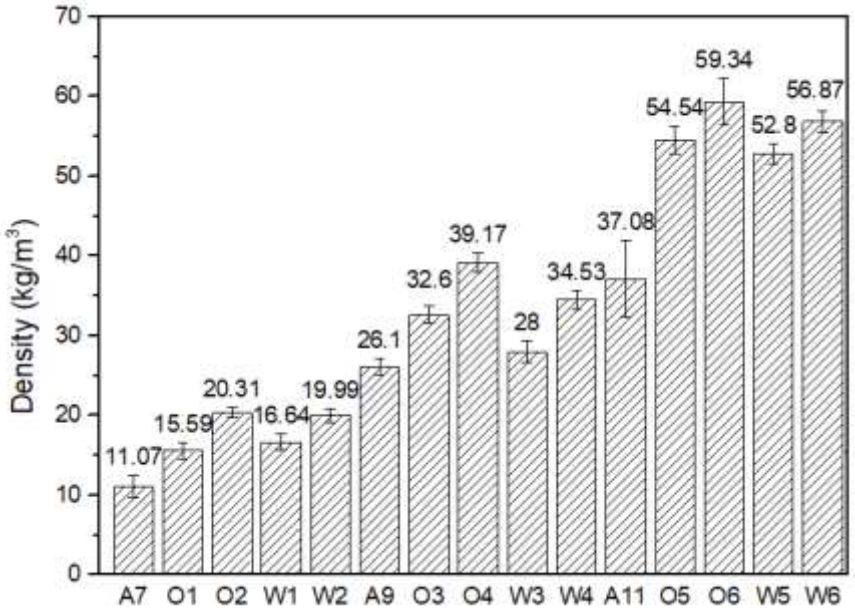

Figure 6.7. DENSITY OF GELATINE-SURFACTANT "A"-FIBRE COMPOSITE FOAMS AND COMPARISON WITH THE BASE FOAMS A7, A9 AND A11

The ANOVA test (see Table A.21 in Appendix A) for density gave F statistics=3,723.97, $p<0.001$, F=34.77, $p<0.001$, F=194.50, $p<0.001$ for gelatine content, fibre type and fibre content, respectively. Thus, it can be said that there is a strong evidence that the density varied with the three studied parameters.

As found in Section 5.4.3 (Chapter 5), density increased as gelatine content increased ($p<0.001$). The use of straw fibre (instead of oat) and lower fibre contents led to lower densities. The main effect plots can be seen in Figure B.19 (Appendix B).

There was also evidence of gelatine content-fibre type ($p<0.001$) and gelatine content-fibre content ($p<0.05$) interaction. The incorporation of fibre had a more significant effect on density (i.e. stronger effect on increasing density) at higher gelatine concentrations. The increase of fibre content was more significant at lower gelatine contents.

6.2.3.2 Composite foams based on gelatine-surfactant C2 formulations

Density ranged from min 25.45 kg/m^3 (sample W7; 10 *wt%* gelatine, 1 *wt%* straw fibre) to max 52.77 kg/m^3(sample O10; 15 *wt%* gelatine, 3 *wt%* oat fibre), as illustrated in Figure 6.8.

The 10 *wt%* foams densities increased by 22.11% and 42.49% when oat fibre was used at 1% and 3 *wt%* contents, respectively; and by 25.45% and 29.39% when straw was used at 1% and 3% concentrations, respectively.

The 15 *wt%* foams densities increased by 20.67% and 42.70% when oat fibre was used at 1% and 3 *wt%* concentrations, respectively; and by 23.08% and 31.45% when straw was used at 1% and 3% contents, respectively.

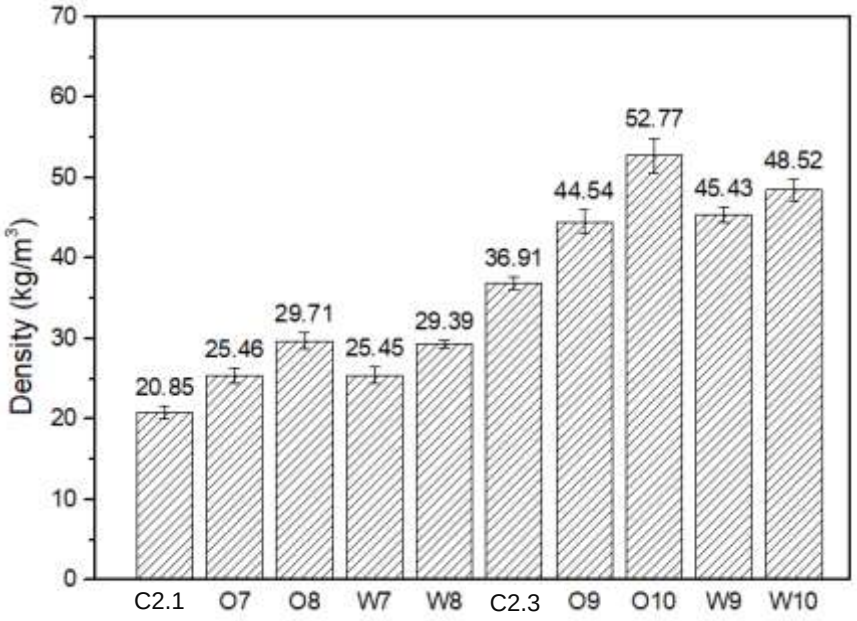

Figure 6.8. DENSITY OF GELATINE-SURFACTANT C2-FIBRE COMPOSITE FOAMS AND COMPARISON WITH THE BASE FOAMS C2.1 AND C2.3

The ANOVA analysis (see Table A.22 in Appendix A) gave F statistics=2496.28, $p<0.001$, $F=5.05$, $p=0.032$, $F=143.57$, $p<0.001$ for gelatine content, fibre type and fibre content, respectively. Thus, there is a strong evidence that density varies with the three studied parameters.

The use of straw and lower gelatine and fibre contents led to lower composite foams. As expected from the results from Subsections 6.2.1.2 and 6.2.2.2, the average density of the foams prepared with straw was slightly lower than its oat counterparts (see Figure 6.7B). It was also expected from THE MER results to associate higher fibre content with higher densities. Figure B.20 in Appendix B shows the main effect plots for the density of foams made with surfactant C2.

The fibre type-fibre content ($p<0.05$) and the gelatine content-fibre content-fibre type ($p<0.05$) interactions also had a significant influence on density. Not a significant effect on density was found at low fibre concentrations with fibre type (i.e. both oat and straw produced similar foam densities at low concentrations). However, at higher

fibre concentrations the foams containing straw were lighter than those made with oat.

The three-way interaction relates the fibre type-fibre content interaction with gelatine content. Higher oat concentrations at 15 *wt%* gelatine content were the composite foams exhibiting the highest density.

6.2.4 FOAM STRUCTURE

All the composite foams exhibited open-cell structures, as observed in Section 5.4.4, in Chapter 5.

The fibres were dispersed into the solutions by mechanical stirring so their dispersion in the cellular structure was generally random. ranging from areas with a relatively low number of particles to areas exhibiting clusters of particles. These areas with clusters may exhibit greater heterogeneous porosity as fibres shaped the cellular structure. In some areas, the fibres shaped the cells in relatively big cell sizes (>0.2 *mm*).

Figures 6.9A and 6.9B presents SEM images of sample **O2** (20.31 kg/m^3,10 *wt%* gelatine content, 3*wt%* oat) at different magnifications. Figure 6.9A shows an oat fibre within the plateau border, joining cell edges. In contrast, Figures 6.9C and 6.10D show that for sample **O6** (59.34 kg/m^3, 20 *wt%* gelatine content, 3 *wt%* oat) the oat fibres were mostly embedded within the much thicker cell walls.

Figures 6.10A and 6.10B show images of samples **W2** (19.99 kg/m^3, *10 wt%* gelatine, 3 *wt%* straw fibre). The higher aspect ratios straw fibres were mostly embedded within the plateau border of the low-density cell structure whereas Figures 6.10C and 6.10D showed that **W6** (56.80 kg/m^3, 20 *wt%* gelatine, 3 *wt%* straw fibre) fibres were embedded in the much thicker cell walls.

The intimate interface between the matrix and the filler fibres suggested good adhesion between the 2 phases.

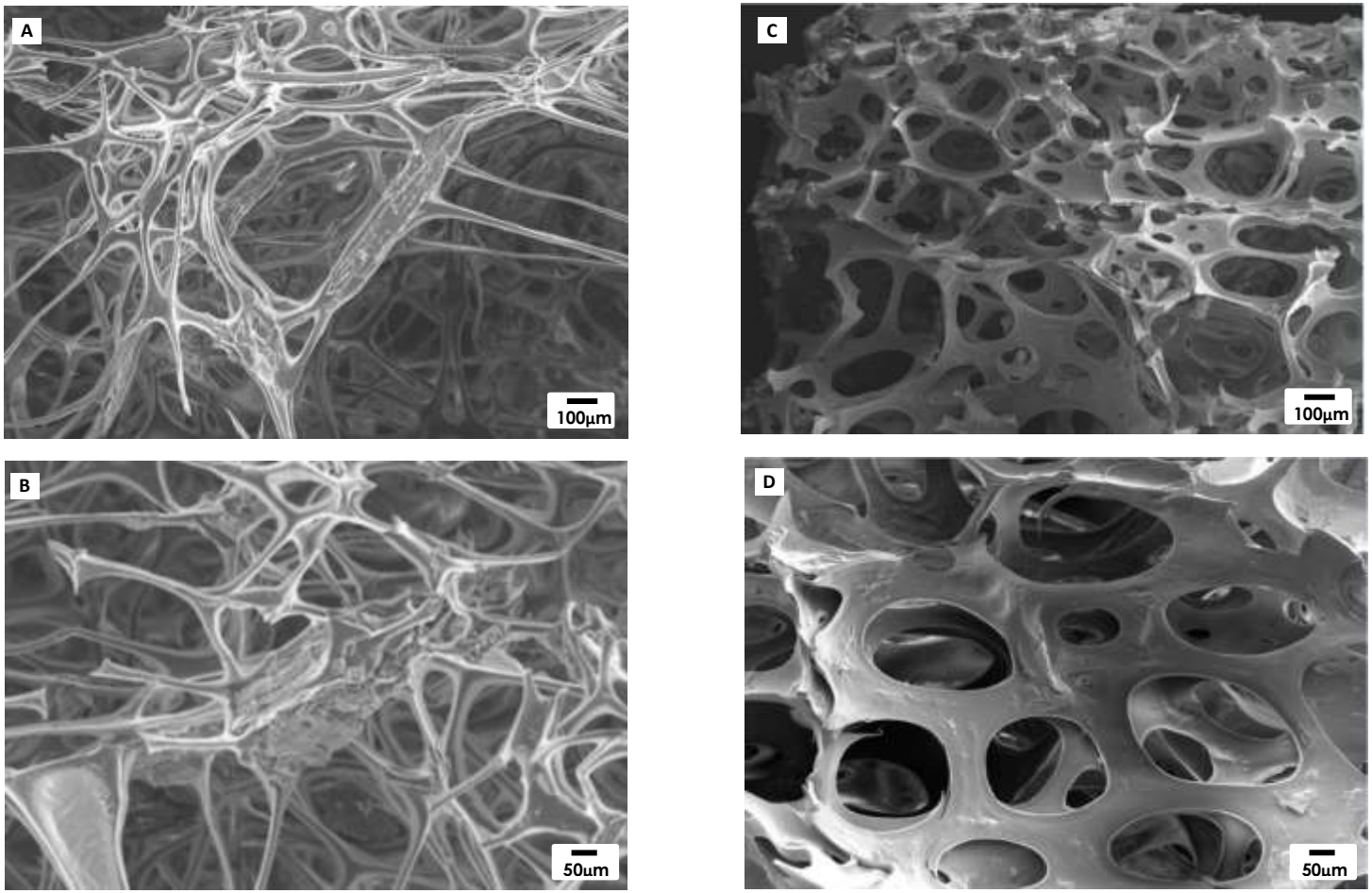

Figure 6.9. SEM IMAGES OF GELATINE-SURFACTANT "A"-OAT FIBRE COMPOSITE FOAMS SHOWING THE CELL STRUCTURE AND FIBRE DISTRIBUTION OF (A) (C) SAMPLE O2 (DENSITY=20.31 *kg·m*$^{-3}$, 10 *wt%* GELATINE CONTENT, 3 *wt%* OAT) AND (C) (D) SAMPLE O6 (DENSITY=59.34 kg·m^{-3}, 20 *wt%* GELATINE CONTENT, 3 *wt%* OAT)

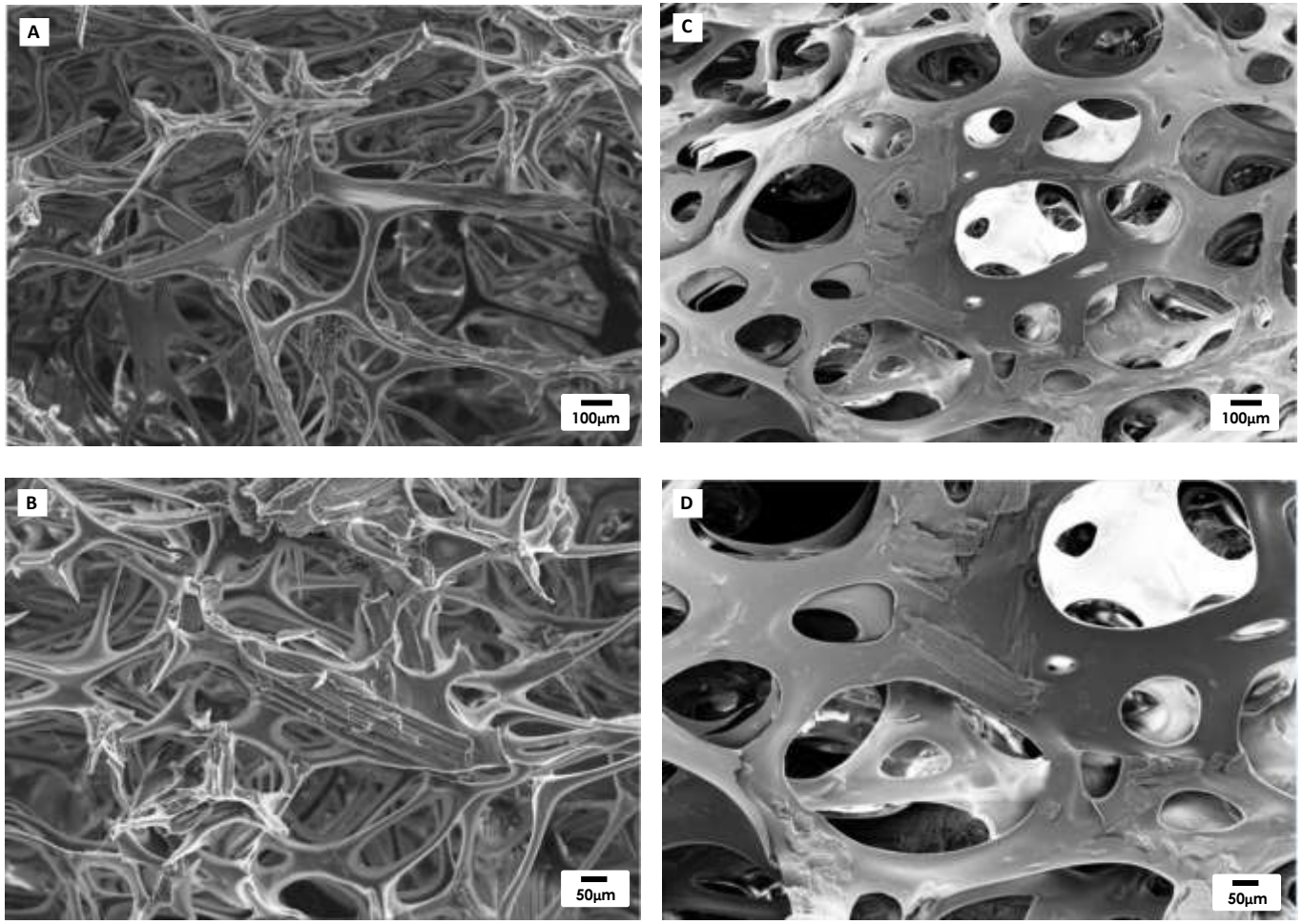

Figure 6.10. SEM IMAGES OF GELATINE-SURFACTANT "A"-STRAW FIBRE COMPOSITE FOAMS SHOWING THE CELL STRUCTURE AND FIBRE DISTRIBUTION OF (A) (C) SAMPLE W2 (DENSITY=19.99 *kg·m*$^{-3}$, 10 *wt%* GELATINE CONTENT, 3 *wt%* STRAW) AND (C) (D) SAMPLE O6 (DENSITY=56.80 kg·m^{-3}, 20 *wt%* GELATINE CONTENT, 3 *wt%* STRAW)

6.2.5 MECHANICAL PROPERTIES

As demonstrated by the foams without fibre fillers (discussed in Chapter 5), compression properties of the composite foams were dependent on foam densities. The variation of compression modulus, yield strength and compression strength at 3 different strains (10, 25 and 50%) is compared in Table 6.3.

Table 6.3. SUMMARY OF COMPRESSION PROPERTIES AND THERMAL CONDUCTIVITIES FOR GELATINE-SURFACTANT "A"/C2-FIBRE COMPOSITE FOAMS

ID	DENSITY (kg/m³)	E (kPa)	YIELD STRENGTH (kPa)	STRESS AT 10% (kPa)	STRESS AT 25% (kPa)	STRESS AT 50% (kPa)
O1	15.59	94.64±15.23	4.23	4.77±1.76	6.83±1.76	12.70±1.28
O2	20.31	152.30±34.30	3.97	5.20±1.44	8.20±1.68	18.13±2.01
O3	32.60	515.88±143.42	33.43	33.10±4.76	42.67±3.31	64.30±4.70
O4	39.17	877.33±89.27	42.15	41.10±0.71	44.90±1.70	56.05±4.45
O5	54.54	2581.50±146.79	62.95	68.00±30.83	80.25±27.79	114.80±21.07
O6	59.34	3705.22±617.58	115.47	120.05±51.55	134.93±36.40	203.23±31.26
O7	25.46	446.97±52.36	6.05	9.60±1.41	15.90±3.11	29.95±6.01
O8	29.71	403.12±52.36	4.15	7.65±0.92	14.95±3.18	33.45±4.74
O9	44.54	1124.83±80.45	11.05	16.45±0.64	27.60±2.26	69.35±1.20
O10	52.77	2120.17±391.13	50.80	53.70±22.63	69.70±18.95	116.85±8.84
W1	16.64	94.50±38.88	1.60	2.85±0.92	5.65±1.34	14.25±3.61
W2	19.99	131.43±22.35	3.50	5.27±2.54	9.10±2.95	20.10±3.10
W3	28.00	827.56±194.01	10.57	15.97±7.13	23.10±6.88	47.77±2.64
W4	34.53	1064.50±85.80	23.00	25.25±1.06	33.75±0.35	65.55±2.47
W5	52.80	3310.00±559.12	72.55	63.60±28.01	94.15±34.74	159.75±55.51
W6	56.87	2649.83±285.15	73.00	78.25±63.14	95.90±63.07	179.95±72.90
W7	25.45	212.63±38.88	2.35	3.05±0.93	6.67±2.34	17.67±2.38
W8	29.39	294.41±22.35	4.62	5.74±2.38	14.38±2.95	26.93±5.98
W9	45.43	1655.11±194.01	13.63	24.91±6.38	36.04±8.45	74.04±10.34
W10	48.52	2522.87±85.80	28.06	39.90±6.38	46.91±7.43	68.83±14.54

6.2.6 THERMAL CONDUCTIVITY

The thermal conductivity of the composite foams made with surfactant "A" (see Table 6.4) was measured as described in section 3.6.7 in Chapter 3.

The thermal conductivity obtained was comparable to that obtained in Section 5.4.5.2 (Chapter 5) for gelatine-surfactant "A" and, thus falling into a good alternative for conventional plastic foams used for thermal insulation applications.

The lowest density did not necessarily mean better insulating, as shown for gelatine-surfactant "A" foams. In fact, the sample exhibiting the highest thermal conductivity was sample A1, that with the lowest density. This is attributable to the large standard deviation obtained in the measurements, which depended not only in the matrix composition but also the foam cell structure. As discussed in Section 6.2.4 the

composite foams exhibited a greater number of cells with a cell size>0.2 *mm* than those made without fibres and the erratic presence of these bigger cells may considerably affect the foams thermal conductivity.

Table 6.4. THERMAL CONDUCTIVITIES FOR GELATINE-SURFACTANT "A"/C2-FIBRE COMPOSITE FOAMS

ID	DENSITY (kg/m^3)	THERMAL CONDUCTIVITY (W/mK)
O1	15.59	0.0456 ± 0.0028
O2	20.31	0.0445 ± 0.0028
O3	32.60	0.0383 ± 0.0021
O4	39.17	0.0378 ± 0.0024
O5	54.54	0.0389 ± 0.0011
O6	59.34	0.0382 ± 0002
W1	16.64	0.0423 ± 0.0017
W2	20.00	0.0392 ± 0.0004
W3	28.00	0.0404 ± 0.0008
W4	34.53	0.0396 ± 0.0005
W5	52.80	0.0428 ± 0.0005
W6	56.87	0.0399 ± 0.0004

Figures 6.11 shows the relationship between thermal conductivity and density. The oat samples showed a thermal conductivity decrease as density increased. The straw samples did not show a clear trend.

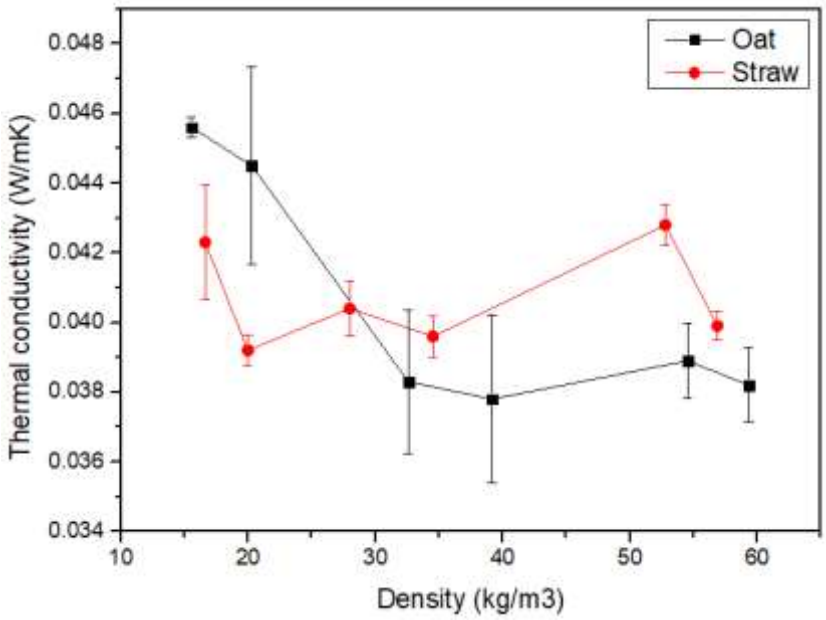

Figure 6.11. DENSITY-THERMAL CONDUCTIVITY RELATIONSHIP FOR GELATINE-FIBRE COMPOSITE FOAMS

6.2.7 SUMMARY

This section studied the incorporation of lignocellulose powders into the gelatine foams in attempt to produce a more cost-effective product for different applications.

Fibre incorporation lowered the expansion ratio of the surfactant "A" ($p<0.05$) and surfactant C2 ($p>0.05$) foams. For surfactant "A" foams, higher MER values were achieved with straw and lower fibres concentrations ($p<0.05$). The maximum MER obtained (corresponding to 10 *wt%* gelatine content) were 9.91 and 7.37 for foams made with surfactants "A" and C2, respectively. The minimum MER obtained (corresponding to the higher gelatine content studied for each surfactant) were 4.96 and 5.78 for surfactants "A" and C2, respectively.

The shrinkage obtained for surfactant "A" foams ranged from 20.83 to 42.71%. When fibres were incorporated into the surfactant "A" containing foams, shrinkage tended to decrease. There are two possible explanations for this behaviour. An increase in solid content may favoured the cell structure integrity and the filler powder did not absorb in the matrix and helped to maintain the cell structure. However, the opposite trend was found for surfactant C2 containing foams which shrinkage increased compared to that for foams made without fibres (their shrinkage ranged from 26.46-43.54%, considerably higher than the minimum value found for the system without fibres, ≈10%). The use of straw powder led to lower shrinkage levels compared to that for oat for both surfactants ($p<0.001$) but higher fibre content gave rise to slightly lower shrinkage in surfactant "A" containing foams ($p<0.05$) and slightly higher shrinkage in surfactant C2 foams. Further research needs to be done about the influence of fibres on shrinkage, especially regarding the fibre content and the influence on gelatine concentration.

The density of the composite foams made with surfactant A ranged from 15.59 kg/m^3 (10 *wt%* gelatine) to 59.34 kg/m^3 (20 *wt%* gelatine), while the density of composite foams made with surfactant C2 ranged from 25.46 kg/m^3 (10 *wt%* gelatine) to 52.77 kg/m^3 (15 *wt%* gelatine). Compared to the base foams all the formulations including fibres exhibited a considerable increase in density. The density increase was more remarkable in 10 *wt%* gelatine foams including oat fibres. The use of straw fibre (instead of oat) ($p<0.05$) and lower fibre contents ($p<0.05$) led to lower densities for both surfactants.

The fibre content in the dry gelatine-fibre composite foams ranged from ~4 wt% to ~20 wt%. This fibre content could be further increase in foams containing 10 *wt%* gelatine, where the increase in fibre content may produce relatively high-density foams (30-40

kg/m³) with a considerably lower gelatine content, which would lead to a reduce in cost.

The foams exhibited an open-cell structure, as previously observed for the foams without fibres, and the SEM images showed a good adhesion between the two phases (gelatine-fibres). However, the fibre dispersion was generally random, with areas exhibiting cluster of particles and areas with a relatively low number of particles which shape the cell structure producing cells with a relatively big size (>2 *mm*).

The mechanical properties depended on foam density and higher fibre content usually led to higher compression modulus and yield strength.

The thermal conductivity was not heavily depended on density and the values obtained (0.039-0.046 *W/m·K*) were comparable to that for gelatine-surfactant "A" foams, which mean gelatine-fibre composite foams are also a good alternative to conventional plastic polymers, like EPS.

The lowest density did not necessarily mean better insulating, as shown for gelatine-surfactant "A" foams. In fact, the sample exhibiting the highest thermal conductivity was sample A1, that with the lowest density. This is attributable to the large standard deviation obtained in the measurements, which depended not only in the matrix composition but also the foam cell structure. As discussed in Section 6.2.4 the composite foams exhibited a greater number of cells with a cell size>0.2 *mm* than those made without fibres and the erratic presence of these bigger cells may considerably affect the foams thermal conductivity.

In conclusion, it was feasible to produce low-density gelatine-fibres composite foams with relatively low shrinkage and good thermal properties. However, further research is needed to explore a greater fibre inclusion for those samples exhibiting higher expansion ratios.

6.3 GELATINE-SURFACTANT C2–SiO_2 AEROGEL COMPOSITE FOAMS

This section studies the influence of the incorporation of silica aerogel powders on the thermal conductivity properties of the gelatine-SDS2 foams.

As discussed in section 3.3.3.4.4 in Chapter 3, the SiO_2 aerogel powder was incorporated into the formulation C2.1 (10 *wt%* gelatine content, 0.75 *wt%* surfactant content) and C2.3 (15 *wt%* gelatine content, 0.75 *wt%* surfactant content). Table 6.5 shows the experimental matrix, the density and the thermal conductivity of the foams prepared with the aerogel powders.

Table 6.5. EXPERIMENTAL MATRIX, DENSITY AND THERMAL CONDUCTIVITY OF AEROGEL FOAMS

ID	GELATINE CONTENT (*wt%*)	AEROGEL TYPE	AEROGEL CONTENT* (*wt%*)	DENSITY (kg/m³)	THERMAL CONDUCTIVITY (W/m·K)
C2.1	10	-	0	20.85±0.79	0.0381±0.0016
P1	10	Hydrophobic	1	30.16±1.66	0.0348±0.000679
P2	10	Hydrophobic	3	46.30±3.83	0.0333±0.000955
P3	10	Hydrophilic	1	29.65±2.99	0.0342±0.001004
P4	10	Hydrophilic	3	35.82±0.32	0.0330±0.000156
C2.3	15	-	0	36.91±0.77	0.0387±0.0021
P5	15	Hydrophobic	1	56.15±2.69	0.0345±0.000191
P6	15	Hydrophobic	3	73.33±1.32	0.0344±0.000566
P7	15	Hydrophilic	1	56.59±3.22	0.0350±0.000481
P8	15	Hydrophilic	3	57.05±1.19	0.0351±0.001018

**Content based on the total weight of the gelatine-water solution*
Note: Surfactant C2 content was constant at 0.75 wt% on the total weight of the gelatine-water solution

The considerably increase in density may be due to cell structure changes due to the aerogel incorporation. This can be proved if cell morphology is carefully assessed for the foam but it is beyond this study due to timescale.

Figure 6.12 shows the relationship between density and thermal conductivity of the gelatine-surfactant C2-aerogel foams.

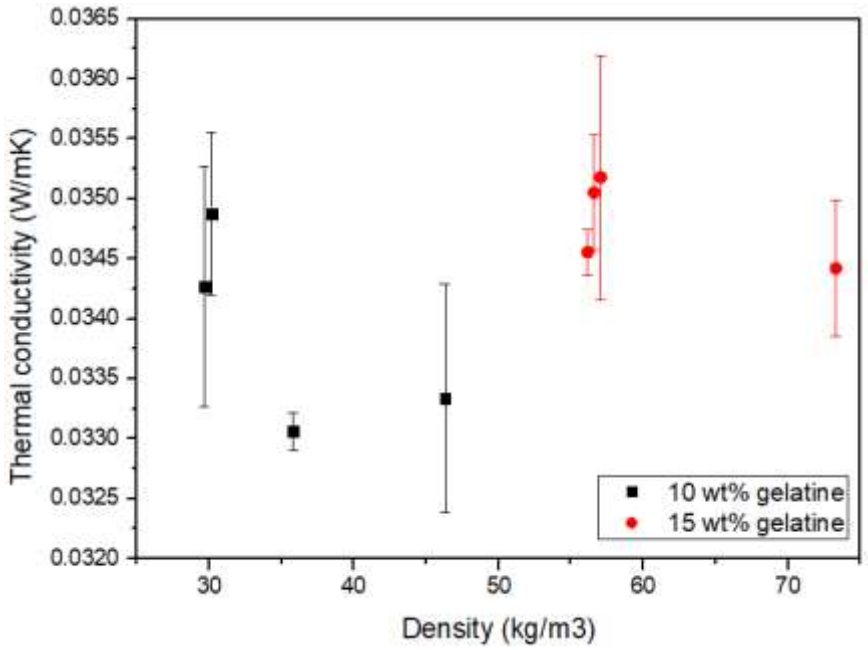

Figure 6.12. THERMAL CONDUCTIVITY VARIATION WITH FOAM DENSITY FOR THE GELATINE-SURFACTANT C2-AEROGEL COMPOSITE FOAMS

To investigate the statistical significance of the incorporation of aerogel powders, an ANOVA test at 2 factors was carried out. These factors were:

- Gelatine content, at 2 levels: 10 and 15 wt%
- Aerogel incorporation at 3 levels: 0 wt%, 1wt% hydrophilic powder, 1wt% hydrophobic powder

The ANOVA table (see Table A.23 in Appendix A) gave statistics F=7.03 and p=0.027 for aerogel incorporation, so it can be said that there was a strong evidence for thermal conductivity varying with aerogel incorporation as low as 1 *wt%*. A second ANOVA test (not shown) confirmed the positive influence of the powders incorporation at 3 *wt%*.

A third ANOVA test was carried out to assess the statistical significance of the impact of the type of aerogel powder used and its concentration. Three factors at two levels were studied:

- *Gelatine content,* at 2 levels: 10 and 15 *wt%*
- *Aerogel type,* at 2 levels: hydrophobic and hydrophilic
- *Aerogel content,* at two levels: 1*wt%* and 3*wt%*

The second ANOVA table for aerogel foams (see Table A.24 in Appendix A) gave statistics F=6.65 and p=0.033, F=0.07 and p=0.801 and F=3.78 and p=0.088 for gelatine content, aerogel type and aerogel content, respectively. Thus, the only statistically significant factor on thermal conductivity was gelatine content.

Thus, any type of aerogel added at any of the concentrations studied made a positive impact on thermal conductivity of hydrogel foams based in gelatine. However, this positive impact did not significantly improve with the increase in concentration of the aerogel powders and the performance of the two different powders was similar.

Figures 6.13 shows SEM images of the foam cell structures. The particles were trapped in the cell walls which give them a rough appearance. They did not show a good wetting/adhesion between the particles, specially the hydrophobic, and the matrix and the particles were mostly wrapped by a film of the matrix. This help to explain the reduction in thermal conductivity by the aerogel inclusion. The thermal conductivity of the composite cell walls depended on the thermal conductivity of the aerogel powder (which is much lower than that of the matrix) and the powder volume fraction in the cell walls. It is foreseeable that further increase of aerogel content will lead to difficulties for liquid foaming and thus the scope for more drastic reduction is rather limited.

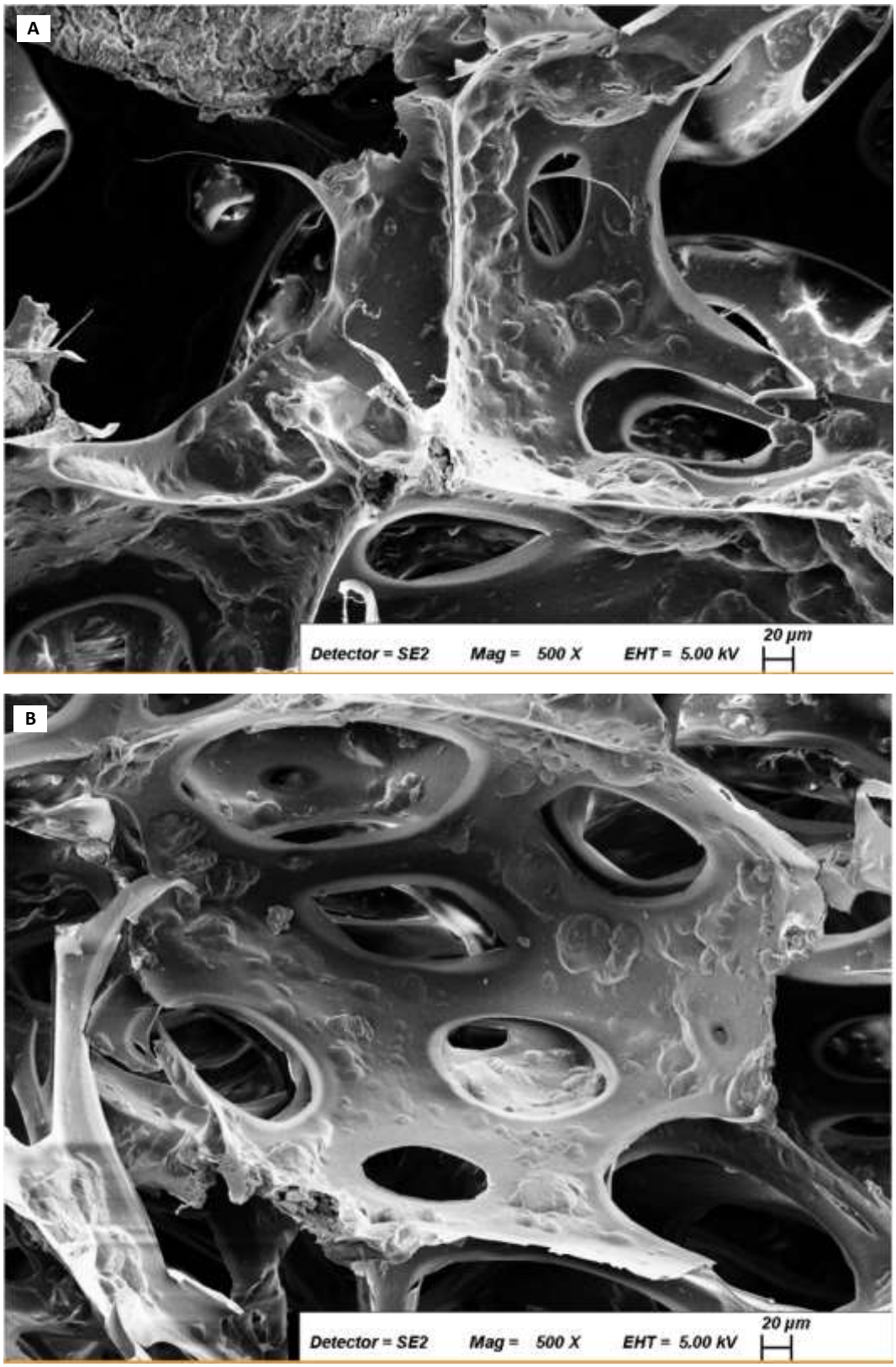

Figure 6.13. SEM IMAGES OF FOAM CELL WALLS EMBEDDED WITH (A) P2, HYDROPHOBIC AEROGEL (B) P4, HYDROPHILIC AEROGEL

6.4 GELATINE-EXPANDED VERMICULITE COMPOSITE FOAMS

This section investigates the effect of inclusion of expanded vermiculate particles into formulations A7, A9 and A11 (see their formulation in Table 3.35 in Chapter 3). The main objective was to assess the thermal insulation and fire resistance of the composite foams for e.g. construction applications. Table 6.6 summarises the experimental matrix of the gelatine-surfactant "A"-vermiculite composite foams, their dry density, total shrinkage and compression modulus. The formulation table can be seen in Section 3.3.3.4.3.

As the composite foams were made by blending the vermiculite particles, at a given *vol%,* into the base liquid foams at maximum expansion ratio, no attempt was made to record the volume change in the liquid composite foams.

Table 6.6. DRY COMPOSITE FOAM DENSITY, TOTAL SHRINKAGE (%), AND COMPRESSION MODULUS OF THE COMPOSITE FOAMS BASED ON A7, A9 AND A11

ID	VERM*. TYPE	VERM*. CONTENT (wt%)	GELATINE CONTENT (wt%)	DENSITY (kg/m^3)	TOTAL SHRINKAGE (%)	COMPRESSION MODULUS (kPa)	RECOVERY AFTER 50% STRAIN (%)
A7**	-	-	10	11.09	43	19.37	94.29
A9**	-	-	15	26.10	31	660	73
A11**	-	-	20	37.08	43	1795	76.26
VS1	Fine	6.5	10	50.23±3.85	31.46	26	96.13
VS2			15	69.18±3.67	34.38	299	76.74
VS3			20	93.19±5.96	35.21	880	75.49
VS4		13	10	90.9±3.88	36.46	7	94.84
VS5			15	103.35±4.3	35.63	116	81.94
VS6			20	99.36±2.78	32.08	878	73.89
VS7		19.5	10	104.22±3.00	30.35	18	88.89
VS8			15	105.81±3.34	29.79	96	82.2
VS9			20	125.56±4.96	27.33	377	68.06
VB1	Coarse	6.5	10	47.27±2.19	41.46	26	95.83
VB2			15	54.31±2.05	36.63	315	82.99
VB3			20	79.88±6.04	38.13	1166	72.11
VB4		13	10	64.79±5.24	34.33	23	98.89
VB5			15	69.42±2.78	30	116	83.96
VB6			20	94.42±1.71	32.92	2359	75.49
VB7		19.5	10	81.63±3.79	31.25	24	89.31
VB8			15	93.54±3.76	29.38	89	81.25
VB9			20	101.26±4.09	27.5	1256	76.96

*Vermiculite
** See complete formulation in Table 3.35 (Chapter 3)

The incorporation of the expanded vermiculite considerably increased the density and reduced the total shrinkage of the composite foams compared with the base foams A7, A9 and A11. This can be attributed to the relatively higher density of the vermiculite particles, which did not contribute to the shrinkage and maintained the cell structure bonded as the liquid foam dried.

Sample VS9 (20 *wt%* gelatine content, 19.5 *vol%* fine vermiculite) exhibited the highest density, 125.56*kg/m*^{3,} while sample VB1 (10 *wt%* gelatine content, 6.5 *vol%* coarse vermiculite) exhibited the lowest density, 47.27 *kg/m*^{3}.

As expected, higher gelatine contents tended to produce higher density foams for a given vermiculite *vol%* concentration. Higher vermiculite levels incorporated into the base formula and the use of small vermiculite particles (smaller air gaps between particles) also produced foams with higher density.

Sample VB1 (10 *wt%* gelatine content, 6.5 *vol%* vermiculite) exhibited the highest shrinkage value, 41.46%. Sample VS9 (20 *wt%* gelatine content, 19.5 *vol%* vermiculite) had the lowest shrinkage value, 27.33%.

Sample VB6 (20 *wt%* gelatine content, 13.5 *vol%* vermiculite) exhibited the highest compression modulus (2356 *kPa*) and sample VS4, the lowest (*7 kPa)*. Sample VB4 had the highest recovery ratio at 98.89% and sample VS9 had the lowest recovery ratio at 68.06%.

The thermal conductivity of samples VS2 (*15 wt%* gelatine content, 6.5 vol% fine vermiculite) and VS8 (15 *wt%* gelatine content, 19.5 *vol%* fine vermiculite) was 0.0534 and 0.0603*W/m·K*, respectively. Thus, vermiculite incorporation, while still creating a good insulating material, had a relatively higher thermal conductivity than the base gelatine foams.

The gelatine-vermiculite composites foams were assessed in a simplified fire test procedure, as decribed in section 3.6.9 in Chapter 3, in comparison with the base foams and some conventional plastic foams.

Polystyrene caught fire after 1 second of flame exposure (Fig. 6.14A). After 3 seconds the flame was removed (Fig 6.14B) but the PS foam continued burning and escalating with time (Figure 6.14.C).

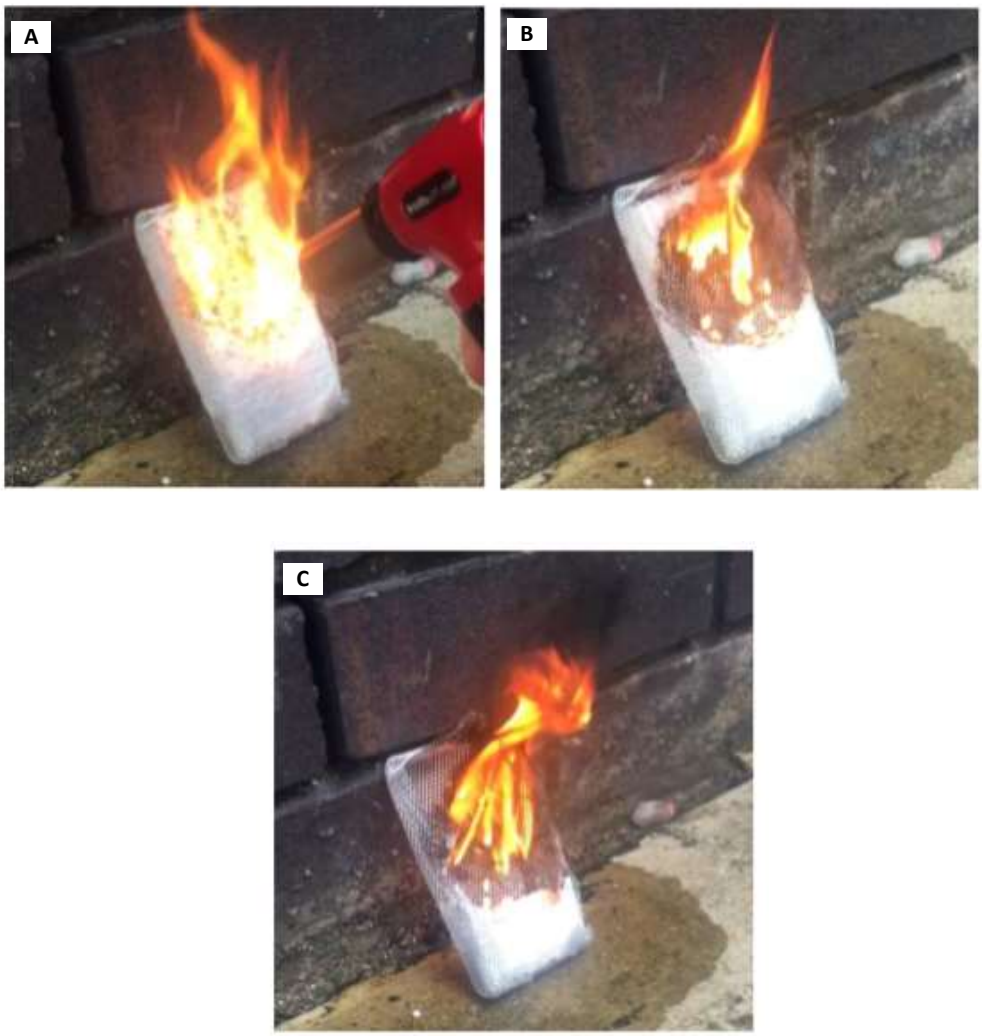

Figure 6.14. RESPONSE OF POLYSTYRENE FOAM IN DIRECT FLAME EXPOSURE (1300°C) FOR THE LENGTH OF TIME (SECONDS) (A) 1 (B) 3 AND (C) 10

Polyurethane foam also caught fire after 1 second, as soon as the flame reached the material surface (Fig 6.15A, B and C). After the flame was removed, the flames were sustained and considerably more violent than the ones observed in PS (Figure 6.15D).

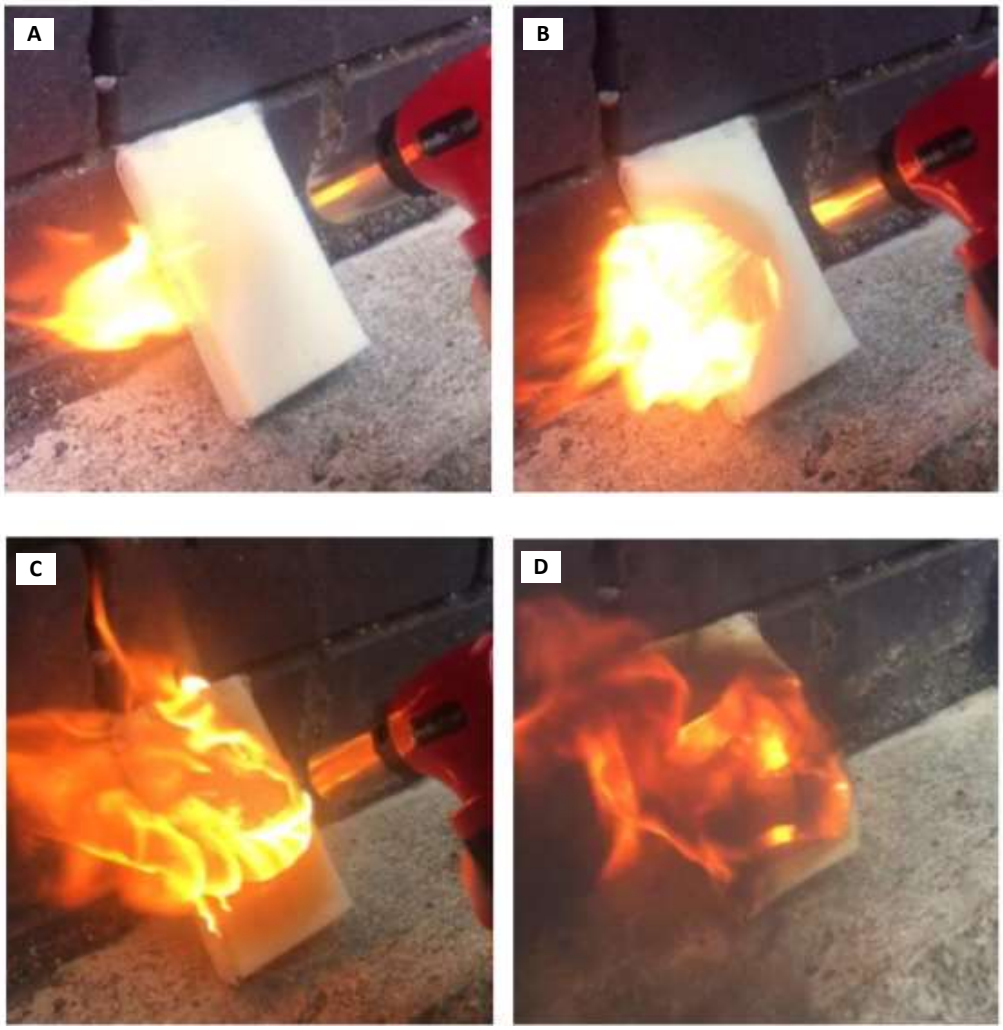

Figure 6.15. RESPONSE OF POLYURETHANE FOAM IN DIRECT FLAME EXPOSURE (1300°C) FOR THE LENGTH OF TIME (SECONDS) (A) 1 (B) 3 AND (C) 10

Figure 6.16 shows the images of the fire test performed on the base foam A11 (20 *wt%* gelatine). The foam was tested in continued exposure to flame for 20 second, a much harsher condition than the earlier tests. The material burned while exposed to the flame, but in a much less violently manner compared with the PS and PU foams. As soon as the flame torch was withdrawn at 20 *seconds*, the fire extinguished spontaneously. There was no melting and dripping of the material but only charring (Figure 6.16D), demonstrating relatively good fire resistance characteristics.

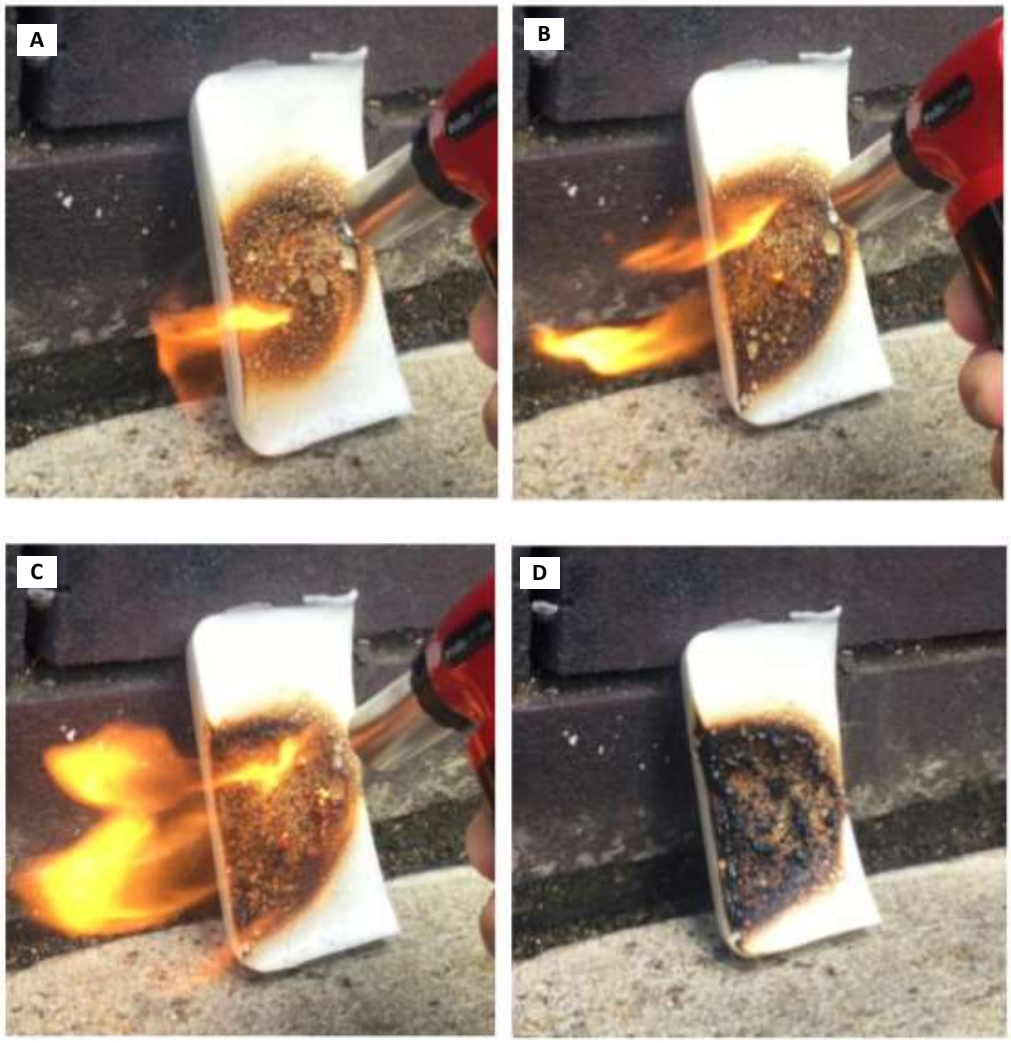

Figure 6.16. RESPONSE OF BASE GELATINE FOAM (SAMPLE A11) FOAM IN DIRECT FLAME EXPOSURE (1300°C) FOR THE LENGTH OF TIME (SECONDS) (A) 5 (B) 10 (C) 15 (D) 20

Finally, four samples of the gelatine-vermiculite composite foams: VB9, VS9, VS3 and VB7 were selected in direct fire exposure tests. Figure 6.17 illustrates their fire-resistant performance after 5 seconds exposure to the flame. All the samples burned only at the surfaces and charred.

After 5 seconds exposure to flame, sample VB7 (10% gelatine content, 6.5 *vol%* coarse vermiculite) generated more smoke than the others (Fig 6.17A). Sample VS3 (20% gelatine content, 6.5 *vol%* fine vermiculite) emitted out a small fire flame from a different location to where the flame torch was focusing which implies the flame was generated by the heated material (Fig 6.17B). Samples VS9 (20% gelatine content, 19.5 *vol%* fine vermiculite) and VB9 (20 *wt%* gelatine content, 19.5 *vol%* coarse vermiculite) withstood the flame much better. They neither emitted flame nor smoke (Fig 6.17C and D).

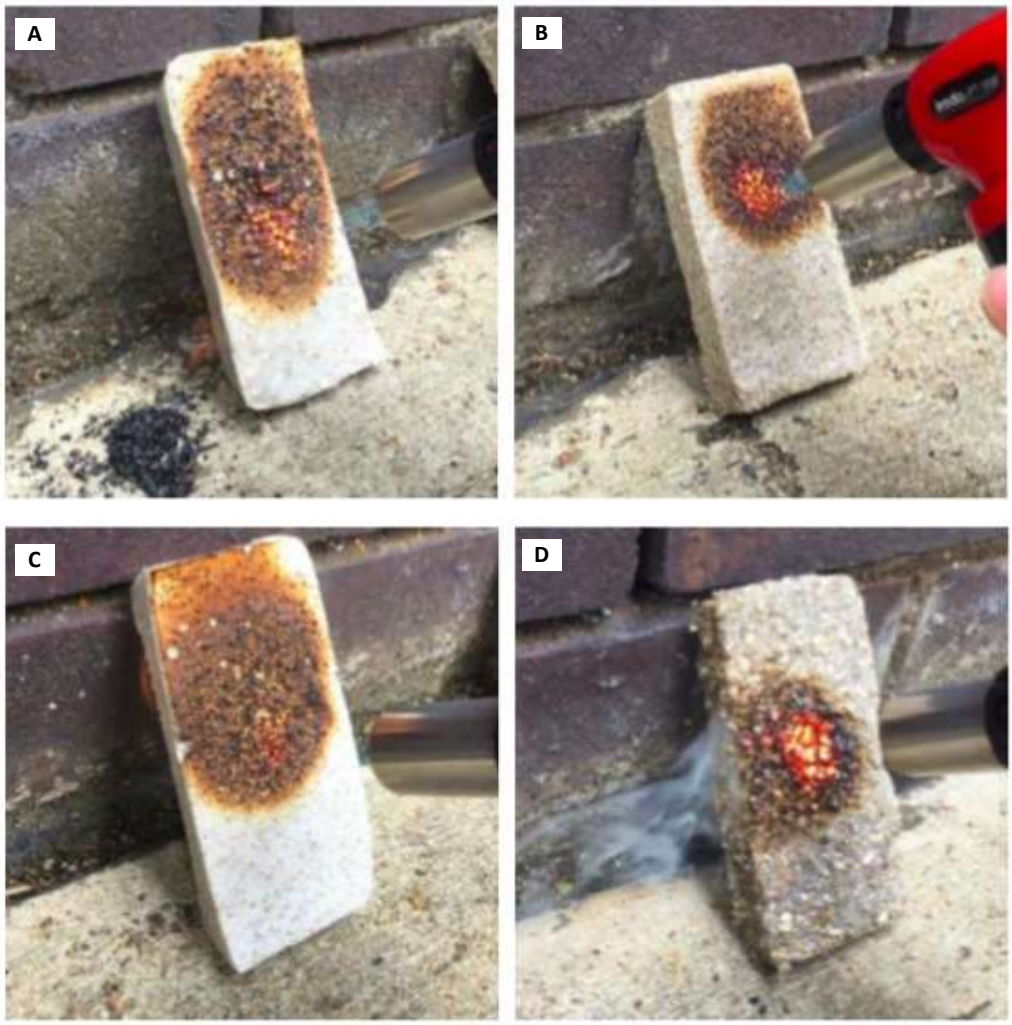

FIGURE 6.17. RESPONSE OF THE GELATINE VERMICULITE COMPOSITE FOAMS TO DIRECT FLAME EXPOSURE FOR 5 SECONDS: (A) SAMPLE VB9; 20 *wt%* GELATINE, 19.5VOL% COARSE VERMICULITE (B) SAMPLE VS9; 20 *wt%* GELATINE, 19.5 VOL% FINE VERMICULITE (C) SAMPLE VS3; 20 *wt%* GELATINE CONTENT, 6.5 VOL% FINE VERMICULITE (D) SAMPLE VB7; 10 *wt%* GELATINE CONTENT, 6.5 VOL% COARSE VERMICULITE

After 15 *seconds* of flame exposure, Sample VB7 (10% gelatine content, 6.5 *vol%* coarse vermiculite) emitted a relatively high amount of smoke (Fig 6.18A) and VS3 (20% gelatine content, 6.5 *vol%* fine vermiculite) exhibited a small flame (Fig 6.18B). Samples VS9 (20% gelatine content, 19.5 *vol%* fine vermiculite) and VB9 (20 *wt%* gelatine content, 19.5 *vol%* coarse vermiculite) exhibited a similar state as observed after 5 *seconds* flame exposure (Fig 6.18C and D).

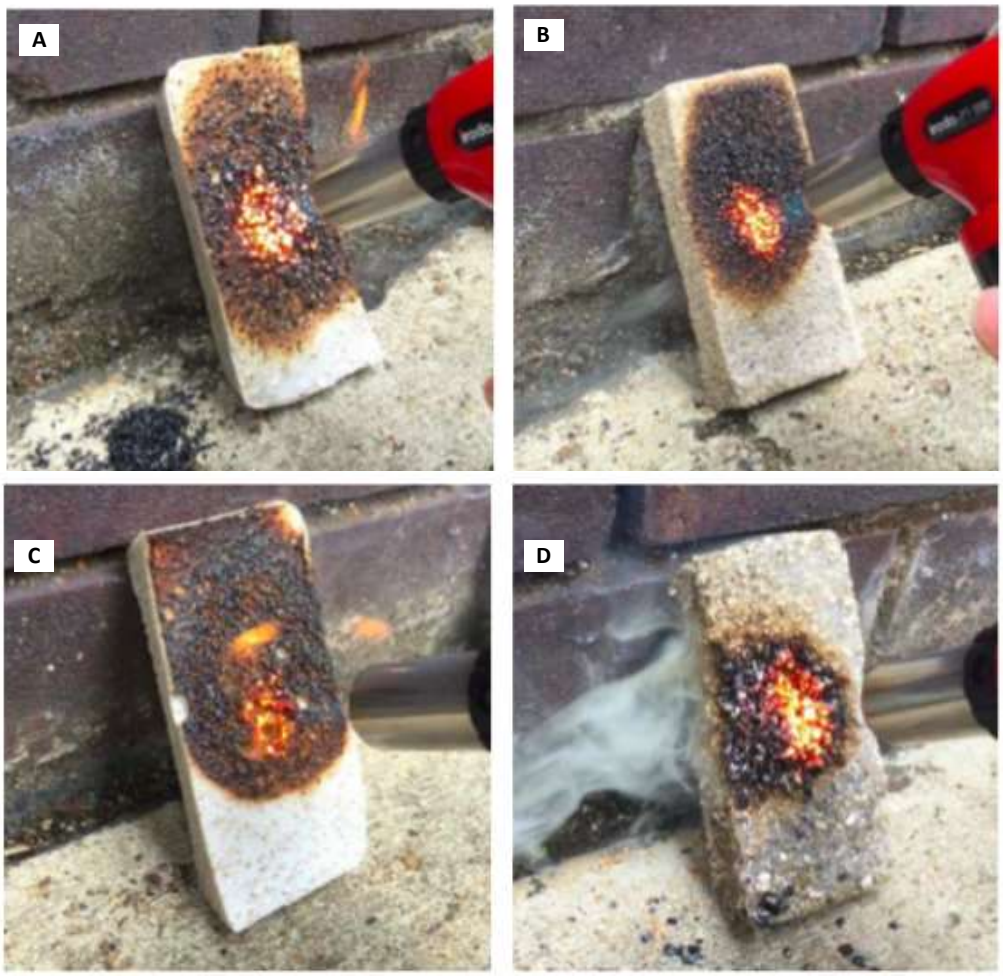

Figure 6.18. RESPONSE OF THE GELATINE VERMICULITE COMPOSITE FOAMS TO DIRECT FLAME EXPOSURE FOR 15 SECONDS: (A) SAMPLE VB9; 20 *wt%* GELATINE, 19.5VOL% COARSE VERMICULITE (B) SAMPLE VS9; 20 *wt%* GELATINE, 19.5 VOL% FINE VERMICULITE (C) SAMPLE VS3; 20 *wt%* GELATINE CONTENT, 6.5 VOL% FINE VERMICULITE (D) SAMPLE VB7; 10 *wt%* GELATINE CONTENT, 6.5 VOL% COARSE VERMICULITE

Figure 6.19 shows the states of the samples after 20 seconds of flame exposure. As soon as the fire torch was removed, the samples stopped burning simultaneously. All the samples had their surface charred during the tests, a good characteristic for fire resistance, as the charring protected the internal foam.

Sample VB7 was the most damaged, exhibiting a hole from the front to the back where the flame was focused and there was considerable distortion (Figure 6.19 A). VS3 also exhibits a small hole but not as deep (Figure 6.19B) VB9 and VS9 are in much better states (Figure 6.19C and D).

Comparing VB7 and VB9, both had the same vermiculite content but VB9 had a higher gelatine content than VB7. This suggest higher gelatine content was beneficial

for fire resistance, due probably to the better bonding and better structural integrity during burning.

Comparing VS3 with VS9, both had 20 *wt%* gelatine but VS9 (19.5 vol% vermiculite) had three times more vermiculite than VS3 (6.5 vol% vermiculite), contributing to the much better fire resistance.

In conclusion, the fireproofing performance of the foams may be enhanced by high gelatine and vermiculite contents. Higher gelatine content implied higher sample integrity which implies a stronger structure which withstands deformation on burning.

Vermiculite had excellent thermal and fire-resistant properties and thus higher *vol%* contributed to the fire resistance. However, excessively high vermiculite content may lead to the composite foam processing difficulties and compromise the sample integrity.

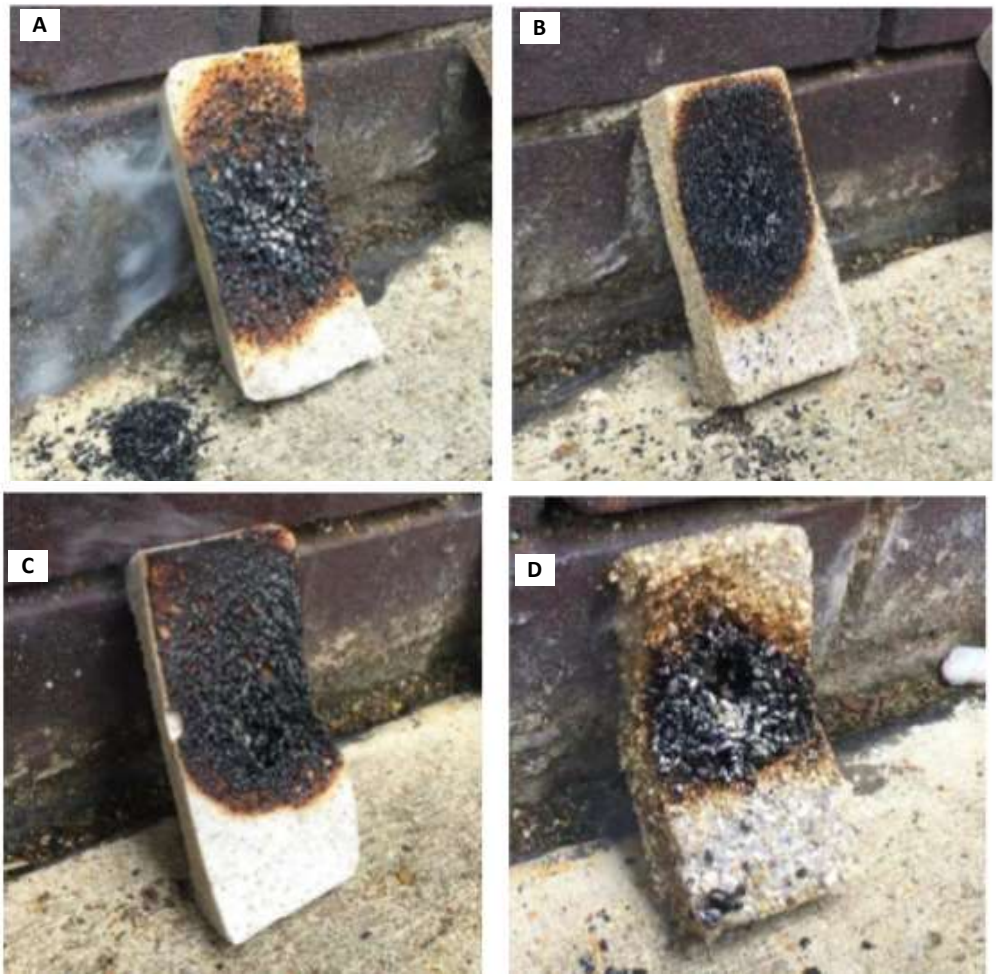

Figure 6.19. RESPONSE OF THE GELATINE VERMICULITE COMPOSITE FOAMS TO DIRECT FLAME EXPOSURE FOR 15 SECONDS: (A) SAMPLE VB9; 20 *wt%* GELATINE, 19.5VOL% COARSE VERMICULITE (B) SAMPLE VS9; 20 *wt%* GELATINE, 19.5 VOL% FINE VERMICULITE (C) SAMPLE VS3; 10 *wt%* GELATINE CONTENT, 6.5 VOL% FINE VERMICULITE (D) SAMPLE VB7; 20 *wt%* GELATINE CONTENT, 6.5 VOL% COARSE VERMICULITE

6.5 FOAM-FILLED HONEYCOMB PANELS

One of the key features of the hydrogel liquid foaming, the low foam viscosity in comparison with molten polymer foams, enables filling of complex cavities such as honeycomb structures.

This section evaluates the potential enhancement in properties of Nomex® and cardboard honeycomb panels using formulation A11 (density =37.08 kg/m^3, for further details see Table 3.35 in Chapter 3) as the filling foam. Table 6.7 show the experimental matrix for the foam-filled honeycomb panels.

Table 6.7. EXPERIMENT MATRIX FOR HONEYCOMB BOARDS FILLED WITH HYDRO-GEL FOAMS.

ID	HONEYCOMB BOARD MATERIAL	HONEYCOMB BOARD CELL SIZE (mm)	FOAM FILLING (Y/N)
H1.1	Cardboard	15	N
H1.2			Y
H2.1		27	N
H2.2			Y
N1.1	Nomex®	3.2	N
N1.2			Y
N2.1		4.8	N
N2.2			Y

Note: The filling material was Sample A11 (see Table 3.35 in Chapter 3)

Post foam filling, the panels were left 10 days in laboratory conditions to dry naturally, no attempt was made to accelerate the drying, but the drying of the foams may be benefitted from using air-circulating drying.

Figure 6.20 shows the bonding between the open-celled structure of the foam (formulation A11)) and cell walls of the honeycomb boards.

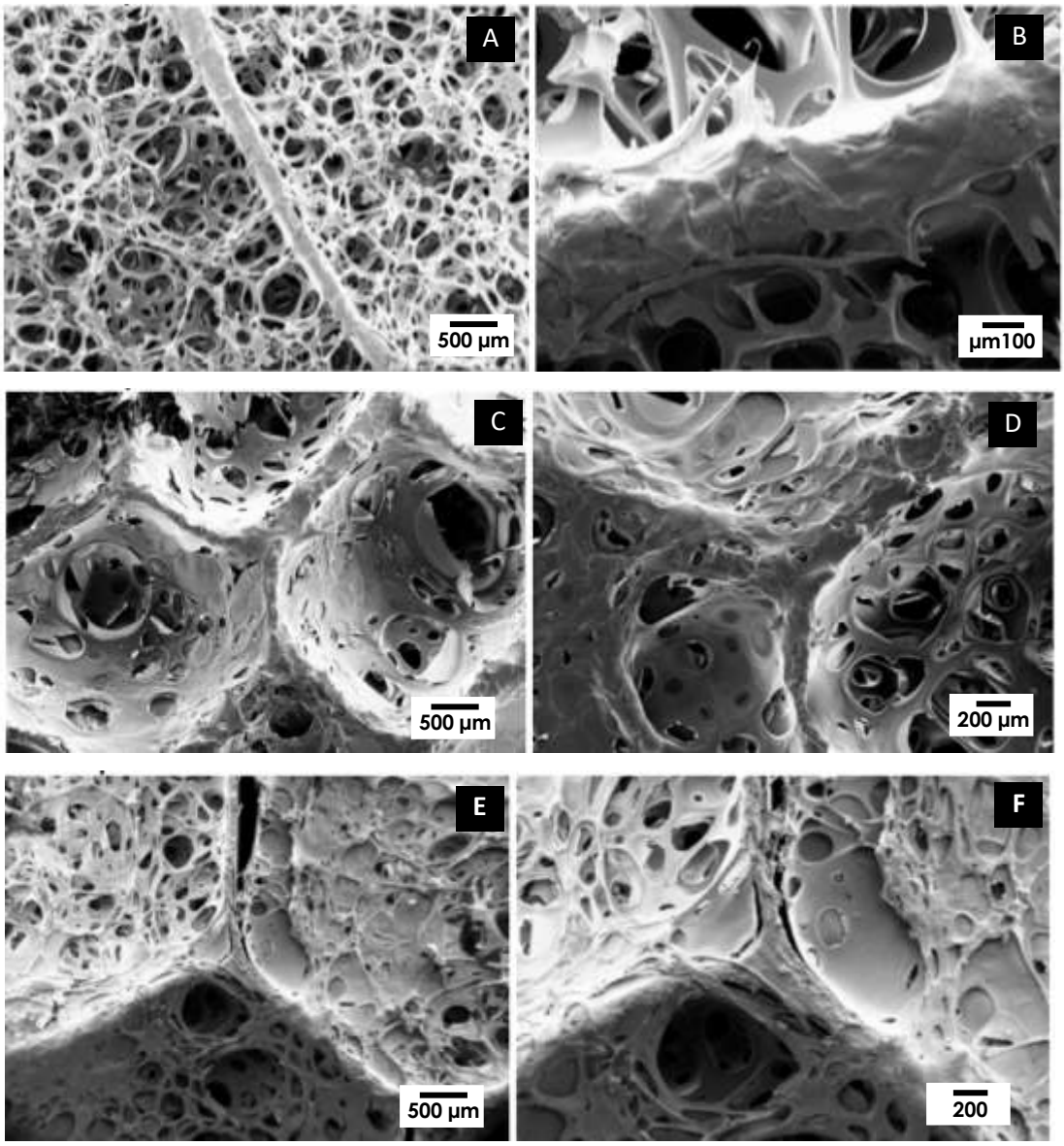

Figure 6.20. SEM IMAGES OF FILLED HONEYCOMB PANELS AT DIFFERENT MAGNIFICATIONS (A) (B) SAMPLE H2.2 (C) (D) SAMPLE N1.2 (E) (F) SAMPLE N2.2

As seen in Figures 6.20, the foam filling into the cardboard honeycomb cell structure was uniform and no large cavities or filling defects were found.

Figures 6.20C and 6.20D show the foam filling of sample N1.2 (Nomex® panel with 3.2 *mm* cell size) and N2.2 (Nomex® panel with 4.8 *mm* cell size), respectively. The foam exhibited a strong bonding with the cell walls of the honeycomb without large cavities despite some minor de-bonding was observed. Filling into the much smaller honeycomb cells seemed to have densified the base foam considerably. The densification may have resulted from the slightly higher pressure and shear applied to the liquid foams during filling the smaller cells.

Table 6.8 shows the density of the filled and unfilled honeycomb boards. As expected, bigger honeycomb cell sizes resulted in lower densities owing to the less differences in the densification of the foam during the filling process, as discussed earlier. However, the overall density increase of the honeycomb boards depended also on the original board densities. For the relatively lighter cardboard honeycomb boards (H2.1. and H1.1), density increase of the filled panels, ranged from 46% and 42% for H2.2 and H1.2, respectively. Whereas, for the relatively heavier Nomex® honeycomb (N2.1 and N1.1), it increased by 36% and 19%. (N2.2 and N1.2), respectively.

Table 6.8. DRY PANEL DENSITY OF THE FOAM FILLED (AND UNFILLED) CARDBOARD AND NOMEX® HONEYCOMBS WITH OUTER CARBOARD SHEETS

ID	HONEYCOMB BOARD MATERIAL	HONEYCOMB BOARD CELL SIZE (mm)	FOAM FILLING (Y/N)	PANEL DENSITY (kg/m^3)	DENSITY INCREASE (%)
H1.1	Cardboard	15	N	102.80 ± 0.16	-
H1.2			Y	146.30 ± 0.27	42.3
H2.1		27	N	92.00 ± 0.10	-
H2.2			Y	133.90 ± 0.23	45.6
N1.1	Nomex®	3.2	N	218.80 ± 1.67	-
N1.2			Y	259.20 ± 0.13	18.5
N2.1		4.8	N	120.16 ± 0.26	-
N2.2			Y	163.20 ± 2.56	35.8

Figure 6.21 presents the stress-strain curves from compression testing of the foam honeycomb panels with and without foam filling.

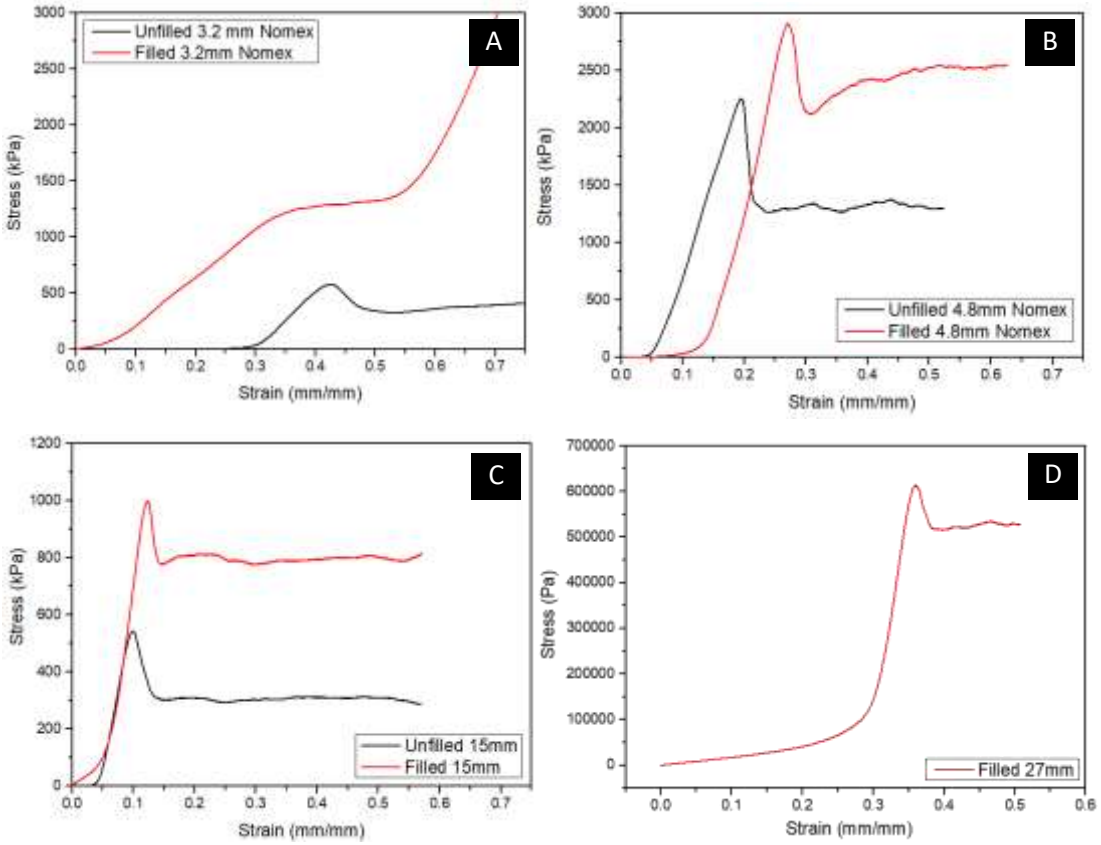

Figure 6.21. STRESS-STRAIN CURVES FOR HONEYCOMB PANELS (A) SAMPLES N1.1 AND N1.2 (B) SAMPLES N2.1 AND N2.2 (C) SAMPLES H.1.1 AND H1.2 (D) SAMPLES H2.1 AND H2.2

Table 6.9 compares the compression modulus (E) and the maximum compressive strength (σ_{max}) of the honeycomb panels filled with sample A11. Foam filling considerably improved both *E* and σ_{max} of the honeycomb panels due to the foam cell walls sharing the stress applied under compression. The percentage increase in σ_{max} and *E* due to filling was 109 and 169%, for the former, and 52.5 and 109% for the latter, for H1.2 and H2.2, respectively. H2.1 exhibited greater properties improvement after filling because of its lower relatively density and, consequently, greater space to fill by the foam, what gives more room for properties enhancement.

An 80% increase in cell size for unfilled cardboard honeycombs, resulted in a 31% and 56% decrease in σ_{max} and *E,* respectively. H2.1 exhibited lower mechanical properties than H1.1 due to a lower relative density of the panel, in other words, for the sample surface area, there is less axial support during compression.

Unlike cardboard honeycomb panels, Nomex® panels are not comparable due to differences in panel and cell wall thickness. An increase in cell size for unfilled Nomex® honeycombs, resulted in a 355% and 302% increase in *E* and σ_{max},

respectively. N1.1 exhibited lower mechanical properties than N2.1 due to a smaller cell thickness compared to N2.1.

For Nomex®, filled samples σ_{max} and *E* increased 150 and 40%, for the former, and 92 and 40% for the latter, for N1.2 and N2.2, respectively. N1.2 panel mechanical properties considerably increased compared to N2.2 when filled. This is also attributable to the small cell thickness of sample N1.2

Table 6.9. COMPRESSION MODULUS (kPa) AND YIELD STRENGTH (kPa) OF HONEYCOMB PANELS FILLED WITH SAMPLE A11

ID	DENSITY (kg/m³)	COMPRESSION MODULUS (kPa)	MAX. COMPRESSIVE STRENGTH (kPa)
N1.1	218.80 ± 1.67	3,179.33 ± 74.85	417.33 ± 9.24
N1.2	259.20 ± 0.13	6,111.00 ± 37.75	951.33 ± 136.18
N2.1	120.16 ± 0.26	14,477.58 ± 359.93	1,677.00 ± 22.87
N2.2	163.20 ± 2.56	18,745.22 ± 1,012.76	2,501.67 ± 184.34
H.1.1	102.80 ± 0.16	8,036.27 ± 385.08	455.89 ± 9.74
H1.2	146.30 ± 0.27	12,231.97 ± 979.47	913.67 ± 48.17
H2.1	92.00 ± 0.1	4,537.39 ± 168.90	233 ± 14.11
H2.2	133.90 ± 0.23	9,485.76 ± 2,041.39	645.33 ± 43.14

Figure 6.22 presents the load-displacement curves obtained from 3-point bending testing for the Nomex® honeycomb panels.

N1.2 and N2.2 panels initial failure may be attributable to the compressive forces exceeding the micro-buckling strength of the cardboard skins. The ultimate failure may be due to forces exceeding the tensile strength of the bottom cardboard skin, leading to the skin tearing and lost in load bearing capacity.

N1.1 panels exhibited micro-buckling failure and cells crushing. Wrinkling was observed in the top cardboard skin.

N2.1 panels exhibited instantly de-bonding in the top skin underneath the roller. However, de-bonding did not imply force decrease (see Figure 6.34.C), what suggests the adhesive did not provide a significant load bearing capacity.

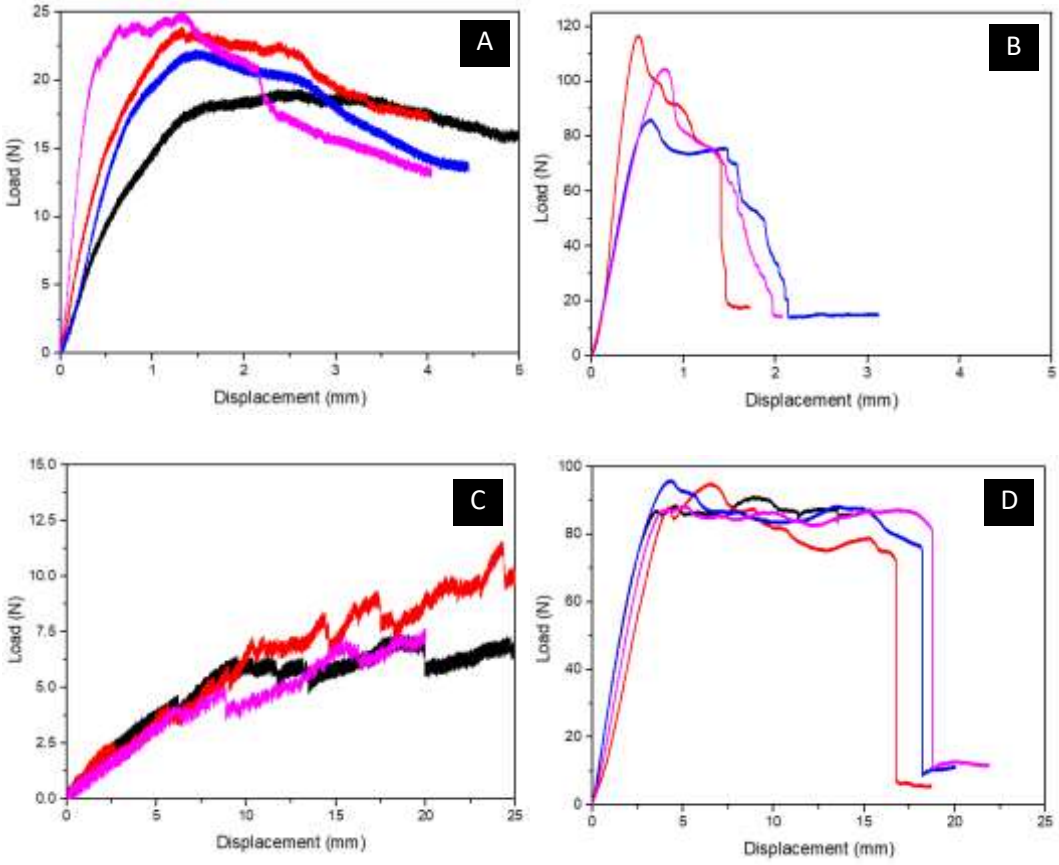

Figure 6.22. 3-POINT BENDING LOAD-DISPLACEMENT CURVES FOR HONEYCOMB PANNELS (A) UNFILLED 3.2*mm* NOMEX® PANELS (B) FILLED 3.2*mm* NOMEX® PANELS (C) UNFILLED 4.8*mm* NOMEX® PANELS (D) FILLED 4.8*mm* NOMEX® PANELS

Figure 6.23 presents the load-displacement curves obtained from 3-point bending testing for the cardboard honeycomb panels.

Figures 6.23A and 6.23B compares the force-strain curves of samples H1.1 and H1.2, respectively. The combination of thin skins and large cell size causes the intra cell buckling failure mechanisms in H1.1, what lead to the wrinkling of the top face sheet. The sharp decreases/increases in force after the yield point were due to the formation of wrinkles in the cardboard skin. H1.1 and H2.1 panels exhibited higher and lower, respectively, load bearing capability after yield. This may be attributable to the panel density: higher densities depict higher load bearing.

H2.2 and, more considerably, H2.1 panels exhibited gradually skins debonding due to a relatively low adhesion area to the honeycomb core. However, adhesion forces maintained the panel integrity which eventually failed by face microbuckling.

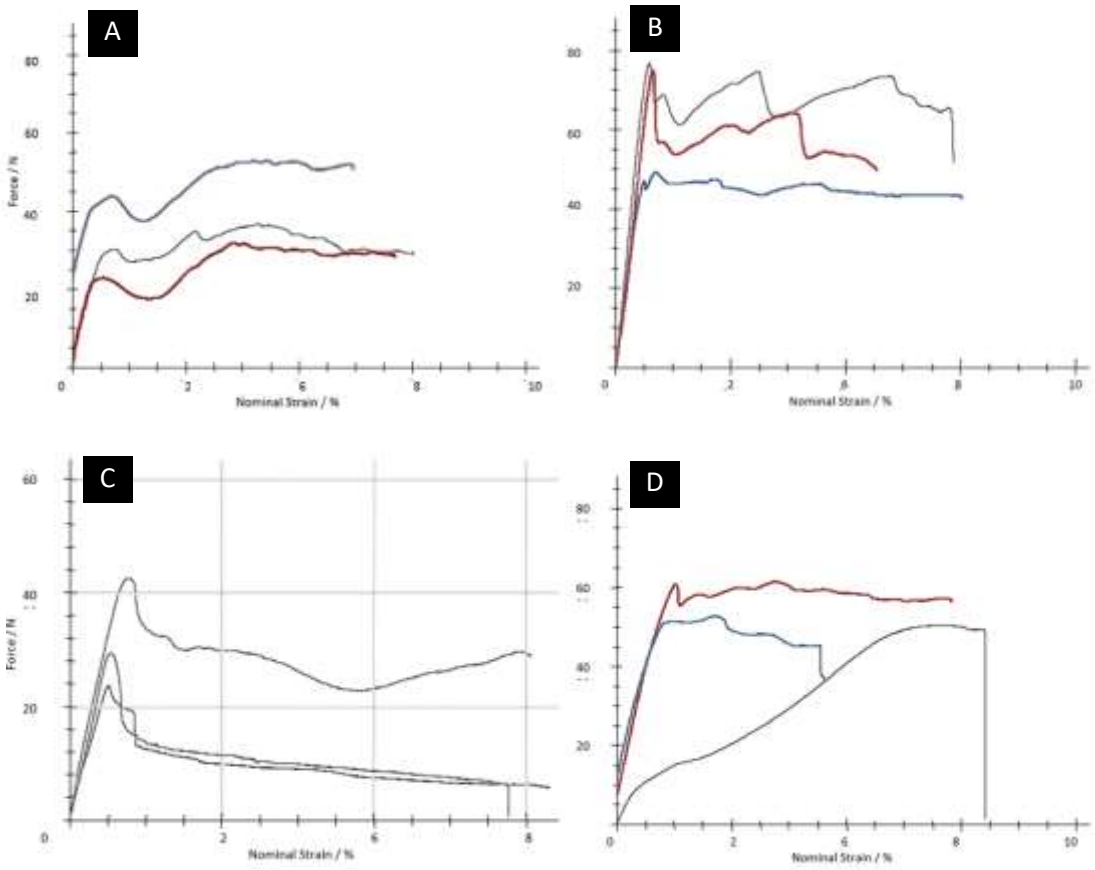

Figure 6. 23 3-POINT BENDING LOAD-DISPLACEMENT CURVES FOR HONEYCOMB PANELS (A) UNFILLED 15*mm* CARDBOARD PANELS (B) FILLED 15*mm* CARDBOARD PANELS (C) UNFILLED 27*mm* CARDBOARD PANELS (D) FILLED 27*mm* CARDBOARD PANELS

Table 6.10 compares the flexural modulus and the flexural strength of the honeycomb panels filled with sample A11.

The filing of the cardboard honeycomb panels increased more significantly the flexural modulus of H1 panels (54%) than H2 panels (27%). However, flexural strength increased more significantly in H2 panels (77%) than in H1 panels (27%) due to the greater cell size, what implies a larger volume of filling and thus, more significantly increase in both lateral and axial support.

The filing of the Nomex® honeycomb panels exhibited the same trend observed for cardboard panels. The flexural modulus of N1 panels (573%) increased more significantly than that in N2 panels (123%) and the flexural strength increased more significantly in H2 panels (528%) than in H1 panels (364%).

Table 6.10 FLEXURAL MODULUS (MPa) AND FLEXURAL STRENGTH (MPa) OF HONEYCOMB PANELS FILLED WITH SAMPLE A11

ID	DENSITY (kg/m^3)	FLEXURAL MODULUS (kPa)	FLEXURAL STRENGTH (kPa)
N1.1	218.80 ± 1.67	159 ± 104	8.8 ± 0.902
N1.2	259.20 ± 0.13	1070 ± 373	40.8 ± 4.45
N2.1	120.16 ± 0.26	282 ± 108	1.14 ±0.23
N2.2	163.20 ± 2.56	629 ± 77	7.12 ± 0.29
H.1.1	102.80 ± 0.16	443 ± 17.2	2.96 ± 0.39
H1.2	146.30 ± 0.27	680 ± 123	3.75 ± 0.79
H2.1	92.00 ± 0.1	270 ± 21.6	1.72 ± 0.111
H2.2	133.90 ± 0.23	343 ± 17.3	3.05 ± 0.22

7. CHAPTER 7.
CONCLUSION

Chapter 7.
CONCLUSION

7.1 INTRODUCTION

This project has laid the groundwork for the scale-up of (economic and environmental) sustainable alternative materials to conventional plastic foams. The foams produced in this work has several advantages over their commercial fossil-fuel based counterparts (e.g. polystyrene and polyethylene, among others) including their compostability and their bio-based origin.

This work has made important contributions to the development of a novel process for producing commercially viable bio-based and compostable foams and the understanding of their processing, structure and properties. There is some literature available regarding hydrogel foams but it is mainly focused on the development of tissue engineering materials. Little work has been made on the development of hydrogel foams for packaging applications.

Different bio-based formulations which produced high expansion ratios and low density solid foams on drying were designed and their feasibility was proved. The key parameters of formulation and process conditions were identified and investigated in detail.

This research started with the study of starch-based foams, systems 1 (starch-PVAc-calcium sulfate) and 2 (starch-gelatine foams). Then, the concept of liquid foaming for the production of low-density bio-foams was proved for the system 3, hydrogel-gelatine foams, and was pursued as the main focus of this project. The key parameters in both formulation and processing conditions of hydrogel-gelatine foams were identified and investigated.

The investigation of hydrogel-gelatine foams was then extended beyond packaging applications. Other applications aspects were studied in four cases studies (system 4, gelatine-composite foams): the inclusion of bio-foams powders from agricultural waste, the incorporation of silica aerogel powders, the inclusion of expanded vermiculite particles and the filling of honeycomb structures.

Finally, a preliminary exploration of two other bio-based hydrogels, agar and gellan gum, was carried out (system 5).

7.2 PRELIMINARY STUDY LEADING TO HYDROGEL FOAMS

Starch was initially selected as the main biopolymer for this initial exploration due to its commercial availability, low cost and high biodegradability. Two starch-based formulations systems were explored for liquid foaming and their key outcomes are summarised below.

7.2.1 SYSTEM 1. STARCH-PVAc-CALCIUM SULFATE FOAMS

System 1, starch-PVAc-calcium sulfate foams proved the liquid foaming process achieving stable foams leading to dry foams. The biopolymer used for this system was starch due to its high biodegradability and relatively high commercial availability. The starch-PVAc-calcium sulfate liquid foams were stabilised by the incorporation of PVAc, which improved the cell walls stretchability, and calcium sulfate, which stabilised the liquid foams via solidification. Detergent was utilised to assist the foaming process.

Four main limitations were identified for this system: the high density of the foams produced (135 kg/m^3), the long drying time (16 days), the starch preparation process (proved insufficient) and the relatively low biodegradability associated with the high calcium sulfate content of the foams produced.

7.2.2 SYSTEM 2. STARCH-GELATINE FOAMS

System 2 was developed in attempt to improve the biodegradability and reduce the foam density and drying timescale of the foams produced in system 1. Table 7.1 summarises the main properties of the best starch-gelatine foams produced (e.g. lowest density and drying shrinkage).

Table 7.1 FOAMING AND FOAM CHARACTERISTICS OF SELECTED STARCH-GELATINE FOAMS

ID	STARCH-GELATINE CONTENT	SOLID CONTENT (*wt%*)*	ACETIC ACID (Y/N)	MER	DENSITY (kg/m^3)	VOLUME SHRINKAGE (*vol%*)**	E (kPa)
ST9	30/70	14	N	4.22 ± 0.06	31.86 ± 4.81	35.83 ± 3.54	1861.67 ± 263.60
ST10	30/70	14	Y	4.00 ± 0.18	34.31 ± 3.14	42.29 ± 0.88	2068.67 ± 445.35
ST11	30/70	18	N	3.89 ± 0.09	47.17 ± 5.01	25.42 ± 2.36	2505.33 ± 402.06
ST12	30/70	18	Y	3.83 ± 0.06	47.51 ± 4.24	37.29 ± 0.88	2409.67 ± 542.26
ST13	50/50	14	N	3.40 ± 0.07	41.12 ± 7.27	40.42 ± 1.18	-
ST14	50/50	14	Y	3.38 ± 0.08	42.28 ± 3.65	40.83 ± 2.36	-
ST15	50/50	18	N	2.91 ± 0.06	62.33 ± 16.08	40.00 ± 0.59	-
ST16	50/50	18	Y	2.66 ± 0.05	73.08 ± 13.87	46.88 ± 0.29	-

Note: surfactant C2 was incorporated at 0.75wt% of the total starch-gelatine solution weight

*based on the starch-gelatine solution weight; **for a cast foam ~ 300cm^3 in volume

The substitution of calcium sulfate with gelatine, as foam stabiliser, and detergent with surfactant C2, as surface tension modifier, led to higher MER (~4) and lower density (approximately 32 kg/m^3) than the system discussed in Section 7.2.1. The shrinkage level of the system was also relatively low (~38% for a casted foam ~ 300cm^3 in volume) and the drying time at ambient conditions considerably decreased to 4 *days*.

Starch-gelatine foams exhibited an open-cell structure with cell size ranging from 50 to 600 μm. The mechanical properties were comparable to that on HDPE foams (Young's modulus, ~2 *MPa* and yield strength, ~100 kPa for ~32.5 kg/m^3 density foams).

The thermal conductivity was reasonably low (~0.036 $W/m{\cdot}K$), exhibiting a comparable performance to PS foams and slightly better than LDPE and HDPE foams, with same densities.

Thus, starch-gelatine foams proved the feasibility of hydrocolloids use as foam stabilisers. However, further improvement was required. As observed in system 1, the starch preparation process was proved effective but not sufficient to produced TPS. The relatively high density compared to that to conventional plastics foams for packaging applications (approximately 20 kg/m^3) and the drying time suggested the exploration of other materials as the main biopolymer.

7.3 HYDROGEL FOAMS BASED ON GELATINE

Starch was removed from the liquid foams formulation in attempt to reduce the solid foams density. The feasibility of hydrogel foams based on gelatine and two selected surfactants ("A" and C2) was proved and the role of the different formulation (e.g. gelatine content, surfactant, surfactant type and content and plasticiser) and processing factors (foaming temperature, expansion ratio, drying conditions) was investigated.

7.3.1 FUNDAMENTALS OF GELATINE SOLUTIONS AND GELS

The study of MER and total shrinkage showed the importance of relatively low changes in viscosity and rheological properties.

Higher gelatine concentrations increased the equilibrium modulus, the gelation temperature($p<0.001$) and the melting temperature ($P=0.051$) and decreased gelling time. Higher gelatine strength slightly increased the equilibrium modulus but did not seem to considerably affect gelling time, gelation temperature ($P=0.068$) and melting temperature ($P=0.643$). Thus, high gelatine concentrations may produce more stable gelatine foams. However, a gelatine content-stabilisation balance was desirable

because as gelatine content increased, the density of the dry foam was also expected to increase.

Higher curing temperatures (>23°C), extreme pH and surfactant type and content negatively affected gelation kinetics. Gelatine is a thermo-sensitive polymer, and thus, higher curing temperatures delayed gelling time, affecting the stabilisation of gel foams. This limits the use of heating drying methods.

Surfactant C2 and, more significantly, surfactant "A" considerably increased the gelling time of gelatine. This negative effect was more significant as surfactant concentration increased. This partially explained (in conjunction with the viscosity influence) the lower shrinkage levels achieved with foams made surfactant C2.

7.3.2 INFLUENCE OF FOAMING TEMPERATURE, SURFACTANT TYPE AND GELATINE AND SURFACTANT CONTENT ON THE FOAMING BEHAVIOUR AND PROPERTIES OF HYDROGEL-GELATINE FOAMS

Gelatine foams made with both surfactants "A" and C2 exhibited desirable properties for being strong alternatives to conventional plastic foams. Low densities (<20 kg/m^3), thermal conductivity (≈0.039 $W/k{\cdot}m$), and relatively low shrinkage level were achieved.

The influence of different experimental factors on the main hydrogel foams properties based on gelatine was investigated. Table 7.1 summarises the main properties of the best hydrogel-gelatine foams produced.

Table 7.2 FOAMING AND FOAM CHARACTERISTICS OF SELECTED HYDROGEL-GELATINE FOAMS

ID	MER	SHRINKAGE (%)	DENSITY (kg/m^3)	YOUNG'S MODULUS (KPa)	RECOVERY (%)	THERMAL CONDUCTIVITY (W/m·K)
A1	8.67	40	14.03 ± 0.72	43.15±24.50	97.00±2.87	-
A3	6.46	31	25.99 ± 1.46	504.11±89.12	79.86±2.08	-
A7	9.70	43	11.09 ± 1.43	19.37±2.00	94.29±2.47	0.0398 ± 0.0019
A9	7.39	31	26.10 ± 1.02	660.53±117.05	73.00±2.89	0.0403 ± 0.0025
C2.1	7.17	11.3	20.85 ± 0.79	446.50±77.03	89.84	0.0381 ± 0.0016
C2.3	6.64	22.7	36.91 ± 0.77	1297.91±429.78	74.40	0.0387 ± 0.0021
C2.7	7.68	15.6	19.60 ± 1.69	3646.40±681.41	72.63	-
C2.9	6.84	15.5	33.17 ± 0.79	1213.83±161.12	69.19	**-**

7.3.2.1 MER

The study of MER and total shrinkage showed the importance of relatively small changes in viscosity and surface tension. Considerably higher MERs were achieved for both gelatine foams made with surfactant "A" (~6-10) and C2 (~4.5-8.5).

MER increased as gelatine content decreased ($p<0.001$) and foaming temperature increased ($p<0.001$) for both surfactants "A" and C2.

The surfactant influence on MER was driven by low surface tension and viscosity. MER increased as surfactant content increased ($p<0.001$) for surfactant "A" foams. However, there was a gelatine content-surfactant content ($p<0.05$) interaction in surfactant "A" foams. Lower gelatine content and higher surfactant content exhibited higher expansion ratios. However, the surfactant content had a stronger positive effect on MER when increasing from lower to medium concentrations than medium to higher concentrations due to the surfactant reaching CMC at relatively low surfactant content. This trend was less remarkable at higher gelatine concentrations.

Surfactant C2 foams achieved the highest MER at intermediate surfactant levels due to an optimum viscosity-surface tension balance. Surfactant C2 foams exhibited a gelatine content-foaming temperature interaction ($p<0.05$). At 50°C, their MER decrease as gelatine content increased was virtually linear, but at 80°C, the MER decreased less sharply due to the higher viscosity at higher temperature.

7.3.2.2 Shrinkage

Gelatine-surfactant C2 foams exhibited less shrinkage (11.22-33.97%) level than foams made with surfactant "A" (31% to 56%), but all the samples exhibited the same drying shrinkage deformation patterns (concave, on the top surface, and convex, on the bottom).

Both surfactants systems generally exhibited lower shrinkage values at lower foaming temperature ($p<0.001$) due to shorter gelling time and lower viscosity.

Shrinkage was minimum at intermediate gelatine content for surfactant "A" foams ($p<0.001$) but surfactant content did not considerably influence these foams shrinkage ($p>0.05$). Gelatine content-foaming temperature ($p<0.05$), gelatine content-surfactant content ($p<0.05$) and surfactant content-foaming temperature ($p<0.05$) interactions also affected their shrinkage. Total shrinkage tended to be higher with foams processed at higher temperatures and lower gelatine content. However, the increase of foaming temperature had a less negative impact on the shrinkage of higher gelatine foams. As previously mentioned, surfactant content had little effect

on the shrinkage of surfactant "A" foams. However, at higher gelatine concentrations (20 *wt%*), intermediate surfactant concentration (1.5 *wt %*) exhibited a slightly more negative response in shrinkage. tThe shrinkage of surfactant "A" foams was minimum at lower foaming temperatures ($p<0.001$), especially at lower gelatine concentrations ($p<0.001$).

For surfactant C2 foams, shrinkage was maximum at intermediate gelatine concentration ($p<0.001$) and miminum at intermediate surfactant concentration. Gelatine content-foaming temperature ($p<0.05$), gelatine content-surfactant content ($p<0.05$) and surfactant content-foaming temperature ($p<0.05$) interactions also affected their shrinkage. C2 foams exhibited similar shrinkage levels when processed at 50°C. However, at higher foaming temperature, the surfactant content influenced the level of shrinkage, being maximum at lower surfactant content, where solution viscosity was minimum. Gelatine-C2 foams shrinkage decreased when increasing the surfactant content from low to intermediate contents. However, when surfactant was further increased the shrinkage level had an erratic response due to the formation of central voids, especially for the foams produced at the lower foaming temperature.

7.3.2.3 Density

The low density achieved was considered remarkable for bio-foams which tend to have a higher density than conventional plastic foams. Density <10 $kg \cdot m^{-3}$ or >99% porosity, enters the range of low-density expanded polystyrene (EPS), and thus, a breakthrough achievement enabling the bio-foams to compete in similar applications.

Surfactant "A" exhibited lower densities (from 8.8 kg/m^3 to 47.32 kg/m^3) than surfactant C2 (19.60 kg/m^3 to 59.70 kg/m^3). Both systems produced low-density bio-foams, which may have different applications at different densities.

The most significant factors influencing density were the solution foaming content, MER and shrinkage. Both surfactant "A" and C2 foams achieved lower densities at lower gelatine concentrations ($p<0.001$).

Surfactant "A" foams achieved lower densities at intermediate and higher surfactant content ($p<0.001$) and higher foaming temperature ($p<0.001$). Density exhibited two two-way interactions: gelatine content-surfactant content ($p<0.05$) and gelatine content-foaming temperature ($p<0.05$). An intermediate surfactant content was the optimum to achieve lower density foams, closely followed by the highest surfactant content. This was mainly due to the more significant effect of surfactant content on foams made with higher gelatine content. Surfactant content increase had little

effect on the density of lower and intermediate gelatine content foams. The effect of foaming temperature on density increased at higher gelatine concentrations.

Surfactant C2 foams exhibited lower densities at intermediate surfactant concentrations ($p<0.001$) and lower foaming temperatures ($p<0.001$). These foams had two two-way interactions: gelatine content-surfactant content ($p<0.05$) and gelatine content-foaming temperature ($p<0.05$).

7.3.2.4 Structure

All the foams exhibited an open-cell structure, but the foams made with surfactant C2 exhibited a greater number of closed-cells due to the higher viscosity of both the plateau borders and the cell walls. The cell size ranged from 0.05 to 0.8 *mm*.

The foam structure mainly consisted of macropores and interconnecting micropores. Foams made at higher foaming temperatures, lower gelatine content and surfactant "A" exhibited relatively bigger macropores and thinner plateau borders than that processed at lower temperature, higher gelatine content and containing surfactant C2.

7.3.2.5 Other properties

The stress-strain response of gelatine foams made with surfactants "A" and C2 was elastomeric. The compression modulus ranged from 10-2000 *kPa* and 280-5200 *kPa*, for foams made with surfactant "A" and C2, respectively. Higher gelatine content and the use of surfactant C2 led to higher compression modulus and, generally, lower recovery rates. Lower gelatine foams were more flexible, especially those made with surfactant "A".

The thermal conductivity achieved was considered remarkably low as it was comparable to that in conventional plastic foams (e.g. EPS, PE). The thermal conductivity of ≈0.039 $W/m \cdot K$ enters the range of relatively high-insulating foams.

The bio-foams did not generally exhibit a considerable sound blocking, but they may be used in combination with other materials in sandwiched structures to mitigate this.

7.3.3 OPTIMISATION OF THE EXPANSION RATIO

The maximum expansion ratios (MER) gave rise to lower total shrinkage and, generally, lighter foams. Higher expansion ratios exhibited shorter drying time, which minimised total shrinkage, and higher porosity, which reduced density.

MER was identified as the optimum expansion ratio.

7.3.4 INFLUENCE OF PLASTICISER TYPE AND CONTENT

The plastification effect of glycerol and sorbitol was proved as compression modulus generally decreased as plasticiser content increased.

7.3.5 STUDY OF THE DRYING PROCESS

There was a considerable improvement in drying timescale from the previous systems studied but drying time was still a limiting factor for liquid foaming.

There are several processing parameters which may affect the drying of the hydrogel foams. The use of perforated moulds was proved to reduce slightly (by approximately 25%) the drying time by allowing water migration from all the mould walls.

Freeze-drying was proved as an effective method to produce highly-porous materials.

7.4 CASE STUDIES: APPLICATIONS OF GELATINE BIO-FOAMS

Some potential applications for hydrogel-gelatine foams were explored. However, further work may focus on others, like vacuum superinsulators.

7.4.1 FULLY BIODEGRADABLE COMPOSITE GELATINE BIOFOAMS CONTAINING POWDERED BIOMASS FILLERS

It was feasible to produce low-density (15.59 kg/m^3-59.34 kg/m^3) cost-effective gelatine-fibres composite foams with relatively low shrinkage (20.83-42.71%) and good thermal properties (0.039-0.046 $W/m{\cdot}K$).

Table 7.3 summarises the main properties of a selection of hydrogel-gelatine foams produced with biomass fillers.

Table 7.3 FOAMING AND FOAM CHARACTERISTICS OF SELECTED HYDROGEL-GELATINE FOAMS CONTAINING BIOMASS FILLERS AND THE FOAMS THEY WERE BASED UPON

ID	FIBRE TYPE	FIBRE CONTENT* (%)	GELATINE CONTENT (wt%)	SURFACTANT CONTENT (wt%)	SURFACTANT TYPE	MER	SHRINKAGE (%)	DENSITY (kg/m^3)	THERMAL CONDUCTIVITY (W/m·K)
A7	-	-	10	1.5	A	9.7	43	11.07	0.0398 ± 0.0019
O1	Oat	1	10	1.5	A	9.41	39.24	15.59	0.0456 ± 0.0028
O2	Oat	3	10	1.5	A	8.84	27.92	20.31	0.0445 ± 0.0028
W1	Straw	1	10	1.5	A	9.18	34.58	16.64	0.0423 ± 0.0017
W2	Straw	3	10	1.5	A	8.84	27.08	19.99	0.0392 ± 0.0004
A9	-	-	15	1.5	A	7.39	31	26.10	0.0403 ± 0.0025
O3	Oat	1	15	1.5	A	6.72	42.71	32.60	0.0383 ± 0.0021
O4	Oat	3	15	1.5	A	6.31	40.21	39.17	0.0378 ± 0.0024
W3	Straw	1	15	1.5	A	7.39	23.54	28	0.0404 ± 0.0008
W4	Straw	3	15	1.5	A	6.53	20.83	34.53	0.0396 ± 0.0005
C2.1	-	-	10	0.75	C2	7.17	11.25	20.85	0.0381 ± 0.0016
O7	Oat	1	10	0.75	C2	6.31	35.63	25.46	-
O8	Oat	3	10	0.75	C2	6.23	36.67	29.71	-
W7	Straw	1	10	0.75	C2	7.37	30	25.45	-
W8	Straw	3	10	0.75	C2	6.65	28.33	29.39	-
C2.3	-	-	1	0.75	C2	6.64	22.69	36.91	0.0387 ± 0.0021
O9	Oat	3	15	0.75	C2	6.26	36.67	44.54	-
O10	Oat	1	15	0.75	C2	5.78	43.54	52.77	-
W9	Straw	3	15	0.75	C2	6.14	26.46	45.43	-
W10	Straw	1	15	0.75	C2	5.69	30	48.52	-

7.4.2 GELATINE-SURFACTANT C2–SiO_2 AEROGEL COMPOSITE FOAMS

Aerogel powders incorporation into the gelatine-hydrogel foams made a positive impact on the thermal conductivity of hydrogel foams based on gelatine. However, this positive impact did not significantly improve with the increase in the concentration of the aerogel powders.

In addition to this, further thermal conductivity decreasing is limited by aerogel content, which may lead to mixing difficulties at higher concentrations.

Table 7.4 summarises the result obtained for hydrogel-gelatine-aerogel foams.

Table 7.4 EXPERIMENTAL MATRIX, DENSITY AND THERMAL CONDUCTIVITY OF AEROGEL FOAMS AND THE FOAMS THEY WERE BASED UPON

ID	GELATINE CONTENT (*wt%*)	AEROGEL TYPE	AEROGEL CONTENT* (*wt%*)	DENSITY (kg/m^3)	THERMAL CONDUCTIVITY (W/m·K)
C2.1	10	-	0	20.85±0.79	0.0381±0.0016
P1	10	Hydrophobic	1	30.16±1.66	0.0348±0.000679
P2	10	Hydrophobic	3	46.30±3.83	0.0333±0.000955
P3	10	Hydrophilic	1	29.65±2.99	0.0342±0.001004
P4	10	Hydrophilic	3	35.82±0.32	0.0330±0.000156
C2.3	15	-	0	36.91±0.77	0.0387±0.0021
P5	15	Hydrophobic	1	56.15±2.69	0.0345±0.000191
P6	15	Hydrophobic	3	73.33±1.32	0.0344±0.000566
P7	15	Hydrophilic	1	56.59±3.22	0.0350±0.000481
P8	15	Hydrophilic	3	57.05±1.19	0.0351±0.001018

**Content based on the total weight of the gelatine-water solution*
Note: Surfactant C2 content was constant at 0.75 wt% on the total weight of the gelatine-water solution

7.4.3 GELATINE-EXPANDED VERMICULITE COMPOSITE FOAMS

The incorporation of vermiculite considerably increased the density and reduced the total shrinkage of the dry composite foams.

The gelatine and gelatine-vermiculite foams exhibited much better fire resistance performances than PS and PU foams. They:

a) were not flame-escalating;

b) generate charred layers to protect the internal areas;

c) produced less amount (or less harmful) smoke;

d) did not melt or drip to spread the fire; and

e) were self-distinguishing

Table 7.5 summarises the main properties of the gelatine-expanded vermiculite foams.

Table 7.5 DRY COMPOSITE FOAM DENSITY, TOTAL SHRINKAGE (%), AND COMPRESSION MODULUS OF THE HYDROGEL-GELATINE-VERMICULITE COMPOSITE FOAMS BASED ON A7, A9 AND A11

ID	VERM*. TYPE	VERM*. CONTENT (wt%)	GELATINE CONTENT (wt%)	DENSITY (kg/m^3)	TOTAL SHRINKAGE (%)	COMPRESSION MODULUS (kPa)	RECOVERY AFTER 50% STRAIN (%)
A7**	-	-	10	11.09	43	19.37	94.29
A9**	-	-	15	26.10	31	660	73
A11**	-	-	20	37.08	43	1795	76.26
VS1	Fine	6.5	10	50.23±3.85	31.46	26	96.13
VS2			15	69.18±3.67	34.38	299	76.74
VS3			20	93.19±5.96	35.21	880	75.49
VS4		13	10	90.9±3.88	36.46	7	94.84
VS5			15	103.35±4.3	35.63	116	81.94
VS6			20	99.36±2.78	32.08	878	73.89
VS7		19.5	10	104.22±3.00	30.35	18	88.89
VS8			15	105.81±3.34	29.79	96	82.2
VS9			20	125.56±4.96	27.33	377	68.06
VB1	Coarse	6.5	10	47.27±2.19	41.46	26	95.83
VB2			15	54.31±2.05	36.63	315	82.99
VB3			20	79.88±6.04	38.13	1166	72.11
VB4		13	10	64.79±5.24	34.33	23	98.89
VB5			15	69.42±2.78	30	116	83.96
VB6			20	94.42±1.71	32.92	2359	75.49
VB7		19.5	10	81.63±3.79	31.25	24	89.31
VB8			15	93.54±3.76	29.38	89	81.25
VB9			20	101.26±4.09	27.5	1256	76.96

*Vermiculite
** See complete formulation in Table 3.35 (Chapter 3)

7.4.4 FOAM-FILLED HONEYCOMB PANELS

The low foam viscosity in comparison with molten polymer foams enabled filling of honeycomb structures, in which mechanical properties (compression and flexural bending) were enhanced after filling, as seen in Table 7.6.

Table 7.6 DENSITY, COMPRESION AND FLEXURAL PROPERTIES OF HONEYCOMB BOARDS FILLED WITH HYDROGEL FOAMS

ID	DENSITY (kg/m^3)	COMPRESSION MODULUS (kPa)	MAX. COMPRESSIVE STRENGTH (kPa)	FLEXURAL MODULUS (kPa)	FLEXURAL STRENGTH (kPa)
N1.1	218.80 ± 1.67	3,179.33 ± 74.85	417.33 ± 9.24	159 ± 104	8.8 ± 0.902
N1.2	259.20 ± 0.13	6,111.00 ± 37.75	951.33 ± 136.18	1070 ± 373	40.8 ± 4.45
N2.1	120.16 ± 0.26	14,477.58 ± 359.93	1,677.00 ± 22.87	282 ± 108	1.14 ±0.23
N2.2	163.20 ± 2.56	18,745.22 ± 1,012.76	2,501.67 ± 184.34	629 ± 77	7.12 ± 0.29
H.1.1	102.80 ± 0.16	8,036.27 ± 385.08	455.89 ± 9.74	443 ± 17.2	2.96 ± 0.39
H1.2	146.30 ± 0.27	12,231.97 ± 979.47	913.67 ± 48.17	680 ± 123	3.75 ± 0.79
H2.1	92.00 ± 0.1	4,537.39 ± 168.90	233 ± 14.11	270 ± 21.6	1.72 ± 0.111
H2.2	133.90 ± 0.23	9,485.76 ± 2,041.39	645.33 ± 43.14	343 ± 17.3	3.05 ± 0.22

7.5 BIO-BASED HYDROGEL FOAMS ALTERNATIVES TO GELATINE

7.5.1 AGAR FOAMS

It was feasible to product liquid agar foams. However, the dry agar cell structure collapsed significantly after gelling and drying.

Rheological characterisation suggested that the loss of gelling power was due to the surfactant incorporation

No attempt for further investigation was made, but the focus of future research should ensure the compatibility of processing additives with the hydrogel of interests. Agar could also benefit from the use of cross-linkers or process, such as freeze-drying.

7.5.2 GELLAN GUM FOAMS

It was feasible to produce both liquid and solid gellan gum foams. Gellan gum is a promising bio-material as it gels at very low concentrations and can be dried by convective methods (≈70°C).

Further work needs to focus on minimise shrinkage (e.g. use of crosslinkers) and processing improvement (e.g. vacuum foaming).

Table 7.7 PHYSICAL AND THERMAL PROPERTIES OF SELECTED GELLAN GUM FOAMS

ID	HA GELLAN GUM (*wt%*)	LA GELLAN GUM (*wt%*)	FOAM DENSITY (kg/m^3)	TOTAL SHRINKAGE (*vol%*)	THERMAL CONDUCTIVITY ($W/m \cdot K$)
GG3	3	1	31.04	34.67	0.0347
GG4	3	1.5	32.23	35.33	0.0329
GG6	4	0.5	38.59	41.33	0.035
GG7	4	1	35.82	32	0.0373

7.6 FURTHER WORK

The work carried out in this thesis raised some topics requiring further investigation in order to assist the future development of the foams studied. It is suggested that further research focus on the following:

- System 1, starch-PVAc-calcium sulfate foams. This system can be further explored for applications different to packaging, such as alternatives to plasterboards used for construction applications.

- System 2, starch-gelatine foams. Further optimisation is required. As observed in system 1, the starch preparation process was proved effective but not sufficient to produced TPS. The relatively high density compared to that from conventional plastics foams for packaging applications (approximately 20 kg/m^3) and the drying time suggested the exploration of other materials as the main biopolymer. A proper destruction of the starch granules can create more homogeneous blends which can lead to lower density foams.

- Drying process. The use of convection drying is limited by the thermo-sensitivity of gelatine. This may be addressed by using stronger chemical crosslinking (e.g. formaldehyde (Shyamkuwar *et al.*, 2010), glutaraldehyde (Kang, Tabata and Ikada, 1999) or carbodiimides (Kim, Knowles and Kim, 2005)) of the hydrogels. In addition to this, there is also considerable scope for increasing the vapour transport rate to speed up drying, by, for example, forced gas flow techniques, such as fans. Freeze-drying may be another route to explore for further work, which may not only reduce shrinkage to minimum, but can also significantly affect the foam microstructure. Improvements in the drying process may also bring shrinkage reduction.

- Plasticisers use. Further investigations need to be carried out regarding the influence of plasticisers use on gelatine-hydrogel foams.

- Gelatine foams with biomass fillers. Further research is needed to explore a greater fibre inclusion for those samples exhibiting higher expansion ratios.
- Gellan gum. Further work needs to focus on minimise shrinkage (e.g. use of crosslinkers) and processing improvement (e.g. vacuum foaming).
- Foam generation. This work focused on lab-scale foam generation. Industrial foaming generators need to be explore for the scale-up.
- Further material characterisation should focus on the study of the foam isotropic properties, chemical homogeneity (using chemical mapping techniques such as μFTIR, μRaman and EDX) and the solvent (water) quality.
- Material hydrophilicity. Methods to control the foams hydrophilicity can be explored to control fungus growth in system 2, starch-gelatine foams.
- Further applications. Some potential applications for hydrogel-gelatine foams were explored. However, further work may focus on others, like vacuum superinsulators.

REFERENCES

REFERENCES

A

Affinity Water (2017) *Water information and reports*. Available at: https://www.affinitywater.co.uk/water-quality-in-your-area.aspx.

Affinity Water (2017) *Water information and reports*. Available at: https://www.affinitywater.co.uk/water-quality-in-your-area.aspx.

Akkineni, A. *et al.* (2016) 'Highly Concentrated Alginate-Gellan Gum Composites for 3D Plotting of Complex Tissue Engineering Scaffolds', *Polymers*, 8(5), p. 170. doi: 10.3390/polym8050170.

Amaral, M. H. *et al.* (2008) 'Foamability of detergent solutions prepared with different types of surfactants and waters', *Journal of Surfactants and Detergents*, 11(4), pp. 275–278. doi: 10.1007/s11743-008-1088-0.

Antony, J. (2003) *Design of Experiments for Engineers and Scientists*, *Materials & Mechanical*. doi: 10.1198/tech.2006.s381.

Avérous, L. (2004) 'Biodegradable multiphase systems based on plasticized starch: A review', *Journal of Macromolecular Science - Polymer Reviews*, pp. 231–274. doi: 10.1081/MC-200029326.

Aydinli, M. and Tutas, M. (2000) 'Water Sorption and Water Vapour Permeability Properties of Polysaccharide (Locust Bean Gum) Based Edible Films', *LWT - Food Science and Technology*, 33(1), pp. 63–67. doi: 10.1006/fstl.1999.0617.

Ayoub, A. S. and Rizvi, S. S. H. (2009) 'An overview on the technology of cross-linking of starch for nonfood applications', *Journal of Plastic Film and Sheeting*, pp. 25–45. doi: 10.1177/8756087909336493.

B

Balakrishnan, B. *et al.* (2014) 'Self-crosslinked oxidized alginate/gelatin hydrogel as injectable, adhesive biomimetic scaffolds for cartilage regeneration', *Acta Biomaterialia*, 10(8), pp. 3650–3663. doi: 10.1016/j.actbio.2014.04.031.

Banerjee, S. and Bhattacharya, S. (2012) 'Food Gels: Gelling Process and New Applications', *Critical Reviews in Food Science and Nutrition*, 52, pp. 334–346. doi:

10.1080/10408398.2010.500234.

Barnard, A. R. and Rao, M. D. (2004) 'Measurement of Sound Transmission Loss Using a Modified Four Microphone Impedance Tube', in *Noise-Con 04. The 2004 National Conference on Noise Control Engineering*. Baltimore Maryland, United States, pp. 209–216.

BASF (2016) *Envio EA-certified compostable expandable particle foam*. Available at: https://www.basf.com/en/microsites/BASFatK2016/must_sees/ecovio-EA.html (Accessed: 28 April 2018).

Bergeret, A. and Benezet, J. C. (2011) 'Natural fibre-reinforced biofoams', *International Journal of Polymer Science*, 2011. doi: 10.1155/2011/569871.

Bhakta, A. and Ruckenstein, E. (1997) 'Decay of standing foams: drainage, coalescence and collapse', *Advances in Colloid and Interface Science*, 70, pp. 1–124. doi: 10.1016/S0001-8686(97)00031-6.

Bian, X. C., Tang, J. H. and Li, Z. M. (2008) 'Flame retardancy of hollow glass microsphere/rigid polyurethane foams in the presence of expandable graphite', *Journal of Applied Polymer Science*, 109(3), pp. 1935–1943. doi: 10.1002/app.27786.

Bing, L. *et al.* (2010) 'Batch Foam Processing of Polypropylene/Polydimethylsiloxane Blends', *International Journal of Polymeric Materials*, 60(1), pp. 51–61. doi: 10.1080/00914037.2010.504157.

Biopower Technologies (2016a) *Gret Grain Straw Tecnical Specification*. UK.

Biopower Technologies (2016b) *Oat Husk Fibre Technical Specification*. UK.

Bitzer, T. (1997) *Honeycomb Technology: Materials, Design, Manufacturing, Applications And Testing*, *Chapman & Hall, London*. doi: 10.1007/978-94-011-5856-5.

Blanshard, J. M. V. (1987) *Starch granule structure and function. A physicochemical approach*. London: John Wiley & Sons.

Bonin, M. (2010) *An Investigation into the Properties of Starch-Based Foams*.

Boral, S. and Bohidar, H. B. (2009) 'Hierarchical structures in agar hydrogels', *Polymer*, 50(23), pp. 5585–5588. doi: 10.1016/j.polymer.2009.09.033.

Brodin, M. *et al.* (2017) 'Lignocellulosics as sustainable resources for production of

bioplastics – A review', *Journal of Cleaner Production*, pp. 646–664. doi: 10.1016/j.jclepro.2017.05.209.

Brooks, R. (1881) 'Gelatine Prepared in the form of dried foam'. US.

Bruel & Kjaer (2018) *TRANSMISSION LOSS AND IMPEDANCE TUBE KITS. Product Data*. Available at: https://www.bksv.com/-/media/literature/Product-Data/bp1039.ashx.

Bule, A. (1998) 'Starch granules : structure and biosynthesis', 23, pp. 85–112.

Buléon, A. *et al.* (1998) 'Starch granules: structure and biosynthesis', *International Journal of Biological Macromolecules*, 23, pp. 85–112.

Burlayenko, V. N. and Sadowski, T. (2010) 'Effective elastic properties of foam-filled honeycomb cores of sandwich panels', *Composite Structures*, 92(12), pp. 2890–2900. doi: 10.1016/j.compstruct.2010.04.015.

C

Cai, C. and Wei, C. (2013) 'In situ observation of crystallinity disruption patterns during starch gelatinization.', *Carbohydrate polymers*. Elsevier Ltd., 92(1), pp. 469–78. doi: 10.1016/j.carbpol.2012.09.073.

Callister Jr., W. and Rethwisch, D. (2013) *Fundamentals of Materials Science and Engineering*, *Book*.

Calvert, P. (1997) 'The structure of starch', 389(September).

Cao, N., Yang, X. and Fu, Y. (2009) 'Effects of various plasticizers on mechanical and water vapor barrier properties of gelatin films', *Food Hydrocolloids*, 23(3), pp. 729–735. doi: 10.1016/j.foodhyd.2008.07.017.

Cao, W. *et al.* (2015) 'Thermal conductivity of highly porous ceramic foams with different agar concentrations', *Materials Letters*, 139, pp. 66–69. doi: 10.1016/j.matlet.2014.08.096.

Ceglia, G. *et al.* (2012) 'Formulation and mechanical properties of emulsion-based model polymer foams.', *The European physical journal. E, Soft matter*, 35(4), p. 9708. doi: 10.1140/epje/i2012-12031-0.

Cha, J. . *et al.* (2001) 'Physical properties of starch-based foams as affected by extrusion temperature and moisture content', *Industrial Crops and Products*, 14(1),

pp. 23–30. doi: 10.1016/S0926-6690(00)00085-6.

Chandrashekar, A., Savitri, A. and Somashekar, K. (1987) 'Optical Interference Studies on Single Starch Granules', in *Cereal Carbohydrate Conference*. West Lafayette, Indiana.

Chattopadhyay, H., De, A. K. and Datta, S. (2015) 'Novel Starch-PVA Polymer for Microparticle Preparation and Optimization Using Factorial Design Study', *International Scholarly Research Notices*, 2015, pp. 1–8. doi: 10.1155/2015/261476.

Chen, Q. Z. (2011) 'Foaming technology of tissue engineering scaffolds - a review', *Bubble Science, Engineering & Technology*, 3(2), pp. 34–47. doi: 10.1179/1758897911Y.0000000003.

Chen, S. C., Liao, W. H. and Chien, R. Der (2012) 'Structure and mechanical properties of polystyrene foams made through microcellular injection molding via control mechanisms of gas counter pressure and mold temperature', *International Communications in Heat and Mass Transfer*, 39(8), pp. 1125–1131. doi: 10.1016/j.icheatmasstransfer.2012.06.015.

Cheng, Y. H., Yang, S. H. and Lin, F. H. (2011) 'Thermosensitive chitosan-gelatin-glycerol phosphate hydrogel as a controlled release system of ferulic acid for nucleus pulposus regeneration', *Biomaterials*, 32(29), pp. 6953–6961. doi: 10.1016/j.biomaterials.2011.03.065.

Choi, Y. H., Lim, S. T. and Yoo, B. (2004) 'Measurement of dynamic rheology during ageing of gelatine-sugar composites', *International Journal of Food Science and Technology*, 39(9), pp. 935–945. doi: 10.1111/j.1365-2621.2004.00871.x.

Classroom, T. P. (2017) *Sound is a Pressure Wave*. Available at: http://www.physicsclassroom.com/class/sound/u11l1c.cfm (Accessed: 5 October 2017).

Coles, R. *et al.* (2014) 'Design of biomaterial packaging systems for the chilled fish/ seafood and meat industry sectors.

Coles, R. and Kirwan, M. (2011) *Food and Beverage Packaging Technology*, *Wiley-Blackwell*. Available at: https://leseprobe.buch.de/images-adb/45/82/4582a88d-dc39-4bfb-93ea-07eac1ea0724.pdf.

Cotts, S. (2016) *Fundamentals of Polymer Rheology*. Available at:

http://www.tainstruments.com/wp-content/uploads/TA-Instruments-CUICAR-presentation-201609-Polymer-Rheology.pdf.

Coutinho, D. F. *et al.* (2010) 'Modified Gellan Gum hydrogels with tunable physical and mechanical properties', *Biomaterials*, 31(29), pp. 7494–7502. doi: 10.1016/j.biomaterials.2010.06.035.

CR (2004) *Technical Note. Rings are for fingers, plates are for surface tension*. Available at: https://www.kruss-scientific.com/fileadmin/user_upload/website/literature/kruss-tn308-en.pdf.

Crochet, P. *et al.* (2005) 'Starch crystal solubility and starch granule gelatinisation.', *Carbohydrate research*, 340(1), pp. 107–13. doi: 10.1016/j.carres.2004.11.006.

D

Danks, A. E., Hall, S. R. and Schnepp, Z. (2016) 'The evolution of "sol–gel" chemistry as a technique for materials synthesis', *Mater. Horiz.*, 3(2), pp. 91–112. doi: 10.1039/C5MH00260E.

Derkach, S. R. (2015) 'Interfacial layers of complex-forming ionic surfactants with gelatin', *Advances in Colloid and Interface Science*, pp. 172–198. doi: 10.1016/j.cis.2014.05.001.

Dufaylite Ltd (2017) *Ultraboard*. Available at: http://ultraboard.co.uk/.

E

Easy Composites Ltd (2017) *Nomex Aramid Honeycombs*. Available at: http://www.easycomposites.co.uk/#!/core-materials/nomex-aramid-honeycomb/3mm-29kg-aerospace-nomex-honeycomb.html.

Edwards, W. (2000) 'Sugar-free Confectionery', in *The Science of Sugar Confectionary*, pp. 131–143. doi: 10.1016/j.(73).

Enguix, C., Imbernon, A. and Ferrer, J. (2008) 'Legislation and certification of environmentally compatible packaging in the European Union', in *Environmentally Compatible Food Packaging*, pp. 521–556. doi: 10.1533/9781845694784.3.521.

European Bioplastics Association (2015) *European Bioplastics Association Webpage*. Available at: https://www.european-bioplastics.org/bioplastics/.

European Bioplastics Association (2018) *Bioplastics Market Data*. Available at: https://www.european-bioplastics.org/market/.

European Comission (2015) *Internal Market, Industry, Entrepreneurship and SMEs*. Available at: http://ec.europa.eu/growth/sectors/biotechnology/bio-based-products/index_en.htm.

European Comittee for standardisation (CEN) (2014) *European Standards supporting the market for bio-based products*. Available at: https://www.cen.eu/news/brochures/brochures/CEN_Bio-based-products_2014.pdf.

Fakhouri, F. M. *et al.* (2013) 'Comparative study of processing methods for starch/gelatin films', *Carbohydrate Polymers*, 95(2), pp. 681–689. doi: 10.1016/j.carbpol.2013.03.027.

F

Fang, Q. and Hanna, M. A. (2001) 'Characteristics of biodegradable Mater-Bi®-starch based foams as affected by ingredient formulations', *Industrial Crops and Products*, 13(3), pp. 219–227. doi: 10.1016/S0926-6690(00)00079-0.

Fidler, C. and Simonton, T. C. (2000) 'Aerogel-in-foam thermal insulation and its preparation'. US.

Fisher Scientific (2015a) *Acetic acid, 99.5%, pure, ACROS Organics Specification*. Available at: https://www.fishersci.co.uk/shop/products/acetic-acid-99-5-pure-acros-organics-4/p-3212329.

Fisher Scientific (2015b) *Sodium Hydroxide, Extra Pure, SLR, Pellets, Fisher Chemical Specification*. Available at: https://www.fishersci.co.uk/shop/products/sodium-hydroxide-extra-pure-slr-pellets-5/p-7073537.

Fisher Scientific (2016) *Glycerol, 99% extra pure, ACROS Organics Spec*. Available at: https://www.fishersci.co.uk/shop/products/glycerol-99-extra-pure-acros-organics-5/10152970.

Foegeding, E. A., Luck, P. J. and Davis, J. P. (2006) 'Factors determining the physical properties of protein foams', in *Food Hydrocolloids*, pp. 284–292. doi: 10.1016/j.foodhyd.2005.03.014.

Frazier, S. D., Aday, A. N. and Srubar, W. V. (2018) 'On-Demand Microwave-Assisted

Fabrication of Gelatin Foams', *Molecules*, 23(5).

Frazier, S. D. and Srubar, W. V. (2016) 'Evaporation-based method for preparing gelatin foams with aligned tubular pore structures', *Materials Science and Engineering C*, 62, pp. 467–473. doi: 10.1016/j.msec.2016.01.074.

Freedman, H. H. (1985) 'Crosslinked Gelatine Foams'.

Frydrych, M. *et al.* (2011) 'Structure and mechanical properties of gelatin/sepiolite nanocomposite foams', *Journal of Materials Chemistry*, 21(25), pp. 9103–9111.

G

Gelardi, G. *et al.* (2015) 'Chemistry of chemical admixtures', in *Science and Technology of Concrete Admixtures*, pp. 149–218. doi: 10.1016/B978-0-08-100693-1.00009-6.

Gibas, I. and Janik, H. (2010) 'Review : Synthetic Polymer Hydrogels for Biomedical', *Chemical Technology*, 4(4), pp. 297–304. Available at: http://www.nbuv.gov.ua/Portal/Chem_Biol/Chemistry/2010_4/07.pdf.

Gibson, L. J. and Ashby, M. F. (1997) *Cellular Solids*, *Cellular Solids: Structure and Properties, Second Edition*. doi: 10.1017/CBO9781139878326.

GMIA (2012) *Gelatin Handbook*. Available at: http://www.gelatin-gmia.com/images/GMIA_Gelatin_Manual_2012.pdf.

Gomez-Gomez, F. J. *et al.* (2013) 'Influence of the injection moulding parameters on the microstructure and thermal properties of microcellular polyethylene terephthalate glycol foams', *Journal of Cellular Plastics*, 49(1), pp. 47–63. doi: 10.1177/0021955X12460044.

Granta (2017) *Granta's teaching resources for materials and process education*, *CES EduPack*. Available at: http://www.grantadesign.com/education/edupack/%0Ahttp://www.grantadesign.com/education/edupack/index.htm.

Green Cell Foam (2018) *Green Cell Foam*. Available at: https://www.greencellfoam.com/green-cell-foam/ (Accessed: 28 April 2018).

Grundke, K. *et al.* (1996) 'Studies on the wetting behaviour of polymer melts on solid surfaces using the Wilhelmy balance method', in *Colloids and Surfaces A:*

Physicochemical and Engineering Aspects, pp. 93–104. doi: 10.1016/0927-7757(96)03624-2.

Gunther, S., Borgschulte, K. and Hanns, P. (1992) 'Hydrogel foams and a process for their preparation'. US. Patent number: US5147344A

H

Hartranft, R. G. *et al.* (1994) 'Thermal foam insulator'. UD.

Herman, F. M. (2003) *Encyclopedia of Polymer Science and Technology*, *http://mrw.interscience.wiley.com/emrw/9780471440260/home/*. Available at: http://mrw.interscience.wiley.com/emrw/9780471440260/home/.

Hixon, K. R., Lu, T. and Sell, S. A. (2017) 'A comprehensive review of cryogels and their roles in tissue engineering applications', *Acta Biomaterialia*, pp. 29–41. doi: 10.1016/j.actbio.2017.08.033.

Hu, R. Y. Z., Wang, A. T. A. and Hartnett, J. P. (1991) 'Surface tension measurement of aqueous polymer solutions', *Experimental Thermal and Fluid Science*, 4(6), pp. 723–729. doi: 10.1016/0894-1777(91)90079-7.

Huo, W. *et al.* (2017) 'Strength enhancement of ultralight alumina-dried foams from particle-stabilized foams with assistance of agar and PVA', *International Journal of Applied Ceramic Technology*, 14(5), pp. 928–937. doi: 10.1111/ijac.12724.

Hyono, A. *et al.* (2004) 'Overshoot and oscillation in surface tension of gelatin solutions', *Colloids and Surfaces B: Biointerfaces*, 39(1–2), pp. 65–68. doi: 10.1016/j.colsurfb.2004.09.001.

I

Iannace, S., Di Maio, E. D. and Nicolais, L. (2001) 'Preparation and Characterization of Polyurethane Porous Membranes by Particulate-leaching Method', *Cellular Polymers*, 20(5), pp. 321–338.

Iannace, S. and Park, C. B. (2014) *Biofoams. Science and applications of biobased cellular and porous materials*. Boca Raton: CRC Press, Taylor & Francis Group.

Iannace, S. and Sorrentino, A. (2016) 'Bio-based and Bio-inspired Cellular Materials', in Park, Salvatore, I. C. B. (ed.) *Biofoams. Science and Applications of Bio-Based*

Cellular and Porous Materials. Boca Raton: CRC Press. Taylor & Francis Group, pp. 1–25.

ICEE (2017) *ICEE folding box*. Available at: http://iceefoldingbox.com/en/ (Accessed: 3 April 2017).

Imam, S. *et al.* (2008) 'Types, production and assessment of biobased food packaging materials', in *Environmentally Compatible Food Packaging*, pp. 29–62. doi: 10.1533/9781845694784.1.29.

J

Jaipan, P., Nguyen, A. and Narayan, R. J. (2017) 'Gelatin-based hydrogels for biomedical applications', *MRS Communications*, 7(3), pp. 416–426. doi: 10.1557/mrc.2017.92.

Jardim, I. M. *et al.* (2016) 'Preparation of amine-impregnated silica foams using agar as the gelling agent', *Materials Characterization*, 120, pp. 175–184. doi: 10.1016/j.matchar.2016.09.002.

K

Kaewtatip, K., Tanrattanakul, V. and Phetrat, W. (2013) 'Preparation and characterization of kaolin/starch foam', *Applied Clay Science*. Elsevier B.V., 80–81, pp. 413–416. doi: 10.1016/j.clay.2013.07.011.

Kaisangsri, N., Kerdchoechuen, O. and Laohakunjit, N. (2012) 'Biodegradable foam tray from cassava starch blended with natural fiber and chitosan', *Industrial Crops and Products*, 37(1), pp. 542–546. doi: 10.1016/j.indcrop.2011.07.034.

Kang, H. W., Tabata, Y. and Ikada, Y. (1999) 'Fabrication of porous gelatin scaffolds for tissue engineering.', *Biomaterials*, 20(14), pp. 1339–1344. doi: 10.1016/S0142-9612(99)00036-8.

Kelly, C. A. *et al.* (2014) 'Production of Biodegradable Foams Using Supercritical CO2', *Polymer - Plastics Technology and Engineering*, 53(11), pp. 1169–1177. doi: 10.1080/03602559.2014.886114.

Khomutov, L. I. *et al.* (1995) 'Temperature-composition phase diagram and gel properties of the gelatin-starch-water system', *Carbohydrate Polymers*, 28(4), pp. 341–345. doi: 10.1016/0144-8617(96)00001-X.

Khomutov, L. I. *et al.* (1996) 'Temperature-composition phase diagram and gel properties of the gelatin-starch-water system', 8617(96), pp. 341–345.

Kim, H. W., Knowles, J. C. and Kim, H. E. (2005) 'Hydroxyapatite and gelatin composite foams processed via novel freeze-drying and crosslinking for use as temporary hard tissue scaffolds', *Journal of Biomedical Materials Research - Part A*, 72(2), pp. 136–145. doi: 10.1002/jbm.a.30168.

Kristen, N. *et al.* (2009) 'No charge reversal at foam film surfaces after addition of oppositely charged polyelectrolytes?', *Journal of Physical Chemistry B*, 113(23), pp. 7986–7990. doi: 10.1021/jp902369d.

Kruss (2018) *Kruss Webpage*, *Wilhelmy plate method*. Available at: https://www.kruss-scientific.com/services/education-theory/glossary/wilhelmy-plate-method/.

L

Laftah, W. A., Hashim, S. and Ibrahim, A. N. (2011) 'Polymer hydrogels: A review', *Polymer - Plastics Technology and Engineering*, pp. 1475–1486. doi: 10.1080/03602559.2011.593082.

Lagarrigue, S. and Alvarez, G. (2001) 'The rheology of starch dispersions at high temperatures and high shear rates: a review', *Journal of Food Engineering*, 50(4), pp. 189–202. doi: 10.1016/S0260-8774(00)00239-9.

Lai, S.-M., Sun, W.-W. and Don, T.-M. (2015) 'Preparation and characterization of biodegradable polymer blends from poly(3-hydroxybutyrate)/poly(vinyl acetate)-modified corn starch', *Polymer Engineering and Science*, 55(6), pp. 1321–1329. doi: 10.1002/pen.24071.

Landrock, A. H. (1995) *Handbook of Plastic Foams: Types, Properties, Manufacture and Applications*, *Handbook of Plastic Foams*. doi: 10.1016/B978-081551357-5.50004-8.

Lavorgna, M., Verdolotti, L. and Mascia, L. (2016) 'Organic-Inorganic Bio-Hybrid Materials by Sol-Gel Processing', in Park, S. I. and B., C. (eds) *Biofoams. Science and Applications of Bio-Based Cellular and Porous Materials*. Boca Raton: CRC Press. Taylor & Francis Group, pp. 39–57.

Lee, J. P. and Lee, K. H. (1997) 'Manufacture of biodegradable packaging foams from agar by freeze-drying', *Journal of materials science*, 32, pp. 5825–5832. doi:

10.1023/A:1018642406530.

Lee, S.-T. (2004) 'Introduction: Polymeric Foams, Mechanism, and Materials', in *Polymeric Foams: Mechanisms and Materials*, pp. 1–16. doi: 10.1109/MEI.2005.1412232.

Liang, J. Z. and Jiang, X. H. (2012) 'Sound insulation in polymer/inorganic particle composites. I. Theoretical model', *Journal of Applied Polymer Science*, 125(1), pp. 676–681. doi: 10.1002/app.34824.

Liu, P. S. *et al.* (2014) 'Chapter Ten – Characterization Methods: Physical Properties', in *Porous Materials*, pp. 493–532. doi: 10.1016/B978-0-12-407788-1.00010-1.

Liu, X. and Ma, P. X. (2009) 'Phase separation, pore structure, and properties of nanofibrous gelatin scaffolds', *Biomaterials*, 30(25), pp. 4094–4103. doi: 10.1016/j.biomaterials.2009.04.024.

Ludmila, A. and Dyshlyuk, L. (2016) 'Study of viscosity of aqueous solutions of natural polysaccharides', *Science Evoluton*, 1, pp. 11–19.

Lund, B., Baird-Parker, A. C. and Grahame W., G. (2000) *Microbiological Safety and Quality of Food*. 1st edn. Springer US.

Luong, D. D. *et al.* (2014) 'High Strain Rate Compressive Behavior of Polyurethane Resin and Polyurethane/Al2O3 Hollow Sphere Syntactic Foams', *Journal of Composites*, 2014, pp. 1–10. doi: 10.1155/2014/795984.

M

Maity, G. C. (2007) 'Low Molecular Mass Gelators of Organic Liquids', *Journal of Physical Sciences*, 11, pp. 156–171.

Majzoobi, M. and Beparva, P. (2014) 'Effects of acetic acid and lactic acid on physicochemical characteristics of native and cross-linked wheat starches', *Food Chemistry*, 147, pp. 312–317. doi: 10.1016/j.foodchem.2013.09.148.

Manda, M. G. *et al.* (2018) 'Gellan gum-hydroxyapatite composite spongy-like hydrogels for bone tissue engineering', *Journal of Biomedical Materials Research - Part A*, 106(2), pp. 479–490. doi: 10.1002/jbm.a.36248.

Marr, P. C. and Marr, A. C. (2015) 'Ionic liquid gel materials: applications in green and sustainable chemistry.', *Green Chem.*, 18, pp. 105–128. doi:

10.1039/C5GC02277K.

Martucci, J. F., Espinosa, J. P. and Ruseckaite, R. A. (2015) 'Physicochemical Properties of Films Based on Bovine Gelatin Cross-linked with 1,4-Butanediol Diglycidyl Ether', *Food and Bioprocess Technology*, 8(8), pp. 1645–1656. doi: 10.1007/s11947-015-1524-x.

McRae, J. D., Naguib, H. E. and Atalla, N. (2010) 'Mechanical and acoustic performance of compression-molded open-cell polypropylene foams', *Journal of Applied Polymer Science*, 116(2), pp. 1106–1115. doi: 10.1002/app.31581.

Mills, N. (2007) *Polymer Foams Handbook*, *Polymer Foams Handbook*. doi: 10.1016/B978-0-7506-8069-1.X5000-4.

Misra, P. K., Meher, J. and Maharana, S. (2016) 'Investigation on the gelatin-surfactant interaction and physiochemical characteristics of the mixture', *Journal of Molecular Liquids*, 224, pp. 900–908. doi: 10.1016/j.molliq.2016.10.043.

Mitra, D., Bhattacharya, S. C. and Moulik, S. P. (2009) 'A LB film morphological study with reference to biopolymer-surfactant interaction taking gelatin-CTAB system as a model', *Biophysical Chemistry*, 139(2–3), pp. 123–136. doi: 10.1016/j.bpc.2008.10.012.

Montgomery, R. (2004) 'Development of biobased products', *Bioresource Technology*, 91(1), pp. 1–29. doi: 10.1016/S0960-8524(03)00154-8.

Morris, E. R., Nishinari, K. and Rinaudo, M. (2012) 'Gelation of gellan - A review', *Food Hydrocolloids*, pp. 373–411. doi: 10.1016/j.foodhyd.2012.01.004.

Morrison, R. L. (1995) 'Biofoam'. US.

N

Nafchi, A. M. *et al.* (2013) 'Thermoplastic starches: Properties, challenges, and prospects', *Starch/Staerke*, pp. 61–72. doi: 10.1002/star.201200201.

Neuman, P. (1976) 'Gelatin-Based Compositions and a method for the generation of stabilised foams therefrom'. US-4086331-A

Nishinari, K. (2009) 'Some thoughts on the definition of a gel', *Progress in Colloid and Polymer Science*, 136, pp. 87–94. doi: 10.1007/2882_2009_12.

Niu, F. *et al.* (2014) 'Ovalbumin-gum arabic interactions: effect of pH, temperature,

salt, biopolymers ratio and total concentration.', *Colloids and surfaces. B, Biointerfaces*. Elsevier B.V., 113, pp. 477–82. doi: 10.1016/j.colsurfb.2013.08.012.

Nofar, M. and Park, C. B. (2016) 'Heterogeneous Cell Nucleation Mechanisms in Polylactide Foaming', in Park, S. I. & C. B. (ed.) *Biofoams. Science and Applications of Bio-Based Cellular and Porous Materials*. Boca Raton: CRD Press. Taylor & Francis Group, pp. 153–174.

Novamont (2018) *Mater-bi*. Available at: http://www.novamont.com/eng/mater-bi (Accessed: 24 May 2018).

Nur Hanani, Z. A., Roos, Y. H. and Kerry, J. P. (2014) 'Use and application of gelatin as potential biodegradable packaging materials for food products', *International Journal of Biological Macromolecules*, 71, pp. 94–102. doi: 10.1016/j.ijbiomac.2014.04.027.

O

Oliviero, M. *et al.* (2015) 'Foaming behavior of bio-based blends based on thermoplastic gelatin and poly(butylene succinate)', *Journal of Applied Polymer Science*, 132(48). doi: 10.1002/app.42704.

Osama Al, A. B. (2015) 'Foamability and Foam Stability of Several Surfactants Solutions: The Role of Screening and Flooding', *Journal of Petroleum & Environmental Biotechnology*, 06(04). doi: 10.4172/2157-7463.1000227.

Osorio, F. A. *et al.* (2007) 'Effects of concentration, bloom degree, and pH on gelatin melting and gelling temperatures using small amplitude oscillatory rheology', *International Journal of Food Properties*, 10(4), pp. 841–851. doi: 10.1080/10942910601128895.

P

Pang, Z. *et al.* (2014) 'Rheology, texture and microstructure of gelatin gels with and without milk proteins', *Food Hydrocolloids*, 35, pp. 483–493. doi: 10.1016/j.foodhyd.2013.07.007.

Paperfoam (2018) *Paperfoam webpage*. Available at: https://www.paperfoam.com/ (Accessed: 23 April 2018).

Park, C. B. and Cheung, L. K. (1997) 'A study of cell nucleation in the extrusion of

polypropylene foams', *Polymer Engineering and Science*, 37(1), pp. 1–10. doi: 10.1002/pen.11639.

Peng, L. (2016) 'Sound absorption and insulation functional composites', in *Advanced High Strength Natural Fibre Composites in Construction*, pp. 333–373. doi: 10.1016/B978-0-08-100411-1.00013-3.

Peng, X. *et al.* (2013) 'Microwave foaming of starch-based materials (I) dielectric performance', *Journal of Cellular Plastics*, 49(3), pp. 245–258. doi: 10.1177/0021955X13477438.

Pera Technology (2014) *Pera technology webpage*. Available at: www.peratechnology.com/casestudies/materials/PLA-foam (Accessed: 5 April 2014).

Petkova, R., Tcholakova, S. and Denkov, N. D. (2012) 'Foaming and foam stability for mixed polymer-surfactant solutions: Effects of surfactant type and polymer charge', *Langmuir*, 28(11), pp. 4996–5009. doi: 10.1021/la3003096.

Philp, J. C., Ritchie, R. J. and Guy, K. (2013) 'Biobased plastics in a bioeconomy', *Trends in Biotechnology*, pp. 65–67. doi: 10.1016/j.tibtech.2012.11.009.

Pinto, J. *et al.* (2013) 'Characterization of the cellular structure based on user-interactive image analysis procedures', *Journal of Cellular Plastics*, 49(7), pp. 555–575. doi: 10.1177/0021955X13503847.

Plastics Today (2009) 'Ten years on: biomaterials use surges at Toyota'. Available at: https://www.plasticstoday.com/content/ten-years-on-biomaterials-use-surges-toyota/7365428413206.

Preechawong, D. *et al.* (2004) 'Preparation and Properties of Starch/Poly(vinyl alcohol) Composite Foams', *Macromolecular Symposia*, 216(1), pp. 217–228. doi: 10.1002/masy.200451221.

Prociak, A. (2016) 'Bio-based Polyurethane foams', in B.Park, S. I. and Chul (eds) *Biofoams. Science and Applications of Bio-Based Cellular and Porous Materials*. Boca Raton: CRC Press. Taylor & Francis Group, pp. 267–282.

Pushpadass, H. A. *et al.* (2008) 'Extrusion of starch-based loose-fill packaging foams: Effects of temperature, moisture and talc on physical properties', *Packaging Technology and Science*, 21(3), pp. 171–183. doi: 10.1002/pts.809.

R

Ramos, M. *et al.* (2016) 'Gelatin-Based Films and Coatings for Food Packaging Applications', *Coatings*, 6(4), p. 41. doi: 10.3390/coatings6040041.

Razza, F. *et al.* (2015) 'Environmental profile of a bio-based and biodegradable foamed packaging prototype in comparison with the current benchmark', *Journal of Cleaner Production*. Elsevier, 102, pp. 493–500. doi: 10.1016/J.JCLEPRO.2015.04.033.

Reddy, M. M. *et al.* (2013) 'Biobased plastics and bionanocomposites: Current status and future opportunities', *Progress in Polymer Science*. Elsevier Ltd, 38(10–11), pp. 1653–1689. doi: 10.1016/j.progpolymsci.2013.05.006.

Rio, E. *et al.* (2014) 'Unusually stable liquid foams', *Advances in Colloid and Interface Science*. Elsevier B.V., 205, pp. 74–86. doi: 10.1016/j.cis.2013.10.023.

Robertson, G. (2008) 'State-of-the-art biobased food packaging materials', in *Environmentally Compatible Food Packaging*, pp. 3–28. doi: 10.1533/9781845694784.1.3.

Rohsenow, W. M., Hartnett, J. P. and Cho, Y. I. (1998) *Handbook of heat transfer media*, *International Journal of Heat and Mass Transfer*. doi: 10.1016/0017-9310(64)90164-4.

Roy, R. *et al.* (2014) 'Characterization of Nomex honeycomb core constituent material mechanical properties', *Composite Structures*, 117(1), pp. 255–266. doi: 10.1016/j.compstruct.2014.06.033.

Ruiz-Cabrera, M. a. *et al.* (2005) 'Assessment of water diffusivity in gelatine gel from moisture profiles. I—Non-destructive measurement of 1D moisture profiles during drying from 2D nuclear magnetic resonance images', *Journal of Food Engineering*, 68(2), pp. 209–219. doi: 10.1016/j.jfoodeng.2004.05.033.

Ruiz-Hitzky, E. *et al.* (2016) 'Clay-Based Bionanocomposite Foams', in Park, S. I. and B., C. (eds) *Biofoams. Science and Applications of Bio-Based Cellular and Porous Materials*. Boca Raton: CRC Press. Taylor & Francis Group, pp. 251–262.

Rusch, K. C. (1970) 'Load-compression behavior of brittle foams', *Journal of Applied Polymer Science*, 14(5), pp. 1263–1276. doi: 10.1002/app.1970.070140514.

Russell, B. P. *et al.* (2011) 'Quasi-Static Three-Point Bending of Carbon Fiber Sandwich Beams With Square Honeycomb Cores', *Journal of Applied Mechanics*, 78(3), p. 031008. doi: 10.1115/1.4003221.

S

Salgado, P. R. *et al.* (2008) 'Biodegradable foams based on cassava starch, sunflower proteins and cellulose fibers obtained by a baking process', *Journal of Food Engineering*, 85(3), pp. 435–443. doi: 10.1016/j.jfoodeng.2007.08.005.

Satish, K. and KS, T. (2017) 'Bioplastics-classification, production and their potential food applications', *Journal of Hill Agriculture*, 8, pp. 118–129.

Schrieber, R. and Gareis, H. (2007) *Gelatine Handbook: Theory and Industrial Practice*, *Wiley-VCH Verlag GmbH & Co. KGaA*. doi: 10.1002/9783527610969.gloss.

Seafish Industry Authority (2009) *Fresh Fish Wholesale Packaging*. Available at: http://www.seafish.org/media/Publications/datasheet_96_03_FT.pdf.

Sharma, C., Dinda, A. K. and Mishra, N. C. (2013) 'Fabrication and characterization of natural origin chitosan-gelatin- alginate composite scaffold by foaming method without using surfactant', *Journal of Applied Polymer Science*, 127(4), pp. 3228–3241. doi: 10.1002/app.37755.

Shey, J. *et al.* (2006) 'Properties of baked starch foam with natural rubber latex', *Industrial Crops and Products*, 24(1), pp. 34–40. doi: 10.1016/j.indcrop.2005.12.001.

Shogren, R. . *et al.* (1998) 'Structure and morphology of baked starch foams', *Polymer*, 39(25), pp. 6649–6655. doi: 10.1016/S0032-3861(97)10303-2.

Shyamkuwar, A. L. *et al.* (2010) 'Synthesis, Characterization, and Drying of Absorbable Gelatin Foam', *Drying Technology*, 28(5), pp. 659–668. doi: 10.1080/07373931003799137.

Sierra Suppy and Packaging (2018) *Sierra Supply and Packaging webpage*. Available at: http://www.sierrapackaging.net/productdetaill2.aspx?dataid=TSP-15S (Accessed: 28 April 2018).

da Silva, A. *et al.* (2013) 'Cassava starch-based foams reinforced with bacterial cellulose', *Journal of Applied Polymer Science*, 130(5), pp. 3043–3049. doi: 10.1002/app.39526.

Singh, N. B. and Middendorf, B. (2007) 'Calcium sulphate hemihydrate hydration leading to gypsum crystallization', *Progress in Crystal Growth and Characterization of Materials*, pp. 57–77. doi: 10.1016/j.pcrysgrow.2007.01.002.

Sobral, P. J. do A. *et al.* (2011) 'Phase transitions in biodegradable films based on blends of gelatin and poly (vinyl alcohol)', *Ciência e Tecnologia de Alimentos*, 31(2), pp. 372–379. doi: 10.1590/S0101-20612011000200015.

Song, J. (2014) 'Starch foams', in Park, S. I. and B., C. (eds) *Biofoams. Science and Applications of Bio-Based Cellular and Porous Materials*. Boca Raton: CRC Press. Taylor & Francis Group, pp. 2017–226.

Soykeabkaew, N., Thanomsilp, C. and Suwantong, O. (2015) 'A review: Starch-based composite foams', *Composites Part A: Applied Science and Manufacturing*, 78, pp. 246–263. doi: 10.1016/j.compositesa.2015.08.014.

Steeves, C. A. and Fleck, N. A. (2004) 'Collapse mechanisms of sandwich beams with composite faces and a foam core, loaded in three-point bending. Part II: Experimental investigation and numerical modelling', *International Journal of Mechanical Sciences*, 46(4), pp. 585–608. doi: 10.1016/j.ijmecsci.2004.04.004.

Stepto, R. F. T. (2009) 'Thermoplastic starch', *Macromolecular Symposia*, 279(1), pp. 163–168. doi: 10.1002/masy.200950525.

Suh, K. W. and Skochdopole, R. E. (1980) 'Foamed Plastics', in Kirl-Othmer (ed.) *Encyclopedia of Chemical Technology*. 3rd edn. New York: Wiley.

Suhanek, M., Jambroši, K. and Horvat, M. (2008) 'A comparison of two methods for measuring the sound absorption coefficient using impedance tubes', *50th International Symposium ELMAR-2008*, 2(September), pp. 321–324.

Sundaram, J., Durance, T. D. and Wang, R. (2008) 'Porous scaffold of gelatin-starch with nanohydroxyapatite composite processed via novel microwave vacuum drying', *Acta Biomaterialia*, 4(4), pp. 932–942. doi: 10.1016/j.actbio.2008.01.019.

Svagan, A. J., Samir, M. A. S. A. and Berglund, L. A. (2008) 'Biomimetic foams of high mechanical performance based on nanostructured cell walls reinforced by native cellulose nanofibrils', *Advanced Materials*, 20(7), pp. 1263–1269. doi: 10.1002/adma.200701215.

Swain, M. V. *et al.* (2014) 'Projectile penetration into ballistic gelatin', *Journal of the*

Mechanical Behavior of Biomedical Materials, 29, pp. 385–392. doi: 10.1016/j.jmbbm.2013.09.024.

Synbra Technology (no date) *Biofoam*. Available at: https://www.synbratechnology.com/biofoam/ (Accessed: 28 April 2018).

T

TA Instruments (2017) *TA Instruments Webinars*. Available at: http://www.tainstruments.com/support/webinars/.

Tau, T. and Gunasekaran, S. (2016) 'Thermorheological evaluation of gelation of gelatin with sugar substitutes', *LWT - Food Science and Technology*, 69, pp. 570–578. doi: 10.1016/j.lwt.2016.02.015.

Temperature Control Packaging (2016) *Temperature Control Packaging*. Available at: http://www.temperature-controlled-packaging.co.uk/ (Accessed: 16 December 2016).

Tereos Syral (2014) *Meritena 200 Technical Specification*. France.

Tester, R. F., Karkalas, J. and Qi, X. (2004) 'Starch—composition, fine structure and architecture', *Journal of Cereal Science*, 39(2), pp. 151–165. doi: 10.1016/j.jcs.2003.12.001.

The Coca-Cola Company (2015) *Coke unveils PET bottle made entirely from plants*. Available at: http://www.coca-colacompany.com/plantbottle-technology/plantbottle-20-coca-cola-unveils-worlds-first-pet-plastic-bottle-made-entirely-from-plants#TCCC (Accessed: 6 March 2015).

The Engineering Toolbox (2005) *Surface Tension*. Available at: https://www.engineeringtoolbox.com/surface-tension-d_962.html (Accessed: 22 April 2018).

Topa Thermal (2017) *Topa Thermal Wepbage*. Available at: http://www.topathermal.com/ (Accessed: 5 April 2017).

Trček, J., Mira, N. P. and Jarboe, L. R. (2015) 'Adaptation and tolerance of bacteria against acetic acid', *Applied Microbiology and Biotechnology*, pp. 6215–6229. doi: 10.1007/s00253-015-6762-3.

Turuallo, G. and Soutsos, M. N. (2015) 'Supplementary cementitious materials:

Strength development of self-compacting concrete under different curing temperature', in *Procedia Engineering*, pp. 699–704. doi: 10.1016/j.proeng.2015.11.109.

U

Ullah, F. *et al.* (2015) 'Classification, processing and application of hydrogels: A review', *Materials Science and Engineering C*, 57, pp. 414–433. doi: 10.1016/j.msec.2015.07.053.

Unibond (2015) *Unibond Super PVA Glue*. Available at: https://www.screwfix.com/p/unibond-super-pva-glue-5ltr/29912.

V

Vieira, S. *et al.* (2007) 'Natural-Based Hydrogels: From Processing to Applications', in *Encyclopedia of Polymer Science and Technology, 1*. John Wiley & Sons.

W

Waje, S. S. *et al.* (2005) 'Drying and shrinkage of polymer gels', *Brazilian Journal of Chemical Engineering*, 22(2).

Wang, J., Lee, P. C. and Park, C. B. (2011) 'Visualization of initial expansion behavior of butane-blown low-density polyethylene foam at extrusion die exit', *Polymer Engineering and Science*, 51(3), pp. 492–499. doi: 10.1002/pen.21803.

Wang, Y. *et al.* (2010) 'Assessment of Technical and Environmental Performances of Wheat-Based Foams in Thermal Packaging Applications', *Packaging Technology and Science*, 23(7), pp. 363–382. doi: Doi 10.1002/Pts.897.

Weaire, D. and Hutzler, S. (1999) 'The physics of foams', *Foam collapse*, p. 246.

Whistler, J. B. and R. (2009) *Starch: Chemistry and Technology*. 3rd edn. Edited by J. B. and R. Whistler. Elsevier Inc.

Willett, J. . and Shogren, R. . (2002) 'Processing and properties of extruded starch/polymer foams', *Polymer*, 43(22), pp. 5935–5947. doi: 10.1016/S0032-3861(02)00497-4.

Wu, Q. *et al.* (2017) 'Freeze-dried wheat gluten biofoams; scaling up with water welding', *Industrial Crops and Products*, 97, pp. 184–190. doi:

10.1016/j.indcrop.2016.12.010.

Wu, X. *et al.* (2010) 'Preparation of aligned porous gelatin scaffolds by unidirectional freeze-drying method', *Acta Biomaterialia*, 6(3), pp. 1167–1177. doi: 10.1016/j.actbio.2009.08.041.

Y

Yahia, Lh. (2015) 'History and Applications of Hydrogels', *Journal of Biomedical Sciencies*, 04(02). doi: 10.4172/2254-609X.100013.

Yan, C. and Pochan, D. J. (2010) 'Rheological properties of peptide-based hydrogels for biomedical and other applications', *Chemical Society Reviews*, 39(9), p. 3528. doi: 10.1039/b919449p.

Yan, L. L. *et al.* (2014) 'Three-point bending of sandwich beams with aluminum foam-filled corrugated cores', *Materials and Design*, 60, pp. 510–519. doi: 10.1016/j.matdes.2014.04.014.

Yao, J. and Rodrigue, D. (2012) 'Density graded polyethylene foams produced by compression moulding using a chemical blowing agent', *Cellular Polymers*, 31(4), pp. 189–206.

Yildirim, N. *et al.* (2014) 'Cellulose nanofibril (CNF) reinforced starch insulating foams', *Cellulose*, 21(6), pp. 4337–4347. doi: 10.1007/s10570-014-0450-9.

Z

Zanto, E. J., Al-Muhtaseb, S. A. and Ritter, J. A. (2002) 'Sol-gel-derived carbon aerogels and xerogels: Design of experiments approach to materials synthesis', *Industrial and Engineering Chemistry Research*, 41(13), pp. 3151–3162. doi: 10.1021/ie020048g.

Zeng, Q. *et al.* (2014) 'Characterizing pore structure of cement blend pastes using water vapor sorption analysis', *Materials Characterization*. Elsevier B.V., 95, pp. 72–84. doi: 10.1016/j.matchar.2014.06.007.

Zhang, J.-F. and Sun, X. (2007) 'Biodegradable foams of poly(lactic acid)/starch. II. Cellular structure and water resistance', *Journal of Applied Polymer Science*, 106(5), pp. 3058–3062. doi: 10.1002/app.26697.

Zhang, N. *et al.* (2013) 'Developing gelatin-starch blends for use as capsule materials.', *Carbohydrate polymers*. Elsevier Ltd., 92(1), pp. 455–61. doi: 10.1016/j.carbpol.2012.09.048.

Zhang, Y. *et al.* (2014) 'Gelcasting of alumina suspension using gellan gum as gelling agent', *Ceramics International*, 40(4), pp. 5715–5721. doi: 10.1016/j.ceramint.2013.11.010.

Zhao, R., Torley, P. and Halley, P. J. (2008) 'Emerging biodegradable materials: Starch- and protein-based bio-nanocomposites', *Journal of Materials Science*, 43(9), pp. 3058–3071. doi: 10.1007/s10853-007-2434-8.

Zhou, J. (2004) *Microwave assisted moulding of starch-based foams. A thesis submitted for the degree of Doctor of Philosophy by Jiang Zhou Department of Mechanical Engineering Brunel University*.

Zhou, J. and Hanna, M. (2006) 'Shrinkage and re-expansion of extruded starch acetate foams', *Journal of Applied Polymer Science*, 102(5), pp. 4264–4268. doi: 10.1002/app.24781.

Zhou, J., Song, J. and Parker, R. (2006) 'Structure and properties of starch-based foams prepared by microwave heating from extruded pellets', *Carbohydrate Polymers*, 63(4), pp. 466–475. doi: 10.1016/j.carbpol.2005.09.019.

Zinno, A. *et al.* (2011) 'Experimental characterization of phenolic-impregnated honeycomb sandwich structures for transportation vehicles', *Composite Structures*, 93(11), pp. 2910–2924. doi: 10.1016/j.compstruct.2011.05.012.

Zuidema, J. M. *et al.* (2014) 'A protocol for rheological characterization of hydrogels for tissue engineering strategies', *Journal of Biomedical Materials Research - Part B Applied Biomaterials*, 102(5), pp. 1063–1073. doi: 10.1002/jbm.b.33088.

APPENDIX A.
ANOVA TABLES

Appendix A.

ANOVA TABLES

Table A.1 ANOVA TABLE FOR THE GELLING TEMPERATURE OF GELATINE SOLUTIONS (SIGNIFICANCE LEVEL α=0.05)

SOURCE	DF	ADJ SS	ADJ MS	F-VALUE	P-VALUE
Model	5	19.1346	3.8269	7.16	0.003
Linear	3	18.7804	6.2601	11.71	0.001
Gelatine strength	**1**	**2.1549**	**2.1549**	**4.03**	**0.068**
Gelatine content	**2**	**16.6255**	**8.3127**	**15.55**	**0.000**
2-Way Interactions	2	0.3542	0.1771	0.33	0.724
Gelatine Strength*Gelatine content	**2**	**0.3542**	**0.1771**	**0.33**	**0.724**
Error	12	6.4141	0.5345		
Total	17	25.5487			

Table A.2 ANOVA TABLE FOR THE MELTING POINT OF GELATINE SOLUTIONS (SIGNIFICANCE LEVEL α=0.05)

SOURCE	DF	ADJ SS	ADJ MS	F-VALUE	P-VALUE
Model	5	4.1088	0.8218	1.67	0.215
Linear	3	3.8825	1.2942	2.64	0.098
Gelatine strength	**1**	**0.1112**	**0.1112**	**0.23**	**0.643**
Gelatine content	**2**	**3.7713**	**1.8856**	**3.84**	**0.051**
2-Way Interactions	2	0.2262	0.1131	0.23	0.798
Gelatine Strength*Gelatine content	**2**	**0.2262**	**0.1131**	**0.23**	**0.798**
Error	12	5.8932	0.4911		
Total	17	10.0020			

Table A.3 ANOVA TABLE FOR THE MER OF GELATINE-SURFACTANT "A" FOAMS (SIGNIFICANCE LEVEL a=0.05)

SOURCE	DF	ADJ SS	ADJ MS	F-VALUE	P-VALUE
Model	17	110.837	6.5198	29.57	0.000
Linear	5	103.487	20.70	93.87	0.000
Gelatine content	**2**	**64.062**	**32.03**	**145.27**	**0.000**
Surfactant content	**2**	**26.287**	**13.14**	**59.61**	**0.000**
Foaming temperature	**1**	**13.138**	**13.14**	**59.59**	**0.000**
2-Way Interactions	8	5.866	0.73	3.33	0.006
Gelatine content*surfactant content	**4**	**4.623**	**1.16**	**5.24**	**0.002**
Gelatine content*Foaming temperature	**2**	**0.993**	**0.50**	**2.25**	**0.572**
Surfactant content*Foaming temperature	**2**	**0.25**	**0.12**	**0.57**	**0.120**
3-Way Interactions	4	1.485	0.37	1.68	0.175
Gelatine content*Surfactant content *Foaming temperature	**4**	**1.485**	**0.37**	**1.68**	**0.175**
Error	36	7.938	0.22		
Total	53	118.775			

Table A.4 ANOVA TABLE FOR THE MER OF GELATINE-SURFACTANT C2 FOAMS (SIGNIFICANCE LEVEL a=0.05)

SOURCE	DF	ADJ SS	ADJ MS	F-VALUE	P-VALUE
Model	17	47.522	2.7954	16.35	0.000
Linear	5	41.6973	8.3395	48.77	0.000
Gelatine content	**2**	**27.3857**	**13.6928**	**80.08**	**0.000**
Surfactant content	**2**	**8.8582**	**4.4291**	**25.90**	**0.000**
Foaming temperature	**1**	**5.4533**	**5.4533**	**31.89**	**0.000**
2-Way Interactions	8	2.7052	0.3381	1.98	0.078
Gelatine content*surfactant content	**4**	**1.5497**	**0.3874**	**2.27**	**0.081**
Gelatine content*Foaming temperature	**2**	**0.0173**	**0.0086**	**0.05**	**0.047**
Surfactant content*Foaming temperature	**2**	**1.1382**	**0.5691**	**3.33**	**0.951**
3-Way Interactions	4	3.12	0.780	4.56	0.004
Gelatine content*Surfactant content *Foaming temperature	**4**	3.12	0.780	4.56	0.004
Error	36	6.155	0.1710		
Total	53	53.678			

Table A.5 ANOVA TABLE FOR THE COMPARISON OF THE MER OF GELATINE FOAMS CONTAINING SURFACTANTS C1 AND C2 (SIGNIFICANCE LEVEL α=0.05)

SOURCE	DF	ADJ SS	ADJ MS	F-VALUE	P-VALUE
Model	11	23.858	2.16895	17.16	0.000
Linear	4	7.159	1.78976	14.16	0.000
Surfactant type	**1**	**0.1895**	**0.18946**	**1.50**	**0.233**
Gelatine content	**2**	**6.1924**	**3.09621**	**24.49**	**0.000**
Surfactant content	**1**	**0.7772**	**0.77715**	**6.15**	**0.021**
2-Way Interactions	5	9.2976	1.85952	14.71	0.000
Surfactant type*Gelatine content	**2**	**3.3526**	**1.67631**	**13.26**	**0.000**
Surfactant type*Surfactant content	**1**	**0.0354**	**0.03543**	**0.28**	**0.601**
Gelatine content*Surfactant content	**2**	**5.9095**	**2.95477**	**23.37**	**0.000**
3-Way Interactions	2	7.4018	3.70090	29.28	0.000
Gelatine content*Surfactant content *Foaming temperature	**2**	7.4018	3.70090	29.28	0.000
Error	24	3.0340	0.12641		
Total	35	26.8924			

Table A.6 ANOVA TABLE FOR THE SHRINKAGE OF GELATINE-SURFACTANT "A" FOAMS (SIGNIFICANCE LEVEL α=0.05)

SOURCE	DF	ADJ SS	ADJ MS	F-VALUE	P-VALUE
Model	17	2035.13	119.714	11.97	0.000
Linear	5	36.278	7.2556	42.43	0.000
Gelatine content	**2**	**1098.43**	**549.21**	**54.91**	**0.000**
Surfactant content	**2**	**1.64**	**0.82**	**0.08**	**0.921**
Foaming temperature	**1**	**361.51**	**361.51**	**36.14**	**0.000**
2-Way Interactions	8	485.19	60.65	6.06	0.000
Surfactant content*Gelatine content	**4**	**224.72**	**56.18**	**5.62**	**0.001**
Surfactant content*Foaming temperature	**2**	**75.25**	**37.62**	**3.76**	**0.033**
Gelatine content*Foaming temperature	**2**	**185.23**	**92.61**	**9.26**	**0.001**
3-Way Interactions	4	88.36	22.09	2.21	0.088
Gelatine content*Surfactant content *Foaming temperature	4	88.36	22.09	2.21	0.088
Error	36	360.1	10.00		
Total	53	2395.23			

Table A.7 ANOVA TABLE FOR THE SHRINKAGE OF GELATINE-SURFACTANT C2 FOAMS (SIGNIFICANCE LEVEL α=0.05)

SOURCE	DF	ADJ SS	ADJ MS	F-VALUE	P-VALUE
Model	17	2183.17	128.42	11.59	0.000
Linear	5	1442.88	288.58	26.04	0.000
Surfactant content	2	302.69	151.34	13.66	0.000
Gelatine content	2	416.81	208.41	18.81	0.000
Foaming temperature	1	723.38	723.38	65.27	0.000
2-Way Interactions	8	476.05	59.51	5.37	0.000
Surfactant content*Gelatine content	4	305.91	76.48	6.90	0.000
Surfactant content*Foaming temperature	2	102.92	51.46	4.64	0.016
Gelatine content*Foaming temperature	2	67.22	33.61	3.03	0.061
3-Way Interactions	4	264.24	66.06	5.96	0.001
Surfactant content*Gelatine content *Foaming temperature	4	264.24	66.06	5.96	0.001
Error	36	398.96	11.08		
Total	53	2582.13			

Table A.8 ANOVA TABLE FOR THE DENSITY OF GELATINE-SURFACTANT "A" FOAMS (SIGNIFICANCE LEVEL α=0.05)

SOURCE	DF	ADJ SS	ADJ MS	F-VALUE	P-VALUE
Model	17	12768.8	741.36	176.75	0.000
Linear	5	12169.7	23.67.8	572.74	0.000
Surfactant content	2	366.6	190.12	43.13	0.000
Gelatine content	2	11531.9	5567.88	1356.82	0.000
Foaming temperature	1	271.2	323.00	63.81	0.000
2-Way Interactions	8	516.7	77.74	15.2	0.000
Surfactant content*Gelatine content	4	317.5	85.18	18.68	0.000
Surfactant content*Foaming temperature	2	25.6	24.78	3.01	0.056
Gelatine content*Foaming temperature	2	173.6	115.83	20.42	0.000
3-Way Interactions	4	82.4	35.53	4.85	0.002
Surfactant content*Gelatine content *Foaming temperature	4	82.4	35.53	4.85	0.002
Error	72	306	4.58		
Total	89	13074.7			

Table A.9 ANOVA TABLE FOR THE DENSITY OF GELATINE-SURFACTANT C2 FOAMS (SIGNIFICANCE LEVEL α=0.05)

SOURCE	DF	ADJ SS	ADJ MS	F-VALUE	P-VALUE
Model	17	17584.7	1034.39	299.46	0.000
Linear	5	17099.5	3419.91	990.06	0.000
Surfactant content	2	462.8	231.41	66.99	0.000
Gelatine content	2	16531.2	8265.59	2392.88	0.000
Foaming temperature	1	105.6	105.55	30.56	0.000
2-Way Interactions	8	413.3	51.66	14.96	0.000
Surfactant content*Gelatine content	4	373.8	93.44	27.05	0.000
Surfactant content*Foaming temperature	2	1.3	0.64	0.18	0.832
Gelatine content*Foaming temperature	2	38.2	19.12	5.54	0.006
3-Way Interactions	4	71.8	17.95	5.2	0.001
Surfactant content*Gelatine content *Foaming temperature	4	71.8	17.95	5.2	0.001
Error	72	248.7	3.45		
Total	89	17833.4			

Table A.10 ANOVA TABLE FOR THE THERMAL CONDUCTIVITY OF GELATINE SOLUTIONS MADE WITH SURFACTANTS "A" AND C2 (SIGNIFICANCE LEVEL α=0.05)

SOURCE	DF	ADJ SS	ADJ MS	F-VALUE	P-VALUE
Model	5	0.000023	0.000005	0.91	0.504
Linear	3	0.000022	0.000007	1.49	0.267
Gelatine content	2	0.00007	0.000003	0.67	0.532
Surfactant type	2	0.000016	0.000016	3.15	0.051
2-Way Interactions	2	0.00000	0.00000	0.05	0.956
Gelatine content*Surfactant type	2	0.00000	0.00000	0.05	0.956
Error	12	0.000060	0.000005		
Total	17	0.00083			

Table A.11 ANOVA TABLE FOR THE MER OF GELATINE-SURFACTANT "A"-PLASTICISER FOAMS (SIGNIFICANCE LEVEL a=0.05)

SOURCE	DF	ADJ SS	ADJ MS	F-VALUE	P-VALUE
Model	11	17.6628	1.6057	4.60	0.007
Linear	4	17.2734	4.3184	12.36	0.000
Gelatine content	1	16.4673	16.4673	47.14	0.000
Plasticiser type	1	0,7994	0,7994	2.29	0.156
Plasticiser content	2	0.0068	0.0034	0.01	0.990
2-Way Interactions	5	0.3653	0.0731	0.21	0.952
Gelatine content*Plasticiser type	1	0.0182	0.0731	0.05	0.824
Gelatine content*Plasticiser content	2	0.3410	0.1705	0.49	0.625
Plasticiser type*Plasticiser content	2	0.0062	0.0031	0.01	0.991
3-Way Interactions	2	0.0240	0.0120	0.03	0.966
Gelatine content*Plasticiser type *Plasticiser content	2	0.0240	0.0120	0.03	0.966
Error	12	4.1922	0.3493		
Total	23	21.855			

Table A.12 ANOVA TABLE FOR THE MER OF GELATINE-SURFACTANT C2-PLASTICISER FOAMS (SIGNIFICANCE LEVEL a=0.05)

SOURCE	DF	ADJ SS	ADJ MS	F-VALUE	P-VALUE
Model	7	1.66987	0.23855	3.76	0.041
Linear	3	1.54942	0.51647	8.15	0.008
Gelatine content	1	1.28823	1.28823	20.33	0.002
Plasticiser type	1	0.06760	0.06760	1.07	0.332
Plasticiser content	1	0.19360	0.19360	3.06	0.119
2-Way Interactions	3	0.07422	0.02474	0.39	0.763
Gelatine content*Plasticiser type	1	0.01440	0.01440	0.23	0.646
Gelatine content*Plasticiser content	1	0.02560	0.02560	0.40	0.543
Plasticiser type*Plasticiser content	1	0.03422	0.03422	0.54	0.483
3-Way Interactions	1	0.04622	0.04622	0.73	0.418
Gelatine content*Plasticiser type *Plasticiser content	1	0.04622	0.04622	0.73	0.418
Error	8				
Total	15				

Table A.13 ANOVA TABLE FOR THE TOTAL SHRINKAGE OF GELATINE-SURFACTANT "A"-PLASTICISER FOAMS (SIGNIFICANCE LEVEL α=0.05)

SOURCE	DF	ADJ SS	ADJ MS	F-VALUE	P-VALUE
Model	11	1625.31	147.756	16.68	0.000
Linear	4	1138.94	284.734	32.14	0.000
Gelatine content	1	422.51	422.508	47.69	0.000
Plasticiser type	1	282.52	282.52	31.89	0.000
Plasticiser content	2	433.91	216.954	24.49	0.000
2-Way Interactions	5	455.78	91.155	10.29	0.000
Gelatine content*Plasticiser type	1	48.23	48.233	5.44	0.028
Gelatine content*Plasticiser content	2	388.06	169.03	19.08	0.000
Plasticiser type*Plasticiser content	2	69.48	34.742	3.92	0.034
3-Way Interactions	2	30.60	15.3	1.73	0.199
Gelatine content*Plasticiser type *Plasticiser content	2	30.60	15.3	1.73	0.199
Error	24	212.61			
Total	35	1837.93			

Table A.14 ANOVA TABLE FOR THE TOTAL SHRINKAGE OF GELATINE-SURFACTANT C2-PLASTICISER FOAMS (SIGNIFICANCE LEVEL α=0.05)

SOURCE	DF	ADJ SS	ADJ MS	F-value	P-value
Model	7	246.782	35.255	7.51	0.000
Linear	3	189.464	63.155	13.45	0.000
Gelatine content	1	55.173	55.173	11.75	0.003
Plasticiser type	1	4.401	4.401	0.94	0.347
Plasticiser content	1	129.89	129.89	27.67	0.000
2-Way Interactions	3	49.598	16.533	3.52	0.039
Gelatine content*Plasticise content	1	36.809	36.809	7.84	0.013
Gelatine content*Plasticiser type	1	12.76	12.76	2.72	0.119
Plasticiser*Plasticiser content	1	0.029	0.029	0.01	0.938
3-Way Interactions	1	7.719	7.719	1.64	0.218
Gelatine content*Plasticiser *Plasticiser content	1	7.719	7.719	1.64	0.218
Error	16	75.103	4.694		
Total	23	321.885			

Table A.15 ANOVA TABLE FOR THE DENSITY OF GELATINE-SURFACTANT "A"-PLASTICISER FOAMS (SIGNIFICANCE LEVEL α=0.05)

SOURCE	DF	ADJ SS	ADJ MS	F-VALUE	P-VALUE
Model	11	3095.88	281.44	81.28	0.000
Linear	4	3034.02	758.51	219.06	0.000
Gelatine content	1	2935.29	2935.29	847.71	0.000
Plasticiser type	1	0.02	0.02	0.01	0.939
Plasticiser content	2	98.71	49.35	14.25	0.000
2-Way Interactions	5	49.70	9.94	2.87	0.024
Gelatine content*Plasticiser type	1	13.59	13.59	3.92	0.053
Gelatine content*Plasticiser content	2	35.74	17.87	5.16	0.009
Plasticiser type*Plasticiser content	2	0.37	0.18	0.05	0.949
3-Way Interactions	2	12.16	6.08	1.76	0.184
Gelatine content*Plasticiser type *Plasticiser content	2	12.16	6.08	1.76	0.184
Error	48	166.20	3.46		
Total	59	3262.09			

Table A.16 ANOVA TABLE FOR THE DENSITY OF GELATINE-SURFACTANT C2-PLASTICISER FOAMS (SIGNIFICANCE LEVEL α=0.05)

SOURCE	DF	ADJ SS	ADJ MS	F-VALUE	P-VALUE
Model	7	3862.59	551.80	243.39	0.000
Linear	3	3777.24	1259.08	555.36	0.000
Gelatine content	1	3042.5	3042.5	1342	0.000
Plasticiser type	1	56.42	56.42	24.89	0.000
Plasticiser content	1	678.32	678.32	299.19	0.000
2-Way Interactions	3	55.93	18.64	8.22	0.000
Gelatine content*Plasticiser type	1	42.24	42.24	18.63	0.000
Gelatine content*Plasticiser content	1	0.99	0.99	0.44	0.513
Plasticiser type*Plasticiser content	1	12.70	12.70	5.60	0.024
3-Way Interactions	1	29.42	29.42	12.98	0.001
Gelatine content*Plasticiser type *Plasticiser content	1	29.42	29.42	12.98	0.001
Error	32	72.55	2.27		
Total	39	3935.13			

Table A.17 ANOVA TABLE FOR THE MER OF GELATINE-SURFACTANT "A"-FIBRE COMPOSITE FOAMS (SIGNIFICANCE LEVEL α=0.05)

SOURCE	DF	ADJ SS	ADJ MS	F-VALUE	P-VALUE
Model	11	55.66	5.06	43.87	0.000
Linear	4	54.40	13.60	117.92	0.000
Gelatine content	2	52.26	26.13	226.58	0.000
Fibre type	1	0.97	0.97	8.4	0.013
Fibre content	1	1.17	1.17	10.13	0.008
2-Way Interactions	5	1.15	0.23	2	0.152
Gelatine content*Fibre type	2	1.00	0.50	4.35	0.038
Gelatine content*Fibre content	2	0.14	0.07	0.59	0.569
Fibre type*Fibre content	1	0.01	0.01	0.1	0.752
3-Way Interactions	2	0.11	0.05	0.47	0.639
Gelatine content*Fibre type *Fibre content	2	0.11	0.05	0.47	0.639
Error	12	1.38	0.12		
Total	23	57.04			

Table A.18 ANOVA TABLE FOR THE MER OF GELATINE-SURFACTANT C2-FIBRE COMPOSITE FOAMS (SIGNIFICANCE LEVEL α=0.05)

SOURCE	DF	ADJ SS	ADJ MS	F-VALUE	P-VALUE
Model	7	3.89	0.57	0.73	0.654
Linear	3	2.97	0.99	1.3	0.339
Gelatine content	1	1.82	1.82	2.38	0.161
Fibre type	1	0.41	0.41	0.54	0.485
Fibre content	1	0.75	0.75	0.98	0.351
2-Way Interactions	3	0.81	0.27	0.36	0.789
Gelatine content*Fibre type	1	0.71	0.72	0.94	0.361
Gelatine content*Fibre content	1	0.01	0.01	0.01	0.945
Fibre type*Fibre content	1	0.10	0.01	0.12	0.733
3-Way Interactions	1	0.11	0.11	0.14	0.718
Gelatine content*Fibre type *Fibre content	1	0.11	0.11	0.14	0.718
Error	8	6.10	0.76		
Total	15	9.99			

Table A.19 ANOVA TABLE FOR THE SHRINKAGE OF GELATINE-SURFACTANT "A"-FIBRE COMPOSITE FOAMS (SIGNIFICANCE LEVEL α=0.05)

SOURCE	DF	ADJ SS	ADJ MS	F-VALUE	P-VALUE
Model	11	985.81	89.619	7.65	0.001
Linear	4	531.04	132.760	11.33	0.000
Gelatine content	2	6.88	3.440	0.29	0.751
Fibre type	1	419.66	419.663	35.82	0.000
Fibre content	1	104.50	104.496	8.92	0.011
2-Way Interactions	5	443.83	88.766	7.58	0.002
Gelatine content*Fibre type	2	357.04	178.519	15.24	0.001
Gelatine content*Fibre content	2	86.67	43.333	3.70	0.056
Fibre type*Fibre content	1	0.13	0.127	0.01	0.919
3-Way Interactions	2	10.94	5.469	0.47	0.638
Gelatine content*Fibre type *Fibre content	2	10.94	5.469	0.47	0.638
Error	12	140.58	11.715		
Total	23	1126.38			

Table A.20 ANOVA TABLE FOR THE SHRINKAGE OF GELATINE-SURFACTANT C2-FIBRE COMPOSITE FOAMS (SIGNIFICANCE LEVEL α=0.05)

SOURCE	DF	ADJ SS	ADJ MS	F-VALUE	P-VALUE
Model	7	452.055	64.579	16.38	0.000
Linear	3	388.404	129.468	32.84	0.000
Gelatine content	1	9.120	9.120	2.31	0.167
Fibre type	1	355.322	355.322	90.12	0.000
Fibre content	1	23.961	23.961	6.08	0.039
2-Way Interactions	3	63.552	21.184	5.37	0.026
Gelatine content*Fibre type	1	23.961	23.961	6.08	0.039
Gelatine content*Fibre content	1	30.470	30.47	7.73	0.024
Fibre type*Fibre content	1	9.120	9.12	2.31	0.167
3-Way Interactions	1	0.099	0.099	0.03	0.878
Gelatine content*Fibre type *Fibre content	1	0.099	0.099	0.03	0.878
Error	8	31.544	3.943		
Total	15	483.599			

Table A.21 ANOVA TABLE FOR THE DENSITY OF GELATINE-SURFACTANT "A"-FIBRE COMPOSITE FOAMS (SIGNIFICANCE LEVEL α=0.05)

SOURCE	DF	ADJ SS	ADJ MS	F-VALUE	P-VALUE
Model	11	14940.5	1358.23	701.84	0.000
Linear	4	14857.2	3714.29	1919.30	0.000
Gelatine content	2	13313.5	7206.73	3723.97	0.000
Fibre type	1	67.3	67.29	34.77	0.000
Fibre content	1	376.4	376.40	194.50	0.000
2-Way Interactions	5	82.3	16.45	8.50	0.000
Gelatine content*Fibre type	2	62.2	31.08	16.06	0.000
Gelatine content*Fibre content	2	18.2	9.10	4.70	0.014
Fibre type*Fibre content	1	1.9	1.92	0.99	0.325
3-Way Interactions	2	1.1	0.55	0.28	0.753
Gelatine content*Fibre type *Fibre content	2	1.1	0.55	0.28	0.753
Error	48	92.9	1.94		
Total	59	15033.4			

Table A.22 ANOVA TABLE FOR THE DENSITY OF GELATINE-SURFACTANT C2-FIBRE COMPOSITE FOAMS (SIGNIFICANCE LEVEL α=0.05)

SOURCE	DF	ADJ SS	ADJ MS	F-VALUE	P-VALUE
Model	7	4358.21	622.60	388.14	0.000
Linear	3	4314.83	1438.28	896.64	0.000
Gelatine content	1	4004.20	4004.20	2496.28	0.000
Fibre type	1	8.11	8.11	5.05	0.032
Fibre content	1	230.29	230.29	143.57	0.000
2-Way Interactions	3	30.54	10.18	6.35	0.002
Gelatine content*Fibre type	1	5.56	5.56	3.47	0.072
Gelatine content*Fibre content	1	5.84	5.84	3.64	0.066
Fibre type*Fibre content	1	18.22	18.22	11.36	0.002
3-Way Interactions	1	14.33	14.33	8.94	0.005
Gelatine content*Fibre type *Fibre content	1	14.33	14.33	8.94	0.005
Error	31	49.73	1.60		
Total	38	4407.94			

Table A.23 ANOVA TABLE FOR THERMAL CONDUCTIVITY OF AEROGEL FOAMS. AEROGEL INCLUSION SIGNIFICANCE (SIGNIFICANCE LEVEL α=0.05)

SOURCE	DF	ADJ SS	ADJ MS	F-VALUE	P-VALUE
Model	5	0.000038	0.000008	2.89	0.114
Linear	3	0.000037	0.000012	4.73	0.05
Gelatine content	1	0.000000	0.000000	0.14	0.719
Aerogel content	2	0.000037	0.000018	7.03	0.027
2-Way Interactions	2	0.000001	0.000000	0.13	0.877
Gelatine Strength*Gelatine content	2	0.000001	0.000000	0.13	0.877
Error	6	0.000016	0.000003		
Total	11	0.000053			

Table A.24 ANOVA TABLE FOR THERMAL CONDUCTIVITY OF AEROGEL FOAMS. AEROGEL TYPE AND CONTENT SIGNIFICANCE (SIGNIFICANCE LEVEL α=0.05)

SOURCE	DF	ADJ SS	ADJ MS	F-VALUE	P-VALUE
Model	7	0.000008	0.000001	2.39	0.123
Linear	3	0.000005	0.000002	3.50	0.070
Gelatine content	1	0.000003	0.000003	6.65	0.033
Aerogel type	1	0.000000	0.000000	0.07	0.801
Aerogel content	1	0.000002	0.000002	3.78	0.088
2-Way Interactions	3	0.000003	0.000001	2.07	0.183
Gelatine content*Aerogel type	1	0.000001	0.000001	2.27	0.170
Gelatine content*Aerogel content	1	0.000002	0.000002	3.75	0.089
Aerogel type*Aerogel content	1	0.000000	0.000000	0.18	0.684
3-Way Interactions	1	0.000000	0.000000	0.00	0.962
Gelatine content*Aerogel type*Aerogel content	1	0.000000	0.000000	0.00	0.962
Error	7	0.000008	0.000001	2.39	0.123
Total	3	0.000005	0.000002	3.50	0.070

APPENDIX B.
FIGURES

Appendix B. FIGURES

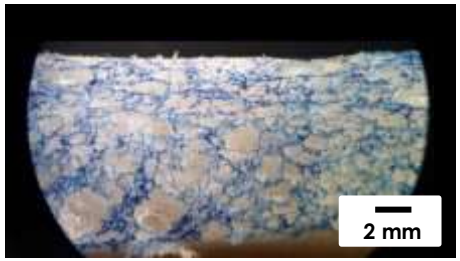

FH2.
15 *wt%* Gelatine. 0.05 *wt%* SURFACTANT C2

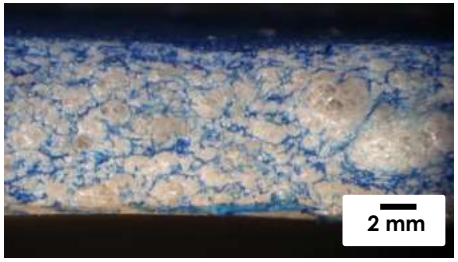

FH5.
15 *wt%* Gelatine. 0.05 *wt%* SURFACTANT B

FH8.
15 *wt%* Gelatine. 0.05 *wt%* SURFACTANT A

FH3.
15 *wt%* Gelatine. 0.5*wt%* SURFACTANT C2

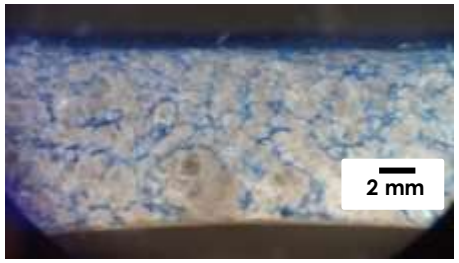

FH6.
15 *wt%* Gelatine. 0.5*wt%* SURFACTANT B

FH9.
15 *wt%* Gelatine. 0.5*wt%* SURFACTANT A

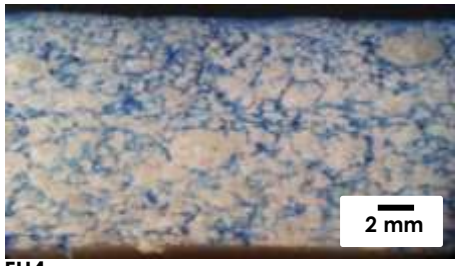

FH4.
15 *wt%* Gelatine. 5*wt%* SURFACTANT C2

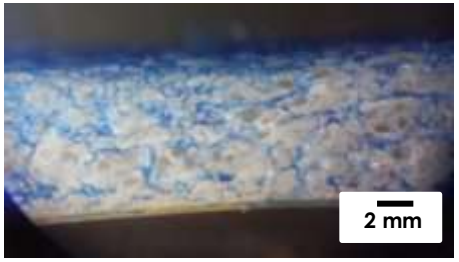

FH7.
15 *wt%* Gelatine. 5*wt%* SURFACTANT B

FH10.
15 *wt%* Gelatine. 5*wt%* SURFACTANT A

Figure B.1 OPTICAL MICROSCOPE IMAGES OF CROSS-SECTIONS SHOWING INFLUENCE OF SURFACTANT TYPE AND CONTENT ON THE CELL STRUCTURE OF DRY FOAMS

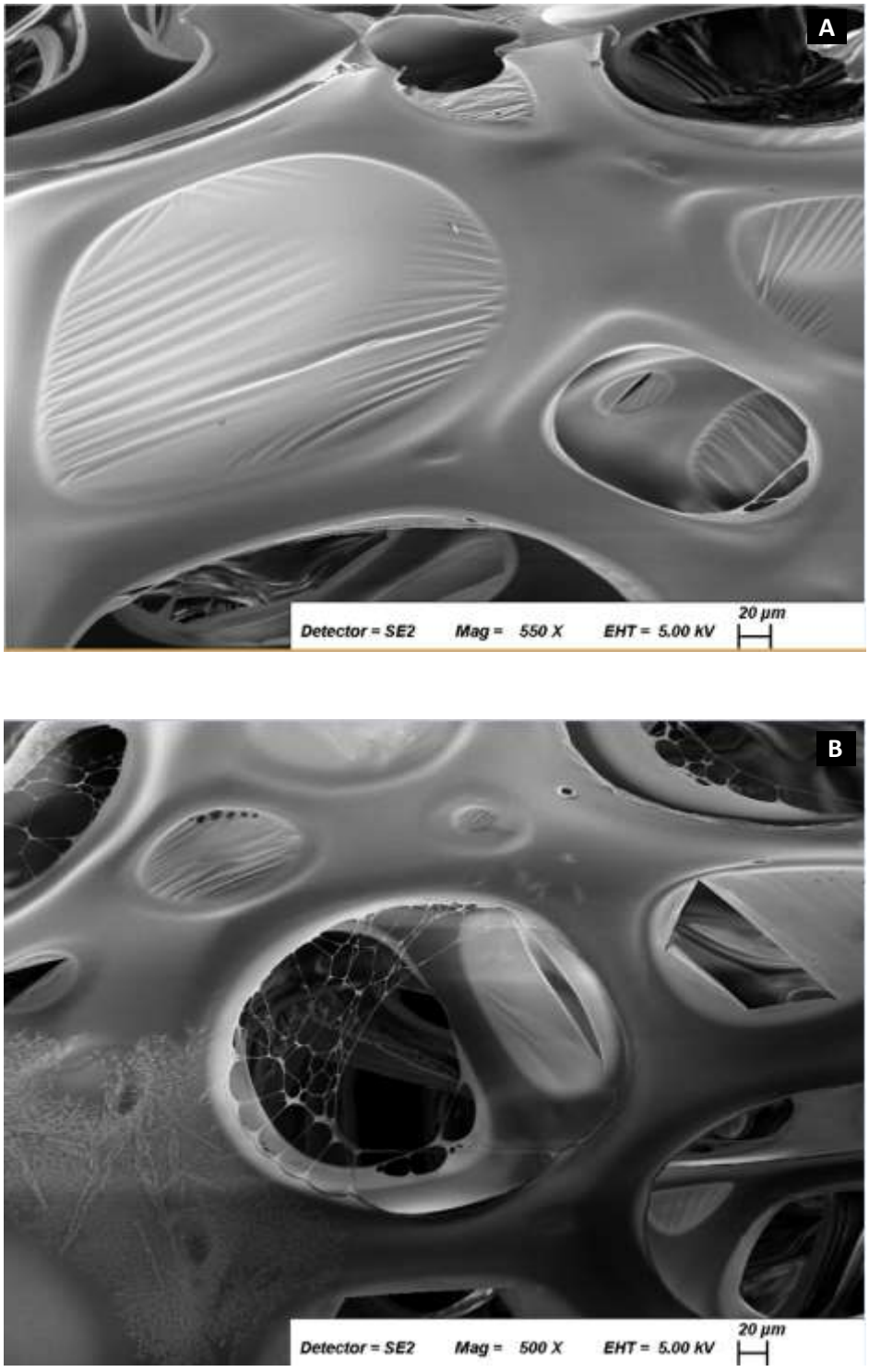

Figure B.2 SEM IMAGES SHOWING DETAILS OF SAMPLE C2.1 FOAM STRUCTURE (A) CELL WALL (B) WALLS DEFECTS

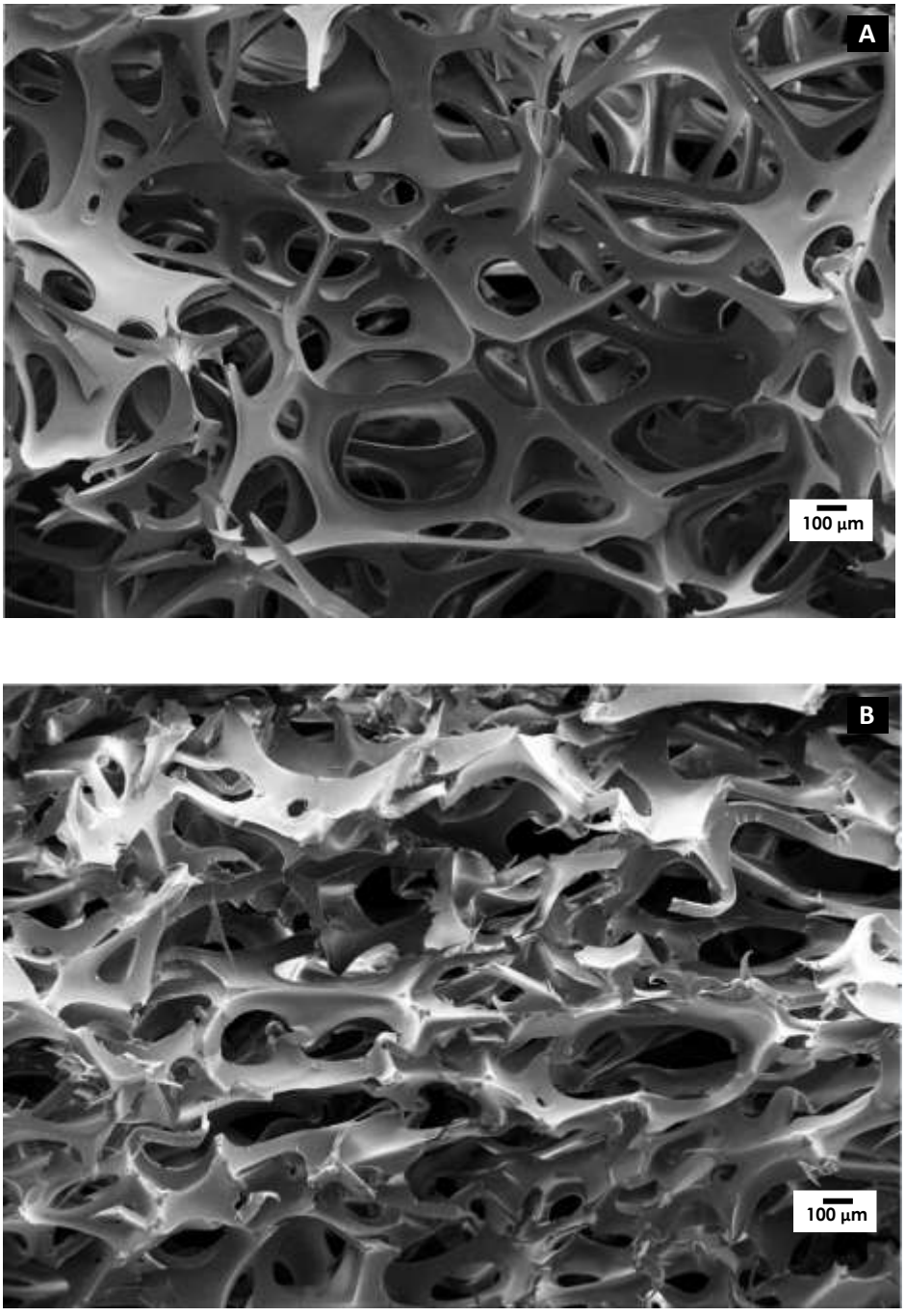

Figure B.3 SEM IMAGES COMPARISON OF GELATINE-SURFACTANT "A" FOAMS (A) NO COMPRESSED FOAM (B) COMPRESSED FOAM AT 50% STRAIN

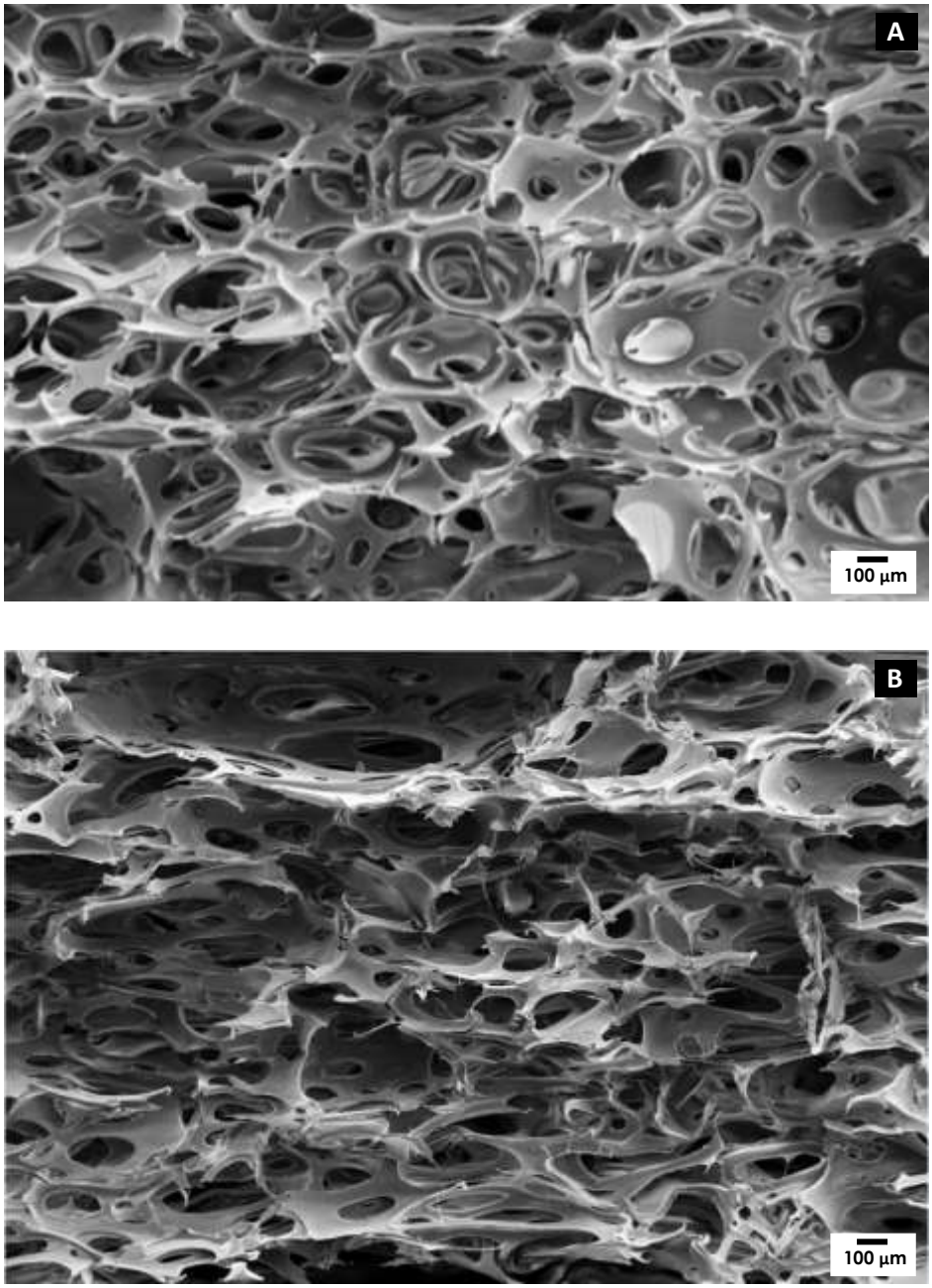

Figure B.4 SEM IMAGES COMPARISON OF GELATINE-SURFACTANT C2 FOAMS (A) NO COMPRESSED FOAM (B) COMPRESSED FOAM AT 50% STRAIN

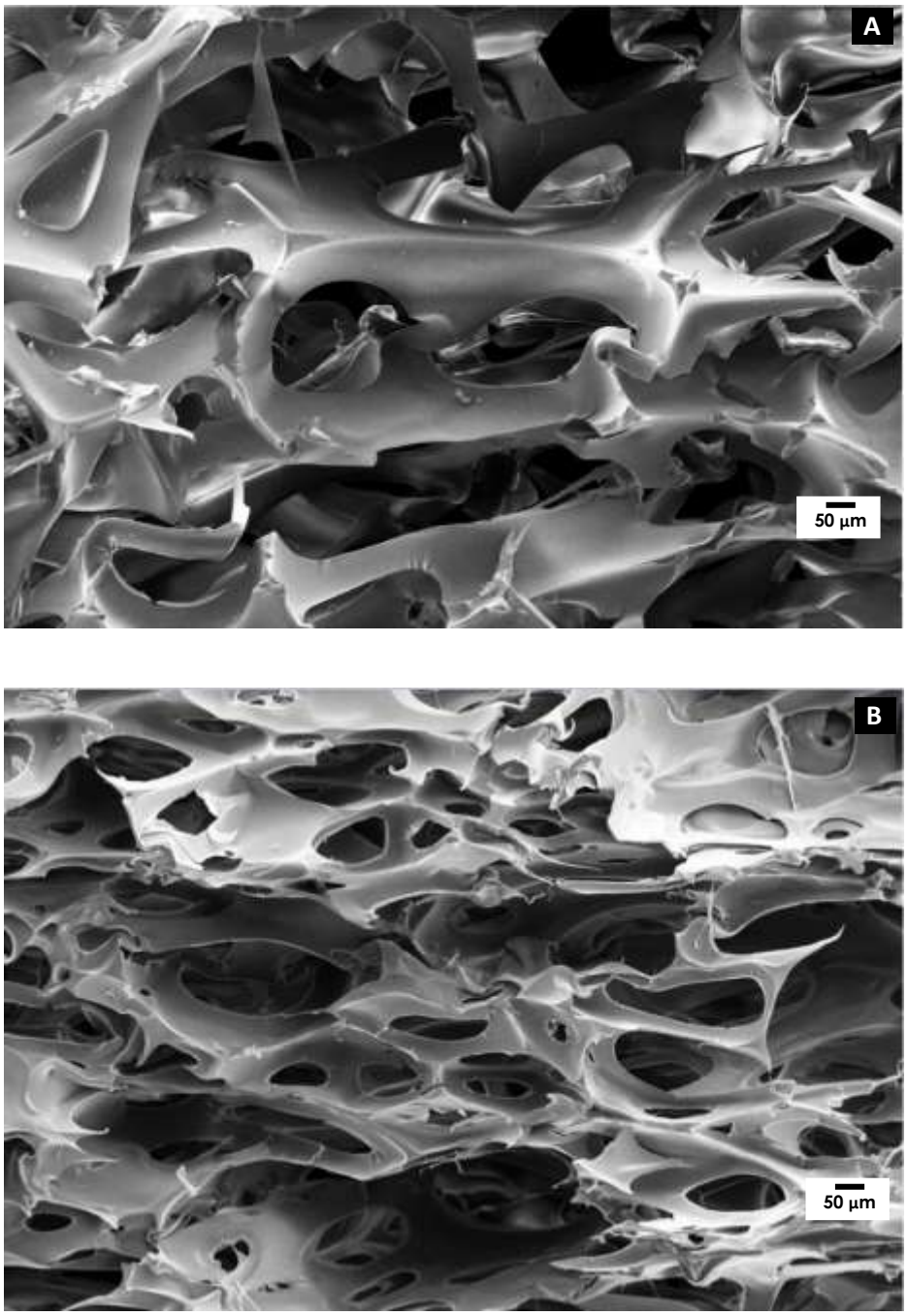

Figure B.5 SEM IMAGES OF (A) GELATINE-SURFACTANT "A" FOAM (B) GELATINE-SURFACTANT C2 FOAM COMPRESSED AT 50% STRAIN (CLOSE-UP)

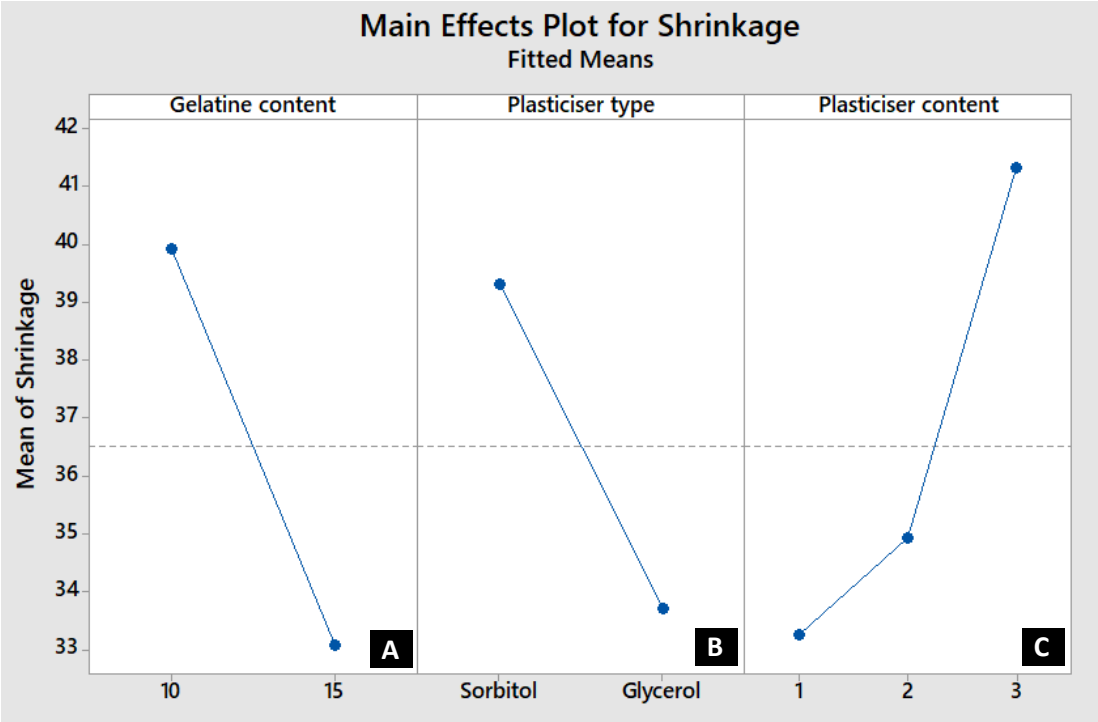

Figure B.6 MAIN EFFECTS PLOTS FOR TOTAL SHRINKAGE OF GELATINE-SURFACTANT "A"-PLASTICISER FOAMS (A) GELATINE CONTENT (*wt%*); (B) PLASTICISER TYPE; (C) PLASTICISER CONTENT (wt%)

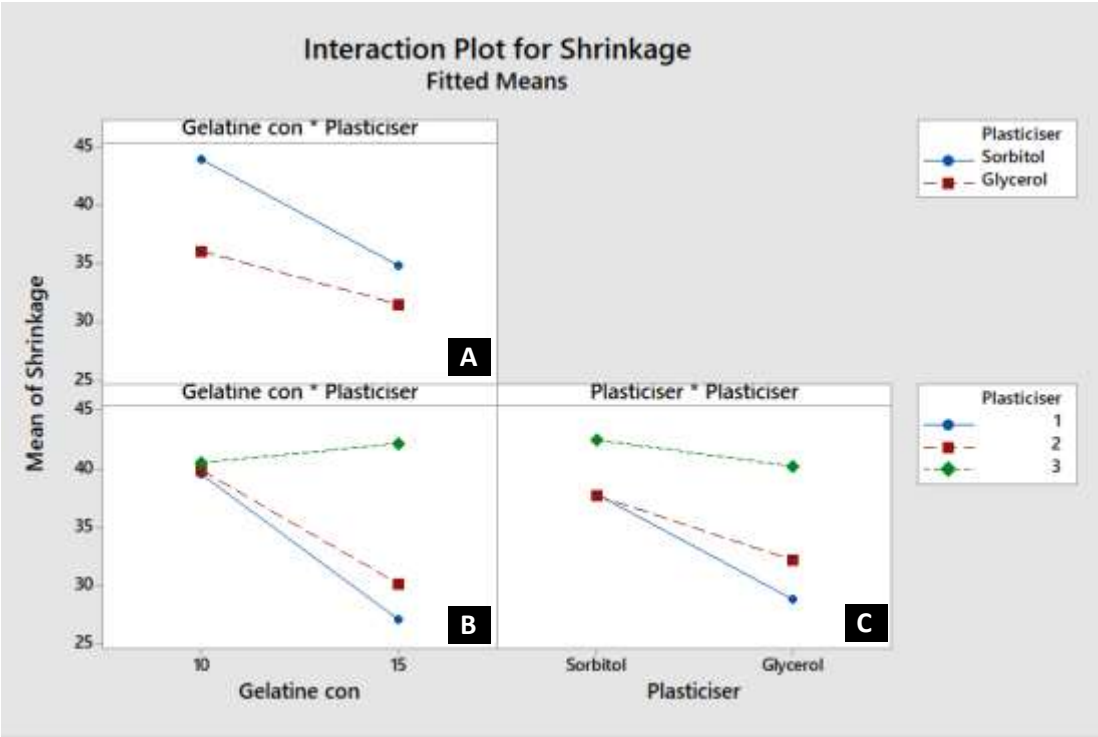

Figure B.7 INTERACTION PLOTS FOR GELATINE-SURFACTANT "A"-PLASTICISERS TOTAL SHRINKAGE (A) GELATINE CONTENT-PLASTICISER TYPE INTERACTION (B) GELATINE CONTENT-PLASTICISER CONTENT INTERACTION (C) PLASTICISER TYPE-PLASTICISER CONTENT INTERACTION

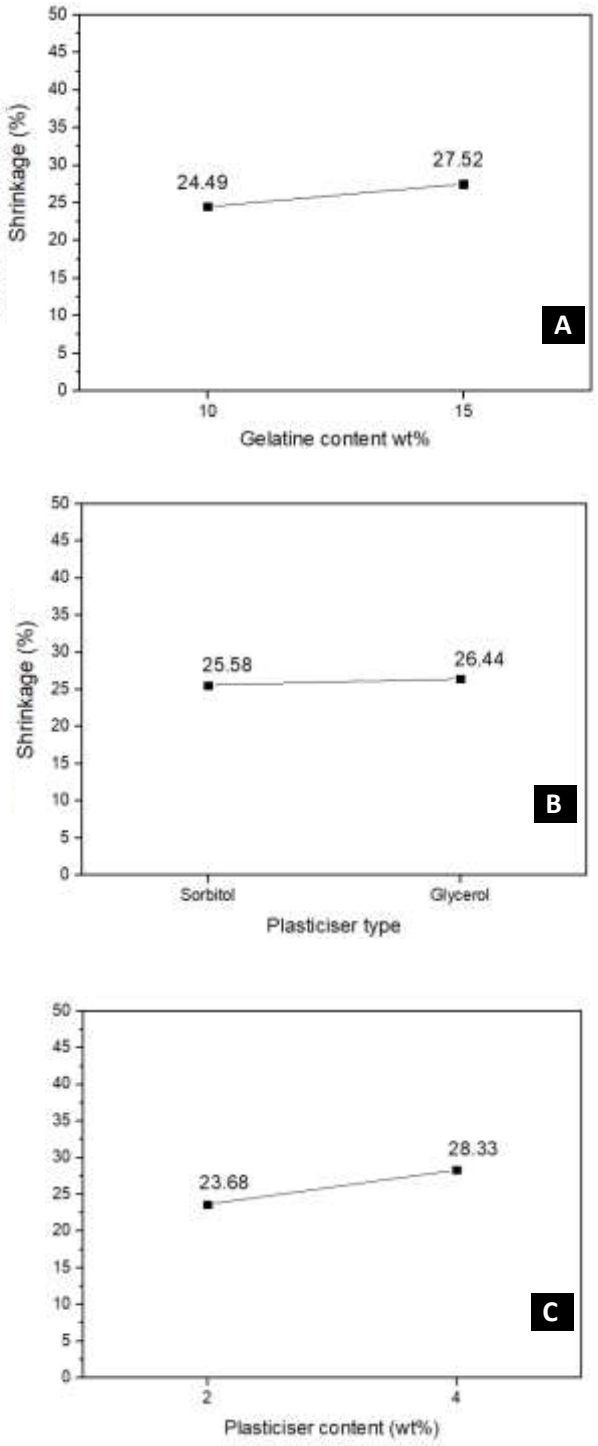

Figure B.8 MAIN EFFECTS PLOTS FOR TOTAL SHRINKAGE OF GELATINE-SURFACTANT C2-PLASTICISER FOAMS (A) GELATINE CONTENT (*wt%*); (B) PLASTICISER TYPE; (C) PLASTICISER CONTENT (wt%)

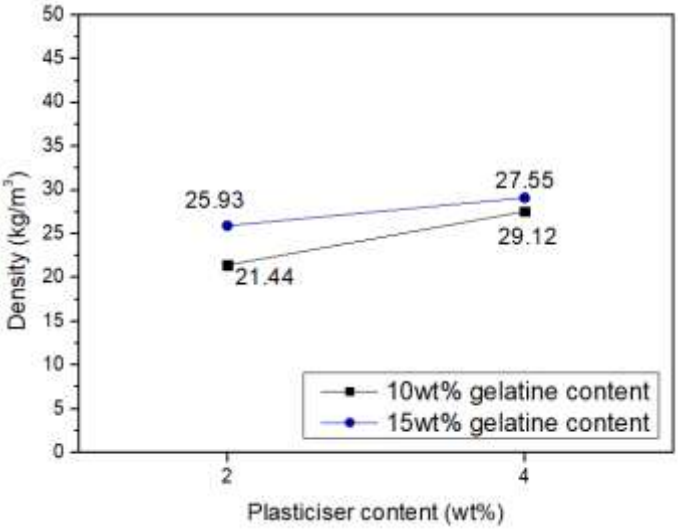

Figure B.9 GELATINE-PLASTICISER CONTENTS INTERACTION PLOT FOR GELATINE-SURFACTANT C2-PLASTICISERS TOTAL SHRINKAGE

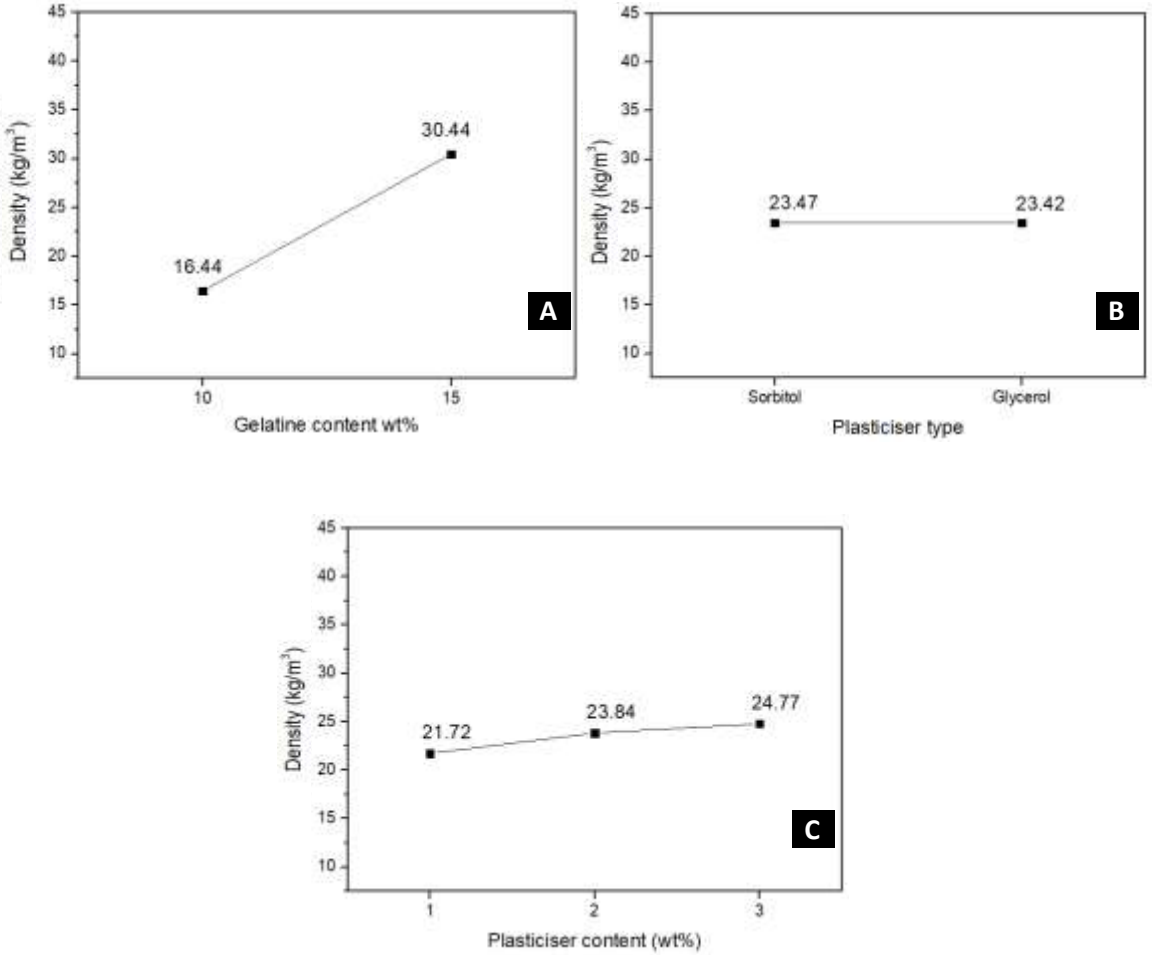

Figure B.10 MAIN EFFECTS PLOTS FOR DENSITY OF GELATINE-SURFACTANT "A"-PLASTICISER FOAMS (A) GELATINE CONTENT (*wt%*); (B) PLASTICISER TYPE; (C) PLASTICISER CONTENT (wt%)

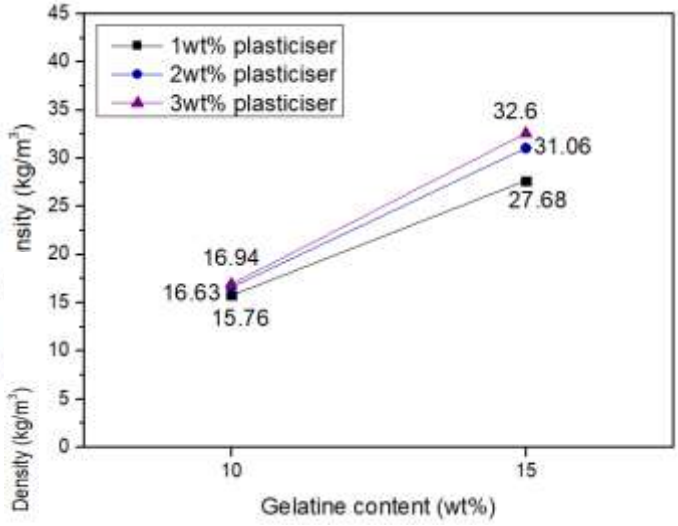

Figure B.11 GELATINE-PLASTICISER CONTENTS INTERACTION PLOT FOR GELATINE-SURFACTANT C2-PLASTICISERS TOTAL SHRINKAGE

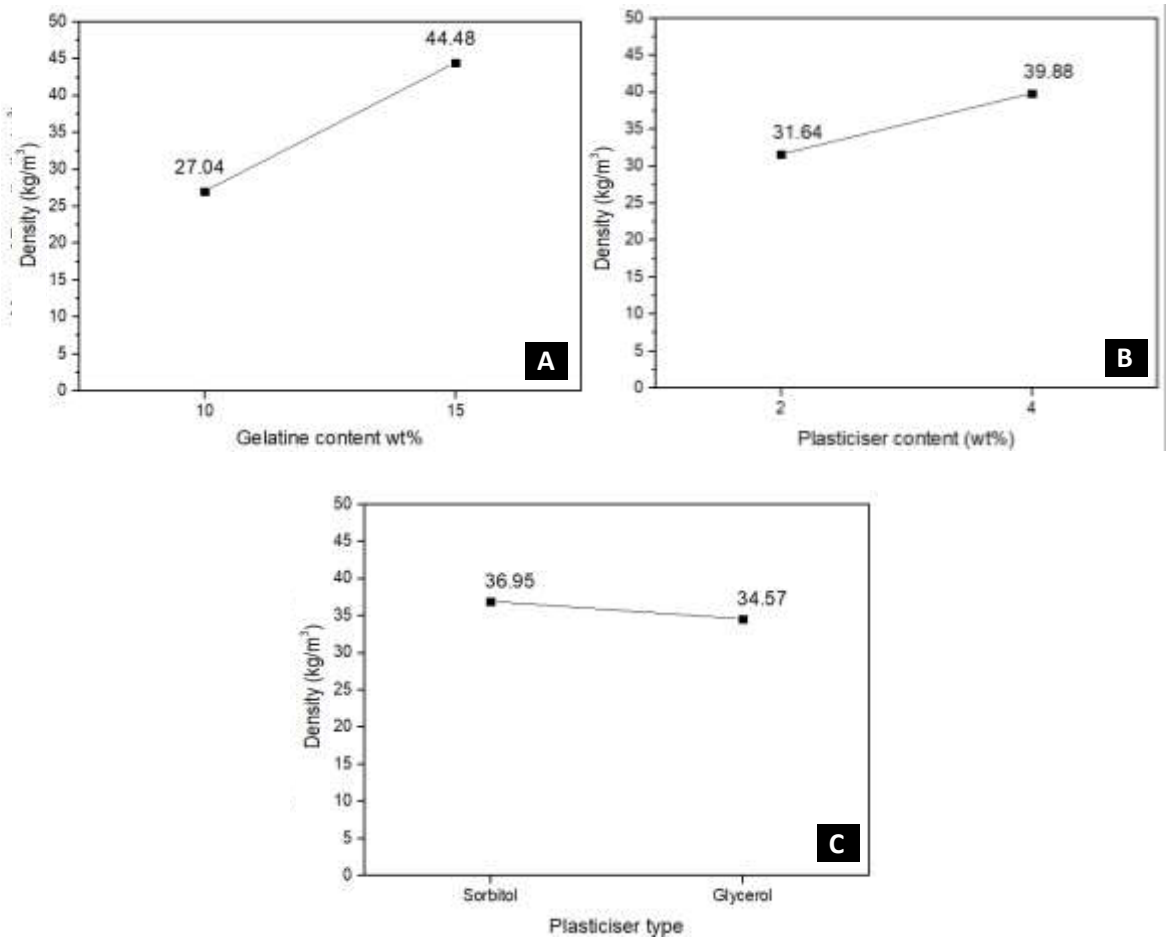

Figure B.12 MAIN EFFECTS PLOTS FOR DENSITY OF GELATINE-SURFACTANT C2-PLASTICISER FOAMS (A) GELATINE CONTENT (*wt*%); (B) PLASTICISER CONTENT (wt%) (C) PLASTICISER TYPE

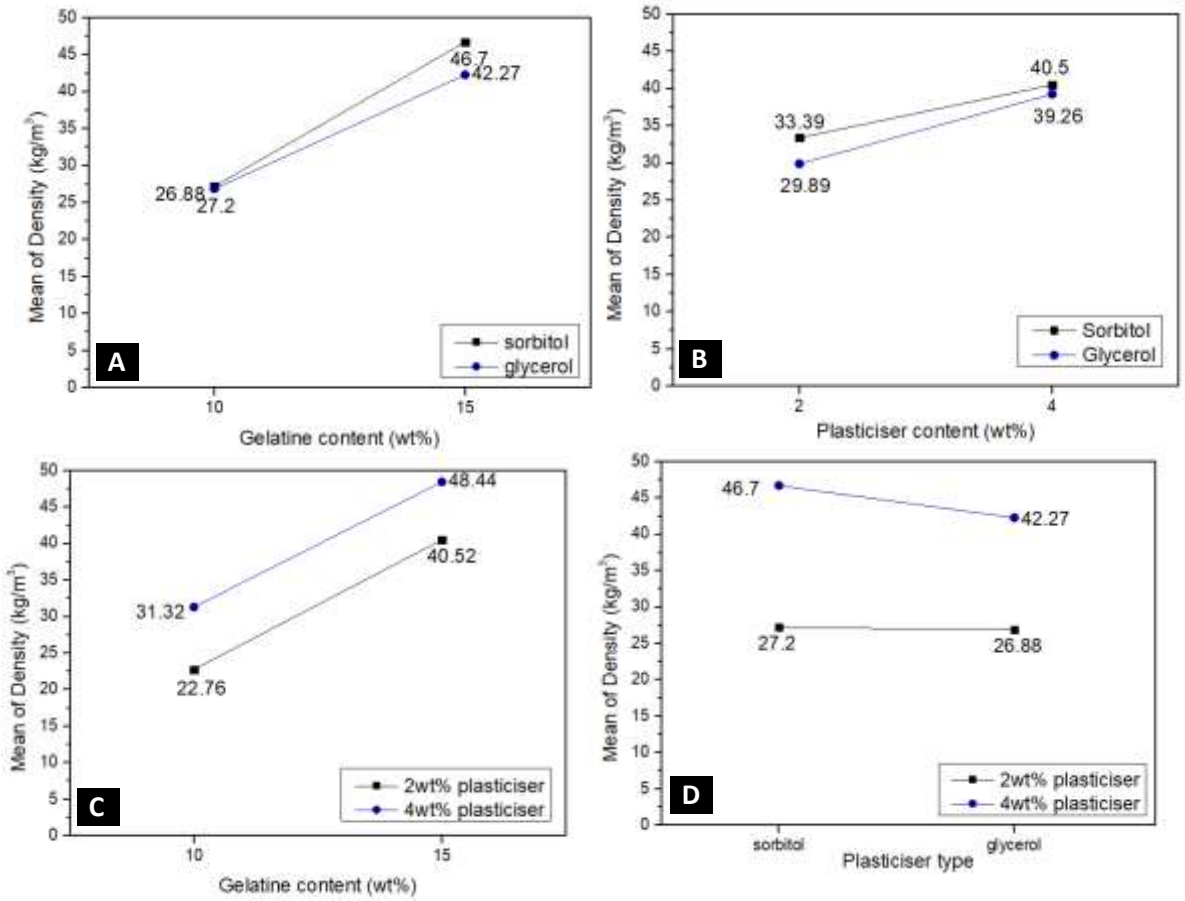

Figure B.13 INTERACTION PLOTS FOR GELATINE-SURFACTANT C2-PLASTICISERS DENSITY (A) GELATINE CONTENT-PLASTICISER TYPE INTERACTION (B) GELATINE CONTENT-PLASTICISER CONTENT INTERACTION (C) PLASTICISER TYPE-PLASTICISER CONTENT INTERACTION

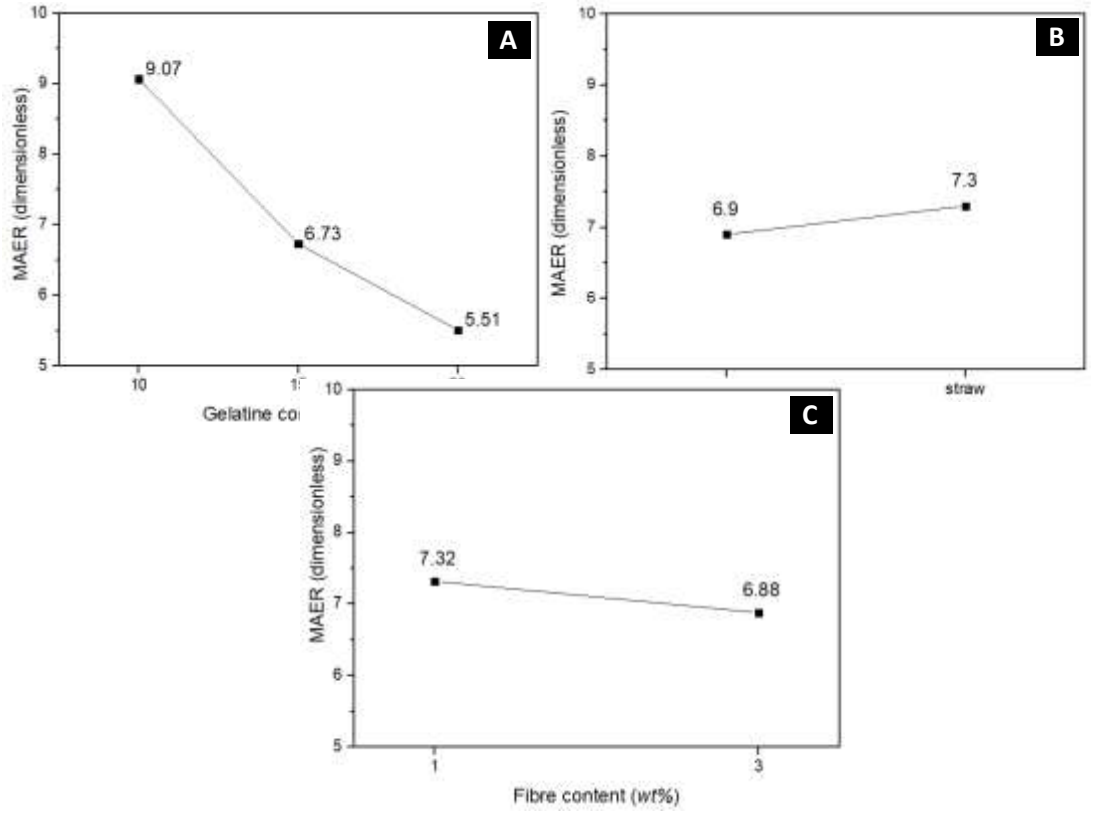

Figure B.14 MAIN EFFECTS PLOTS FOR MER OF GELATINE-SURFACTANT "A"-FIBRE COMPOSITE FOAMS (A) GELATINE CONTENT (*wt%*); (B) FIBRE TYPE (C) FIBRE CONTENT (*wt%*)

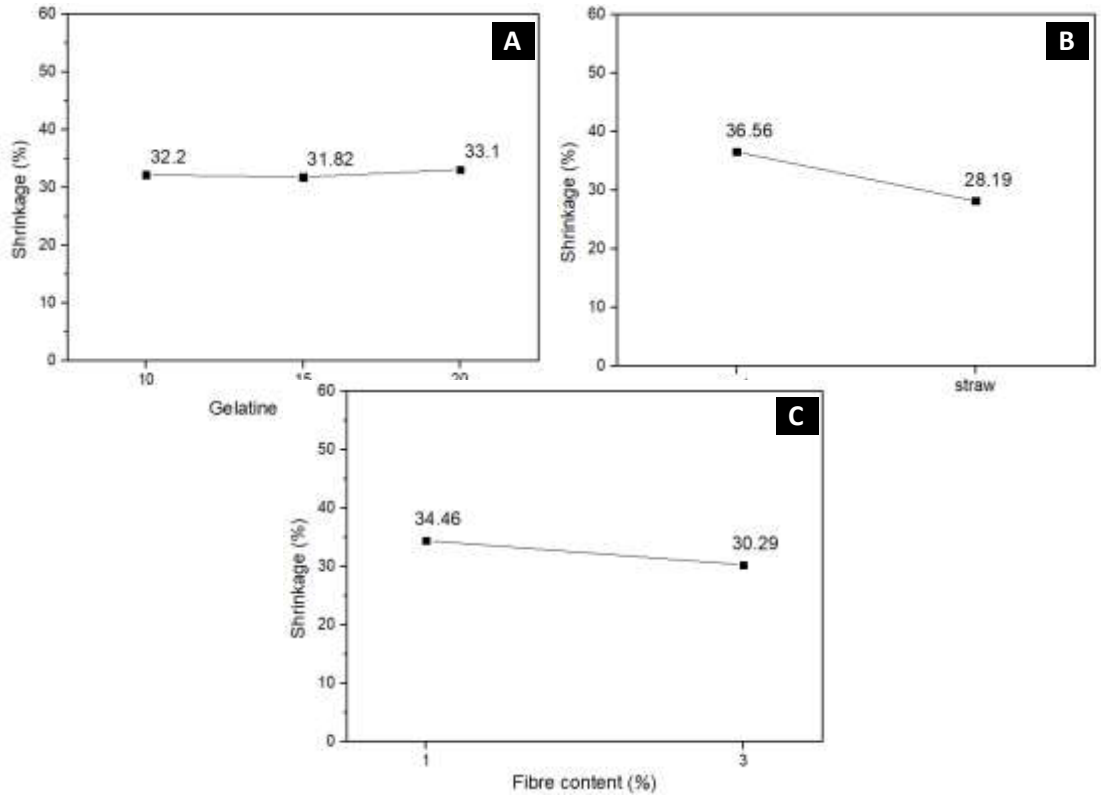

Figure B.15 MAIN EFFECTS PLOTS FOR SHRINKAGE OF GELATINE-SURFACTANT "A"-FIBRE COMPOSITE FOAMS (A) GELATINE CONTENT (*wt%*); (B) FIBRE TYPE (C) FIBRE CONTENT (*wt%*)

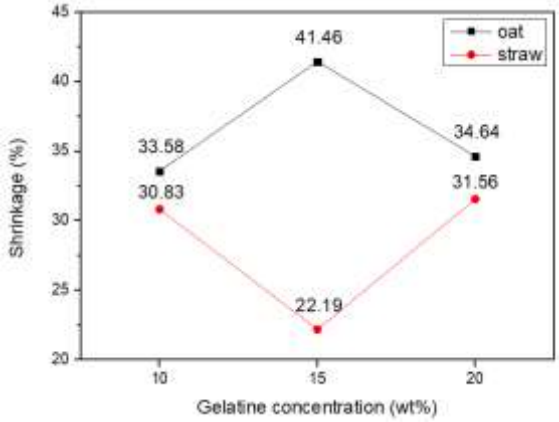

Figure B.16 GELATINE CONTENT-FIBRE TYPE INTERACTION PLOT FOR THE SHRINKAGE OF GELATINE-SURFACTANT "A"-FIBRE COMPOSITE FOAMS

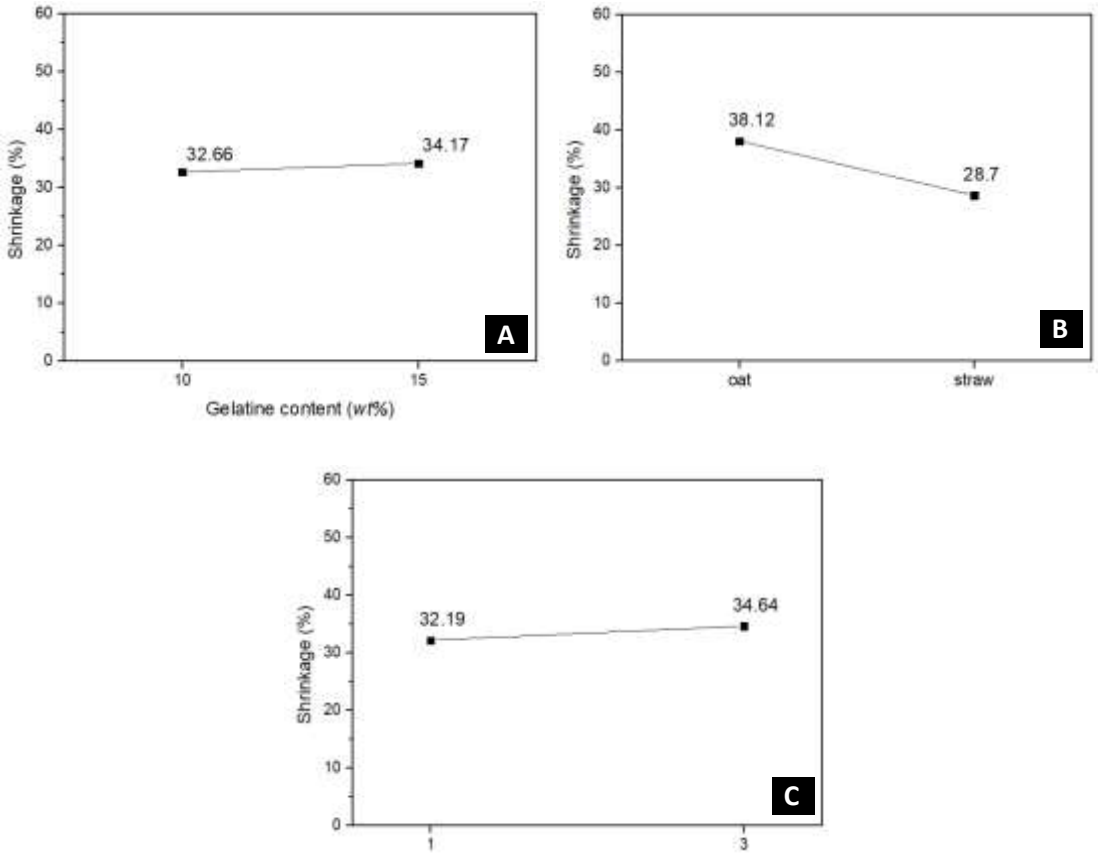

Figure B.17 MAIN EFFECTS PLOTS FOR SHRINKAGE OF GELATINE-SURFACTANT C2-FIBRE COMPOSITE FOAMS (A) GELATINE CONTENT (*wt%*); (B) FIBRE TYPE (C) FIBRE CONTENT (wt%)

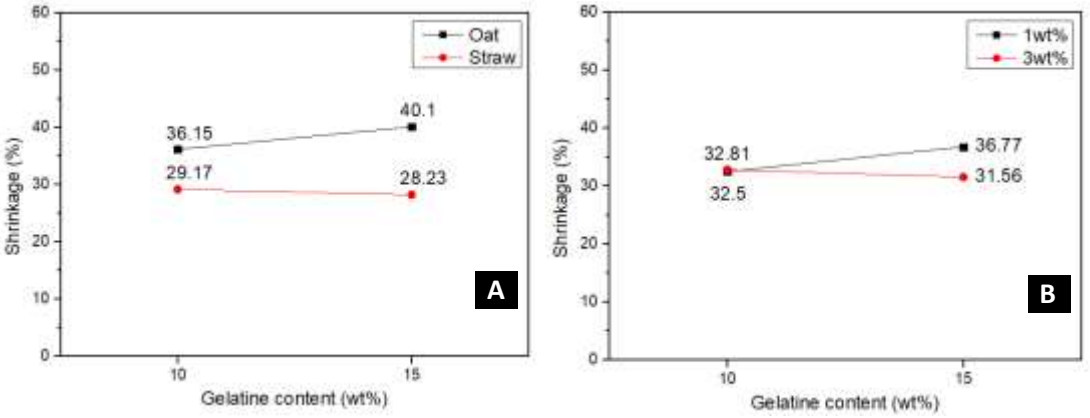

Figure B.18 INTERACTION PLOTS FOR GELATINE-SURFACTANT C2-FIBRE COMPOSITES SHRINKAGE (A) GELATINE CONTENT-FIBRE TYPE INTERACTION (B) GELATINE CONTENT-FIBRE CONTENT INTERACTION

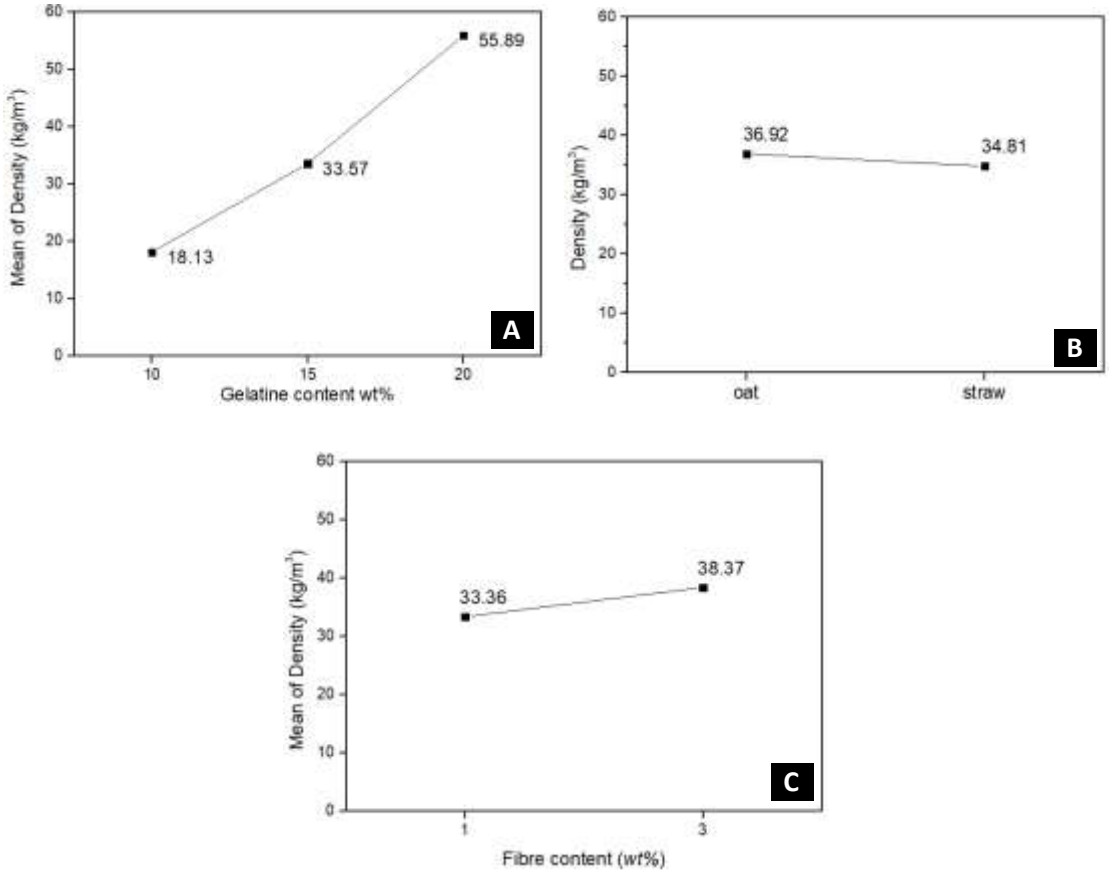

Figure B.19 MAIN EFFECTS PLOTS FOR DENSITY OF GELATINE-SURFACTANT "A"-FIBRE COMPOSITE FOAMS (A) GELATINE CONTENT (*wt%*); (B) FIBRE TYPE (C) FIBRE CONTENT (wt%)

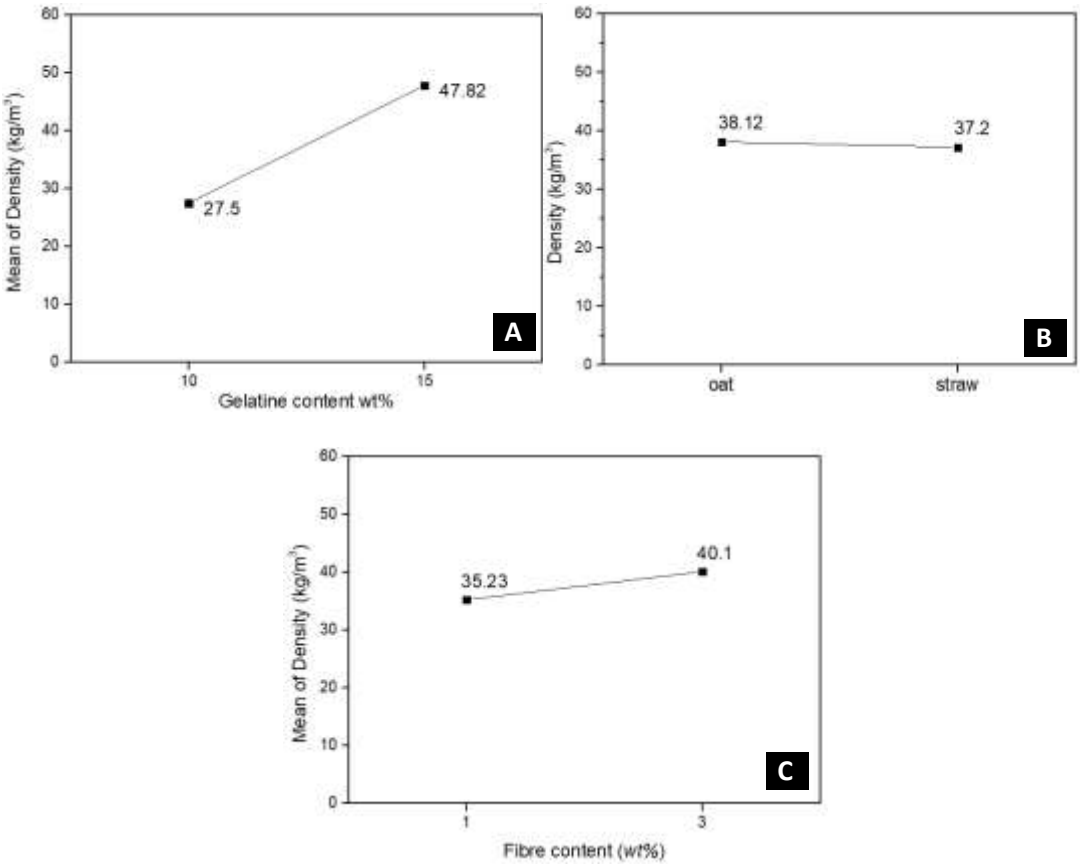

Figure B.20 MAIN EFFECTS PLOTS FOR DENSITY OF GELATINE-SURFACTANT C2-FIBRE COMPOSITE FOAMS (A) GELATINE CONTENT (*wt%*); (B) FIBRE TYPE (C) FIBRE CONTENT (wt%)

APPENDIX C.
TABLES

Appendix C. TABLES

Table C.1 VARIATION OF EXPANSION RATIO WITH FOAMING TIME FOR HYDROGEL-SURFACTANT "A" FOAMS

	EXPANSION RATIO (dimensionless)									
TIME (min)	**A1**	**A2**	**A3**	**A4**	**A5**	**A6**	**A7**	**A8**	**A9**	**TIME (min)**
0	1.00 ± 0.00	1.00 ± 0.00	1.00 ± 0.00	1.00 ± 0.00	1.00 ± 0.00	1.00 ± 0.00	1.00 ± 0.00	1.00 ± 0.00	1.00 ± 0.00	**0**
0.25	4.83 ± 0.24	5.14 ±0.26	4.37 ± 0.27	4.01 ±0.23	2.93 ±0.15	3.72 ±0.46	6.87 ±0.95	6.55 ±1.22	5.07 ±0.14	**0.25**
1	7.13 ± 0.29	8.07 ±0.46	5.19 ±0.25	5.90 ±0.20	3.61 ±0.19	4.73 ±0.77	7.78 ±0.75	8.35 ±1.73	6.19 ±0.52	**1**
2	7.88 ± 0.29	9.01 ±0.44	5.69 ±0.22	6.00 ±0.15	4.14 ±0.33	5.31 ±0.87	8.42 ±0.95	10.14 ±1.03	6.36 ±0.28	**2**
3	7.98 ± 0.05	9.67 ±0.39	5.99 ±0.19	6.08 ±0.14	4.86 ±0.42	5.52 ±0.56	9.02 ±0.10	9.87±0.41	6.56 ±0.37	**3**
4	8.12 ± 0.05	9.73 ±0.37	6.01 ±0.22	6.01 ±0.25	5.08 ±0.12	5.52 ±0.56	9.30 ±0.10	10.27 ±0.03	6.66 ±0.70	**4**
5	8.17 ± 0.07	9.67 ±0.40	6.13 ±0.09	6.19 ±0.31	5.17 ±0.06	5.59 ±0.56	9.65 ±0.40	10.26±0.56	5.70 ±0.67	**5**
10	**8.67 ±0.05**	**9.85 ±0.7**	**6.46±0.30**	**6.99 ±0.23**	**5.70±0.23**	**6.45 ±0.74**	**9.70 ±0.43**	**10.20±0.84**	**7.39 ±0.50**	**10**

	EXPANSION RATIO (dimensionless)									
TIME (min)	**A10**	**A11**	**A12**	**A13**	**A14**	**A15**	**A16**	**A17`**	**A18**	**TIME (min)**
0	1.00 ± 0.00	1.00 ± 0.00	1.00 ± 0.00	1.00 ± 0.00	1.00 ± 0.00	1.00 ± 0.00	1.00 ± 0.00	1.00 ± 0.00	1.00 ± 0.00	**0**
0.25	6.29 ± 0.00	3.41 ±0.09	4.90 ± 0.54	6.05 ±1.04	6.65 ±0.51	5.18 ±0.29	6.58 ±0.35	4.05 ±0.49	4.68 ±0.76	**0.25**
1	7.47 ± 0.72	4.66 ±0.82	7.09 ±0.86	7.63 ±0.30	10.51 ±0.40	6.24 ±0.15	7.69 ±0.74	5.48 ±0.54	7.38 ±0.35	**1**
2	8.59 ± 0.96	5.06 ±0.14	7.54 ±0.52	8.11 ±0.21	11.04 ±0.26	6.98 ±0.53	8.49 ±0.10	5.59 ±0.39	7.89 ±0.76	**2**
3	8.59 ± 0.57	5.44 ±0.77	7.96 ±0.81	9.10 ±0.30	10.90 ±0.06	7.26 ±0.34	8.91 ±0.59	5.73 ±0.30	8.03 ±0.35	**3**
4	8.62 ± 0.05	5.50 ±0.67	7.75 ±0.62	9.55 ±0.15	10.67 ±0.33	7.46 ±0.43	9.05 ±0.30	6.14 ±0.00	7.74 ±0.56	**4**
5	8.65 ± 0.48	5.65 ±0.58	7.68 ±0.52	9.55 ±0.05	10.63 ±0.27	7.62 ±0.59	9.03 ±0.36	7.02 ±0.25	7.92 ±0.20	**5**
10	**8.65 ±0.48**	**6.23 ±0.32**	**7.88 ±0.22**	**9.84 ±0.36**	**10.25 ±0.78**	**7.27 ±0.72**	**9.15 ±0.25**	**7.63 ±0.50**	**9.23 ±0.25**	**10**

Table C2. VARIATION OF EXPANSION RATIO WITH FOAMING TIME FOR HYDROGEL-SURFACTANT C2 FOAMS

	EXPANSION RATIO (dimensionless)									
TIME (min)	**C2.10**	**C2.11**	**C2.12**	**C2.13**	**C2.14**	**C2.15**	**C2.16**	**C2.17**	**C18**	**TIME (min)**
0	1.00 ± 0.00	1.00 ± 0.00	1.00 ± 0.00	1.00 ± 0.00	1.00 ± 0.00	1.00 ± 0.00	1.00 ± 0.00	1.00 ± 0.00	1.00 ± 0.00	**0**
0.25	3.38 ± 0.81	2.84 ±0.36	4.01 ± 0.82	4.43 ± 0.67	4.38 ± 1.40	3.42 ± 0.58	4.04 ±0.14	2.30 ±0.18	2.70 ±0.40	**0.25**
1	4.71 ± 1.50	4.03 ±0.40	5.75 ±0.97	5.32 ±0.42	5.86 ± 1.68	4.85 ± 1.01	5.40 ±0.26	3.83 ±0.40	3.79 ±0.19	**1**
2	4.99 ± 1.18	4.82 ±0.19	6.12 ±0.71	5.86 ± 0.01	6.61 ± 1.47	5.07 ± 0.97	6.14 ±0.10	4.17 ±0.40	4.46 ±0.26	**2**
3	5.79 ± 0.87	5.26 ±0.41	6.50 ±0.38	6.39 ± 0.30	7.18 ± 1.11	6.12 ± 0.34	6.36 ±0.35	4.28 ±0.33	5.24 ±0.20	**3**
4	5.96 ± 0.57	5.47 ±0.37	6.50 ±0.43	6.93 ± 0.90	7.63 ± 0.98	6.19 ± 0.20	6.39 ±0.40	4.41 ±0.35	5.42 ±0.14	**4**
5	6.24 ± 0.10	5.80 ±0.72	6.46 ±0.28	7.00 ±0.93	7.67 ± 0.96	6.25 ± 0.19	6.37 ±0.38	4.50 ±0.48	5.52 ±0.28	**5**
10	**6.63 ±0.41**	**6.84 ±0.71**	**7.93 ±0.81**	**7.29 ±0.37**	**7.89 ± 0.40**	**6.34 ±0.28**	**7.08 ±0.16**	**4.50 ±0.46**	**6.27 ±0.50**	**10**

	EXPANSION RATIO (dimensionless)									
TIME (min)	**C2.1**	**C2.2**	**C2.3**	**C2.4**	**C2.5**	**C2.6**	**C2.7**	**C2.8**	**C2.9**	**TIME (min)**
0	1.00 ± 0.00	1.00 ± 0.00	1.00 ± 0.00	1.00 ± 0.00	1.00 ± 0.00	1.00 ± 0.00	1.00 ± 0.00	1.00 ± 0.00	1.00 ± 0.00	**0**
0.25	4.16 ± 1.55	4.37 ± 1.56	3.66 ± 0.56	3.59 ±0.85	2.17 ±0.17	2.56 ±0.17	5.03 ±0.10	6.18 ± 0.18	3.94 ±0.99	**0.25**
1	5.66 ± 1.34	6.17 ± 1.26	4.78 ±0.48	5.26 ±0.81	3.58 ±0.55	3.77 ±0.49	5.97 ±0.61	7.34 ± 0.51	4.92 ± 1.15	**1**
2	5.77 ± 0.60	6.99 ± 1.11	5.06 ±0.28	6.15 ±0.42	4.18 ±0.37	4.29 ±0.35	6.23 ±0.25	7.97 ± 0.31	5.84 ± 1.34	**2**
3	6.25 ± 0.17	7.47 ± 0.44	5.82 ±0.22	6.68 ±0.25	4.91 ±0.21	5.09 ±0.46	6.33 ±0.36	8.42 ±0.27	6.20 ± 1.06	**3**
4	6.57 ± 0.15	7.52 ± 0.21	5.87 ±0.47	6.69 ±0.32	5.29 ±0.19	5.57 ±0.45	6.53 ±0.32	8.48 ±0.22	6.89 ± 0.43	**4**
5	6.80 ± 0.30	7.60 ±0.13	6.00 ±0.49	6.80 ±0.43	5.40 ±0.28	5.84 ±0.67	6.77 ±0.11	8.41 ±0.10	5.90 ± 0.41	**5**
10	**7.17 ±0.05**	**7.60 ±0.09**	**6.64 ±0.17**	**6.86 ±0.53**	**5.44±0.28**	**5.86 ±0.55**	**7.68 ±0.28**	**8.52 ±0.22**	**7.02 ±0.21**	**10**

Table C.2 CELL SIZE DISTRIBUTION OF THE GELATINE-SURFACTANT "A" FOAMS

CELL Ø (*mm*)	ER1		ER2		ER3		ER4		ER5	
	FREQ. (%)	CELLS/ cm^2	FREQ. (%)	CELLS/ cm^2	FREQ. (%)	CELLS/ cm^2	FREQ. (%)	CELLS/ cm^2	FREQ. (%)	CELLS/ cm^2
<0.5	84.87	947.56	82.74	656.00	83.89	666.67	93.2	1436.4	90.80	1192.9
0.5-1	12.26	136.89	13.45	106.67	11.41	90.67	6.01	94.22	8.25	108.44
1-1.5	1.27	14.22	1.79	14.22	1.79	14.22	0.23	3.56	0.54	7.11
1.5- 2	0.64	7.11	0.45	3.56	0.23	1.78	0.00	0.00	0.14	1.78
>2	0.96	10.67	1.57	12.44	2.68	21.33	0.58	8.89	0.27	3.56
TOTAL	**100**	**1116.5**	**100**	**792.89**	**100**	**794.67**	**100**	**1543.1**	**100**	**1313.8**

Table C.3 SUMMARY OF CELL DISTRIBUTION DATA SHOWING AVERAGE, MINIMUM AND MAXIMUM CELL SIZES OF THE GELATINE-SURFACTANT "A" FOAMS

	ER1	ER2	ER3	ER4	ER5
Average Cell Diameter (*mm*)	0.28	0.31	0.33	0.24	0.25
Minimum cell size (*mm*)	0.08	0.08	0.08	0.08	0.08
Maximum cell size (*mm*)	4.42	5.49	4.79	4.77	4.86